01 Oct 1969

Channel and Z-sections braced by diaphragms

Nuri Celebi

George Winter

CCFSS LIBRARY Celebi, Nuri, Winter, George
22 3 * 136 CHANNEL AND Z-SECTIONS BRACED BY
1969 DIAPHRAGMS

=

DATE	ISSUED TO

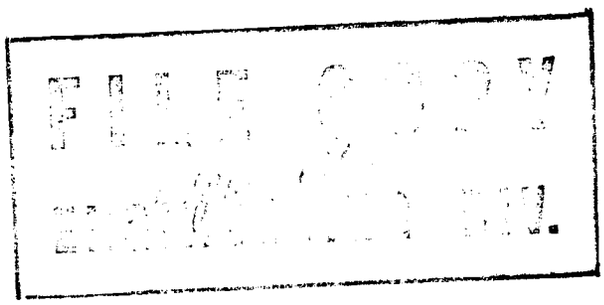

Department of Structural Engineering
School of Civil Engineering
Cornell University

Informal Progress Report on

CHANNEL AND Z-SECTIONS BRACED BY DIAPHRAGMS

by Nuri Celebi

George Winter, Project Director

October 9, 1969

CHANNEL AND Z-SECTION BEAMS BRACED BY DIAPHRAGMS

1. General

The differential equations of bending under distributed loading for thin-walled singly or point symmetrical open sections (like channels or Z-sections), braced by a diaphragm have been derived. The equations have been solved by the Galerkin Method using infinite series for hinged boundary conditions and uniformly distributed load acting (downward or uplift) through the web of the beam. The case of one discrete bracing at mid-span is also being treated. The bracing prevents the lateral deflection v and the rotation ϕ at midspan. Because of the symmetry of loading also v' and ϕ' vanish at that point.

Based on these solutions computer programs have been developed to compute the yield load capacity of channel, lipped channel, Z- and lipped Z-section beams for a given shear rigidity Q of the diaphragm bracing. The stresses at midspan and the max deflections v and ϕ are also computed. Before presenting some numerical examples, the effect of the diaphragm bracing will be discussed qualitatively.

2. Influence of diaphragm stiffness:

Since the bracing restrains the points where it is connected to the beam from sidesway displacement, its effectiveness largely depends on how much and in which direction these points tend to displace. Consider a beam first without bracing. Suppose that the diaphragm will later be connected to the upper flange at point A.

a) Channel or lipped channel: On the figures below, the load is partitioned into three components.

Downward loading:

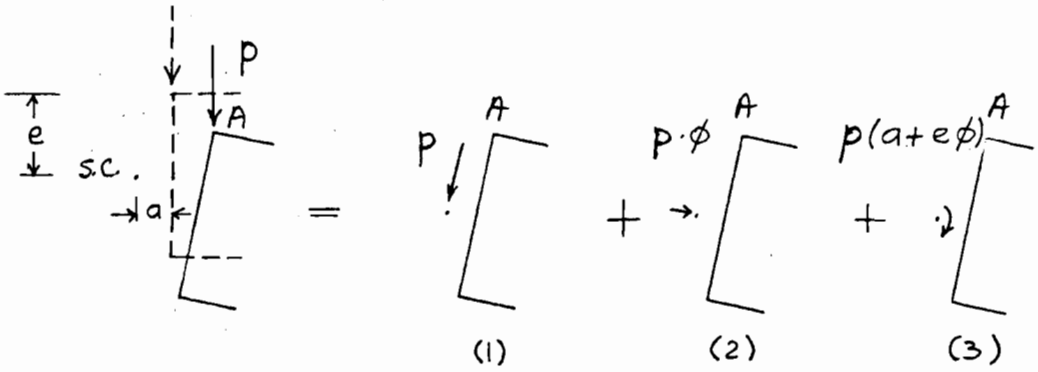

The effects of components (2) and (3) add, hence point A moves clearly to the right. The bracing force therefore is as follows:

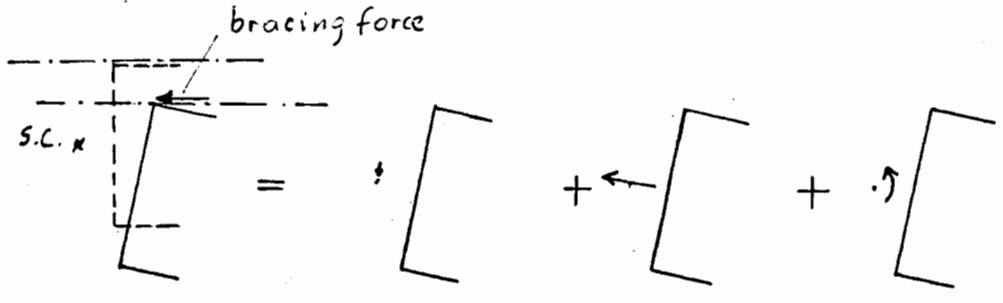

Hence, component (1) is slightly increased while the other two are greatly reduced. Hence the yield load capacity will clearly be increased by diaphragm bracing.

Uplift loading :

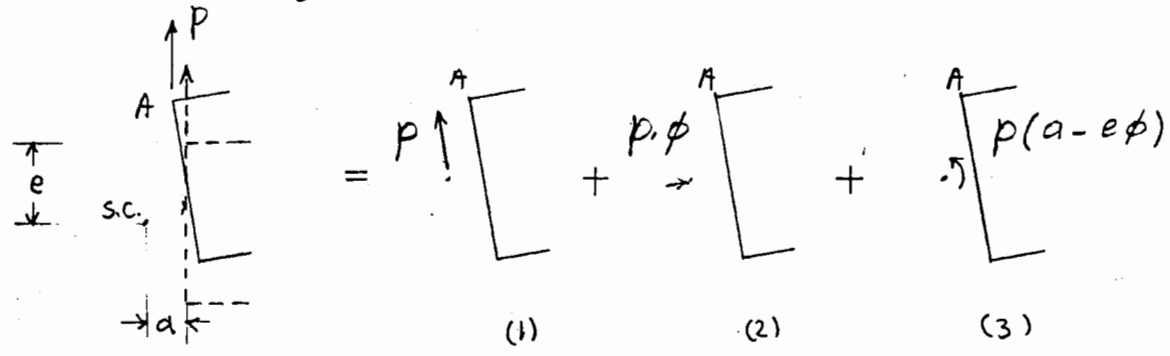

The situation is more complex for this case. Point A has the tendency to move to the right due to the component (2) and to the left due to the component (3). However when we increase the load continuously from zero , φ will be small at the outset and the comp. (2) can be neglected. Therefore at first, point A will move to the left as shown on the figure above. The diaphragm forces then are as follows :

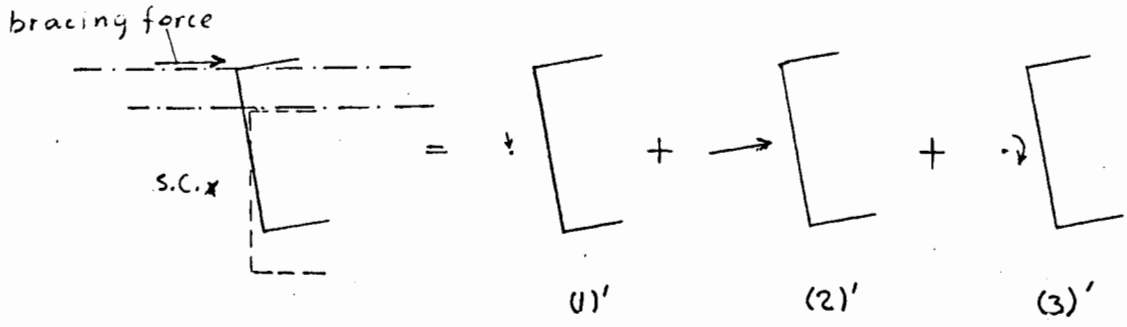

It is observed that diaphragm forces increase the comp. (2) but decrease (1) and (3). Hence depending on section properties bracing may increase or decrease the capacity if yielding occurs at this stage.

When the load can increase further, the comp. (2) will be dominant, and point A will eventually move to the right. This in turn changes the sign of the bracing forces. Now the comp (2) will be reduced while the components (1) and (3) are increased. It depends again on the section properties whether the yielding capacity will be increased or decreased.

An interesting situation arises when the dimensions and the length of the beam are such that yielding occurs at the level of the load where point A has just come back from the left to its initial position. For this case, the diaphragm forces are zero. Hence yielding capacity cannot be affected by the stiffness of the diaphragm.

b) <u>Z- or lipped Z-sections</u> : The carrying capacity of Z-sections can be greatly increased by diaphragm bracing, because bracing supplies horizontal supporting

3. Computer results

Summing up the discussion in the previous chapter, diaphragm bracing increases the carrying capacity of channels under downward loading; but may increase, decrease or not affect it for the uplift loading case. On the other hand, the carrying capacity of Z-sections will be increased for downward as well as uplift loading. These conclusions are confirmed by the computer results as shown on Tables I-A through I-D.

In Tables I-A (through) I-D the midspan moment $M = \frac{PL^2}{\delta}$ (under yield load) is shown for $\frac{Q}{P_r}$ values from 0 to 1000 and for various span lengths ranging from 30" to 120". Q is the shear stiffness of the diaphragm bracing and $P_r = \pi^2 E I_y / L^2$ is the Euler buckling load. There is an important point which can be observed in these Tables: The capacity M practically does not vary over a range extending from a relatively small finite value for shear stiffness, say $Q = 4P_r$, up to infinity. ($4P_r$ is an approximate number valid only for the presented examples. It may change for sections with different dimensions).

As will be shown in the next chapter, a relatively simple design procedure can be developed for beams braced by a rigid diaphragm. This procedure then can be used safely for beams braced by diaphragms of reasonable stiffness.

On Figures 1-A through 1-D the ratios $\frac{M_o}{M_{bend.}}$ and $\frac{M_\infty}{M_{bend.}}$ versus span length are shown. The subscripts "o" and "∞" show "no" and "rigid" bracing respectively. M_o and M_∞ are compared here with the theoretical capacity $M_{bend} = \frac{\sigma_y I_x}{e}$. The numbers in circles indicate where in the cross-section yielding has occur. The dotted lines indicate where the max. angle of rotation is larger than 10°.

In the computations the yield stress σ_y is assumed to be 33 ksi. However, since the stresses are generally variable along the flanges and lips, 15% overstressing is allowed. This results in a max. stress of 37.95 ksi at the peaks. Examples for stress distribution are given on Figures 2-A through 2-D. They imply that the allowance of overstressing is generally justified for uplift loading case. But for downward loading, it seems justified only for unbraced beams. For braced beams under downward loading the max. stress should be limited to σ_y, unless the

designer computes the stresses at all corners and shows that overstressing is justified.

Figures 3-A through 3-D show the lateral deflections and the angles of rotation at the mid-span of unbraced and rigidly braced beams versus the total load $p \cdot L$ for uplift loading case. It is observed that v_o for channel and ϕ_o for Z-sections are tangential to the load axis at $pL = 0$. This is because there is no load component at the outset to cause these deflections.

From Tables II-A through II-D, it is seen that the rotations are generally reduced for downward but increased for uplift loading with increasing stiffness of the bracing. Z beams display generally less rotation than channel beams. However, when the stiffness is increased, there is not much difference between them. Note that all the deflections are computed under yield load of that particular case.

Then

$$E\Gamma'\phi^{IV} = p\left(a + \frac{I_{xy}}{I_x} e\right)$$

This is very similar to the differential equation of ordinary bending. Namely:

$$E I_x v^{IV} = p$$

Let us define a quantity called bimoment B_z analogous to bending moment M_x:

$$B_z = -E\Gamma'\phi'' = -\iint p\left(a + \frac{I_{xy}}{I_x} e\right) dz^2$$

analogous to

$$M_x = -E I_x v'' = -\iint p\, dz^2$$

The stress due to B_z is

$$\sigma = \frac{B_z}{\Gamma'} w' \qquad \text{analogous to} \qquad \sigma = \frac{M_x}{I_x} y$$

where

$$w' = \frac{I_{xy}}{I_x} y e - x e + w$$

w = warping

The computation of bimoment B_z is same as the bending moment. Thus for example, for simply supported boundary conditions (i.e. $\phi = \phi'' = 0$ at $z = 0$ and $z = L$), the max. bimoment is at midspan and equal to

$$p\left(a + \frac{I_{xy}}{I_x} e\right) \cdot \frac{L^2}{8}$$

4- Design formula for rigid bracing :

Rigid bracing will prevent point A from moving sidesway. This gives :

$$u_A = u + \phi e = 0$$

$$\therefore \quad u = -\phi \cdot e$$

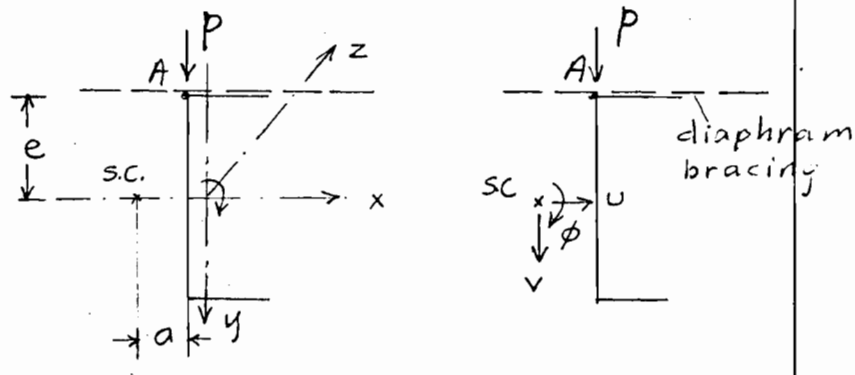

Thus the lateral deflection u can be eliminated and after modifications, one obtains a fourth order differential equation for the angle of rotation ϕ.

$$E\Gamma'\phi^{IV} - GK\phi'' + F\phi - [M_x\phi'' + (M_x\phi)'']e - pe\phi = p\left(a + \frac{I_{xy}}{I_x}e\right)$$

where

$$\Gamma' = \Gamma + \frac{I_x I_y - I_{xy}^2}{I_x} e^2$$

Γ = Warping constant = C_w

K = Saint-venant's torsion constant

F = Resistance of the diaphragm against rotation of beam. (Taken zero in the numerical computation.)

M_x = Bending moment due to p

a) Definition of Bimoment

In order to define the term "bimoment" suppose we temporarily neglect the terms with less than the fourth derivative in the differential equation above.

b) Solution of the differential equation:

An approximate solution of the differential equation on Page 9 is obtained by Galerkin Method with one term of series $\phi = \sum_1^{\infty} \phi_i f_i$. Namely:

$$\phi = \phi_1 f_1$$

(where f_1 is chosen as the first eigenfunction of free vibriation of a beam with the same boundary conditions as the beam under consideration. λ_1 is the eigenvalue).

The function g_1 is defined in the curvature expression

$$\phi'' = \phi_1 \lambda_1^2 g_1$$

Applying the method

$$\phi_1 = \frac{L^2}{\lambda_1^2} \frac{\int_0^1 f_1 \, dz}{\lambda_1^2 \int_0^1 f_1^2 \, dz} \frac{pL^2(a + \frac{I_{xy}}{I_x} e)}{E\Gamma'} \frac{1}{1 + k^2 L^2} \frac{1}{1 - M/Mcr}$$

Substituting ϕ_1 into curvature expression and doing some modifications, the stress becomes

$$\sigma = \frac{M_x}{I_x} y + \frac{Bz}{\Gamma'} w' \frac{1}{1+k^2L^2} \frac{1}{1 - M/Mcr}$$

where

$$k^2 = \frac{-GK \int_0^1 g_1 f_1 \, dz + \frac{FL^2}{\lambda_1^2} \int_0^1 f_1^2 \, dz}{E\Gamma' \lambda_1^2 \int_0^1 f_1^2 \, dz}, \quad z = \frac{z}{L}$$

$$Mcr = - \frac{E\Gamma' \lambda_1^2 (1 + k^2 L^2) \int_0^1 f_1^2 \, dz}{T \cdot L^2 e}$$

T = a constant depending on boundary conditions.

For simply supported boundary conditions and F=0

$$k^2 = \frac{GK}{\pi^2 E\Gamma'}$$

$$M_{cr} \approx -\frac{1.08}{e}\left(\frac{\pi^2 E\Gamma'}{L^2} + GK\right)$$

c) Discussion :

The stress $\frac{B_z}{\Gamma'} w'$ is due to warping as well as bending strains (except the primary bending stress $\frac{M_x}{I_x} y$). As mentioned before, computation of B_z is similar to a routine bending moment analysis, and should not present any difficulties.

The factor $\frac{1}{1+k^2L^2}$ shows the influence of the saint-venant torsion. Note that k^2 depends on boundary conditions.

The term $\frac{1}{1-M/M_{cr}}$ is like a magnification factor. When M approaches M_{cr}, the deflections and stresses will increase indefinitely. The situation is somewhat similar to that of a beam-column : In a beam-column, the axial force causes additional bending moment due to the bending deformations. In this case however, additional torsion moments

are caused by the rotation and the lateral deflection of the cross-section.

Note that Mcr is a negative quantity. Therefore the magnification factor is greater than unity only for negative values of M, that is for uplift. For downward loading, magnification factor is less than one. The situation is then similar to a beam-column with a tensile force.

d) Summary of the formulas for stress

$$\sigma = \frac{M_x}{I_x} y + \frac{B_z}{\Gamma'} w' \frac{1}{1+k^2L^2} \frac{1}{1 - M/M_{cr}}$$

$$M_x = -\iint p\, dz^2 \quad , \quad B_z = -\iint p\left(a + \frac{I_{xy}}{I_x} e\right) dz^2$$

$$\Gamma' = \Gamma + \frac{I_x I_y - I_{xy}^2}{I_x} \cdot e^2 \quad , \quad \Gamma = \text{warping constant} = \int w^2 t\, ds = C_w$$

$$w' = \frac{I_{xy}}{I_x} ye - xe + w \quad , \quad w = \text{warping (Simple formulas available)}$$

Note that in formula for σ and w', the quantities x, y, and w may have different values for different points of the cross-section.

$$k^2 = \frac{-GK \int_0^1 q_i f_i\, dz + \frac{FL^2}{\lambda_i^2} \int_0^1 f_i^2\, dz}{E\Gamma' \lambda_i^2 \int_0^1 f_i^2\, dz}$$

$$M_{cr} = -\frac{E\Gamma' \lambda_i^2 (1 + k^2L^2) \int_0^1 f_i^2\, dz}{T L^2 e}$$

For Simply Supported Ends: $k^2 = \frac{GK}{\pi^2 E\Gamma'}$

(and for $F = 0$) $\qquad M_{cr} \approx \frac{1.08}{e} \left(\frac{\pi^2 E\Gamma'}{L^2} + GK\right)$

5- Summary and conclusions

... The stress and deflections of channel, lipped channel, Z- and lipped Z-section beams braced by diaphragms have been investigated under downward as well as uplift loading. It is found that the carrying capacity is generally increased by diaphragm bracing except for channel or lipped channels under uplift loading. For this case the capacity may be increased or slightly decreased.

The influence of shear stiffness Q on yield load capacity is investigated numerically through computer. The capacity increases rapidly for small values of Q but does not vary appreciably over a range extending from a finite value of Q up to infinity. For examples considered here, a reasonable value for Q seems to fall into this range.

Finally a design formula for computing the stress has been developed for beams braced by rigid diaphragms. As discussed before, this formula can also be used safely for beams braced by diaphragms of reasonable rigidity. A formula to define "reasonable rigidity" is yet to be developed.

Table I-A : Midspan moment $M = \frac{pL^2}{8}$ [ki] (under yield load) for different values of Q/P_Y and L

Channel Section Example

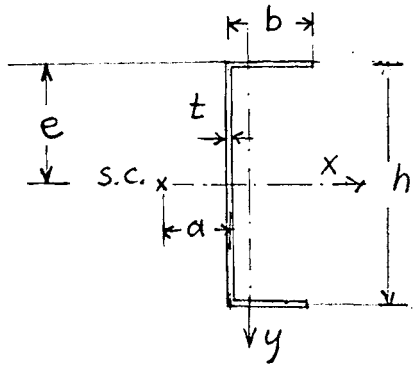

$a = .42574''$
$e = 3.0''$

$h = 5.865''$
$b = 1.432''$
$t = .135''$

$M_{bend} = \frac{\sigma_y I_x}{e} = 61.55$ k

$I_x = 5.596$ in^4
$I_y = .199$ in^4
$\Gamma = 1.261$ in^6
$\Gamma' = 3.056$ in^6
$K = .0072$ in^4

L \ Q/P_Y	0	1.	4	9	16	1000	
30"	36.248	46.121	47.696	48.073	48.212	48.393	DOWNWARD LOAD.
45"	32.580	48.705	50.850	51.360	51.533	51.754	
60"	26.594	50.566	54.136	54.783	55.006	55.283	
90"	19.672	41.887	58.921	60.203	60.569	60.977	
120"	15.765	32.104	57.501	63.299	63.901	64.445	
30"	-42.815	-43.741	-44.083	-44.170	-44.202	-44.244	UPLIFT LOADING
45"	-43.933	-43.566	-43.373	-43.309	-43.282	-43.245	
60"	-42.832	-42.381	-42.108	-42.016	-41.978	-41.928	
90"	-34.765	-36.681	-37.768	-38.219	-38.425	-38.744	
120"	-25.518	-28.178	-31.240	-32.938	-33.848	-35.486	

Table I-B: Midspan moment $M = \frac{pL^2}{8}$ [ki] (under yield load) for different values of Q/P_Y and L

Z-Section Example

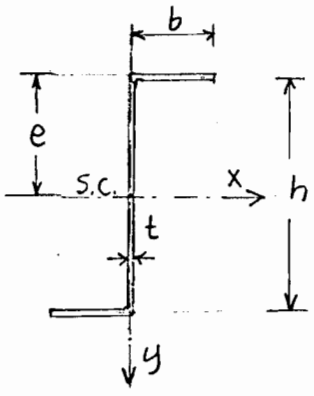

$a = 0$
$e = 3.0''$

$h = 5.865''$
$b = 1.432''$
$t = .135''$

$M_{bend} = \frac{\sigma_y I_x}{e} = 61.55$ ki

$I_x = 5.596$ in^4
$I_y = .265$ in^4
$I_{xy} = -.812$ in^4
$\Gamma = 1.179$ in^6
$\Gamma' = 3.035$ in^6
$K = .0072$ in^4

L \ Q/P_Y	0	1	4	9	16	1000	
30"	36.602	47.191	48.609	48.914	49.023	49.163	DOWNWARD LOADING
45"	32.790	50.347	51.953	52.254	52.356	52.489	
60"	25.228	53.472	55.443	55.734	55.527	55.944	
90"	17.293	49.448	60.988	61.287	61.362	61.450	
120"	13.339	37.370	64.141	64.626	64.697	64.769	
30"	- 37.128	- 42.335	- 44.094	- 44.561	- 44.740	- 44.980	UPLIFT LOADING
45"	- 34.852	- 40.252	- 42.584	- 43.277	- 43.552	- 43.931	
60"	- 31.718	- 37.480	- 40.511	- 41.522	- 41.944	- 42.543	
90"	- 22.550	- 29.385	- 34.850	- 37.088	- 37.910	- 39.182	
120"	- 17.330	- 23.156	- 28.554	- 31.286	- 32.703	- 35.187	

Table I-C : Midspan moment $M = \frac{PL^2}{8}$ [ki] (under yield load) for different values of Q/P_Y and L

Lipped Channel Example

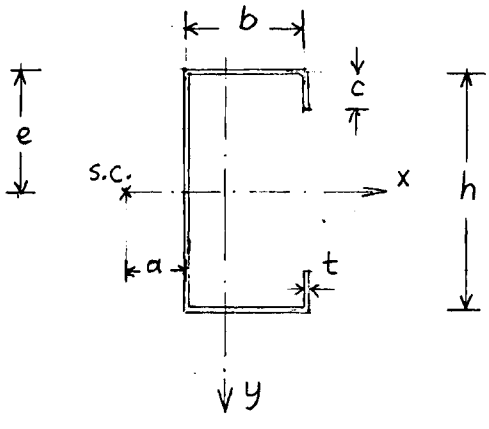

$a = 1.10937''$
$e = 3.0''$

$h = 5.865''$
$b = 2.365''$
$c = .633''$
$t = .135''$

$M_{bend} = \frac{\sigma_y I_x}{e} = 98.3$ ki

$I_x = 8.935$ in^4
$I_y = 1.307$ in^4
$\Gamma = 9.354$ in^6
$\Gamma' = 21.115$ in^6
$K = .0097$ in^4

L \ Q/P_Y	0	1	4	9	16	1000	
30"	51.172	58.166	59.947	60.400	60,570	60.793	DOWNWARD LOADING
45"	50.028	59.413	61.346	61.833	62,015	62.255	
60"	48,458	61,057	63.231	63.771	63.973	64.236	
90"	44.299	65.061	68,119	68.844	69.110	69.455	
120"	39,480	68.890	73,737	74.788	75,162	75.639	
30"	- 53.445	- 57.356	- 58.692	- 59.037	- 59.166	- 59.336	UPLIFT LOADING
45"	- 54,846	- 57,578	- 58.546	- 58.796	- 58.690	- 59.014	
60"	- 56.326	- 57. 780	- 58.316	- 58.453	- 58.503	- 58.570	
90"	- 58.254	- 57. 764	- 57,520	- 57.439	- 57.406	- 57.360	
120"	- 57. 646	- 56.681	- 56.143	- 55.968	- 55.897	- 55.802	

Table I-D: Midspan moment $M = \frac{pL^2}{8}$ [ki] (under yield load) for different values of Q, p_y and L

Lipped Z-Section Example

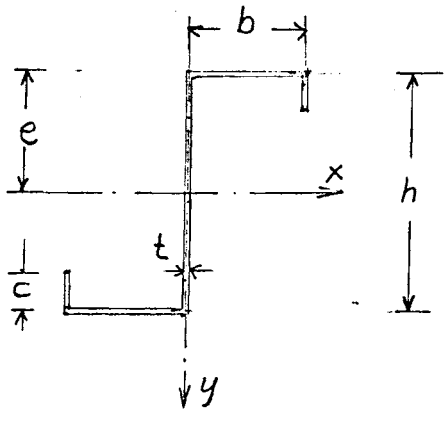

$a = 0$
$e = 3.0''$

$h = 5.865''$
$b = 2.365''$
$c = .633''$
$t = .135''$

$M_{bend} = \frac{\sigma_y I_x}{e} = 98.3$ ki.

$I_x = 8.935$ in^4
$I_y = 2.146$ in^4
$I_{xy} = -3.271$ in^4
$\Gamma = 12.584$ in^6
$\Gamma' = 21.119$ in^6
$K = .0097$ in^4

L \ Q/p_y	0	1	4	9	16	1000	
30"	48.833	59.078	60.970	61.395	61.550	61.752	DOWNWARD LOADING
45"	47.977	60.491	62.436	62.865	63.020	63.221	
60"	46.674	62.414	64.427	64.857	65.011	65.210	
90"	42.666	67.507	69.677	70.095	70.241	70.428	
120"	37.414	73.545	75.905	76.285	76.412	76.573	
30"	-48.866	-57.402	-59.405	-59.874	-60.047	-60.274	UPLIFT LOADING
45"	-48.137	-56.754	-58.450	-59.480	-59.677	-59.936	
60"	-47.140	-55.862	-58.318	-58.934	-58.974	-59.472	
90"	-44.447	-53.411	-56.557	-57.418	-57.752	-58.202	
120"	-41.075	-50.248	-54.218	-55.418	-55.900	-56.567	

Table II-A : Angle of rotation ϕ at midspan [degrees] (under yield load) for different values of Q/P_Y and L

Channel Section Example

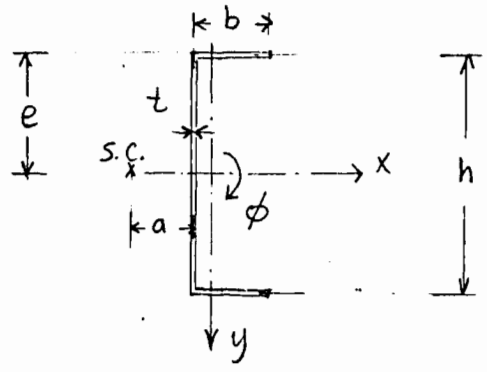

Dimensions are same as on Table I-A

L \ Q/P_Y	0	1	4	9	16	1000	
30"	2.35°	1.49°	1.15°	1.07°	1.04°	1.00°	DOWNWARD LOADING
45"	5.23°	3.30°	2.33°	2.12°	2.04°	1.94°	
60"	7.75°	6.22°	3.69°	3.22°	3.06°	2.56°	
90"	12.88°	14.97°	7.28°	5.37°	4.83°	4.23°	
120"	17.98°	26.85°	14.34°	7.97°	6.44°	5.04°	
30"	- 1.87°	- 1.44°	- 1.26°	- 1.22°	- 1.20°	- 1.17°	UPLIFT LOADING
45"	- 3.45°	- 3.09°	- 2.83°	- 2.77°	- 2.75°	- 2.72°	
60"	- 5.35°	- 5.17°	- 5.07°	- 5.03°	- 5.02°	- 5.00°	
90"	- 10.78°	- 11.77°	- 11.99°	- 12.06°	- 12.09°	- 12.13°	
120"	- 14.59°	- 16.88°	- 19.40	- 20.75°	- 21.46°	- 22.72°	

Table II-B: Angle of rotation at midspoin [degrees] (under yield load) for different values of Q/P_y and L

Z-Section Example

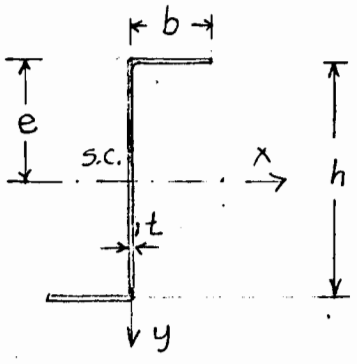

Dimensions are same as on Table I-B

L \ Q/P_y	0	1	4	9	16	1000	
30"	.40°	.70°	.95°	1.00°	1.02°	1.05°	DOWNWARD LOADING
45"	1.80°	1.12°	1.78°	1.91°	1.96°	2.02°	
60"	3.36°	.93°	2.50°	2.76°	2.85°	2.95°	
90"	7.23°	4.61°	3.08°	3.88°	4.10°	4.34°	
120"	11.64°	18.87°	1.70°	4.25°	4.72°	5.15°	
30"	.31°	.92°	1.13°	1.18°	1.20°	1.23°	UPLIFT LOADING
45"	1.16°	2.22°	2.63°	2.74°	2.79°	2.86°	
60"	2.71°	4.22°	4.89°	5.08°	5.17°	5.28°	
90"	5.80°	9.21°	11.66°	12.50°	12.67°	12.90°	
120"	9.40°	14.34°	18.38°	20.27°	21.22°	22.80°	

Table II-C: Angle of rotation ϕ at midspan [degrees] (under yield load) for different values of Q/P_y and L

Lipped Channel Example

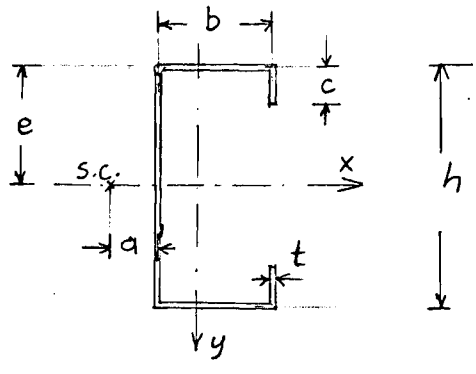

Dimensions are same as on Table II-C

L \ Q/P_y	0	1	4	9	16	1000	
30"	1.11°	.75°	.62°	.59°	.58°	.56°	DOWNWARD LOADING
45"	2.47°	1.68°	1.37°	1.29°	1.26°	1.22°	
60"	4.31°	2.97°	2.38°	2.23°	2.17°	2.10°	
90"	9.38°	6.67°	4.98°	4.59°	4.44°	4.25°	
120"	16.15°	12.42°	8.17°	7.29°	6.97°	6.57°	
30"	- 1.07°	- .74°	- .63°	- .60°	- .59°	- .57°	UPLIFT LOADING
45"	- 2.27°	- 1.64°	- 1.41°	- 1.35°	- 1.33°	- 1.29°	
60"	- 3.74°	- 2.85°	- 2.50°	- 2.40°	- 2.36°	- 2.31°	
90"	- 7.11°	- 6.06°	- 5.57°	- 5.42°	- 5.37°	- 5.29°	
120"	- 10.93°	- 10.22°	- 9.83°	- 9.70°	- 9.65°	- 9.58°	

Table II-D: Angle of rotation ϕ at midspan [degrees] (under yield load) for different values of Q/P_Y and L

Lipped Z-Section Example

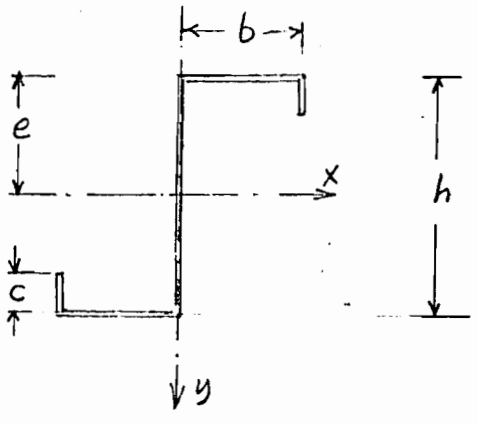

Dimensions are same as on Table II-c

L \ Q/P_Y	0	1	4	9	16	1000	
30"	.04°	.42°	.52°	.54°	.55°	.56°	DOWNWARD LOADING
45"	.18°	.90°	1.13°	1.18°	1.21°	1.23°	
60"	.53°	1.51°	1.93°	2.02°	2.06°	2.10°	
90"	2.38°	2.76°	3.85°	4.07°	4.15°	4.25°	
120"	6.23°	3.38°	5.79°	6.22°	6.37°	6.55°	
30"	.03°	.44°	.53°	.56°	.56°	.58°	UPLIFT LOADING
45"	.16°	1.00°	1.21°	1.26°	1.28°	1.30°	
60"	.44°	1.79°	2.16°	2.25°	2.27°	2.33°	
90"	1.73°	4.15°	4.93°	5.14°	5.22°	5.33°	
120"	4.14°	7.65°	8.96°	9.32°	9.47°	9.67°	

Table II-D: Angle of rotation ϕ at midspan [degrees] (under yield load) for different values of Q/P_Y and L

Lipped Z-Section Example

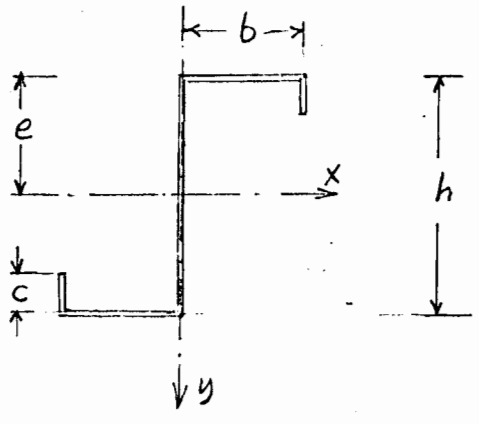

Dimensions are same as on Table II-c

L \ Q/P_Y	0	1	4	9	16	1000	
30"	.04°	.42°	.52°	.54°	.55°	.56°	DOWNWARD LOADING
45"	.18°	.90°	1.13°	1.18°	1.21°	1.23°	
60"	.53°	1.51°	1.93°	2.02°	2.06°	2.10°	
90"	2.38°	2.76°	3.85°	4.07°	4.15°	4.25°	
120"	6.23°	3.38°	5.79°	6.22°	6.37°	6.55°	
30"	.03°	.44°	.53°	.56°	.56°	.58°	UPLIFT LOADING
45"	.16°	1.00°	1.21°	1.26°	1.28°	1.30°	
60"	.44°	1.79°	2.16°	2.25°	2.27°	2.33°	
90"	1.73°	4.15°	4.93°	5.14°	5.22°	5.33°	
120"	4.14°	7.65°	8.96°	9.32°	9.47°	9.67°	

Figure 1-A : Comparison of $M = \frac{pL^2}{8}$ (under yield load) with $M_{bend} = \frac{\sigma_y I_x}{e}$ for downward and uplift loading. The diaphragm stiffness is taken as zero and infinity.

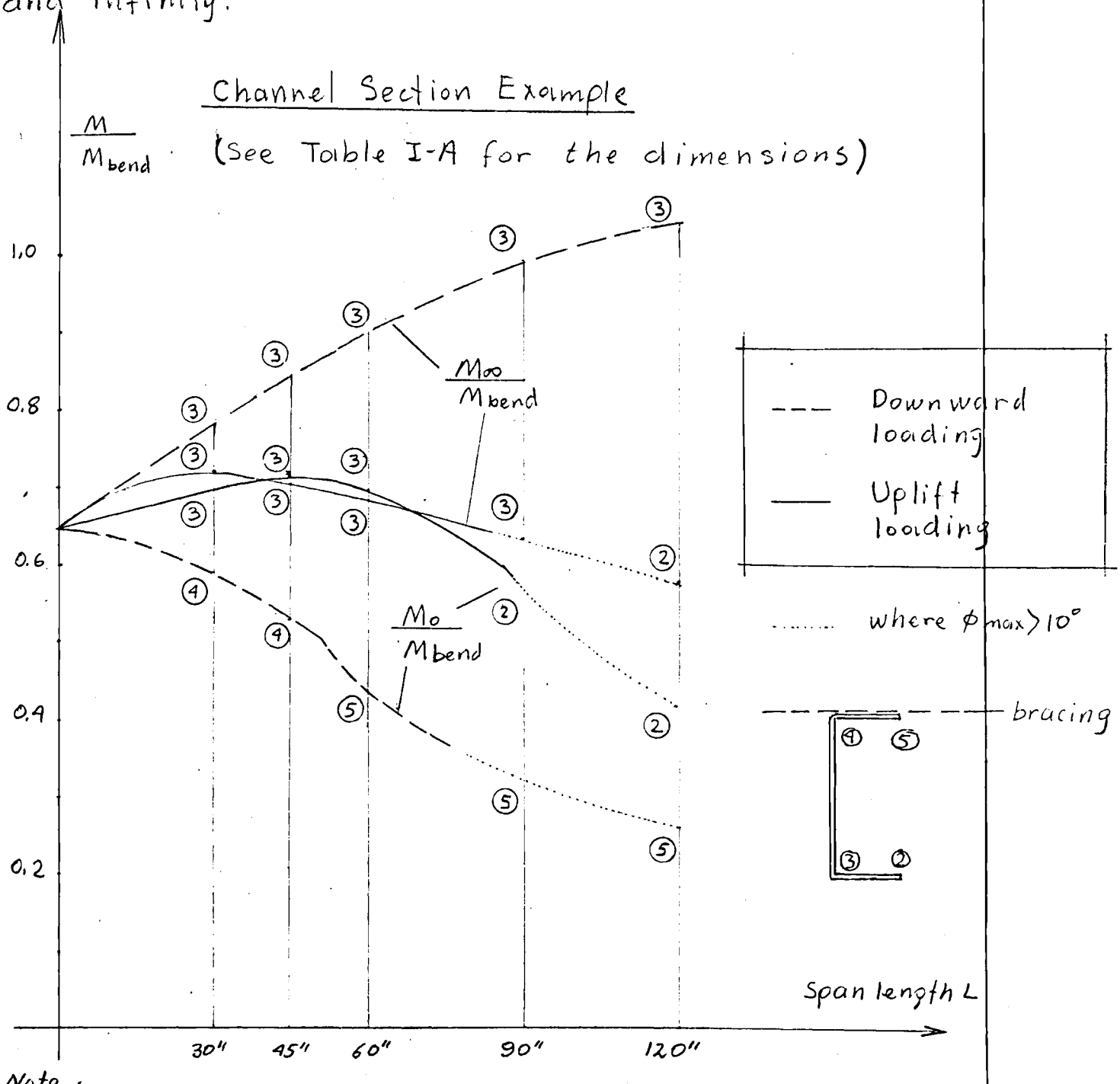

Note :
The numbers in circles indicate where in the cross-section yielding

Figure 1-B : Comparison of $M = \frac{pL^2}{8}$ (under yield load) with $M_{bend} = \frac{\sigma_y I_x}{e}$ for downward and uplift loading. The diaphragm stiffness is taken as zero and infinity

Z-Section Example

(See Table I-B for the dimensions)

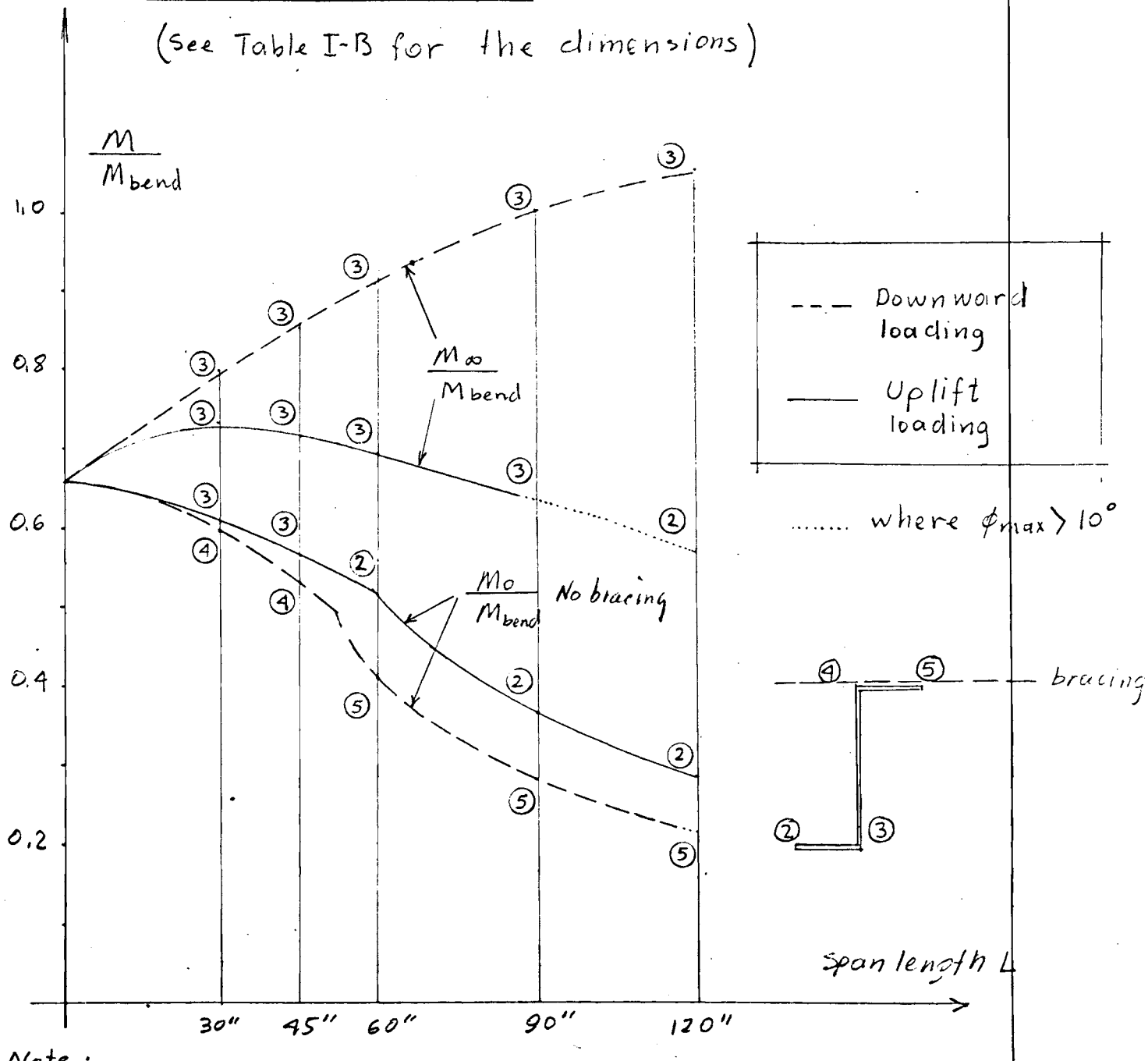

Note :

Figure I-C: Comparison of $M = \frac{pL^2}{8}$ (under yield load) with $M_{bend} = \frac{\sigma_y I_x}{e}$ for downward and uplift loading. The diaphragm stiffness is taken as zero and infinity.

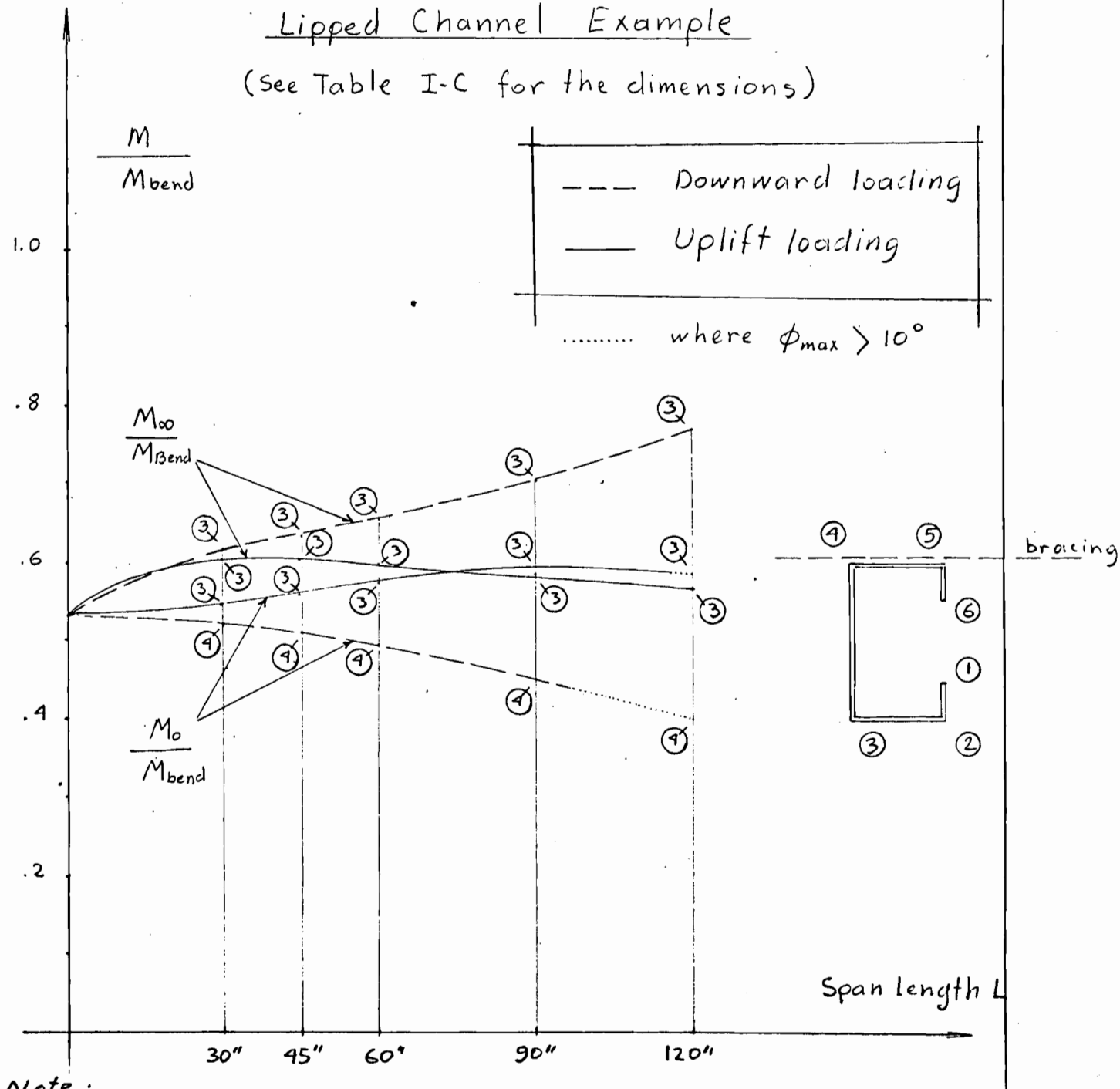

Note:
The numbers in circles indicate where in the cross-section

Figure I-D: Comparison of $M = \frac{pL^2}{8}$ (under yield load) with $M_{bend} = \frac{\sigma_y I_x}{e}$ for downward and uplift loading. The diaphragm stiffness is taken as zero and infinity

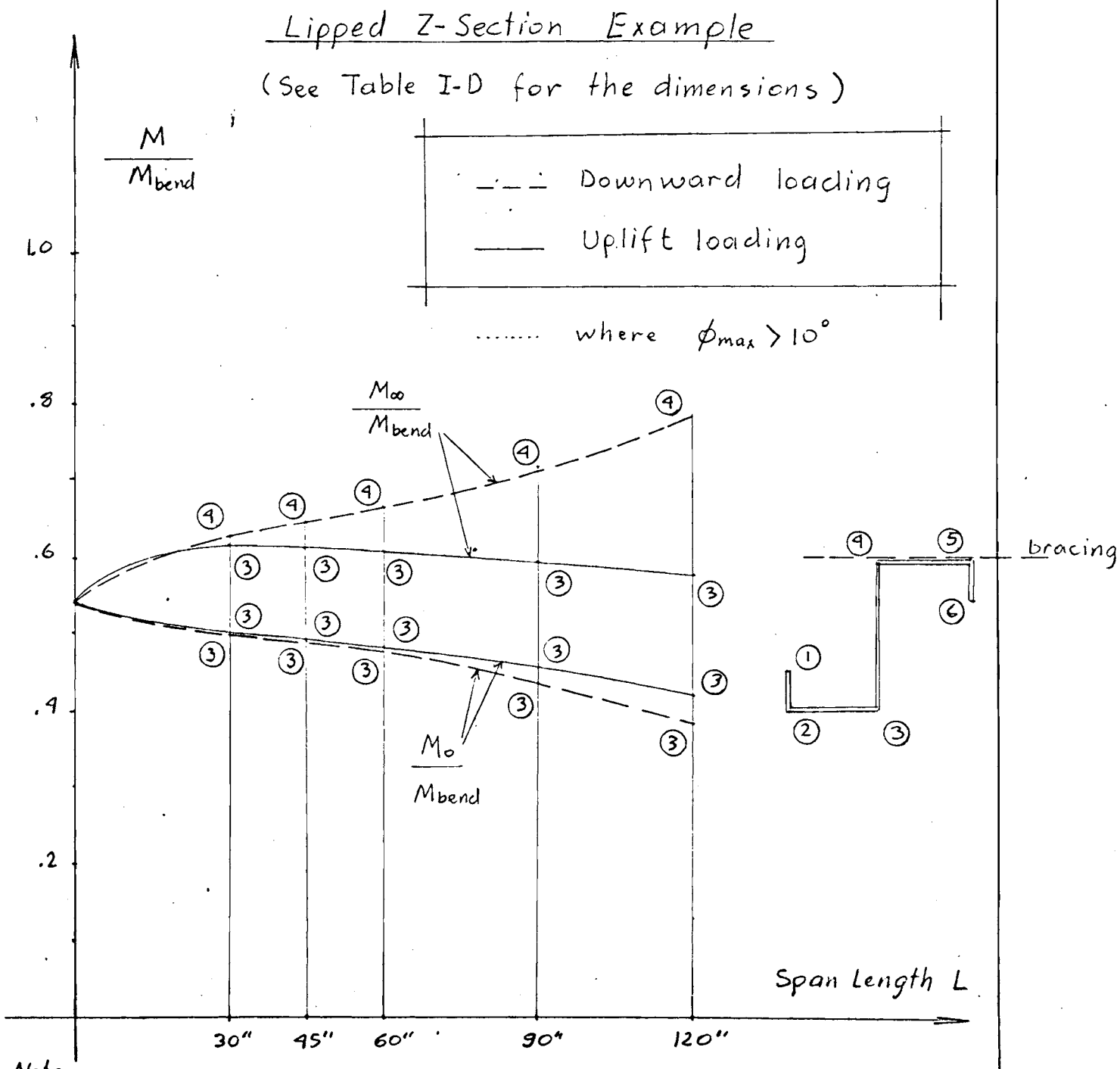

Note:

The numbers in circles indicate where in the cross-section

Figure 2-A - Stress distribution (under yield load)

Channel Section Example

(See Table I-A for the dimensions)

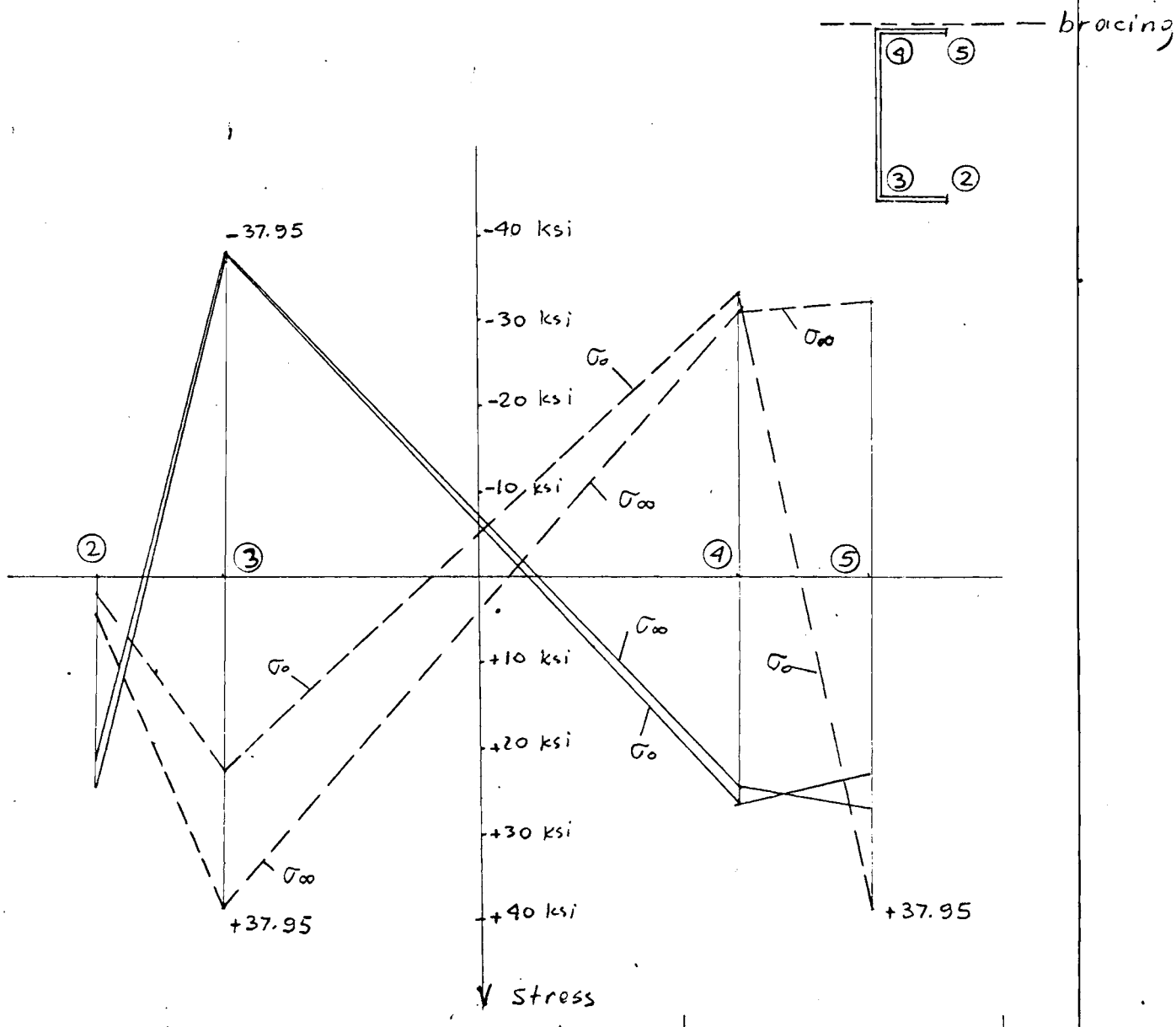

Figure 2-A - Stress distribution (under yield load)

Channel Section Example

(See Table I-A for the dimensions)

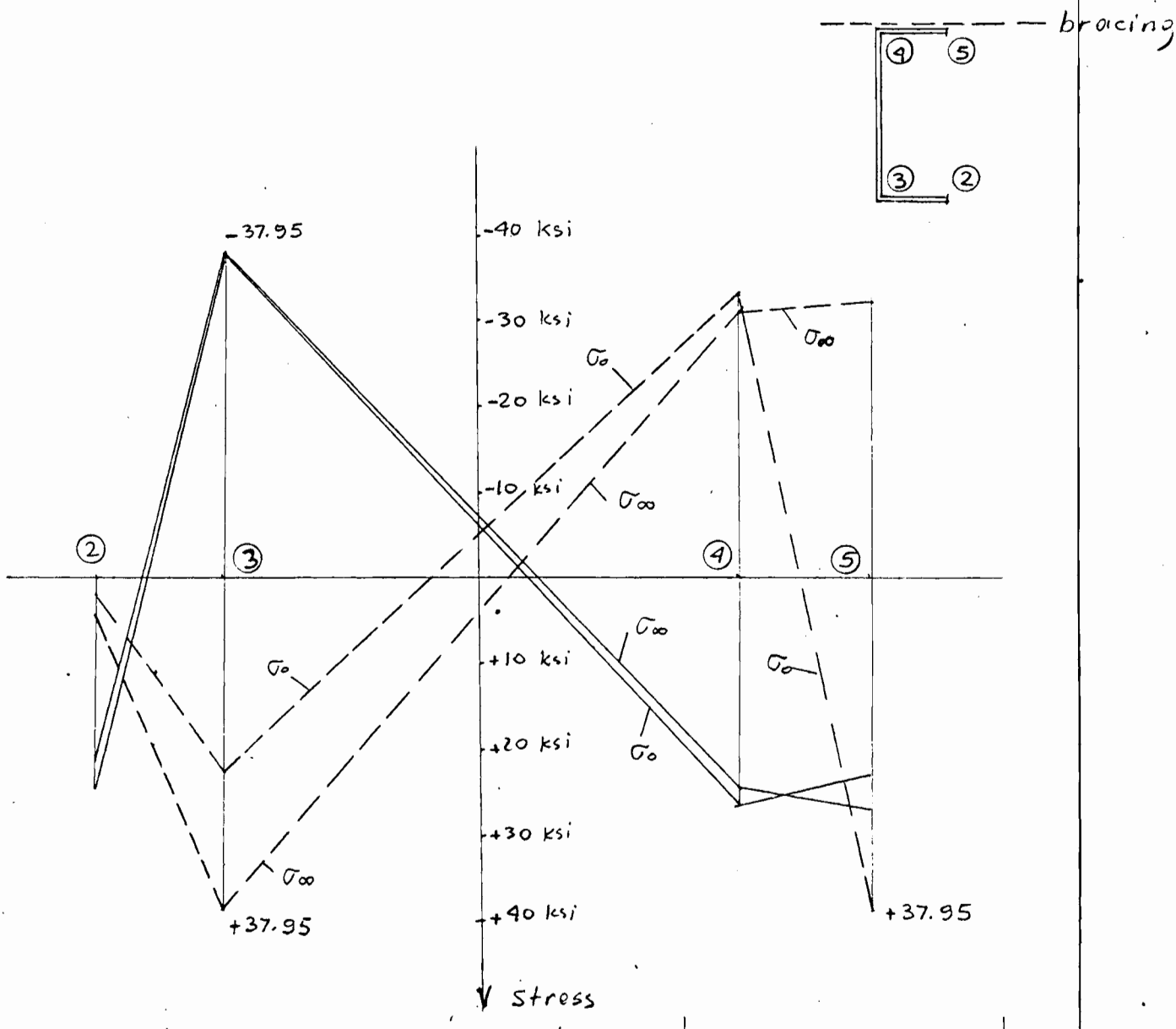

Figure 2-B Stress distribution (under yield load)

Z-Section Example

(See Table I-B for the dimensions)

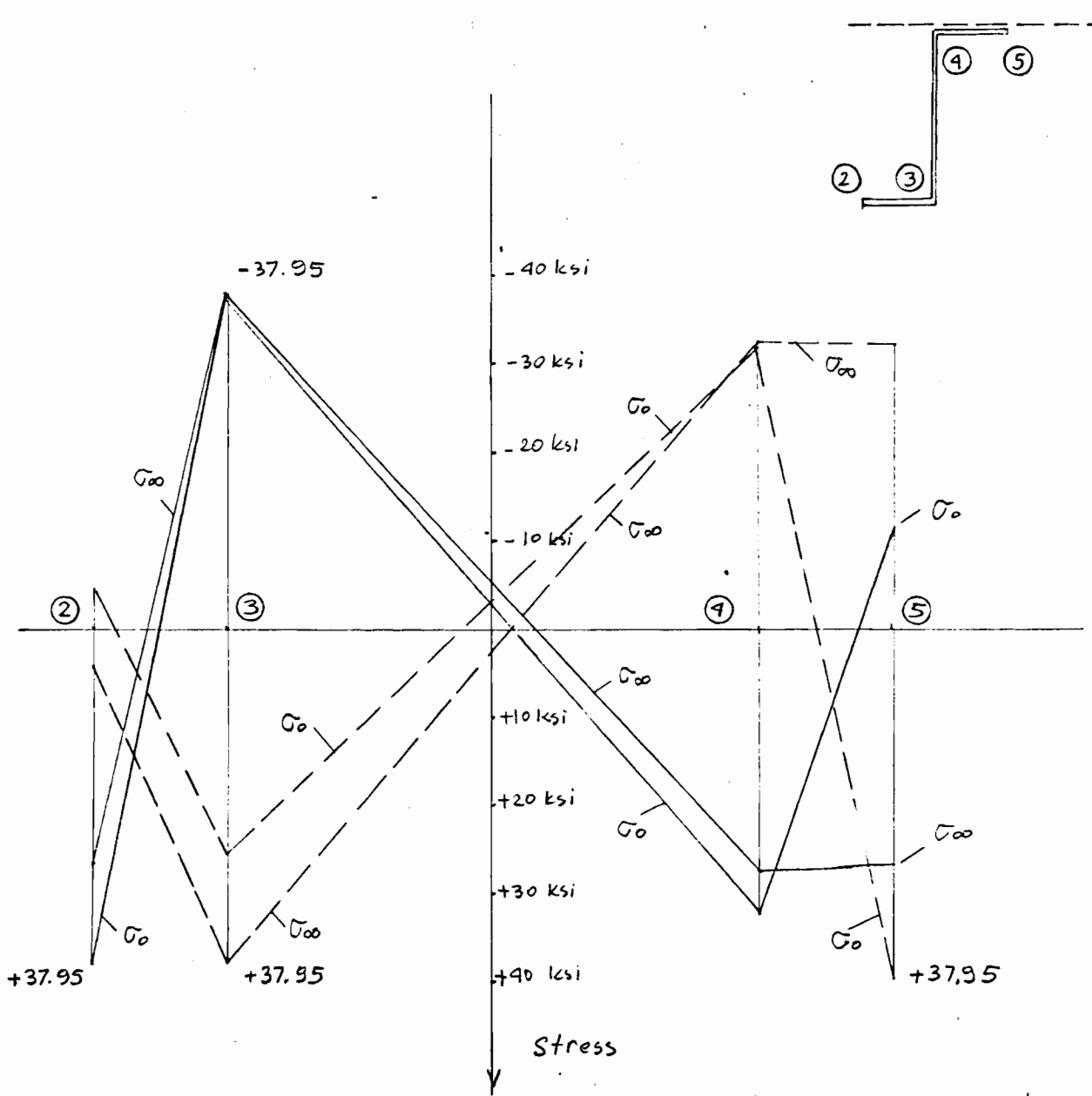

--- Downward loading

___ Uplift loading

Span length
60"

Figure 2-C : Stress distribution (under yield load)

Lipped Channel Section Example:

(See Table I-B for the dimensions)

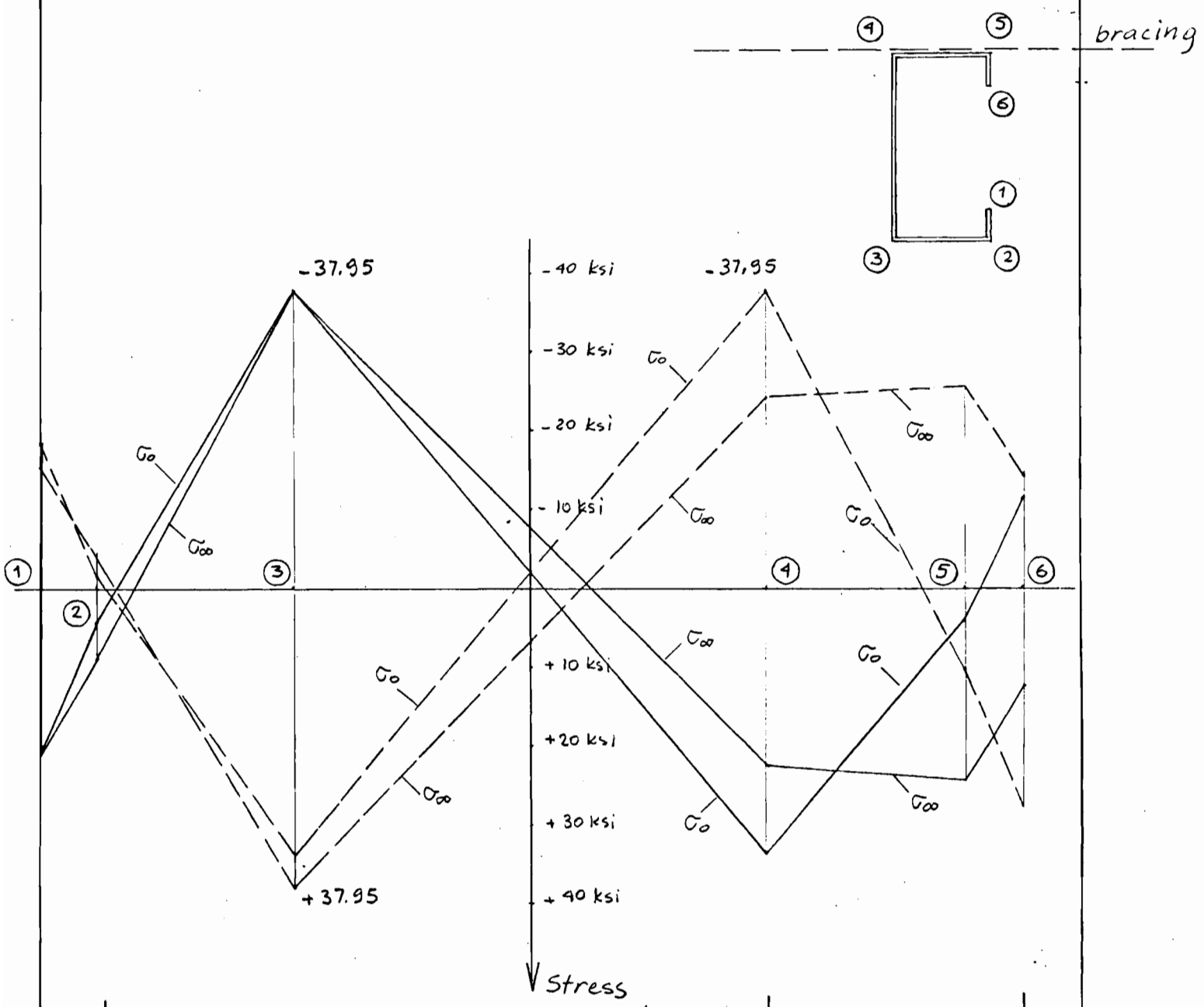

Figure 2-C : Stress distribution (under yield load)

Lipped Channel Section Example

(See Table I-B for the dimensions)

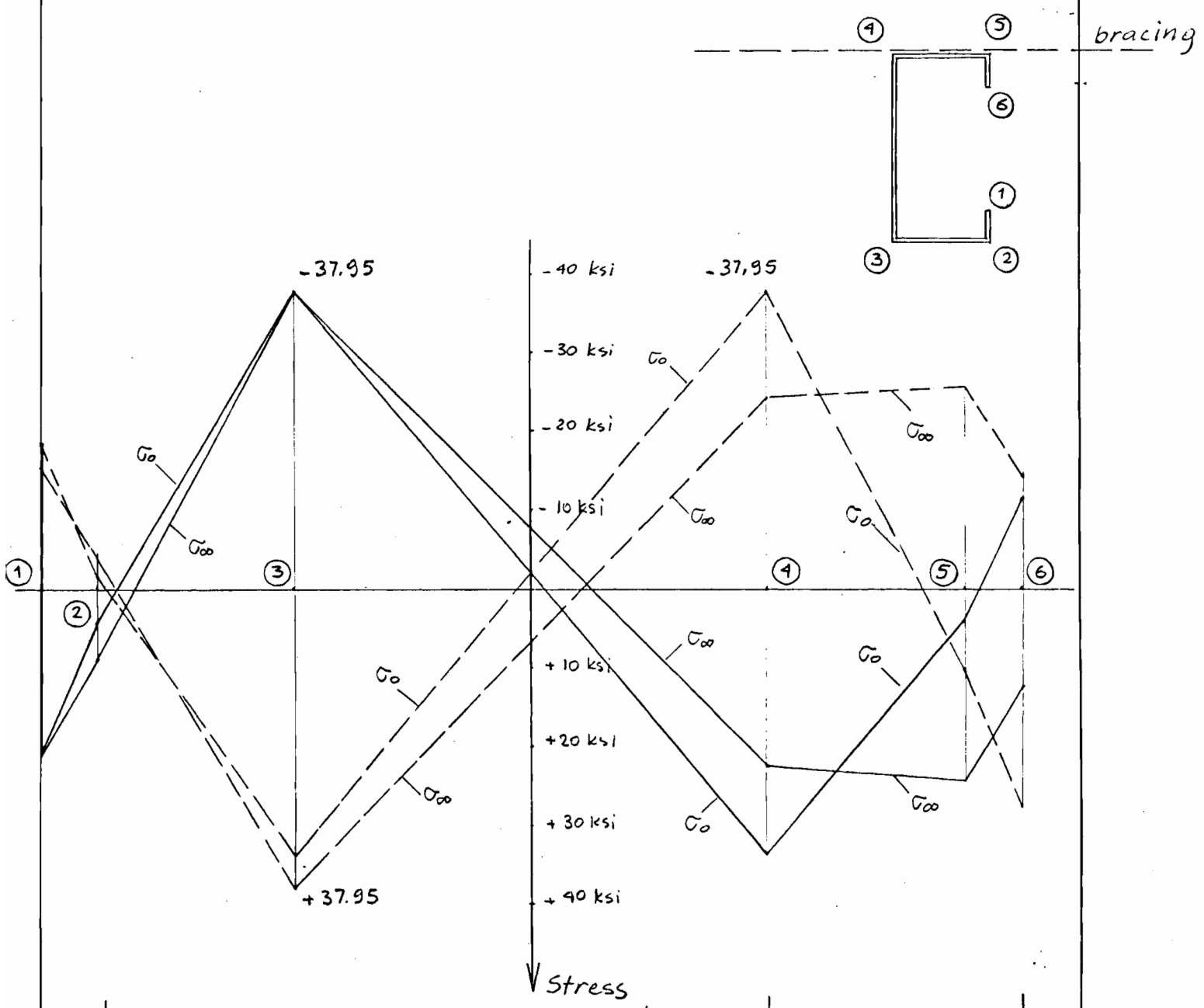

---- Downward loading	Span Length
____ Uplift loading	60"

Figure 2-D : Stress distribution (under yield load)

Lipped Z-section Example

(See Table I-B for the dimensions)

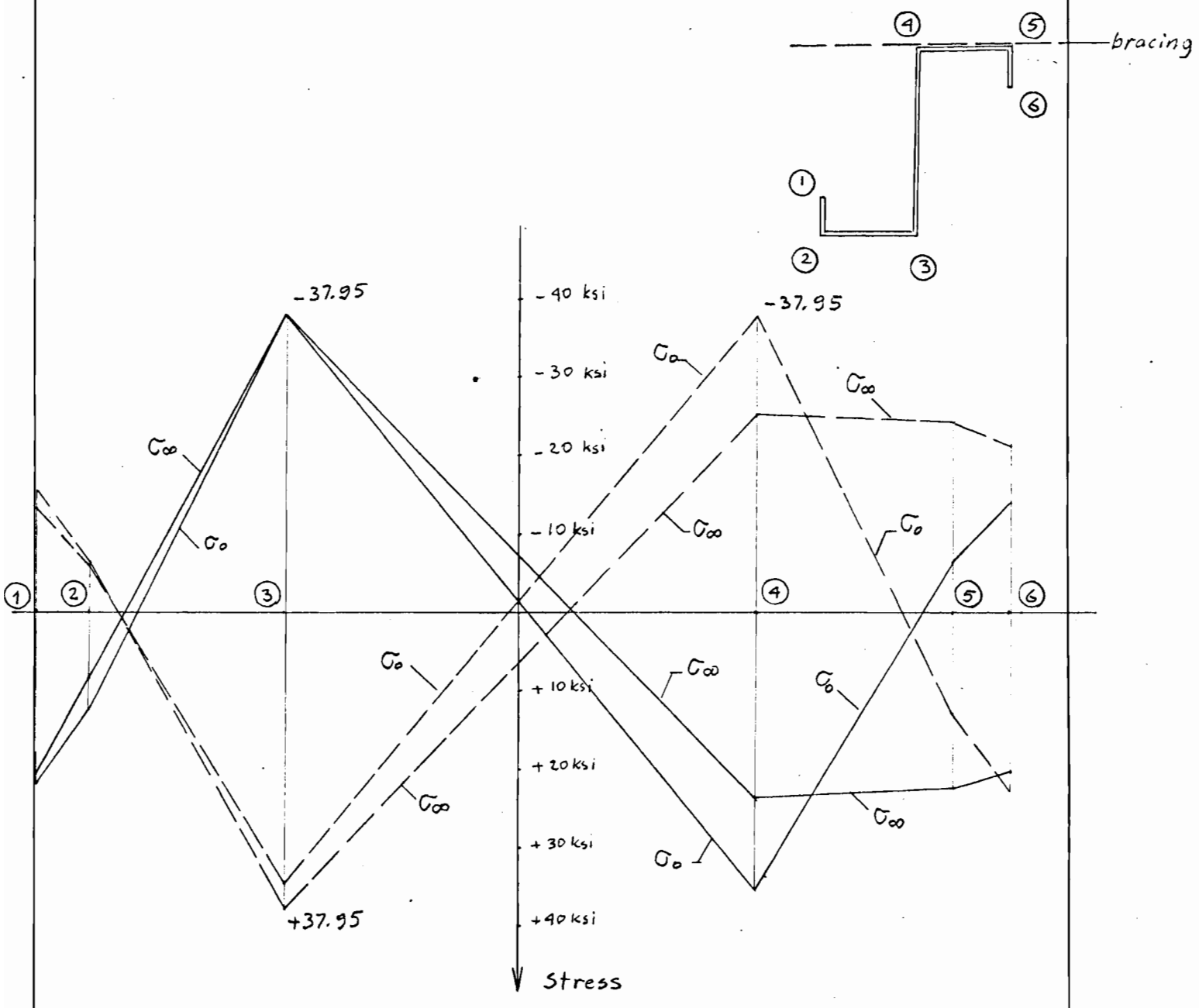

---- Downward loading —— Uplift loading	Span Length 60"

Figure 3-A : Deflections ϕ and u versus $p.L$ up to yield load

Channel Section Example

(See Table I-A for the dimensions)

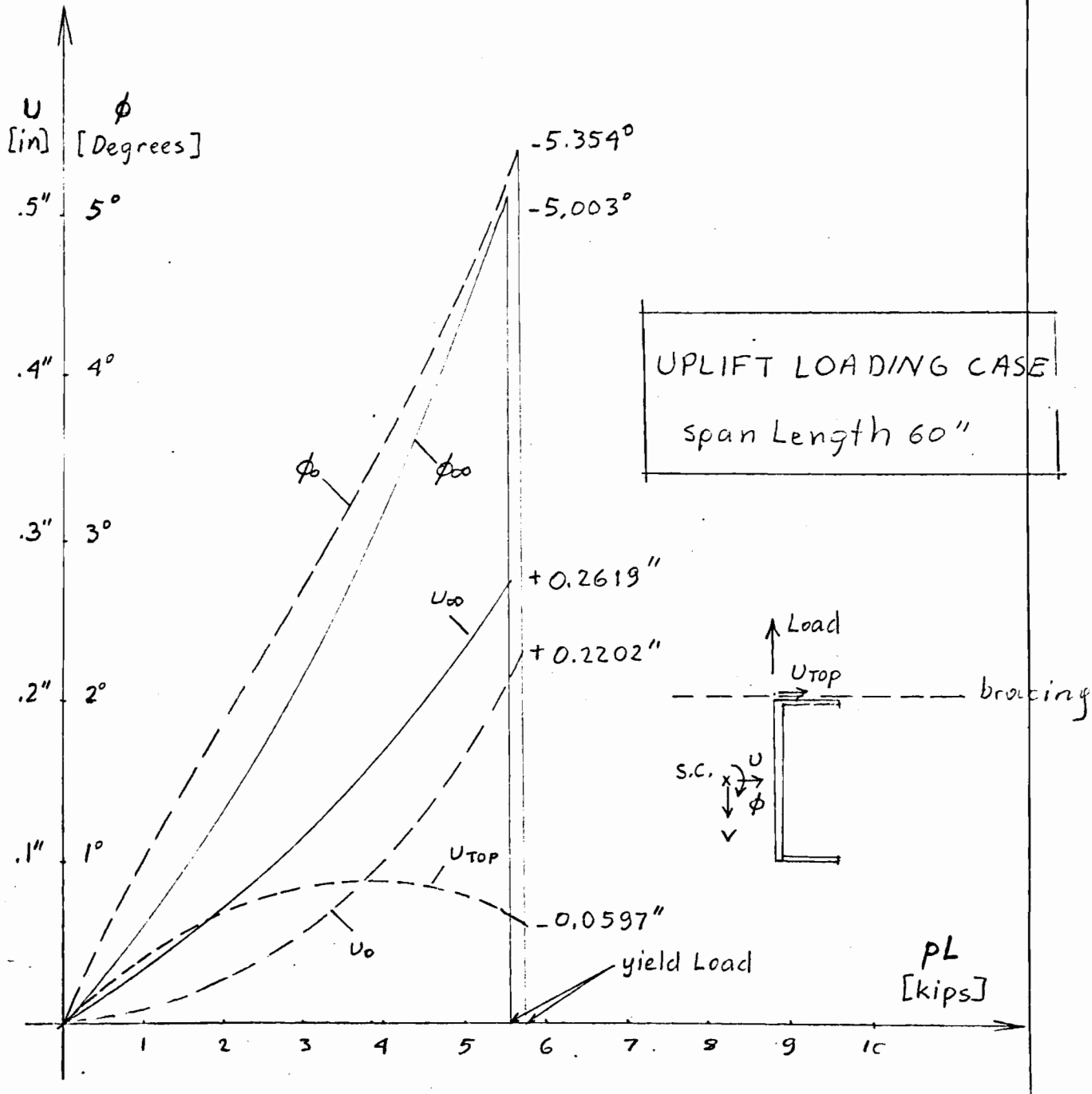

Note : (+) and (-) values are shown in the same quadrant

Figure 3-B: Deflections ϕ and u versus $p \cdot L$ up to yield load

Z-Section Example

(See Table I-B for the dimensions)

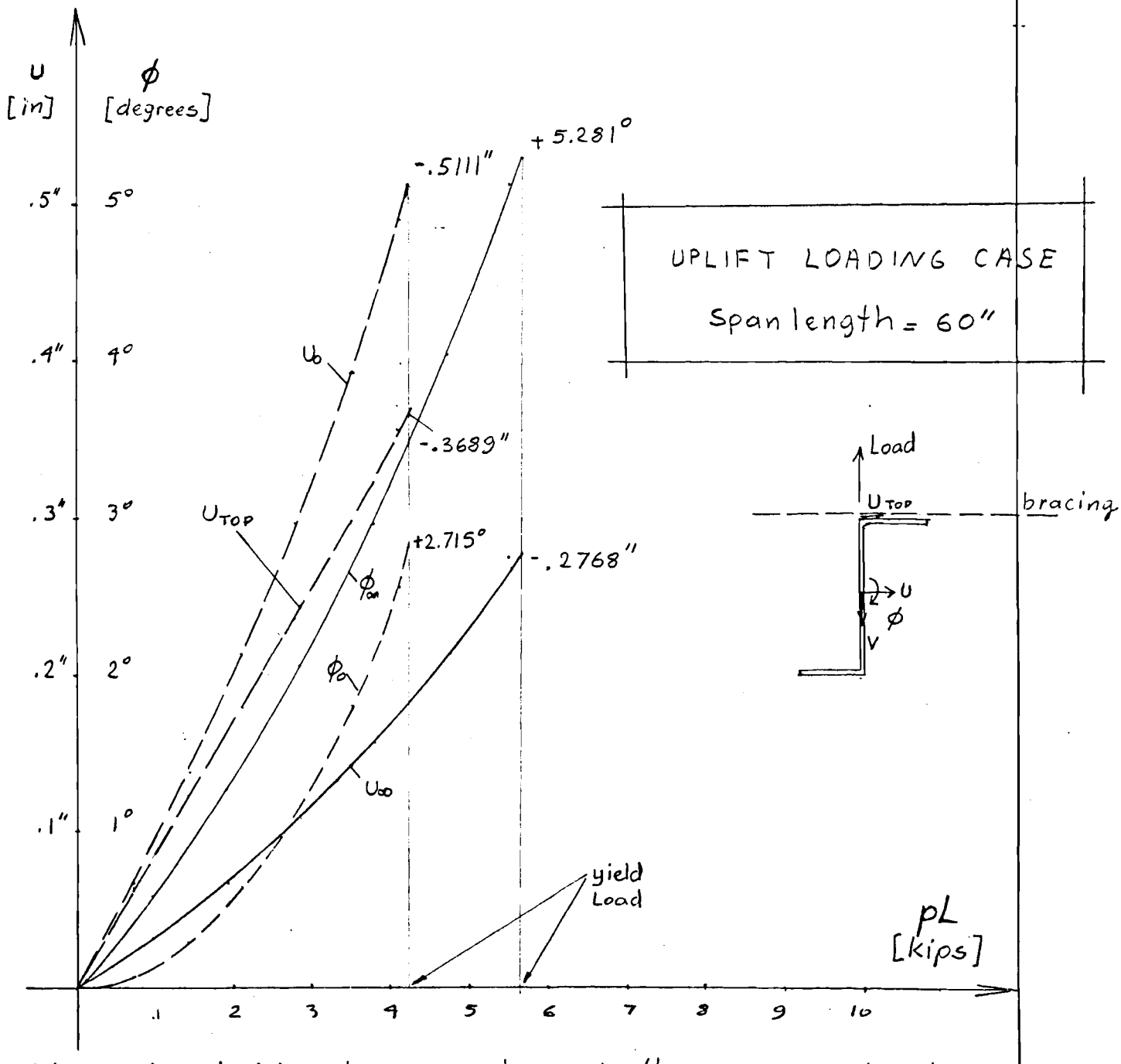

Note: (+) and (-) values are shown in the same quadrant

Figure 3-C : Deflections ϕ and u versus $p \cdot L$ up to yield load

Lipped Channel Example

(See Table I-C for the dimensions)

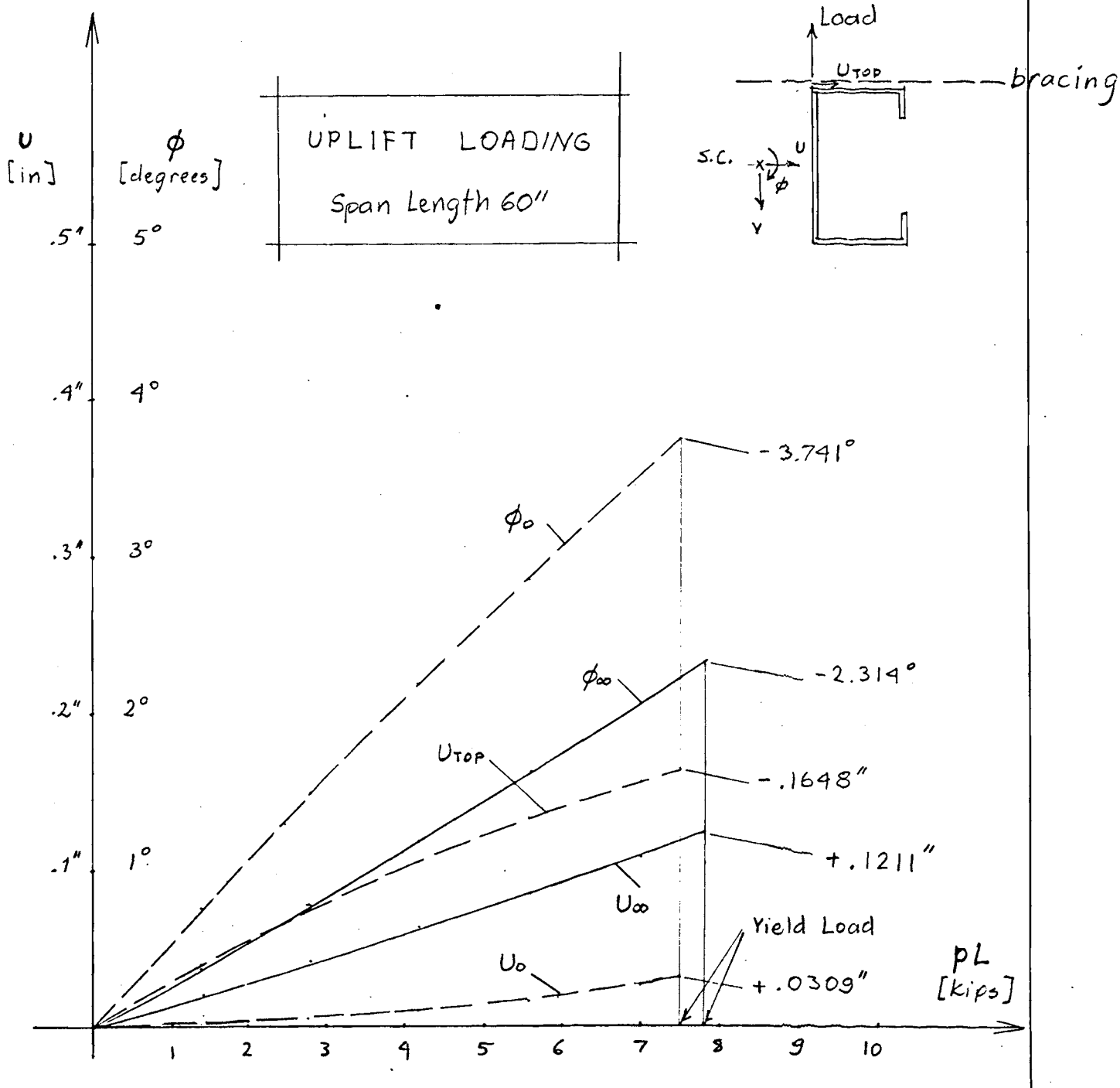

Note : (+) and (-) values are shown in the same quadrant

Figure 3-D : Deflections ϕ and u versus $p \cdot L$ up to yield load

Lipped Z-Section Example

(See Table I-D for the dimensions)

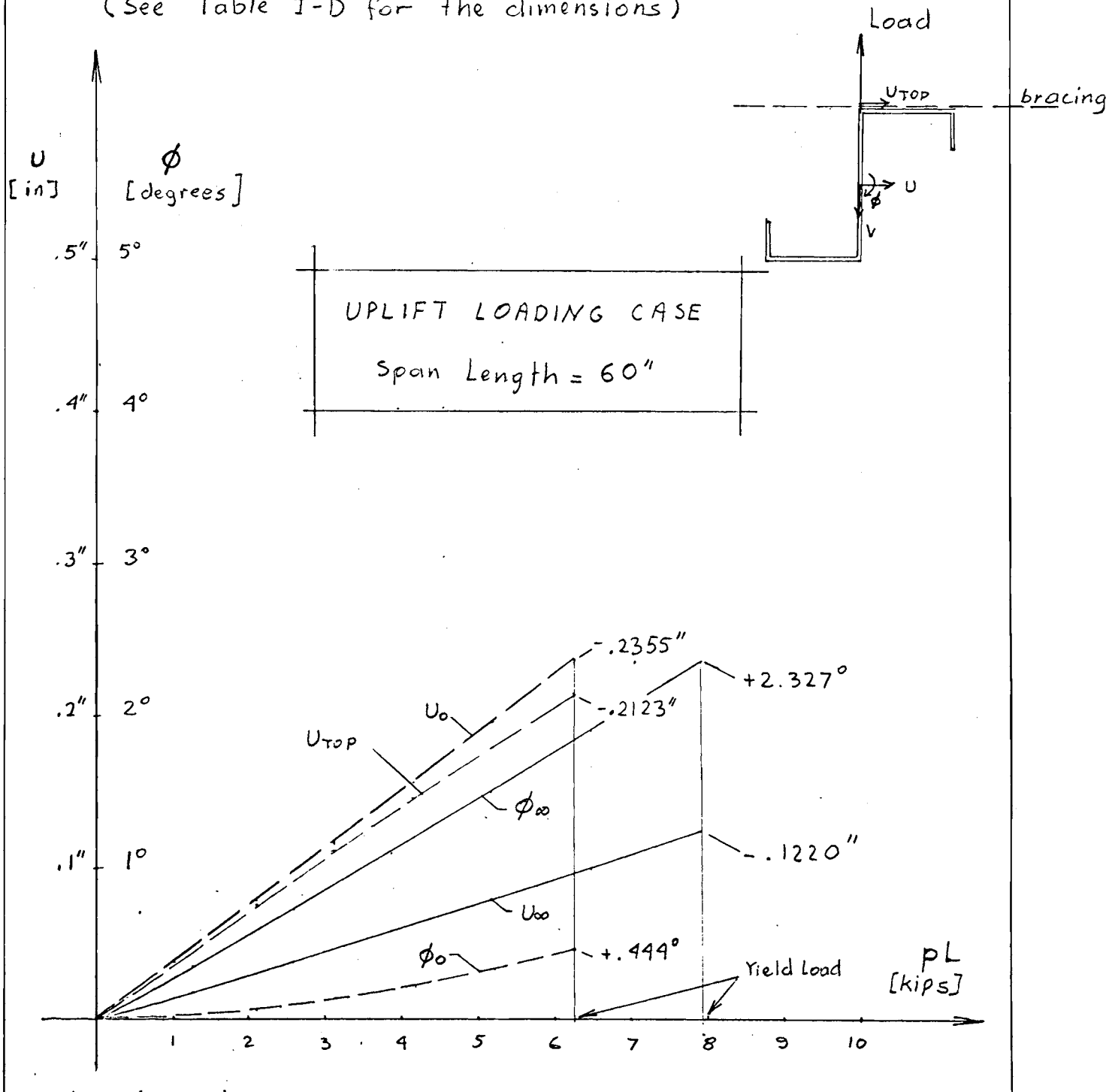

Note: (+) and (-) values are shown in the same quadrant

FILE 12-D (c)

DEPARTMENT OF STRUCTURAL ENGINEERING
SCHOOL OF CIVIL ENGINEERING
CORNELL UNIVERSITY

Report No. 344

DIAPHRAGM BRACED CHANNEL AND Z-SECTION BEAMS

by

Nuri Celebi
Research Assistant

George Winter
Teoman Pekoz
Project Directors

A Research Project Sponsored by the
American Iron and Steel Institute

Ithaca, New York October, 1971

PREFACE

Cold-formed channels and Z-shapes are widely used as purlins supporting roof surfaces which consist of light-gage steel panels or other material. If the panels are interconnected to form diaphragms, they brace the purlins and increase their carrying capcity sizeably. It is the purpose of this investigation to explore this bracing effect and provide tools for its utilization in design.

The author wishes to express his gratitude to Professors George Winter and Teoman Pekoz, Project Directors. Their suggestions, criticism and guidance made this work possible.

The research project covered by this report was sponsored at Cornell University by the American Iron and Steel Institute. The valuable cooperation of Dr. Albert L. Johnson, Senior Research Engineer, American Iron and Steel Institute, Dr. J. Scalzi, Chairman of the Research and Specifications Subcommittee, Mr. T.J. McCabe, Chairman of Diaphragm Tasle Force and of the entire sponsoring organization is gratefully acknowledged.

This report was originally a thesis presented to the Faculty of the Graduate School of Cornell University as a partial requirement for the Degree of Doctor of Philosophy to be awarded in January. 1972.

TABLE OF CONTENTS

NOMENCLATURE

A = Cross sectional area.

A_s = Defined by Eq. A.16.

A_1, A_2, A_3, A_4 = Coefficients defined by Eq. C.2a.

$\bar{A}_1, \bar{A}_2, \bar{A}_3, \bar{A}_4$ = Coefficients defined by Eq. C.2b.

A_{mn} = Coefficients of u_n in Eq. 2.17a.

a = Positive number showing the horizontal distance between p_y and shear center (Fig. 10).

a_1, a_2 = Constants defined by Eq. 4.9.

a'_o, a'_1, a'_2, a'_3 = Constants defined by Eq. 4.19.

$a''_o, a''_1, a''_2, a''_3$ = Constants defined by Eq. 4.21.

B = Bimoment defined by Eq. 2.5.

B_{mn} = Coefficients of ϕ_n in Eq. 2.17a.

B_s = Simplified bimoment defined by Eq. 4.57b.

b = Width of flanges of lipped or plane channel and Z-sections.

b_1, b_2 = Constants defined by Eq. 4.9.

b'_o, b'_1, b'_2 = Constants defined by Eq. 4.19.

b''_o, b''_1 = Constants defined by Eq. 4.21.

C.G = Center of gravity.

C_{mn} = Coefficients of u_n in Eq. 2.17b.

c = Width of lips of lipped channel and Z-sections.

C_0, C_1 = Integration constants in Eq. C.15 or Eq. C.23.

C_w = Warping constant, defined by Eq. A.28.

C'_w = Modified warping constant for rigid bracing case, defined by Eq. 2.15.

D, D_1, D_2 = Determinants of Eq. 4.2, defined by Eqs. 4.7a, b, c respectively.

D_{mn} = Coefficients of ϕ_n in Eq. 2.17b.

d = y_3, i.e., the coordinate y for corner 3.

E = Young's modulus.

E_m = Right hand side of Eq. 2.17a.

e = Positive number showing the vertical distance between p_y and shear center (Fig. 10).

e_D = Positive number showing the vertical distance between the diaphragm bracing and shear center (Fig. 10).

F = Rotational restraint supplied by diaphragm bracing.

F_m = Right hand side of Eq. 2.17b.

f_1 = Vibration eigenfunction of first mode representing u and/or ϕ as a function of ζ along the beam, defined by Eq. 4.1.

f_1'' = Second derivative of f_1 with respect to ζ.

G = Shear modulus.

G_{eff} = Effective shear modulus of diaphragm bracing.

H_x, H_y, H_w = Defined by Eqs. A.39b, c, d respectively.

h = Height of lipped or plane channel or Z-section.

$h(\zeta)$ = Moment distribution function defined in Eq. C.7a.

$\bar{h}(\zeta)$ = Load distribution function defined in Eq. C.7b.

I_o = Polar moment of inertia with respect to shear center.

I_x = Moment of inertia with respect to x-axis.

I_y = Moment of inertia with respect to y-axis.

I_{xy} = Product of inertia with respect to x and y axes.

K = Saint Venant torsion constant.

K_{11}, K_{33}, K'_{33} = Constants defined by Eqs. 4.4a and 4.4b, see Table 11.

L = Span length.

L_1 = Distance between the discrete braces.

M = Load parameter defined by Eq. 4.3a.

M_{bend} = The bending capacity of a beam which is guided or braced such that the only possible deformation is bending in the plane of the load with no rotation or lateral deflection, defined by Eq. 4.13c.

M_x, M_y = Bending moments with respect to x and y axes.

M_z = Torsional moment with respect to z axis.

M_ζ, M_η = Bending moments with respect to ζ and η axis.

M_ζ = Torsional moment with respect to ζ axis.

M_t = Torsional moment defined by Eq. A.36.

M_{tw} = Flexural twist, i.e., torsional moment carried by the beam due to its warping rigidity, see Eqs A.30c and A.31c.

M_{yd} = Incipient yield moment.

m_t, m_z = Distributed torsional moments.

N = Normal force

N = Maximum number of terms considered in series solution.

n = Coordinate axis normal to profile line of cross-section (Fig. 4).

n = Subscript.

P = Concentrated force.

P_x = Euler buckling load about the x axis.

P_Y = Euler buckling load about the y axis.

P'_Y = Defined by Eq. 4.3b.

P_ϕ = Defined by Eq. 4.3d

p = Uniformly distributed load acting in a plane parallel to web.

p_x, p_z = Bracing forces in x and z axes directions.

p_y = Distributed loads in y axis direction.

Q = Shear rigidity of diaphragm bracing.

Q_L = Limiting shear rigidity, defined by Eq. 4.36.

$Q_{L,con}$ = Defined by Eq. 4.37.

Q_x, Q_y, Q_w = Defined by Eqs. A.17, A.18 and A.19 respectively.

q = Defined by Eq. 4.15.

r = Distance from shear center (Fig. 4).

r_n = Distance of shear center from the line tangent to the center line of the cross section (Fig. 4).

r_o^2 = Defined by Eq. 4.3e.

s = Coordinate axis tangential to the center line of the cross section (Fig. 4).

T_o = Shear force at $s = 0$.

T_i = Definite integrals defined by Eqs. C.9 and C.18.

T_u, T_ϕ = Defined by Eqs. F.2a and b respectively.

t = Wall-thickness of the sections.

u = Deflection in x-axis direction.

u_o = u for no bracing case, i.e., Q = 0.

u_∞ = u for rigid bracing case, i.e., Q = ∞.

u_s, u_n = Deflection in tangential and normal directions to the center line respectively.

u_1 = Amplitude of u.

V = Shear force in diaphragm contributory to the bracing of one beam.

V_x, V_y = Shear forces in x and y axes directions.

v = Deflection in y axis direction.

W_1, W_2, W_3 = Defined by Eq. 4.4, see Table 11 .

W_4, W_5 = Defined by Eq. 4.24, see Table 11 .

W_6 = Defined by Eq. 4.27, see Table 11 .

W_7, W_8 = Defined by Eq. 4.39, see Table 11 .

W_9 = Defined by Eq. 4.49, see Table 11 .

W_{10}, W_{11} = Defined by Eq. 4.49, see Table 11 .

W_{12} = Defined by Eq. 4.52, see Table 11 .

w = Width of the diaphragm contributory to one of the beams.

w = Displacements in z-axis direction.

w_o = Displacement due to normal force.

X_n = Series terms defined by Eq. C.3a.

x, y, z = Fixed coordinate axis, (Fig. 2).

$\bar{x}, \bar{y}$ = Coordinates of the shear center.

Z_n = Series terms defined by Eq. C.3b.

α = Defined by Fig. 4 .

α = Defined by Eq. 4.28a.

α_{ch} = α for channels, defined by Eq. 4.28a or 4.69a.

α_z = α for Z-sections, defined by Eq. 4.28a or 4.73a.

β = Defined by Eq. 4.28b.

β_{ch} = β for channels, defined by Eq. 4.28b or 4.69b

β_z = β for Z-sections, defined by Eq. 4.28 or 4.73b

$\beta_x, \beta_y, \beta_w$ = Defined by Eqs. A.41a, b, c respectively.

γ = Shear strain.

γ_{ch} = Defined by Eq. 4.44a.

γ_z = Defined by Eq. 4.51a.

δ_{nm} = Kronecker delta.

δ_{ch} = Defined by Eq. 4.44b.

δ_z = Defined by Eq. 4.51b.

ε = Defined by Eq. 4.13b.

$\varepsilon, \varepsilon_z$ = Longitudinal strain.

$\zeta = \frac{z}{L}$ = Dimensionless length parameter.

η = Defined by Eq. 4.16.

κ = Defined by Eq. 4.3a.

λ_x, λ_z = Eigen values defined by Eqs. C.1a and b respectively.

λ_1 = Eigenvalue corresponding to eigenfunction f_1, see Table 11 .

ξ, η, ζ = Coordinate axis in deformed state (Fig. 2).

$\mu_1, \mu_2, \mu_3, \mu_4$ = Defined by Eqs. 4.17d through 4.17g.

ν_x, ν_y, ν_z = Defined by Eqs. 4.17a through 4.17c.

ρ = Dimensionless yield load parameter defined by Eq. 4.13a.

ρ_∞ = ρ for rigid bracing, i.e., Q = ∞, defined by Eq. 4.33.

ρ_L = ρ for Q = Q_L, defined by Eq. 4.47 or Eq. 4.53a.

σ, σ_z = Longitudinal stress.

$\sigma_u, \sigma_v, \sigma_\phi$ = Stress components due to curvatures u", v", ϕ" respectively.

σ_{yd} = Yield stress.

τ = Shear stress.

ϕ = Angle of rotation (Fig. 2).

ϕ_o = ϕ for no bracing case, i.e., Q = 0.

ϕ_∞ = ϕ for rigid bracing case, i.e., Q = ∞.

ω = Warping displacement or sectorial area, defined by Eq. A9; (Fig. 6).

ω_A, ω_C = ω at Location A and location C (See Fig. 2).

ω_3 = ω for corner 3, see Fig. 6 .

ω' = Modified sectorial area for rigid bracing case defined by Eq. 4.26

ABSTRACT

The behavior of thin-walled cold formed channel and Z-sections, braced on their upper flange by light-gage steel diaphragms under static loading is studied.

The objective of the study is to obtain mathematical solutions, to verify these solutions by tests, and to derive design formulations for the bending behavior of channel and Z-section beams with verious boundary conditions.

This type of structural element is encountered as purlins and girts to support the roof cover and siding of metal buildings.

The roof cover is connected to the upper flange of the purlins and gives rise to the case of braced compression flange when the system is under gravity loading. Similarly, for the uplift caused by wind forces, the beam is braced on its tension flange.

The bracing capability of the diaphragms is due to their shear rigidity and/or due to the rotational restraints at the beam diaphragm connection.

The effect of the shear rigidity as well as of the rotational restraint on the load carrying capacity of the beams have been investigated.

Since in some applications, the lower flange of the beam which is not connected to the diaphragm is braced by X-bracings

or sag rods, the additional effect of this discrete bracing is also included in this study.

The differential equation of the diaphragm braced channel and Z-section beams have been derived and a series solution has been obtained by the Galerkin Method. Based on these studies, a computer program is written for the determination of the yield load of the beam. The program is capable of considering any desired number of terms in the series solution and in many cases, it is sufficient to use but a few terms of the series.

The computer program is sufficiently general to include the effect of all geometric parameters. Using a single term solution of the differential equation, design formulas for the yield moment are derived for the beams considered. The designer is thus given the choice of using these simple formulas or the computer program if he desires more accurate analysis.

Based on theoretical and experimental results, pertinent conclusions are obtained and recommendations for further studies are included.

CHAPTER I

INTRODUCTION

1.1 General

Thin-walled cold-formed channel and Z-sections are widely used as purlins and girts due to their easy and economical fabrication and light weight. They are subjected to gravity and wind loading transferred by roof covering or siding of the structure. A typical roof assembly is shown in Figure 1. Generally, the cover or siding material is a light-gage steel diaphragm. Since the channel and Z-section members are weak against torsion and bending in the lateral direction, they should be braced in order to use their bending capacity in their strong direction.

A diaphragm which is properly connected to purlin and girts provides a firm bracing to the individual members, thereby increasing their strength and/or stability. The result is an economical engineering concept. It has been brought to the attention of the author by reliable sources that there have been recent failures of roof structures due to improper design of the purlins. The investigation reported here is aimed at obtaining rational and theoretically sound approaches to the treatment of diaphragm braced, thin-walled channel and Z-section beams which are most commonly used as purlins. A critical review of the previous investigations and the objective of the present study are given in this chapter. Theoretical analysis, design consid-

erations, and experimental programs are discussed in the following chapters.

1.2 Previous Studies

Torsional-flexural behavior of thin-walled prismatic members with open cross-sections has been studied by several investigators. Maillart introduced the concept of shear center in 1922 [35]. Extending the ideas of Wagner and Kappus, in 1941 and 1942, Goodier [15,16] developed the differential equations for stability of such sections under bending and eccentric thrust.

The most extensive investigation of the subject was performed by Vlasov [35]. He derived the differential equations for stability of thin-walled sections under general loading conditions. He also suggested their solution by Galerkin's Method and presented some examples. Vlasov also treated the torsional bending of thin-walled open sections. The concepts of bimoment and flexural twist have been introduced by him. However, he did not consider the coupling of flexural and torsional bending. Rather, he treated them separately and superposed the resulting stresses. The practical implications of his findings were discussed by K. Z. Koscia [41].

Combined torsional-flexural bending has been investigated at Cornell by Lansing [20] in 1949 and McCalley [24] in 1952. McCalley has derived pertinent differential equations in non-principal coordinates. He also studied the second order terms in the longitudinal strain expression and found that under non-uniform torsion, the cross-section does not rotate about the

shear center but about the "rotation center" which is defined in his thesis. However, he has found that these second order terms can be neglected for engineering purposes.

Patterson [26] has studied singly and doubly symmetrical I-beams loaded parallel to the plane of symmetry. He developed expressions for the maximum angle of rotation ϕ_o and for ϕ_o'' to be used in design. Dabrowski [10,11] has conducted similar studies using an energy method. He also investigated torsional-flexural bending of beams under doubly eccentric thrust.

Torsional-flexural bending of channel beams braced by discrete braces has been investigated by Winter, Lansing, and McCalley [37]. They have presented a simple method to determine the spacing and strength of bracing to counteract the twisting tendency of such members. Zetlin and Winter [42] have given a design method for Z-beams with and without lateral bracing under unsymmetrical bending where there are no primary torsional loads and the twisting of the beam is restricted so that the secondary torsional moments can be neglected.

Beams and columns are often braced by other elements of the construction. There is a large volume of research dealing with the stability of discretely or continuously braced beams and columns. Goodier studied the stability of a bar attached to a flexible sheet which prevented the displacements in the plane of the sheet. Vlasov presented the differential equations for the stability of thin-walled beams, continuously braced by elastic springs against displacement and rotation.

K. Kloppel and B. Unger [18] have studied the lateral buck-

ling of a doubly symmetrical I beam whose compression flange is braced by elastic springs against lateral and rotational movements. They used the Runge-Kutta method for integration of the differential equations.

Winter [38] also has studied the stability of braced members. He has developed a method to obtain the lower limits of the strength and rigidity of lateral bracing which provide "full bracing" of beams and columns. The term "full bracing" means that the bracing is equivalent to an immovable lateral support. Larson [21] extended Winter's analysis to shear type lateral supporting media. In this case, the restraint is a function of the slope of the member rather than the lateral deflection itself.

The behavior of shear diaphragms and diaphragm-braced columns and beams have been investigated at Cornell University by L. Luttrell [22,23], G. Pincus [31,32], S. Errera [13,14], and T.V.S.R. Apparao [3,4]. Pincus studied concentrically loaded columns symmetrically braced at both flanges by shear diaphragms. Errera has derived the differential equations of diaphragm-braced beams and columns from energy considerations. He presented solutions for (1) a column braced by a diaphragm on one flange, (2) a column with enforced axis of rotation, and (3) diaphragm-braced beams under uniform bending moment with hinged and fixed boundary conditions. Errera has also considered the stability behavior of diaphragm-braced beams and columns in the inelastic range. Apparao extended the theory to initially imperfect beams and columns. He obtained solutions for (1) axial-

ly loaded columns braced by girts, which in turn are braced by diaphragms, with hinged (i.e. $v = v'' = u = u'' = \phi = \phi'' = 0$) and torsionally fixed but flexurally hinged (i.e. $v = v'' = u = u' = \phi = \phi' = 0$) boundary conditions, and (2) I, channel and Z-beams with hinged or fixed ends, subjected to uniform bending moment and braced by a shear diaphragm at one flange. Both cases include ideally perfect and initially imperfect situations. For the imperfect case, either the beam may yield first, or the diaphragm may fail. Diaphragm failure is defined as the condition when the shear strains exceed a limiting value determined by test [5]. Many tests on diaphragm-braced beams and columns have been carried out by Pincus, Errera and Apparao to verify their computations.

These authors have utilized the shear rigidity of the diaphragm, but neglected the rotational restraint supplied by the diaphragm bracing with the justification of being on the safe side.

On the other hand, Pelikan [30] has performed full scale tests on purlins braced by well-eternit deck and substantiated the value of the rotational restraint of the diaphragm. Vogel [36] has derived approximate formulas for the critical load of a continuous purlin of doubly symmetrical I-section, taking only the rotational restraint into consideration. He also derived a simple formula for the required rotational restraint, setting the critical lateral buckling load of purlin equal to its flexural carrying capacity. If the existing rotational restraint provided by the diaphragm to the beam is larger than

the one defined by Vogel, failure is not caused by instability and the optimum strength of the beam is obtained.

In this study, both the shear rigidity and the rotational rigidity of the diaphragm in bracing of channel and Z-purlins have been considered.

1.3 Objective of this Study

1. Establish a theoretical basis for the design of diaphragm-braced thin-walled channel and Z-section beams.

2. Obtain the solution to the differential equation of the diaphragm-braced thin-walled beams.

3. Investigate the effect of various parameters, computerizing the solutions obtained.

4. Obtain closed form and relatively simple design formulas.

5. Verify the theoretical findings by model and full-scale tests.

The objectives are achieved as follows: In the second chapter, the elastic theory for combined bending and torsion of thin-walled beams with open cross sections is discussed. The differential equations for diaphragm-braced channel and Z-beams are presented and their solution is outlined. The derivation of the general theory is given in Appendix A where, among others, the works of Vlasov [35] and McCalley [24] have been used extensively without specific reference. Derivation of the differential equations for diaphragm-braced beams and a detailed treatment of their solution is presented in Appendices B and C respectively. Appendix D describes an experimental procedure to determine the rotational restraint of the diaphragm.

The third chapter deals with numerical studies through computers. The results are discussed qualitatively. The flow chart of the computer program is given in Appendix E.

Some possibilities for design simplifications are described in the fourth chapter.

Experiments are discussed in the fifth chapter.

Finally, in the sixth chapter, the results are summarized and future research is outlined.

CHAPTER II

THEORETICAL ANALYSIS

2.1 General

Ordinary beam theory with the assumption of plane sections remaining plane is, in general, unsatsifactory for thin-walled beams with open cross sections. Such beams warp when loaded, and the corresponding stresses and deformations are of the same order as the ones due to ordinary beam theory. Hence, a more advanced theory which considers warping is necessary.

2.2 Theory of Thin-Walled Open Section Beams

The theory for thin-walled beams is described in Appendix A. Coordinate axes and the positive directions of the forces are given on Figures 2 through 4. Equilibrium of an element in the z-axis direction is shown on Figure 5.

The longitudinal stress as determined in Appendix A is:

$$\sigma_z = \frac{Edw_o}{dz} - \frac{Ed^2u}{dz^2} x - \frac{Ed^2v}{dz^2} y - \frac{Ed^2\phi}{dz^2} \omega \qquad (2.1)$$

The last term is due to warping. The quantity ω is called sectorial area or warping displacement. For channel and Z-sections, ω is shown in Figure 6.

The shear stress when there are no longitudinal tractions along the surface and along the free edges of the beam is:

$$\tau_{zs} = \frac{E}{t} Q_y \frac{d^3u}{dz^3} + \frac{E}{t} Q_x \frac{d^3v}{dz^3} + \frac{E}{t} Q_w \frac{d^3\phi}{dz^3} \qquad (2.2)$$

where Q_x, Q_y, and Q_w are statical moments whose values depend upon the coordinates of the point of the cross section where the stress is sought. The last term represents stresses due to warping. Warping stresses are assumed to be constant over the thickness. Saint Venant shear stress, which is zero at mid-thickness and varies linearly over the thickness is not included above.

When the shear stresses are integrated over the cross section, the component due to warping results in torsional moment M_{tw}.

$$M_{tw} = -EC_w \frac{d^3\phi}{dz^3} \qquad (2.3)$$

This is called flexural twist in distinction from Saint Venant twist. The latter is

$$M_{ts} = GK \frac{d\phi}{dz} \qquad (2.4)$$

Thus, an external twist will be resisted by both warping and St. Venant rigidities. The significance of the warping rigidity increases as the wall thickness and the span length of the beam decrease.

When the normal stresses are integrated to find the stress resultants, the component due to warping has no contribution to normal force or bending moments. However, the virtual work of these normal stresses acting over the warping displacements does not vanish. It is useful to introduce the following quantity, called bimoment [35], to represent warping stresses in a

cross section.

$$B = \int_A \sigma\omega \, dA = -EC_w \frac{d^2\phi}{dz^2} \tag{2.5}$$

A system which has zero force and zero moment resultants but has a bimoment is shown in Fig. 7a. It is intuitively clear that such a force system will warp a thin-walled beam with open cross section.

The external loads which do work along warping displacements create external bimoments. For example, a longitudinal force P acting at a point A (where ω_A is not zero) constitutes a bimoment of $P\omega_A$. A bimoment is always accompanied by warping and twisting of the beam or column. Hence, a concentrically loaded column of Z-section will twist in a continuous manner due to the bimoments $P\omega_c$ at the ends. On the other hand, a column of channel section loaded concentrically will remain straight until the buckling load because $\omega_c = 0$ for this case [35,41]. Some examples for loads causing bimoments in a member are shown on Figures 7a through 7d. In summary, both torsional moments and external bimoments lead to warping of the cross-section and twisting of the beam or column, producing warping stresses.

Note that flexural twist is the derivative of the bimoment as can be seen from Eqs. 2.3 and 2.5,

$$M_{tw} = \frac{d}{dz} B$$

The differential equations of channel and Z-beams loaded in a plane parallel to the web are

$$EI_{xy} \frac{d^2u}{dz^2} + EI_x \frac{d^2v}{dz^2} = -M_\xi \tag{2.6a}$$

$$EI_y \frac{d^2u}{dz^2} + EI_{xy} \frac{d^2v}{dz^2} = M_\eta \tag{2.6b}$$

$$EC_w \frac{d^3\phi}{dz^3} - GK \frac{d\phi}{dz} = -M_\zeta \tag{2.6c}$$

The derivation of these equations is given in Appendix A. The curvatures in Eq. 2.1 will be obtained by solving the differential equations for combined bending and torsion [20,24]. The moments M_ξ, M_η and M_ζ are in the direction of the deflected axes. M_ξ and M_η act at the centroid while M_ζ is at the shear center. They can be expressed in terms of the moments M_x, M_y, and M_z in the direction of undeformed axes as follows

$$M_\xi = M_x + \phi M_y - \frac{du}{dz} M_z \tag{2.7a}$$

$$M_\eta = -\phi M_x + M_y - \frac{dv}{dz} M_z \tag{2.7b}$$

$$M_\zeta = \frac{du}{dz} M_x + \frac{dv}{dz} M_y + M_z \tag{2.7c}$$

2.3 Theory of Diaphragm-Braced Beams

The behavior of diaphragm-braced beams depends on the cross-sectional configuration of the beam and the type of the loading. The main types of loading in a roof structure are gravity loads and wind suction forces. They are transmitted from diaphragm to the members by bearing for downward loading and through the connectors for uplift loading.

If doubly symmetrical shapes such as I section or singly symmetrical shapes such as ⊓ or ⊤ are used in the diaphragm-

beam assembly, the loads act in the plane of symmetry. Thus, the beam deflects only vertically without any rotation or lateral deflection until the bending capacity is reached or lateral instability occurs. This behavior will also be observed for channel and Z-section beams, when the load plane passes through the shear center and the load is applied parallel to one of the principal axes. However, in the analyzed structure, the loads do not act through the shear center in the case of channels and are not in the direction of principal axes for Z-sections. Hence, in addition to the vertical bending, these sections rotate and deflect laterally with increasing load. Evidently, this is not a stability problem. It is rather a problem of combined bending and torsion.

2.3.1 Diaphragm Bracing

Diaphragms usually consist of thin-walled corrugated or orthotropic metal plates with open configuration. Because of its orthotropic characteristics, one can assume that along the corrugations, the axial stiffness is infinite, but perpendicular to the corrugations, it is zero. Consequently, in the latter direction, no axial force and moments in the plane of the diaphragm can be carried. The bracing capacity of a diaphragm in its plane is then only due to the shear strength and shear rigidity. When the beam where the bracing is attached deflects sideways, the diaphragm undergoes shear deflections. Consequently, shear forces arise in the diaphragm. The rate of change in the shear force along the z-axis is equivalent to a distributed load acting on the upper flange of the beam. This

distributed load restrains the deflection of the beam in the plane of the diaphragm bracing. Previous research at Cornell University indicates that this model is adequate to describe the behavior of diaphragm-braced members within engineering accuracy. The shear forces in the diaphragm, and the lateral bracing force between the diaphragm and the beam are shown on Figure 8.

It should be noted that shear type deflection of the diaphragm is not due only to actual shear strains in the material. Cross-sectional deformations of the diaphragm and deflections at the fasteners generally contribute the larger portion of the macroscopic shear deformations. Hence, shear rigidity depends on several factors, such as cross-sectional configuration, the length of the diaphragm along the corrugations, and material thickness, fastener type and spacing, etc. Research is in progress [12] to predict the shear rigidity Q of a given diaphragm analytically. But for the time being, no established analytical formulation is available; therefore, Q must be determined experimentally [22,23].

In addition to shear rigidity, the diaphragm has a cross-bending stiffness along its corrugations. This may provide rotational bracing to the members. The rotation of the diaphragm and the purlins are sketched on Figure 9. Three types of deformation are possible:

(1) Rotation ϕ_b caused by beam type deflection of the diaphragm.

(2) Rotation ϕ_{fl} caused by deformation of the flange with

respect to the web,

(3) Rotation ϕ_{dia} caused by local deformation at the connections of the diaphragm. The local rotation then consists of the sum of ϕ_{fl} and ϕ_{dia}, i.e. $\phi_{local} = \phi_{fl} + \phi_{dia}$. The total rotation of the cross-section of the purlin is the sum of ϕ_b and ϕ_{local}. The corresponding components of the rotational rigidity F are designated as F_b and F_{local}. Thus

$$\frac{1}{F} = \frac{1}{F_b} + \frac{1}{F_{local}}$$

Since the local deformations depend on the connection detail and on the type of deck panel, it is proposed to find the corresponding rotational restraint by a test. A possible test set-up is discussed in Appendix D.

2.3.2 The Differential Equation

Previous investigations of diaphragm braced beams considered only either the shear rigidity Q [14,4] or only the rotational stiffness F [36], and were generally confined to doubly or singly symmetrical sections with the loading in the axis of symmetry. This research includes the effect of both of the parameters at the same time.

The differential equations of diaphragm-braced I, channel and Z-beams loaded in a plane parallel to the web are derived in Appendix B. They are

$$E \frac{(I_x I_y - I_{xy}^2)}{I_x} \frac{d^4u}{dz^4} - Q \frac{d^2u}{dz^2} - Qe_D \frac{d^2\phi}{dz^2} + \frac{d^2}{dz^2}(M_x\phi) = - \frac{I_{xy}}{I_x} p_y \qquad (2.8a)$$

$$EC_w \frac{d^4\phi}{dz^4} - (GK + Qe_D^2) \frac{d^2\phi}{dz^2} - p_y e\phi + F\phi + M_x \frac{d^2u}{dz^2} - Qe_D \frac{d^2u}{dz^2} = p_y a \tag{2.8b}$$

where

Q = shear rigidity of the diaphragm

F = cross-bending rigidity of the diaphragm

e_D = a positive number showing the vertical distance of the diaphragm from the shear center (Figure 10)

p_y = distributed load in the plane of the web (positive for downward, negative for uplift loading case)

a, e = positive numbers indicating respectively the horizontal and vertical distances of the application point of p_y from the shear center (Figure 10)

$M_x = \iint p_y dz^2$, i.e. bending moment due to p_y

For I beams $I_{xy} = a = 0$, thus the equations are homogeneous indicating a stability problem. For channel sections $I_{xy} = 0$ but $a \neq 0$, whereas Z beams have $I_{xy} \neq 0$ and $a \neq 0$. Hence, Eqs. 2.8 remain nonhomogeneous for both channels and Z beams so that stable deflections will arise continuously with increasing loads

Eqs. 2.8 are repeated below in terms of a dimensionless variable ζ, where

$$\zeta = \frac{Z}{L}$$

In the remainder of this study, primes will indicate differentiation with respect to ζ, except when otherwise specified.

$$\frac{E(I_x I_y - I_{xy}^2)}{I_x L^2} u^{IV} - Qu'' - Qe\phi'' + (M_x\phi)'' = -\frac{I_{xy}}{I_x} p_y L^2 \tag{2.9a}$$

$$\frac{EC_w}{L^2}\phi^{IV} - GK\phi'' - Qe^2\phi'' - p_y eL^2\phi + FL^2\phi + M_x u'' - Qeu'' = p_y L^2 a \tag{2.9b}$$

where $e_D = e$ is substituted assuming that the distance of the bracing force p_x and external load p_y from the shear center is the same.

The parameter Q influences both the lateral and rotational stiffness of the beam-diaphragm assembly since the bracing forces cause stabilizing torsional moments about the shear center. In contrast, F increases only the torsional stiffness of the purlin. Thus Q appears in both of the equations 2.9 while F is present only in 2.9b.

The vertical deflection can be found from

$$\frac{d^4v}{dz^4} = \frac{p_y}{EI_x} - \frac{I_{xy}}{I_x}\frac{d^4u}{dz^4} \tag{2.10}$$

2.3.3 Special Cases

For two limiting values of the shear stiffness Q, the coupled equation system 2.9 can be reduced to one fourth order differential equation for ϕ.

2.3.3.1 No bracing, i.e. Q = 0

For this case

$$\frac{EC_w}{L^2}\phi^{IV} - GK\phi'' - \left[p_y e + \frac{I_x M_x^2}{E(I_x I_y - I_{xy}^2)}\right] L^2\phi + FL^2\phi = \left[p_y a - \frac{I_{xy} M_x^2}{E(I_x I_y - I_{xy}^2)}\right] L^2 \tag{2.11}$$

After ϕ is found, u" is given by

$$u'' = \frac{L^2}{E(I_x I_y - I_{xy}^2)}(-M_x I_x \phi + M_x I_{xy}) \tag{2.12}$$

2.3.3.2 Rigid bracing, i.e., $Q = \infty$

For this case the displacements u and ϕ are no longer independent. Specifically, $u_D = 0$ gives

$$u = -e_D\phi = -e\phi \tag{2.13}$$

The differential equation is

$$\frac{EC'_w}{L^2}\phi^{IV} - GK\phi'' + FL^2\phi - M_x\phi''e - (M_x\phi)''e - p_y eL^2\phi = p_y L^2\left(a + \frac{I_{xy}}{I_x}e\right) \tag{2.14}$$

where

$$C'_w = C_w + \frac{I_x I_y - I_{xy}^2}{I_x}e^2 \tag{2.15}$$

2.3.4 Solution of the Differential Equations

The differential equations are solved by the Galerkin Method. The displacements u and ϕ are represented by infinite series of the form

$$u = \sum_{n=1}^{\infty} u_n X_n \tag{2.16a}$$

$$\phi = \sum_{n=1}^{\infty} \phi_n Z_n \tag{2.16b}$$

where the functions X_n and Z_n satisfy the boundary conditions. By the Galerkin Method the differential equations are converted into algebraic equation systems for u_n and ϕ_n. Thus Eqs. 2.9 become

$$\sum_{n=1}^{\infty}(A_{mn}u_n + B_{mn}\phi_n) = E_m \tag{2.17a}$$

$$\sum_{n=1}^{\infty}(C_{mn}u_n + D_{mn}\phi_n) = F_m \tag{2.17b}$$

$$m = 1, 2, \ldots\infty$$

where A_{mn} through F_m are constants which depend on beam dimensions, boundary conditions, diaphragm stiffness, and load distribution and intensity. The details of the procedure and formulas for A_{mn} through F_m are presented in Appendix C.

2.3.5 Stress Calculations

The curvatures are used to compute stresses. The vertical curvature is

$$\frac{Ed^2v}{dz^2} = -\frac{M_x}{I_x} - \frac{Ed^2u}{dz^2}\frac{I_{xy}}{I_x} \tag{2.18}$$

using this equation, and assuming that there are no longitudinal forces on the beam, Eq. 2.1 becomes

$$\sigma = \frac{M_x}{I_x}y - \frac{E}{L^2}[(x - \frac{I_{xy}}{I_x}y)u'' + \omega\phi''] \tag{2.19}$$

The following summarizes how the terms u" and v" are determined.

a) General case

From Eqs. 2.16,

$$u'' = \sum_{n=1}^{\infty} u_n X_n'' \tag{2.20a}$$

$$\phi'' = \sum_{n=1}^{\infty} \phi_n Z_n'' \tag{2.20b}$$

Coefficients u_n and ϕ_n can be determined using Eqs. 2.17

b) No bracing, i.e., Q = 0

Here u" may be found from Eq. C.22 (Appendix C) as a function of M_x and ϕ. For a given number of terms in the series solution, this will give better accuracy than Eq. 2.20a, because the series for deflection converges more rapidly than that for curvature.

c) Rigid bracing, i.e., $Q = \infty$

Since $u'' = -e\phi''$, Eq. 2.19 becomes

$$\sigma = \frac{M_x}{I_x} y - \frac{E}{L^2} \omega' \phi'' \tag{2.21}$$

where

$$\omega' = \omega - (x - \frac{I_{xy}}{I_x} y)e \tag{2.22}$$

The curvature ϕ'' is given by Eq. 2.20b for both $Q = 0$ and $Q = \infty$.

CHAPTER III

PHYSICAL BEHAVIOR AND DISCUSSION OF COMPUTER SOLUTION

3.1 General

In general, channel and Z-section beams undergo lateral displacement and rotation when loaded parallel to the plane of the web. Diaphragm bracing which is connected to the upper flange of the beams resists these deformations, thereby generally increasing the yield load capacity of the purlins and reducing their deflections. The evident but important consequence of the above statement is that the effectiveness of the diaphragm depends on the deflection tendency of the upper flange and rotation tendency of the cross-section. Detailed examples illustrating this statement are presented in this chapter.

A computer program has been prepared on the basis of the series solution of the differential equations for lipped and plain channel and Z-section beams braced by diaphragms. This program determines the incipient yield load, lateral deflection u and angle of rotation ϕ at midspan (for both yield load and service loads) as well as stresses at the cross-section where yielding starts. All plots and tables are based on using three terms of the series solution for u and ϕ each.

Though the numerical results are given for hinged boundaries, extension of the program to other boundary conditions should not cause any basic difficulty. Both uplift and downward gravity loads are investigated. The load is taken as uniformly distributed.

The coupling of bending and torsion generally results in a nonlinear relationship between the load and the stresses. Hence, the yield load cannot be found directly, but only through iteration. In the computer examples, the theoretical failure is defined as the load resulting in a maximum stress of 37.95 or 46 ksi. The value of 37.95 ksi as maximum stress is obtained by applying a 15% overstressing to the basic yield stress of 33 ksi. This overstressing factor was first proposed in Ref. 37 where localized maximum stresses appeared at the corners of the cross-section. This also has been observed by the author in unbraced channel and Z-section beams or in braced beams of relatively small L/h (length/depth) ratios, particularly for uplift loading case. On the other hand, as the L/h ratio increases, the stress distribution on the flange becomes more and more uniform, since the main contribution to the stress comes from the bending about the strong axis. In these cases, an overstressing is not justified. Thus, in the latter phases of this investigation, where relatively large L/h ratios were studied, the maximum stress was taken as 46 ksi without any overstressing considerations. In the opinion of the author, the designer should be the one to decide whether or not he can increase the maximum stress after checking the stress distribu-

tion. Further considerations are discussed in Chapter IV in connection with the determination of stress distribution.

The two important characteristics of diaphragm bracing are the shear rigidity Q and the rotational restraint F. Separate and combined effects of both of these parameters are investigated in this study. The studies also include the case where both parameters vanish, namely, the unbraced case.

It should be noted that an extensive discussion of physical behavior is also included in Chapter IV.

3.2 Influence of Shear Rigidity Q on Behavior

3.2.1 General

Light gage steel diaphragms usually have both shear rigidity Q and offer rotational restraint F. However, there may be cases where the rotational restraint is not reliable. In order to cover this separately, and to simplify the explanation of some of the phenomena connected mainly with the shear rigidity, the discussion here will be confined to the case F=0. The dimensions of the members involved in the discussions are given in Fig. 11.

3.2.2 Deformations

Figures 12-15 show the lateral deflections and the angles of rotation at midspan for the sections in question for uplift loading with L = 60". It is seen that Z-section beams display, in general, less rotation than channel beams with identical dimensions. However, when the diaphragm stiffness is increased, there is not much difference between them. It is also observed that u_o for channels and ϕ_o for Z-sections are tangential to

the load axis at the origin. (Subscripts o and ∞ refer to no bracing and rigid bracing cases, respectively). This is so because there is no load component at the outset to cause these deformations. Slight non-linearity can be observed in these diagrams. The reason is that new components of the loads are created by the deformation u and ϕ of the beam. The effects of these secondary components may add to or subtract from the primary loading effects depending upon the parameters involved.

In general, for uplift loading, both diaphragm-braced or unbraced channel and Z-beams will have pL - ϕ diagrams with decreasing slopes at failure. No examples for the downward case are included here. However, for the unbraced case the pL - ϕ diagrams will be more non-linear and will have a decreasing slope as above. On the other hand, for the rigidly braced case, a stiffening-type pL - ϕ curve will emerge for downward loading. (This will also be the case for a reasonable stiffness of the diaphragm bracing).

3.2.2 Yield Load Capacity versus Span Length

On Figures 16 through 19, the ratio M/M_{bend} versus span length is shown for no and rigid bracing cases. M is the bending moment at midspan due to uniformly distributed load p, i.e., $M = \frac{pL^2}{8}$. It is compared here with the theoretical bending capacity $M_{bend} = \frac{\sigma_y I_x}{d}$. M_{bend} represents the capacity of a beam which is guided or braced such that the only possible deformation is bending in the plane of the load with no rotation or lateral deflection. Thus M_{bend} for I, channel

and Z beams of the same flange and web dimensions is the same. (Of course for an I beam there is no need for guides or bracing, provided that M_{bend} does not cause instability). The corner where the stress has reached 37.95 ksi first, is indicated on these figures.

The dotted lines indicate where the maximum angle of rotation is larger than 10°, assumed here as an arbitrary practical limit. Both uplift and downward loading cases are presented.

It may be of interest to note how M/M_{bend} attains some definite value as the span length approaches zero. Of course zero span length has no physical meaning and may be viewed just as a mathematical limit. The calculation of M/M_{bend} for L=0 is given in Appendix F. Here this matter will be considered qualitatively. For example, for an I beam the ratio of M/M_{bend} is equal to unity for any span length. (If we use 1.15 σ_y as the failure criterion M/M_{bend} would be 1.15 for all L). As L approaches zero, p will approach infinity so that $M = \frac{pL^2}{8}$ will be equal to the yield load capacity which is finite. If a channel beam were loaded through the shear center, the same result as that for an I beam would be obtained. However, if the load is acting in the plane of the web, primary torsional moment $m_t = pa$ exist. When L is small, the Saint Venant torsion resistance can be neglected. External torsion is then resisted by flexural twist M_{tw} only and the bimoment at the midspan will be simply $B = \frac{paL^2}{8} = Ma$. Since it was shown that M remains finite as L approaches zero, B

also will be finite. The bimoment causes additional stresses in the cross section and reduces M/M_{bend} to some definite value less than 1.15. The amount of the reduction will depend on the section properties.

In the case of a Z-section loaded in the plane of the web, there is also a reduction. Since the load is not in the principal plane, the beam experiences lateral deflections in addition to the vertical ones. For convenience these deflections can be thought of as caused by fictitious lateral loads[11] equal to $p \frac{I_{xy}}{I_x}$. These loads result in a lateral bending moment of $M\ I_{xy}/I_x$ which remains finite as L goes to zero. Thus the ratio M/M_{bend} will be reduced due to the additional stresses caused by this moment.

3.2.4 Yield Load Capacity for Gravity or Uplift Loading

Figures 16 through 19 illustrate the effect of diaphragm bracing on yield load capacity.

First, it can be observed that for the downward loading, due to the shear rigidity of the diaphragm bracing, there is a definite increase in yield load capacity of channel and Z-beams.

For the uplift case, however, only Z and lipped Z sections show a definite improvement. The yield load capacity of channel and lipped channel beams under uplift loading may not be effected by the shear rigidity of the diaphragm bracing.

This puzzling behavior can be explained, qualitatively, with the aid of Figures 20a and 20b. First a channel beam

without bracing will be considered. For this case, on Figure 20a, the uplift load is decomposed into three components with respect to the deformed configuration. The signs of the corresponding component stresses are also indicated in this figure and it can be observed that all component stresses at corner 3 are of the same sign. Thus, it is concluded that for this loading the stress at corner 3 will govern the initiation of yielding. As far as the displacements are concerned, the upper flange has a tendency to move to the right due to component B on Figure 20a and to the left due to component C. If the load is increased continuously from zero until yielding, it would be observed that at first ϕ will be small and component B can be neglected. Therefore, at first, the upper flange will move to the left. The bracing forces corresponding to this displacement if the beam were connected to a diaphragm along its upper flange is illustrated in Figure 20b. The diaphragm force component B' adds to while component C' subtracts from the corresponding components in Figure 20a. (Component A' of the diaphragm forces is of higher order and can be neglected in this discussion). The stress at corner 3 will be affected similarly. If the stress at corner 3 due to the bracing force components B' is larger than the stress due to bracing force component C', then the stress in the braced case is likewise larger than in the unbraced case. The reverse is true if component B' is smaller than C'. Thus, if the former case leads to yielding, then the yield load capacity of the braced beam will be smaller than that of the

unbraced beam. In the latter case the reverse will be true. However, since for small values of ϕ the stresses due to bracing force components B' and C' are of the same order of magnitude, their difference will be small and the net effect of bracing on the yield load capacity will also be small.

If yielding does not occur at relatively small ϕ and the load is increased further, the force component B of Figure 20a will become dominant and eventually the upper flange will move to the right. This in turn changes the sign of the bracing forces. Now component B' of Figure 20a will be reduced while C' is increased. The stress at corner 3 in the braced case may again be larger or smaller than that of the unbraced case. Hence, the yield load capacity again may be increased or decreased by the diaphragm bracing depending on the section geometry, the span length and the magnitude of the yield stress.

The behavior of diaphragm braced channels under downward loading and Z-section beams under both uplift and downward loading cases could be discussed in a similar manner as above. However, intuitively it is clear that for these cases the upper flange of the unbraced beam will move only in one direction with increasing load. Thus, the diaphragm will always restrain this movement, thereby increasing the capacity.

3.2.5 Stress Distribution Example

Figures 21 and 22 show the stress distribution in unbraced and rigidly braced channel and Z-beams under uplift or downward loading at failure. Numerical values of failure

moments, that is the moment causing 1.15 times the yield stress, are given in these figures in parentheses. The span length is 60". On Figure 21, it can be observed that shear rigidity of the bracing has almost no effect on the stress distribution in the channel section for the uplift loading case for this particular span length. This is in accordance with the previous statement on the yield load capacity of channels under uplift load.

Comparing Figures 21 and 22, one sees that rigidly braced channel and Z-beams have similar stress distributions. Since the magnitude of the angle of rotation is almost the same but of opposite sign for channel and Z-beams, the unbraced flange in both cases has similar stress distributions. In this flange the stress due to twist (second component in Eq. 2.21) increases the stress at corner 3 while reducing it at corners 2 and 1. In the braced flange, however, the stress is nearly constant and mainly due to vertical bending.

3.2.6 Yield Load Versus the Shear Rigidity

In Figures 23-26, plots of M/M_{bend} versus Q/P_Y are given. P_Y is the Euler buckling load, that is

$$P_Y = \frac{\pi^2 E I_y}{L^2}$$

These figures consist of several curve segments each indicating yielding at a particular corner of the cross section. Only the curves determining the yield load are shown.

On these figures it can be seen that for downward loading yielding initiates at corner 3 for a wide range of values

of Q, varying from a relatively small finite value up to infinity. For smaller values of Q, yielding at corner 4 governs. As Q decreases further, yielding at corners 5 or 6 may govern. The value of the diaphragm shear rigidity where the curves for corners 3 and 4 intersect is designated Q_L. It can be observed that there is a rapid increase in the yield load capacity for the range $0 \leq Q \leq Q_L$. On the other hand, for $Q > Q_L$ the change in the yield load capacity is quite small. Obviously, to provide diaphragm shear rigidities less than Q_L would be uneconomical in practical design. Approximate determination of Q_L and the corresponding yield load will be discussed in Chapter IV.

3.2.7 Tables

In Tables 1 through 10, the load carrying capacity and the angle of rotation of channels and Z-beams are investigated for a wider range of parameters than in the plots mentioned above. The parameters are:

$$Q/P_Y,\ h/t,\ b/h,\ c/b,\ \text{and}\ L/h$$

where

h = depth of the beam

b = width of flange

c = width of the lip

t = thickness

L = span length

Both downward and uplift loading are considered. Most of the information listed in these Tables is qualitatively the same as that given in Figures previously discussed. Below is a brief description of these Tables.

(1) Tables 1a, 1b, 2a and 2b: The ratio $p/p_{bend} = M/M_{bend}$ at theoretical failure

(2) Tables 1c and 2c: The point of maximum stress at theoretical failure

(3) Tables 3a, 3b, 4a and 4b: The midspan rotation ϕ at theoretical failure

(4) Tables 5a, 5b, 6a and 6b: The midspan rotation $\phi_{1.67}$ at 1/1.67th of the theoretical failure load

(5) Tables 7a, 7b, 8a and 8b: The ratio p/p_{∞} at theoretical failure

(6) Tables 9a, 9b, 10a and 10b: The ratio ϕ/ϕ_{∞} at theoretical failure.

Some of the values in Tables 7 through 10 are plotted in Figures 27 and 28 to illustrate the effect of various parameters more clearly.

The angle of rotation at service loads is of special interest in design. In preparing Tables 5 and 6, an arbitrary safety factor of 1.67 against theoretical failure was assumed to obtain service loads. The most important parameter appears to be the span length. Below is a summary of the magnitudes of $\phi_{1.67}$:

$0.00° < \phi_{1.67} < 1.32°$ for L/h = 5

$0.06° < \phi_{1.67} < 3.67°$ for L/h = 10

$0.25° < \phi_{1.67} < 6.32°$ for L/h = 15

3.3 Influence of Rotation Restraint F on Behavior

3.3.1 The Rotation Restraint Due to Local Deformation of The Diaphragm

As mentioned earlier F consists of the two components F_b and F_{local}. F_b is the rotational restraint offered by the cross-bending rigidity of the diaphragm and may be computed by ordinary beam theory from the cross-sectional properties of the diaphragm and purlin spacing. On the other hand F_{local} may be determined experimentally (Figures 29 and 30) as proposed in Appendix D. In general, F_{local} is smaller than F_b as has been observed in full scale tests with purlins by light gage steel diaphragms.

When the beam rotates, the diaphragm develops counter acting torsional moments on the beam at the connection points. This moment is partly created through the bending rigidity of the mechanical connector itself. The couple consist of a compressive force at the corner where contact is established between the beam and the diaphragm, and a tensile force in the screw. The screw connection must be strong enough to take this force in addition to the tensile force due to uplift loading.

The factors which influence F_{local} may be deduced from the physical model described above:

(1) If the contact between the diaphragm and the purlin is incomplete or if there is an intermediate layer of soft (insulation) material, the realization of either one of the forces constituting the couple and thus of the torsional restraint, may be doubtful.

(2) On the other hand, if the couple can be materialized, the distance between the forces of the couple will be of importance. The position of the screw relative to the web influences the rotational restraint F. This will be discussed in the subsequent section in some detail.

(3) The sheet thickness and the cross-sectional configuration of the diaphragm may also influence F_{local}.

3.3.2 The Position of the Screws

The forces which constitute the restraining couple are shown on Figures 31 and 32 for channel and Z-sections, respectively. The tensile force component acts at the screw and the compressive force component acts at the contact points between the purlin and the diaphragm. The point of contact depends on the direction of rotation of the cross-section.

For channels, as illustrated in Figure 31, the angle of rotation is clockwise for gravity and counter-clockwise for uplift loading cases. Hence the contact point of purlin and diaphragm changes from web to lip side when the loading type changes from gravity to uplift. Unless the screw is exactly at the middle of the flange, the lever arm of the forces of the couple will be different for these two loading cases. Consequently, the respective rotational restraints will be different for gravity and uplift loadings. The research reported here indicates that F is more beneficial for uplift loading. Thus, it is preferable to have the screws closer to web than to lip for channel section purlins. Also, if the screws are placed closer to web, the distance of the point of application of the uplift

load from the shear center is smaller and hence the primary torsional loading is reduced. Thus, it is seen that the location of screws affects both the primary torsional moment and the rotational restraint F.

As for Z-section purlins, for gravity loading, the direction of rotation is also influenced by the shear rigidity of the diaphragm. If the load is assumed to be acting in the plane of the web, for $Q > Q_L$ as shown in Figure 32a, the rotation is counter-clockwise. (The direction of rotation changes to clockwise at $Q = Q_L$). A counter-clockwise rotation is likely to shift the loading point to the right of the web which in turn should reduce the angle of rotation of the section.

In the uplift loading case of Z-sections, there are two possibilities as shown in Figures 32b and 32c. If the screw (hence the load application point) is very close to the web, the rotation is clockwise, while if the screw is very close to the lip, the rotation is counter-clockwise. For both of these extreme cases, the lever arm of the resisting couple is quite small. On the other hand, as the screw location is brought to the mid-section of the flanges, the rotation tendency of the section decreases. At the same time, the lever arm of the resisting couple, hence F increases. Consequently, the optimum placement of the screws for Z-sections is approximately at the middle of the flange.

In summary, it is advantageous to have the screws close to the web for channels and at mid-flange for Z-section purlins.

3.3.3 The Effect of F

The diaphragm beam assembly constitutes a statically indeterminate system. If the diaphragm can supply a rotational restraint F, it directly participates in carrying the primary torsional moments which arise when the beam is loaded outside the shear center as in the cases of channel section purlins under uplift and gravity loading and of Z-section purlins under uplift loading.

The primary loads for channel section purlins consist of vertical and torsional loads. As was discussed in section 3.2.3, secondary loads arise due to lateral and rotational deformations. In particular, a secondary load in the weak axis direction (i.e., $M_x\phi$ in Eq. 2.9a) becomes more significant as the rotation of the section increases. This is the only load which causes deflections in the weak axis direction of channel section purlins.

When F is increased, the angle of rotation ϕ is reduced. This, in turn causes a reduction in the lateral deflection of channel section purlins. Hence, with increasing F, the ratio M/M_{bend} approaches unity asymptotically as can also be observed for example in Figures 34a or 35a.

On the other hand, for Z-sections, there is also a lateral primary load of intensity $p_y\ I_{xy}/I_x$, in addition to the primary loads mentioned above. As the term "primary" implies, this load is independent of ϕ. Therefore, even for values of F approaching infinity, there will be lateral deflections in addition to the bending in the strong axis direction while ϕ

approaches zero. Associated stresses with the lateral deflection reduce the yield load capacity. Thus the asymptotic value of M/M_{bend} cannot be unity. (It can be shown that it is equal to $1-I_{xy}^2/I_xI_y$).

On the basis of the above discussion, it can be concluded that channel sections are generally more effected by F than Z-sections. In particular, channels under uplift loads which have a relatively large tendency to rotate are beneficially influenced by the rotational restraint of the diaphragm. On the other hand, for Z-sections braced by a diaphragm with a reasonable shear rigidity, the angle of rotation is relatively small, thus reducing the influence of F. As can be seen in Figures 33 through 56 the effect of F is most pronounced when the shear rigidity is equal to zero.

3.3.4 Reliability of F

Unlike the shear rigidity Q, the rotational restraint F seems to be quite sensitive to the usual inaccuracies of practice. Screws are usually applied through the top of the deck. Thus, their location on the flange of the purlin is quite irregular and somewhat unpredictable.

The resisting torsional moments act at discrete points along the purlin. Therefore, omission or unfavorable placing of screws at a crucial cross-section (such as at mid-span for simply supported purlins) may reduce the load carrying capacity greatly, especially if the beam has a low torsional rigidity as is common in thin-walled purlins with large span lengths.

Since the yield load capacity may vary fairly rapidly with F for certain cases, utilization of F must be undertaken with considerable caution.

3.4 Combined Effect of Q and F

3.4.1 General

The influence of Q and F alone were discussed in the previous sections of this chapter. Here, the combined effect of Q and F on the yield load capacity and the corresponding angle of rotation at mid-span will be discussed. The effect of various parameters were studied using the computer program discussed in Appendix E. The results are plotted in Figures 33a and b through 56a and b. These figures also contain the cases of Q = 0 and/or F = 0. Parameters and their ranges of values that were considered are listed below:

(1) F from 0 to .40 ki/in/rad

(2) Q = 0, Q_L, $2Q_L$ and ∞

(3) L/h = 15, 30 and 45

(4) Two sets of cross-sectional parameters were considered

a) b/h = 1/4, c/b = .4, b/t = 20

b) b/h = 1/2, c/b = .5, b/t = 20

In these figures the cases of diaphragm braced lipped channel and Z-section purlins with hinged ends under uniformly distributed uplift and gravity loads are covered. In the uplift case of channels two sets of curves are shown. The full-line curves in Figures 39 through 41 and Figures 51 through 53 are for loads applied at midflange while the dotted line curves are for loads acting in the plane of the web. On the other

hand, for Z-sections, curves are given only for the case of loading in the plane of web. Since for Z-sections the capacity increases when the load application point is moved towards mid-flange, the given curves constitute a conservative representation of practical cases.

The plots consist of several segments, each indicating the start of yielding at a particular corner as designated in the figures. The segment designated by $\phi = 30°$ which appears in some plots indicates that the failure criterion is changed from yielding to the arbitrarily set limiting value of 30° for the angle of rotation at mid-span. As a consequence of the large twist angle, the yield load parameter M/M_{bend} decreases rapidly along this segment. (For example see Figure 34a). This limit has been introduced for two reasons: First, when the angle of rotation becomes excessively large the theory used in the present study is not accurate. The second reason concerns the computational difficulties. The iterational scheme used for the determination of the yield load occasionally converged to a wrong value when the angle of rotation was too large. This is not surprising, since the largeness of ϕ may indicate that the yield load is quite near the value of the critical load (instability).

The critical load is the smallest positive or negative root of the main determinant of the equation system given by the Eqs. 2.17a and b. (The positive root is for gravity and the negative is for uplift loading case). It is well known that in the inhomogeneous problem, the deformations and the

stresses grow without bounds as the load approaches the critical value. Of course, yielding occurs before reaching this value. The region beyond the critical load has no physical meaning, but it is mathematically defined. Thus, occasionally, during the iterational process for the determination of the yield load, convergence to a value in this region beyond the critical load value occurred.

3.4.2 Yield load parameter M/M_{bend}

In Figures 33 through 44, the yield load parameter M/M_{bend} versus F is plotted for the parameters mentioned above.

In the beginning of this chapter, it was stated that the effectiveness of a diaphragm depends on the lateral deflection tendency of the upper flange of the beam and the rotational tendency of the cross-section. These tendencies depend primarily on the stiffnesses of the beam and the direction of loading, i.e., whether it is uplift or downward. The effect of the direction of loading was discussed earlier. In the following, the effect of beam stiffness will be discussed, in two stages.

The length parameter L/h

As L/h increases, the warping rigidity and the lateral stiffness of the beam decrease with the square of L, while the Saint Venant rigidity remains constant. Also, the shear rigidity Q and the rotational restraint F remain the same. Hence, as the beam with increasing span becomes weaker in torsion and lateral bending, the diaphragm can restrain the rotation and the lateral displacement of the beam more effectively. Consequently, for longer spans the yield load parameter

M/M_{bend} approaches the asymptotic value at smaller values of F and Q.

Cross-sectional dimensions

Figures 33 through 44 are given for two channels of cross-sectional dimensions as given below.

Section (a)	Section (b)	
h = 6"	h = 6"	
b = 1.5"	b = 3"	Ratio of $\frac{I \text{ of (b)}}{I \text{ of (a)}}$
c = .6"	c = 1.5"	
t = .075"	t = .150"	
I_x = 3.78 in^4	I_x = 11.98 in^4	3.15
I_y = .216 in^4	I_y = 3.038 in^4	14.10
C_w = 1.581 in^6	C_w = 32.878 in^6	20.80
a = .629 in	a = 1.67	2.66

The first one designated as (a) is much weaker than the one designated as (b). While the bending stiffness in the strong direction increases 3.15 times, the lateral and warping stiffness increases 14.10 and 20.80 times respectively. The horizontal distance of the load from shear center increases only 2.66 times.

The stronger section (b) has, of course, a larger yield load capacity than section (a). However, if one compares their respective M/M_{bend} ratios it can be observed that (a) has larger values if Q and/or F do not get too small. (If the beam is unbraced, the stronger section has a more favorable M/M_{bend} ratio).

3.4.3 Angle of Rotation

In Figs. 45 through 56, the angle of rotation ϕ at midspan versus F is plotted at failure loads for the parameters mentioned in Sec. 3.4.1. As can be observed, ϕ is reduced by increasing F in every case. This reduction is more significant for cases with larger rotational tendency. Hence, the torsionally weaker section (a) is influenced more favorably than section (b) by the same amount of increase in F. Also the cases with larger span lengths are more affected by F.

F strengthens the purlin only torsionally; Q, however, reduces the lateral deflections as well as torsional rotations. Hence, the effect of Q on ϕ is more complex.

For channels under gravity loads, increase in Q reduces ϕ. For channels under uplift loading, Q has no appreciable influence.

For Z-sections under gravity loads the angle of rotation is positive for Q=0 and negative for $Q=\infty$. The angle of rotation changes sign near $Q=Q_L$, that is, for $Q=Q_L$, ϕ almost vanishes. This is also discussed in Sec. 4.5.2. For Z-sections under uplift loads, ϕ is computed assuming the load in the plane of the web. The actual values of ϕ should be much smaller since the load really acts through the screws which are placed inside the flange. In this case the primary torsion is in the opposite direction of the torsion which is caused by the lateral bracing forces. For the case where the loads are assumed in the plane of the web, one observes on Fig. 54a as well as on Figs. 54b through 56b that ϕ increases with increasing Q. On the other hand for the relatively weaker purlins ϕ decreases with increasing Q as can be seen on Figs. 55a and 56a.

CHAPTER IV

DESIGN CONSIDERATIONS

4.1 General

Design procedures for diaphragm braced channel and Z-section beams are presented. The prime objectives of the procedures are to find the shear rigidity of an efficient diaphragm for a given beam and carrying capacity as measured by the yield moment of that beam. Maximum deflections are also to be determined. Two possibilities are developed for the designer: One possibility is to use simple and conservative design formulas. The other is to make use of the prepared computer program. Both methods will be described and discussed below.

In some applications, the lower flange of the purlin, which is not connected to a diaphragm, is braced at discrete points. The additional effect of such discrete bracing is also included in this chapter.

4.2 Computer Program as Design Tool

The program is based on the series solution of the differential equations of equilibrium. Though it written to consider any number of terms, three terms are found to give sufficiently accurate results for practical problems. Included in the program are the two parameters: the shear rigidity Q and the rotational

restraint F. These may have any positive value or be zero. In addition to Q and F, the cross sectional dimensions, the span length, and the yield stress of the purlin are given as input.

The program calculates the yield moment of uniformly loaded, simple span,diaphragm braced channel or Z-section purlins. It further calculates the deflection u and the angle of rotation ϕ under yield and working (service) loads. A flow chart of the computer program is given in Appendix E.

4.3 Derivation of Approximate Formulas

In the previous section, the computer program was mentioned as a possible design tool. As an alternative design tool, the following closed form formulas will be derived using only one term of the series solution.

4.3.1 Analytical Procedure

For identical boundary conditions of u and ϕ, one has

$$\begin{aligned} u &= u_1 f_1 \qquad \text{and} \qquad & u'' &= u_1 f_1'' \\ \phi &= \phi_1 f_1 & \phi'' &= \phi_1 f_1'' \end{aligned} \tag{4.1}$$

where u is the lateral deflection and ϕ is the angle of rotation. Primes indicate derivation with respect to the dimensionless length parameter $\zeta = z/L$. For hinged ends, $f_1 = \sin \pi\zeta$.

The amplitudes u_1 and ϕ_1 are found from the following equation system:

$$\begin{bmatrix} P_Y' + Q & Qe - MW_1 \\ Qe - MW_1 & r_o^2 P_\phi + K_{33}' FL^2 + Qe^2 - MeW_2 \end{bmatrix} \begin{Bmatrix} u_1 \\ \phi_1 \end{Bmatrix} = \begin{Bmatrix} -I_{xy}/I_x \\ a \end{Bmatrix} MW_3 \tag{4.2}$$

with

$$M = \frac{pL^2}{\kappa} \tag{4.3a}$$

where κ is the appropriate constant for determining the maximum bending moment in the beam ($\kappa = 8$ for hinged boundary conditions). M is defined positive for downward and negative for uplift loads.

$$P_Y' = P_Y \left(1 - \frac{I_{xy}^2}{I_x I_y}\right) \tag{4.3b}$$

where P_Y is the Euler buckling load

$$P_Y = K_{11} \frac{\pi^2 E I_y}{L^2} \tag{4.3c}$$

and

$$P_\phi = \frac{1}{r_o^2} \left(K_{33} \frac{\pi^2 E C_w}{L^2} + GK\right) \tag{4.3d}$$

where

$$r_o^2 = \frac{I_o}{A} \tag{4.3e}$$

(which is introduced to make the dimension of P_ϕ a force) and

$$K_{11} = K_{33} = \frac{\lambda_1^4 \int_0^1 f^2 d\zeta}{\pi^2 - \int_0^1 f f'' d\zeta} \tag{4.4a}$$

$$K_{33}' = \frac{\int_0^1 f^2 d\zeta}{-\int_0^1 f f'' d\zeta} \tag{4.4b}$$

$$W_1 = \frac{\kappa \int_0^1 f f'' h \, d\zeta}{\int_0^1 f f'' d\zeta} \tag{4.4c}$$

$$W_2 = \frac{\kappa \int_0^1 f^2 \, d\zeta}{-\int_0^1 f f'' \, d\zeta} \tag{4.4d}$$

$$W_3 = \frac{\kappa \int_0^1 f h \, d\zeta}{-\int_0^1 f f'' \, d\zeta} \tag{4.4e}$$

where h is a function of ζ indicating the bending moment distribution. For hinged boundary conditions, $h = \frac{1}{2}(\zeta - \zeta^2)$ so that $M = pL^2 h$. The constants K_{11}, K_{33}, K_{33}', W_1, W_2, W_3, and λ_1 are

given in Table 11.

The longitudinal stress σ is the sum of three components due to the curvatures associated with vertical displacement v, lateral displacement u, and the angle of rotation φ.

$$\sigma = (M + I_{xy} \frac{Eu''}{L^2}) \frac{y}{I_x} - \frac{Eu''}{L^2} x - \frac{E\phi''}{L^2} \omega \qquad (4.5a)$$

Substituting u" and φ" from Eq. 4.1 and modifying slightly, Eq. 5a becomes

$$\sigma = \frac{M}{I_x} y + \frac{E}{L^2} [(x - \frac{I_{xy}}{I_x} y)u_1 + \omega\phi_1](-f_1'') \qquad (4.5b)$$

For given values of M, Q, and F, u_1 and ϕ_1 can be determined using Eq. 4.2. Stresses are then computed, substituing these into Eq. 4.5b. For the cross-sections under consideration, the stress at any point is found using the pertinent values of x, y, and ω (the latter being the so-called warping displacement or sectorial area). The sign convention for x, y, and the formulas for ω for channel and Z-sections are given in Figure 6. As can be seen in this same figure, a number from 1-6 is assigned to each corner beginning with the lower lip of the section. These numbers are used as subscripts for the parameters x, y, ω, or σ to indicate for which corner the particular parameter is calculated.

4.3.2 Deformations

The solution of Eq. 4.2 in determinant form is

$$u_1 = \frac{D_1}{D} \qquad (4.6a)$$

$$\phi_1 = \frac{D_2}{D} \qquad (4.6b)$$

where

$$D_1 = MW_3 \{(\frac{I_{xy}}{I_x} eW_2 + aW_1)M - [\frac{I_{xy}}{I_x} (r_o^2 P_\phi + K'_{33} FL^2) + (\frac{I_{xy}}{I_x} e + a)Qe] \quad (4.7a)$$

$$D_2 = MW_3 \{- \frac{I_{xy}}{I_x} W_1 M + aP'_Y + (\frac{I_{xy}}{I_x} e + a)Q\} \quad (4.7b)$$

$$D = -W_1^2 M^2 + [-P'_Y eW_2 + (2W_1 - W_2)Qe]M + (r_o^2 P_\phi + K'_{33} FL^2)P'_Y + (r_o^2 P_\phi + K'_{33} FL^2 + P'_Y e^2)Q \quad (4.7c)$$

The expressions for D_1, D_2, and D are zero or first degree polynomials in F and Q. Note that in determinant D, terms with Q^2 cancel each other. On the other hand, they are second order polynomials in M. Hence

$$u_1 = \frac{(a_2 M + a_1)M}{c_2 M^2 + c_1 M + c_o} \quad (4.8a)$$

$$\phi_1 = \frac{(b_2 M + b_1)M}{c_2 M^2 + c_1 M + c_o} \quad (4.8b)$$

where

$$a_1 = -W_3 [\frac{I_{xy}}{I_x} (r_o^2 P_\phi + K'_{33} FL^2) + (\frac{I_{xy}}{I_x} e + a)Qe] \quad (4.9a)$$

$$a_2 = W_3 (\frac{I_{xy}}{I_x} eW_2 + aW_1) \quad (4.9b)$$

$$b_1 = W_3 [aP'_Y + (\frac{I_{xy}}{I_x} e + a)Q] \quad (4.9c)$$

$$b_2 = -W_3 \frac{I_{xy}}{I_x} W_1 \quad (4.9d)$$

$$c_o = (r_o^2 P_\phi + K'_{33} FL^2)P'_Y + (r_o^2 P_\phi + K'_{33} FL^2 + P'_Y e^2)Q \quad (4.9e)$$

$$c_1 = -P'_Y eW_2 + (2W_1 - W_2)Qe \quad (4.9f)$$

$$c_2 = -W_1^2 \tag{4.9g}$$

4.3.3 Failure Criterion

Failure is defined herein as the initiation of yielding at any point in the section, i.e., reaching plus or minus σ_{yd} at any point of the purlin. The yield condition at the corners of the governing cross-section may be represented as surfaces in the coordinate system consisting in Q, F, and M_{yd}. A possible case is sketched in Figure 57 where only the regions of the surface giving the lowest yield load are shown.

Although one is primarily interested in the initial yield load, the stress distribution in the cross-section is also of interest. This aids one to assess the reserve load capacity after the initiation of yielding. In Figure 58, the qualitative stress distribution in channel and Z-sections due to v, u, and ϕ are shown. In fact, the relative magnitudes of the component stresses are influenced by many factors: (1) x, y, and ω which are functions of cross-sectional dimensions only; and (2) M, u, and ϕ which depend on (a) boundary conditions and span length (concerning the purlin), (b) the shear rigidity Q and rotational restraint F (concerning the diaphragm), (c) horizontal distance a of load from the shear center, and the sign of the load which is positive for downward and negative for uplift cases (concerning the load). Since σ_v is a linear function of M whereas σ_u and σ_ϕ are not, the relative magnitudes of the component stresses are also influenced indirectly by the value of the yield stress (It can be noted that the amplitudes u_1 and ϕ_1 approach infinity as

the load approaches the critical load, indicating the nonlinear nature of the associated curvatures). Hence, for a high yield stress value, the true load may be closer to the critical load and the components σ_u and σ_ϕ may contribute larger amounts to the total stress when compared to the case with a low yield stress

Although the above discussion implies that the maximum stress may in general occur in any one of the corners of the cross-section, numerical computations for the hinged boundary conditions indicate that for most practical cases of diaphragm braced channel and Z-section purlins, yielding occurs at corner 3. This somewhat simplifies the reverse problem in which the bending moment M which causes incipient yielding is sought. Hence σ_3 may be set equal to $\pm\sigma_{yd}$ (plus sign for downward loading) as the first trial. The stresses at the other corners may be checked later to determine if yielding has been reached elsewhere in the section.

Calculation of the stress distribution in the cross-section has other advantages as well. If the maximum stress occurs at a sharp peak localized at one particular corner, it is justified to raise the maximum nominal failure stress above the stipulated yield stress because (a) the corners have higher yield stresses than the flat portions as a consequence of cold forming and (b) there may be favorable stress redistribution when the corners start yielding. For instance, the 15% increase now in the AISI Specifications would be applicable to such cases. The knowledge of compressive stress distribution may also be helpful in the consideration of local buckling. For example, concentration of high compressive stresses along a stiffened edge is more favorabl

with respect to buckling than concentration at an unstiffened edge.

4.4 Possible Design Parameters

The design criterion is the maximum stress reaching $\pm\sigma_{yd}$. The corner where incipient yielding occurs needs not be specified at the outset. The information that corner 3 governs for simply supported purlins braced by diaphragms will be utilized later to simplify more general equations. Substituting u_1 and ϕ_1 from Eqs. 4.8 into Eq. 4.5b, an expression for stresses is obtained.

$$\sigma = \frac{M}{I_x} y + \frac{E}{L^2}\left[(x - \frac{I_{xy}}{I_x} y)\frac{(a_2M + a_1)M}{c_2M^2 + c_1M + c_o} + \omega \frac{(b_2M + b_1)M}{c_2M^2 + c_1M + c_o}\right](-f_1'') \tag{4.10}$$

The constants a_i, b_i, and c_i are defined by Eqs. 4.9. Eq. 4.10 contains among others, M, Q, and F as parameters and may be arranged for one of them in terms of the others. Hence, there are three possibilities for a design procedure.

4.4.1 Yield Moment

The yield moment M is sought for given values of the diaphragm parameters, Q and F. This is straightforward, except that one obtains the following cubic equation in M.

$$\begin{aligned} c_2yM^3 + \; & c_1y - c_2\sigma I_x + P_x \frac{-f_1''}{\pi^2}\left[(x - \frac{I_{xy}}{I_x} y)a_2 + \omega b_2\right] M^2 \\ + \; & c_oy - c_1\sigma I_x + P_x \frac{-f_1''}{\pi^2}\left[(x - \frac{I_{xy}}{I_x} y)a_1 + \omega b_1\right] M \\ - \; & c_o\sigma I_x = 0 \end{aligned} \tag{4.11}$$

where

$$P_x = \frac{\pi^2 EI_x}{L^2} \tag{4.12}$$

Introducing the dimensionless yield load parameter

$$\rho = \frac{M}{M_{bend}} \varepsilon \tag{4.13a}$$

with

$$\begin{aligned} \varepsilon &= 1 \text{ for gravity loading} \\ \varepsilon &= -1 \text{ for uplift loading} \end{aligned} \tag{4.13b}$$

and

$$M_{bend} = \frac{\sigma_y I_x}{d} \tag{4.13c}$$

where d is equal to y_3, i.e. the y-coordinate of corner 3 as shown in Figure 6. Substituting the constants a_i, b_i, and c_i from Eqs. 4.9, Eq. 4.11 is transformed to a dimensionless form. Thus

$$\varepsilon\rho^3 + [\frac{W_1}{W_2}\nu_y + \eta\varepsilon + \nu_x\mu_1 - \frac{2W_1 - W_2}{W_1} q]\rho^2 + \varepsilon[-\nu_z\nu_y - \nu_y \frac{W_2}{W_1} \eta\varepsilon]\rho$$

$$+ \varepsilon[\nu_x(\nu_z\mu_3 + \nu_y\mu_4) - (\nu_y\nu_z - \frac{2W_1 - W_2}{W_1} \eta\varepsilon + \nu_x\mu_2)q]\rho$$

$$- [\nu_z\nu_y + (\nu_z + \nu_y)q]\eta\varepsilon = 0 \tag{4.14}$$

where

$$q = \frac{Qe}{W_1 M_{bend}} \tag{4.15}$$

$$\eta = \frac{\sigma}{\sigma_y} \varepsilon \frac{d}{y} \tag{4.16}$$

and

$$\nu_x = \frac{P_x e}{M_{bend}} (\frac{-f_1''}{\pi^2}) \frac{W_3}{W_1} \tag{4.17a}$$

$$\nu_y = \frac{P_y' e}{M_{bend}} \frac{1}{W_1} \tag{4.17b}$$

$$\nu_z = \frac{r_o^2 P_\phi + K'_{33} F L^2}{e M_{bend}} \frac{1}{W_1} \tag{4.17c}$$

$$\mu_1 = \left(\frac{a}{e} + \frac{I_{xy}}{I_x}\frac{W_2}{W_1}\right)\left(\frac{x}{y} - \frac{I_{xy}}{I_x}\right) - \frac{\omega}{ed}\frac{d}{y}\frac{I_{xy}}{I_x} \tag{4.17d}$$

$$\mu_2 = \left(\frac{a}{e} + \frac{I_{xy}}{I_x}\right)\left[\frac{\omega}{ed}\frac{d}{y} - \left(\frac{x}{y} - \frac{I_{xy}}{I_x}\right)\right] \tag{4.17e}$$

$$\mu_3 = \left(\frac{x}{y} - \frac{I_{xy}}{I_x}\right)\frac{I_{xy}}{I_x} \tag{4.17f}$$

$$\mu_4 = -\frac{\omega}{ed}\frac{a}{e}\frac{d}{y} \tag{4.17g}$$

However, by limiting the range of the shear rigidity Q to two specific values, one can obtain a quadratic equation involving M instead of the above cubic. The details of this procedure will be discussed later on. Thus, Q can be eliminated from the formula for M as a parameter. On the other hand, the rotational restraint F remains in the equation and may have any positive value or may be zero.

4.4.2 Shear Rigidity Q

For a given value of F and a prescribed value of M, the necessary shear rigidity Q may be computed and compared with the one provided. Such an expression for Q can be obtained by solving Eq. 4.14 for q, where q is a dimensionless parameter defined by Eq. 4.15 involving shear rigidity Q. This gives

$$Q = \frac{W_1}{2W_1 - W_2}\frac{W_1 M_{bend}}{e}\frac{a'_o + a'_1\rho + a'_2\rho^2 + a'_3\rho^3}{b'_o + b'_1\rho + b'_2\rho^2} \tag{4.18}$$

where

$$a'_o = -\nu_z \nu_y \eta\varepsilon \tag{4.19a}$$

$$a_1' = [-\nu_z\nu_y - \nu_y \frac{W_2}{W_1} \eta\varepsilon + \nu_x(\nu_z\mu_3 + \nu_y\mu_4)]\varepsilon \qquad (4.19b)$$

$$a_2' = \frac{W_2}{W_1} \nu_y + \eta\varepsilon + \nu_x\mu_1 \qquad (4.19c)$$

$$a_3' = \varepsilon \qquad (4.19d)$$

$$b_o' = \frac{W_1}{2W_1 - W_2} (\nu_z + \nu_y)\eta\varepsilon \qquad (4.19e)$$

$$b_1' = -\eta + \frac{W_1}{2W_1 - W_2} (\nu_z + \nu_y + \nu_x\mu_2)\varepsilon \qquad (4.19f)$$

$$b_2' = 1 \qquad (4.19g)$$

4.4.3 Rotational Restraint F

Alternatively, the rotational restraint F may be calculated for a given value of Q and prescribed value of M. To this end, Eq. 4.14 is solved first for ν_z.

$$\nu_z = \frac{a_o'' + a_1''\rho + a_2''\rho^2 + a_3''\rho^3}{b_o'' + b_1''\rho} \qquad (4.20)$$

where

$$a_o'' = -\nu_y q\eta\varepsilon \qquad (4.21a)$$

$$a_1'' = -\nu_y \frac{W_1}{W_2} + \nu_y\nu_x\mu_4\varepsilon - (\nu_y - \frac{2W_1 - W_2}{W_1} \eta\varepsilon + \nu_x\mu_2)q\varepsilon \qquad (4.21b)$$

$$a_2'' = \frac{W_1}{W_2} \nu_y + \eta\varepsilon + \nu_x\mu_1 - \frac{2W_1 - W_2}{W_1} q \qquad (4.21c)$$

$$a_3'' = \varepsilon \qquad (4.21d)$$

$$b_o'' = (\nu_y + q)\eta\varepsilon \tag{4.21e}$$

$$b_1'' = (\nu_y + q - \nu_x\mu_3)\varepsilon \tag{4.21f}$$

Substituting ν_z from Eq. 4.17c into Eq. 4.20, an expression for F is obtained.

$$F = \frac{W_1}{K_{33}'}\frac{eM_{bend}}{L^2}\frac{a_o'' + a_1''\rho + a_2''\rho^2 + a_3''\rho^3}{b_o'' + b_1''\rho} - \frac{r_o^2 P_\phi}{K_{33}' L^2} \tag{4.22}$$

In the second or third possibility, if the given value is less than the necessary one, either a more rigid diaphragm may be used or a different purlin may be tried. The disadvantage of these two design possibilities is the difficulty of carrying out accurate computations. As can be observed in Figure 57, for a range of values of Q and F up to infinity, the surface determining the yield moment M_{yd} becomes very flat. This means that one may obtain very different Q and F values when the prescribed M is changed very little. (Of course, if the prescribed value of M is larger than a certain value, the plane through the corresponding point on the M-axis may never cut the pertinent surface and the answers from the equation for Q or F will be wrong). Only for cases where M changes rapidly with Q and/or F may these equations be accurate. In general, this corresponds to a region consisting of small values of Q and F. It seems to be more economical to use a somewhat stronger diaphragm avoiding the steep region of M_{yd} surface. Thus, it is not practical to use the formula for Q or F in order to calculate their required values exactly so that M attains a prescribed value. However, it would be very practical to have simple, approximate formulas giving the lower limits for

Q and F (or a limit for the combination of the two) so that M safely attains a certain percentage of the bending capacity $M_{bend} = \sigma_{yd} I_x/d$.

4.5 Determination of Yield Moment

It was mentioned above that for two specific values of Q, the cubic equation (Eq. 4.11 or Eq. 4.14) can be reduced to a quadratic. These values of Q are (1) infinite, that is rigid bracing and (2) Q_L, which is a limiting shear rigidity as will be discussed subsequently.

4.5.1 Rigidly Braced Channel and Z-Sections

A rigid diaphragm prevents the lateral displacement of the upper flange. For this case, u can be expressed in terms of ϕ as

$$u = -e\phi$$

Considering one term of the series leads to

$$\phi_1 = \frac{(a + \frac{I_{xy}}{I_x} e)MW_5}{W_4(r_o^2 P_\phi + P'_Y e^2 + K'_{33} FL^2) + Me} \qquad (4.23a)$$

and

$$u_1 = -e\phi_1 \qquad (4.23b)$$

where

$$W_4 = \frac{1}{2W_1 - W_2} \qquad (4.24a)$$

$$W_5 = \frac{W_3}{2W_1 - W_2} \qquad (4.24b)$$

Substituting u_1 and ϕ_1 from Eqs. 4.23 into Eq. 4.5b

$$\sigma = \frac{M}{I_x} y + \frac{E}{L^2} [-(x - \frac{I_{xy}}{I_x} y)e + \omega](-f_1'') \frac{(a + \frac{I_{xy}}{I_x} e)MW_5}{W_4(r_o^2 P_\phi + P_Y' e^2 + K_{33}' FL^2) + Me} \quad (4.25a)$$

or in dimensionless form

$$\frac{\sigma}{\varepsilon\sigma_y} = \frac{M}{\varepsilon M_{bend}} \frac{y}{d} + \frac{P_x W_6}{M_{bend}} \frac{\omega'}{\varepsilon d} (\frac{a}{e} + \frac{I_{xy}}{I_x}) \frac{M/\varepsilon M_{bend}}{\frac{W_4(r_o^2 P_\phi + P_Y' e^2 + K_{33}' FL^2)}{eM_{bend}\varepsilon} + \frac{M\varepsilon}{M_{bend}}} \quad (4.25b)$$

where

$$\omega' = \omega - (x - \frac{I_{xy}}{I_x} y)e \quad (4.26)$$

and

$$W_6 = \frac{W_5(-f_1'')}{\pi^2} \quad (4.27)$$

Eq. 4.25b can be simplified by introducing the following positive and dimensionless parameters

$$\alpha = \frac{W_4(r_o^2 P_\phi + P_Y' e^2 + K_{33}' FL^2)}{eM_{bend}} \quad (4.28a)$$

$$\beta = W_6(\frac{a}{e} + \frac{I_{xy}}{I_x}) \frac{P_x \omega'}{M_{bend} d} \quad (4.28b)$$

Using these parameters and with ρ as defined in Eq. 4.13a, Eq. 4.25 b becomes

$$\frac{\sigma}{\varepsilon\sigma_y} = \rho \frac{y}{d} + \frac{\beta}{\varepsilon} \frac{\rho}{\rho + \alpha/\varepsilon} \quad (4.29)$$

Provided that $\rho \neq -\alpha/\varepsilon$, Eq. 4.29 can be rearranged to result in the following quadratic equation for the yield load parameter:

$$\rho^2 + \left(-\frac{\sigma}{\varepsilon\sigma_y}\frac{d}{y} + \frac{\alpha}{\varepsilon} + \frac{d}{y}\frac{\beta}{\varepsilon}\right)\rho - \frac{d}{y}\frac{\alpha}{\varepsilon}\frac{\sigma}{\varepsilon\sigma_y} = 0 \qquad (4.30)$$

Eq. 4.30 is general in the sense that one might assume incipient yielding at any corner and obtain the corresponding yield load by substituting the values of y and ω' of that corner and setting σ equal to plus or minus σ_{yd}. ε is +1 for gravity and -1 for uplift loading. Since ρ is defined only for positive values, negative or imaginary roots can be ignored. In the case of two positive roots, the smaller one is to be taken. If there is no positive root, this means that the stress will not reach the yiel stress level at that corner.

It would be a lengthy calculation if all the corner yield possibilities had to be checked individually. However, numerical computations indicate that for purlins of usual dimensions braced by diaphragms with reasonable shear rigidities, generally corner 3 governs for hinged boundary conditions. Hence substituting

$$\frac{d}{y_3} = 1 \text{ and } \sigma = \sigma_3 = \varepsilon\sigma_y$$

into Eq. 4.30 gives

$$\rho^2 + \left(-1 + \frac{\alpha}{\varepsilon} + \frac{\beta}{\varepsilon}\right) - \frac{\alpha}{\varepsilon} = 0 \qquad (4.31)$$

The positive root of this equation is

$$\rho = \frac{1}{2}\left[1 - \frac{\alpha}{\varepsilon} - \frac{\beta}{\varepsilon} + \varepsilon\sqrt{\left(1 - \frac{\alpha}{\varepsilon} - \frac{\beta}{\varepsilon}\right)^2 + 4\,\frac{\alpha}{\varepsilon}}\,\right] \qquad (4.32)$$

Or written separately for gravity loading

$$\rho_\infty = \frac{1}{2}\left[1 - \alpha - \beta + \sqrt{(1 - \alpha - \beta)^2 + 4\alpha}\,\right] \qquad (4.33)$$

and for uplift loading

$$\rho_\infty = \frac{1}{2}\left[1 + \alpha + \beta - \sqrt{(1 + \alpha + \beta)^2 - 4\alpha}\,\right] \qquad (4.34)$$

where the subscript ∞ indicates rigid bracing.

4.5.2 Limiting Shear Rigidity

For downward loading, it is also possible to obtain a quadratic equation for the yield load if the shear rigidity equals the so-called limiting shear rigidity Q_L. Q_L is so defined that for the range $Q_L \leq Q \leq \infty$, the increase in the yield load is comparatively small and does not increase significantly with increasing Q. On the other hand, for $Q < Q_L$, the yield load decreases rapidly with decreasing Q. Hence, in design, it would not be economical as far as the purlins are concerned to use shear rigidities less than Q_L.

Extensive computer calculations have shown that Q_L can be defined as that shear rigidity which makes the stresses at the two corners 3 and 4 simultaneously equal to σ_{yd} in absolute value. By the following qualitative considerations, it may be deduced when this is the case, i.e. when $\sigma_3 = -\sigma_4$.

The stress σ at any point consists of the sum of the three component stresses σ_v, σ_ϕ, and σ_u. For channel and Z-sections, σ_v is antisymmetrical with respect to the midpoint of the web; that is, $\sigma_{v,3} = -\sigma_{v,4}$. For channel sections, σ_ϕ is antisymmetrical and σ_u is symmetrical, while for Z-sections, the reverse is true. Hence, in order to have $\sigma_3 = -\sigma_4$, that stress component which is symmetrical must vanish, namely, for channels $\sigma_u = 0$ and for Z-sections $\sigma_\phi = 0$. Since these stresses are proportional

to the curvatures u" and ϕ" respectively, the corresponding curvature must also vanish.

In the series solution, u" and ϕ" consist of the summation of the terms $u_k f_k''$ and $\phi_k f_k''$, respectively. Hence, it is possible that for certain values of Q, certain combinations of u_k's and ϕ_k's will make u" and ϕ" zero, respectively. However, when only one term is considered, u" and ϕ" will vanish only if $u_1 = 0$ and $\phi_1 = 0$, respectively. Since $u = u_1 f_1$ and $\phi = \phi_1 f_1$, the respective deformation also vanishes for $Q = Q_L$. In summary, if one term of the series is considered and the shear rigidity is equal to the limiting shear rigidity Q_L, σ_3 will be equal to $-\sigma_4$ and at the same time for channels, the deformation u and for Z-sections, the deformation ϕ, will vanish.

The formula for Q_L will now be derived using these conditions. The amplitudes u_1 and ϕ_1 are given by Eq. 4.2. For channel sections $I_{xy} = 0$; therefore, an expression for u_1 can be obtained substituting $I_{xy} = 0$ into the first of Eqs. 4.2.

$$u_1 = - \frac{Qe - M_{yd}W_1}{P_Y + Q} \tag{4.35a}$$

where M_{yd} indicates the yield moment. On the other hand, for Z-sections, if a = 0, i.e. if the load acts in the plane of the web, the second of Eqs. 4.2 gives

$$\phi_1 = - \frac{Qe - M_{yd}W_1}{r_o^2 P_\phi + K'_{33} FL^2 + Qe^2 - MeW_2} \tag{4.35b}$$

Setting $u_1 = 0$ for channels and $\phi_1 = 0$ for Z-sections leads to an expression for Q_L as

$$Q_L = \frac{M_{yd}W_1}{e} \tag{4.36}$$

As seen from Eq. 4.36,which is valid for both channel and Z-sections, Q_L is proportional to the yield moment M_{yd} if only one term is considered. Since a negative shear rigidity has no physical meaning, Q_L is defined only for positive values of M_{yd}, i.e. for the gravity loading case. On the other hand, if more terms are taken, it may well be possible that for uplift loading, a positive Q_L may also be obtained. However, this would probably not lead to a simple expression for design purposes and is not considered here.

A conservative estimate for Q_L is obtained by substituting $M_{yd} = M_{bend}$ in Eq. 4.36

$$Q_{L,con} = \frac{M_{bend} W_1}{e} \tag{4.37}$$

4.5.3 Channel Section

Substituting $Q = Q_L$, where Q_L is as defined by Eq. 4.36, into Eq. 4.2, expressions for the amplitudes u_1 and ϕ_1 can be obtained

$$u_1 = 0 \tag{4.38a}$$

$$\phi_1 = \frac{aMW_3}{r_o^2 P_\phi + K'_{33} FL^2 + (W_1 - W_2)Me} \tag{4.38b}$$

Letting

$$W_7 = \frac{1}{W_1 - W_2} \tag{4.39a}$$

$$W_8 = \frac{W_3}{W_1 - W_2} \tag{4.39b}$$

which are tabulated in Table 11, Eq. 4.38b becomes

$$\phi_1 = \frac{aMW_8}{W_7(r_o^2 P_\phi + K'_{33} FL^2) + Me} \tag{4.40}$$

Substituting u_1 and ϕ_1 into Eq. 4.56, the expression for stress becomes:

$$\sigma = \frac{M}{I_x} y + \frac{E}{L^2} \omega \frac{aMW_8(-f_1'')}{W_7(r_o^2 P_\phi + K_{33}' FL^2) + Me} \tag{4.41}$$

Due to the definition of the limiting shear rigidity Q_L, simultaneous yielding at corners 3 and 4 occurs. Hence, considering the stress at corner 3

$$y = y_3 = d$$

$$\omega = \omega_3$$

and setting $\sigma_3 = \sigma_{yd}$ and $M = M_{yd}$

$$\sigma_{yd} = \frac{d}{I_x} \left[M_{yd} + P_x \frac{W_8(-f_1'')}{\pi^2} \frac{\omega_3}{d} \frac{a}{e} \frac{M_{yd}}{W_7(r_o^2 P_\phi + K_{33}' FL^2)/e + M_{yd}}\right]$$

or setting

$$W_9 = \frac{W_8(-f_1'')}{\pi^2} \tag{4.42}$$

the above equation can be written as

$$1 = \frac{M_{yd}}{M_{bend}} + \frac{P_x W_9}{M_{bend}} \frac{\omega_3}{d} \frac{a}{e} \frac{M_{yd}/M_{bend}}{W_7(r_o^2 P_\phi + K_{33}' FL^2)/eM_{bend} + M_{yd}/M_{bend}} \tag{4.43}$$

This equation can also be written in the form

$$1 = \rho + \delta_{ch} \frac{\rho}{\gamma_{ch} + \rho} \tag{4.44}$$

where

$$\gamma_{ch} = \frac{W_7(r_o^2 P_\phi + K_{33}' FL^2)}{eM_{bend}} \tag{4.45a}$$

$$\delta_{ch} = W_9 \frac{a}{e} \frac{P_x \omega_3}{M_{bend}^d} \tag{4.45b}$$

Since both γ_{ch} and ρ are positive, the denominator $\gamma_{ch} + \rho$ cannot be zero. Therefore, Eq. 4.44 may be transformed into a quadratic equation by multiplying both sides by the expression in the denominator.

$$\rho^2 - (1 - \gamma_{ch} - \delta_{ch})\rho - \gamma_{ch} = 0 \tag{4.46}$$

The positive root is

$$\rho_L = \frac{1}{2} \left[1 - \gamma_{ch} - \delta_{ch} + \sqrt{(1 - \gamma_{ch} - \delta_{ch})^2 + 4\,\gamma_{ch}}\right] \tag{4.47}$$

where the subscript L indicates that $Q = Q_L$. Once $M_{yd} = \rho_L M_{bend}$ is determined, Q_L can be found using Eq. 4.36.

4.5.4 Z-section

The derivation is similar to that of channel section. The following expressions can be obtained for the deformation components ϕ_1 and u_1.

$$\phi_1 = 0 \tag{4.48a}$$

$$u_1 = - \frac{I_{xy}}{I_x} \frac{MW_3}{P'_Y + MW_1/e} \tag{4.48b}$$

letting

$$W_{10} = \frac{1}{W_1} \tag{4.49a}$$

$$W_{11} = \frac{W_3}{W_1} \tag{4.49b}$$

the expression for deflection u_1 becomes

$$u_1 = - \frac{I_{xy}}{I_x} \frac{MW_{11}e}{W_{10}P'_Y e + M} \tag{4.50}$$

Substituting this expression for u_1 with $\phi_1 = 0$ as well as

$$x = x_3 = 0 \; ; \; y = y_3 = d$$

$$\sigma = \sigma_3 = \sigma_{yd} \; ; \; M_{yd} \text{ for } M$$

into Eq. 4.5b to obtain stress σ

$$\sigma_y = \frac{d}{I_x} \left[M + P_x e \frac{W_{11}(-f_1'')}{\pi^2} \left(\frac{I_{xy}}{I_x}\right)^2 \frac{M}{W_{10} P_Y' e + M} \right]$$

After some modifications and using the dimensionless parameters

$$\rho = \frac{M}{M_{bend}}$$

$$\gamma_z = \frac{W_{10} P_Y' e}{M_{bend}} \tag{4.51a}$$

$$\delta_z = \frac{W_{12} P_x e}{M_{bend}} \left(\frac{I_{xy}}{I_x}\right)^2 \tag{4.51b}$$

where

$$W_{12} = \frac{W_{11}(-f_1'')}{\pi^2} \tag{4.52}$$

one obtains

$$1 = \rho + \delta_z \frac{\rho}{\gamma_z + \rho} \tag{4.53}$$

This may be brought into a quadratic of the same form as Eq. 4.46. The positive root of this equation is

$$\rho_L = \frac{1}{2} \left[1 - \gamma_z - \delta_z + \sqrt{(1 - \gamma_z - \delta_z)^2 + 4\gamma_z} \right] \tag{4.53a}$$

where the subscript L indicates that $Q = Q_L$.

Again, once $M_{yd} = \rho_L M_{bend}$ is known, the limiting diaphragm rigidity Q_L can be found from Eq. 4.35.

4.6 Discussion of the Approaches

In the preceding sections, formulas for the yield moment M_{yd} of channel and Z-section purlins have been derived using one term of the series solution and assuming yielding at corner 3. In order to obtain a quadratic equation for M, the shear rigidity Q has been limited to two specific values, namely $Q = \infty$ or $Q = Q_L$.

The latter constitutes the lower limit for the useful shear rigidity of a given purlin. The rotational resistance F is included in the design procedure as a parameter. The exceptions are Z-sections under gravity loading with $Q = Q_L$ and $a = 0$, i.e. loaded in the web plane where the angle of rotation ϕ, happens to be zero, thus eliminating F from the formulas.

For gravity loading, two formulas giving the upper and lower limits of practical purlin capacity have been derived using $Q = \infty$ and $Q = Q_L$ respectively. However, to have matters simple, only the yield load based on Q_L is proposed for design use. This gives the lower limit for the desirable range $Q > Q_L$ and, at the same time, it is not too conservative when compared with the case of maximum value of $Q = \infty$.

In the case of uplift loading, a simplified formula for the yield moment M_{yd} can be obtained when $Q = \infty$. It is safe to use this formula also for actual (i.e. finite) shear rigidities. The safety justifications of the given formula differ for channel and for Z-sections, as explained below.

The behavior of channel sections under uplift loads is such that the lateral deflection of the upper flange where the diaphragm is connected to the purlin is generally negligible.

Hence, the shear rigidity of the diaphragm cannot influence the yield load capacity of the purlin appreciably. In other words, a plot of yield load versus Q is almost horizontal. Thus, the formula for $Q = \infty$ is safe to use also for cases where Q is finite but reasonable, e.g. $Q \geq Q_L$.

For Z-sections, the shear rigidity does affect the yield load capacity. However, by a compensating conservative assumption concerning another parameter which also influences the yield load, one may obtain a safe formula. This parameter is a, that is,the lateral distance between the point of load application and the shear center. Uplift loading is transmitted through the screws which are located near the mid-portion of the flange. However, since the yield load capacity is smaller if the loading is applied at the corners rather than near mid-flange, a conservative estimate of the yield load is obtained by assuming $a = 0$. This is justified also, because the exact locations of the screws are never known in practice. Incidently, this also simplifies the formulas for Z-sections. It should be noted that for channel sections, a cannot be assumed zero, because this would mean applying the load at the shear center.

The lower practical limit for the shear rigidity is Q_L for gravity loading. For design computations, it is proposed to use the conservative value $Q_L = W_1 M_{bend}/e$ for uplift as well as for gravity loading (see Eq. 4.37)). This is justified not only because of simplicity, but also because the same roof generally must be able to resist both gravity and uplift loading.

4.7 Discrete Bracing in Addition to the Diaphragm

4.7.1 General

The behavior of channels with discrete bracing is studied and reported in Ref. 37. Similar studies for Z-sections are in Ref. 42. Diaphragm bracing was not included in those investigations. In the following, an approximate analysis will be developed for diaphragm braced channel and Z-section purlins which are additionally braced at discrete locations between supports.

4.7.2 Theory

In the case of additional discrete bracing, the rotation and lateral deflection of the purlin is small. The differential equations can, therefore, be simplified by neglecting the terms which couple the deflection u and rotation ϕ.

When discrete bracing is used, the beam is divided into smaller sections which have zero rotation at each end. This reduces the effect of the term GK due to Saint Venant torsion and F due to rotational restraint supplied by the diaphragm. Thus, these terms are neglected in the differential equation which, incidentally, is conservative.

The shear rigidity of the diaphragm is assumed to be infinite. With the simplifications discussed above, Eq. 2.14 takes the form of

$$\frac{EC'_w}{L^2}\,\phi^{IV} = p_y L^2\left(a + \frac{I_{xy}}{I_x}\,e\right) \qquad (4.54)$$

Eq. 4.54 can also be written in the form

$$EC'_w\,\frac{d^4\phi}{dz^4} = p_y\left(a + \frac{I_{xy}}{I_x}\,e\right) \qquad (4.55)$$

This is analogous to the usual beam differential equation of bending where

ϕ corresponds to v

C_w' corresponds to I_x

Integrating Eq. 4.55

$$EC_w' \frac{d^3\phi}{dz^3} = p_y(a + \frac{I_{xy}}{I_x} e)dz \qquad (4.56a)$$

$$EC_w' \frac{d^2\phi}{dz^2} = p_y(a + \frac{I_{xy}}{I_x} e)dzdz \qquad (4.56b)$$

The right hand side of Eq. 4.56a is equal to the torsional moment while the right hand side of Eq. 4.56b is equal to the simplified bimoment B_s

$$M_t = -\int p_y(a + \frac{I_{xy}}{I_x} e)dz \qquad (4.57a)$$

$$B_s = -\iint p_y(a + \frac{I_{xy}}{I_x} e)dzdz \qquad (4.57b)$$

Extending the previous analogy

B_s corresponds to M

M_t corresponds to V

$p_y(a + \frac{I_{xy}}{I_x} e)$ corresponds to p_y

Formulas and tables for the bending moment M and shear force V may also be used for the determination of B_s and M_t as described in the following section.

4.7.3 The Yield Moment

The stress is

$$\sigma = \frac{M}{I_x} y + \frac{B_s}{C_w'} \omega' \qquad (4.58)$$

From the correspondence between B_s and bending moment M, B_s can be calculated. For example, in the case of single midspan discrete bracing, the analogous system for bending moment is a two span continuous beam for which the support moment is

$$M = -\frac{1}{8} p_y L_1^2$$

$$L_1 = \frac{L}{2}$$

Therefore,

$$B_s = -\frac{1}{8} p_y (a + \frac{I_{xy}}{I_x})(\frac{L}{2})^2$$

$$B_s = -\frac{1}{4} (\frac{p_y L^2}{8})(a + \frac{I_{xy}}{I_x}) \qquad (4.59)$$

or in general

$$B_s = (W_B)\ M\ (a + \frac{I_{xy}}{I_x}\ e) \qquad (4.60)$$

where $M = \frac{p_y L^2}{8}$ and W_B is constant depending on the number of braces (Table 12). Hence

$$\sigma = \frac{M}{I_x}\ y + \frac{(W_B)\ M\ (a + \frac{I_{xy}}{I_x}\ e)\omega'}{C'_w} \qquad (4.61)$$

After substituting σ_{yd} for σ and M_{yd} for M, Eq. 4.61 can be solved for M_{yd}

$$M_{yd} = \frac{\sigma_{yd}}{\frac{y}{I_x} + \frac{W_B}{C'_w}\ (a + \frac{I_{xy}}{I_x}\ e)(-\omega')} \qquad (4.62)$$

Or with

$$\rho = \frac{1}{1 + (W_B)\ \frac{I_x}{C'_w}\ (a + \frac{I_{xy}}{I_x}\ e)(\frac{-\omega'}{y})} \qquad (4.63)$$

The yield moment is

$$M_{yd} = \rho M_{bend} \tag{4.64}$$

When diaphragm bracing alone was considered, it was pointed out that yielding usually occurs at corner 3 at midspan (Fig. 6). This may not be true in the case of additional discrete bracing. One should find the corner for which the absolute value of ρ is the smallest. By substituting the values of ω' and y for each corner, the proper sign of the terms should be used as indicated on Fig. 6. It should also be noted that I_{xy} has a sign.

In the denominator of Eq. 4.63, the term which is added to 1.0 is the ratio of the stress due to warping to the stress due to bending. When bending stress dominates, this term has a positive sign and a value less than unity for the governing corner. This corner is most likely corner 1 or 2.

4.8 Proposed Design Procedure

4.8.1 Diaphragm Braced Channel and Z-section Beams

a) Use either the explicit computer program, which gives the yield moment for any values of the diaphragm rigidity parameters Q and F, or

b) use the simplified and conservative formulas given below, or

c) use an even further simplified procedure if diaphragm shear rigidity Q and rotational restraint F are larger than set limits.

Formulas for Design for Alternative b above:

$$\text{Minimum shear rigidity for all cases} \quad Q_L = \frac{W_1 M_{bend}}{d} \tag{4.65}$$

where

$$M_{bend} = \frac{\sigma_{yd} I_x}{d} \tag{4.66}$$

If the maximum stress is restricted to a particular corner in a localized manner, then raising the nominal failure stress above the stipulated yield stress, such as the 15% increase in the AISI Specification, is justified.

1. Uplift Loading

a) Channel Section

$$\text{Yield Moment } M_{yd} = -\rho M_{bend} \tag{4.67}$$

with

$$\rho = \frac{1}{2}\{(1+\alpha_{ch}+\beta_{ch}) - \sqrt{(1+\alpha_{ch}+\beta_{ch})^2 - 4\alpha_{ch}}\} \tag{4.68}$$

where

$$\alpha_{ch} = \frac{W_4(r_o^2 P_\phi + P_Y e^2 + K'_{33} F L^2)}{e M_{bend}} \tag{4.69a}$$

$$\beta_{ch} = W_6 \frac{a}{e} \frac{P_x \omega'}{e M_{bend} d} \tag{4.69b}$$

Angle of Rotation

$$\phi_{ch} = \frac{M/M_{bend}}{\alpha_{ch} - M/M_{bend}} W_5 \frac{a}{e} \tag{4.70}$$

b) Z-Section

$$\text{Yield Moment } M_{yd} = -\rho M_{bend} \tag{4.71}$$

with

$$\rho = \frac{1}{2}\{(1+\alpha_z+\beta_z) - \sqrt{(1+\alpha_z+\beta_z)^2 - 4\alpha_z}\} \tag{4.72}$$

where

$$\alpha_z = \frac{W_4(r_o^2 P_\phi + P_Y' e^2 + K_{33}' FL^2)}{eM_{bend}} \tag{4.73a}$$

$$\beta_z = W_6 \frac{I_{xy}}{I_x} \frac{P_x \omega'}{eM_{bend} d} \tag{4.73b}$$

Angle of rotation

$$\phi_z$$

small, no need to compute

2. Gravity Loading

a) Channel Section

$$\text{Yield Moment } M_{yd} = \rho M_{bend} \tag{4.74}$$

with

$$\rho = \frac{1}{2}\{(1-\gamma_{ch}-\delta_{ch}) + \sqrt{(1-\gamma_{ch}-\delta_{ch})^2 + 4\gamma_{ch}}\} \tag{4.75}$$

where

$$\gamma_{ch} = \frac{W_7(r_o^2 P_\phi + K_{33}' FL^2)}{eM_{bend}} \tag{4.76a}$$

$$\delta_{ch} = W_9 \frac{a}{e} \frac{P_x \omega}{M_{bend} d} \tag{4.76b}$$

Angle of rotation

$$\phi_{ch} = \frac{M/M_{bend}}{\gamma_{ch} + M/M_{bend}} W_8 \frac{a}{e} \tag{4.77}$$

b) Z-Section

$$\text{Yield Moment } M_{yd} = \rho M_{bend} \tag{4.78}$$

with

$$\rho = \frac{1}{2}\{(1-\gamma_z-\delta_z) + \sqrt{(1-\gamma_z-\delta_z)^2 + 4\gamma_z}\} \quad (4.79)$$

where

$$\gamma_z = \frac{W_{10}P'_Y e}{M_{bend}} \quad (4.80a)$$

$$\delta_z = W_{12}\left(\frac{I_{xy}}{I_x}\right)^2 \frac{P_x e}{M_{bend}} \quad (4.80b)$$

Angle of rotation

$$\phi_z$$

small, no need to compute

4.8.2 Diaphragm Braced Channel and Z-Section Beams with Additional Discrete Bracing

Uplift and Gravity Loading

$$\text{Yield Moment } M_{yd} = \pm\rho M_{bend} \quad (4.81)$$

with

$$\rho = \frac{1}{1 + W_B \frac{I_x}{C'_w}\left(a + \frac{I_{xy}}{I_x} e\right)\left(-\frac{\omega'}{y}\right)} \quad (4.82)$$

Note: Find the corner for which the ratio $-\frac{\omega'}{y}$ is the largest. The most likely corners are 1 or 2.

Angle of rotation

$$\phi$$

small, no need to compute

4.8.3 Nomenclature for Design Procedure

a = Positive number showing the horizontal distance between the uniformly distributed line loading and shear center (Fig. 10).

C_w = Warping constant, defined by Eq. A.28

C_w' = Modified warping constant for rigid bracing case, defined by Eq. 2.15

d = y_3, i.e. distance of the outer fiber at corner 3 from the x-axis

e = Positive number showing the vertical distance between the shear center and the diaphragm (also between shear center and the uniformly distributed loads transmitted by the diaphragm).

F = Rotational restraint provided by the diaphragm bracing.

I_o, I_x, I_y, I_{xy} = Moment of inertia.

K_{33}' = Constant defined by Eq. 4.4b (see Table 11).

M = Bending moment

M_{bend} = The bending capacity of a beam which is guided or braced such that the only possible deformation is bending in the plane of the load with no rotation or lateral deflection, defined by Eq. 4.13c

M_{yd} = Bending moment causing start of yielding.

P_x = Euler buckling load, defined by Eq. 4.12.

P_y = Euler buckling load defined by Eq. 4.3c.

P_ϕ = Defined by Eq. 4.3d.

Q = The shear rigidity of the diaphragm bracing.

Q_L = Limiting shear rigidity, defined at section 4.8.2

r_o^2 = Defined by Eq. 4.3e

W_i (where i = 1,12) = Constants concerning boundary conditions (see Table VI).

W_B = A constant concerned with the bimoment at midspan when there are one or several discrete braces in addition to diaphragm bracing (see Table VII).

x,y = Coordinates of a point.

α_{ch},β_{ch} = Parameters for channel uplift case.

α_z,β_z = Parameters for Z-section uplift case.

γ_{ch},δ_{ch} = Parameters for channel gravity case.

γ_z,δ_z = Parameters for Z-section gravity case.

ρ = dimensionless yield load parameter.

σ_{yd} = Yield stress.

ϕ = Angle of rotation

ϕ_{ch} = Angle of rotation at midspan for channel sections.

ϕ_z = Angle of rotation at midspan for Z-sections.

ω = Warping displacement or sectorial area (see Fig. 6).

ω' = Modified ω for rigid bracing case

CHAPTER V

EXPERIMENTAL PROGRAM

5.1 General

In previous chapters, an elastic theory of diaphragm braced beams under combined torsion and bending has been presented. During its development, several assumptions and simplifications were made. To check the theory and to obtain some information on the behavior of diaphragm braced beams, a number of tests were performed.

The experimental program consisted of two parts:

1) Model tests

2) Full-scale tests.

In the following, the test set-up and the results will be presented for both the model and full-scale tests.

5.2 Model Tests

5.2.1 General

Tests were performed to study the effect of the bracing on channel and Z-section beams under gravity and uplift load conditions. The term "model test" here does not refer to the usual scaling down of the geometrical configuration. These tests were not intended to replace the full-scale tests nor to be a preliminary study for them. The prime objective was to check the theo-

retical results for the two limiting cases of the diaphragm shear rigidity, that is, zero ($Q = 0$) or infinite ($Q = \infty$). An unbraced beam is represented by $Q = 0$ (Fig. 59).

The case $Q = \infty$ is simulated in (Fig. 60) the model test by bracing either the upper or the lower flanges of two beams laterally against each other (Figs. 60 through 64). The braces were placed at four discrete locations (Fig. 60). Though the beams were intended to have the same properties, they were not identical because of fabrication inaccuracies. Therefore, due to these inaccuracies, the braced flange of the beam, which is supposed to be fully restrained laterally, would deflect sideways when this flange is in compression as in the case of gravity loading. Such a deflection was prevented by means of some additional external bracing (Figs. 62 through 64). On the other hand, in the tests where the braced flange was in tension, as in the case of uplift, no additional bracing was necessary.

5.2.2 Test Specimens

The virgin material for the specimen was hot rolled steel sheets with a sharp yielding $\sigma - \varepsilon$ diagram. The sheets were bent into channel or Z-shapes by cold forming. Several tension coupons out of the virgin material were machined to the 3" standard size. The yield stress values for the model test beams are given in Table 13.

5.2.3 Test Set-up

Four channel and four Z-section beams, each representing a different bracing and loading condition, were tested. All speci-

mens were simply supported.

Loading cases and test numbering as referred to in Figs. 15a through 15f are shown below:

Test #1: Channel, unbraced, uplift loading

Test #2: Z-section, unbraced, uplift loading

Test #3: Channel, rigid bracing, uplift loading

Test #4: Z-section, rigid bracing, uplift loading

Test #5: Channel, rigid bracing, gravity loading

Test #6: Z-section, rigid bracing, gravity loading

Test #7: Channel, rigid bracing, gravity loading

(a) one discrete brace at midspan, loaded within elastic range

(b) 5 discrete braces, loaded until failure

Test #8: Z-beam, rigid bracing, downward load

(a) 5 discrete braces, loaded within elastic ranges

(b) one discrete brace at midspan, loaded until failure

5.2.4 Results and Discussion

The horizontal and vertical displacements at midspan were measured by dial gages. From them, the angle of rotation ϕ and the shear center deflections $\bar{u}$ and $\bar{v}$ were computed. Here $\bar{u}$ and $\bar{v}$ indicate deflections in the direction of the coordinates ξ and η of the deflected section. These values agree well with the theoretical values u and v. Figs. 66 through 71 show the comparison of test and theory. The test values for ϕ are in general somewhat less than the predicted values.

The behavior of channel beams under uplift loading was dis-

cussed in Chapter 3. It was mentioned that the points where the diaphragm bracing is attached to the beam have a tendency to move first in one direction, and then come back to zero and begin to move in the other direction, under increasing loads. This was actually observed in Test #1 and is shown in Fig. 66.

The strains have been measured at four to six locations at midspan by Type A-12 SR-4 strain gages (Gage locations can be seen on Figs. 72 and 73). At the flange tips, gages also have been placed on the inside in order to detect any local buckling or bending during the loading. The sections were dimensioned not to buckle locally in the elastic range and they did not. Fig. 74 shows the predicted and measured strains at locations 2 and 3. The agreement is quite satisfactory in the elastic range where the theory is valid.

The inelastic behavior for the uplift and downward loading cases was quite different. In the former, the stress distribution is such that there is tension everywhere except at the corner of the web and "compression" flange. Hence, no local buckling was possible and failure occurred by yielding. The beams under downward loading failed due to a combination of yielding at the tension flange and plastic local buckling of the compression flange.

The experimental strain and stress distribution at failure on the midspan cross-section for tests #1 and #2 are shown on Figs. 72 and 73, respectively. For tests #1 through #4 (uplift loading), one observes that a plastic hinge was forming at the compression flange. On the other hand, for tests #5 through #8 (downward loading), the stresses at the flanges were fairly uniform on the

flat portions; at the corners, the strains were usually large enough to develop the increased yield strength due to cold forming. A partial plastification of the web is also observed.

In Table X, the experimental failure loads in Column (1) are compared with the following computed ones:

a) Column (2): Incipient yield loads

b) Column (3): Load when 15% overstressing is allowed for Tests #5 through #8 only

c) Column (4): Yield load assuming the beam to be braced such that only vertical bending is possible, i.e. M_{bend}

d) Column (5): The load of column (4) plus the additional capacity due to increased corner strength

e) Column (6): The load computed from the experimental stress distribution at failure (which includes the effects of cold forming and partial plastification of the web).

It is seen that the experimental failure loads for Tests #1 through #4 (uplift loads) are closely predicted by criterion (a) or (b). This may be explained as follows: In the uplift cases, there is considerable angle of rotation in the elastic range. Hence, the strains are highly nonlinear, especially at the tip of the compression flange. A small addition to the load causes large strains. Therefore, the ultimate load capacity was not much higher than the incipient yield load. On the other hand, the beams in the downward load case (Tests #5 and #6) displayed comparatively small rotations and the strains were almost linear for increasing loads. These beams have shown large reserve strength

beyond the predicted values of criterion (a) or (b), as indicated in Table 15. Hence, although the theory is valid only in the elastic range, the nonlinearity in the strain-load relationship may indicate whether or not there is reserve strength in the beam. However, it is felt that this conclusion cannot be generalized. In beams with other dimensions and material properties, local buckling may occur at loads not too much above the incipient yield load.

Tests #7 and #8 had discrete braces on the tension flange in addition to the simulated rigid bracing on the compression flange. The bracing arrangements for these tests are shown on Figs. 63 and 64. The brace at midspan was the most effective, reducing the angle of rotation of the beam almost to zero (Fig. 65). Additional braces were then not of much value for the test beams since the displacements were probably of the order of the play present in the braces (No figures are given in series 16 for the deflection of these tests since they are very small, i.e. $\phi << 1^{o}$).

For test beams #7a and #8b with a discrete brace at midspan, the incipient yield loads turn out to be somewhat smaller than that of a beam without that brace. Since the brace at midspan changes the sign of bimoment and the corresponding warping stresses at the brace location, the maximum stress occurs at the open side of the tension flange instead of the corner, and incipient yielding occurs at a lower load. However, local plastification wipes out this effect and the failure load is of about the same magnitude as for the beam without the discrete brace (Compare the experimental failure loads of Tests #6 to #8b).

Tests #7b and #8b suggest that the main advantage of discrete bracing for downward loading is not that it may increase the strength of the diaphragm-braced channel and Z-beam, but rather that the angle of rotation is greatly reduced. For the uplift loading case also, the angle of rotation will be reduced by discrete braces (which would now support the compression flange at one or more points). But when ϕ is small, the torsional load due to $\pm p(e\phi)$ may be insignificant and therefore the difference between the capacities corresponding to uplift or downward loading cases diminishes. Hence, discrete bracing may increase the capacity of diaphragm-braced channels and Z-beams for the uplift loading case.

5.3 Full-Scale Tests

5.3.1 General

Full-scale tests were performed to study the behavior of diaphragm-braced channel and Z-section purlins. Since the theory was checked for some limiting values of the parameters Q and F in the model tests, the main purpose of the full-scale tests was to duplicate the conditions in practice and find out the problems associated with practical applications.

5.3.2 Specimens

The first specimen was used to develop and improve the test set-up. Subsequently, there were three channel and two Z-beam tests. Each specimen consisted of two purlins, 4' apart (Fig. 78 braced on one flange by a narrow-rib light gage steel diaphragm of 26 gage material with 24" cover width, as shown in Fig. 79.

The panels were connected to the purlins by self-tapping screws at every valley, resulting in a screw spacing of 8". This provided a diaphragm shear rigidity of Q = 50 kips as determined experimentally by the standard procedure given in Refs. 22 and 23.

Rotational restraint F was determined by the test procedure described in Appendix D. The values of F ranged from .060 to .180 in-k/in/rad depending on the position of the screws with respect to the web. As it was discussed in Section 3.3 in some detail, the value of F is very sensitive to the position of the screws. Since in the purlin test specimens, the screws were placed from the top of the deck panels, as it is the case in practice, the position of the screws varied considerably, apparently resulting in different rotational restraints in different test assemblies. Usually effectively different values of F are obtained, even for the beams A and B of the same assembly. Therefore, for comparison, on the plots for test results, analytical computations are given for a range of values of the rotational restraint F, between zero and .180 in-k/in/rad.

The specimens were simply supported. X-bracings were supplied at the supports to prevent any rotation of this cross-section. The web was stiffened by a $\frac{1}{4}$" plate at the supports to eliminate web crippling.

The mechanical properties of the steel used to manufacture the specimens were determined by tension coupon tests on the material of same heat. The coupons were machined to 3" gage lengths according to ASTM 370-65. The values of the yield stress for full-scale test beams are given in Table 14.

5.3.3 Test Set-up

The test set-ups for gravity and uplift loading cases are shown on Figures 80 and 81, respectively. The load was applied at four points on the beams through a wiffle tree. The weight of the wiffle tree was 800 lbs. The load was applied by a tension jack coupled to a gravity simulator which was developed at Lehigh University. As can be seen on Figure 82, this device consists of a mechanism which enables the unobstructed sideways translation of the load with the deflection of the beams. During this translation, no lateral resistance is created and the load remains almost vertical as long as the lateral displacement is not too large (say less than 3" for the device used in these tests). The magnitudes of the loads were measured by a calibrated tension bar.

In the case of uplift loading, the load is transmitted to the web by a rigid piece of channel section in order to avoid the distortion of the tension flange which would occur if the load were applied to the flange directly.

The tests are summarized below:

Test #F1: Channel, uplift, loaded until failure (span = 20 ft

Test #F2: Z-section, uplift, loaded in the elastic range (span = 16 ft. 8 in)

Test #F3: Z-section, uplift, one discrete brace at midspan, loaded until failure (span = 16 ft. 8 in)

Test #F4: Channel, gravity, one discrete brace at midspan, loaded in the elastic range (span = 20 ft)

Test #F5: Channel, gravity, loaded until failure (span = 20 ft)

As can be seen above, identical specimens were used for Tests #F2 and #F3 as well as for Tests #F4 and #F5, except for the midspan brace.

5.3.4 Results and Discussion

Full-scale tests were helpful in bringing out the significance of the rotational restraint of the diaphragm bracing. This is best demonstrated in Fig. 83 for Test #F1. While for F = 0 the angle of rotation at midspan would be 16° due to the mere weight of the wiffle tree, it was limited to 1° at the same load when the rotational restraint of F = .180 in-k/in/rad. was considered in the calculations. The latter agrees with the experiments.

Fig. 84 shows the angle of rotation for test #F2. In this test, the stresses were in the elastic range and the beam was unloaded at the load of 1700 lb/beam in order to be used in the subsequent test. Although the tests #F1 and #F2 are not directly comparable due to differences in the span length, wall thickness of the purlins and the rotational restraint F, their results support the conclusion that Z-beams generally display less rotation than channels. In test #F2, the angle of rotation ϕ for beams A and B are very close to each other and to the theoretical result for F = .060 ki/in/rad. The theoretical predictions corresponding to F = .180 ki/in/rad is also given on this Figure for comparison.

In addition to the diaphragm bracing, test #F3 had a discrete brace at midspan, providing zero angle of rotation. Furthermore, an additional external restraint was provided to secure

zero lateral displacement at midspan. The discrete bracing limited the angle of rotation to values less than 1.5^{o} elsewhere in the span (Fig. 85).

In test #F4, an assembly of 20 ft. long channel purlins with a discrete brace at midspan in addition to the diaphragm bracing was tested under gravity loads. This test was terminated at a total load of 2000 lb/beam before inelastic deformations occurred. The maximum angle of rotation was less than 2^{o} because of the discrete brace (Fig. 86).

In test #F5, Fig. 87, the difference between the angle of rotations belonging to F = 0 and F = .060 to .180 in-k/in/rad. are again very significant.

In Fig. 88, the stress distribution for test #F4 with discrete brace is shown. As was discussed at the end of Section 4.7.3, the maximum stress for this case occurs at corner 2. On the other hand, for #F5 without discrete brace, the stress distribution on the flanges are almost uniform for F = .180 in-k/in/rad., as shown in Fig. 89 .

It is seen from Figs. 88 and 89 that measured and computed stresses are in satisfactory agreement. The seeming discrepancy at high loads for test #F4 (Fig. 88) comes from the fact that calculated results assume elastic behavior while actual stresses at these high loads were already in the inelastic range. At these inelastic strains, local flange waving was visible, which increased discrepancies between actual and elastic calculated strains.

CHAPTER VI

CONCLUSIONS

6.1 Summary

The principal objective of this investigation was to study the behavior of thin-walled cold formed channel and Z-sections braced by light gage steel diaphragms.

Though there were previous studies dealing with the behavior of similar types of elements, none had included the combined action of the shear rigidity and rotational restraints by the diaphragm bracing. This study established the mathematical background and gave numerical solutions to include the interactive effect of the mentioned parameters upon the carrying capacity of the braced beams.

The solution was computerized so that the included parameters could easily be varied and accurate results could be obtained.

The study proposes practical and fairly simple design formulas. It also includes the additional effect of discrete bracing, if the diaphragm braced beams were x-braced or connected to each other by sag rods.

The theoretical results were verified by model experiments. Full-scale specimens were tested to obtain more insight into the behavior of the braced purlins.

A method was suggested to determine experimentally the ro-

tational restraint supplied by the diaphragm.

6.2 Conclusions

The following conclusions are based on both the theoretical and experimental findings:

1. The overall elastic behavior of the diaphragm braced beams can reasonably be predicted by the given solution of the differential equation.

2. The model tests showed that the incipient yield load predicted by the theory generally constitutes a conservative estimate of the failure load. This reserve strength depends mainly on the plastic local buckling tendency of the compression flange. For purlins with dimensions as in the full-scale tests, the reserve strength does not seem to be appreciable.

3. The usefulness of a light gage unbraced purlin is limited by its low resistance to torsion.

4. Theory and experiments clearly showed that diaphragm bracing considerably increases the carrying capacity of light gaged, cold formed purlins.

5. For gravity loading, the shear rigidity of the diaphragm caused a definite increase in the yield load capacity of both channel and Z-section beams. For the uplift case however, only Z-sections showed definite improvement due to shear rigidity. For channel beams under uplift loading, the load carrying capacity generally did not increase with the shear rigidity.

6. The rotational restraint F is most effective for channel sections. For Z-sections, it is helpful only for uplift loading, provided that $Q \geq Q_L$.

7. The influence of diaphragm bracing increases with the increase in beam span length, since the parameters Q and F do not change with L while the beam stiffness decreases. Ignoring either Q or F may lead to results which are too conservative.

8. The computer program based on the series solution of the differential equation showed that consideration of three terms was sufficient for quite accurate results.

9. Simplified and conservative design formulas could be obtained using one term in the series solution.

10. Analytical studies showed that the governing design stress for channel and Z-sections will occur at the corner between the web and the lower flange, if the diaphragm bracing has a shear rigidity above a specified value Q_L which is a function of the bending stiffness of the beam.

11. In none of the tests was there a fracture type of failure. There were also no shear or bearing failures at the diaphragm attachment locations.

6.3 Recommendations for Further Study

The following recommendations are made for further investigations:

1. The elastic behavior of the thin-walled sections with unsymmetrical configurations may be studied.

2. The effect of the different types of connections of diaphragm to the beam could be critically examined.

3. Theoretical and experimental work is encouraged in order to study the inelastic behavior of diaphragm braced light gage sections.

4. The interaction between the combined torsion and bending and the local buckling at the compression flange or lip needs further studies.

APPENDIX A

GENERAL THEORY

A1 Assumptions

The theory of nonuniform torsion for the prismatical beams of thin-walled open sections is based on the following assumptions:

a) The shape of the section is undeformable. Hence the displacements in the plane of the cross section for any point can be described through the translation of a reference point and the rotation about this point.

b) The shear deformation of the middle surface is negligible. Hence the angle between the generator of the middle surface and a cross section is assumed not to change during deformation. Since thin-walled beams of open sections are very flexible under torsional moments, the contribution of shear strains to the deformations are indeed small. In contrast to this is tubular beams which are geometrically many times more rigid than open sections under torsion. Here the shear deformations might be quite important.

c) Deflections are assumed to be small. Thus

$$\sin \phi = \phi \text{ and } \cos \phi = 1$$

Non-linear terms in the differential equations have been neglected.

d) Hooke's law is assumed to hold.

A2 Coordinates

A right handed coordinate system is adopted. (Fig. 2). The positive signs of deflections, angles, slopes, curvatures, forces and moments consistent with this system are described in Ref. 24 in detail (Fig. 3). Several sets of coordinates will be employed. The first set x,y,z will stay fixed in space in the unloaded position of the beam. The origin of the coordinates need not be specified at the outset; but later it will be shown that it is to be chosen at the centroid to simplify the expressions. The z axis will be taken along the beam axis. The second set ξ,η,ζ will be attached to the beam to deflect with it under load, the ζ axis being tangent to the deflected axis of the beam. Yet another coordinate system is useful in specifying the points in the cross section. As shown in Fig. 4 a curvilinear orthogonal system s and n will be established. Note that s and n are in accordance with the right hand rule.

The deflections in the x, y and z axes directions are u, v and w. Usually u and v will show the deflection of a specific reference point with the coordinates $\bar{x}$ and $\bar{y}$. Later we will see that it is advantageous to choose the shear center as this reference point. The angle of rotation is ϕ. The deflections in directions of axes s and n are u_s and u_n.

A3 Warping Deformation

Using the first assumption of a rigid cross section we can find the deflection of any point in the tangential direction s in terms of the deflections u, v of the reference

point and ϕ. Let u_A and v_A denote the displacement of point A in the direction of x and y axes (Figure 4).

$$u_A = u - (y-\bar{y})\phi \tag{A.1}$$

$$v_A = v + (x-\bar{x})\phi \tag{A.2}$$

The displacement of A in the direction s is:

$$\begin{aligned} u_s &= -u_A \sin\alpha + v_A \cos\alpha \\ &= -u \sin\alpha + v \cos\alpha + [(y-\bar{y})\sin\alpha + (x-\bar{x})\cos\alpha]\phi \\ &= -u \sin\alpha + v \cos\alpha + r_n\phi \end{aligned} \tag{A.3}$$

where r_n is the distance of the reference point to the tangent drawn to the center line of the section at point A. The angle between this tangent and the y axis is indicated by α.

$$\gamma_{sz} = \frac{\partial w}{\partial s} + \frac{\partial u_s}{\partial z} = 0$$

$$\frac{\partial w}{\partial s} = -\frac{\partial u_s}{\partial z} = -(-\frac{du}{dz}\sin\alpha + \frac{dv}{dz}\cos\alpha + r_n\frac{d\phi}{dz}) \tag{A.4}$$

$$w = -\int(-\frac{du}{dz}\sin\alpha + \frac{dv}{dz}\cos\alpha + r_n\frac{d\phi}{dz})ds + w_o \tag{A.5}$$

But

$$dx = -ds \sin\alpha \tag{A.6}$$

$$dy = ds \cos\alpha \tag{A.7}$$

Therefore,

$$w = -(\frac{du}{dz}x + \frac{dv}{dz}y + \frac{d\phi}{dz}\int r_n\, ds) + w_o \tag{A.8}$$

Let

$$\omega = \int r_n\, ds \tag{A.9}$$

This quantity is called sectorial area in accordance with Vlasov. Substituting ω in Eq. A.8 we obtain the longitudinal displacement

$$w = w_o - \left(\frac{du}{dz} x + \frac{dv}{dz} y + \frac{d\phi}{dz} \omega\right) \qquad (A.10)$$

The first three terms in Eq. A.10 correspond to the hypothesis of plane sections remaining plane. The last term characterizes the warping of the cross section.

A4 Strains and Stresses

If warping and displacements are constant along the beam and not restrained at the ends, they will cause no stresses. Otherwise strains and consequently stresses arise. Taking only the linear terms in the strain displacement relations, the longitudinal strain is

$$\varepsilon_z = \frac{\partial w}{\partial z} = \frac{dw_o}{dz} - \left(\frac{d^2u}{dz^2} x + \frac{d^2v}{dz^2} y + \frac{d^2\phi}{dz^2} \omega\right) \qquad (A.11)$$

Hooke's law states

$$\varepsilon_z = \frac{1}{E} \sigma_z - \frac{\nu}{E} (\sigma_n + \sigma_s)$$

Assuming $\sigma_n = \sigma_s = 0$,

$$\sigma_z = E \frac{dw_o}{dz} - E\left(\frac{d^2u}{dz^2} x + \frac{d^2v}{dz^2} y + \frac{d^2\phi}{dz^2} \omega\right) \qquad (A.12)$$

Now the shear stresses will be determined considering the equilibrium of an element in the longitudinal direction (Figure 5)

$$d\sigma \; ds \; t + d\tau \; dz \; t + p_z \; ds \; dz = 0$$

dividing by ds dz,

$$\frac{\partial(\sigma t)}{\partial z} + \frac{\partial(\tau t)}{\partial s} + p_z = 0 \qquad (A.13)$$

Solving this for the shear stress gives

$$\tau = \frac{1}{t}\left[T_o(z) - \int_o^s \frac{\partial(\sigma t)}{\partial z}\, ds - \int_o^s p_z\, ds\right] \qquad (A.14)$$

For $s = 0$ we get $\tau = T_o/t$. Hence T_o/t means the shear stress at the longitudinal section $s = 0$. Substituting σ from Eq. A.12

$$\tau = \frac{1}{t}\left[T_o(z) - \int_o^s p_z\, ds - E\frac{d^2w_o}{dz^2}\int_o^s dA + E\frac{d^3u}{dz^3}\int_o^s x\, dA + E\frac{d^3v}{dz^3}\int_o^s y\, dA + E\frac{d^3\phi}{dz^3}\int_o^s \omega\, dA\right] \qquad (A.15)$$

Let

$$A_s = \int_o^s dA \qquad (A.16)$$

$$Q_x = \int_o^s y\, dA \qquad (A.17)$$

$$Q_y = \int_o^s x\, dA \qquad (A.18)$$

$$Q_w = \int_o^s \omega\, dA \qquad (A.19)$$

Then the shear stress becomes

$$\tau = \frac{T_o(z)}{t} - \frac{1}{t}\int_o^s p_z \, ds - \frac{E}{t}\frac{d^2 w_o}{dz^2} A_s + \frac{E}{t}\frac{d^3 u}{dz^3} Q_y + \frac{E}{t}\frac{d^3 v}{dz^3} Q_x + \frac{E}{t}\frac{d^3 \phi}{dz^3} Q_w \quad (A.20)$$

If $p_z = 0$ and there is no shear stress at the free edge, the shear stress is given as follows:

$$\tau = \frac{E}{t} Q_y \frac{d^3 u}{dz^3} + \frac{E}{t} Q_x \frac{d^3 v}{dz^3} + \frac{E}{t} Q_w \frac{d^3 \phi}{dz^3} \quad (A.21)$$

A5 Stress Resultants

In analyzing beams it is convenient to integrate the stresses into equivalent internal forces and moments. This can be done in a systematic manner if we demand the virtual work of these forces to be equal to that of the stresses. The corresponding virtual displacements are found when we examine the kinematical degrees of freedom of the system. There are seven degrees of freedom, namely u, v, ϕ, w_o, $\frac{du}{dz}$, $\frac{dv}{dz}$, and $\frac{d\phi}{dz}$, because the displacement of any point of the beam is described uniquely in terms of these quantities (refer to Eqs. A.1, A.2 and A.10).

A5.1 Resultants of σ

The degrees of freedom in the longitudinal direction are w_o, $\frac{du}{dz}$, $\frac{dv}{dz}$, $\frac{d\phi}{dz}$. Setting one of them equal to unity and the others to zero we obtain the following displacement states from Eq. A.10.

$$w_o = 1, \quad w = 1 \quad (A.22a)$$

$$\frac{du}{dz} = -1, \quad w = x \quad (A.22b)$$

$$\frac{dv}{dz} = -1, \quad w = y \tag{A.22c}$$

$$\frac{d\phi}{dz} = -1, \quad w = \omega \tag{A.22d}$$

The stress resultants are obtained considering the virtual work of σ dA on these displacements.

$$N = \int_A \sigma \, 1 \, dA \tag{A.23a}$$

$$M_y = -\int_A \sigma \, x \, dA \tag{A.23b}$$

$$M_x = \int_A \sigma \, y \, dA \tag{A.23c}$$

$$B = \int_A \sigma \, \omega \, dA \tag{A.23d}$$

Substituting σ from Eq. A.12, we get

$$N = E\left(\frac{dw_o}{dz}\int_A dA - \frac{d^2u}{dz^2}\int_A x \, dA - \frac{d^2v}{dz^2}\int_A y \, dA - \frac{d^2\phi}{dz^2}\int_A \omega \, dA\right) \tag{A.24a}$$

$$M_y = E\left(-\frac{dw_o}{dz}\int_A x \, dA + \frac{d^2u}{dz^2}\int_A x^2 \, dA + \frac{d^2v}{dz^2}\int_A x \, y \, dA + \frac{d^2\phi}{dz^2}\int_A \omega \, x \, dA\right) \tag{A.24b}$$

$$M_x = E\left(\frac{dw_o}{dz}\int_A y \, dA - \frac{d^2u}{dz^2}\int_A x \, y \, dA - \frac{d^2v}{dz^2}\int_A y^2 \, dA - \frac{d^2\phi}{dz^2}\int_A \omega \, y \, dA\right) \tag{A.24c}$$

$$B = E\left(\frac{dw_o}{dz}\int_A \omega\, dA - \frac{d^2u}{dz^2}\int_A \omega\, x\, dA - \frac{d^2v}{dz^2}\int_A \omega\, y\, dA - \frac{d^2\phi}{dz^2}\int_A \omega^2\, dA\right) \tag{A.24d}$$

Choosing the position of (1) the coordinate axes, and (2) the reference point (where upon the deflections u and v belong) appropriately we may eliminate some of the integrals in Eqs. A.24. Namely, if the origin of the coordinate axes is taken at the centroid the following integrals vanish:

$$\int_A x\, dA = 0, \quad \int_A y\, dA = 0$$

It can be shown that choosing the reference point at the shear center we eliminate the following

$$\int_A \omega\, dA = 0, \quad \int_A \omega\, x\, dA = 0, \quad \int_A \omega\, y\, dA = 0$$

Let

$$I_x = \int_A y^2\, dA \tag{A.25}$$

$$I_y = \int_A x^2\, dA \tag{A.26}$$

$$I_{xy} = \int_A x\, y\, dA \tag{A.27}$$

$$C_w = \int_A \omega^2\, dA \tag{A.28}$$

Then the stress resultants of the normal stress σ are

$$N = AE\,\frac{dw_o}{dz} \tag{A.29a}$$

$$M_y = E\left(\frac{d^2u}{dz^2}\, I_y + \frac{d^2v}{dz^2}\, I_{xy}\right) \tag{A.29b}$$

$$M_x = -E\left(\frac{d^2u}{dz^2} I_{xy} + \frac{d^2v}{dz^2} I_x\right) \qquad \text{(A.29c)}$$

$$B = -EC_w \frac{d^2\phi}{dz^2} \qquad \text{(A.29d)}$$

A5.2 Resultants of τ

The stress resultants of the shear stress will be found in a similar fashion. The virtual displacements in the direction tangential to the center line of the cross section are given by Eq. A.3 with Eqs. A.6, A.7, A.9.

$$u = 1 \rightarrow u_s = -\sin\alpha = dx/ds$$

$$v = 1 \rightarrow u_s = \cos\alpha = dy/ds$$

$$\phi = 1 \rightarrow u_s = r = d\omega/ds$$

Now writing the virtual work of τtds

$$V_x = \int_A (\tau t ds)\, dx/ds = \int_A \tau t dx$$

$$V_y = \int_A (\tau t ds)\, dy/ds = \int_A \tau t dy$$

$$M_{tw} = \int_A (\tau t ds)\, d\omega/ds = \int_A \tau t d\omega$$

Substituting τ from Eq. A.21

$$V_x = E\frac{d^3u}{dz^3}\int_A Q_y dx + E\frac{d^3v}{dz^3}\int_A Q_x dx + E\frac{d^3\phi}{dz^3}\int_A Q_w dx$$

$$V_y = E\frac{d^3u}{dz^3}\int_A Q_y dy + E\frac{d^3v}{dz^3}\int_A Q_x dy + E\frac{d^3\phi}{dz^3}\int_A Q_w dy$$

$$M_{tw} = E\frac{d^3u}{dz^3}\int_A Q_y d\omega + E\frac{d^3v}{dz^3}\int_A Q_x d\omega + E\frac{d^3\phi}{dz^3}\int_A Q_w d\omega$$

The integrals can be modified using integration by parts.

For example

$$\int_A Q_y dx = Q_y x\Big|_A - \int_A x dQ_y = 0 - \int_A x\, x dA = -I_y$$

$$\int_A Q_y dy = Q_y y\Big|_A - \int_A y dQ_y = 0 - \int_A y\, x dA = -I_{xy}$$

$$\int Q_y d\omega = Q_y \omega\Big|_A - \int_A \omega dQ_y = 0 - \int_A \omega\, x dA = 0$$

Similarly

$$\int_A Q_x dx = -I_x \qquad \int_A Q_w dx = 0$$

$$\int_A Q_x dy = -I_{xy} \qquad \int_A Q_w dy = 0$$

$$\int_A Q_x d\omega = 0 \qquad \int_A Q_w d\omega = -C_w$$

Hence the stress resultants are

$$V_x = -EI_y \frac{d^3u}{dz^3} - E\, I_{xy} \frac{d^3v}{dz^3} \tag{A.30a}$$

$$V_y = -EI_{xy} \frac{d^3u}{dz^3} - E\, I_x \frac{d^3v}{dz^3} \tag{A.30b}$$

$$M_{tw} = -EC_w \frac{d^3\phi}{dz^3} \tag{A.30c}$$

Comparison of Eqs. A.29b, c and d with Eqs. A.30a, b, and c, respectively, gives

$$V_x = -\frac{d}{dz} M_y \tag{A.31a}$$

$$V_y = \frac{d}{dz} M_x \tag{A.31b}$$

$$M_{tw} = \frac{d}{dz} B \tag{A.31c}$$

A5.3 Discussion of Bimoment

The bending moments and shear forces determined in the previous section are the same as in elementary beam theory and need no further comment. The bimoment defined in Eq. A.23d or Eq. A.29d was introduced by Vlasov. [25] It is a balanced force system, statically equivalent to zero. An example is shown in Fig. 6a. However, the derivative of bimoment with respect to z is a torsional moment namely M_{tw} as defined in Eq. A.30c. M_{tw} is called flexural twist, as distinguished from Saint Venant twist.

Generally, if a force system (even with zero resultant) can do work on displacements due to the warping of the cross section, it causes bimoment in the beam. Bimoment, and consequently flexural twist, may arise under several different types of loads. Some common examples may be transverse loading outside the shear center, and a single or distributed torsional moment. More unconventional examples are a longitudinal force applied at a point with non-zero sectorial area or a single bending moment applied in a plane parallel to the longitudinal axis at a distance from the shear center. In the former case $B = P\omega$, hence its sign depends on both P and ω. A tensile force is taken positive. The sign of the ω is determined by the sweeping movement of the radius vector r (Fig. 4). If r moves from a point with zero sectorial area to the point in question according to the right hand rule (i.e., in counterclockwise direction in a positive cross section), ω is positive. In the latter case $B = M a$, where a is the

distance between the shear center and the plane in which M is acting. The sign convention for this case is as follows: The bimoment is positive if the moment vector M is pointed towards the shear center as shown in Figure 7b.

It is very important to distinguish whether a bending moment arises due to a force couple perpendicular (Fig. 7b) or parallel (Fig. 7c) to the z axis. The former is what we meant above as a single bending moment M whose bimoment is B = Ma. The bimoment for the latter case is found by adding the bimoments of the single forces. Hence, although the moment is the same for the cases shown on Figures 7b and 7c, the resulting bimoments have opposite signs. The difference between these cases is demonstrated more dramatically in Figure 7d. In one B = 0 whereas in the other B = M 2a.

According to Saint Venant's principle, if a system of forces is equivalent to zero its effects remain localized. This is not the case with bimoment. The stresses and deflections are quite large even at a considerable distance from the application point of an external bimoment.

A.5.4 Stress Resultants in the Deformed State

Thus far the displacements, strains, stresses and stress resultants have been referred to the undeformed state of the beam. However, since the differential equations of equilibrium will be written in the deformed state, we need the corresponding stresses and their resultants. During deformation, normal stresses are oriented in the direction of the bent and twisted fibers of the beam. The shear stresses remain parallel

to the center line of the deflected cross section. The magnitudes of the stresses, however, can be taken, in a first order approximation, equal to the ones referred to the undeformed state. Since the cross section had been assumed rigid, sectional properties will be the same in the deformed and undeformed states. That is $I_\xi = I_x, I_\eta = I_y$, etc. Hence the stress resultants of the normal stress may be obtained from Eqs. A.29 by changing the subscripts of the stress resultants.

$$N_\zeta = AE \frac{dw_o}{dz} \tag{A.32a}$$

$$M_\xi = -E(I_{xy} \frac{d^2u}{dz^2} + I_x \frac{d^2v}{dz^2}) \tag{A.32b}$$

$$M_\eta = E(I_y \frac{d^2u}{dz^2} + I_{xy} \frac{d^2v}{dz^2}) \tag{A.32c}$$

$$B = -EC_w \frac{d^2\phi}{dz^2} \tag{A.32d}$$

Similarly the shear stress resultants are obtained from Eqs. A.30

$$V_\xi = -E\, I_y \frac{d^3u}{dz^3} - E\, I_{xy} \frac{d^3v}{dz^3} \tag{A.33a}$$

$$V_\eta = -E\, I_{xy} \frac{d^3u}{dz^3} - E\, I_x \frac{d^3v}{dz^3} \tag{A.33b}$$

$$M_{\zeta,w} = -EC_w \frac{d^3\phi}{dz^3} \tag{A.33c}$$

A5.5 The Normal Stress in Terms of the Stress Resultants

From Eqs. A.32

$$\frac{dw_o}{dz} = \frac{N_\xi}{EA} \tag{A.34a}$$

$$\frac{d^2u}{dz^2} = \frac{M_\eta I_x + M_\xi I_{xy}}{E(I_x I_y - I_{xy}^2)} \tag{A.34b}$$

$$\frac{d^2v}{dz^2} = -\frac{M_\xi I_y + M_\eta I_{xy}}{E(I_x I_y - I_{xy}^2)} \tag{A.34c}$$

$$\frac{d^2\phi}{dz^2} = -\frac{B}{EC_w} \tag{A.34d}$$

Substituting these into Eq. A.12

$$\sigma_\zeta = \frac{N_\zeta}{A} - \frac{M_\eta I_x + M_\xi I_{xy}}{(I_x I_y - I_{xy}^2)} x + \frac{M_\xi I_y + M_\eta I_{xy}}{(I_x I_y - I_{xy}^2)} + \frac{B}{C_w} \omega \tag{A.35}$$

A6 Torsional Moment due to σ

During torsion every fiber, except the one through the shear center, is twisted into a helix. Consequently, the normal stress at a point is no longer parallel to the axis through the shear center. Let the distance of a point from the shear center be called r. The component of the normal stress perpendicular to both r and the shear center axis is

$$\sigma\, r \frac{d\phi}{dz}$$

Torsional moment of this stress around the shear center is

$$M_t = \int_A (\sigma\, r \frac{d\phi}{dz}) dA\, r = \frac{d\phi}{dz} \int_A \sigma\, r^2\, dA \tag{A.36}$$

where

$$r^2 = (x - \bar{x})^2 + (y - \bar{y})^2 \tag{A.37}$$

Substituting σ from Eq. A.35 into Eq. A.36

$$M_t = \frac{d\phi}{dz}\left[\frac{N_\zeta}{A}\int_A r^2\,dA - \frac{M_\eta I_x + M_\xi I_{xy}}{(I_x I_y - I_{xy}^2)}\int_A x\,r^2\,dA\right.$$

$$\left. + \frac{M_\xi I_y - M_\eta I_{xy}}{(I_x I_y - I_{xy}^2)}\int_A y\,r^2\,dA + \frac{B}{C_w}\int_A \omega\,r^2\,dA\right] \quad (A.38)$$

With r^2 from Eq. A.37, the integrals in Eq. A.38 become

$$I_o = \int_A r^2\,dA \quad (A.39a)$$

$$H_x = \int_A y\,r^2\,dA = \int_A y(x^2+y^2)dA - 2\bar{x}I_{xy} - 2\bar{y}I_x \quad (A.39b)$$

$$H_y = \int_A x\,r^2\,dA = \int_A x(x^2+y^2)dA - 2\bar{x}I_y - 2\bar{y}I_{xy} \quad (A.39c)$$

$$H_w = \int_A \omega\,r^2\,dA = \int_A \omega(x^2+y^2)dA \quad (A.39d)$$

Hence

$$M_t = \frac{d\phi}{dz}\left[N_\zeta\frac{I_o}{A} - \frac{M_\eta I_x + M_\xi I_{xy}}{(I_x I_y - I_{xy}^2)}H_y + \frac{M_\xi I_y + M_\eta I_{xy}}{(I_x I_y - I_{xy}^2)}H_x + \frac{B}{C_w}H_w\right]$$

or

$$M_t = \frac{d\phi}{dz}\left[N_\zeta\frac{I_o}{A} + M_\xi\frac{I_y H_x - I_{xy}H_y}{(I_x I_y - I_{xy}^2)} - M_\eta\frac{I_x H_y - I_{xy}H_x}{(I_x I_y - I_{xy}^2)} + B\frac{H_w}{C_w}\right]$$

$$M_t = \frac{d\phi}{dz}\left[N_\zeta\frac{I_o}{A} + M_\xi\beta_x - M_\eta\beta_y + B\,\beta_w\right] \quad (A.40)$$

where

$$\beta_x = \frac{I_y H_x - I_{xy}H_y}{(I_x I_y - I_{xy}^2)} \quad (A.41a)$$

$$\beta_y = \frac{I_x H_y - I_{xy}H_x}{(I_x I_y - I_{xy}^2)} \quad (A.41b)$$

$$\beta_w = \frac{H_w}{C_w} \qquad (A.41c)$$

Note that if $I_{xy} = 0$

$$\beta_x = \frac{H_x}{I_x} = \frac{1}{I_x} \int_A y(x^2+y^2)dA - 2\bar{y}$$

$$\beta_y = \frac{H_y}{I_y} = \frac{1}{I_y} \int_A x(x^2+y^2)dA - 2\bar{x}$$

Furthermore, for singly symmetrical sections like a channel, if x is the symmetry axis

$$\beta_x = \beta_w = 0 \quad \beta_y \neq 0$$

For point symmetrical sections like a Z-section

$$\beta_x = \beta_y = 0 \quad \beta_w \neq 0$$

For doubly symmetrical sections like an I section

$$\beta_x = \beta_y = \beta_w = 0$$

A7 Differential Equations

Eqs. A.32b and c give the differential equations for bending. For torsion we have to combine Eq. A.33c, Eq. A.40 and the portion carried by Saint Venant torsion. Hence the differential equations for combined bending and torsion are as follows:

$$EI_{xy} \frac{d^2u}{dz^2} + EI_x \frac{d^2v}{dz^2} = -M_\xi \qquad (A.42a)$$

$$EI_y \frac{d^2u}{dz^2} + EI_{xy} \frac{d^2v}{dz^2} = M_\eta \qquad (A.42b)$$

$$EC_w \frac{d^3\phi}{dz^3} - (GK + N_\zeta \frac{I_o}{A} + M_\xi \beta_x - M_\eta \beta_y + B\beta_w)\frac{d\phi}{dz} = -M_\zeta \quad (A.42c)$$

The moments M_ξ, M_η, and M_ζ are in the direction of the deflected axes. In order to determine them, we may first find the moments at the points on the deflected axis through the shear center but in the direction of fixed axes x, y, z and then project the latter into the ξ, η, ζ coordinates. The transformation formulas are

$$M_\xi = M_x + \phi M_y - \frac{du}{dz} M_z \quad (A.43a)$$

$$M_\eta = -\phi M_x + M_y - \frac{dv}{dz} M_z \quad (A.43b)$$

$$M_\zeta = \frac{du}{dz} M_x + \frac{dv}{dz} M_y + M_z \quad (A.43c)$$

To obtain a linear differential equation, we may use N, M_x, and M_y in Eq. A.42c instead of N_ξ, M_η, and M_ζ.

The bimoment B in Eq. A.42c is unknown at the outset. Since it is not a statical quantity, it cannot be found directly from equilibrium equations as can the bending moments. However, it can be determined approximately, using the differential equation of torsion and the pertinent boundary conditions.

$$EC_w \frac{d^4\phi}{dz^4} - GK \frac{d^2\phi}{dz^2} = m_t$$

where m_t indicates the external distributed torsional moments. Substituting B from Eq. A.32d

$$\frac{d^2B}{dz^2} - \frac{GK}{EC_w} B = -m_t$$

Note that the term $B\beta_w$ in Eq. A.42c vanishes for doubly and singly symmetrical sections such as the I and channel, since $\beta_w = 0$. For point symmetrical sections like the Z, it vanishes if the bimoment is zero. This is the case, for example, if a Z beam is under transverse loads through its centroid.

Aβ Summary

In summary, the normal and shear stresses in a thin-walled beam of open cross section are

$$\sigma = E\left(\frac{dw_o}{dz} - \frac{d^2u}{dz^2}\,x - \frac{d^2v}{dz^2}\,y - \frac{d^2\phi}{dz^2}\,\omega\right) \tag{A.12}$$

$$\tau = \frac{E}{t}\left(Q_y \frac{d^3u}{dz^3} + Q_x \frac{d^3v}{dz^3} + Q_w \frac{d^3\phi}{dz^3}\right) \tag{A.21}$$

The stress resultants of σ, in the direction of the deflected coordinates are

$$N_\zeta = AE \frac{dw_o}{dz} \tag{A.32a}$$

$$M_\xi = -E\left(I_{xy} \frac{d^2u}{dz^2} + I_x \frac{d^2v}{dz^2}\right) \tag{A.32b}$$

$$M_\eta = E\left(I_y \frac{d^2u}{dz^2} + I_{xy} \frac{d^2v}{dz^2}\right) \tag{A.32c}$$

$$B = -EC_w \frac{d^2\phi}{dz^2} \tag{A.32d}$$

The stress resultants of τ are

$$V_\xi = -E\left(I_y \frac{d^3u}{dz^3} + I_{xy} \frac{d^3v}{dz^3}\right. \tag{A.33a}$$

$$V_\eta = -E\left(I_{xy} \frac{d^3u}{dz^3} + I_x \frac{d^3v}{dz^3}\right) \tag{A.33b}$$

$$M_{tw} = -EC_w \frac{d^3\phi}{dz^3} \tag{A.33c}$$

The differential equations of combined bending and torsion are

$$EI_{xy} \frac{d^2u}{dz^2} + EI_x \frac{d^2v}{dz^2} = -M_\xi \tag{A.42a}$$

$$EI_y \frac{d^2u}{dz^2} + EI_{xy} \frac{d^2v}{dz^2} = M_\eta \tag{A.42b}$$

$$EC_w \frac{d^3\phi}{dz^3} - (GK + N_\zeta \frac{I_o}{A} + M_\xi\beta_x - M_\eta\beta_y + B\,\beta_w)\frac{d\phi}{dz} = -M_\zeta \tag{A.42c}$$

where

$$M_\xi = M_x + \phi M_y - \frac{du}{dz} M_z \tag{A.43a}$$

$$M_\eta = -\phi\, M_x + M_y - \frac{dv}{dz} M_z \tag{A.43b}$$

$$M_\zeta = \frac{du}{dz} M_x + \frac{dv}{dz} M_y + M_z \tag{A.43c}$$

APPENDIX B

THEORY FOR DIAPHRAGM-BRACED BEAMS

Let the diaphragm be attached to the upper flange of the beam at point D (x_D, y_D) as shown on Figure 10. There is no difficulty in taking the bracing at any other point. The choice is dictated by practical considerations. The diaphragm lies parallel to the x-z plane.

B1 The Forces Between Beam and Diaphragm

In a roof structure external loads are transmitted to the beam through the diaphragm. Having this practical problem in mind more general loading cases where additional loads are applied directly to the beam are not considered.

a) The lateral force p_x

The deflection of the fiber of the beam at point D is called u_D

Let

$$e_D = -y_D$$

$$u_D = u + e_D\phi$$

The shear strain

$$\gamma = \frac{du_D}{dz} = \frac{du}{dz} + e_D \frac{d\phi}{dz} \qquad (B.1)$$

The shear force

$$V = Q\gamma = Q(\frac{du}{dz} + e_D \frac{d\phi}{dz}) \qquad (B.2)$$

where Q is the shear rigidity of the diaphragm contributory to one of the beams.

The bracing force p_x

$$p_x = \frac{dV}{dz} = Q\left(\frac{d^2u}{dz^2} + e_D \frac{d^2\phi}{dz^2}\right) \qquad (B.3)$$

The external loads in the direction of the x axis in the plane of the diaphragm can be assumed to be carried by the diaphragm alone, because its rigidity is usually several times than that of the beam.

b) The vertical force p_y

The vertical and horizontal distances of the application point of p_y from the shear center is indicated by two positive numbers e and a respectively. Downward loading is transferred from the diaphragm to the beam through bearing. Since the section may rotate during the loading, for this case, the contact point may be at the junction of the web and flange rather than point D. On the other hand uplift loading is transmitted by the connectors, hence it acts at the point D. However, in the derivations and numerical computations in this report both uplift and downward loading is assumed acting through the web. For Z-sections this means setting a = 0 which brought certain simplifications such as elimination of $B\,\beta_w$ in Eq. A.42c. This should be taken into account if this assumption is discarded. For channel sections there is no such complication. One can simply substitute the proper value of "a" directly into the computer program.

c) The longitudinal force p_z

There are usually a number of parallel beams braced by the same panel. The middle beams contain only lateral bracing forces. On the other hand, the edge beams have to supply shear forces to the diaphragm along the free edge and get thereby axial loads in addition to the lateral loads. The sign of the axial loading for the two edge beams are opposite to each other.

$$p_z = \pm \frac{V}{w} = \pm \frac{Q}{w}\left(\frac{du}{dz} + e_D \frac{d\phi}{dz}\right) \qquad (B.4)$$

where w is the width of the diaphragm contributory to one of the beams.

d) Torsional moment m_t

$$m_t = F\phi \qquad (B.5)$$

where F is the rotational restraint of the diaphragm per unit length.

B2 Equilibrium Equations

In the following, nonlinear terms have been ignored. The effect of longitudinal forces p_z will not be included. Hence, the equations are valid for the middle beams in an assembly. As mentioned before, the forces with indices x, y, z are at the shear center but in the direction of the fixed coordinates.

Bending in x-direction:

$$\frac{dM_x}{dz} = V_y \qquad (B.6)$$

$$\frac{d^2M_x}{dz^2} = \frac{dV_y}{dz} = -p_y \tag{B.7}$$

Bending in y direction:

$$\frac{dM_y}{dz} = -V_x \tag{B.8}$$

$$\frac{d^2M_y}{dz^2} = -\frac{dV_x}{dz} = p_x \tag{B.9}$$

Torsion:

Torsion is due to p_x, p_y and cross-bending rigidity of the diaphragm. Considering equilibrium along the z axis,

$$dM_z + V_y du + dV_y u + p_y dz(u+e\phi+a) + p_x e_D - F\phi = 0$$

Dividing by dz and using Eqs. B.6 through B.9,

$$\frac{dM_z}{dz} = -\frac{dM_x}{dz}\frac{du}{dz} - p_y(e\phi+a) - p_x e_D + F\phi \tag{B.10}$$

B3 Differential Equations of Diaphragm-Braced Beams

The projections of M_x, M_y, M_z in ξ, η and ζ will be determined by Eqs. A.43. However, the last terms in Eqs. A.43a and b which indicate the projection of M_z on ξ and η, respectively, will be neglected. (This can be justified by the fact that the slopes are small on the major part of the span.)

$$\frac{d^2M_\xi}{dz^2} = -p_y \tag{B.11a}$$

$$\frac{d^2M_\eta}{dz^2} = -\frac{d^2}{dz^2}(M_x\phi) + p_x \tag{B.11b}$$

$$\frac{dM_\zeta}{dz} = \frac{d^2u}{dz^2} M_x + \frac{du}{dz}\frac{dM_x}{dz} - \frac{dM_x}{dz}\frac{du}{dz} - p_y(e\phi+a) - p_x e_D + F\phi$$

(B.11c)

Differentiating Eqs. A.42a and b twice with respect to z and using Eqs. B.11a and b we get

$$E \frac{d^4v}{dz^4} I_x + E \frac{d^4u}{dz^4} I_{xy} = p_y \qquad \text{(B.12a)}$$

$$E \frac{d^4v}{dz^4} I_{xy} + E \frac{d^4u}{dz^4} I_y + \frac{d^2\phi}{dz^2} (M_x\phi) = p_x \qquad \text{(B.12b)}$$

Now Eq. A.42c will be differentiated once and $\frac{dM_\zeta}{dz}$ will be substituted from Eq. B.11c.

$$EC_w \frac{d^4\phi}{dz^4} - GK \frac{d^2\phi}{dz^2} + \frac{d}{dz}\left[\frac{d}{dz}(M_x\beta_x + B\,\beta_w)\right]$$

$$+ M_x \frac{d^2u}{dz^2} - p_y e\phi + F\phi = p_y a + p_x e_D \qquad \text{(B.12c)}$$

The vertical deflection can be eliminated from Eqs. B.12a and b.

$$\frac{d^4v}{dz^4} = \frac{p_y}{EI_x} - \frac{I_{xy}}{I_x}\frac{d^4u}{dz^4} \qquad \text{(B.13)}$$

Substituting,

$$E \frac{(I_x I_y - I_{xy}^2)}{I_x} \frac{d^4u}{dz^4} + \frac{d^2}{dz^2}(M_x\phi) + \frac{I_{xy}}{I_x} p_y = p_x \qquad \text{(B.14a)}$$

I, channel and Z beams:

For I or channel beams $\beta_x = \beta_w = 0$. For Z beams $\beta_x = 0$, and if there is no primary torsion also B = 0. Hence for our case the corresponding terms in Eq. B.12c will vanish

$$EC_w \frac{d^4\phi}{dz^4} - GK \frac{d^2\phi}{dz^2} + M_x \frac{d^2u}{dz^2} - p_y e\phi + F\phi = p_y a + p_x e_D \tag{B.14b}$$

Finally, the bracing force p_x from Eq. B.3 will be substituted into Eqs. B.14a and b.

$$\frac{E(I_x I_y - I_{xy}^2)}{I_x} \frac{d^4u}{dz^4} - Q \frac{d^2u}{dz^2} - Q\, e_D \frac{d^2\phi}{dz^2} + \frac{d^2}{dz^2}(M_x\phi) = -\frac{I_{xy}}{I_x} p_y \tag{B.15a}$$

$$EC_w \frac{d^4\phi}{dz^4} - GK \frac{d^2\phi}{dz^2} - Q\, e_D^2 \frac{d^2\phi}{dz^2} - p_y e\phi + F\phi + M_x \frac{d^2u}{dz^2} - Q\, e_D \frac{d^2u}{dz^2} = p_y a \tag{B.15b}$$

Assuming that p_x and p_y have the same vertical distance from the shear center

$$e_D = e \tag{B.16}$$

Substituting this and introducing the dimensionless variable

$$\zeta = \frac{z}{L} \tag{B.17}$$

Eqs. B.15 become

$$\frac{E(I_x I_y - I_{xy}^2)}{I_x L^2} u^{IV} - Qu'' - Qe\phi'' + (M_x\phi)'' = -\frac{I_{xy}}{I_x} p_y L^2 \tag{B.18a}$$

$$\frac{EC_w}{L^2}\phi^{IV} - GK\phi'' - Qe^2\phi'' - p_y eL^2\phi + FL^2\phi + M_x u'' - Qeu'' = p_y L^2 a \tag{B.18b}$$

where primes denote differentiation with respect to ζ.

B4 Special Cases

The coupled equation system B.18 will be converted to one differential equation in ϕ, for no and rigid bracing cases.

a) No bracing, i.e. Q = 0

For $Q \neq 0$: Eqs. B.18 become

$$\frac{E(I_x I_y - I_{xy}^2)}{I_x L^2} u^{IV} + (M_x \phi)'' = -\frac{I_{xy}}{I_x} p_y L^2 \qquad (B.19a)$$

$$\frac{EC_w}{L^2} \phi^{IV} - GK\phi'' - p_y e L^2 \phi + M_x u'' + FL^2 \phi = p_y L^2 a \qquad (B.19b)$$

Eq. B.19a can be integrated twice and solved for u"

$$u'' = \frac{L^2}{E(I_x I_y - I_{xy}^2)} (-M_x I_x \phi + I_{xy} M_x) \qquad (B.20)$$

Substituting this into Eq. B.19b

$$\frac{EC_w}{L^2} \phi^{IV} - GK\phi'' - (p_y e + \frac{I_x M_x^2}{E(I_x I_y - I_{xy}^2)}) L^2 \phi + FL^2 \phi = (p_y a - \frac{I_{xy} M_x^2}{E(I_x I_y - I_{xy}^2)}) L^2 \qquad (B.21)$$

Eq. B.21 is a special case of a more general differential equation given in Ref. 24, if the term with F is excluded.

b) Rigid bracing, i.e., Q = ∞

For this case the displacements u and ϕ are no longer independent. Specifically, $u_D = 0$ gives

$$u = -e_D \phi = -e\phi \qquad (B.22)$$

Consider Eqs. B.14. The bracing forces p_x can be eliminated between them. Simultaneously $u = -e\phi$ will be substituted. Then

$$\frac{EC'_w}{L^2}\phi^{IV} - GK\phi'' + FL^2\phi - M_x\phi''e - (M_x\phi)''e$$
$$-p_y eL^2\phi = p_y L^2(a+\frac{I_{xy}}{I_x}e) \qquad (B.23)$$

where

$$C'_w = C_w + \frac{I_x I_y - I_{xy}^2}{I_x} e^2 \qquad (B.24)$$

APPENDIX C

SOLUTION METHOD

Consider Eqs. 2.9. These are linear fourth order coupled differential equations with variable coefficients. Their exact solution is difficult if at all possible. Galerkin's Method proves to be very powerful in solving such differential equations approximately.

The displacements u and ϕ will be represented by infinite series. A suitable choice is the eigenfunctions of transverse vibrations of a rod which has the same boundary conditions as our beam. (After separation of variables, the partial differential equation of the vibration problem is reduced to an ordinary differential equation). For transverse and rotational vibrations we have respectively:

$$u^{IV} - \lambda_x^4 u = 0 \qquad (C.1a)$$

$$\phi^{IV} - \lambda_z^4 \phi = 0 \qquad (C.1b)$$

Their solutions are

$$u = A_1 \sin\lambda_x\zeta + A_2 \cos\lambda_x\zeta + A_3 \sinh \lambda_x\zeta + A_4 \cosh \lambda_x\zeta \qquad (C.2a)$$

$$\phi = \bar{A}_1 \sin\lambda_z\zeta + \bar{A}_2 \cos \lambda_z\zeta + \bar{A}_3 \sinh \lambda_z\zeta + \bar{A}_4 \cosh \lambda_z\zeta \qquad (C.2b)$$

From the four boundary conditions for each displacement, homogeneous equation systems for the respective coefficients

are obtained. In order to avoid the trivial solution their determinants are set equal to zero. This results in two transcendental equations for the eigenvalues λ_x and λ_z which have an infinite number of roots. Correspondingly there are an infinite number of eigenfunctions which form an orthogonal and complete set. For the most important boundary conditions, the approximate values for eigenvalues and the corresponding eigenfunctions are given in Ref. 35, Table 33.

C1 Solution for General Case

Let

$$u = \sum_{n=1}^{\infty} u_n X_n \tag{C.3a}$$

$$\phi = \sum_{n=1}^{\infty} \phi_n Z_n \tag{C.3b}$$

Now the Galerkin Method will be applied to Eqs. 2.9

$$\sum_{n=1}^{\infty} \int_o^1 u_n \left[\frac{E(I_x I_y - I_{xy}^2)}{I_x L^2} X_n^{IV} - Q\, X_n''\right] + \phi_n [-Qe Z_n'' + (M_x Z_n)''] X_m \, d\zeta = -\frac{I_{xy}}{I_x} L^2 \int_o^1 p_y X_m d\zeta \tag{C.4a}$$

$$m = 1, 2, \ldots, \infty$$

$$\sum_{n=1}^{\infty} \int_o^1 u_n [M_x X_n'' - Qe X_n''] + \phi_n \left[\frac{EC_w}{L^2} Z_n^{IV} - (GK+Qe^2) Z_n'' - p_y e L^2 Z_n + F L^2 Z_n\right] Z_m d\zeta = a L^2 \int_o^1 p_y Z_m d\zeta \tag{C.4b}$$

$$m = 1, 2, \ldots, \infty$$

For practical computation we can consider of course only a finite number of terms.

From Eqs. C.1

$$X_n^{IV} = \lambda_x^4 X_n$$

$$Z_n^{IV} = \lambda_z^4 Z_n$$

Eqs. C.4 may be written in a more compact form

$$\sum_{n=1}^{\infty} (A_{mn}\, u_n + B_{mn}\, \phi_n) = E_m \qquad (C.5a)$$

$$\sum_{n=1}^{\infty} (C_{mn}\, u_n + D_{mn}\, \phi_n) = F_m \qquad (C.5b)$$

$$m = 1, 2, \ldots, \infty$$

where

$$A_{mn} = \frac{E(I_x I_y - I_{xy}^2)}{I_x L^2} \lambda_x^4 \int_o^1 X_n X_m d\zeta - Q \int_o^1 X_n'' X_m d\zeta \qquad (C.6a)$$

$$B_{mn} = -Qe \int_o^1 Z_n'' X_m d\zeta + \int_o^1 (M_x Z_n)'' X_m d\zeta \qquad (C.6b)$$

$$C_{mn} = -Qe \int_o^1 X_n'' Z_m d\zeta + \int_o^1 M_x X_n'' Z_m d\zeta \qquad (C.6c)$$

$$D_{mn} = \frac{EC_w}{L^2} \lambda_z^4 \int_o^1 Z_n Z_m d\zeta - (GK+Qe^2) \int_o^1 Z_n'' Z_m d\zeta$$

$$- eL^2 \int_o^1 p_y Z_n Z_m d\zeta + FL^2 \int_o^1 Z_n Z_m d\zeta \qquad (C.6d)$$

$$E_m = -\frac{I_{xy}}{I_x} L^2 \int_o^1 p_y X_m d\zeta \qquad (C.6e)$$

$$F_m = aL^2 \int_o^1 p_y Z_m d\zeta \qquad (C.6f)$$

Let

$$M_x = pL^2\, h(\zeta) \tag{C.7a}$$

$$p_y = p\, \bar{h}(\zeta) \tag{C.7b}$$

where p is a load parameter and h, $\bar{h}$ are dimensionless moment and load distribution functions. Then

$$A_{mn} = \frac{E(I_x I_y - I_{xy}^2)}{I_x L^2}\, \lambda_x^4\, T_1 - Q\, T_2 \tag{C.8a}$$

$$B_{mn} = -Qe\, T_3 + pL^2\, T_5 \tag{C.8b}$$

$$C_{mn} = -Qe\, T_4 + pL^2\, T_6 \tag{C.8c}$$

$$D_{mn} = \frac{EC_w}{L^2}\, \lambda_z^4\, T_7 - (GK+Qe^2)\, T_8 - pL^2 e\, T_9 + FL^2\, T_7 \tag{C.8d}$$

$$E_m = -\frac{I_{xy}}{I_x}\, pL^2\, T_{101} \tag{C.8e}$$

$$F_m = apL^2\, T_{102} \tag{C.8f}$$

where T_i indicate the integrals. Some of the integrals may be modified by using integration by parts as shown below

$$T_1 = \int_o^1 X_n X_m d = \delta_{nm} \int_o^1 X_m^2 d \tag{C.9a}$$

$$T_2 = \int_o^1 X_n'' X_m d\zeta = X_n' X_m \Big|_o^1 - \int_o^1 X_n' X_m' d\zeta = -\int_o^1 X_n' X_m' d\zeta \tag{C.9b}$$

$$T_3 = \int_o^1 Z_n'' X_m d\zeta = Z_n' X_m \Big|_o^1 - \int_o^1 Z_n' X_m' d\zeta = -\int_o^1 Z_n' X_m' d\zeta \tag{C.9c}$$

$$T_4 = \int_o^1 X_n'' Z_m d\zeta = X_n' Z_m \Big|_o^1 - \int_o^1 X_n' Z_m' d\zeta = - \int_o^1 X_n' Z_m' d \quad (C.9d)$$

$$T_5 = \int_o^1 (h\, Z_n)'' \, X_m d\zeta = (h\, Z_n)' X_m \Big|_o^1 - \int_o^1 (h\, Z_n)' X_m' d\zeta$$

$$= - \int_o^1 (h\, Z_n)' X_m' d\zeta \quad (C.9e)$$

$$T_6 = \int_o^1 h\, X_n'' Z_m d\zeta = X_n' (h\, Z_m) \Big|_o^1 - \int_o^1 X_n' (h\, Z_m)' d\zeta$$

$$= - \int_o^1 (h\, Z_m)' X_n' d\zeta \quad (C.9f)$$

$$T_7 = \int_o^1 Z_n Z_m d\zeta = \delta_{nm} \int_o^1 Z_m^2 d\zeta \quad (C.9g)$$

$$T_8 = \int_o^1 Z_n'' Z_m d\zeta = Z_n' Z_m \Big|_o^1 - \int_o^1 Z_n' Z_m' d\zeta = - \int_o^1 Z_n' Z_m' d\zeta \quad (C.9h)$$

$$T_9 = \int_o^1 \bar{h}\, Z_n Z_m \, d\zeta \quad (C.9i)$$

$$T_{101} = \int_o^1 \bar{h}\, X_m \, d\zeta \quad (C.9j)$$

$$T_{102} = \int_o^1 \bar{h}\, Z_m \, d\zeta \quad (C.9k)$$

Substituting T_i from Eqs. C.9a through i into Eqs. C.8a through d, the coefficients become:

$$A_{mn} = \frac{E(I_x I_y - I_{xy}^2)}{I_x L^2} \lambda_x^4 \delta_{nm} \int_o^1 X_m^2 d\zeta + Q \int_o^1 X_n' X_m' d\zeta \quad (C.10a)$$

$$B_{mn} = Qe\int_o^1 Z_n'X_m'd\zeta - pL^2\int_o^1 (hZ_n)'X_m'd\zeta \qquad (C.10b)$$

$$C_{mn} = Qe\int_o^1 X_n'Z_m'd\zeta - pL^2\int_o^1 (hZ_m)'X_n'd\zeta \qquad (C.10c)$$

$$D_{mn} = \frac{EC_w}{L^2}\lambda_z^4\,\delta_{nm}\int_o^1 Z_m^2 d\zeta + (GK+Qe^2)\int_o^1 Z_n'Z_m'd\zeta - pL^2e\int_o^1 \bar{h}Z_nZ_m d\zeta + FL^2\int_o^1 Z_nZ_m d\zeta \qquad (C.10d)$$

Eqs. C.6 or C.10 may be used to compute the coefficients. From the latter we observe that A_{mn} and D_{mn} constitute symmetrical matrices and B_{mn} is the transpose of C_{mn}. With matrix description Eqs. C.5 become

$$[A_{mn}]\{u_n\} + [B_{mn}]\{\phi_n\} = \{E_m\} \qquad (C.11a)$$

$$[C_{mn}]\{u_n\} + [D_{mn}]\{\phi_n\} = \{F_m\} \qquad (C.11b)$$

Solving Eq. C.11a for u_n

$$u_n = A_{mn}^{-1}\{E_m - B_{mn}\,\phi_n\} \qquad (C.12a)$$

Substituting this into Eq. C.11b

$$[D_{mn} - C_{mn}\,A_{mn}^{-1}\,B_{mn}]\phi_n = \{F_m - C_{mn}\,A_{mn}^{-1}\,E_m\} \qquad (C.12b)$$

Note that the coefficient matrix in Eq. C.12b is still symmetrical since A_{mn}^{-1} had a congruent transformation. ϕ_n can be found from Eq. C.12b. Then substituting back into Eq. C.12a determines u_n.

Alternatively one may consider Eqs. C.11a and b as one system. In that case the coefficient matrix may be defined

as follows. (Since $C_{mn} = B_{nm}$, this matrix also is symmetrical).

$$\begin{bmatrix} A_{11} & B_{11} & A_{12} & B_{12} & \cdots \\ C_{11} & D_{11} & C_{12} & D_{12} & \\ A_{21} & B_{21} & A_{22} & B_{22} & \\ C_{21} & D_{21} & C_{22} & D_{22} & \\ \vdots & & & \ddots & \end{bmatrix} \begin{Bmatrix} u_1 \\ \phi_1 \\ u_2 \\ \phi_2 \\ \vdots \end{Bmatrix} = \begin{Bmatrix} E_1 \\ F_1 \\ E_2 \\ F_2 \\ \vdots \end{Bmatrix} \qquad (C.13)$$

Hence the deflection components u_n and ϕ_n may be found from Eqs. C.12 or C.13.

The vertical deflection may be found as follows:

$$EI_x \frac{d^2v}{dz^2} = -M_x + EI_{xy} \frac{d^2u}{dz^2} \qquad (C.14)$$

Integrating twice

$$EI_x v = C_o + C_1 z - \int M_x dz^2 + EI_{xy} \sum_{n=1}^{N} u_n X_n \qquad (C.15)$$

where the constants C_o and C_1 are determined from the boundary conditions.

If $I_{xy} = 0$, the vertical deflection is uncoupled from u and ϕ.

Discussion:

The coefficients A_{mn} through D_{mn} for the unbraced case may be found by substituting $Q = 0$ into Eqs. C.12 or C.13. However, the solution presented in the following section should converge faster. On the other hand, the coefficients

for the rigidly braced case cannot be obtained directly from C.12 or C.13. Dividing both sides of Eqs. C.11a and b by Q and setting 1/Q = 0 does not help either. In that case the right hand side becomes zero, i.e., $E_m = F_m = 0$. For the left hand side, inspecting Eqs. C.6 and granting that $X_i = Z_i$ (since the unknowns ϕ and u are no longer independent because $u = -\phi e$) it follows that

$$A_{mn} = e\, B_{mn} = e\, C_{mn} = e^2\, D_{mn}$$

Substituting these into Eq. C.12b results in

$$[o]\{\phi_n\} = \{o\}$$

Hence ϕ_n remains undetermined. The indeterminancy could be eliminated if Eqs. C.11 were first solved without substituting a numerical value for Q. Arranging the determinants D_j and D as polynomials of Q

$$\phi_j = \frac{D_j}{D} = \frac{a_{j,o}+a_{j,1}Q+a_{j,2}Q^2+\ldots+a_{j,n-1}Q^{n-1}}{b_o+b_1Q+b_2Q^2+\ldots.+b_{n-1}Q^{n-1}+b_nQ^n}$$

where $a_{j,n}$ and b_n are some constants. The constant b_n is zero, because it is equal to the following determinant (see Eq. C.6)

$$b_n = \begin{vmatrix} -\int_o^1 X_n''X_m\,d\zeta - e\int_o^1 Z_n''X_m\,d\zeta \\ -e\int_o^1 X_n''Z_m\,d\zeta - -e^2\int_o^1 Z_n''Z_m\,d\zeta \end{vmatrix}$$

This determinant is zero for $X_i = Z_i$. Thus, ϕ_j becomes equal to the ratio of two polynomials of the same order. If we now

let Q approach infinity, we get in the limit

$$\phi_j = \frac{a_{j,n-1}}{b_{n-1}}$$

A direct solution for the rigid bracing case will be obtained from Eq. B.23 as will be shown in section C3.

C2 Solution for Unbraced Case, i.e., Q = 0

Applying the Galerkin Method to Eq. 2.11, we obtain

$$\sum_{n=1}^{\infty} \phi_n \int_o^1 \{\frac{EC_w}{L^2} Z_n^{IV} - GK Z_n'' - (p_y e + \frac{I_x M_x^2}{E(I_x I_y - I_{xy}^2)} + F)L^2 Z_n\} Z_n d\zeta$$

$$= \int_o^1 [p_y a - \frac{I_{xy} M_x^2}{E(I_x I_y - I_{xy}^2)}] L^2 Z_m d\zeta \qquad (C.16)$$

$$m = 1, 2, \ldots \infty$$

with Eqs. C.7a and b

$$\sum_{n=1}^{\infty} \phi_n \{\frac{EC_w}{L^2} \lambda_z^4 \int_o^1 Z_n Z_m d\zeta - GK \int_o^1 Z_n'' Z_m d\zeta - pL^2 e \int_o^1 \bar{h} Z_n Z_m d\zeta$$

$$+ FL^2 \int_o^1 Z_n Z_m d\zeta - \frac{I_x (pL^2)^2 L^2}{E(I_x I_y - I_{xy}^2)} \int_o^1 h^2 Z_n Z_m d\zeta\} = pL^2 a \int_o^1 \bar{h} Z_m d\zeta$$

$$- \frac{I_{xy} (pL^2)^2 L^2}{E(I_x I_y - I_{xy}^2)} \int_o^1 h^2 Z_m d\zeta \qquad (C.17)$$

$$m = 1, 2, \ldots \infty$$

Let

$$T_{10} = \int_o^1 h^2 Z_n Z_m d\zeta \qquad (C.18a)$$

$$T_{103} = \int_o^1 h^2 Z_m d\zeta \qquad (C.18b)$$

In matrix form

$$[D_{mn}]\{\phi_n\} = \{F_m\} \tag{C.19}$$

where

$$D_{mn} = \frac{EC_w}{L^2}\lambda_z^4 T_7 - GK\, T_8 - pL^2 e\, T_9 + FL^2 T_7 - \frac{I_x(pL^2)^2L^2}{E(I_xI_y - I_{xy}^2)} T_{10} \tag{C.20a}$$

$$F_m = pL^2 a\, T_{102} - \frac{I_{xy}(pL^2)^2\, L^2}{E(I_xI_y - I_{xy}^2)}\, T_{103} \tag{C.20b}$$

and T_i is given in Eqs. C.9 and C.18.

Hence the angle of rotation is determined in series form

$$\phi = \sum_{n=1}^{N} \phi_n Z_n \tag{C.21}$$

where N is the number of terms considered.

The curvature for the lateral deflection u" is obtained from Eq. B.20.

$$u'' = \frac{L^2}{E(I_xI_y - I_{xy}^2)}\left(-M_xI_x \sum_{n=1}^{N} \phi_n Z_n + I_{xy} M_x\right) \tag{C.22}$$

Having the curvatures, we are able to determine the normal stress using Eq. 2.19.

If the lateral and vertical deflections are required we may follow one of two ways: the first is to integrate Eq. C.22 twice

$$u = C_o + C_1 L\zeta + \frac{L^2}{E(I_xI_y - I_{xy}^2)}\left(-I_x \sum_{n=1}^{N} \phi_n \iint M_x Z_n d\zeta^2 + I_{xy}\iint M_x d\zeta^2\right) \tag{C.23}$$

However, the functions resulting from these integrations may be cumbersome. The second way is to apply Galerkin's Method

also to Eq. B.19a. Then

$$\sum_{n=1}^{\infty} \int_o^1 \frac{E(I_x I_y - I_{xy}^2)}{I_x L^2} u_n X_n^{IV} + (M_x Z_n)'' \phi_n X_m d\zeta$$

$$= -\frac{I_{xy}}{I_x} L^2 \int_o^1 p_y X_m d\zeta \qquad (C.24)$$

Let

$$A_{mn} = \frac{E(I_x I_y - I_{xy}^2)}{I_x L^2} \lambda_x^4 T_1 \qquad (C.25a)$$

$$B_{mn} = pL^2 T_5 \qquad (C.25b)$$

$$E_m = -\frac{I_{xy}}{I_x} pL^2 T_{101} \qquad (C.25c)$$

Solving Eq. C.24 for u_n gives

$$\{u_n\} = [A_{mn}]^{-1} \{E_m - [B_{mn}]\{\phi_n\}\} \qquad (C.26)$$

Note that A_{mn} is just a diagonal matrix. Thus, we have also the lateral deflection in series form.

$$u = \sum_{n=1}^{N} u_n X_n \qquad (C.27)$$

The vertical deflection can be found from Eq. C.15.

C3 Solution for Rigid Bracing Case, i.e., Q = ∞

The differential equation for this case was given by Eq. 2.14

$$\sum_{n=1}^{\infty} \phi_n \int_o^1 \{ \frac{EC_w'}{L^2} Z_n^{IV} - GK Z_n'' + FL^2 Z_n - M_x Z_n'' e - (M_x Z_n)'' e$$

$$- p_y e L^2 Z_n \} Z_m d\zeta = (a + \frac{I_{xy}}{I_x} e) L^2 \int_o^1 p_y Z_m d\zeta$$

$$m = 1, 2, \ldots \infty \qquad (C.28)$$

$$\sum_{n=1}^{\infty} \phi_n \left\{\left(\frac{EC_w'}{L^2}\lambda_z^4 + FL^2\right)\int_o^1 Z_n Z_m d\zeta - GK\int_o^1 Z_n'' Z_m d\zeta \right.$$

$$- pL^2 e\int_o^1 hZ_n'' Z_m d\zeta - pL^2 e\int_o^1 (hZ_n)'' Z_m d\zeta$$

$$\left. - pL^2 e\int_o^1 \bar{h} Z_n Z_m d\zeta\right\} = \left(a + \frac{I_{xy}}{I_x} e\right) pL^2 \int_o^1 \bar{h} Z_m d\zeta \qquad (C.29)$$

$$m = 1, 2, \ldots \infty$$

Let

$$D_{mn} = \left(\frac{EC_w'}{L^2}\lambda_z^4 + FL^2\right) T_7 - GK\, T_8 - peL^2\,(T_5 + T_6 + T_9) \qquad (C.30a)$$

$$F_m = \left(a + \frac{I_{xy}}{I_x} e\right) pL^2\, T_{102} \qquad (C.30b)$$

Again the problem is reduced to the solution of an algebraic equation system.

$$[D_{nm}]\{\phi_n\} = \{F_m\} \qquad (C.31)$$

Hence the angle of rotation is

$$\phi = \sum_{n=1}^{N} \phi_n Z_n \qquad (C.32)$$

The lateral deflection is simply

$$u = -e\phi \qquad (C.33)$$

The vertical deflection is given by Eq. C.15.

C4 Evaluation of the Integrals

The expressions for the displacements v, u and ϕ have been developed in Sections C1 through C3. They are valid for

a continuous but arbitrary distribution of p_y and for a number of boundary conditions, which may be different for u, v and ϕ. They can be utilized once the values of the definite integrals T_i are known. In this section, these integrals will be evaluated for some specific boundary conditions. For some cases also the coefficients A_{mn}, B_{mn}, etc. will be given after substitution of T_i into them. In the following the load is taken uniformly distributed. Hence

$$p_y = p,\ \bar{h} = 1,\ h = C_o + C_1\zeta - \frac{\zeta^2}{2}$$

For similar boundary conditions $X_n = Z_n$. Hence from Eqs. C.9

$$T_1 = T_7 = T_9$$

$$T_2 = T_3 = T_4 = T_5$$

$$T_{101} = T_{102}$$

C4.1 Hinged boundary

$$v = v'' = 0$$

$$u = u'' = 0 \quad \text{at } \zeta = 0,\ 1 \qquad \text{(C.34)}$$

$$\phi = \phi'' = 0$$

The primary bending moment is

$$M_x = \frac{pL^2}{2}(\zeta - \zeta^2) \qquad \text{(C.35a)}$$

$$h = \frac{1}{2}(\zeta - \zeta^2) \qquad \text{(C.35b)}$$

The eigenfunctions

$$X_n = Z_n = \sin n\pi\zeta \quad n = 1, 3, 5, \ldots \tag{C.36a}$$

$$\lambda_x = \lambda_z = n\pi \tag{C.36b}$$

The integrals T_i from Eqs. C.9 and C.18 are evaluated below

$$T_1 = T_7 = T_9 = \delta_{nm}\int_o^1 \sin^2 n\pi\zeta \, d\zeta = \frac{1}{2}\delta_{nm} \tag{C.37a}$$

$$T_2 = T_3 = T_4 = T_8 = -m^2\pi^2\int_o^1 \sin n\pi\zeta \sin m\pi\zeta \, d\zeta = -\frac{m^2\pi^2}{2}\delta_{nm} \tag{C.37b}$$

$$T_5 = \frac{1}{2}\int_o^1 [(\zeta-\zeta^2)\sin n\pi\zeta]''\sin m\pi\zeta \, d\zeta = \frac{1}{2}\begin{cases} -\frac{m^2\pi^2}{12} - \frac{1}{4} & \text{if } m = n \\ \frac{4m^3n}{(m^2-n^2)^2} & \text{if } m \neq n \end{cases} \tag{C.37c}$$

$$T_6 = \frac{1}{2}\int_o^1 (\zeta-\zeta^2)(-n^2\pi^2)\sin n\pi\zeta \sin m\pi\zeta \, d\zeta = \frac{1}{2}\begin{cases} \frac{-m^2\pi^2}{12} - \frac{1}{4} & \text{if } m=n \\ \frac{4mn^3}{(m^2-n^2)^2} & \text{if } m\neq n \end{cases}$$

$$T_{10} = \frac{1}{4}\int_o^1 (\zeta-\zeta^2)^2 \sin n\pi\zeta \sin m\pi\zeta \, d\zeta = \tag{C.37d}$$

$$T_{101} = T_{102} = \int_o^1 \sin m\pi\zeta \, d\zeta = \frac{2}{m\pi} \tag{C.37f}$$

$$T_{103} = \frac{1}{4}\int_o^1 (\zeta-\zeta^2)^2 \sin m\pi\zeta \, d\zeta =$$

a) General case

The coefficients were given in Eqs. C.6

$$A_{mn} = \left[\frac{E(I_x I_y - I_{xy}^2)}{I_x L^2} \frac{m^4\pi^4}{2} + Q \frac{m^2\pi^2}{2}\right]\delta_{nm} \qquad \text{(C.38a)}$$

$$B_{mn} = \left[Qe \frac{m^2\pi^2}{2} - \frac{pL^2}{2}\left(\frac{m^2\pi^2}{12} + \frac{1}{4}\right)\right]\delta_{nm} + \frac{pL^2}{2} \frac{4m^3 n}{(m^2-n^2)^2}(1-\delta_{nm}) \qquad \text{(C.38b)}$$

$$C_{mn} = \left[Qe \frac{m^2\pi^2}{2} - \frac{pL^2}{2}\left(\frac{m^2\pi^2}{12} + \frac{1}{4}\right)\right]\delta_{nm} + \frac{pL^2}{2} \frac{4mn^3}{(m^2-n^2)^2}(1-\delta_{nm}) \qquad \text{(C.38c)}$$

$$D_{mn} = \left[\frac{EC_w}{L^2} \frac{m^4\pi^4}{2} + (GK + Qe) \frac{m^2\pi^2}{2} - \frac{peL^2}{2} + \frac{FL^2}{2}\right]\delta_{nm} \qquad \text{(C.38d)}$$

$$E_m = -\frac{I_{xy}}{I_x} \frac{2pL^2}{m\pi} \qquad \text{(C.38e)}$$

$$F_m = a \frac{2pL^2}{m\pi} \qquad \text{(C.38f)}$$

where $n = 1, 3, 5, \ldots$

$m = 1, 3, 5, \ldots$

For this case $[A_{mn}]$ and $[D_{nm}]$ are diagonal matrices.

b) No bracing, i.e. Q = 0

The coefficients necessary for ϕ_n (Eqs. C.20)

$$D_{mn} = \left(\frac{EC_w}{L^2} \frac{m^4\pi^4}{2} + GK \frac{m^2\pi^2}{2} - \frac{pL^2 e}{2} + \frac{FL^2}{2}\right)\delta_{nm} - \frac{I_x L^2 (pL^2)^2}{E(I_x I_y - I_{xy}^2)} T_{10} \qquad \text{(C.39a)}$$

$$F_m = a \frac{2pL^2}{m\pi} - \frac{I_{xy} L^2 (pL^2)^2}{E(I_x I_y - I_{xy}^2)} T_{103} \qquad \text{(C.39b)}$$

The coefficients for u_n (Eqs. C.25)

$$A_{mn} = \frac{E(I_x I_y - I_{xy}^2)}{I_x L^2} \frac{m^4\pi^4}{2} \delta_{nm} \qquad (C.40a)$$

$$B_{mn} = \frac{pL^2}{2}\left[-\left(\frac{m^2\pi^2}{12} + \frac{1}{4}\right)\delta_{nm} + \frac{4m^3 n}{(m^2-n^2)^2}(1-\delta_{nm})\right] \qquad (C.40b)$$

$$E_m = -\frac{I_{xy}}{I_x}\frac{2pL^2}{m\pi} \qquad (C.40c)$$

c) Rigid bracing, i.e. $Q = \infty$

From Eqs. C.30

$$D_{nm} = \left[\frac{EC'_w}{L^2} m^4\pi^4 + GK\, m^2\pi^2 + FL^2 + pL^2 e\left(\frac{m^2\pi^2}{6} - \frac{1}{2}\right)\right]\frac{\delta_{nm}}{2} - \frac{pL^2}{2} e \frac{4mn(m^2+n^2)}{(m^2-n^2)^2}(1-\delta_{nm}) \qquad (C.41a)$$

$$F_m = \left(a + \frac{I_{xy}}{I_x} e\right)\frac{2pL^2}{m\pi} \qquad (C.41b)$$

C5 Summary

Galerkin's Method has been used to solve the differential equations for the diaphragm braced I, channel or Z beams and for the two special cases of no bracing and rigid bracing. The displacements u and ϕ have been expressed in infinite series.

$$u = \sum_1^\infty u_n X_n \qquad (C.3a)$$

$$\phi = \sum_1^\infty \phi_n Z_n \qquad (C.3b)$$

X_n and Z_n are chosen to be the eigenfunctions of a vibration problem with the same boundary conditions as the beam. The differential equations are converted into algebraic equation

systems of the following form

a) General case, i.e. $0 < Q < \infty$

$$[A_{mn}]\{u_n\} + [B_{mn}]\{\phi_n\} = \{E_m\} \tag{C.11a}$$

$$[C_{mn}]\{u_n\} + [D_{mn}]\{\phi_n\} = \{F_m\} \tag{C.11b}$$

where

$$A_{mn} = \frac{E(I_x I_y - I_{xy}^2)}{I_x L^2} \lambda_x^4 T_1 - Q T_2 \tag{C.8a}$$

$$B_{mn} = -Qe T_3 + pL^2 T_5 \tag{C.8b}$$

$$C_{mn} = -Qe T_4 + pL^2 T_6 \tag{C.8c}$$

$$D_{mn} = \frac{EC_w}{L^2} \lambda_z^4 T_7 - (GK+Qe^2) T_8 - pL^2 e T_9 + FL^2 T_7 \tag{C.8d}$$

$$E_m = -\frac{I_{xy}}{I_x} pL^2 T_{101} \tag{C.8e}$$

$$F_m = apL^2 T_{102} \tag{C.8f}$$

b) No bracing, i.e. $Q = 0$

$$[D_{mn}]\{\phi_n\} = \{F_m\} \tag{C.19}$$

and

$$\{u_n\} = [A_{mn}]^{-1} \{E_m - [B_{mn}]\{\phi_n\}\} \tag{C.26}$$

where

$$A_{mn} = \frac{E(I_x I_y - I_{xy}^2)}{I_x L^2} \lambda_x^4 T_1 \tag{C.25a}$$

$$B_{mn} = pL^2 T_5 \tag{C.25b}$$

$$D_{mn} = \frac{EC_w}{L^2} \lambda_z^4 T_7 - GK T_8 - pL^2 e T_9 + FL^2 T_7 - \frac{I_x (pL^2)^2 L^2}{E(I_x I_y - I_{xy}^2)} T_{10} \tag{C.20a}$$

$$E_m = -\frac{I_{xy}}{I_x} pL^2 T_{101} \qquad (C.25c)$$

$$F_m = pL^2 a T_{102} - \frac{I_{xy}(pL^2)^2 L^2}{E(I_x I_y - I_{xy}^2)} T_{103} \qquad (C.20b)$$

c) Rigid bracing, i.e. $Q = \infty$

$$[D_{mn}]\{\phi_n\} = \{F_m\} \qquad (C.31)$$

and

$$u = -e\phi \qquad (C.33)$$

where

$$D_{mn} = \frac{EC'_w}{L^2} \lambda_z^4 T_7 - GK T_8 - pL^2 e(T_5+T_6+T_9) + FL^2 T_7 \qquad (C.30a)$$

$$F_m = (a + \frac{I_{xy}}{I_x} e)pL^2 T_{102} \qquad (C.30b)$$

The integrals T_1 through T_{103} are defined by Eqs. C.9 and C.18. They have been evaluated for simply supported boundary conditions and uniformly distributed loads in Eqs. C.37.

APPENDIX D

TEST PROCEDURE FOR THE DETERMINATION OF F_{local}

Since the local deformations depend on the connection detail and on the type of deck panel, it is proposed to find the corresponding rotational restraint F_{local} experimentally. A possible test set-up is shown in Fig. 29. A segment of the purlin is fixed to a rigid support. One panel width of deck is fastened to the purlin. At each edge of the panel, an overlap similar to that in the actual structure is provided. This simulates the continuous nature of the roof decking. The screws are aligned at a certain distance from the web.

The rotational deformation is enforced by loading the roof deck panel by hung weights. At the edge where the weights are applied, a light stiffening angle parallel to the purlin segment is used to obtain a uniform deflection of the end of the cantilevering panel.

In Fig. 29, the panel is extended at both sides of the purlin to provide two possibilities for hanging the weights. When the weights are hung at the right side as in Fig. 29, the direction of the rotation corresponds to that from uplift loading of channel purlins. On the other hand, loading at the left side would simulate the rotations from gravity loading.

δ_{exp}, the total deflection of point A (Fig. 30) is measured during testing. δ_b, the deflection of point A of the diaphragm acting as a cantilever beam, can be calculated from stan-

dard formulae. Subtracting δ_b from δ_{exp}, deflection δ_{local} due to local deformation and hence ϕ_{local} can be obtained. The slope of the experimental curve of cantilever moment per unit width (pl/w) versus ϕ_{local} gives the value of rotational restraint F_{local}.

A limited number of such tests were performed on the narrow ribbed light-gage steel panel with the dimensions shown on Fig. 79. The results of such a test on a panel with screws placed 1/2 inch from the web is given in Fig. 90 (Since the corners of the purlin are rounded, the real distance of the screws from the contact point between the diaphragm and the purlin is somewhat smaller than 1/2 inch). This test gave F = .060 in-k/in/rad. On the other hand, for a distance of 1.0 inch from the web, the rotational restraint was F = .180 in-k/in/rad.

The test should duplicate the connection detail of the structure as close as possible. If in the real structure, the screws are placed randomly, it would be desirable to find F_{local} for two different screw locations, in order to get an idea of how much F is affected by changing the screw location. If insulation material is used between purlin and diaphragm, the test should be performed after a certain period of time so that any loosening in the connections due to creep of the insulation is accounted for in the determination of F.

The influence of F on the behavior of channel and Z-section purlins was discussed in Sec. 3.3. Here, it may be noted that the value of F is different for uplift and gravity loads unless the screws are placed exactly at the middle of the flange. For

example, F obtained by the test shown on Fig. 90 presents an alternative test set-up for measuring F_{local} (of Fig. 29). It is valid only for gravity loading, since the stipulated direction of the rotation between the purlin and diaphragm is that for the gravity loading case.

APPENDIX E

FLOW CHART OF THE COMPUTER PROGRAM

E1. General

The overall flow chart is given below. Some of the individual blocks of this flow chart are explained subsequently and some important parameters are defined. In particular, a more detailed flow chart of the block for determination of the failure load is presented.

E2. Overall Flow Chart

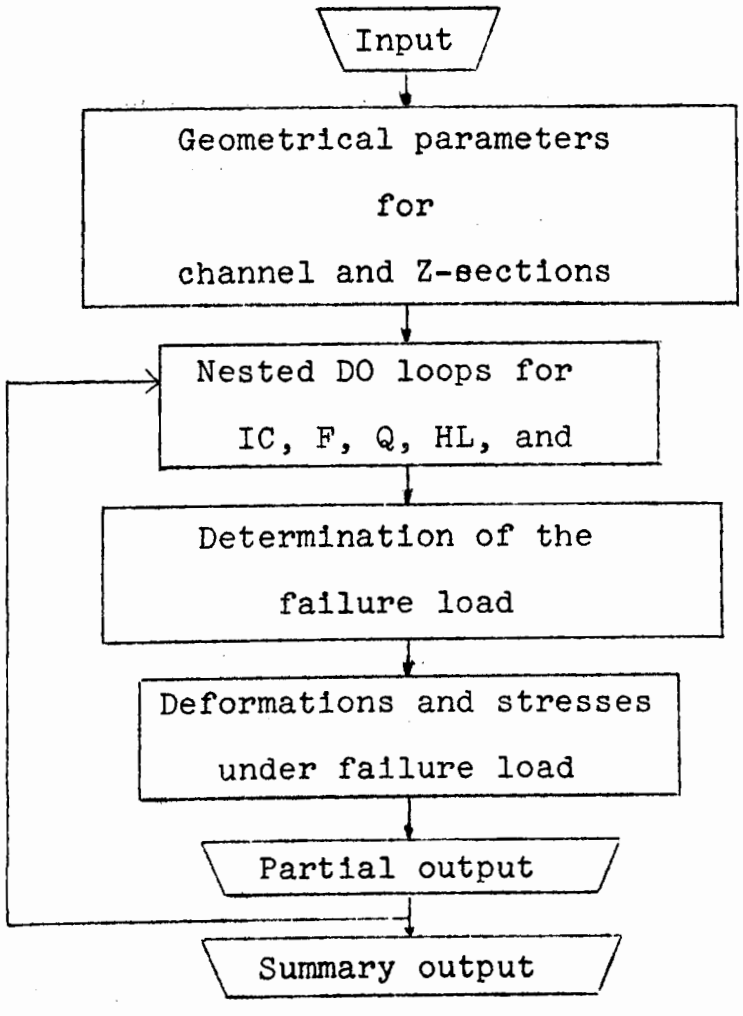

E3. Input, output

Input serves many purposes. These are: (a) Initialization of some parameters, (b) setting the limits of the DO loops, (c) storing the matrices consisting of the values of the definite integrals due to Galerkin's method, and (d) reading the dimensions of the cross-section under consideration.

Output consists of several parts: (a) After finding the failure load for one case, the stresses and values of some integer parameters indicating the flow in the program are printed. (b) After completion of a group of cases for different values of Q and the span length L, a partial summary is printed which includes the values of the yield moment as well as the maximum values of the deformations u and ϕ. (c) A summary table for the ratio of yield moment to M_{bend} and the maximum angle of rotation ϕ is given for gravity and uplift loading cases. The corner where the start of yielding occurred is also indicated.

E4. Definitions

The parameters controlling the do loops are

NPRB = Number of cross-sections

NIC = Number of cases concerning

a) The horizontal distance of the load from the shear center, a = HA

b) The direction of the load, i.e.

IC = 1 for gravity

IC = 2 for uplift

NQF = Number of cases for the rotational rigidity F

IQM = Number of cases for the shear rigidity Q

IHM = Number of cases for the span length L = HL

Some other important paramters are:

M = MM2/2 = Number of series terms considered for each displacement component

L = in general, indicates the index of the corner where stress is equal to σ_{yd}

L = 7 means $\phi = \phi_{limit}$ while $\sigma_i < \sigma_{yd}$

L = 8 means the attempt to find the failure load was unsuccessful

LS = Index of the corner with the largest stress in absolute value

Parameters MJ and MP are discussed in the next section in some detail.

E5. Explanation of the Flow Chart for Failure Load Determination

The flow chart for failure load determination is given in Section E6. Here, some explanation is given to facilitate understanding of this flow chart.

There are two criteria for failure:

1. The maximum angle of rotation $\phi = \phi_{limit}$ can be specified (say 30^{o}).

2. The stress at one of the corners in the governing cross-section is equal to the yield stress.

These criteria may be symbolized as

$$\phi(p) = 0$$

$$\sigma_i(p) = 0 \quad \text{where}$$

$i = 1,2,....,6$ for lipped sections

$i = \quad 2,....,5$ for plain sections

The failure load is determined by successive approximations, starting with a first estimate as

$$\bar{p} = \frac{1}{2} p_{cr} \text{ or } \bar{p} = \pm .6 M_{bend} \frac{8}{L^2}$$

whichever is smaller. p_{cr} is the approximate critical load obtained by setting the main determinant of the equation system equal to zero for MM2 = 2 (see Eq. 4.2). The sign of $\bar{p}$ is positive for gravity and negative for uplift cases, respectively.

The determination of the failure load proceeds in two steps:

1. The values of the functions $\phi(\bar{p})$ and $\sigma_i(\bar{p})$ are computed for at least two $\bar{p}$'s, until there is a change of sign in either $\phi(\bar{p})$ or in any one of $\sigma_i(\bar{p})$. In every cycle, $\bar{p}$ is decreased or increased by $\bar{p}$, whichever brings $\bar{p}$ closer to the zero point of the functions $\phi(\bar{p})$ or $\sigma_i(\bar{p})$. The increment at the beginning is

$$\delta\bar{p} = \frac{1}{2} \bar{p}$$

In the subsequent cycles, however, the value of the increment is taken as half of that for the previous cycle. Of course, a limit for the number of cycles is provided. Hence, if there is no change in the sign of the above mentioned functions within the set limit, the problem is abandoned and the next case is considered. This situation arises when the first estimate $\bar{p}$ and/or the increment $\delta\bar{p}$ are too large or too small when compared to the final value p_{fail}. Hence, the situation may be remedied by substituting better estimates for $\bar{p}$ and $\delta\bar{p}$.

2. Once a sign change occurs, the next value of $\bar{p}$ is found

by linear interpolation. If the sign change occurs in $\sigma_i(\bar{p})$ for one particular value of i = L, linear interpolation is performed only on $\sigma_L(\bar{p})$. If the sign change occurs simultaneously in more than one value of i, the one giving the largest stress is selected as i = L.

The flow of the program is mainly controlled by the two integer parameters MJ and MP. The determination of the failure load proceeds with MJ = 1. The parameter MP determines the details of the flow.

a) MP = 1: First, check ϕ. If $\phi < 0$ set MP = 5. If $\phi > 0$ check σ_i for i=1,...,6. If $\sigma_i < \sigma_y$ increase $\bar{p} = \bar{p} + \delta\bar{p}$, repeat the cycle. If $\sigma_i > \sigma_y$ set MP = 2.

b) MP = 5: Check whether there is a change in the sign of ϕ (needed in case entry is not through MP = 1). If there is none, change the load $\bar{p}$ and repeat. If there is, set MP = 3.

c) MP = 2: Find the yield load by linear interpolation. Set MJ = 2.

d) MP = 3: Find the load for $\phi = \phi_{limit}$ by linear interpolation Set MJ = 2.

For MJ = 2, the program skips the parts described above and proceeds to the determination of stresses.

There is a final checking of the stresses and the angle of rotation ϕ. If the check is unsatisfactory for σ_i, then MP = 4 and if it is unsatisfactory for ϕ, MP = 5; in addition, MJ = 1 and the control returns to the beginning of the block for failure load. If the checks are satisfactory, some of the results

are printed, some of them are stored for the summary table, and one proceeds to the next case.

For MJ = 3, the whole failure determination part of the program is bypassed. This can be useful if the deflections and stresses are sought under a given load (For example, under service loads obtained by dividing the failure load by a constant).

E6. Flow Chart for Failure Load Determination

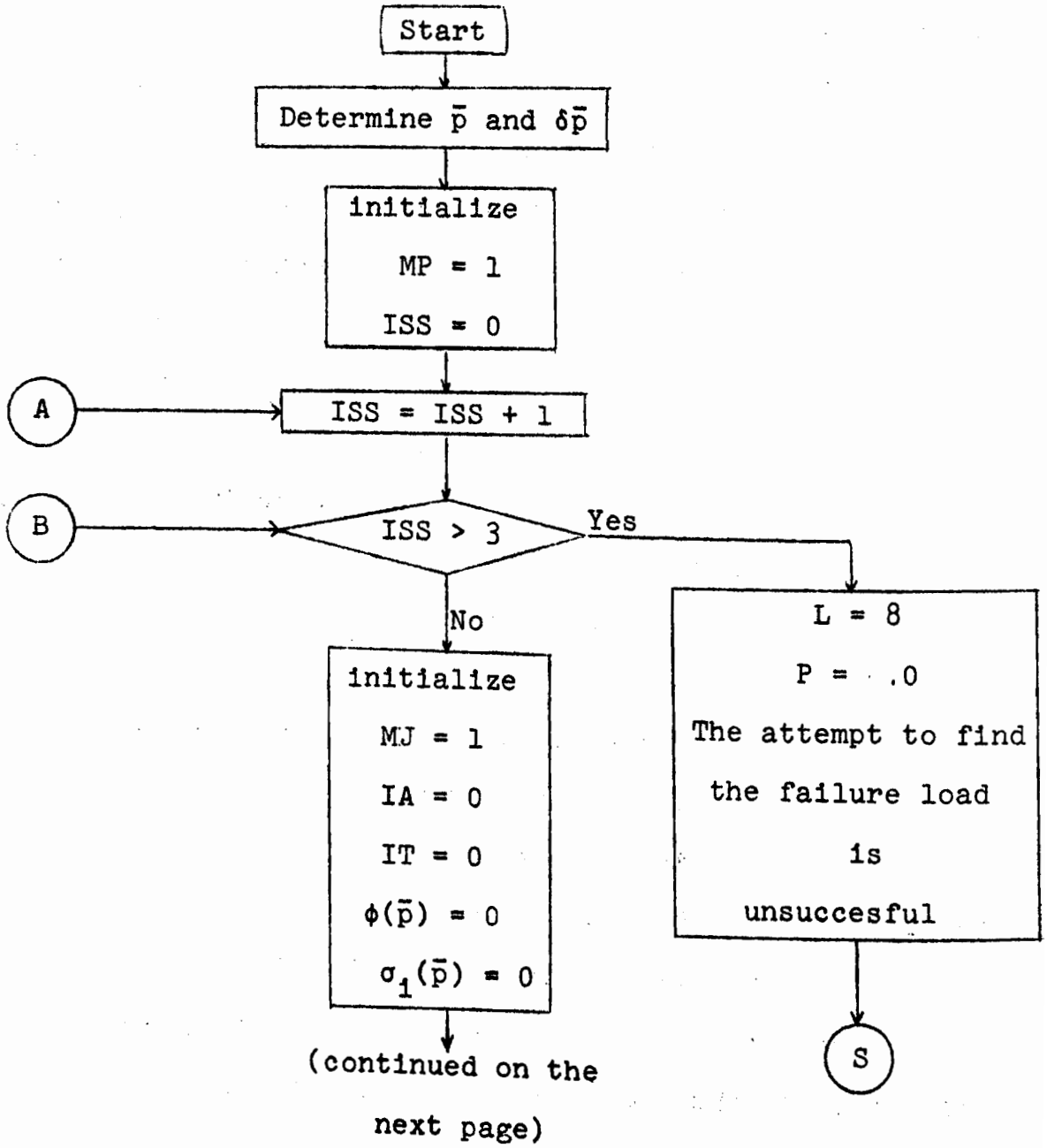

(continuation)

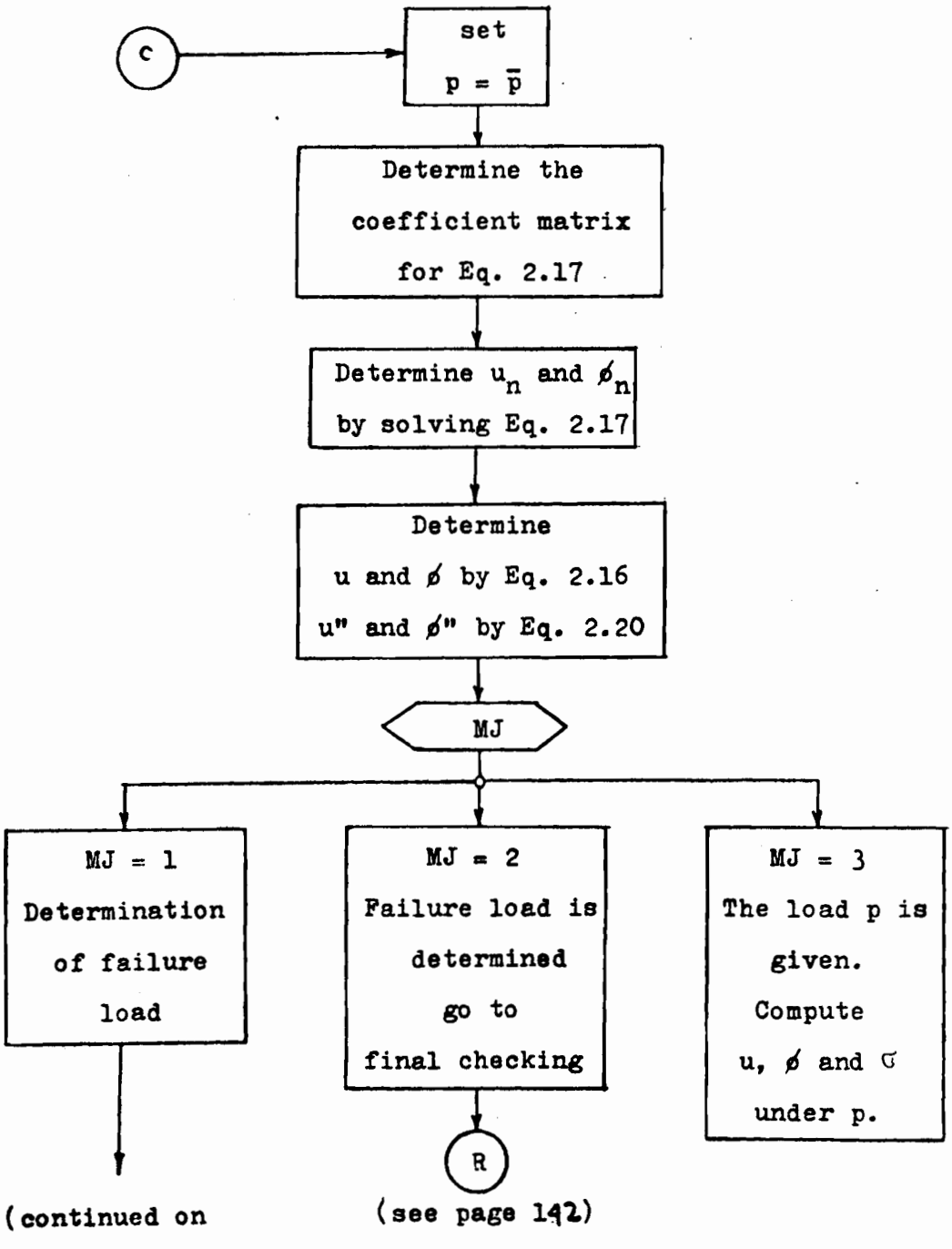

(continued on the next page)

(see page 142)

(continuation)

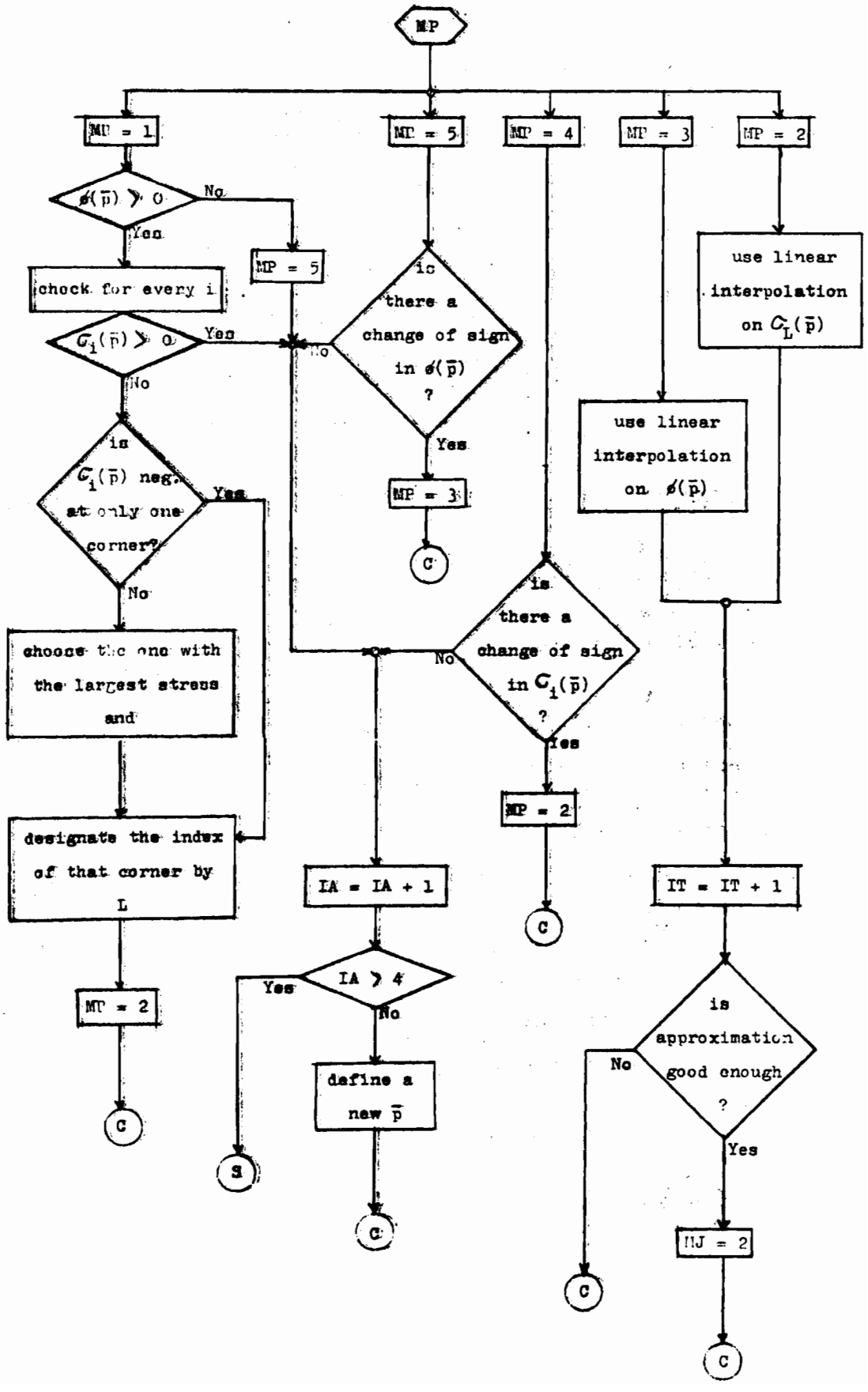

continuation

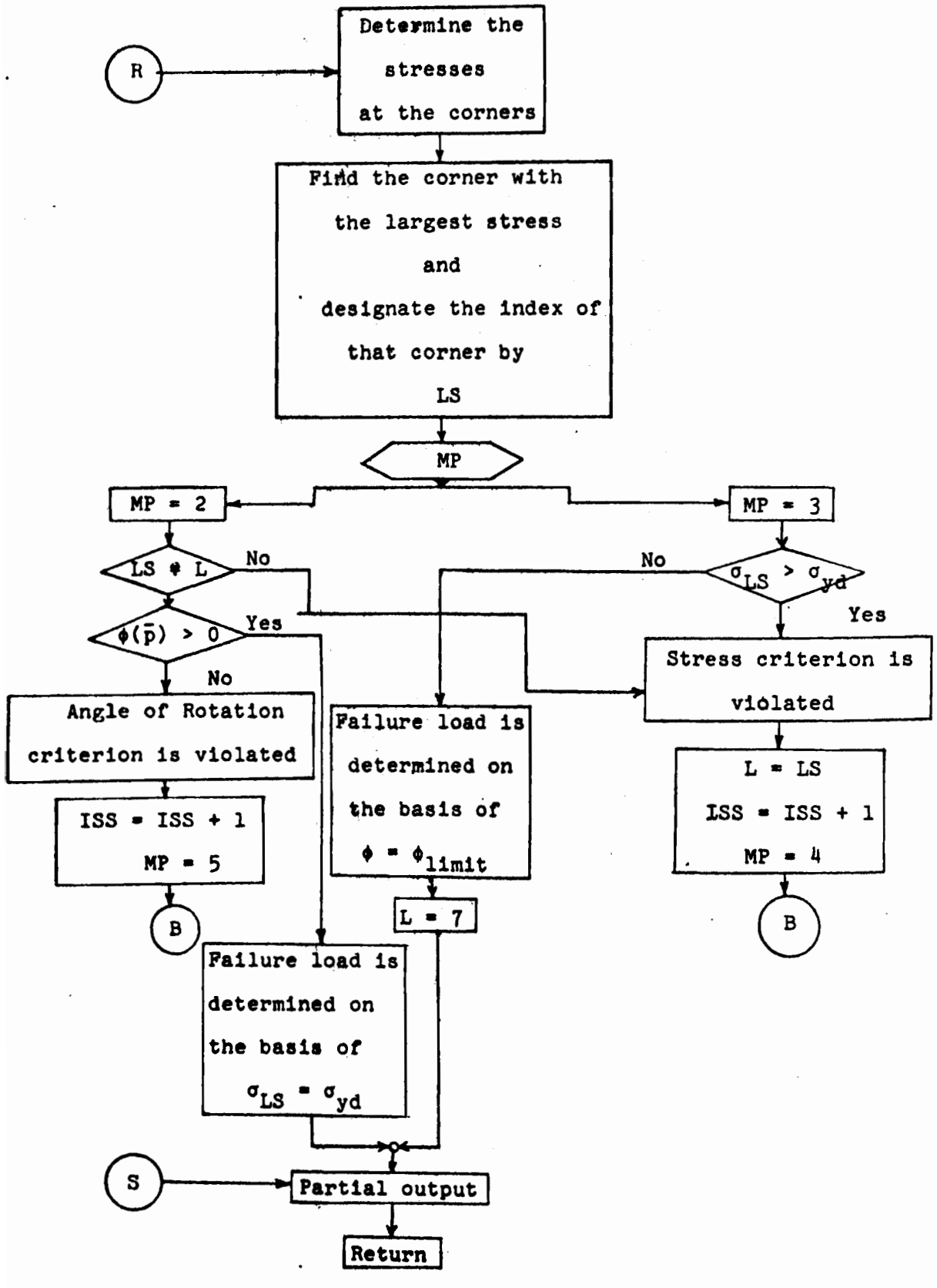

APPENDIX F

FORMULA FOR M/M_{bend}

In Figures 16 through 19 the ratio M/M_{bend} versus span length L is plotted where $M = pL^2/8$ and p is the load causing failure which was defined as the maximum stress attaining a value of $1.15\,\sigma_y$. M_{bend} is the capacity of a beam whose rotations and lateral deflections are eliminated by appropriate bracing, i.e., $M_{bend} = \frac{I_x \sigma_y}{d}$. Here, the value of M/M_{bend} at $L = 0$ will be computed.

Consider Eq. 2.19. Since we demand that the stress is equal to $1.15\,\sigma_y$, the bending moment $M_x = M$ must remain finite as L approaches zero. Next it will be shown that also $\frac{u_n}{L^2}$ and $\frac{\phi_n}{L^2}$ (consequently $\frac{u''}{L^2}$ and $\frac{\phi''}{L^2}$) remain finite.

F1 No Bracing Case

From Eq. C.19

$$L^2[D_{mn}]\{\frac{\phi_n}{L^2}\} = \{F_m\}$$

where for $L = 0$

$$L^2\, D_{mn} = EC_w\, \lambda_z^{\,4}\, T_7 \qquad \text{(from Eq. C.20a)}$$

$$F_m = 8M\, a\, T_{102} \qquad \text{(from Eq. C.20b)}$$

hence

$$\{\frac{\phi_n}{L^2}\} = \frac{8M\, a}{EC_w}\,[\lambda_z^{\,4}\, T_7]^{-1}\{T_{102}\} \qquad \text{(F.1a)}$$

From Eq. C.26

$$\{\frac{u_n}{L^2}\} = \frac{1}{L^2}[A_{mn}]^{-1}\, E_m - L^2[B_{mn}]\{\frac{\phi_n}{L^2}\}$$

where

$$\frac{1}{L^2}[A_{mn}]^{-1} = \frac{I_x}{E(I_xI_y-I_{xy}^2)}\,[\lambda_x^4\ T_1]^{-1}$$

(from Eq. C.25a)

$$L^2\ B_{mn} = 0\cdot 8M\ T_5 = 0 \qquad \text{(from Eq. C.25b)}$$

$$E_m = -\frac{I_{xy}}{I_x}\ 8M\ T_{101} \qquad \text{(from Eq. C.25c)}$$

hence

$$\{\frac{u_n}{L^2}\} = -\frac{I_{xy}\ 8M}{E(I_xI_y-I_{xy}^2)}\,[\lambda_x^4\ T_1]^{-1}\{T_{101}\} \qquad \text{(F.1b)}$$

The curvatures

$$\frac{\phi''}{L^2} = \frac{8\ M_a}{EC_w}\,\{Z_n''\}^T[\lambda_z^4\ T_7]^{-1}\{T_{102}\}$$

$$\frac{u''}{L^2} = -\frac{I_{xy}\ 8M}{E(I_xI_y-I_{xy}^2)}\ \{X_n''\}^T\,[\lambda_x^4\ T_1]^{-1}\{T_{101}\}$$

The matrix multiplications lead to one function of ζ. It reduces to one number when the value of ζ showing the place of yielding is substituted. Let

$$T_\phi = -\{Z_n''\}^T[\lambda_z^4\ T_7]^{-1}\{T_{102}\} \qquad \text{(F.2a)}$$

$$T_u = -\{X_n''\}^T[\lambda_x^4\ T_1]^{-1}\{T_{101}\} \qquad \text{(F.2b)}$$

The values of T_u and T_ϕ are given in the section E4 for simply supported boundary condition.

$$\frac{\phi''}{L^2} = -\frac{8\ Ma}{EC_w}\ T_\phi \qquad \text{(F.3a)}$$

$$\frac{u''}{L^2} = - \frac{8\, M(-I_{xy})}{E(I_x I_y - I_{xy}^2)}\, T_u \qquad (F.3b)$$

Substituting into Eq. 2.19

$$\sigma = \frac{M}{I_x}\, y + \left[\left(x - \frac{I_{xy}}{I_x}\, y\right) \frac{8\, M(-I_{xy})}{(I_x I_y - I_{xy}^2)}\, T_u + \omega\, \frac{8\, Ma}{C_w}\, T_\phi\right]$$

$$\frac{I_x \sigma}{y} = M\left[1 + \frac{I_x}{y}\left(x - \frac{I_{xy}}{I_x}\, y\right) \frac{8\, T_u(-I_{xy})}{(I_x I_y - I_{xy}^2)} + \frac{I_x}{y}\, \frac{\omega\, 8\, T_\phi}{C_w}\, a\right]$$

When σ is equal to 1.15 σ_y and with $\frac{I_x \sigma_y}{y} = M_{bend}$

$$\frac{M}{M_{bend}} = \frac{1.15}{1 + \frac{I_x}{y}\left(x - \frac{I_{xy}}{I_x}\, y\right) \frac{8\, T_u(-I_{xy})}{(I_x I_y - I_{xy}^2)} + \frac{I_x}{y}\, \frac{\omega}{C_w}\, 8\, T_\phi\, a} \qquad (F.4)$$

for channel $I_{xy} = 0$

$$\frac{M}{M_{bend}} = \frac{1.15}{1 + \frac{I_x}{C_w}\, \frac{\omega}{y}\, 8\, T_\phi\, a} \qquad (F.5)$$

for Z section $a = 0$

$$\frac{M}{M_{bend}} = \frac{1.15}{1 + \left(I_x\, \frac{x}{y} - I_{xy}\right) \frac{8\, T_u\, (-I_{xy})}{(I_x I_y - I_{xy}^2)}} \qquad (F.6)$$

The ratio $\frac{M}{M_{bend}}$ is usually the same for downward and uplift loading cases. (More precisely this is so if for these loading cases the incipient yielding in the cross section occurs at the same point or symmetrically located ones in

reference to the x axis for channels and the centroid for Z-sections, respectively, because then the values of $\frac{\omega}{y}$ in Eq. F.5 and $\frac{x}{y}$ in Eq. F.6 do not change.)

F2 Rigid Bracing Case

From Eq. C.31

$$L^2[D_{mn}]\{\frac{\phi_n}{L^2}\} = \{F_m\}$$

where for L = 0

$$L^2 D_{mn} = EC'_w \lambda_z^4 T_7 \qquad \text{(from Eq. C.30a)}$$

$$F_m = (a + \frac{I_{xy}}{I_x} e)8M T_{102} \qquad \text{(from Eq. C.30b)}$$

hence

$$\{\frac{\phi_n}{L^2}\} = \frac{8M}{EC'_w}(a + \frac{I_{xy}}{I_x} e)[\lambda_z^4 T_7]^{-1}\{T_{102}\} \qquad (F.7)$$

With T_ϕ from Eq. F.2a, the curvature is

$$\frac{\phi''}{L^2} = -\frac{8M}{EC'_w}(a + \frac{I_{xy}}{I_x} e)T_\phi \qquad (F.8)$$

Substituting into Eq. 2.21

$$\sigma = \frac{M}{I_x} y + \frac{8M}{C'_w} \omega' (a + \frac{I_{xy}}{I_x} e)T_\phi$$

$$\frac{I_x \sigma}{y} = M[1 + \frac{I_x}{C'_w} \frac{\omega'}{y} (a + \frac{I_{xy}}{I_x} e)8T_\phi]$$

Hence for $\sigma = 1.15\ \sigma_y$

$$\frac{M}{M_{bend}} = \frac{1.15}{1 + \frac{I_x}{C'_w} \frac{\omega'}{y} (a + \frac{I_{xy}}{I_x} e)8T_\phi} \qquad (F.9)$$

C'_w and ω' have been defined by Eqs. 2.15 and 2.22, respectively.

For a channel, $I_{xy} = 0$,

$$\frac{M}{M_{bend}} = \frac{1.15}{1 + \frac{I_x}{C'_w} \frac{\omega'}{y} 8\, T_\phi\, a} \qquad (F.10)$$

For a Z section, a = 0

$$\frac{M}{M_{bend}} = \frac{1.15}{1 + \frac{I_{xy}}{C'_w} \frac{\omega'}{y} 8\, T_\phi\, e} \qquad (F.11)$$

F3 General Case, i.e., $0 < Q < \infty$

The ratio M/M_{bend} for L = 0 and any finite value of Q is the same as for the unbraced case, because if similar calculations as above are made the terms involving Q will vanish as L approaches zero.

F4 The Values of T_ϕ and T_u for Simply Supported Boundary Conditions

For similar boundary conditions $X_n = Z_n$. It follows that

$$T_u = T_\phi \qquad (F.12)$$

From Eq. C.36a

$$X''_n = Z''_n = -n^2\pi^2 \sin n\pi\zeta, \quad n = 1, 3, 5, \ldots \infty \qquad (F.13)$$

Let

$$n = 2k-1 \qquad (F.14)$$

For $\zeta = \frac{1}{2}$, Eq. F.13 becomes

$$X''_n = Z''_n = -(2k-1)^2\, \pi^2\, (-1)^{2k}, \quad k = 1, 2, 3, \ldots \infty$$

Substituting $\lambda_x = \lambda_z = n\pi$ with, $T_1 = T_7$ and $T_{101} = T_{102}$ from

Eqs. C.37; the matrices become

$$\{Z_n''\} = -\pi^2\{(2k-1)^2(-1)^{2k}\}$$

$$[\lambda_x{}^4\ T_1]^{-1} = \frac{2}{\pi^4}\begin{bmatrix} \ddots & & 0 \\ & \frac{1}{(2k-1)^4} & \\ 0 & & \ddots \end{bmatrix}$$

$$\{T_{101}\} = \frac{2}{\pi}\ \{\frac{1}{(2k-1)}\}$$

The matrix multiplication gives

$$T_u = T_\phi = \frac{4}{\pi^3}\sum_1^\infty \frac{1}{(2k-1)^3}\ (-1)^{2k} \qquad \text{(F.15)}$$

The sum is related to "Riemann's zeta function". Its value can be found on page 439 of Ref. 33. Hence

$$T_u = T_\phi = \frac{4}{\pi^3}\ 0.96895 \approx \frac{1}{8} \qquad \text{(F.16)}$$

REFERENCES

1. "Light Gage Cold-Formed Steel Design Manual," American Iron and Steel Institute, New York 1962.

2. "Specification for the Design of Cold-Formed Steel Structural Members," American Iron and Steel Institute, New York 1968.

3. Apparao, T.V.S.R., "Problems in Structural Diaphragm Bracing," Ph.D. Dissertation, Cornell University, 1968.

4. Apparao, T.V.S.R., Errera, S.J., Fisher, G.P., "Columns Braced by Girts and a Diaphragm," Journal of Structural Division, Proc. ASCE, Vol. 95, Paper No. 6576, May 1969.

5. Apparao, T.V.S.R., Errera, S.J., "Design Recommendations for Diaphragm-Braced Beams, Columns and Wall-Studs," Report No. 332, Department of Structural Engineering, Cornell University, October 1968.

6. Black, M.M., Semple, H.M., "Torsion-Bending Analysis of Continuous Thin-Walled Beams," International Journal of Mech. Sci., Vol. 11, Oct. 1969.

7. Bleich, F., "Buckling of Metal Structures," McGraw-Hill Book Co., New York 1952.

8. Celebi, N., Pekoz, T., Winter G., "Behavior of Channel and Z-Section Beams Braced by Diaphragms," Proceedings of the Specialty Conference on Cold-Formed Structures, August 1971, University of Missouri, Rolla Mo.

9. Chilver, A.H., "Thin-Walled Structures," John Wiley and Sons., New York 1967.

10. Dabrowski, R., "Zum Problem der gleichzeitigen Biegung und Torsion dunnwandiger Balken," Der Stahlbau, April 1960.

11. Dabrowski, R., "Dunnwandige Stabe unter zweiachsig auser mittegem Druck," Der Stahlbau, 12/1961.

12. Ellifritt, D.S., "Strength and Stiffness of Steel Deck Shear Diaphragms," Proceedings of the Specialty Conference on Cold-Formed Structures, August 1971, University of Missouri, Rolla Mo.

13. Errera, S.J., "The Performance of Beams and Columns Continuously Braced with Diaphragms," Ph.D. Dissertation, Cornell University, 1965.

14. Errera, S.J., Pincus, G., Fisher, G.P., "Columns and Beams Braced by Diaphragms," Journal of Structural Division, Proc. ASCE, Vol. 93, Paper No. 5103, February 1967.

15. Goodier, J.N., "The Buckling of Compressed Bars by Torsion and Flexure," Cornell University Eng. Exp. Station Bull. No. 27, Dec. 1941.

16. Goodier, J.N., "Flexural-Torsional Buckling of Bars of Open Section," Cornell University Eng. Exp. Station Bull. No. 28, Jan. 1942.

17. Harrison, T., "The Effect of Transverse Straps on the Bending and Torsional Behavior of a Thin-Walled Prismatic Beam of Open Cross-Sectional Profile," International Journal of Mech. Sci., Vol. 11, 1969.

18. Kloppel, K., Unger, B., "Kippen von Durchlauftragern bei seitlich und gegen Verdrehen elastisch gelagertem Obergurt," Der Stahlbau 7/1969.

19. Krajcinovic, D., "A Consistent Discrete Elements Technique for Thin-Walled Assemblages," International Journal of Solids and Structures, Vol. 5, 1969.

20. Lansing, W., "Stresses in Thin-Walled Open Section Beams due to Combined Torsion and Flexure," Ph.D. Dissertation, Cornell University, 1949.

21. Larson, M.A., Discussion of "Lateral Bracing of Columns and Beams," Trans. ASCE, Vol. 125, 1960.

22. Luttrell, L.D., "Structural Performance of Light Gage Steel Diaphragms," Ph.D. Dissertation, Cornell University, 1965.

23. Luttrell, L.D., "Strength and Behavior of Light Gage Steel Shear Diaphragms," Cornell Eng. Research Bulletin 67-1, July 1967.

24. McCalley, Jr., R.B., "Contributions to the Theory of Combined Flexure and Torsion," Ph.D. Dissertation, Cornell University, 1952.

25. Oden, J.T., "Mechanics of Elastic Structures," McGraw-Hill, Inc., New York 1967.

26. Patterson, O., "Combined Bending and Torsion of I-Beams of Monosymmetrical Cross Section," Bulletin No. 10, Div. Blgd. Statics and Struc. Eng. Royal Inst. of Tech., Stockholm, Sweden, 1952.

27. Pekoz, T.B., "Torsional-Flexural Buckling of Thin-Walled Sections Under Eccentric Load," Ph.D. Dissertation, Cornell University, 1967.

28. Pekoz, T.B., Winter G., "Torsional-Flexural Buckling of Thin-Walled Sections under Eccentric Load," Journal of the Structural Division, Proc. ASCE, Vol. 95, Paper No. 6571, May 1969.

29. Pekoz, T.B., Celebi, N., "Torsional-Flexural Buckling of Thin-Walled Sections under Eccentric Load," Cornell Eng. Research Bulletin, 69-1, September 1969.

30. Pelikan, W., "Traglastversuche mit kontinuierlichen Pfetten und Well-eternit-Eindeckung," Der Bauingenier 41, 1966, pp. 440-444.

31. Pincus, G., "The Performance of Columns and Beams Continuously Braced with Diaphragms," Ph.D. Dissertation, Cornell University, 1963.

32. Pincus, G., Fisher, G.P., "Behavior of Diaphragm-Braced Columns and Beams," Journal of Structural Division, Proc. ASCE, Vol. 92, Paper No. 4792, April 1966.

33. Selby, S.M., "CRC Standard Mathematical Tables," 16th Edition The Chemical Rubber Co., Cleveland, Ohio, 1968.

34. Timoshenko, S., Gere, J.M., "Theory of Elastic Stability," 2nd Edition, McGraw-Hill, Inc., New York, 1961.

35. Vlasov, V.Z., "Thin-Walled Elastic Beams," National Science Foundation, Washington, D.C., 2nd Edition, 1961.

36. Vogel, U., "Zur Kippstabilitat durchlaufender Stahlpfetten," Der Stahlbau 3, 1970, pp. 76-82.

37. Winter G., Lansing, W., McCalley, Jr., R.B., "Performance of Laterally Loaded Channel Beams," Cornell University Eng. Exp. Station Reprint No. 33, Nov. 1950.

38. Winter, G., "Lateral Bracing of Columns and Beams," Trans. ASCE, Vol. 125, Part I, Paper No. 3044, 1960.

39. Winter G., "Cold-Formed, Light Gage Steel Construction," Jour. of the Structural Division, Proc. ASCE, Vol. 85, Paper No. 2270, November 1959.

40. Winter, G., "Commentary on the 1968 Edition of the Specification for the Design of Cold-Formed Steel, Structural Members," American Iron & Steel Institute, New York, 1970.

41. Zbirohowski-Koscia, K., "Thin-Walled Beams," Crosby Lockwood & Son, Ltd. London, 1967.

42. Zetlin, L., Winter G., "Unsymmetrical Bending of Beams with and without Lateral Bracing," Proc. ASCE, Vol. 81, Paper No. 774, 1955.

43. Zur Capellen, W.M., "Integral Tafeln," Springer Verlag, Berlin, 1950.

TABLE 1a

THE RATIO $\frac{P}{P_{bend}} = \frac{M}{M_{bend}}$ OF DIAPHRAGM-BRACED CHANNEL BEAMS FOR DOWNWARD LOADING AT THEORETICAL FAILURE

			Q/P_Y						
h/t	b/h	c/b	0	1	4	9	16	1000	L/h
80	1/4	0	.5520	.7273	.7614	.7697	.7727	.7767	5
		1/3	.5447	.6708	.6980	.7048	.7073	.7106	
		1/2	.5461	.6501	.6727	.6785	.6806	.6835	
80		0	.4860	.5783	.6034	.6098	.6121	.6152	
40	1/2	1/3	.5204	.5680	.5805	.5837	.5849	.5865	
40		1/2	.5671	.5877	.5914	.5924	.5928	.5933	
80	1/4	0	.3211	.7439	.8377	.8559	.8621	.8667	10
		1/3	.4119	.6993	.7566	.7695	.7742	.7802	
		1/2	.4387	.6783	.7235	.7342	.7381	.7436	
80		0	.4419	.5936	.6264	.6344	.6374	.6414	
40	1/2	1/3	.5059	.5893	.6032	.6068	.6081	.6098	
40		1/2	.5524	.6047	.6093	.6105	.6109	.6115	
80	1/4	0	.2093	.5689	.8921	.9354	.9476	.9611	15
		1/3	.2697	.6469	.8203	.8474	.8563	.8672	
		1/2	.3023	.6641	.7848	.8068	.8144	.8238	
80		0	.3793	.6126	.6617	.6732	.6775	.6830	
40	1/2	1/3	.4822	.6217	.6388	.6431	.6447	.6467	
40		1/2	.5286	.6313	.6376	.6392	.6398	.6406	

TABLE 1b

THE RATIO $\frac{P}{P_{bend}} = \frac{M}{M_{bend}}$ OF DIAPHRAGM-BRACED CHANNEL BEAMS FOR UPLIFT LOADING AT THEORETICAL FAILURE

			Q/P_Y						
h/t	b/h	c/b	0	1	4	9	16	1000	L/h
80	1/4	0	.6631	.6920	.7027	.7055	.7065	.7079	5
		1/3	.6131	.6479	.6604	.6637	.6649	.6665	
		1/2	.6003	.6307	.6418	.6447	.6458	.6472	
80	1/2	0	.5099	.5708	.5908	.5959	.5978	.6004	
40		1/3	.5339	.5627	.5728	.5754	.5764	.5776	
40		1/2	.5769	.5831	.5854	.5860	.5862	.5865	
80	1/4	0	.6291	.6243	.6215	.6205	.6201	.6196	10
		1/3	.6137	.6134	.6130	.6128	.6127	.6126	
		1/2	.6034	.6039	.6039	.6038	.6038	.6037	
80	1/2	0	.5272	.5634	.5762	.5795	.5807	.5824	
40		1/3	.5548	.5680	.5728	.5741	.5745	.5751	
40		1/2	.5886	.5862	.5853	.5850	.5849	.5865	
80	1/4	0	.4393	.4432	.4467	.4483	.4491	.4504	15
		1/3	.5365	.5334	.5314	.5304	.5305	.5302	
		1/2	.5462	.5411	.5380	.5370	.5360	.5361	
80	1/2	0	.5353	.5467	.5511	.5522	.5526	.5532	
40		1/3	.5761	.5733	.5720	.5716	.5714	.5711	
40		1/2	.6003	.5892	.5844	.5831	.5825	.5818	

TABLE 1c

THE POINT OF MAXIMUM STRESS FOR DIAPHRAGM-BRACED CHANNEL-BEAMS AT THEORETICAL FAILURE

			DOWNWARD LOADING			UPLIFT LOADING			
			Q/P_Y			Q/P_Y			
h/t	b/h	c/b	0	1	4 to 1000	0	1	4 to 1000	L/h
80	1/4	0	4	3	3	3	3	3	5
		1/3	4	3	3	3	3	3	
		1/2	4	3	3	3	3	3	
80	1/2	0	4	3	3	3	3	3	
40		1/3	4	3	3	3	3	3	
40		1/2	4	3	3				
80	1/4	0	5	3	3	3	3	3	10
		1/3	6	3	3	3	3	3	
		1/2	4	3	3	3	3	3	
80	1/2	0	4	3	3	3	3	3	
40		1/3	4	3	3	3	3	3	
40		1/2	4	3	3	3	3	3	
80	1/4	0	5	4	3	2	2	2	15
		1/3	6	4	3	3	3	3	
		1/2	6	4	3	3	3	3	
80	1/2	0	4	3	3	3	3	3	
40		1/3	4	3	3	3	3	3	
40		1/2	4	3	3	3	3	3	

TABLE 2a

THE RATIO $\frac{P}{P_{bend}} = \frac{M}{M_{bend}}$ OF DIAPHRAGM-BRACED Z-BEAMS FOR DOWNWARD LOADING AT THEORETICAL FAILURE

			Q/P_Y						
h/t	b/h	c/b	0	1	4	9	16	1000	L/h
80	1/4	0	.5902	.7565	.7762	.7803	.7818	.7836	5
		1/3	.5561	.6959	.7170	.7216	.7233	.7254	
		1/2	.5420	.6755	.6974	.7023	.7040	.7063	
80	1/2	0	.4917	.5894	.6064	.6102	.6115	.6133	
40		1/3	.4775	.5726	.5907	.5948	.5962	.5982	
40		1/2	.4919	.5845	.6032	.6075	.6091	.6111	
80	1/4	0	.3594	.8568	.8732	.8751	.8757	.8764	10
		1/3	.4577	.7714	.7893	.7922	.7932	.7945	
		1/2	.4666	.7407	.7595	.7629	.7641	.7655	
80	1/2	0	.4681	.6173	.6334	.6368	.6380	.6395	
40		1/3	.4650	.5948	.6140	.6183	.6198	.6212	
40		1/2	.4816	.6022	.6218	.6262	.6277	.6298	
80	1/4	0	.2188	.7671	.9669	.9665	.9663	.9662	15
		1/3	.2937	.8653	.8785	.8792	.8793	.8795	
		1/2	.3314	.8289	.8422	.8433	.8436	.8440	
80	1/2	0	.4198	.6625	.6766	.6792	.6801	.6813	
40		1/3	.4426	.6300	.6509	.6553	.6569	.6589	
40		1/2	.4633	.6306	.6514	.6558	.6574	.6595	

TABLE 2b

THE RATIO $\frac{P}{P_{bend}} = \frac{M}{M_{bend}}$ OF DIAPHRAGM-BRACED Z-BEAMS FOR UPLIFT LOADING AT THEORETICAL FAILURE

			Q/P_Y						
h/t	b/h	c/b	0	1	4	9	16	1000	L/h
80	1/4	0	.5996	.6769	.7020	.7086	.7111	.7145	5
		1/3	.5594	.6447	.6694	.6756	.6780	.6810	
		1/2	.5442	.6330	.6580	.6642	.6666	.6696	
80		0	.4920	.5727	.5907	.5948	.5964	.5984	
40	1/2	1/3	.4776	.5623	.5811	.5855	.5871	.5892	
40		1/2	.4920	.5763	.5957	.6002	.6019	.6040	
80	1/4	0	.4737	.5604	.6026	.6137	.6183	.6247	10
		1/3	.4990	.5766	.6081	.6172	.6209	.6285	
		1/2	.4951	.5768	.6078	.6165	.6199	.6246	
80		0	.4735	.5509	.5711	.5761	.5779	.5804	
40	1/2	1/3	.4668	.5543	.5765	.5818	.5838	.5864	
40		1/2	.4828	.5697	.5919	.5973	.5992	.6019	
80	1/4	0	.3151	.3752	.4148	.4299	.4366	.4468	15
		1/3	.4082	.4773	.5148	.5276	.5330	.5407	
		1/2	.4186	.4924	.5295	.5416	.5466	.5538	
80		0	.4426	.5161	.5394	.5456	.5480	.5512	
40	1/2	1/3	.4500	.5414	.5687	.5757	.5783	.5819	
40		1/2	.4685	.5590	.5857	.5925	.5970	.5985	

TABLE 2c

THE POINT OF MAXIMUM STRESS FOR DIAPHRAGM-BRACED Z-BEAMS AT THEORETICAL FAILURE

			DOWNWARD LOADING Q/P_Y			UPLIFT LOADING Q/P_Y			
h/t	b/h	c/b	0	1	4 to 1000	0	1	4 to 1000	L/h
80	1/4	0	4	3	3	3	3	3	5
		1/3	4	3	3	3	3	3	
		1/2	4	3	3	3	3	3	
80	1/2	0	4	3	3	3	3	3	
40		1/3	4	3	3	3	3	3	
40		1/2	4	3	3	3	3	3	
80	1/4	0	5	3	3	2	2	3	10
		1/3	4	3	3	3	3	3	
		1/2	4	3	3	3	3	3	
80	1/2	0	4	3	3	3	3	3	
40		1/3	4	3	3	3	3	3	
40		1/2	4	3	3	3	3	3	
80	1/4	0	5	4	3	2	2	2	15
		1/3	6	3	3	3	3	3	
		1/2	6	3	3	3	3	3	
80	1/2	0	4	3	3	3	3	3	
40		1/3	4	3	3	3	3	3	
40		1/2	4	3	3	3	3	3	

TABLE 3a

ANGLE OF ROTATION ϕ OF DIAPHRAGM-BRACED CHANNEL BEAMS FOR DOWNWARD LOADING AT THEORETICAL FAILURE

			Q/P_Y						
h/t	b/h	c/b	0	1	4	9	16	1000	L/h
80	1/4	0	2.47°	1.54°	1.20°	1.11°	1.08°	1.04°	5
		1/3	1.89°	1.26°	1.01°	.95°	.93°	.90°	
		1/2	1.67°	1.14°	.93°	.88°	.86°	.83°	
80		0	1.16°	.77°	.63°	.59°	.58°	.56°	
40	1/2	1/3	.85°	.58°	.49°	.46°	.45°	.44°	
40		1/2	.69°	.50°	.42°	.40°	.40°	.39°	
80	1/4	0	7.85°	7.21°	4.21°	3.65°	3.45°	3.21°	10
		1/3	7.83°	5.32°	3.71°	3.36°	3.23°	3.06°	
		1/2	6.96°	4.77°	3.49°	3.19°	3.09°	2.95°	
80		0	4.67°	3.09°	2.45°	2.29°	2.23°	2.15°	
40	1/2	1/3	3.29°	2.31°	1.90°	1.79°	1.75°	1.70°	
40		1/2	2.70°	1.98°	1.66°	1.58°	1.54°	1.50°	
80	1/4	0	14.23°	20.15°	9.25°	6.62°	5.87°	5.06°	15
		1/3	14.54°	14.29°	7.59°	6.40°	5.95°	5.41°	
		1/2	13.97°	12.60°	7.32°	6.25°	5.88°	5.43°	
80		0	10.65°	7.15°	5.28°	4.85°	4.69°	4.48°	
40	1/2	1/3	7.12°	5.14°	4.08°	3.81°	3.71°	3.58°	
		1/2	5.88°	4.41°	3.60°	3.89°	3.31°	3.21°	

TABLE 3b

ANGLE OF ROTATION ϕ OF DIAPHRAGM-BRACED CHANNEL BEAMS FOR UPLIFT LOADING AT THEORETICAL FAILURE

			Q/P_Y						
h/t	b/h	c/b	0	1	4	9	16	1000	L/h
80	1/4	0	-1.98°	-1.50°	-1.31°	-1.26°	-1.24°	-1.22°	5
		1/3	-1.66°	-1.23°	-1.06°	-1.02°	-1.00°	- .98°	
		1/2	-1.51°	-1.12°	- .97°	- .93°	- .91°	- .89°	
80	1/2	0	-1.12°	- .76°	- .64°	- .60°	- .59°	- .58°	
40		1/3	- .82°	- .58°	- .49°	- .46°	- .46°	- .45°	
40		1/2	- .68°	- .50°	- .43°	- .41°	- .40°	- .39°	
80	1/4	0	-6.44°	-6.07°	-5.86°	-5.79°	-5.77°	-5.73°	10
		1/3	-5.47°	-4.80°	-4.48°	-4.38°	-4.34°	-4.29°	
		1/2	-5.06°	-4.36°	-4.03°	-3.93°	-3.89°	-3.84°	
80	1/2	0	-4.06°	-2.98°	-2.58°	-2.47°	-2.43°	-2.37°	
40		1/3	-3.03°	-2.25°	-1.95°	-1.87°	-1.84°	-1.80°	
40		1/2	-2.53°	-1.93°	-1.69°	-1.63°	-1.60°	-1.57°	
80	1/4	0	-11.57°	-11.79°	-11.98°	-12.06°	-12.10°	-12.16°	15
		1/3	-11.36°	-11.16°	-11.04°	-11.00°	-10.98°	-10.96°	
		1/2	-10.26°	-9.92°	-9.71°	-9.64°	-9.62°	-9.58°	
80	1/2	0	-8.06°	-6.57°	-5.93°	-5.74°	-5.67°	-5.57°	
40		1/3	-5.99°	-4.83°	-4.33°	-4.18°	-4.13°	-4.06°	
40		1/2	-5.13°	-4.18°	-3.77°	-3.65°	-3.60°	-3.53°	

TABLE 4a

ANGLE OF ROTATION ϕ OF DIAPHRAGM-BRACED Z-BEAMS FOR DOWNWARD LOADING AT THEORETICAL FAILURE

			Q/P_Y						
h/t	b/h	c/b	0	1	4	9	16	1000	L/h
80	1/4	0	.41°	- .72°	- .96°	-1.02°	-1.04°	-1.07°	5
		1/3	.19°	- .63°	- .82°	- .86°	- .87°	- .89°	
		1/2	.14°	- .58°	- .75°	- .79°	- .80°	- .82°	
80	1/2	0	.04°	- .43°	- .53°	- .55°	- .56°	- .57°	
40		1/3	.02°	- .33°	- .41°	- .42°	- .43°	- .44°	
40		1/2	.01°	- .28°	- .35°	- .36°	- .37°	- .38°	
80	1/4	0	3.60°	-1.24°	-2.85°	-3.09°	-3.17°	-3.27°	10
		1/3	2.91°	-1.77°	-2.72°	-2.90°	-2.97°	-3.04°	
		1/2	2.13°	-1.77°	-2.59°	-2.75°	-2.80°	-2.88°	
80	1/2	0	.58°	-1.60°	-2.01°	-2.10°	-2.13°	-2.18°	
40		1/3	.25°	-1.25°	-1.56°	-1.63°	-1.66°	-1.69°	
40		1/2	.18°	-1.08°	-1.35°	-1.41°	-1.44°	-1.47°	
80	1/4	0	8.34°	6.78°	-4.06°	-4.75°	-4.93°	-5.12°	15
		1/3	8.09°	- .20°	-4.57°	-5.03°	-5.18°	-5.34°	
		1/2	7.65°	-1.55°	-4.56°	-4.97°	-5.10°	-5.26°	
80	1/2	0	2.77°	-3.11°	-4.16°	-4.37°	-4.44°	-4.53°	
40		1/3	1.16°	-2.49°	-3.25°	-3.41°	-3.47°	-3.55°	
40		1/2	.83°	-2.20°	-2.85°	-3.00°	-3.05°	-3.12°	

TABLE 4b

ANGLE OF ROTATION ϕ OF DIAPHRAGM-BRACED Z-BEAMS FOR UPLIFT LOADING AT THEORETICAL FAILURE

			Q/P_Y						
h/t	b/h	c/b	0	1	4	9	16	1000	L/h
80	1/4	0	.31°	.95°	1.15°	1.20°	1.22°	1.25°	5
		1/3	.16°	.74°	.90°	.94°	.96°	.98°	
		1/2	.12°	.66°	.81°	.85°	.86°	.88°	
80	1/2	0	.03°	.45°	.54°	.56°	.57°	.58°	
40		1/3	.02°	.34°	.41°	.43°	.44°	.45°	
40		1/2	.01°	.29°	.35°	.37°	.38°	.38°	
80	1/4	0	2.84°	4.70°	5.51°	5.72°	5.80°	5.92°	10
		1/3	1.83°	3.43°	4.02°	4.18°	4.24°	4.33°	
		1/2	1.44°	3.00°	3.54°	3.68°	3.74°	3.82°	
80	1/2	0	.47°	1.88°	2.24°	2.32°	2.36°	2.40°	
40		1/3	.22°	1.38°	1.66°	1.73°	1.76°	1.79°	
40		1/2	.16°	1.17°	1.42°	1.48°	1.51°	1.55°	
80	1/4	0	6.45°	9.31°	10.96	11.55°	11.81°	12.18°	15
		1/3	6.36°	9.14°	10.39°	10.77°	10.92°	11.14°	
		1/2	5.14°	7.83°	8.95°	9.29°	9.43°	9.62°	
80	1/2	0	1.92°	4.51°	5.27°	5.47°	5.54°	5.64°	
40		1/3	.93°	3.13°	3.75°	3.90°	3.96°	4.04°	
40		1/2	.69°	2.65°	3.21°	3.34°	3.40°	3.47°	

TABLE 5a

ANGLE OF ROTATION $\phi_{1.67}$ OF DIAPHRAGM-BRACED CHANNEL BEAMS FOR DOWNWARD LOADING AT $\frac{1}{1.67}$ OF THE THEORETICAL FAILURE

			Q/P_Y						
h/t	b/h	c/b	0	1	4	9	16	1000	L/h
80	1/4	0	1.32°	.92°	.74°	.69°	.68°	.65°	5
		1/3	1.07°	.75°	.62°	.58°	.57°	.55°	
		1/2	.96°	.68°	.57°	.54°	.53°	.51°	
80		0	.68°	.46°	.38°	.36°	.36°	.34°	
40	1/2	1/3	.50°	.35°	.29°	.28°	.27°	.27°	
40		1/2	.41°	.30°	.26°	.24°	.24°	.23°	
80	1/4	0	3.17°	3.66°	2.68°	2.44°	2.35°	2.23°	10
		1/3	3.51°	3.01°	2.35°	2.17°	2.12°	2.03°	
		1/2	3.32°	2.75°	2.19°	2.05°	1.99°	1.92°	
80		0	2.58°	1.84°	1.50°	1.41°	1.38°	1.34°	
40	1/2	1/3	1.89°	1.38°	1.16°	1.09°	1.07°	1.04°	
40		1/2	1.57°	1.19°	1.01°	.96°	.94°	.91°	
80	1/4	0	4.20°	6.32°	5.33°	4.50°	4.21°	3.85°	15
		1/3	5.05°	6.30°	4.86°	4.34°	4.15°	3.90°	
		1/2	5.21°	6.05°	4.62°	4.19°	4.03°	3.83°	
80		0	5.23°	4.18°	3.32°	3.10°	3.01°	2.90°	
40	1/2	1/3	3.85°	3.05°	2.52°	2.38°	2.32°	2.25°	
40		1/2	3.27°	2.63°	2.21°	2.09°	2.05°	1.99°	

TABLE 5b

ANGLE OF ROTATION $\phi_{1.67}$ OF DIAPHRAGM-BRACED CHANNEL BEAMS FOR UPLIFT LOADING AT $\frac{1}{1.67}$ OF THE THEORETICAL FAILURE

			Q/P_Y						
h/t	b/h	c/b	0	1	4	9	16	1000	L/h
80	1/4	0	-1.25°	- .89°	- .76°	- .72°	- .71°	- .69°	5
		1/3	-1.03°	- .73°	- .62°	- .59°	- .58°	- .57°	
		1/2	- .94°	- .67°	- .57°	- .54°	- .53°	- .52°	
80	1/2	0	- .68°	- .45°	- .38°	- .36°	- .35°	- .34°	
40		1/3	- .50°	- .35°	- .29°	- .28°	- .27°	- .27°	
40		1/2	- .41°	- .30°	- .25°	- .24°	- .24°	- .23°	
80	1/4	0	-3.67°	-3.13°	-2.88°	-2.80°	-2.77°	-2.73°	10
		1/3	-3.38°	-2.70°	-2.41°	-2.33°	-2.30°	-2.25°	
		1/2	-3.15°	-2.50°	-2.22°	-2.14°	-2.11°	-2.07°	
80	1/2	0	-2.55°	-1.77°	-1.50°	-1.43°	-1.40°	-1.36°	
40		1/3	-1.67°	-1.34°	-1.15°	-1.10°	-1.08°	-1.05°	
40		1/2	-1.55°	-1.15°	-1.00°	- .96°	- .94°	- .92°	
80	1/4	0	-4.96°	-4.78°	-4.71°	-4.70°	-4.69°	-4.69°	15
		1/3	-5.76°	-5.25°	-4.98°	-4.89°	-4.86°	-4.81°	
		1/2	-5.58°	-4.98°	-4.67°	-4.58°	-4.54°	-4.49°	
80	1/2	0	-5.11°	-3.80°	-3.30°	-3.16°	-3.11°	-3.04°	
40		1/3	-3.73°	-2.85°	-2.49°	-2.40°	-2.36°	-2.31°	
40		1/2	-3.17°	-2.48°	-2.19°	-2.11°	-2.08°	-2.03°	

TABLE 6a

ANGLE OF ROTATION $\phi_{1.67}$ OF DIAPHRAGM-BRACED Z-BEAMS FOR DOWNWARD LOADING AT $\frac{1}{1.67}$ OF THE THEORETICAL FAILURE

			Q/P_Y						
h/t	b/h	c/b	0	1	4	9	16	1000	L/h
80	1/4	0	.13°	- .47°	- .61°	- .64°	- .65°	- .67°	5
		1/3	.06°	- .40°	- .51°	- .53°	- .54°	- .55°	
		1/2	.05°	- .36°	- .46°	- .48°	- .49°	- .50°	
80		0	.01°	- .26°	- .32°	- .33°	- .34°	- .34°	
40	1/2	1/3	.01°	- .20°	- .25°	- .26°	- .26°	- .26°	
40		1/2	.00°	- .17°	- .21°	- .22°	- .22°	- .23°	
80	1/4	0	.86°	-1.27°	-2.02°	-2.16°	-2.21°	-2.27°	10
		1/3	.79°	-1.32°	-1.83°	-1.94°	-1.98°	-2.02°	
		1/2	.62°	-1.26°	-1.71°	-1.80°	-1.84°	-1.88°	
80		0	.19°	-1.01°	-1.26°	-1.31°	-1.33°	-1.36°	
40	1/2	1/3	.09°	- .77°	- .96°	-1.00°	-1.01°	-1.03°	
40		1/2	.06°	- .66°	- .82°	- .86°	- .88°	- .89°	
80	1/4	0	1.51°	- .78°	-3.28°	-3.66°	-3.77°	-3.91°	15
		1/3	1.66°	-1.76°	-3.40°	-3.66°	-3.75°	-3.86°	
		1/2	1.67°	-1.98°	-3.30°	-3.54°	-3.62°	-3.72°	
80		0	.83°	-2.12°	-2.72°	-2.84°	-2.88°	-2.94°	
40	1/2	1/3	.39°	-1.61°	-2.05°	-2.15°	-2.19°	-2.23°	
40		1/2	.28°	-1.40°	-1.78°	-1.87°	-1.90°	-1.94°	

TABLE 6b

ANGLE OF ROTATION $\phi_{1.67}$ OF DIAPHRAGM-BRACED Z-BEAMS FOR UPLIFT LOADING AT $\frac{1}{1.67}$ OF THE THEORETICAL FAILURE

			Q/P_Y						
h/t	b/h	c/b	0	1	4	9	16	1000	L/h
80	1/4	0	.12°	.53°	.65°	.68°	.69°	.71°	5
		1/3	.06°	.42°	.52°	.55°	.56°	.57°	
		1/2	.04°	.38°	.47°	.49°	.50°	.51°	
80		0	.01°	.26°	.32°	.33°	.34°	.35°	
40	1/2	1/3	.01°	.20°	.25°	.26°	.26°	.27°	
40		1/2	.00°	.17°	.21°	.22°	.22°	.23°	
80	1/4	0	.98°	2.10°	2.56°	2.69°	2.74°	2.81°	10
		1/3	.66°	1.72°	2.08°	2.18°	2.21°	2.27°	
		1/2	.53°	1.55°	1.88°	1.97°	2.01°	2.05°	
80		0	.17°	1.07°	1.28°	1.34°	1.36°	1.38°	
40	1/2	1/3	.08°	.80°	.97°	1.01°	1.03°	1.05°	
40		1/2	.06°	.68°	.83°	.87°	.88°	.90°	
80	1/4	0	1.93°	3.36°	4.14°	4.42°	4.54°	4.72°	15
		1/3	2.03°	3.68°	4.40°	4.63°	4.72°	4.85°	
		1/2	1.72°	3.38°	4.06°	4.27°	4.35°	4.46°	
80		0	.71°	2.39°	2.86°	2.98°	3.02°	3.08°	
40	1/2	1/3	.34°	1.74°	2.12°	2.21°	2.25°	2.30°	
40		1/2	.25°	1.50°	1.83°	1.92°	1.95°	1.99°	

TABLE 7a

THE RATIO P/P_∞ FOR DIAPHRAGM-BRACED CHANNEL BEAMS FOR DOWNWARD LOADING AT THEORETICAL FAILURE

			Q/P_Y						
h/t	b/h	c/b	0	1	4	9	16	1000	L/h
80		0	.711	.936	.980	.991	.995	1.0	
80	1/4	1/3	.766	.944	.982	.992	.995	1.0	
80		1/2	.799	.951	.984	.993	.996	1.0	
80		0	.970	.940	.981	.991	.995	1.0	5
40	1/2	1/3	.887	.968	.990	.995	.997	1.0	
40		1/2	.956	.990	.997	.998	.999	1.0	
80		0	.369	.855	.963	.984	.991	1.0	
80	1/4	1/3	.528	.896	.970	.986	.992	1.0	
80		1/2	.590	.913	.974	.988	.993	1.0	
80		0	.689	.926	.977	.989	.994	1.0	10
40	1/2	1/3	.830	.966	.989	.995	.997	1.0	
40		1/2	.903	.989	.996	.998	.999	1.0	
80		0	.218	.592	.928	.973	.986	1.0	
80	1/4	1/3	.311	.746	.946	.977	.987	1.0	
80		1/2	.367	.806	.953	.979	.989	1.0	
80		0	.555	.897	.969	.986	.992	1.0	15
40	1/2	1/3	.745	.961	.985	.994	.997	1.0	
40		1/2	.825	.985	.995	.998	.999	1.0	

TABLE 7b

THE RATIO P/P_∞ FOR DIAPHRAGM-BRACED CHANNEL BEAMS FOR UPLIFT LOADING AT THEORETICAL FAILURE

			Q/P_Y						
h/t	b/h	c/b	0	1	4	9	16	1000	L/h
80	1/4	0	.937	.978	.993	.997	.998	1.0	5
		1/3	.920	.972	.991	.996	.998	1.0	
		1/2	.927	.974	.992	.996	.998	1.0	
80		0	.849	.951	.984	.993	.995	1.0	
40	1/2	1/3	.924	.974	.992	.996	.998	1.0	
40		1/2	.984	.994	.998	.999	.999	1.0	
80	1/4	0	1.015	1.007	1.003	1.001	1.001	1.0	10
		1/3	1.002	1.001	1.001	1.000	1.000	1.0	
		1/2	1.000	1.000	1.000	1.000	1.000	1.0	
80		0	.095	.967	.989	.995	.997	1.0	
40	1/2	1/3	.965	.988	.996	.998	.999	1.0	
40		1/2	1.007	1.003	1.001	1.000	1.000	1.0	
80	1/4	0	.975	.984	.992	.995	.997	1.0	15
		1/3	1.012	1.006	1.002	1.001	1.001	1.0	
		1/2	1.020	1.009	1.003	1.002	1.001	1.0	
80		0	.968	.988	.996	.998	.999	1.0	
40	1/2	1/3	1.009	1.004	1.002	1.001	1.001	1.0	
40		1/2	1.032	1.013	1.004	1.002	1.001	1.0	

TABLE 8a

THE RATIO P/P_∞ FOR DIAPHRAGM-BRACED Z-BEAMS FOR DOWNWARD LOADING AT THEORETICAL LOADING

			Q/P_Y						
h/t	b/h	c/b	0	1	4	9	16	1000	L/h
80		0	.753	.965	.990	.996	.998	1.0	
80	1/4	1/3	.767	.959	.988	.995	.997	1.0	
80		1/2	.767	.956	.987	.994	.997	1.0	
									5
80		0	.802	.961	.989	.995	.997	1.0	
40	1/2	1/3	.798	.957	.987	.994	.997	1.0	
40		1/2	.805	.956	.987	.994	.997	1.0	
80		0	.410	.978	.996	.998	.999	1.0	
80	1/4	1/3	.576	.971	.993	.997	.998	1.0	
80		1/2	.609	.967	.992	.997	.998	1.0	
									10
80		0	.732	.965	.990	.995	.998	1.0	
40	1/2	1/3	.747	.957	.988	.994	.997	1.0	
40		1/2	.765	.956	.987	.994	.997	1.0	
80		0	.226	.794	1.001	1.000	1.000	1.0	
80	1/4	1/3	.334	.984	.999	1.000	1.000	1.0	
80		1/2	.393	.982	.998	.999	.999	1.0	
									15
80		0	.616	.972	.993	.997	.998	1.0	
40	1/2	1/3	.672	.956	.988	.995	.997	1.0	
40		1/2	.702	.956	.988	.994	.997	1.0	

TABLE 8b

THE RATIO P/P_∞ FOR DIAPHRAGM-BRACED Z-BEAMS FOR UPLIFT LOADING AT THEORETICAL FAILURE

			Q/P_Y						
h/t	b/h	c/b	0	1	4	9	16	1000	L/h
80	1/4	0	.839	.947	.983	.992	.995	1.0	5
		1/3	.821	.947	.983	.992	.995	1.0	
		1/2	.813	.945	.983	.992	.995	1.0	
80		0	.822	.957	.987	.994	.997	1.0	
40	1/2	1/3	.811	.954	.986	.994	.997	1.0	
40		1/2	.815	.954	.986	.994	.996	1.0	
80	1/4	0	.758	.897	.964	.982	.990	1.0	10
		1/3	.797	.921	.972	.986	.992	1.0	
		1/2	.793	.923	.973	.987	.992	1.0	
80		0	.816	.949	.984	.993	.996	1.0	
40	1/2	1/3	.796	.945	.983	.992	.996	1.0	
40		1/2	.802	.947	.983	.992	.996	1.0	
80	1/4	0	.705	.840	.928	.962	.977	1.0	15
		1/3	.755	.883	.952	.976	.986	1.0	
		1/2	.756	.889	.956	.978	.987	1.0	
80		0	.803	.936	.979	.990	.994	1.0	
40	1/2	1/3	.773	.930	.977	.989	.994	1.0	
40		1/2	.783	.934	.979	.990	.994	1.0	

TABLE 9a

THE RATIO ϕ/ϕ_∞ FOR DIAPHRAGM-BRACED CHANNEL BEAMS FOR DOWNWARD LOADING AT THEORETICAL FAILURE

			Q/P_Y						
h/t	b/h	c/b	0	1	4	9	16	1000	L/h
80		0	2.366	1.481	1.150	1.069	1.039	1.000	
80	1/4	1/3	2.113	1.401	1.129	1.060	1.034	1.000	
80		1/2	2.003	1.370	1.120	1.056	1.032	1.000	
									5
80		0	2.069	1.362	1.118	1.055	1.031	1.000	
40	1/2	1/3	1.915	1.322	1.107	1.050	1.028	1.000	
40		1/2	1.787	1.289	1.097	1.046	1.026	1.000	
80		0	2.447	2.248	1.313	1.137	1.076	1.000	
80	1/4	1/3	2.559	1.739	1.213	1.096	1.054	1.000	
80		1/2	2.364	1.619	1.185	1.085	1.047	1.000	
									10
80		0	2.175	1.437	1.139	1.064	1.036	1.000	
40	1/2	1/3	1.935	1.360	1.118	1.055	1.031	1.000	
40		1/2	1.799	1.319	1.106	1.050	1.028	1.000	
80		0	2.815	3.988	1.830	1.309	1.162	1.000	
80	1/4	1/3	2.689	2.644	1.435	1.183	1.100	1.000	
80		1/2	2.573	2.322	1.349	1.151	1.084	1.000	
									15
80		0	2.379	1.599	1.181	1.083	1.047	1.000	
40	1/2	1/3	1.988	1.435	1.138	1.064	1.036	1.000	
40		1/2	1.834	1.377	1.122	1.057	1.032	1.000	

TABLE 9b

THE RATIO ϕ/ϕ_∞ FOR DIAPHRAGM-BRACED CHANNEL BEAMS FOR UPLIFT LOADING AT THEORETICAL FAILURE

			Q/P_Y						
h/t	b/h	c/b	0	1	4	9	16	1000	L/h
80	1/4	0	1.626	1.233	1.080	1.038	1.022	1.0	5
		1/3	1.709	1.257	1.088	1.041	1.024	1.0	
		1/2	1.698	1.255	1.087	1.041	1.024	1.0	
80	1/2	0	1.946	1.317	1.105	1.050	1.028	1.0	
40		1/3	1.848	1.296	1.099	1.047	1.027	1.0	
40		1/2	1.738	1.268	1.091	1.043	1.025	1.0	
80	1/4	0	1.123	1.059	1.023	1.011	1.006	1.0	10
		1/3	1.273	1.119	1.044	1.021	1.012	1.0	
		1/2	1.317	1.136	1.050	1.024	1.014	1.0	
80	1/2	0	1.713	1.257	1.088	1.041	1.024	1.0	
40		1/3	1.684	1.252	1.086	1.041	1.023	1.0	
40		1/2	1.614	1.233	1.081	1.038	1.022	1.0	
80	1/4	0	.951	.970	.985	.991	.995	1.0	15
		1/3	1.036	1.019	1.007	1.004	1.002	1.0	
		1/2	1.071	1.035	1.014	1.007	1.004	1.0	
80	1/2	0	1.447	1.179	1.064	1.030	1.017	1.0	
40		1/3	1.475	1.191	1.067	1.032	1.018	1.0	
40		1/2	1.450	1.183	1.065	1.031	1.018	1.0	

TABLE 10a

THE RATIO ϕ/ϕ_∞ FOR DIAPHRAGM-BRACED Z-BEAMS FOR DOWNWARD LOADING AT THEORETICAL FAILURE

			Q/P_Y						
h/t	b/h	c/b	0	1	4	9	16	1000	L/h
80		0	- .388	.679	.907	.958	.976	1.0	
80	1/4	1/3	- .214	.707	.913	.960	.978	1.0	
80		1/2	- .170	.712	.914	.961	.978	1.0	
									5
80		0	- .064	.760	.929	.968	.982	1.0	
40	1/2	1/3	- .038	.759	.929	.967	.981	1.0	
40		1/2	- .031	.750	.925	.966	.980	1.0	
80		0	-1.101	.381	.872	.946	.971	1.0	
80	1/4	1/3	- .957	.580	.894	.954	.974	1.0	
80		1/2	- .739	.617	.899	.955	.975	1.0	
									10
80		0	- .265	.736	.925	.966	.981	1.0	
40	1/2	1/3	- .149	.739	.923	.965	.980	1.0	
40		1/2	- .121	.734	.921	.964	.980	1.0	
80		0	-1.628	-1.323	.971	.928	.963	1.0	
80	1/4	1/3	-1.515	.037	.855	.942	.969	1.0	
80		1/2	-1.454	.294	.868	.945	.970	1.0	
									15
80		0	- .611	.687	.917	.963	.979	1.0	
40	1/2	1/3	- .327	.702	.915	.962	.978	1.0	
40		1/2	- .266	.704	.914	.961	.978	1.0	

TABLE 10b

THE RATIO ϕ/ϕ_∞ FOR DIAPHRAGM-BRACED Z-BEAMS FOR UPLIFT LOADING AT THEORETICAL FAILURE

			Q/P_Y						
h/t	b/h	c/b	0	1	4	9	16	1000	L/h
80	1/4	0	.252	.762	.922	.963	.979	1.0	5
		1/3	.166	.754	.921	.963	.979	1.0	
		1/2	.138	.751	.921	.963	.979	1.0	
80	1/2	0	.059	.771	.931	.968	.982	1.0	
40		1/3	.036	.766	.929	.967	.982	1.0	
40		1/2	.029	.757	.926	.966	.981	1.0	
80	1/4	0	.481	.794	.931	.966	.981	1.0	10
		1/3	.423	.793	.928	.965	.980	1.0	
		1/2	.376	.785	.926	.965	.980	1.0	
80	1/2	0	.196	.783	.932	.968	.982	1.0	
40		1/3	.125	.769	.928	.967	.981	1.0	
40		1/2	.105	.760	.925	.965	.980	1.0	
80	1/4	0	.528	.764	.900	.948	.969	1.0	15
		1/3	.571	.821	.932	.967	.981	1.0	
		1/2	.535	.814	.932	.967	.981	1.0	
80	1/2	0	.341	.799	.934	.969	.982	1.0	
40		1/3	.231	.774	.927	.966	.980	1.0	
40		1/2	.200	.766	.925	.965	.980	1.0	

TABLE 11

COEFFICIENTS W

(hinged boundary)

$\lambda_1 = \pi$

$K_{11} = 1$

$K_{33} = 1$

$K'_{33} = 1/\pi^2$

$W_1 = \frac{2}{\pi^2}\left(1 + \frac{\pi^2}{3}\right) = .869$

$W_2 = \frac{8}{\pi^2} = .810$

$W_3 = \frac{32}{\pi^3} = 1.032$

$W_4 = 1.078$	$W_7 = 17.02$	$W_{10} = 1.150$
$W_5 = 1.112$	$W_8 = 17.57$	$W_{11} = 1.187$
$W_6 = 1.112$	$W_9 = 17.57$	$W_{12} = 1.187$

TABLE 12

COEFFICIENTS W_B

(hinged end)

$W_B = -.25$ for one brace at middle

$W_B = -.10$ for two braces $\frac{L}{3}$ apart

$W_B = -.036$ for three braces $\frac{L}{4}$ apart

TABLE 13

MATERIAL PROPERTIES OF THE MODEL TEST BEAMS

Test No.	Virgin Properties: Yield Stress* ksi	Ultimate Strength* ksi	$\frac{\sigma_{ult}}{\sigma_y}$	$\frac{\sigma_{corner}}{\sigma_y}$**
1 & 3	33.17	44.65	1.34	
2 & 4	33.71	45.17	1.34	
5 & 7	29.50	40.00	1.35	1.53
6 & 8	29.95	43.50	1.45	1.64

* Found by standard coupon tests

** Tensile yield stress calculated with formulas given in 3.1.1 of Ref. 1

TABLE 14

MATERIAL PROPERTIES OF FULL-SCALE TEST BEAMS

Test No.	Yield Stress*	Ultimate Strength* ksi
F1	52.0	70.5
F2 & F3	59.0	80.0
F4 & F5	51.0	70.0

* Found by standard tension coupon test

TABLE 15

COMPARISON OF EXPERIMENTAL FAILURE LOADS pL WITH THE PREDICTIONS (pounds)

Test No.	1 Exp. Failure Load	2 pL for $\sigma_{max}=\sigma_y$ (a)*	%	3 pL for $\sigma_{max}=1.15\sigma_y$ (b)*	%	4 pL for $M_{max}=M_{bend}$ (c)*	%	5 pL for M_{bend} w.inc.cor.st. (d)*	%	6 pL for σ_{exp} (e)*	%
#1	700	615	-12.1	635	- 9.4	——		———		——	
#2	420	379	- 9.8	402	- 4.3	——		———		——	
#3	830	670	-19.2	700	-15.6	——		———		——	
#4	610	580	- 4.8	608	- 0.1	——		———		——	
#5	1440	980	-32.0	1140	-21.0	1198	-16.9	1278	-11.4	1432	- 0.5
#6	1500	960	-36.0	1110	-26.0	1200	-20.0	1300	-13.4	1440	- 4.0
#7a	——	887	———	1025	——	1200	———	1290	———	——	———
#7b	1550	1200	-22.6	1380	-11.0	1200	-22.6	1290	-16.8	1480	- 4.5
#8a	——	1205	———	1385	———	1205	———	1313	———	———	———
#8b	1450	855	41.0	985	-32.1	1205		1313	-17.0	1480	+ 2.0

* See Text Page 36 For Definitions.

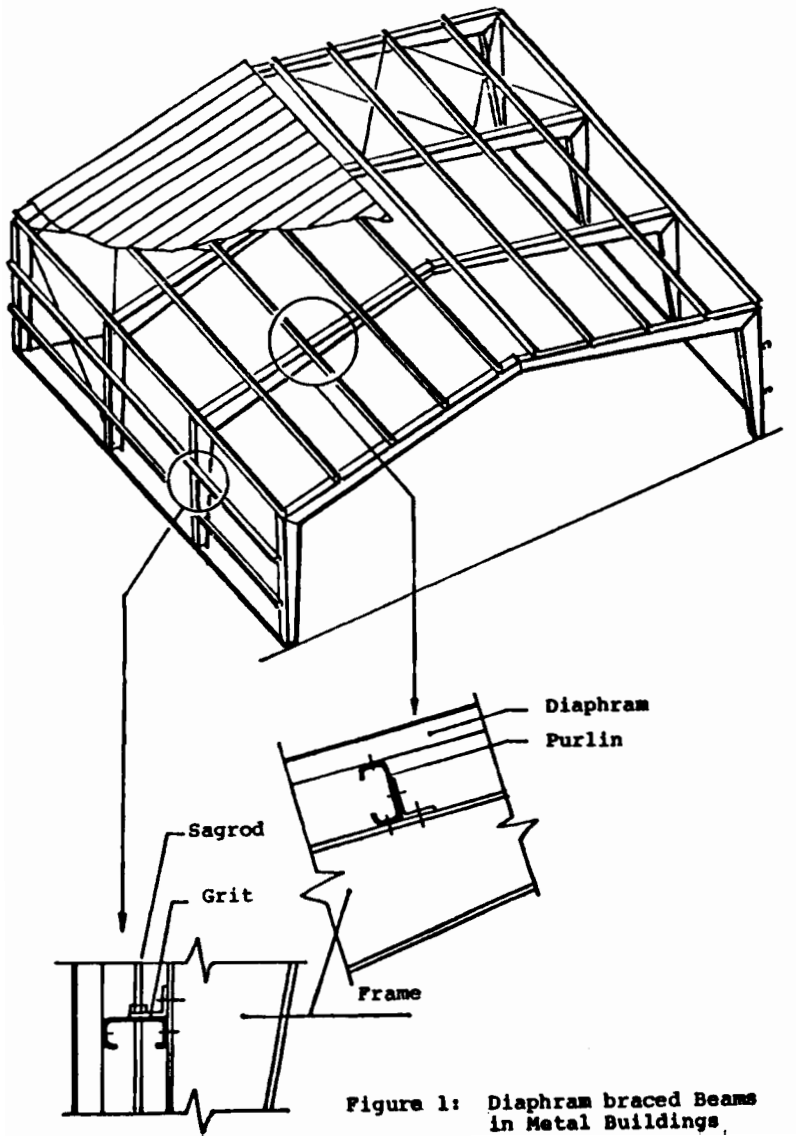

Figure 1: Diaphram braced Beams in Metal Buildings

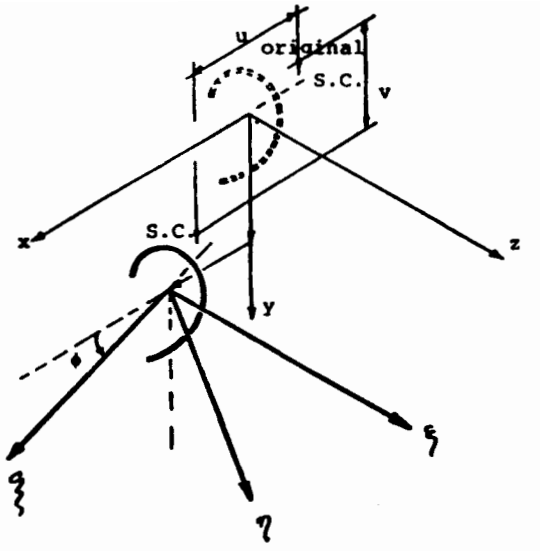

Figure 2: Coordinate Axes, Deflections u, v, ϕ

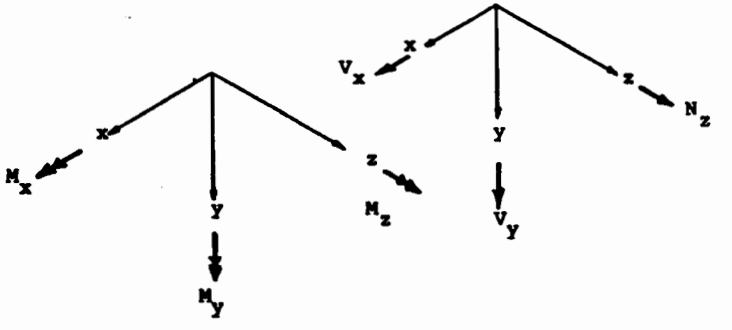

Figure 3: Positive Directions of Moments and Forces

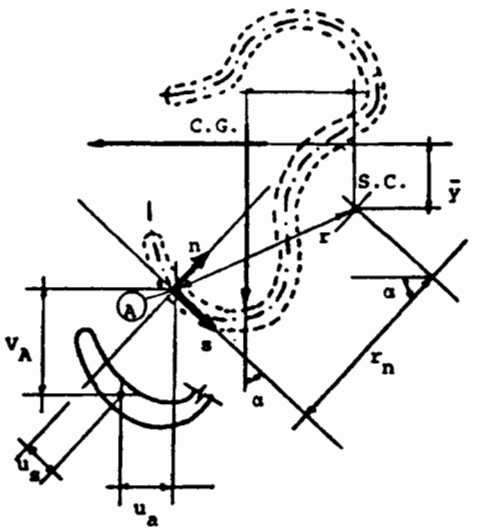

Figure 4: Tangential Displacement u_s

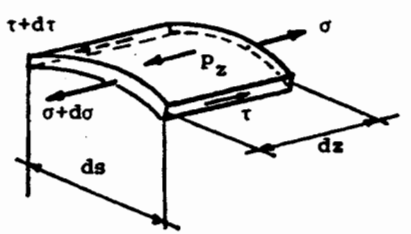

Figure 5: Equilibrium of an Element in Direction z

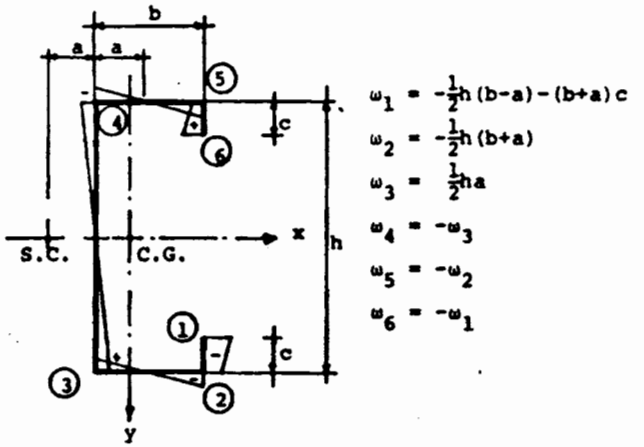

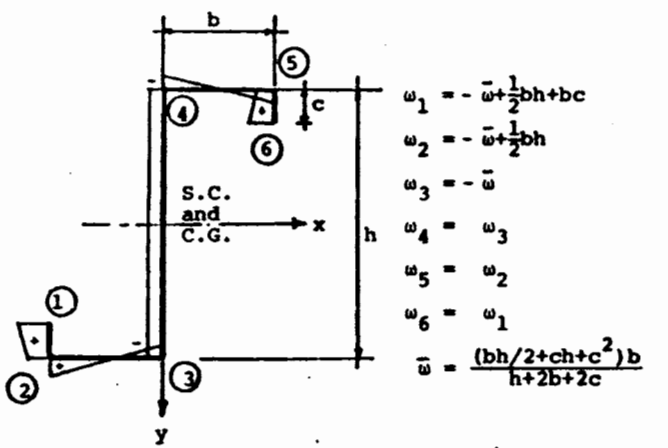

Figure 6: Formulas for Sectional Area (warping-displacement) ω for Channel and Z-Sections

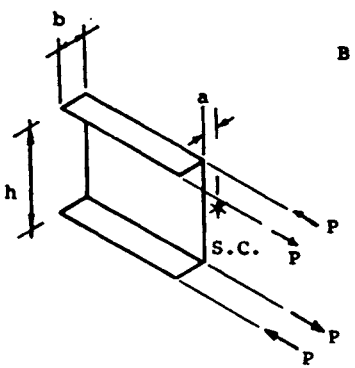

$B = \Sigma P_i \omega_i = Pbh$

Figure 7a: A force system constituting only a bimoment

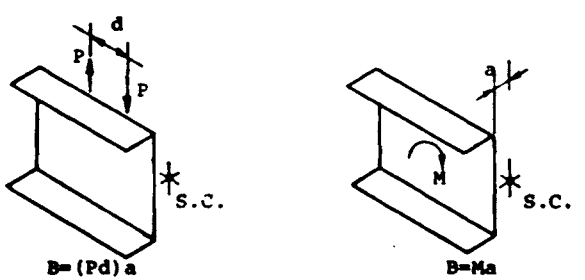

Figure 7b: Bimoment of a couple constiting of forces perpendicular to the z-axis of the beam

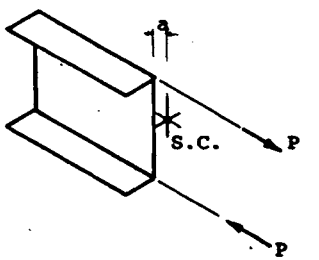

$B=\Sigma P_i \omega_i = P(-\frac{1}{2}ha) - P(\frac{1}{2}ha)$

$= -Pha$

Figure 7c: Bimoment of a couple consisting of forces parallel to the z-axis of the beam

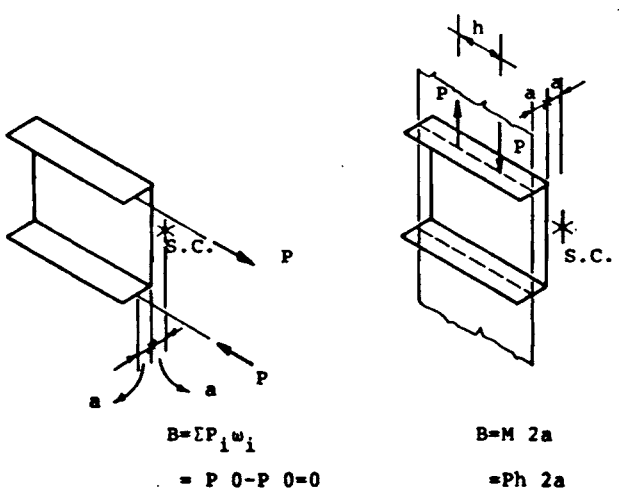

$B=\Sigma P_i \omega_i$

$= P\ 0 - P\ 0 = 0$

$B = M\ 2a$

$= Ph\ 2a$

Figure 7d: Comparison of bimoments of two equal couples, one of them arising due to forces parallel to the z-axis where as the other due to forces perpendicular to the z-axis of the beam.

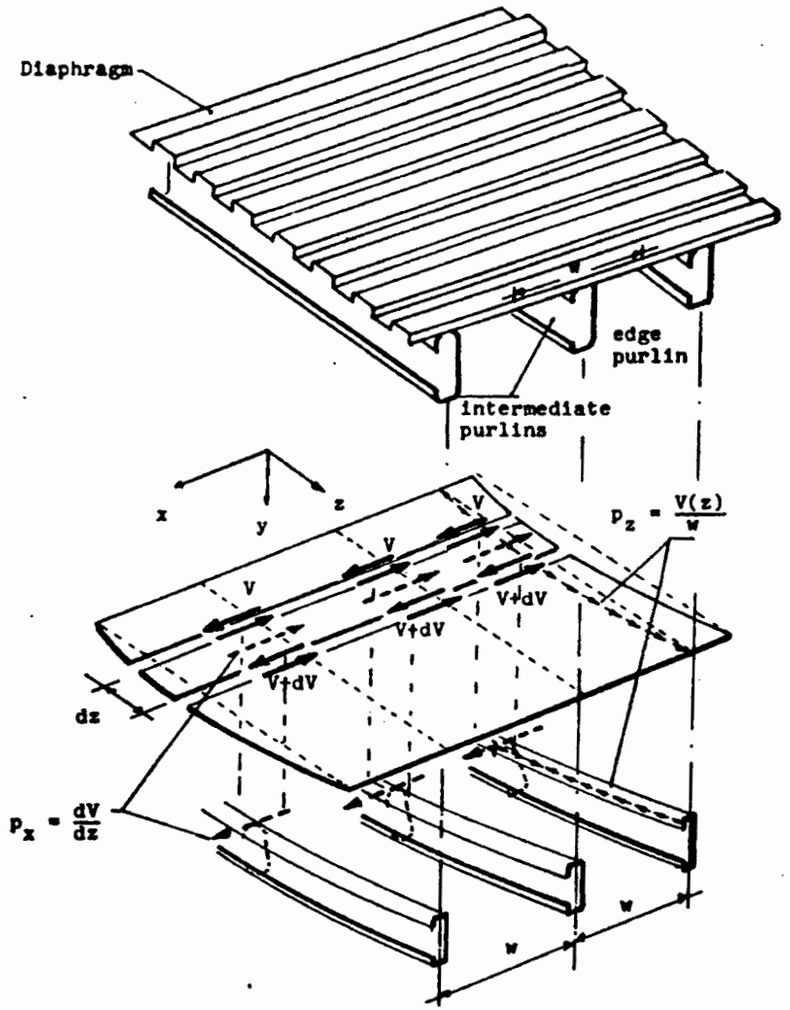

Fig. 8 Shear Forces in the Diaphragm and the Lateral Bracing Force p_x

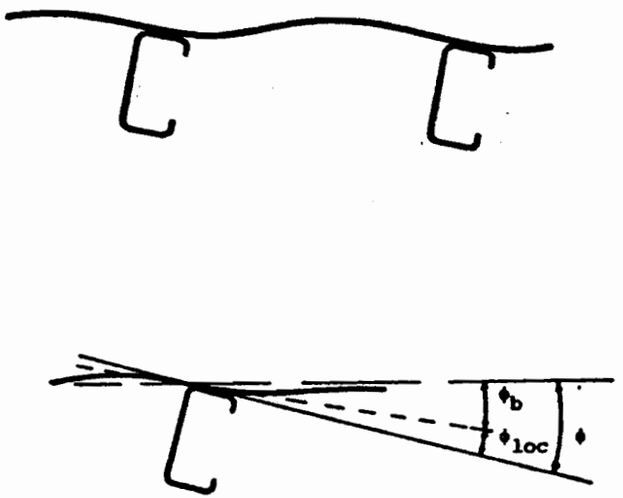

Figure 9: Rotation of Purlin and Diaphragm

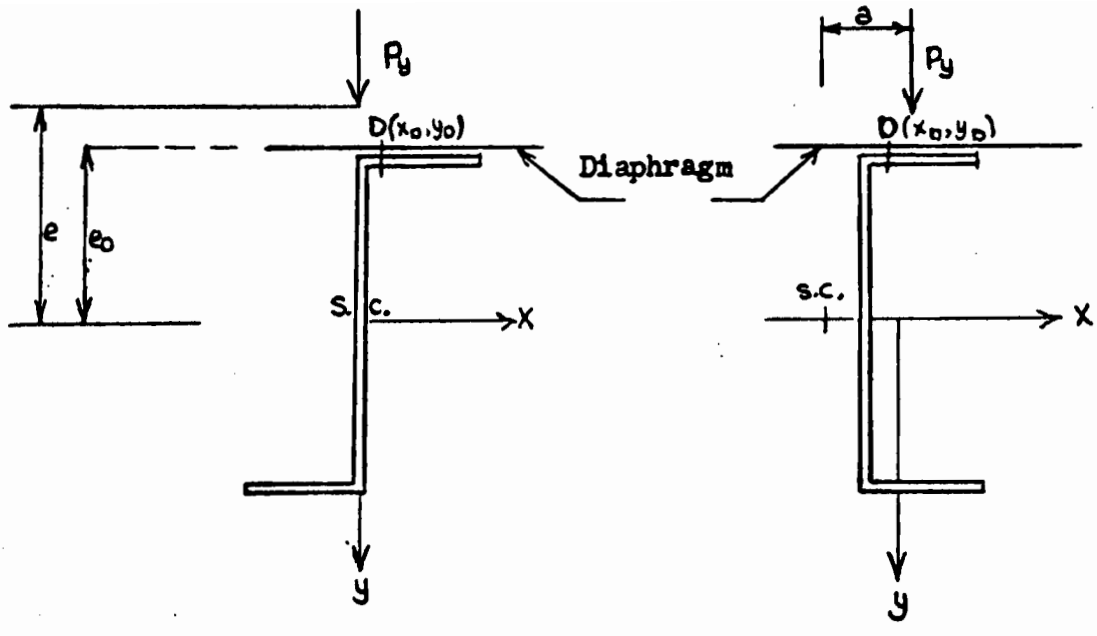

FIG. 10 Notation for the point of application of load

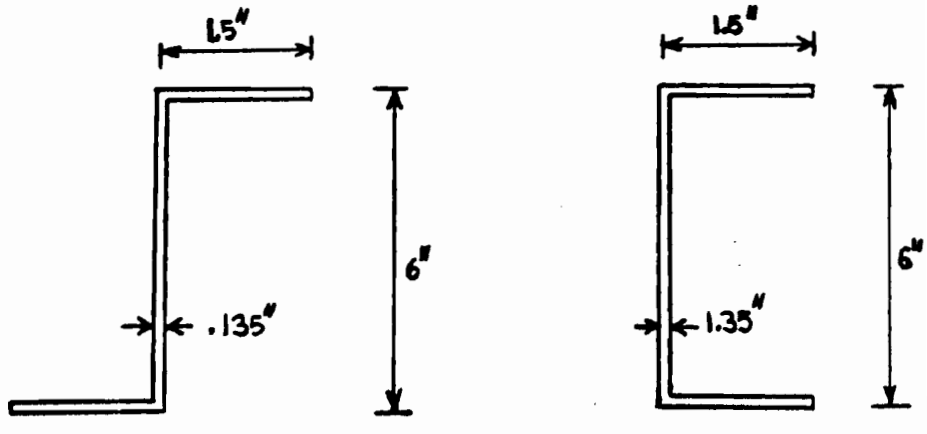

FIG.11 Dimensions of sections discussed in this paper

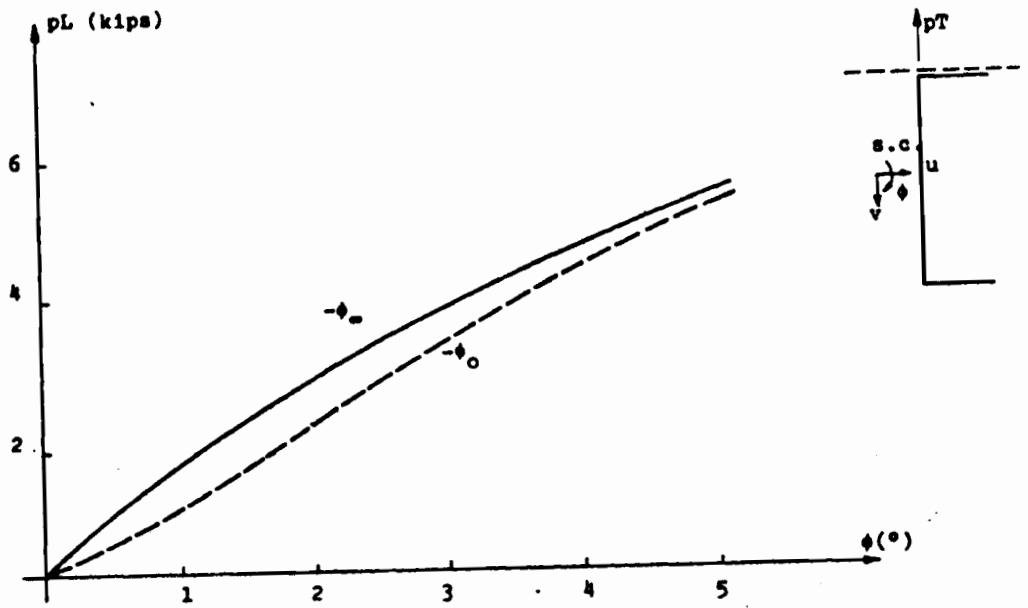

Figure 12. Mid-span rotation ϕ versus pL up to theoretical failure. Uplift, L = 60"

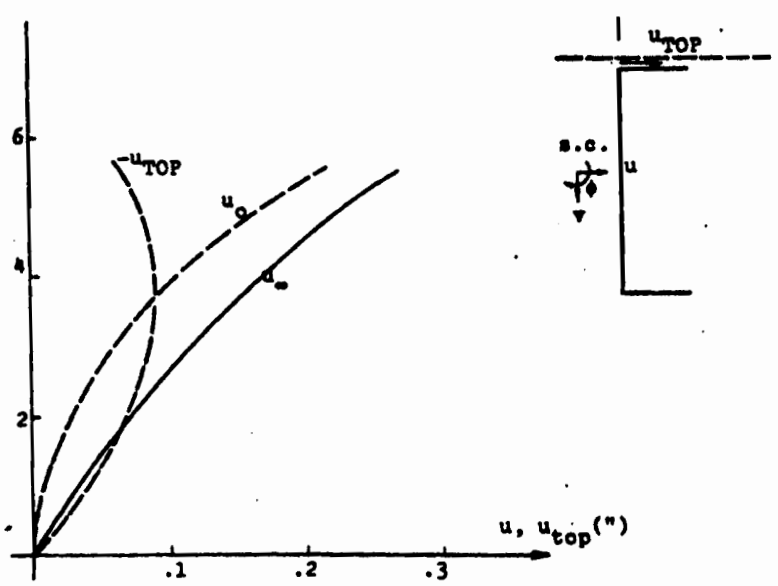

Figure 13. Lateral deflection u versus pL up to theoretical failure Uplift, L = 60"

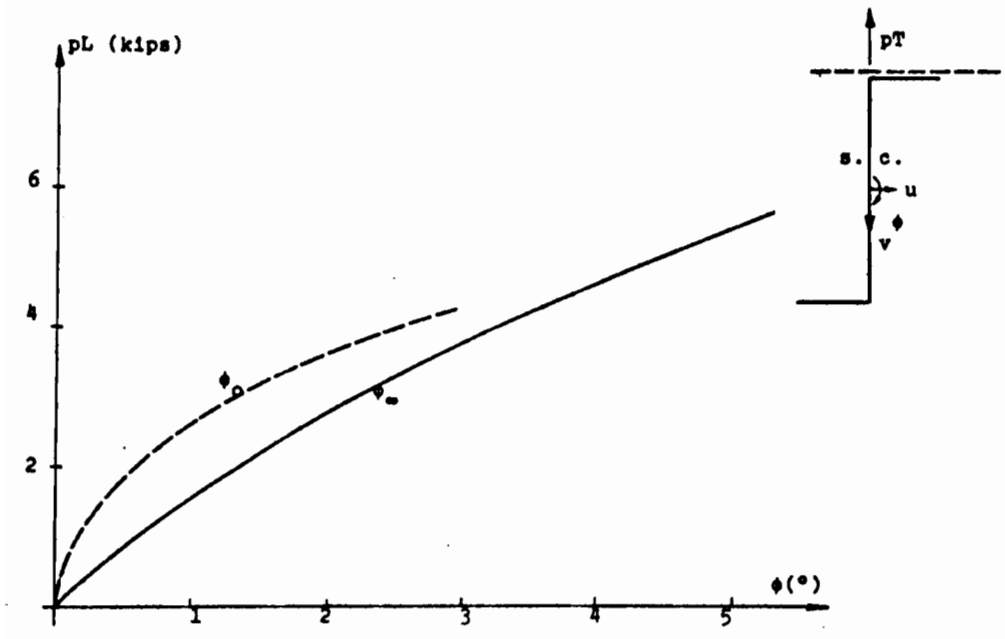

Figure 14. Midspan rotation φ versus pL up to theoretical failure Uplift, L = 60"

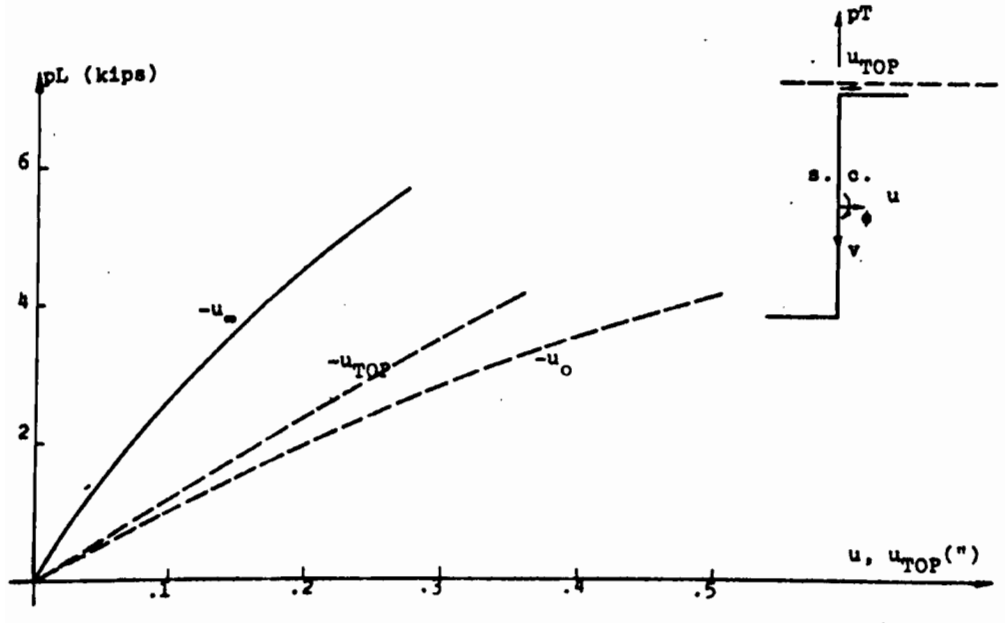

Figure 15. Lateral deflection u versus pL up to theoretical failure Uplift, T. = 60"

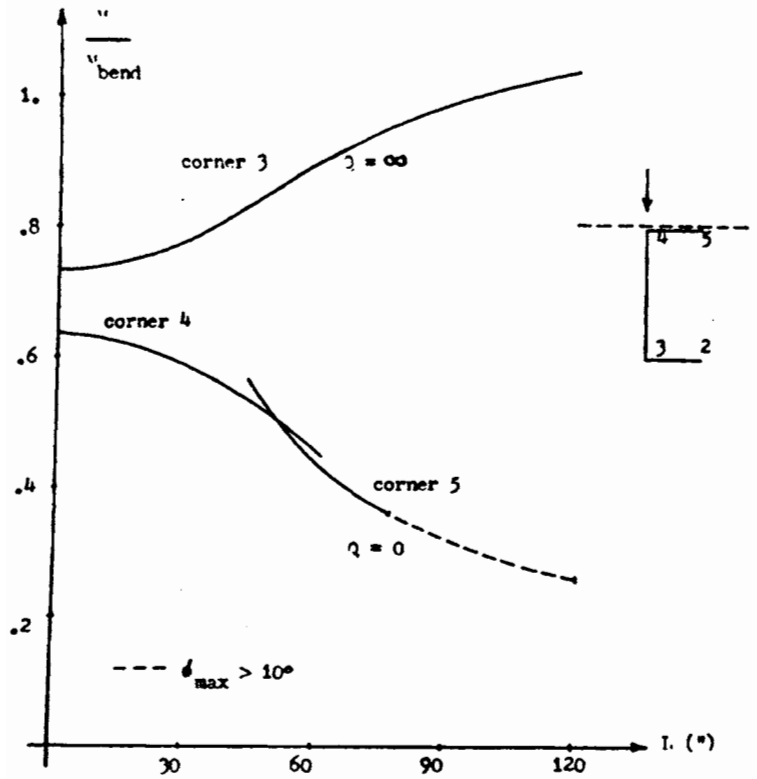

FIG. 16 Comparison of the moment M when stress reaches 1.15 σ_y with yield moment when twist is restrained M_{bend}
Gravity Load, Channel

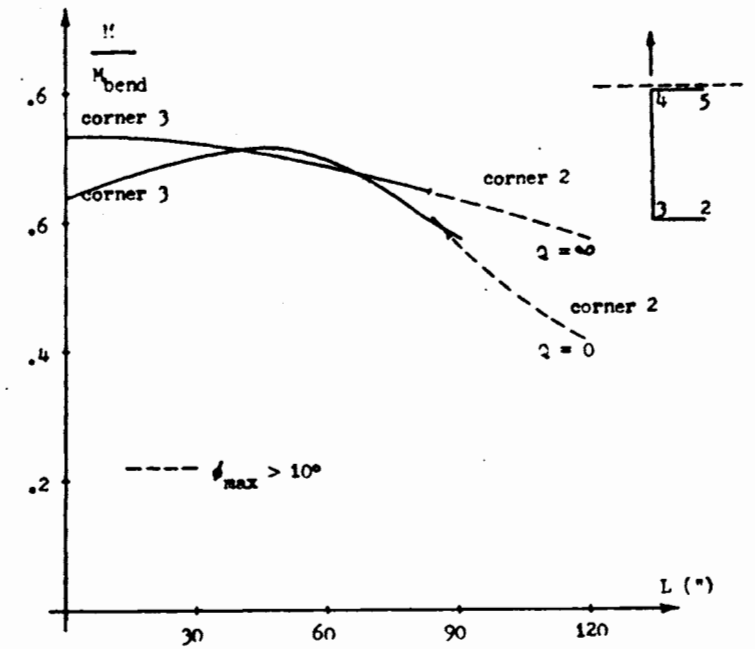

FIG. 17 Comparison of the moment M when stress reaches 1.15 σ_y with yield moment when twist is restrained M_{bend}
Uplift, Channel

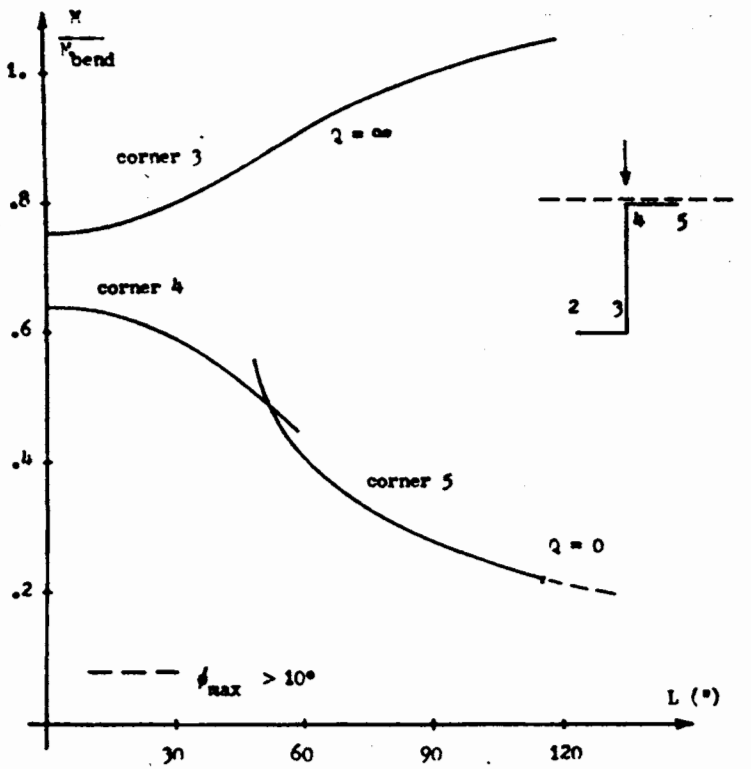

FIG. 18 Comparison of the moment M when stress reaches 1.15 σ_y with yield moment when twist is restrained M_{bend}
Gravity Load, Z-section

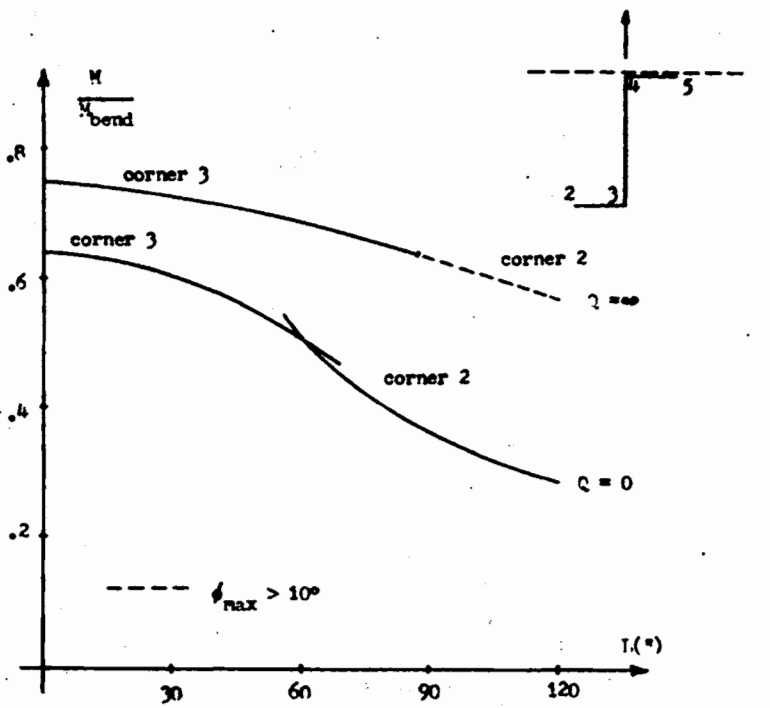

FIG. 19 Comparison of the moment M when stress reaches 1.15 σ_y with yield moment when twist is restrained M_{bend}
Uplift, Z-section

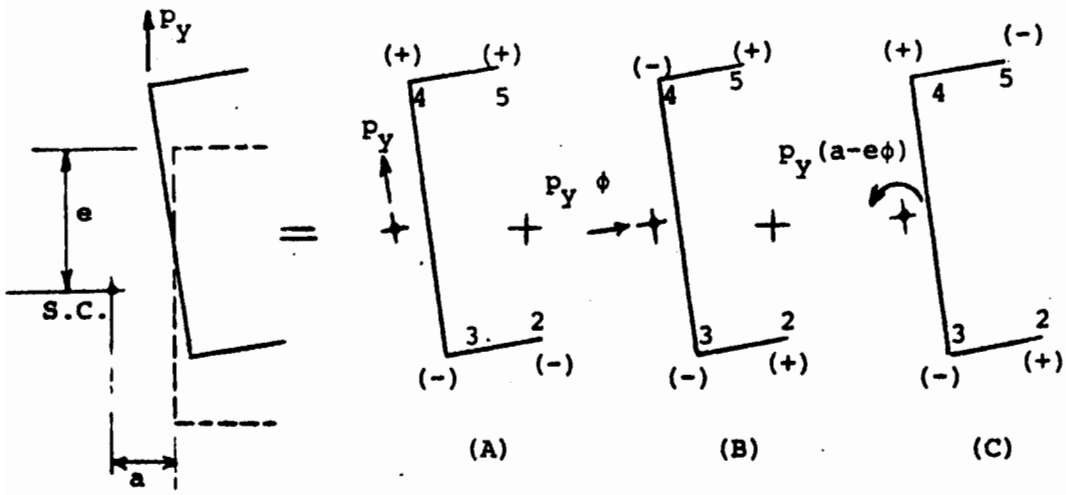

Figure 20: (a) Force Components at Shear Center for Unbraced Channel due to vertical Uplift.

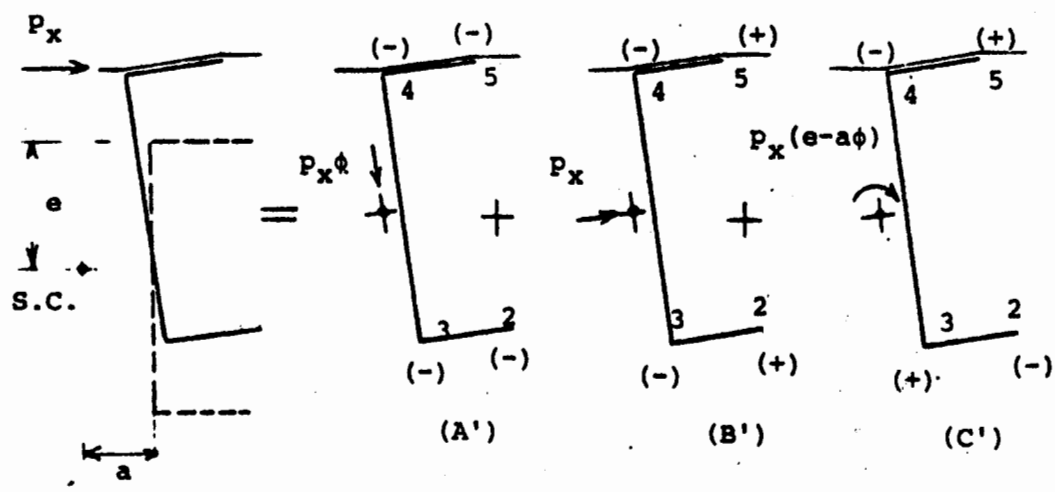

Figure 20: (b) Force Components at Shear Center due to Force P_x in Diaphragm

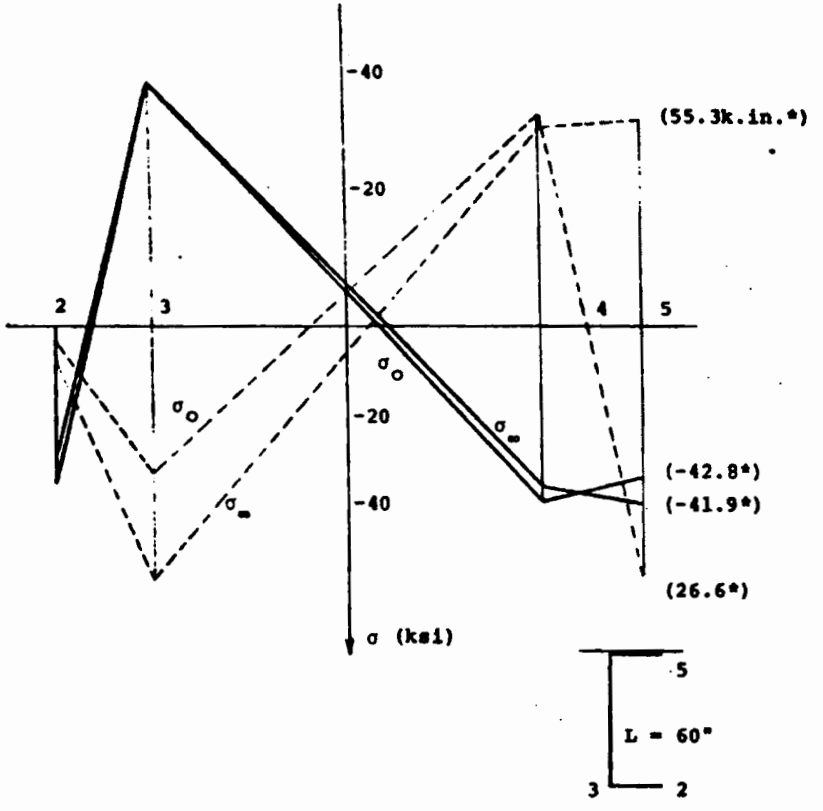

Figure 21: Stress Distribution at Failure

* (Failure moments in parenthesis)

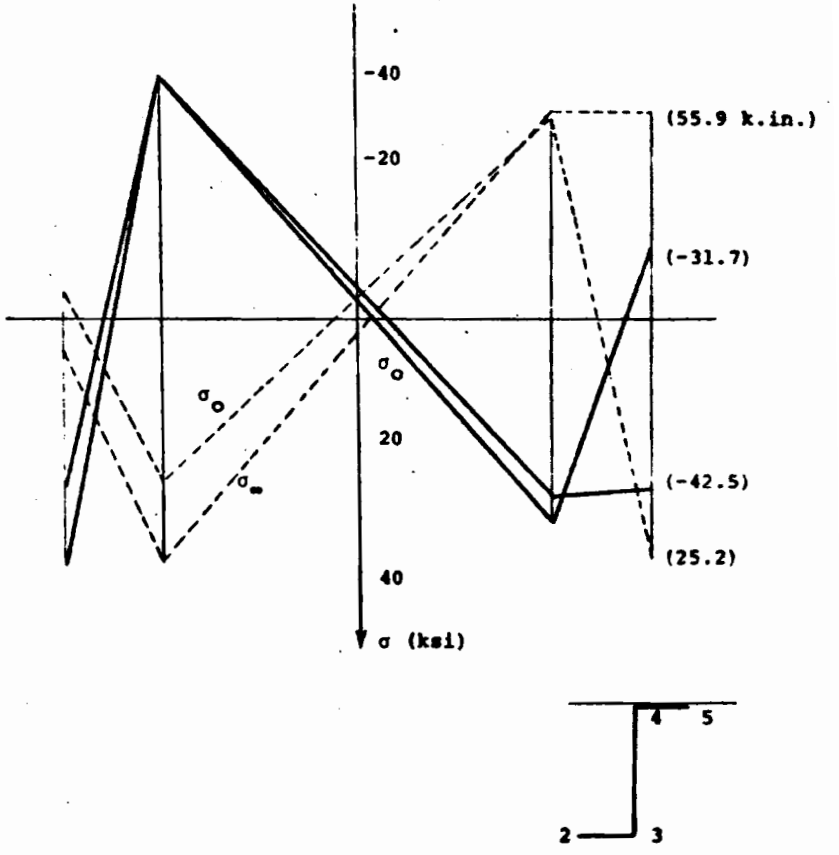

Figure 22: Stress Distribution at Failure
(Failure moments in parentheses)

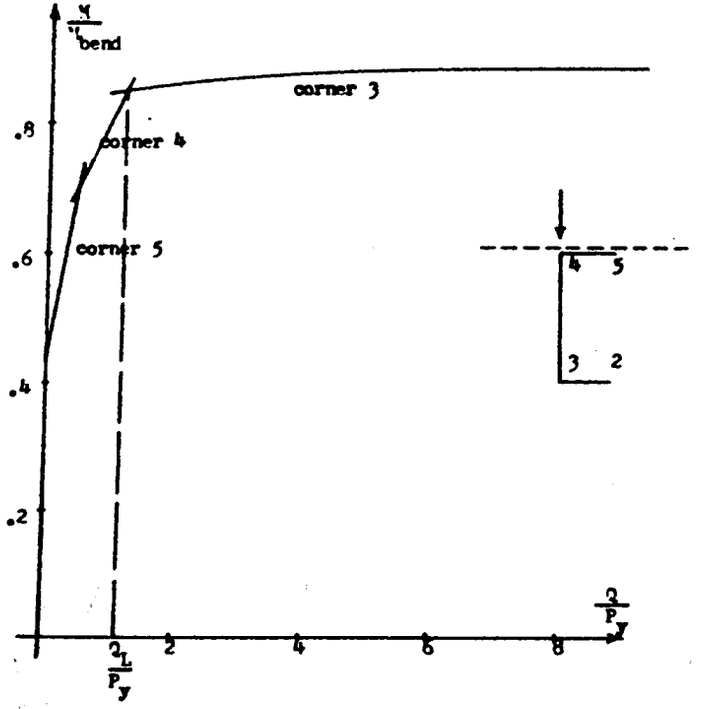

FIG. 23 Comparison of the moment, M, when stress reaches $1.15\sigma_y$ with yield moment when twist is restrained, M_{bend}, versus Q/P_y, gravity load, channel

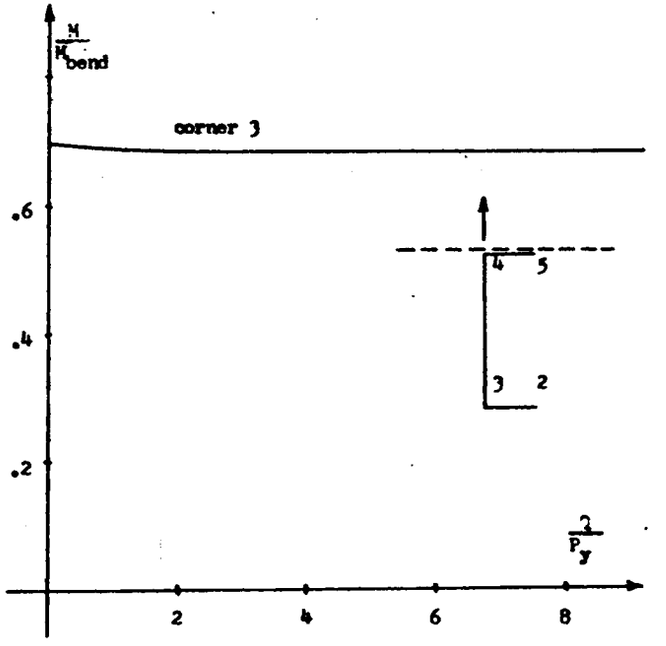

FIG. 24 Comparison of the moment, M, when stress reaches $1.15\sigma_y$ with yield moment when twist is restrained, M_{bend}, versus Q/P_y, uplift, channel

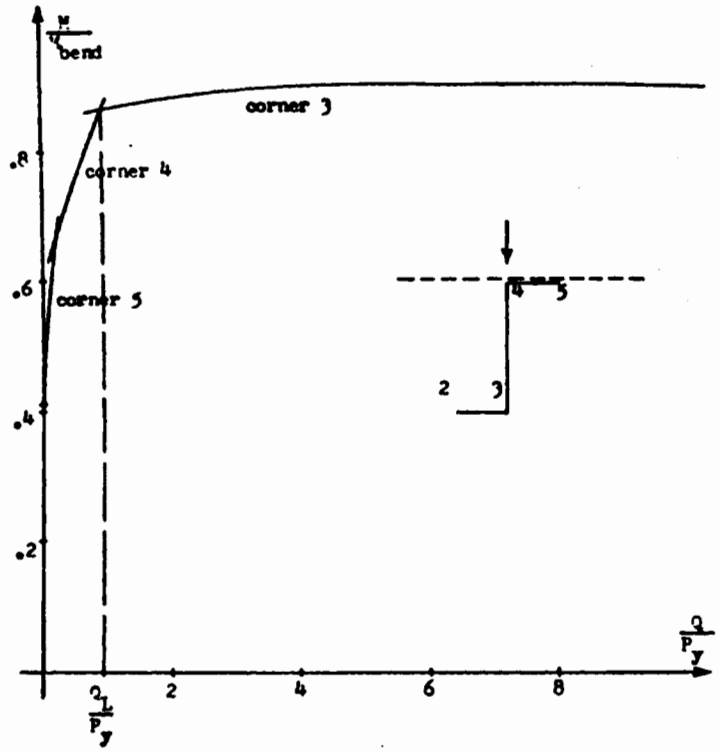

FIG. 25 Comparison of the moment, M, when stress reaches $1.15\sigma_y$ with yield moment when twist is restrained, M_{bend} , versus Q/P_y , gravity, Z-section

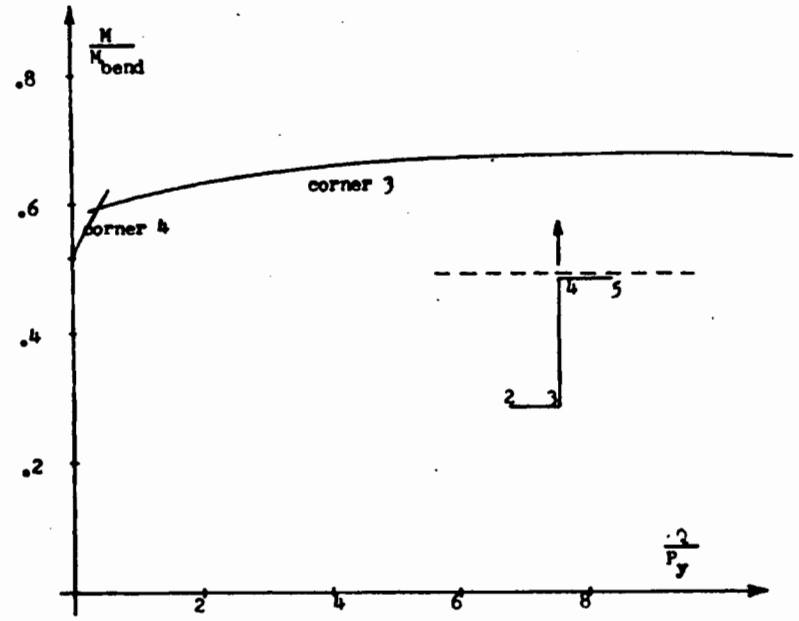

FIG. 26 Comparison of the moment , M, when stress reaches $1.15\sigma_y$ with yield moment when twist is restrained , M_{bend} , versus Q/P_y , uplift, Z-section

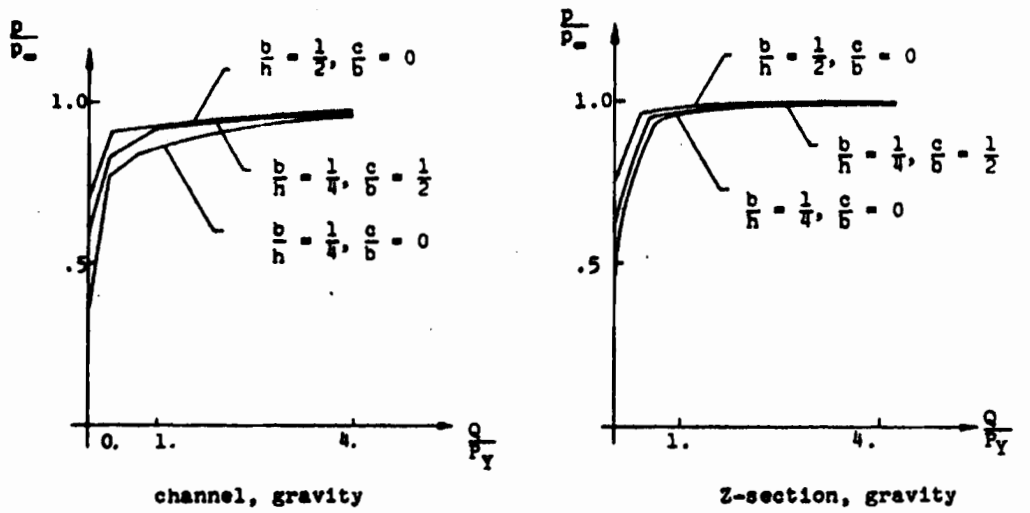

Figure 27 The ratio $\frac{p}{p_\infty}$ versus $\frac{Q}{P_Y}$ at theoretical failure for $\frac{L}{h} = 10$ and $\frac{h}{t} = 80$

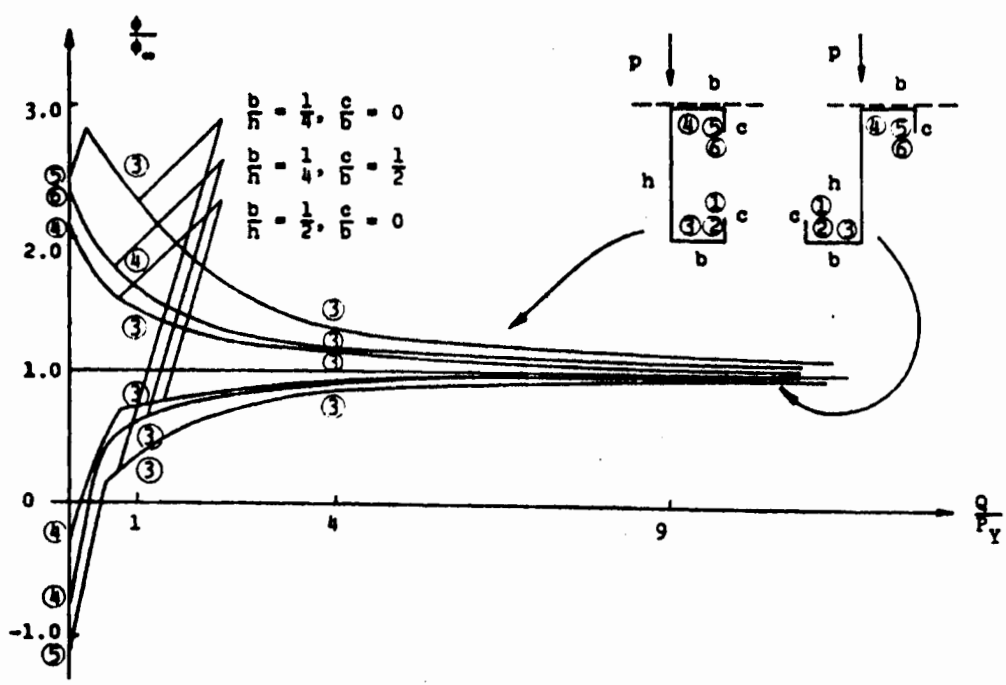

Fig. 28 The ratio $\frac{\phi}{\phi_\infty}$ versus $\frac{Q}{P_Y}$ at theoretical failure for $\frac{L}{h} = 10$ and $\frac{h}{t} = 80$

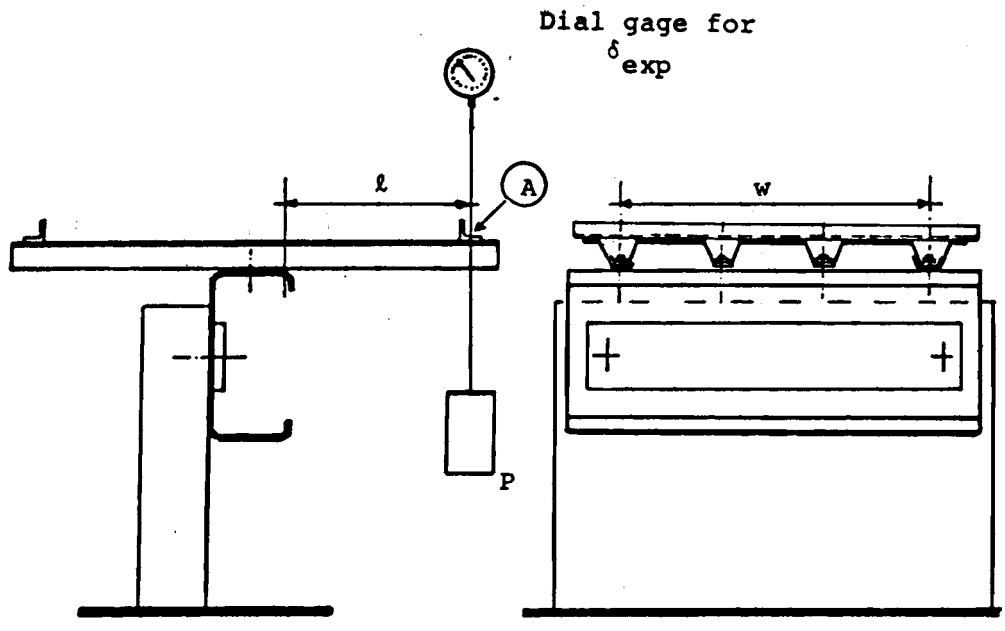

Figure 29: Test Set-up for Determination of F_{local}

(The rotation for this particular arrangement corresponds to uplift loading case of Channels)

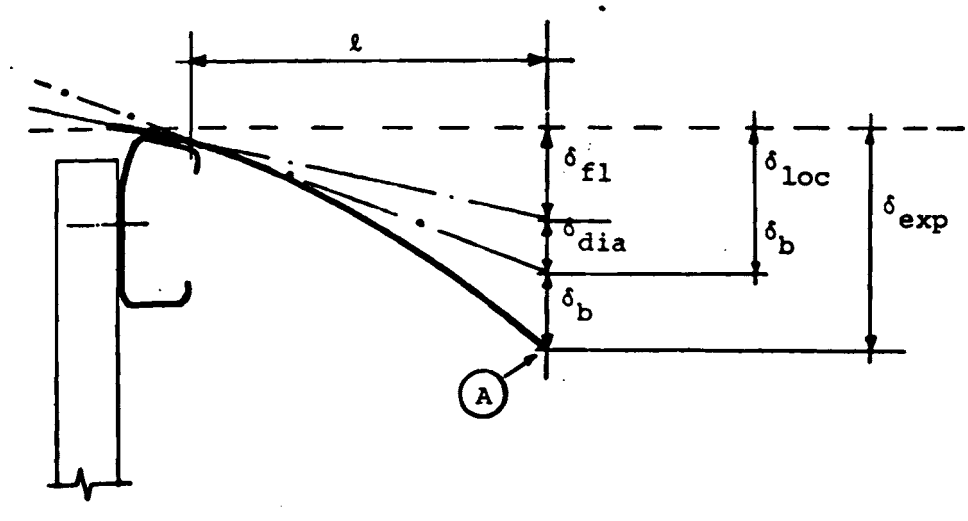

Figure 30: Deflections of Point A

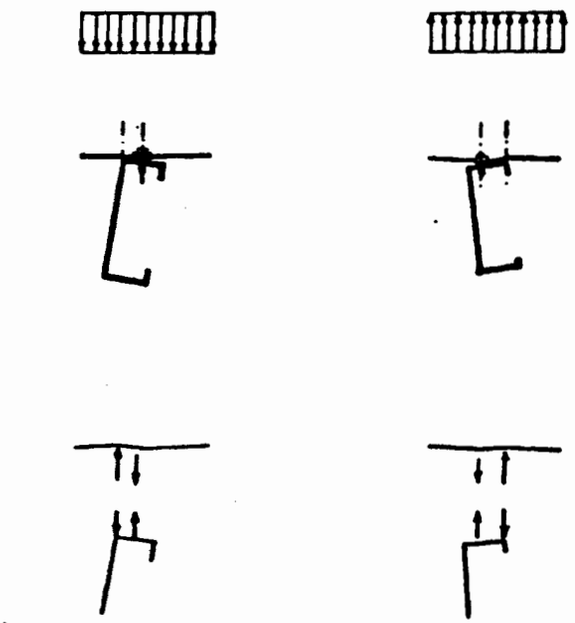

Figure 31: Direction of Rotation and respective Force Couples created between Diaphragm and Purlin Channel Section (bending deformations of diaphragm not shown).

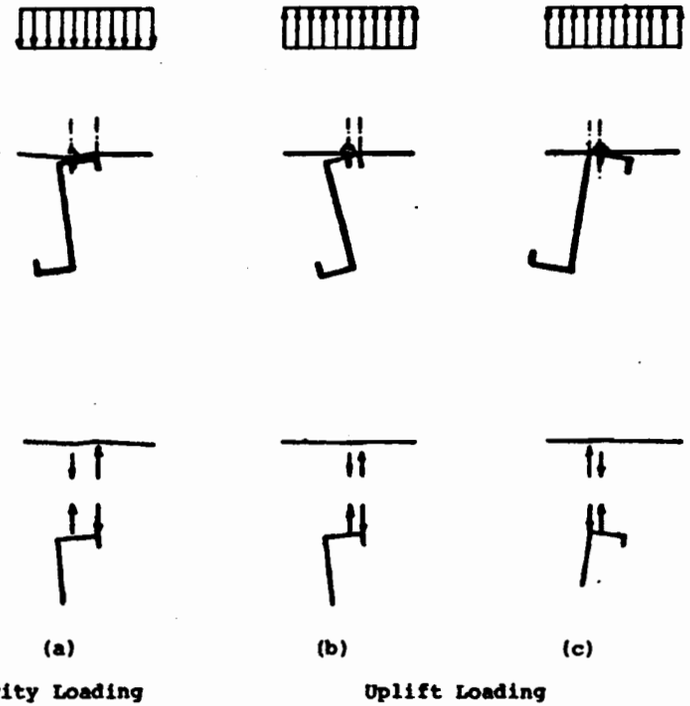

Figure 32: Direction of Rotation and respective Force Couples created between Diaphragm and Purlin,Z-Section (bending deformations of diaphragm not shown).

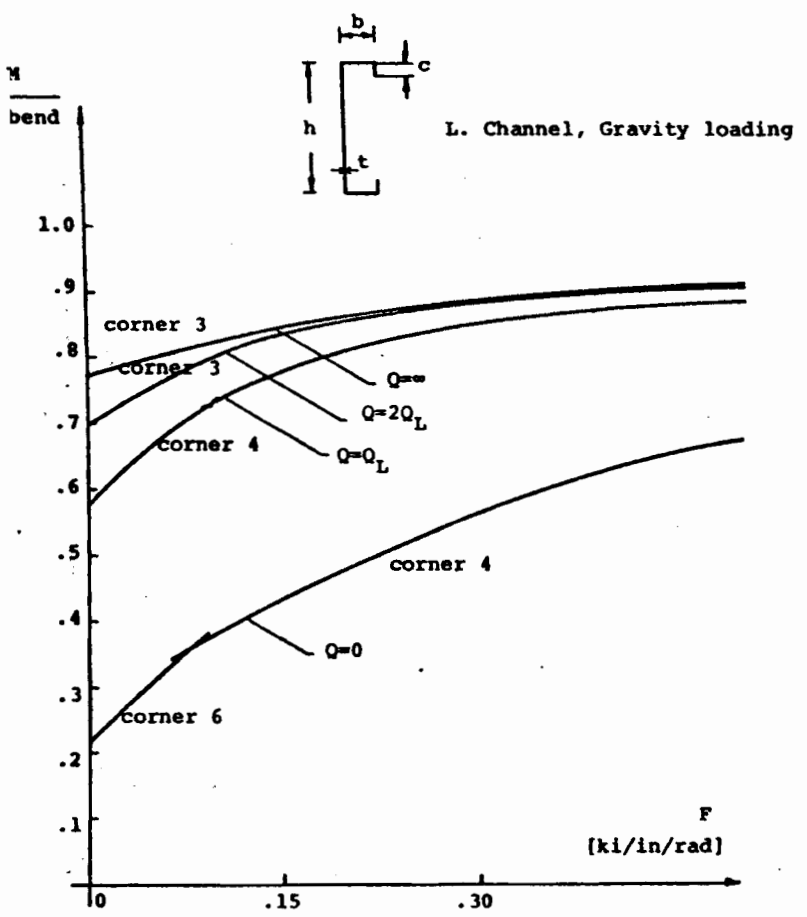

Figure 33a: The ratio M/M_{bend} versus the rotational restraint F for various values of the shear rigidity Q. The geometrical parameters are:

$$\frac{L}{h} = 15 \ , \ \frac{b}{h} = \frac{1}{4} \ , \ \frac{c}{b} = .4 \ , \ \frac{b}{t} = 20$$

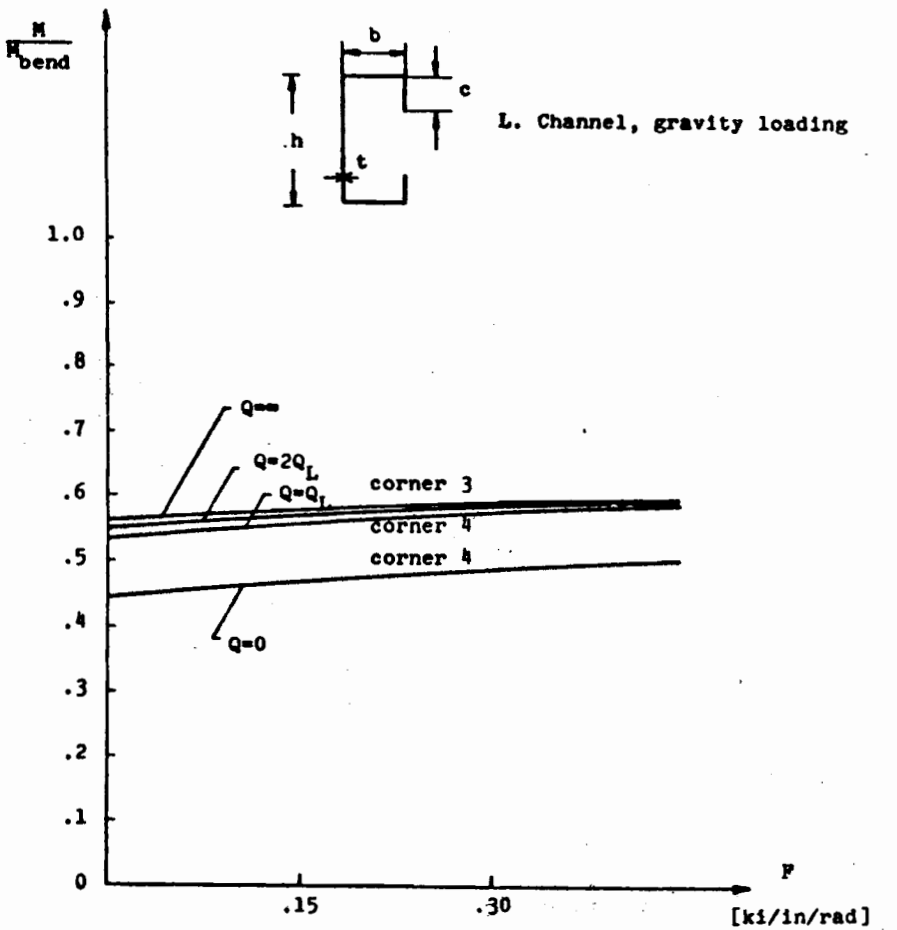

Figure 33b The ratio $\frac{M}{M_{bend}}$ versus the rotational restraint F for various values of the shear rigidity Q. The geometrical parameters are

$$\frac{L}{h} = 15, \ \frac{b}{h} = \frac{1}{2}, \ \frac{c}{b} = \frac{1}{2}, \ \frac{b}{t} = 20$$

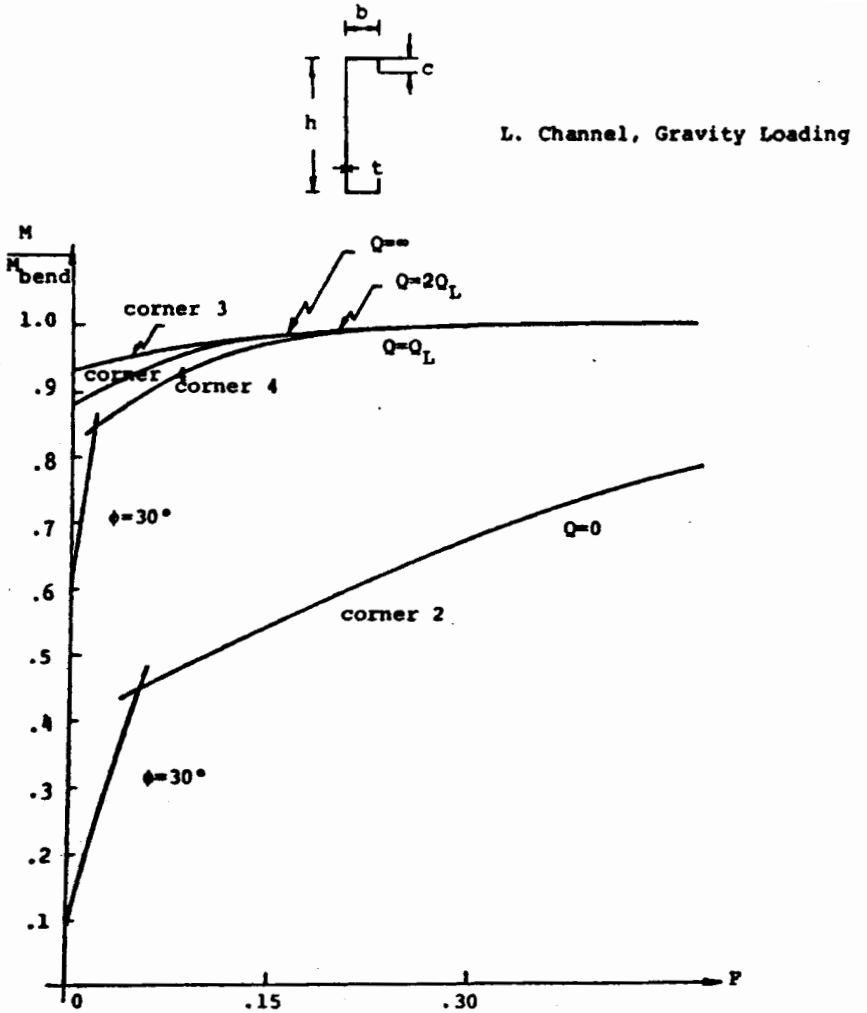

Figure 34a: The ratio M/M_{bend} versus the rotational restraint F for various values of the shear rigidity Q. The geometrical parameters are:

$\frac{L}{h} = 30$, $\frac{b}{h} = \frac{1}{4}$, $\frac{c}{b} = .4$, $\frac{b}{t} = 20$

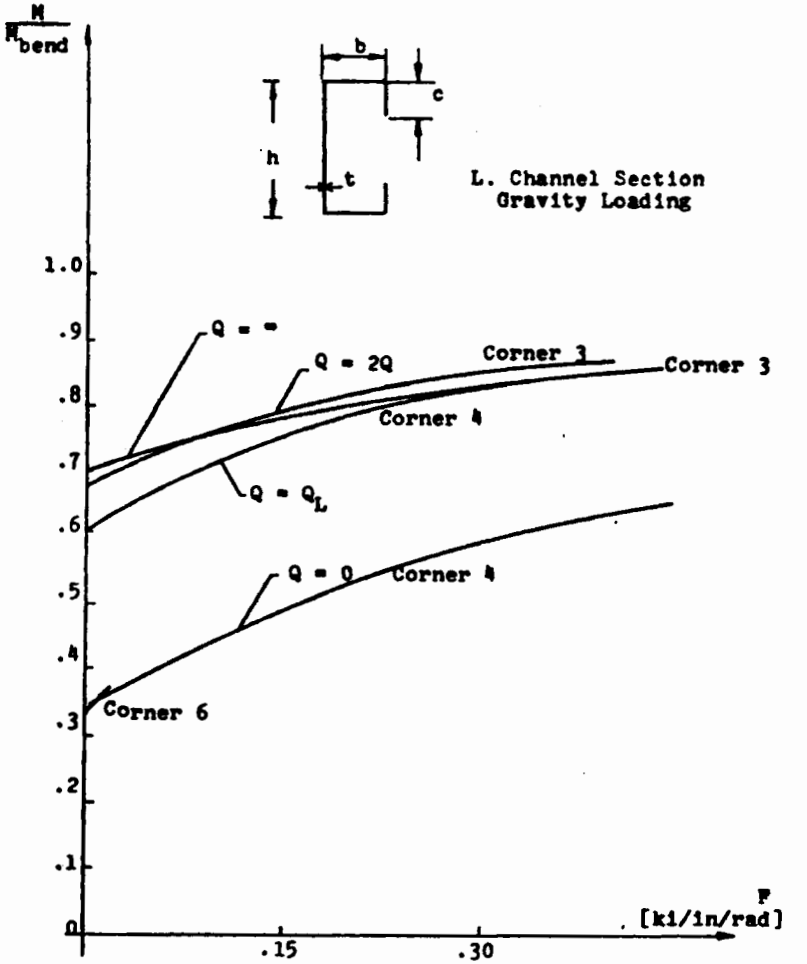

Figure 34.b. The ratio M/M_{bend} versus the rotational restraint F for various values of the shear rigidity Q. The geometrical parameters are:

$\frac{L}{h} = 30$, $\frac{b}{h} = \frac{1}{2}$, $\frac{c}{b} = \frac{1}{2}$, $\frac{b}{t} = 20$

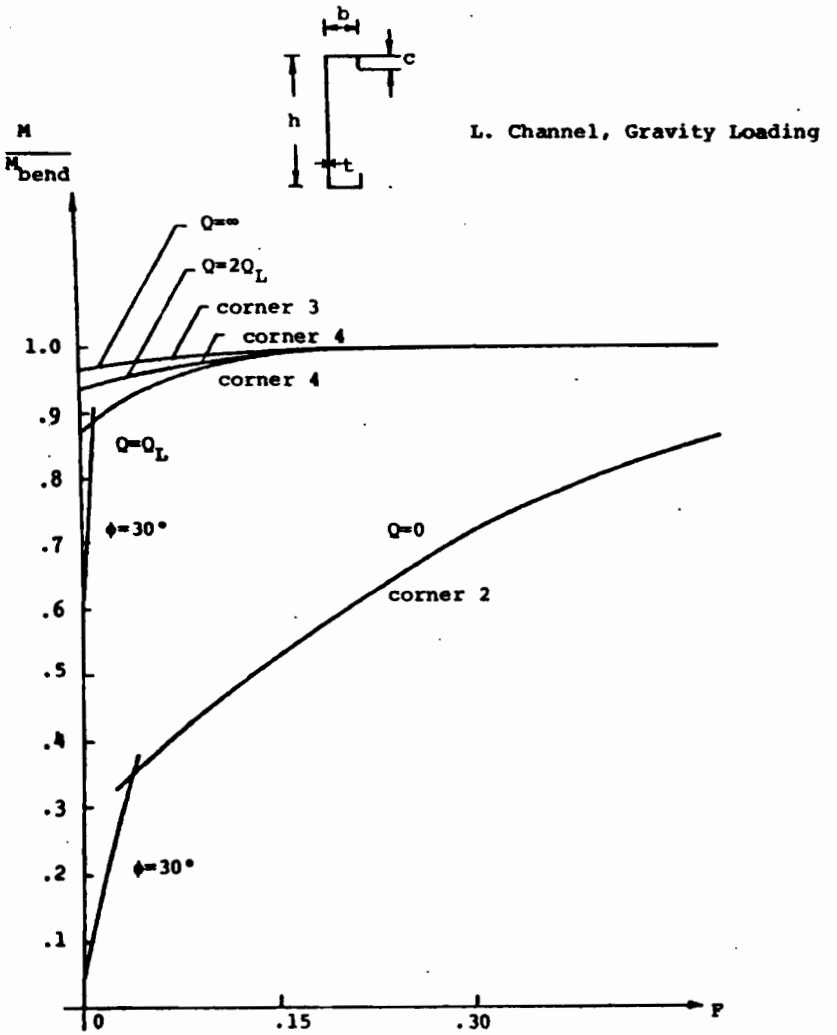

Figure 35a: The ratio M /M_{bend} versus the rotational restraint F for various values of the shear rigidity Q. The geometrical parameters are:

$\frac{L}{h} = 45$, $\frac{b}{h} = \frac{1}{4}$, $\frac{c}{b} = .4$, $\frac{b}{t} = 20$

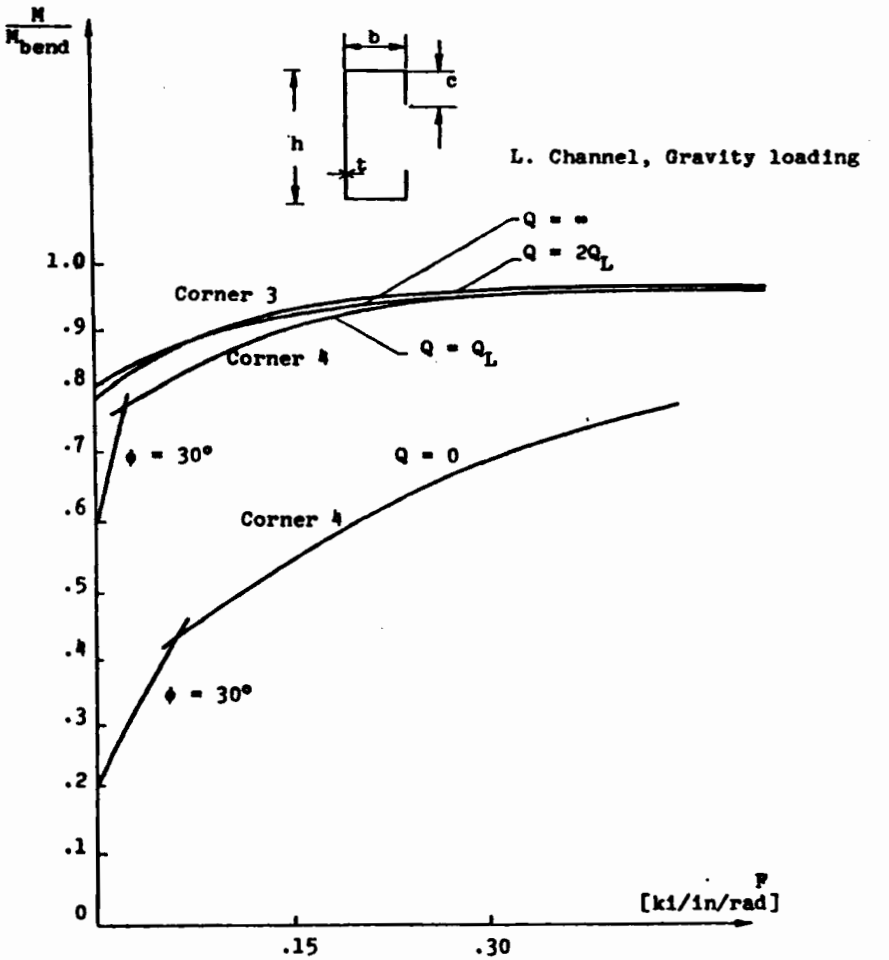

Figure 35.b The ratio M/M_{bend} versus the rotational restraint F for various values of the shear rigidity Q. The geometrical parameters are:

$\frac{L}{h} = 45$, $\frac{b}{h} = \frac{1}{2}$, $\frac{c}{b} = \frac{1}{2}$, $\frac{b}{t} = 20$

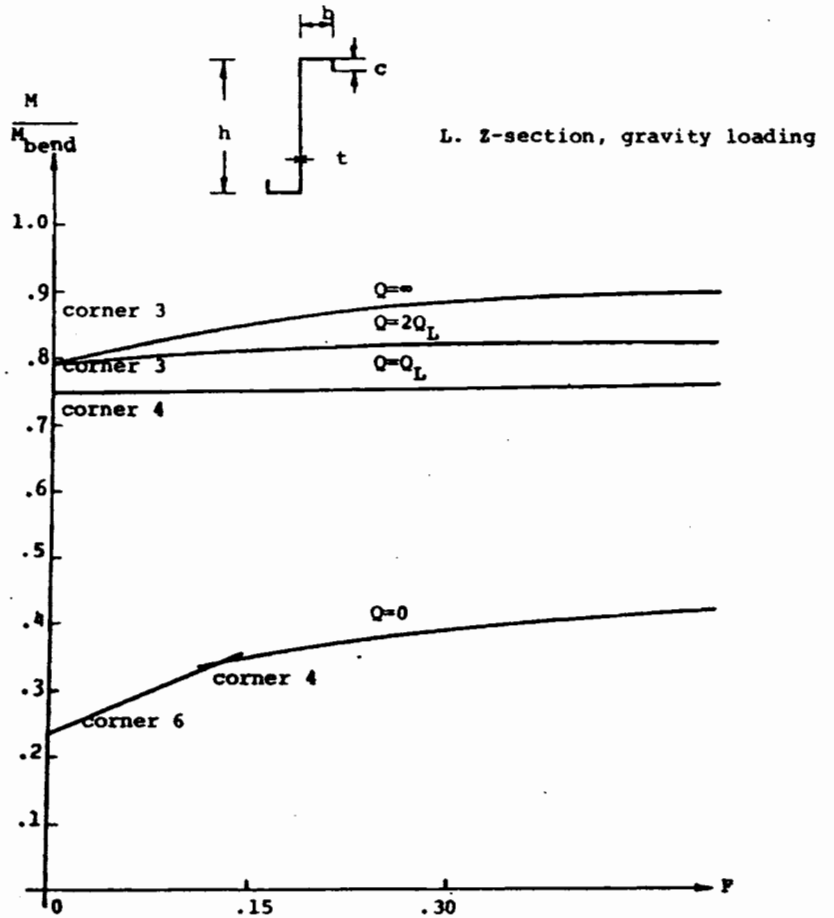

Figure 36a: The ratio M/M_{bend} versus the rotational restraint F for various values of the shear rigidity Q. The geometrical parameters are:

$\frac{L}{h} = 15$, $\frac{b}{h} = \frac{1}{4}$, $\frac{c}{b} = .4$, $\frac{b}{t} = 20$

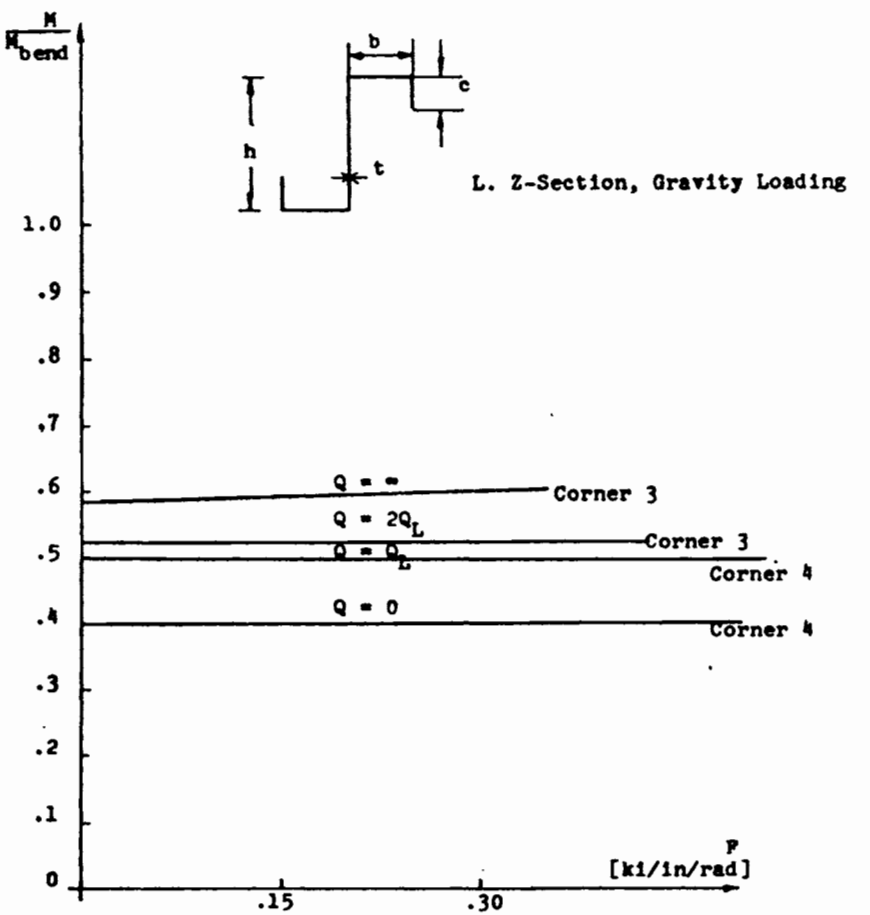

Figure 36.b. The ratio M/M_{bend} versus the rotational restraint F for various values of the shear rigidity Q. The geometrical parameters are:

$\frac{L}{h} = 15$, $\frac{b}{h} = \frac{1}{2}$, $\frac{c}{b} = \frac{1}{2}$, $\frac{b}{t} = 20$

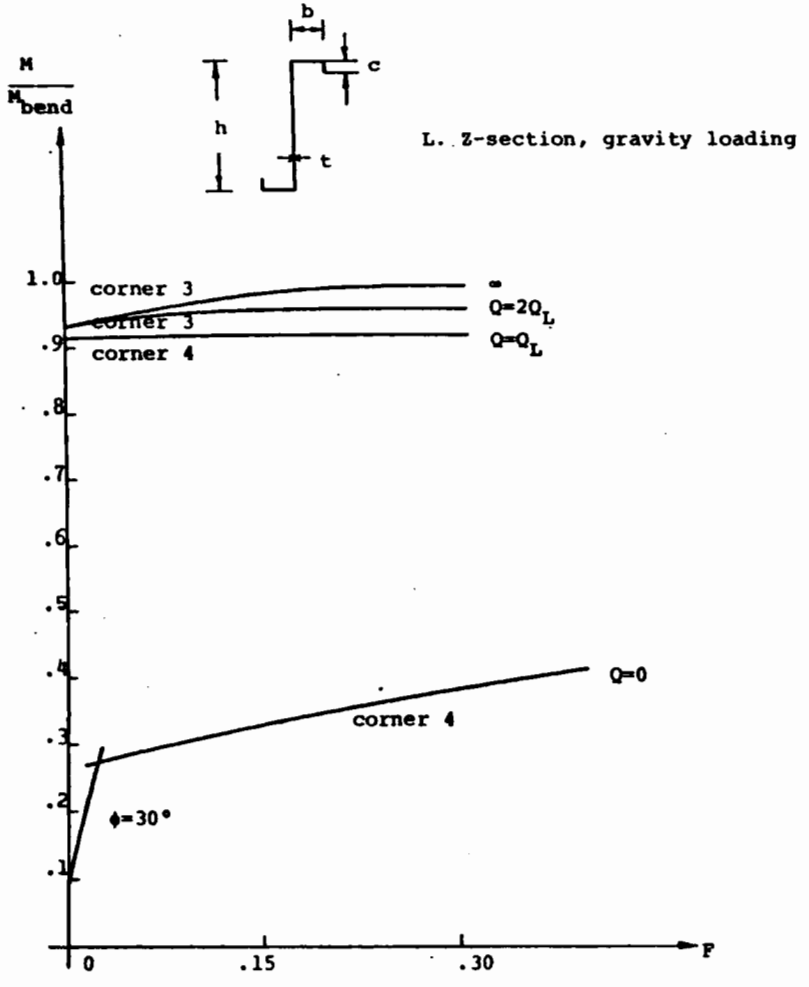

Figure 37a: The ratio M/M_{bend} versus the rotational restraint F for various values of the shear rigidity Q. The geometrical parameters are:

$\frac{L}{h} = 30$, $\frac{b}{h} = \frac{1}{4}$, $\frac{c}{b} = .4$, $\frac{b}{t} = 20$

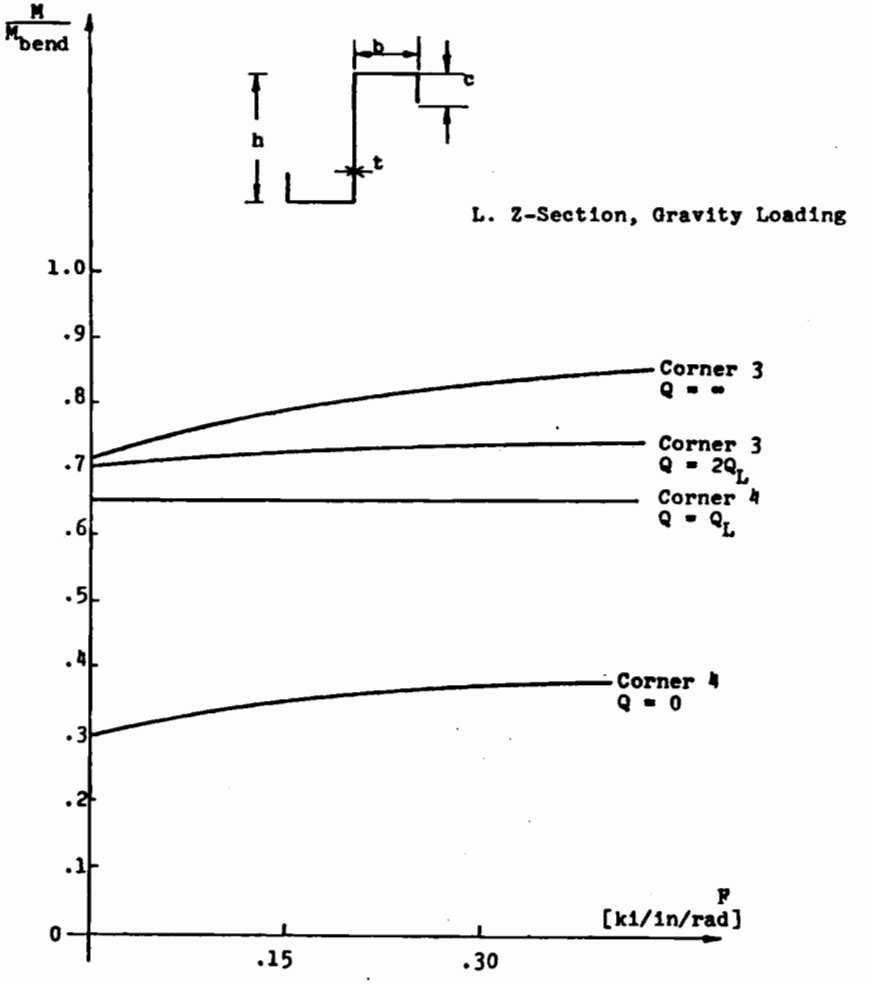

Figure 37.b. The ratio M/M_{bend} versus the rotational restraint F for various values of the shear rigidity Q. The geometrical parameters are:

$\frac{L}{h} = 30$, $\frac{b}{h} = \frac{1}{2}$, $\frac{c}{b} = \frac{1}{2}$, $\frac{b}{t} = 20$

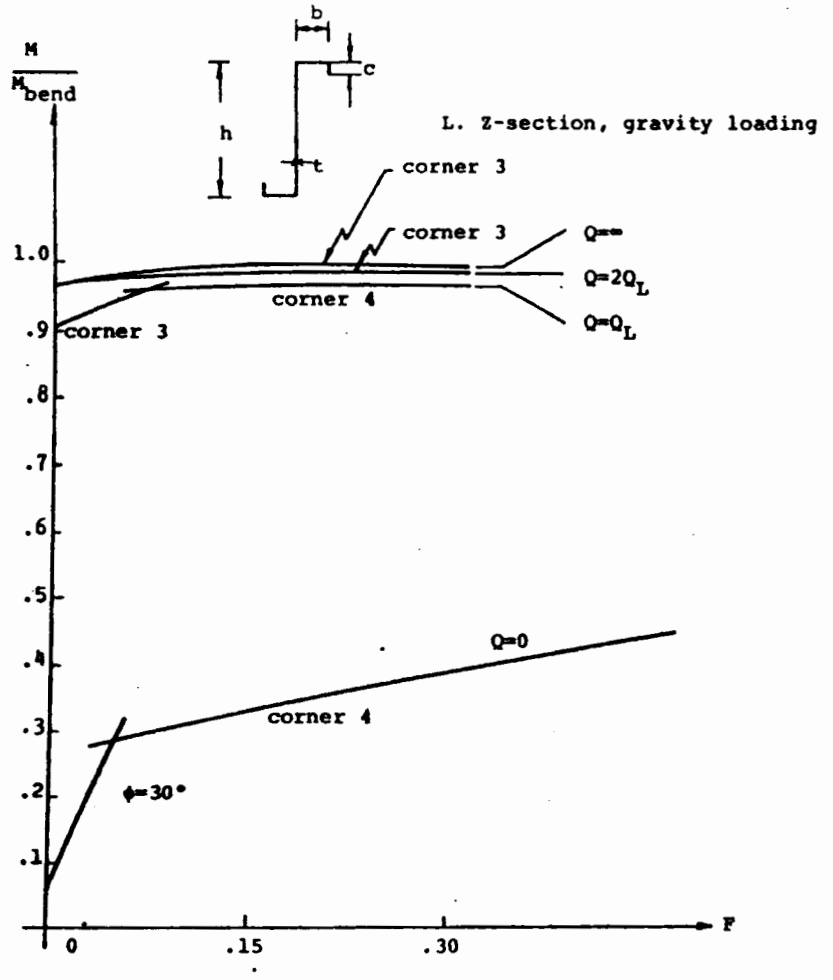

Figure 38a: The ratio M /M_{bend} versus the rotational restraint F for various values of the shear rigidity Q. The geometrical parameters are:

$\frac{L}{h} = 45$, $\frac{b}{h} = \frac{1}{4}$, $\frac{c}{b} = .4$, $\frac{b}{t} = 20$

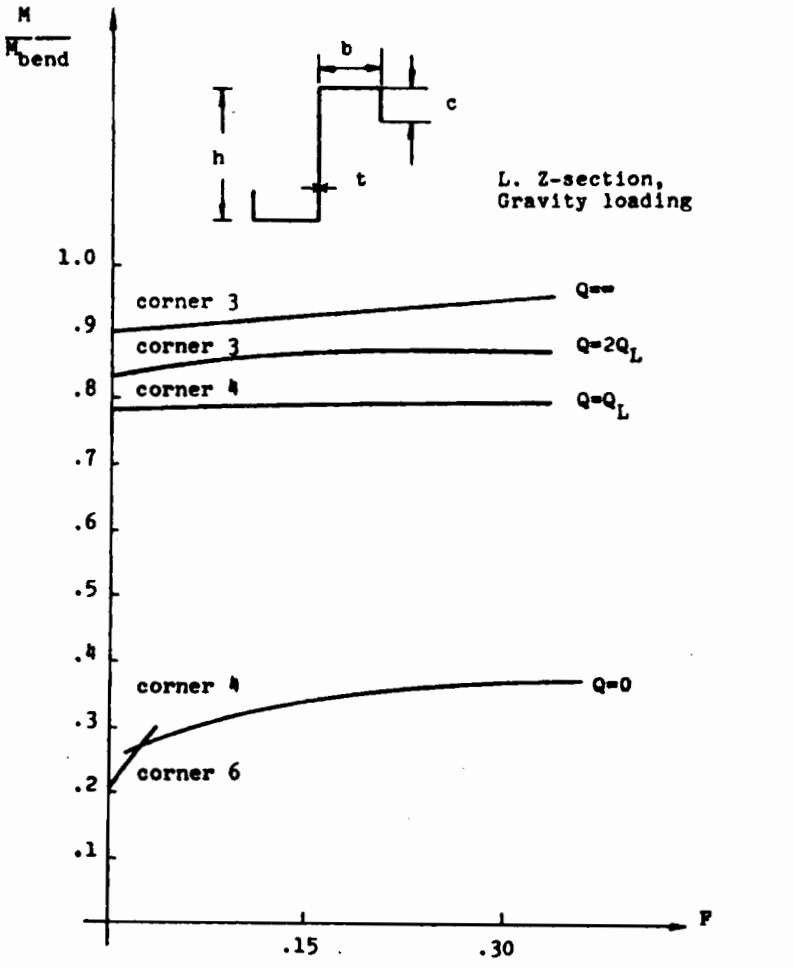

'igure 38b The ratio M/M_{bend} versus the rotational restraint F for various values of the shear rigidity Q. The geometrical parameters are

$\frac{L}{h} = 45$, $\frac{b}{h} = \frac{1}{2}$, $\frac{c}{b} = \frac{1}{2}$, $\frac{b}{t} = 20$

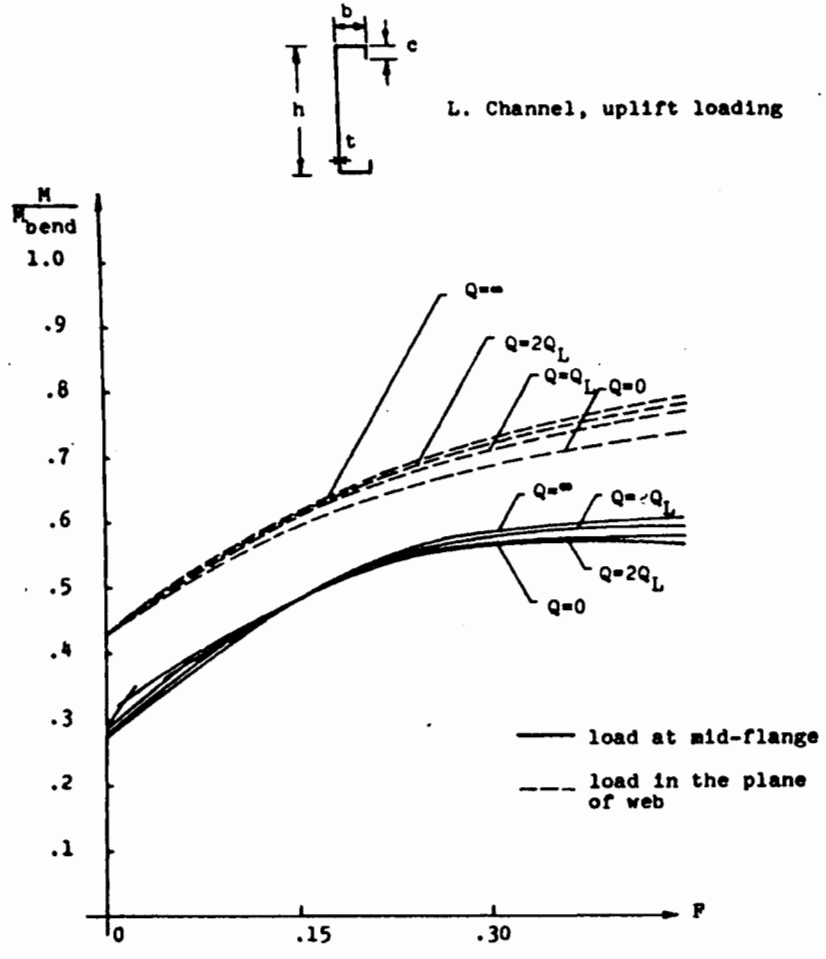

Figure 39a The ratio M/M_{bend} versus the rotational restraint F for various values of the shear rigidity Q. The geometrical parameters are

$$\frac{L}{h} = 15,\ \frac{b}{h} = \frac{1}{4},\ \frac{c}{b} = .40,\ \frac{b}{t} = 20$$

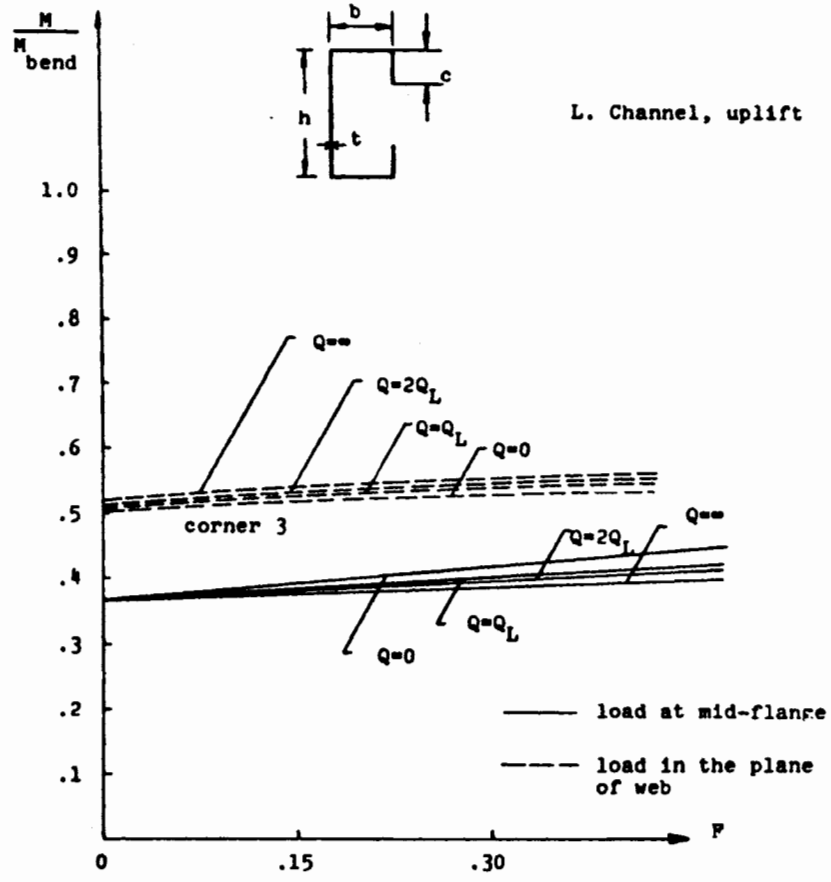

Figure 39b The ratio M/M_{bend} versus the rotational restraint F for various values of the shear rigidity Q. The geometrical parameters are

$$\frac{L}{h} = 15,\ \frac{b}{h} = \frac{1}{2},\ \frac{c}{b} = \frac{1}{2},\ \frac{b}{t} = 20$$

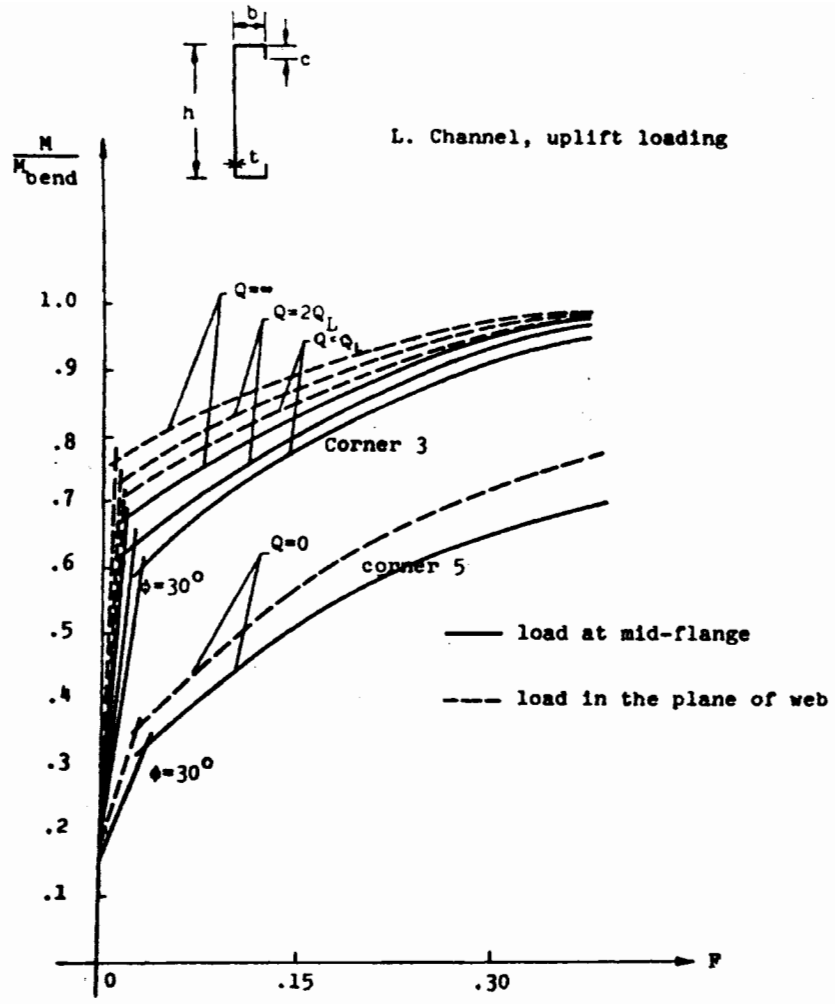

Figure 40a The ratio M/M_{bend} versus the rotational restraint F for various values of the shear rigidity Q. The geometrical parameters are:

$$\frac{L}{h} = 30,\ \frac{b}{h} = \frac{1}{2},\ \frac{c}{b} = 40,\ \frac{b}{t} = 20$$

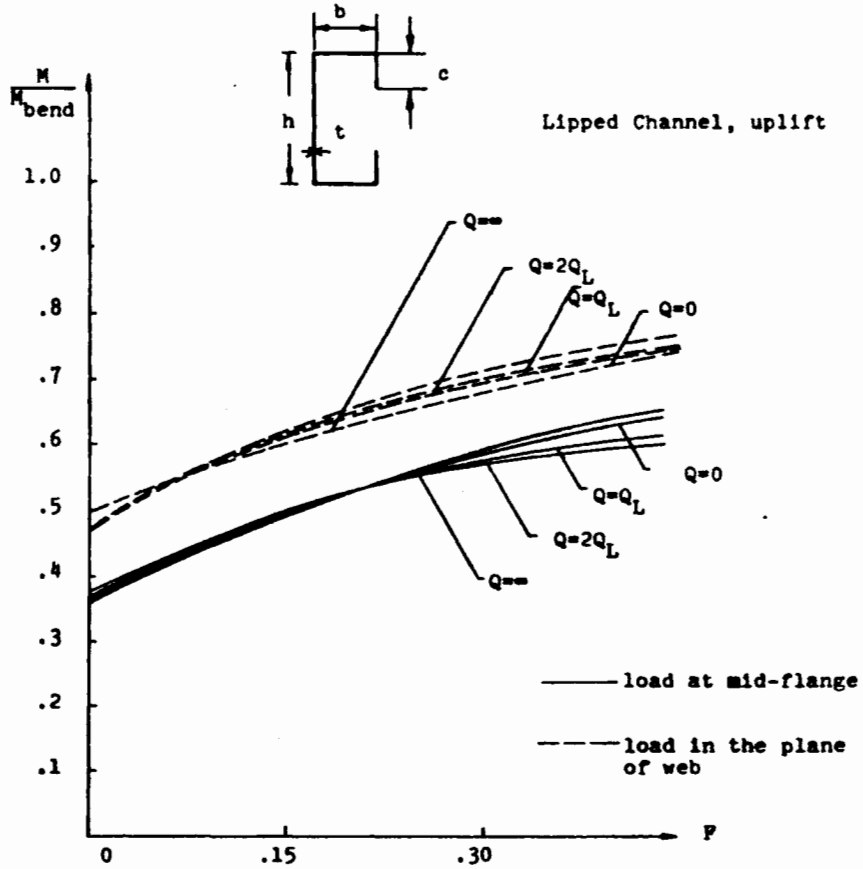

Figure 40b The ratio M/M_{bend} versus the rotational restraint F for various values of the shear rigidity Q. The geometrical parameters are

$$\frac{L}{h} = 30,\ \frac{b}{h} = \frac{1}{2},\ \frac{c}{b} = \frac{1}{2},\ \frac{b}{t} = 20$$

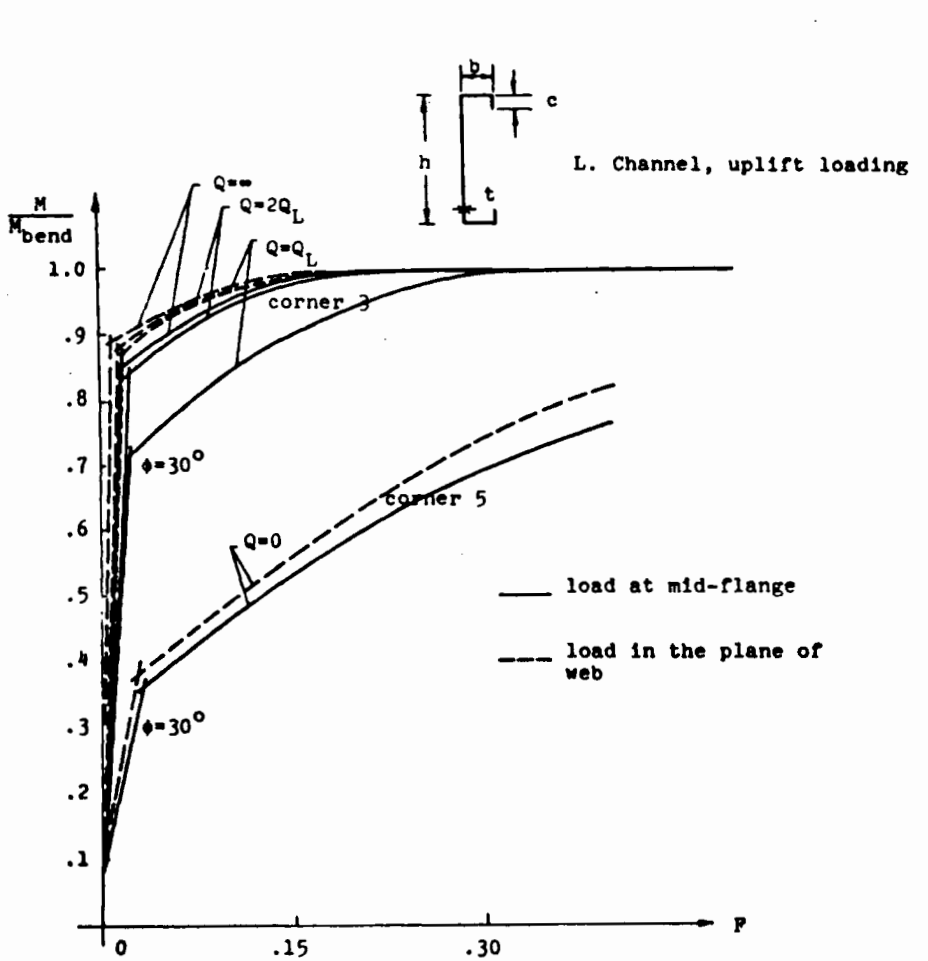

Figure 4.1a The ratio M/M_{bend} versus the rotational restraint F for various values of the shear rigidity Q. The geometrical parameters are

$$\frac{L}{h} = 45,\ \frac{b}{h} = \frac{1}{4},\ \frac{c}{b} = .40,\ \frac{b}{t} = 20$$

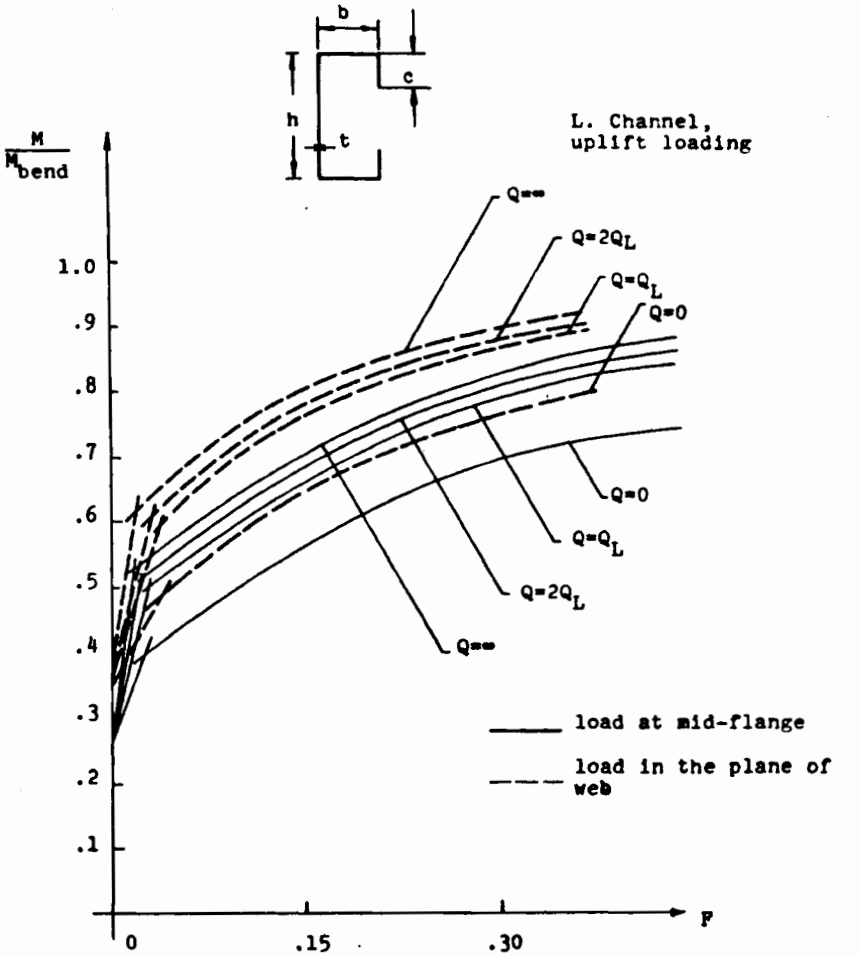

Figure 4.1b The ratio M/M_{bend} versus the rotational restraint F for various values of the shear rigidity Q. The geometrical parameters are

$$\frac{L}{h} = 45,\ \frac{b}{h} = \frac{1}{2},\ \frac{c}{b} = \frac{1}{2},\ \frac{b}{t} = 20$$

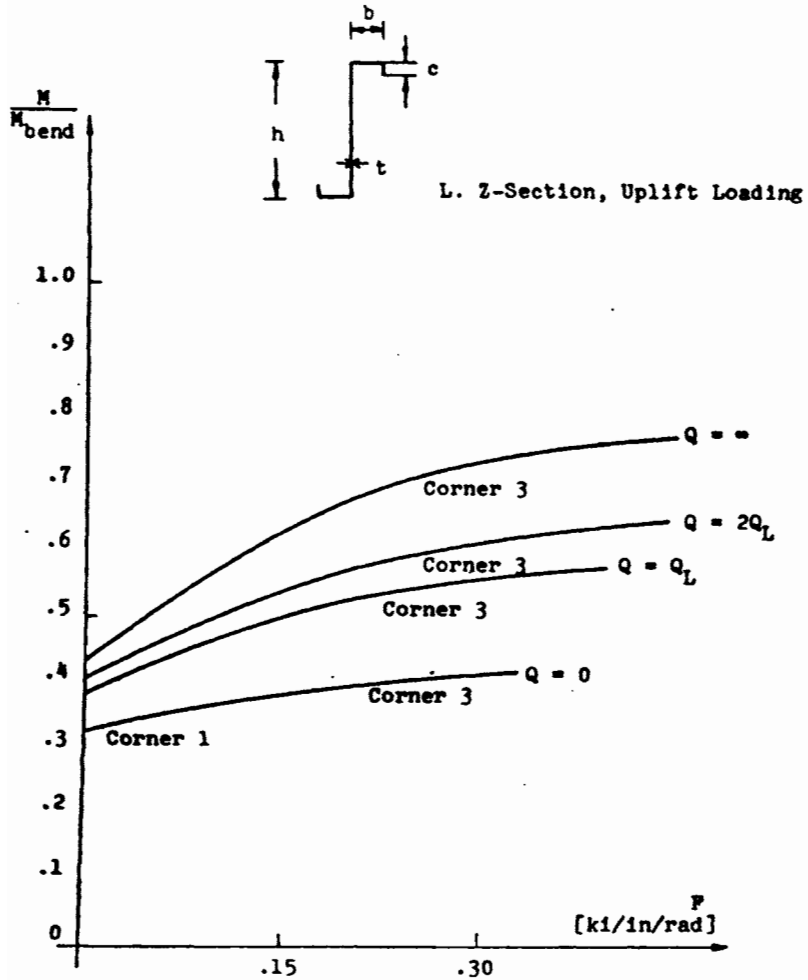

Figure 42.a. The ratio M/M_{bend} versus the rotational restraint F for various values of the shear rigidity Q. The geometrical parameters are:

$\frac{L}{h} = 15$, $\frac{b}{h} = \frac{1}{4}$, $\frac{c}{b} = .4$, $\frac{b}{t} = 20$

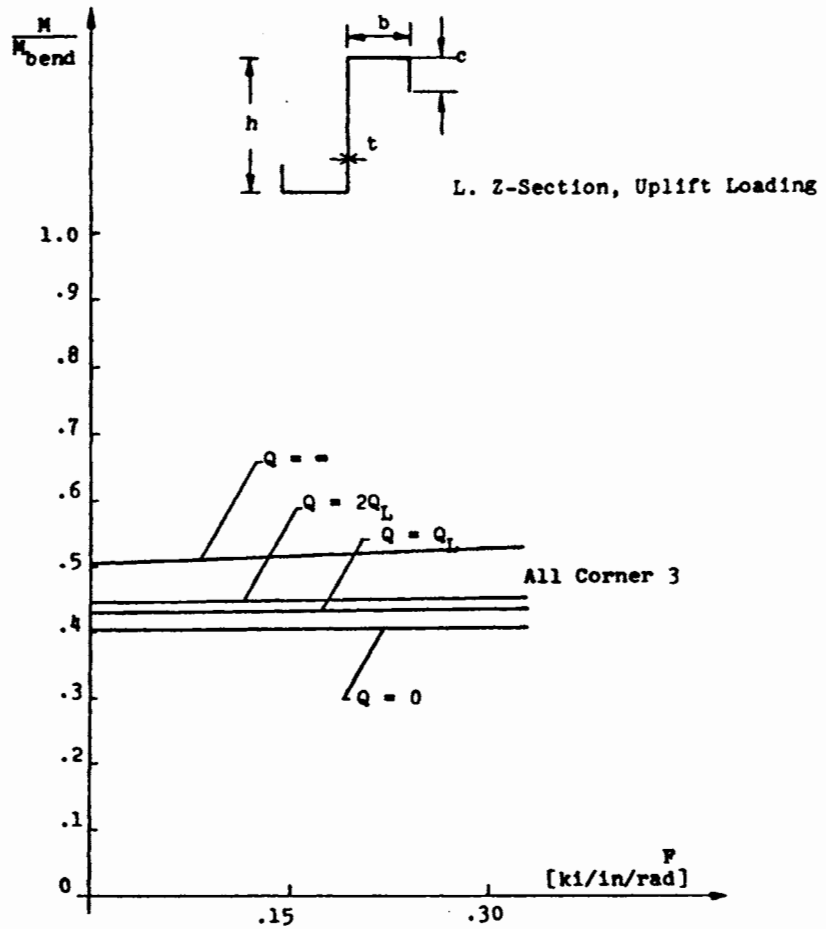

Figure 42.b. The ratio M/M_{bend} versus the rotational restraint F for various values of the shear rigidity Q. The geometrical parameters are:

$\frac{L}{h} = 15$, $\frac{b}{h} = \frac{1}{2}$, $\frac{c}{b} = \frac{1}{2}$, $\frac{b}{t} = 20$

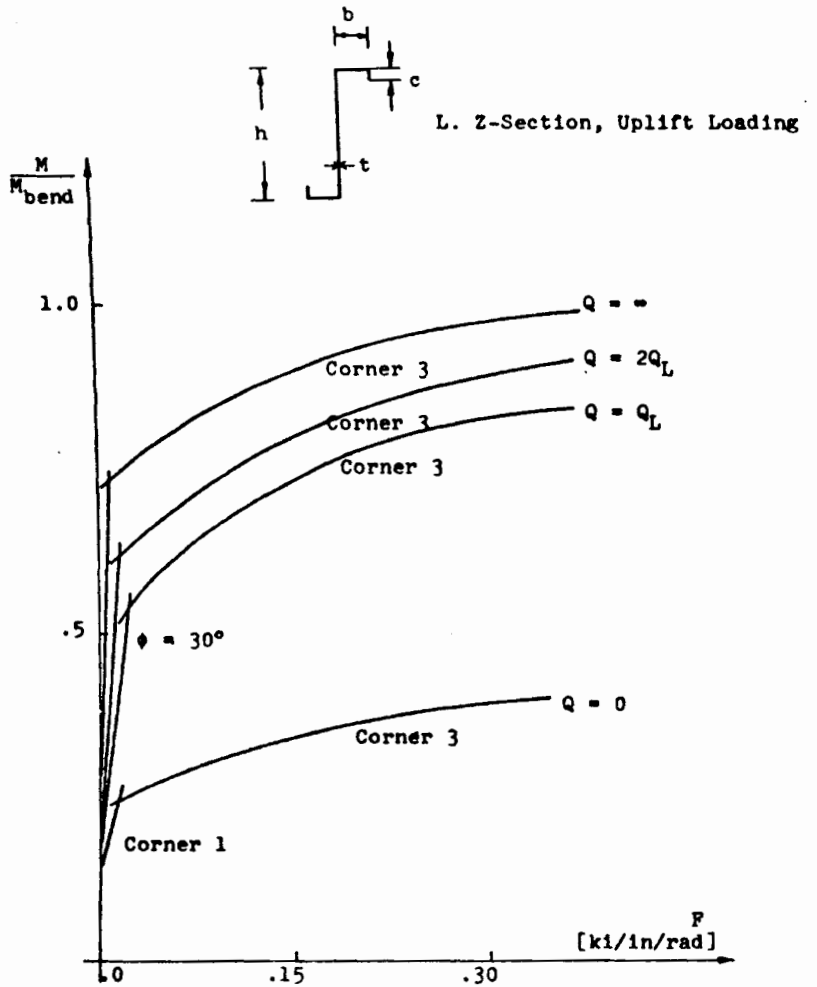

Figure 43.a. The ratio M/M_{bend} versus the rotational restraint F for various values of the shear rigidity Q. The geometrical parameters are:

$\frac{L}{h} = 30$, $\frac{b}{h} = \frac{1}{4}$, $\frac{c}{b} = .4$, $\frac{b}{t} = 20$

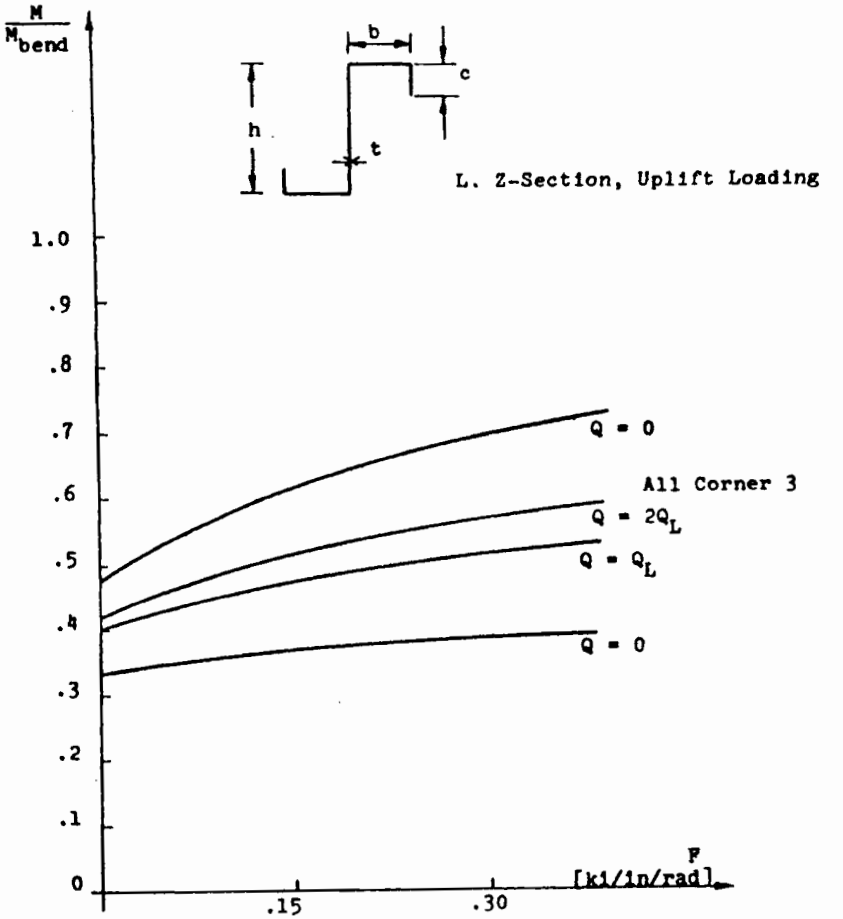

Figure 43.b. The ratio M/M_{bend} versus the rotational restraint F for various values of the shear rigidity Q. The geometrical parameters are:

$\frac{L}{h} = 30$, $\frac{b}{h} = \frac{1}{2}$, $\frac{c}{b} = \frac{1}{2}$, $\frac{b}{t} = 20$

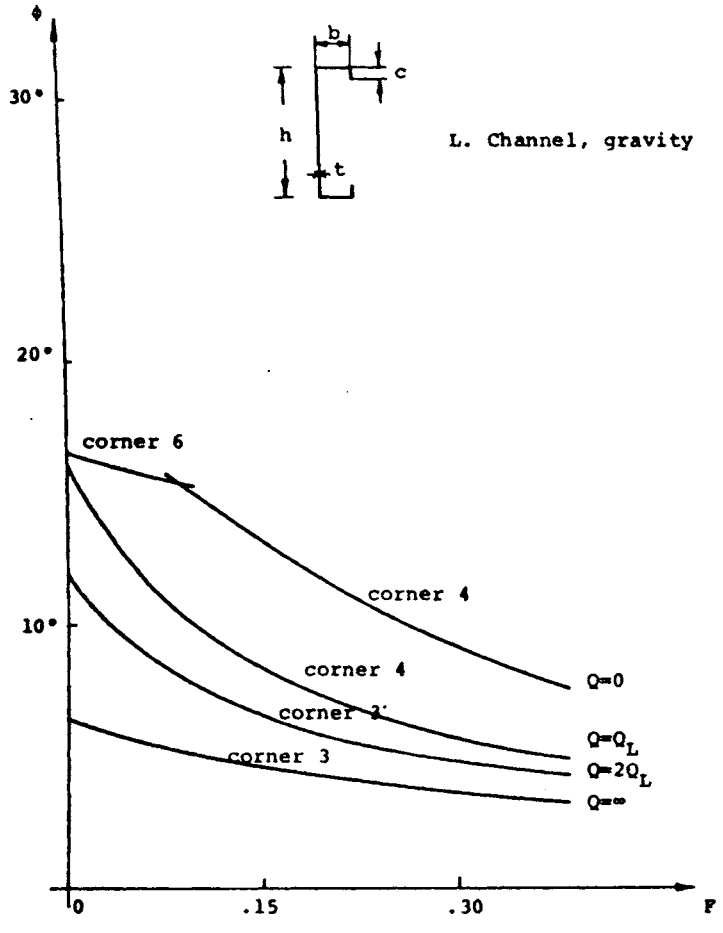

Figure 45a: Angle of Rotation ϕ at mid-span versus the rotational resistance F of the diaphragm at incipient yield load (σ_y = 46 ksi) for various values of the shear rigidity Q.

$\frac{L}{h} = 15$, $\frac{b}{h} = \frac{1}{4}$, $\frac{c}{b} = .4$, $\frac{b}{t} = 20$

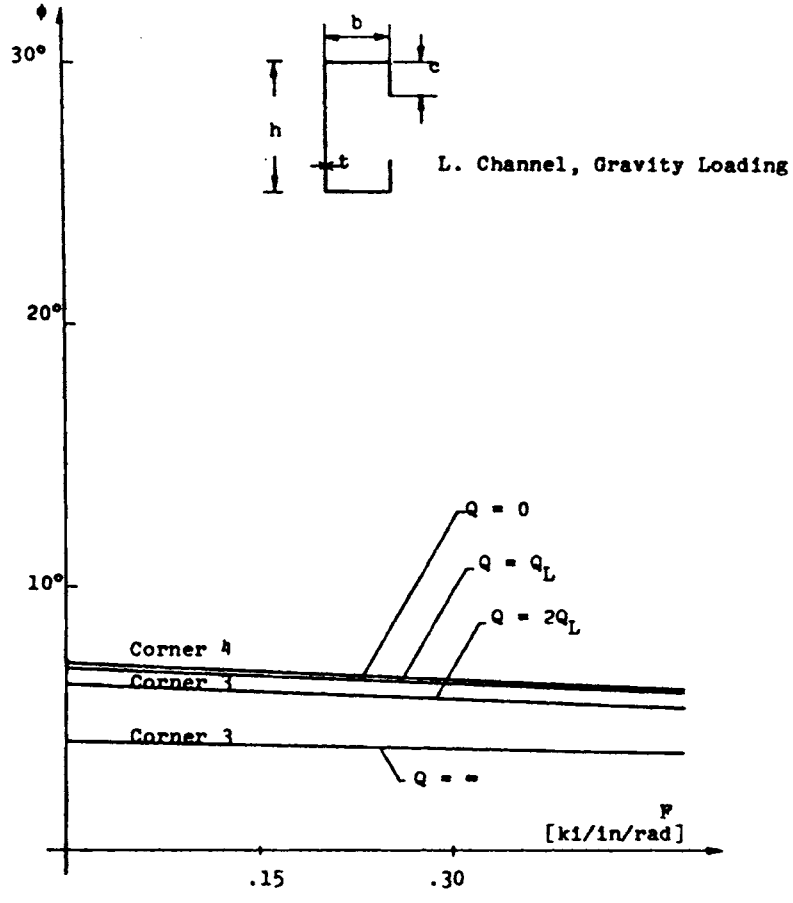

Figure 45.b. Angle of Rotation ϕ at midspan versus the rotational restraint F of the diaphragm at incipient yield load (σ_y = 46 ksi) for various values of the shear rigidity Q.

$\frac{L}{h} = 15$, $\frac{b}{h} = \frac{1}{2}$, $\frac{c}{b} = \frac{1}{2}$, $\frac{b}{t} = 20$

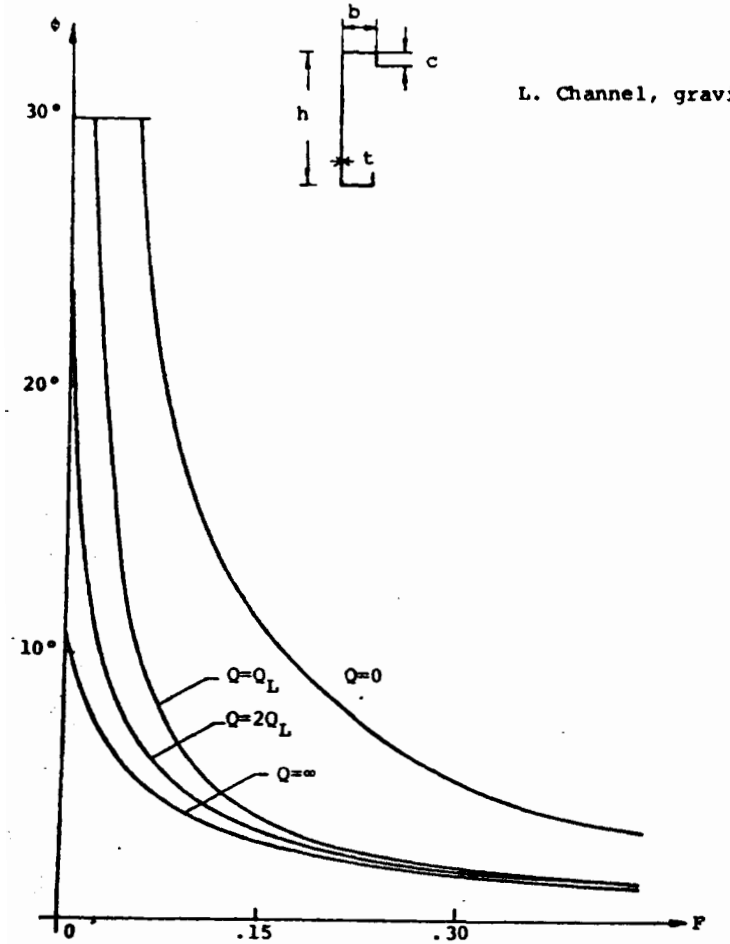

Figure 46a: Angle of Rotation ϕ at mid-span versus the rotational resistance F of the diaphragm at incipient yield load (σ_y = 46 ksi) for various values of the shear rigidity Q.

$\frac{L}{h} = 30$, $\frac{b}{h} = \frac{1}{4}$, $\frac{c}{b} = .4$, $\frac{b}{t} = 20$

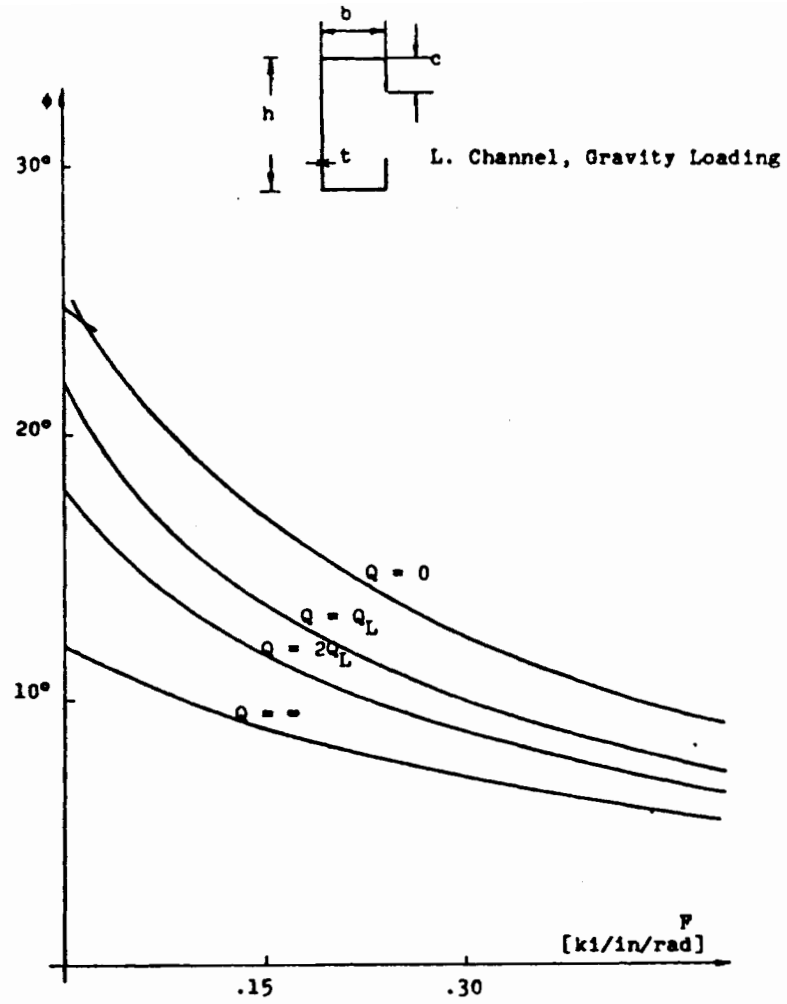

Figure 46.b. Angle of Rotation ϕ at mid-span versus the rotational restraint F of the diaphragm at incipient yield load (σ_y = 46 ksi) for various values of the shear rigidity Q.

$\frac{L}{h} = 30$, $\frac{b}{h} = \frac{1}{2}$, $\frac{c}{b} = \frac{1}{2}$, $\frac{b}{t} = 20$

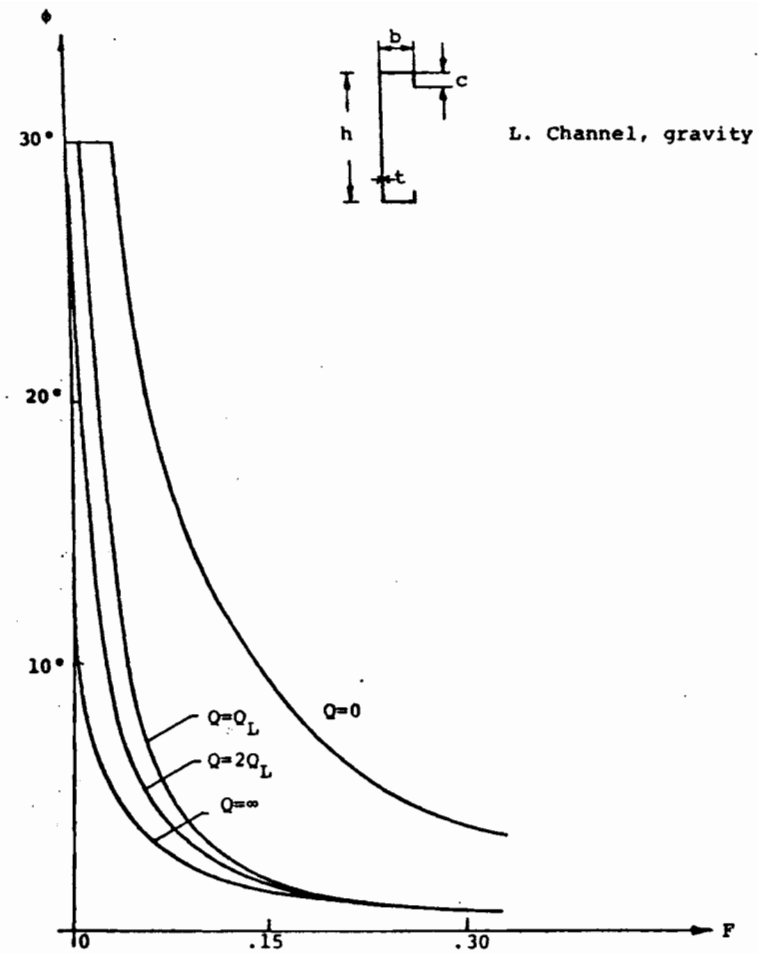

Figure 47a: Angle of Rotation ϕ at mid-span versus the rotational resistance F of the diaphragm at incipient yield load (σ_y = 46 ksi) for various values of the shear rigidity Q.

$\frac{L}{h} = 45$, $\frac{b}{h} = \frac{1}{4}$, $\frac{c}{b} = .4$, $\frac{b}{t} = 20$

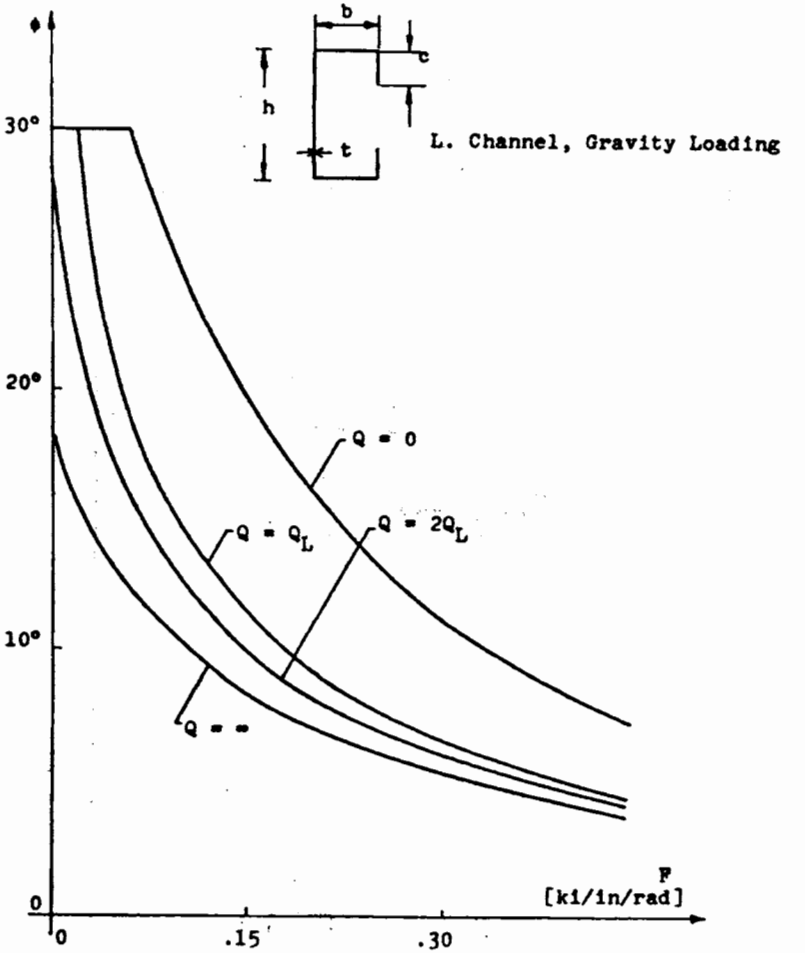

Figure 47.b Angle of Rotation ϕ at mid-span versus the rotational restraint F of the diaphragm at incipient yield load (σ_y = 46 ksi) for various values of the shear rigidity Q.

$\frac{L}{h} = 45$, $\frac{b}{h} = \frac{1}{2}$, $\frac{c}{b} = \frac{1}{2}$, $\frac{b}{t} = 20$

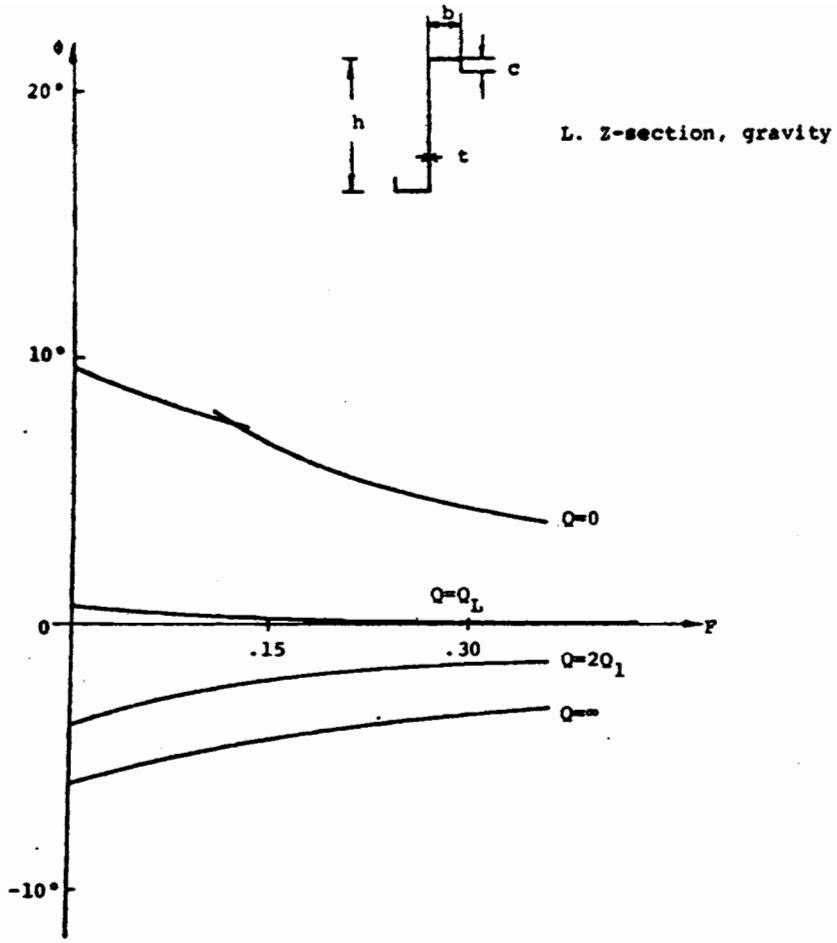

Figure 48a: Angle of Rotation at mid-span versus the rotational resistance F of the diaphragm at incipient yield load (σ_y = 46 ksi) for various values of the shear rigidity Q.

$\frac{L}{h} = 15$, $\frac{b}{h} = \frac{1}{4}$, $\frac{c}{b} = .4$, $\frac{b}{t} = 20$

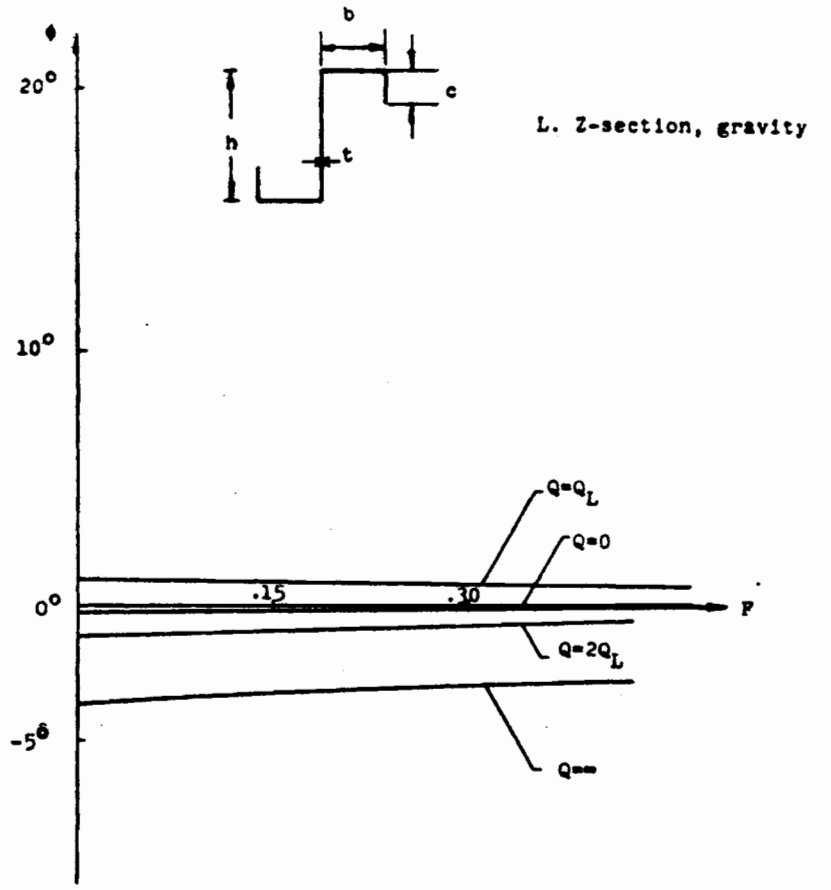

Figure 48b Angle of rotation ϕ at midspan versus the rotational restraint F of the diaphragm at incipient yield load (σ_y = 46 ksi) for various values of the shear rigidity Q

$\frac{L}{h} = 15$, $\frac{b}{h} = \frac{1}{2}$, $\frac{c}{b} = \frac{1}{2}$, $\frac{b}{t} = 20$

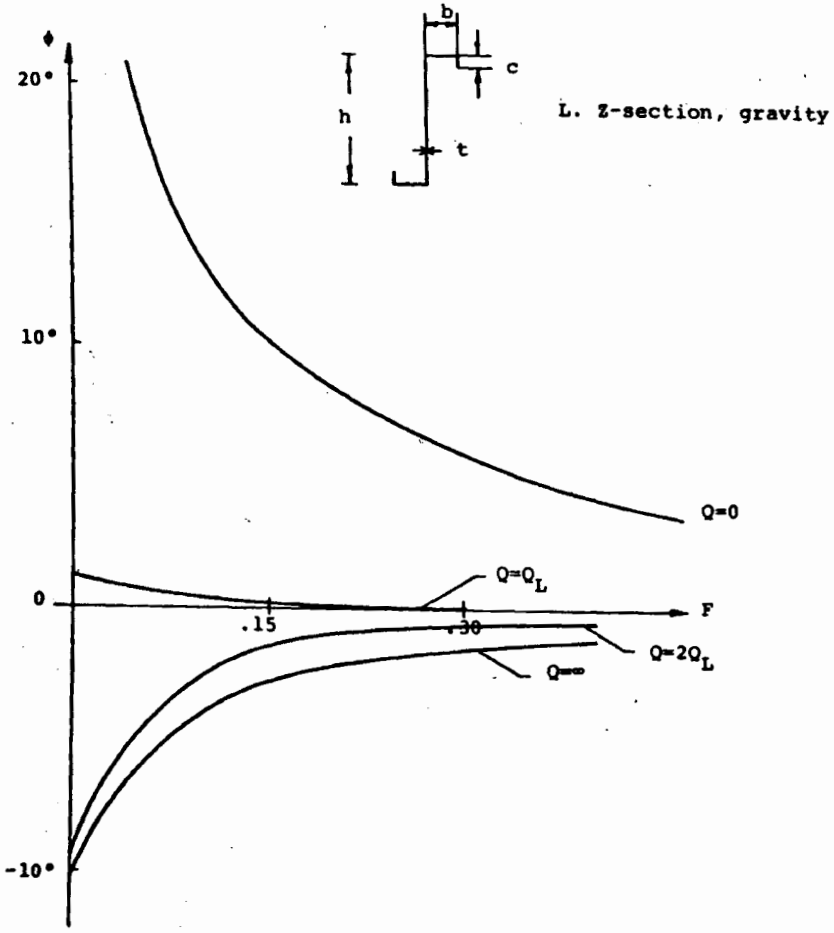

Figure 49a: Angle of Rotation ϕ at mid-span versus the rotational resistance F of the diaphragm at incipient yield load (σ_y = 46 ksi) for various values of the shear rigidity Q.

$\frac{L}{h} = 30$, $\frac{b}{h} = \frac{1}{4}$, $\frac{c}{b} = .4$, $\frac{b}{t} = 20$

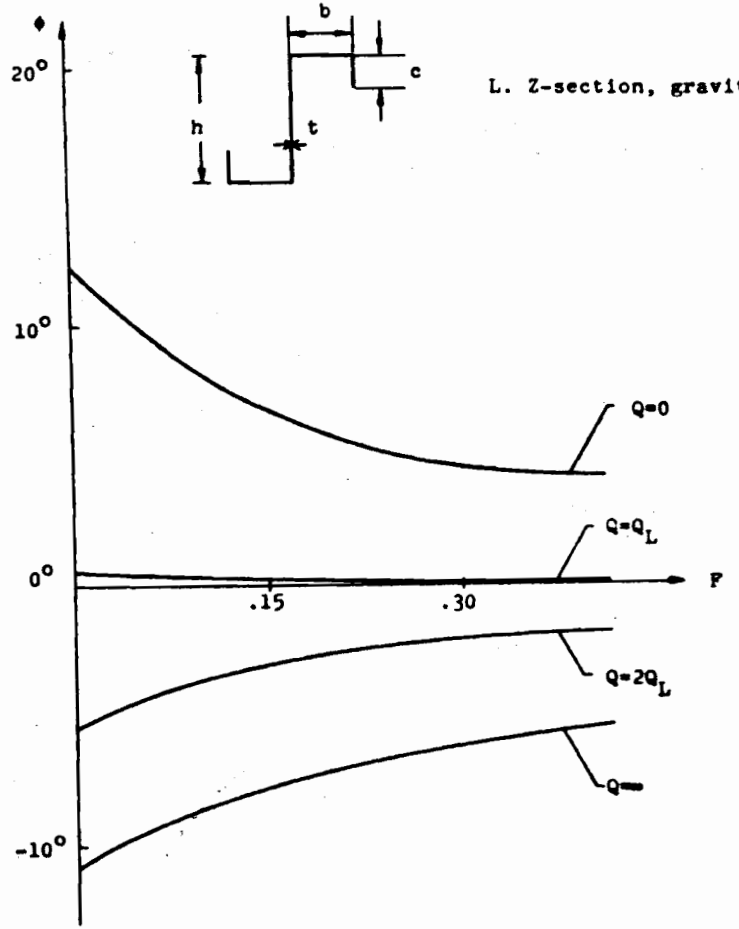

Figure 49b Angle of rotation ϕ at midspan versus the rotational restraint F of the diaphragm at incipient yield load (σ_y = 46 ksi) for various values of the shear rigidity Q

$\frac{L}{h} = 30$, $\frac{b}{h} = \frac{1}{2}$, $\frac{c}{b} = \frac{1}{2}$, $\frac{b}{t} = 20$

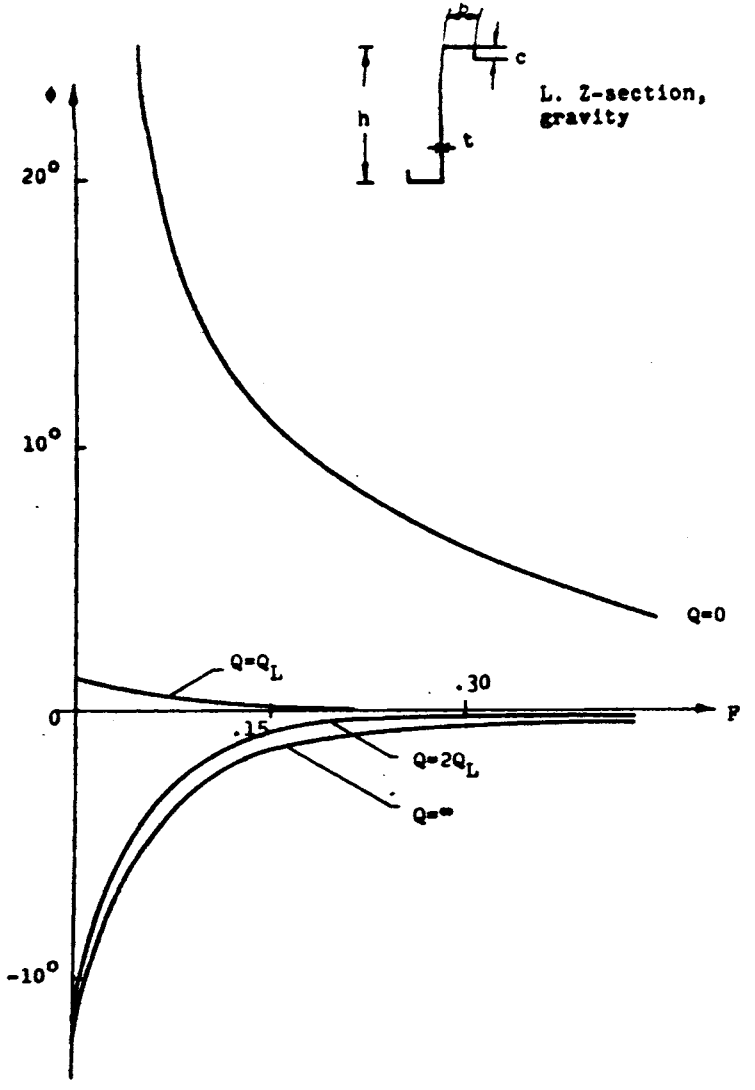

Figure 50a. Angle of rotation ϕ at midspan versus the rotational resistance P of the diaphragm at incipient yield load (σ_y = 46 ksi) for various values of the shear rigidity Q.

$\frac{L}{h} = 45, \frac{b}{h} = \frac{1}{4}, \frac{c}{b} = .4, \frac{b}{t} = 20$

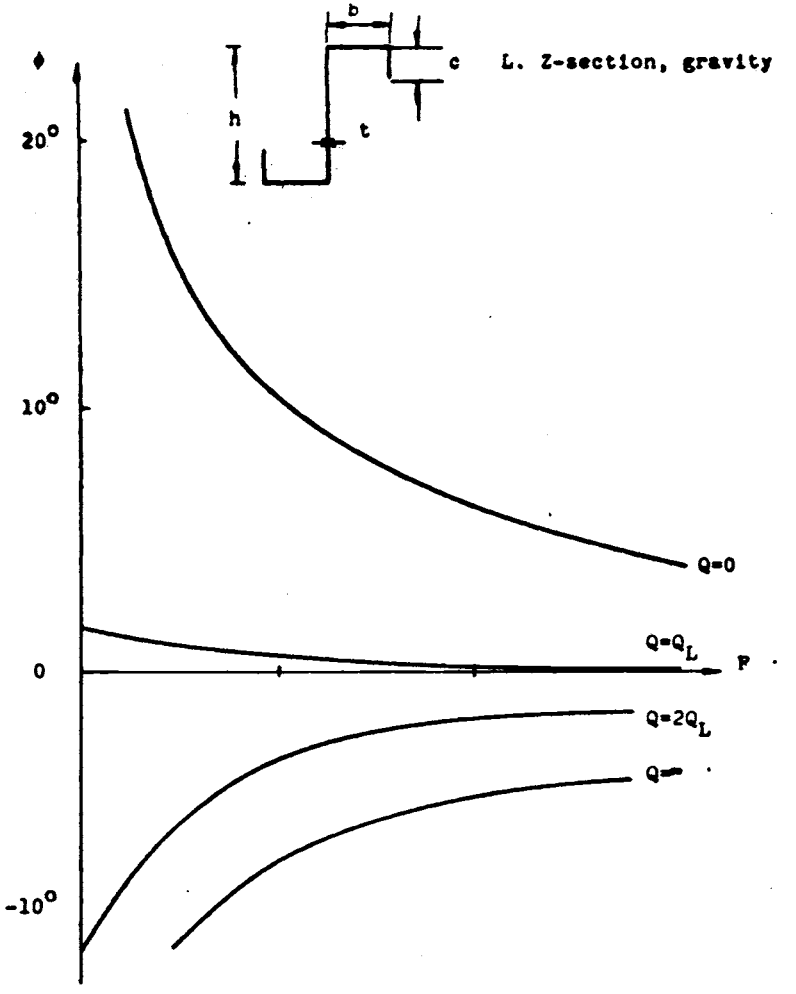

Figure 50b Angle of rotation ϕ at midspan versus the rotational restraint P of the diaphragm at incipient yield load (σ_y = 46 ksi) for various values of the shear rigidity Q.

$\frac{L}{h} = 45, \frac{b}{h} = \frac{1}{2}, \frac{c}{b} = \frac{1}{2}, \frac{b}{t} = 20$

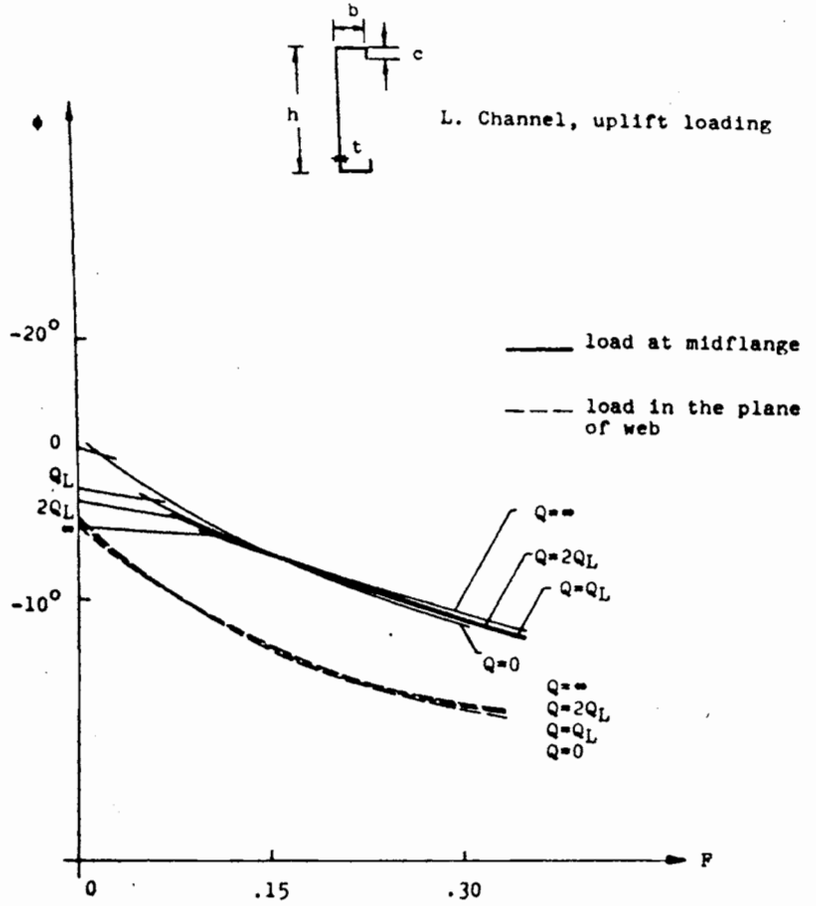

Figure 51a Angle of rotation ϕ at midspan versus the rotational restraint F of the diaphragm at incipient yield load (σ_y = 46 ksi) for various values of the shear rigidity Q.

$\frac{L}{h}$ = 15, $\frac{b}{h}$ = $\frac{1}{4}$, $\frac{c}{b}$ = .40, $\frac{b}{t}$ = 20

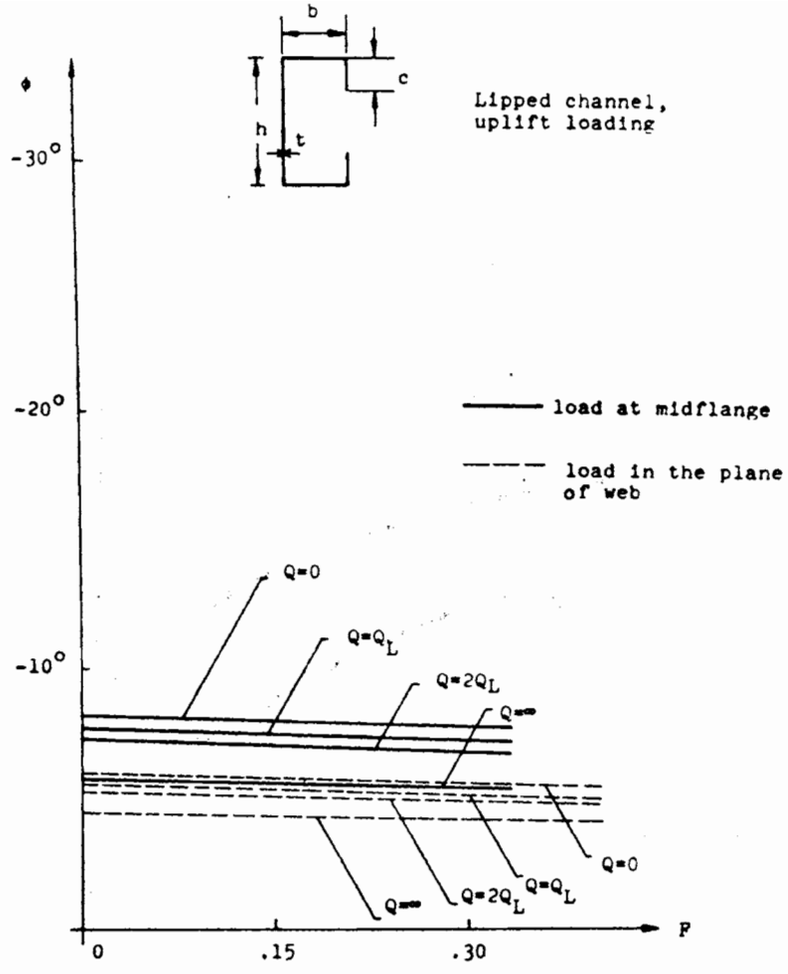

Figure 51b Angle of rotation ϕ at midspan versus the rotational restraint F of the diaphragm at incipient yield load (σ_y = 46 ksi) for various values of the shear rigidity Q.

$\frac{L}{h}$ = 15, $\frac{b}{h}$ = $\frac{1}{2}$, $\frac{c}{b}$ = $\frac{1}{2}$, $\frac{b}{t}$ = 20

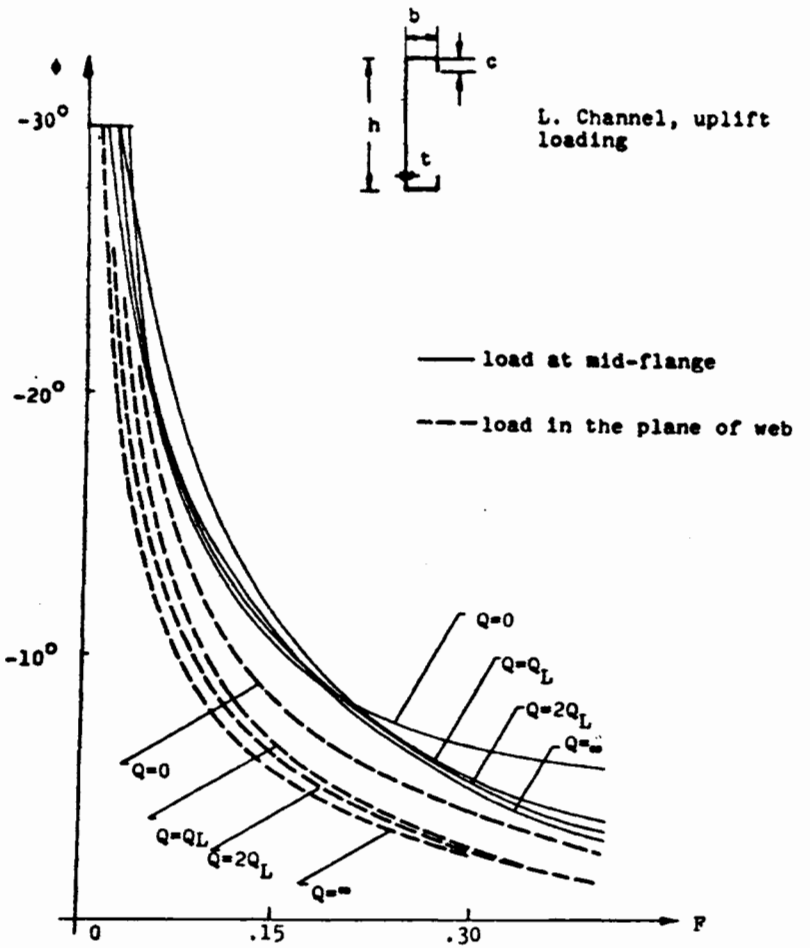

Figure 52a Angle of rotation ϕ at midspan versus the rotational restraint F of the diaphragm at incipient yield load (σ_y = 46 ksi) for various values of the shear rigidity Q_y.

$\frac{L}{h}$ = 30, $\frac{b}{h}$ = $\frac{1}{2}$, $\frac{c}{b}$ = .4, $\frac{b}{t}$ = 20

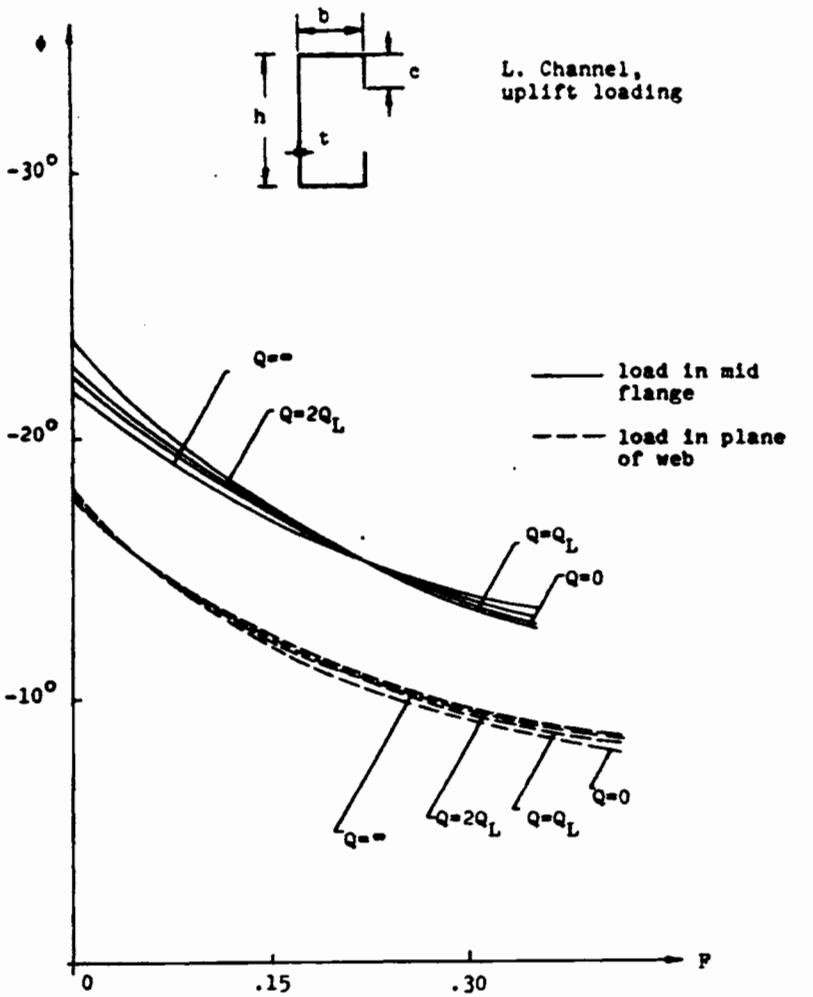

Figure 52b Angle of rotation ϕ at midspan versus the rotational restraint F of the diaphragm at incipient yield load (σ_y = 46 ksi) for various values of the shear rigidity Q_y.

$\frac{L}{h}$ = 30, $\frac{b}{h}$ = $\frac{1}{2}$, $\frac{c}{b}$ = $\frac{1}{2}$, $\frac{b}{t}$ = 20

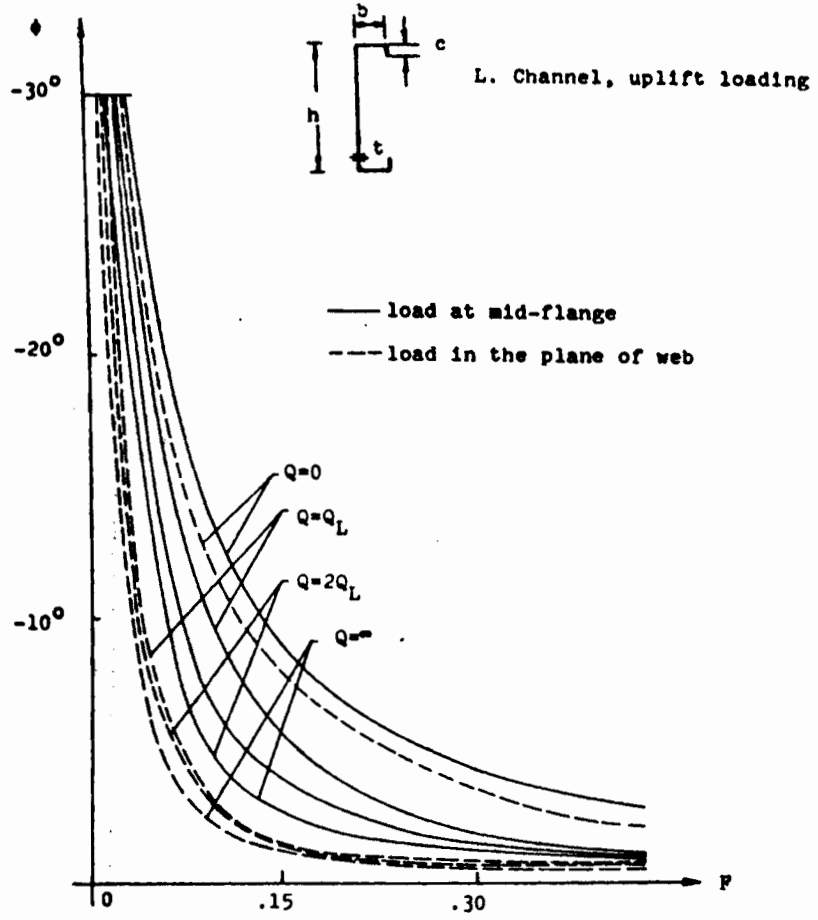

Figure 53a Angle of rotation ϕ at midspan versus the rotational restraint F of the diaphragm at incipient yield load (σ_y = 46 ksi) for various values of the shear rigidity Q.

$\frac{L}{h} = 45, \frac{b}{h} = \frac{1}{4}, \frac{c}{b} = .4, \frac{b}{t} = 20$

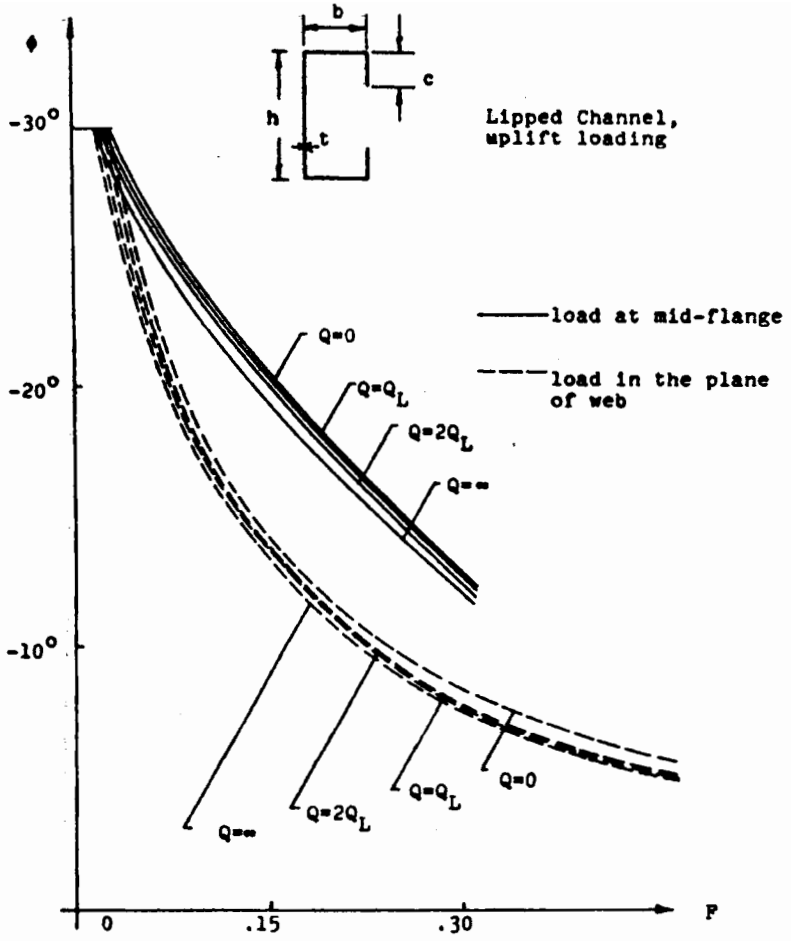

Figure 53b Angle of rotation ϕ at midspan versus the rotational restraint F of the diaphragm at incipient yield load (σ_y = 46 ksi) for various values of the shear rigidity Q.

$\frac{L}{h} = 45, \frac{b}{h} = \frac{1}{2}, \frac{c}{b} = \frac{1}{2}, \frac{b}{t} = 20$

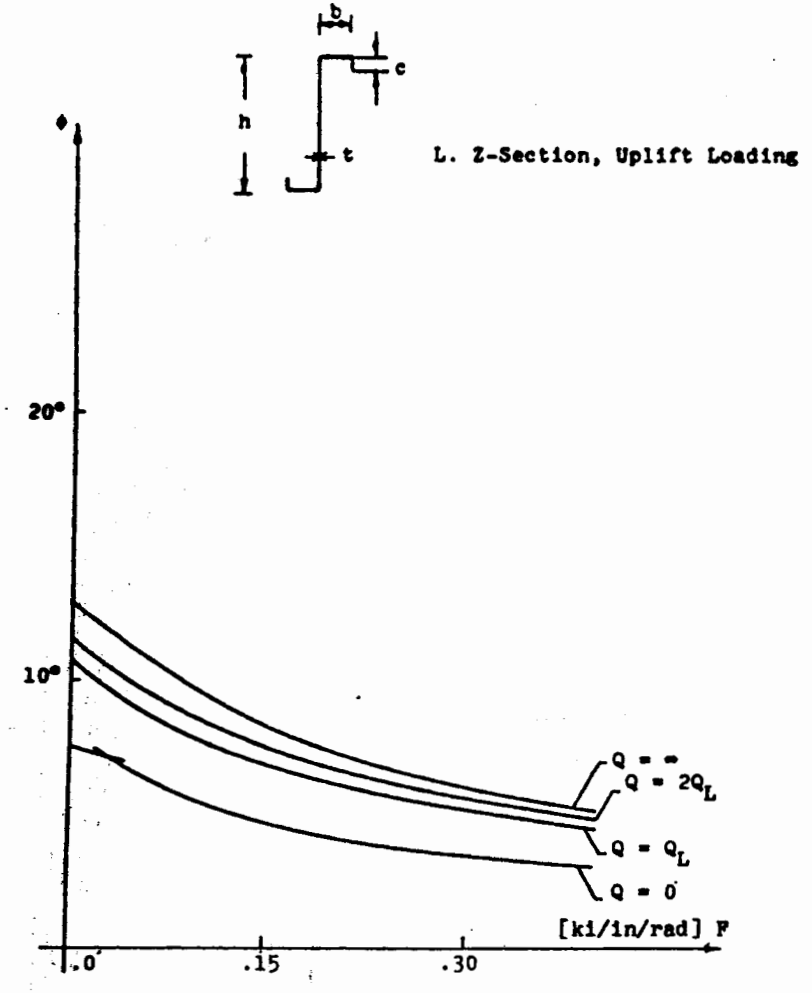

Figure 54.a. Angle of Rotation ϕ at mid-span versus the rotational restraint F of the diaphragm at incipient yield load (σ_y = 46 ksi) for various values of the shear rigidity Q.

$\frac{L}{h}$ = 15, $\frac{b}{h}$ = $\frac{1}{4}$, $\frac{c}{b}$ = .4, $\frac{b}{t}$ = 20

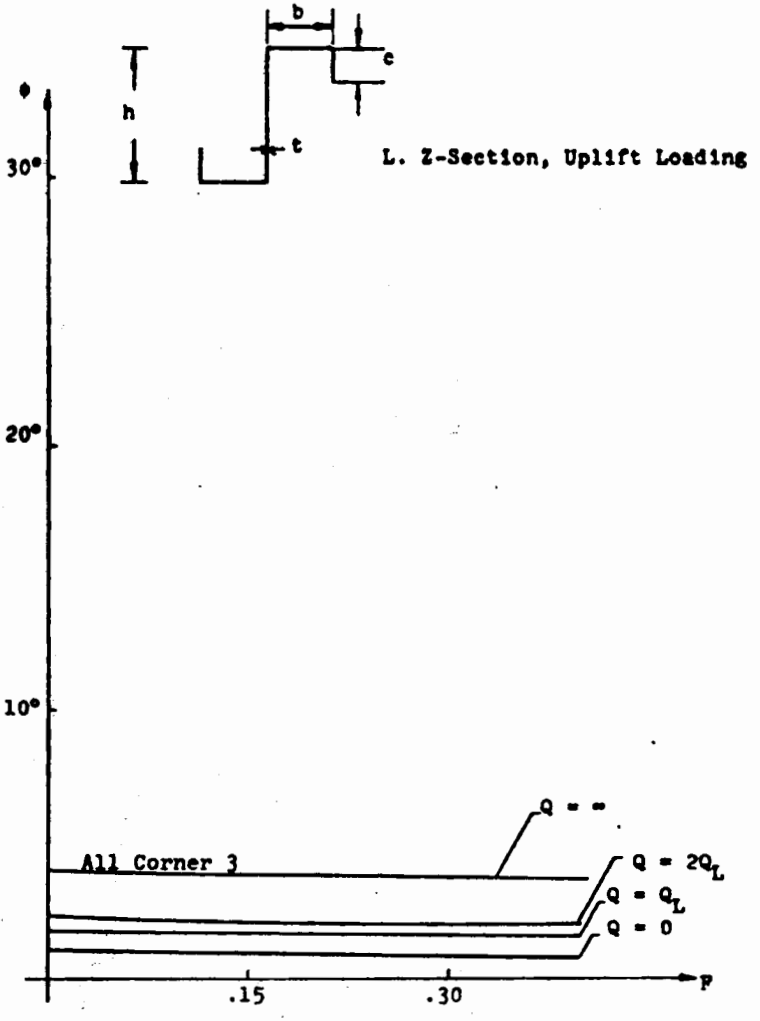

Figure 54.b. Angle of Rotation ϕ at mid-span versus the rotational restraint F of the diaphragm at incipient yield load (σ_y = 46 ksi) for various values of the shear rigidity Q.

$\frac{L}{h}$ = 15, $\frac{b}{h}$ = $\frac{1}{2}$, $\frac{c}{b}$ = $\frac{1}{2}$, $\frac{b}{t}$ = 20

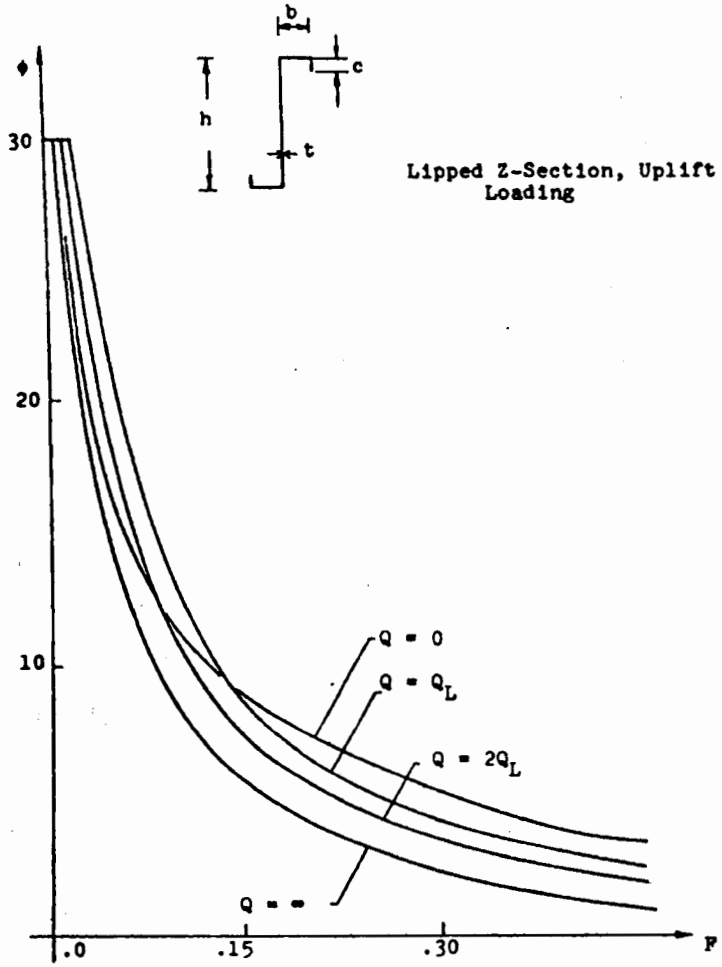

Figure 55.a. Angle of rotation ϕ at mid-span versus the rotational restraint F of the diaphragm at incipient yield load (σ_y = 46 ksi) for various values of the shear rigidity Q.

$\frac{L}{h} = 30, \frac{b}{h} = \frac{1}{4}, \frac{c}{b} = .4, \frac{b}{t} = 20$

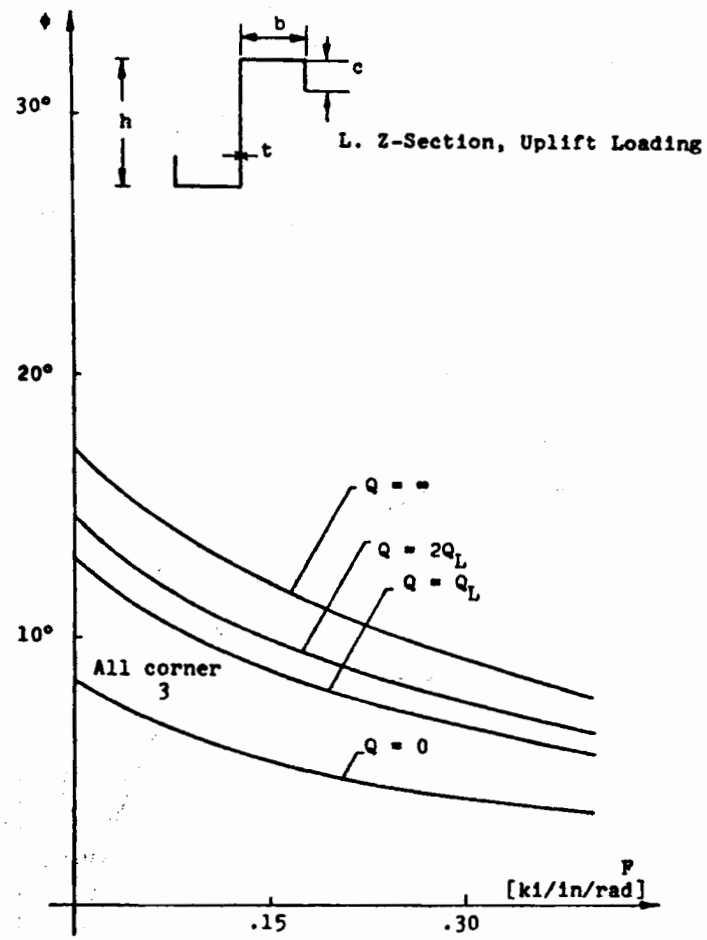

Figure 55.b. Angle of rotation ϕ at mid-span versus the rotational restraint F of the diaphragm at incipient yield load (σ_y = 46 ksi) for various values of the shear rigidity Q.

$\frac{L}{h} = 30, \frac{b}{h} = \frac{1}{2}, \frac{c}{b} = \frac{1}{2}, \frac{b}{t} = 20$

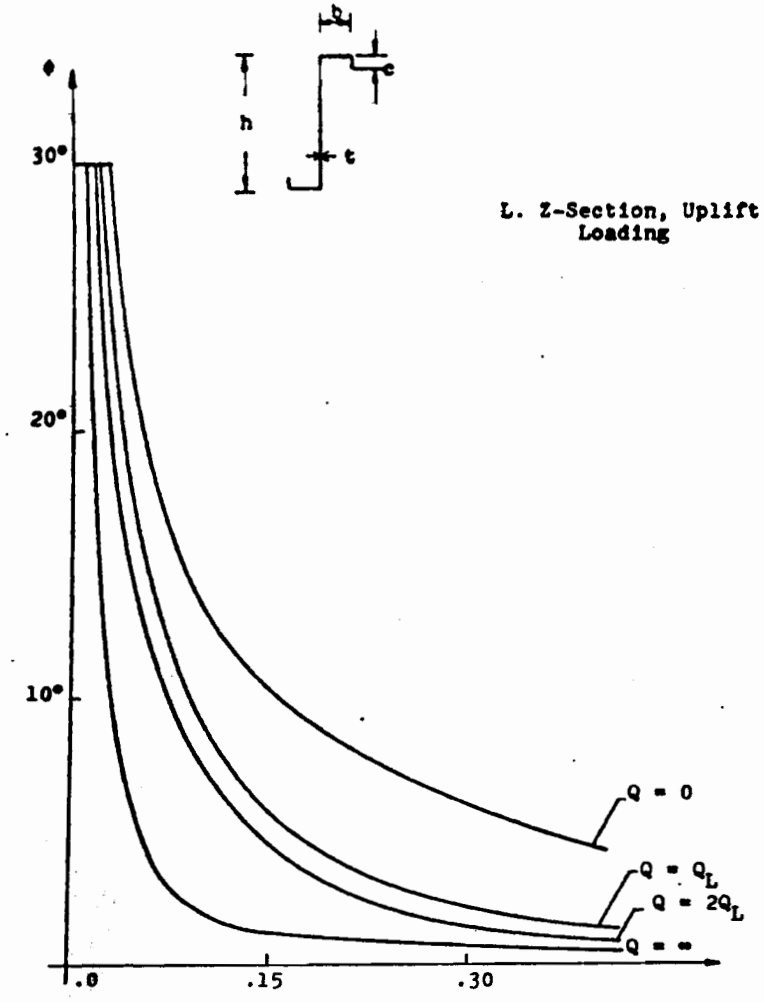

Figure 56.a. Angle of rotation ϕ at mid-span versus the rotational restraint F of the diaphragm at incipient yield load (σ_y = 46 ksi) for various values of the shear rigidity Q.

$\frac{L}{h} = 45,\ \frac{b}{h} = \frac{1}{4},\ \frac{c}{b} = .4,\ \frac{b}{t} = 20$

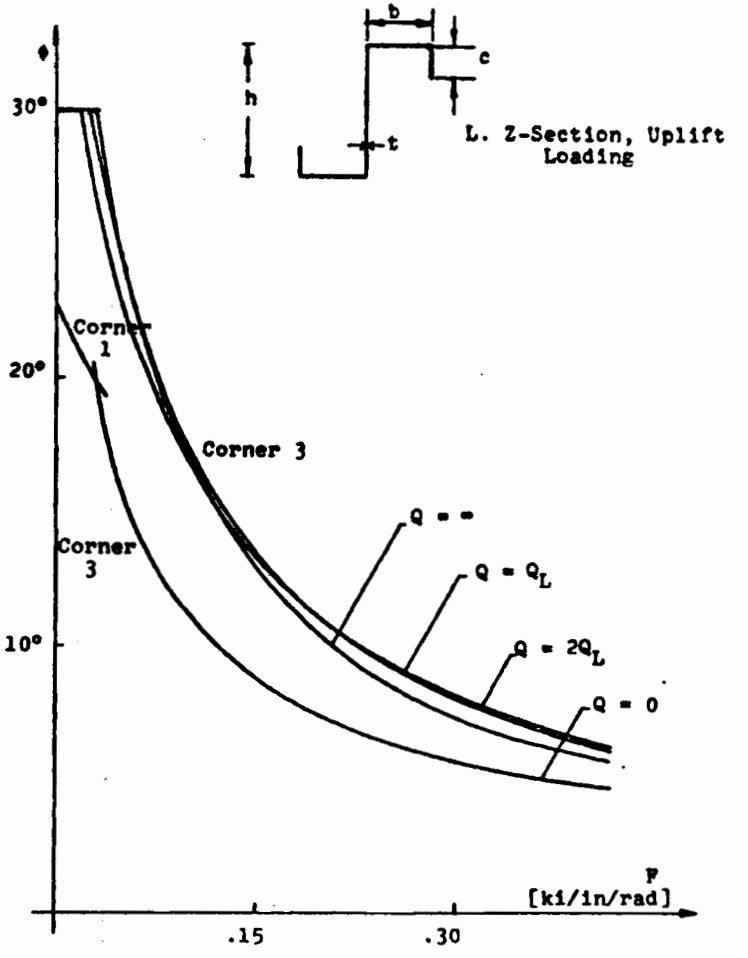

Figure 56.b. Angle of rotation ϕ at mid-span versus the rotational restraint F of the diaphragm at incipient yield load (σ_y = 46 ksi) for various values of the shear rigidity Q.

$\frac{L}{h} = 45,\ \frac{b}{h} = \frac{1}{2},\ \frac{c}{b} = \frac{1}{2},\ \frac{b}{t} = 20$

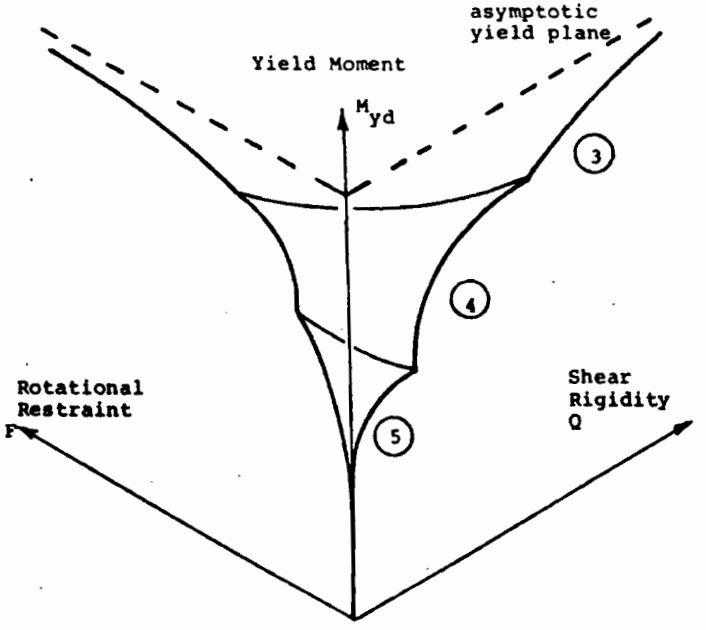

Figure 57: Yield Moment M_{yd} versus Q and F
(a qualitative example)
The circled numbers refer to the corners of the purlin section where incipient yielding occurs first.

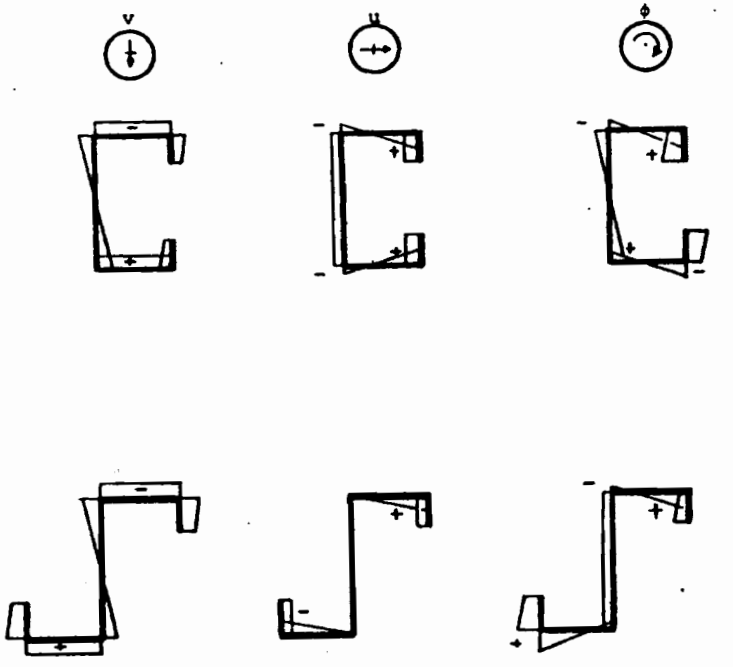

Figure 58: The qualitative stress distribution in channel and Z section due to deformations v, u and ϕ.

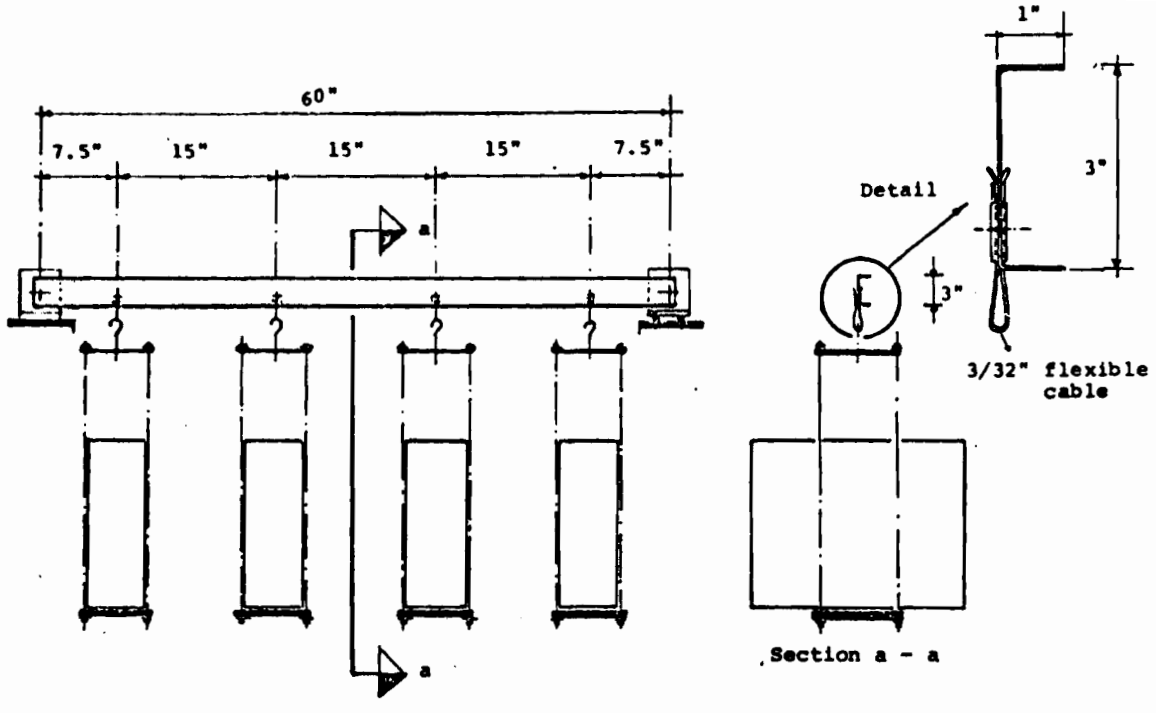

Figure 59: Loading Arrangement for Test 1 and 2

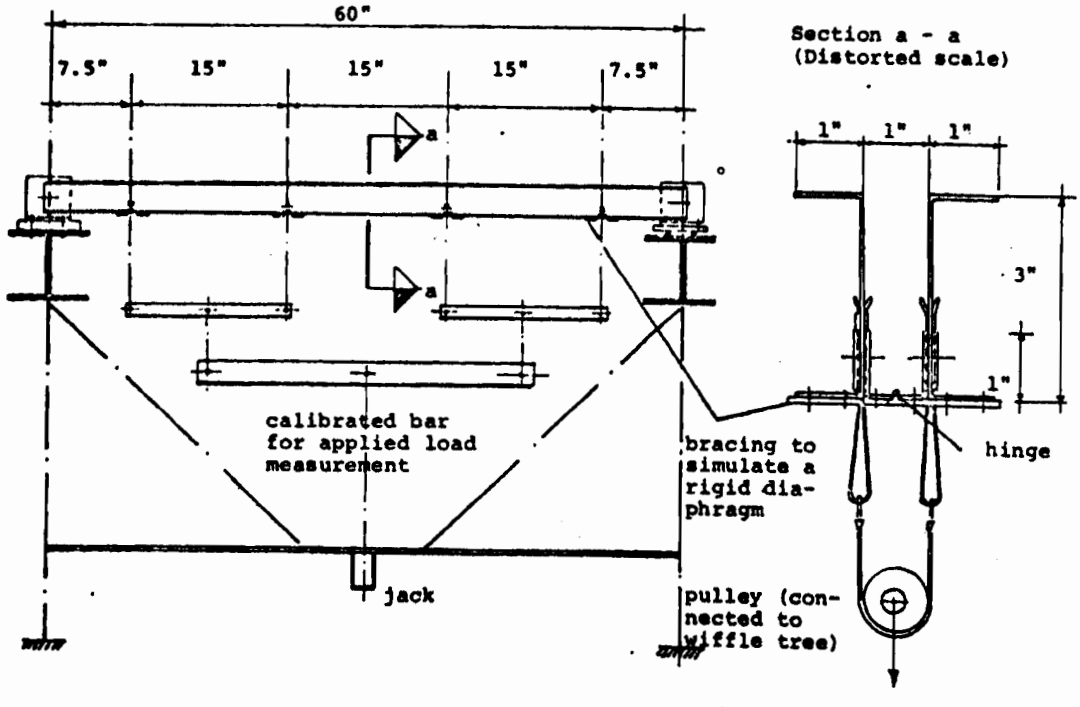

Figure 60: Loading Arrangement for Test 3 through 6.

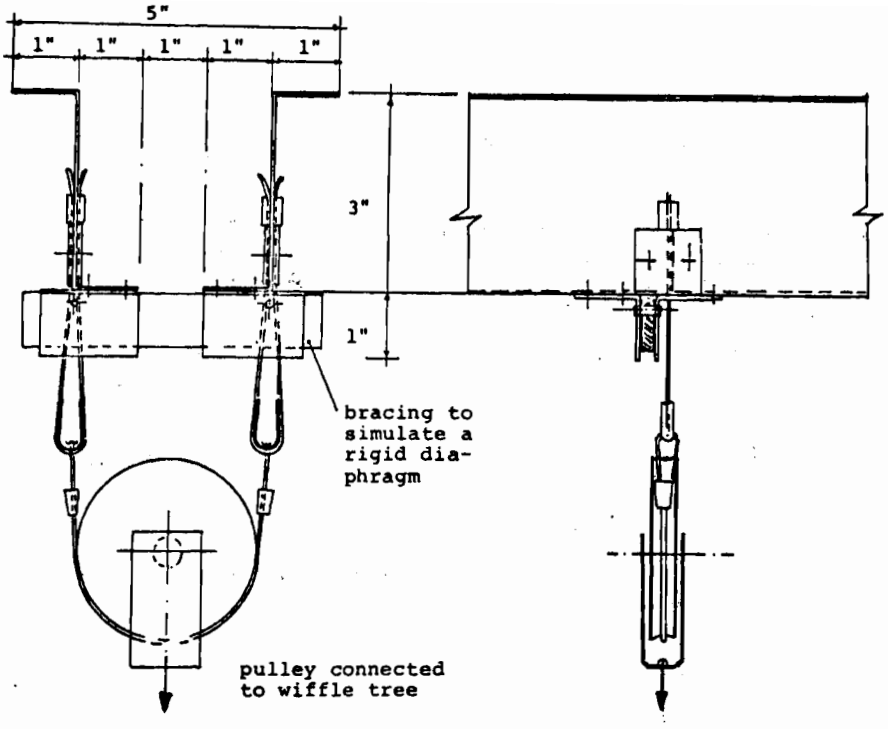

Figure 61: Detail showing the Load Application and Bracing Simulation in Test 4.

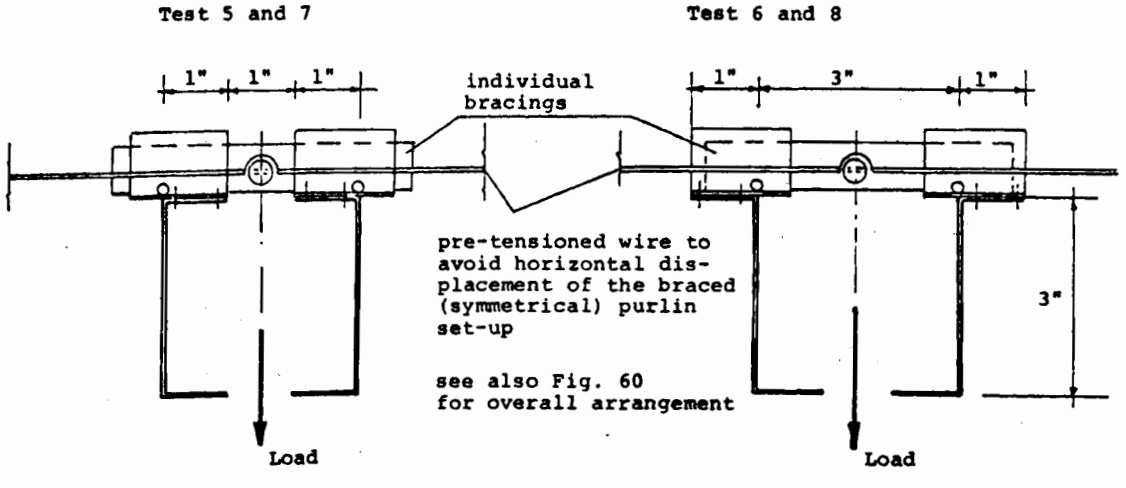

Figure 62: Bracing Detail in Tests 5 through 8

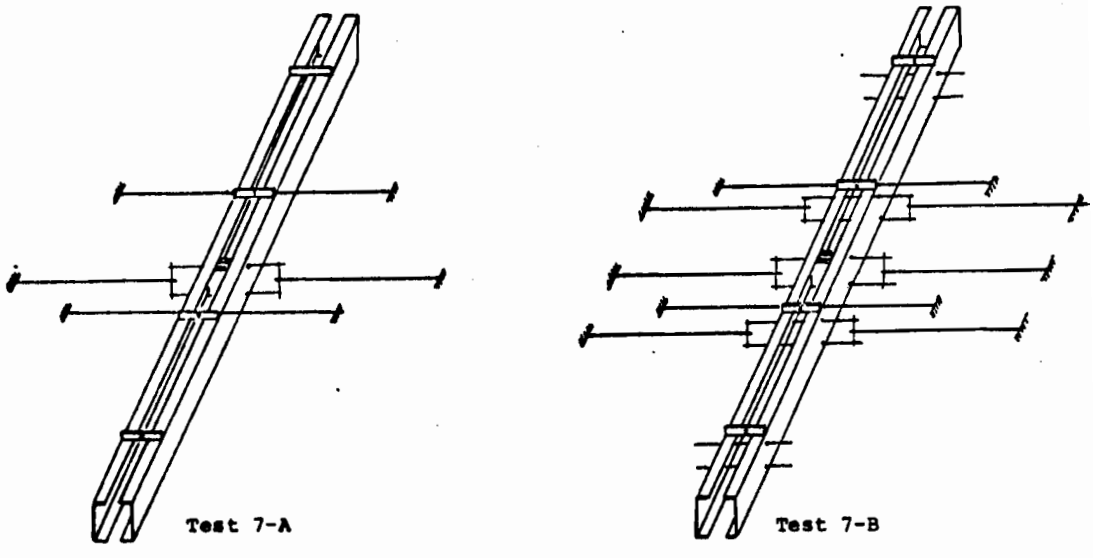

Figure 63: Overall Bracing of the Set-up in Tests 7 A and B with pre-tensioned wires.

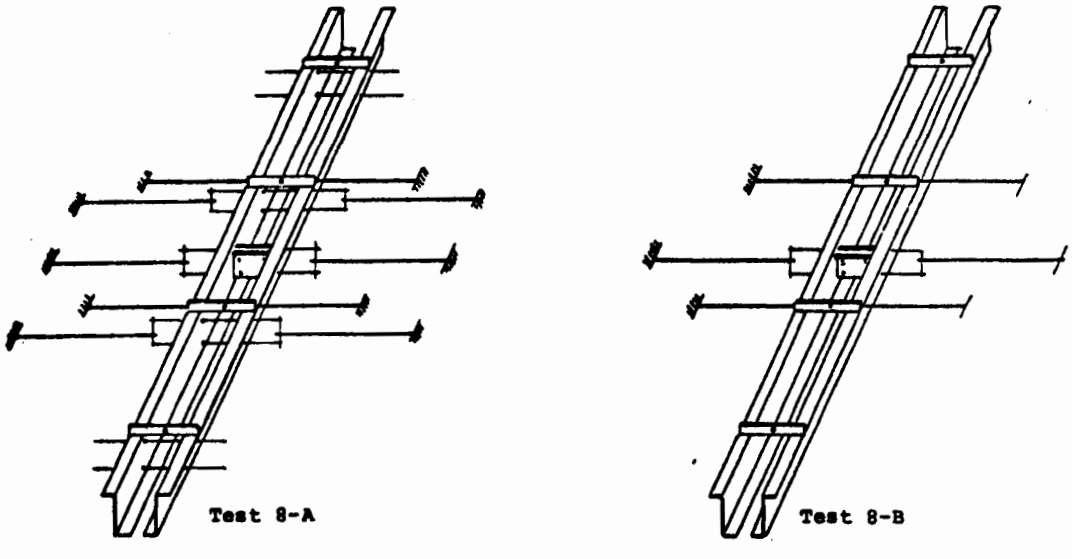

Figure 64: Overall Bracing of the Set-up in Tests 8 A and B with pre-tensioned wires.

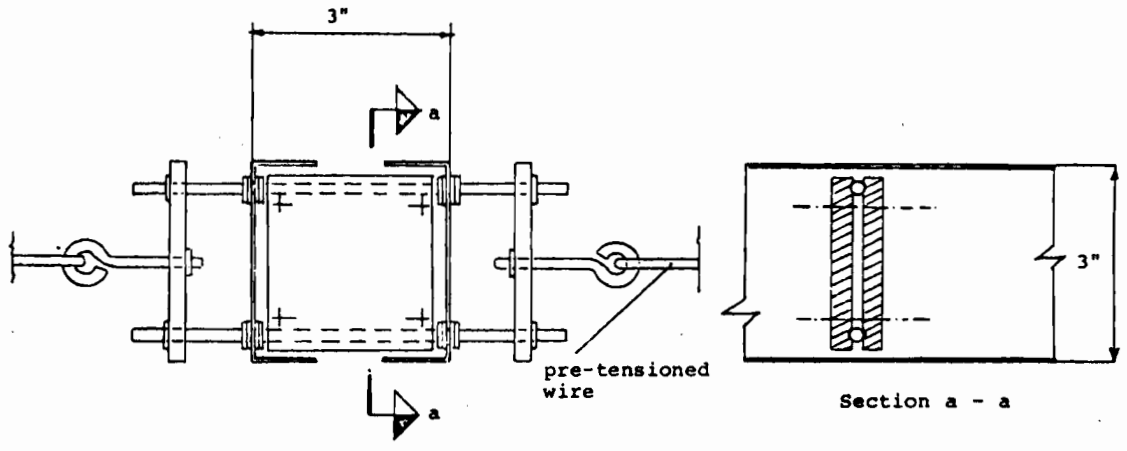

Figure 65: Detail of discrete Bracing at Mid-Span for Test 7 and 8.

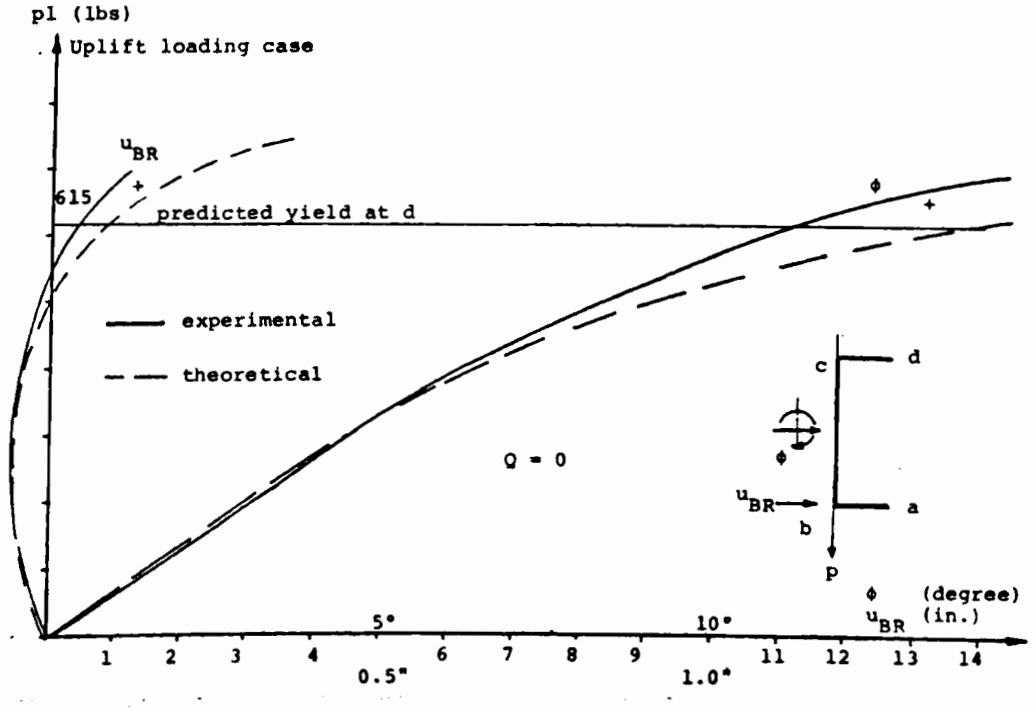

Figure 66: Test 1; theoretical and experimental results for u_{BR} and ϕ.

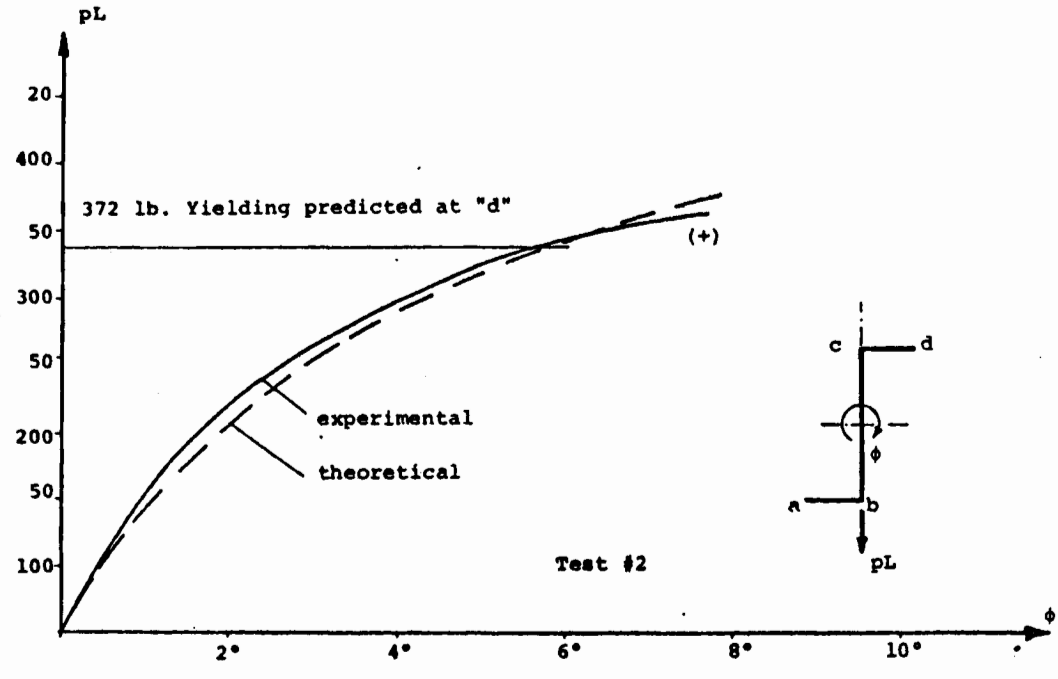

Figure 67a: Comparison of theoretical and experimental results for the angle of rotation ϕ at midspan.
Uplift loading, Q = 0

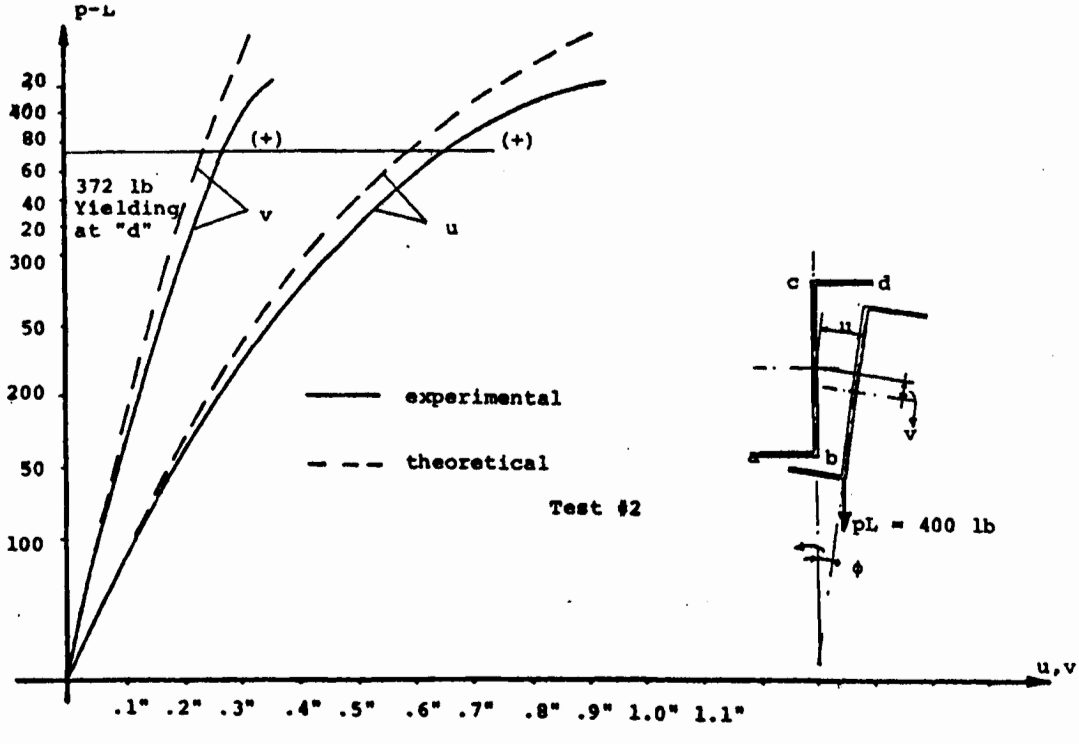

Figure 67b: Comparison of theoretical and experimental results for the deflections u and v.
Uplift loading, Q = 0, Z-Section

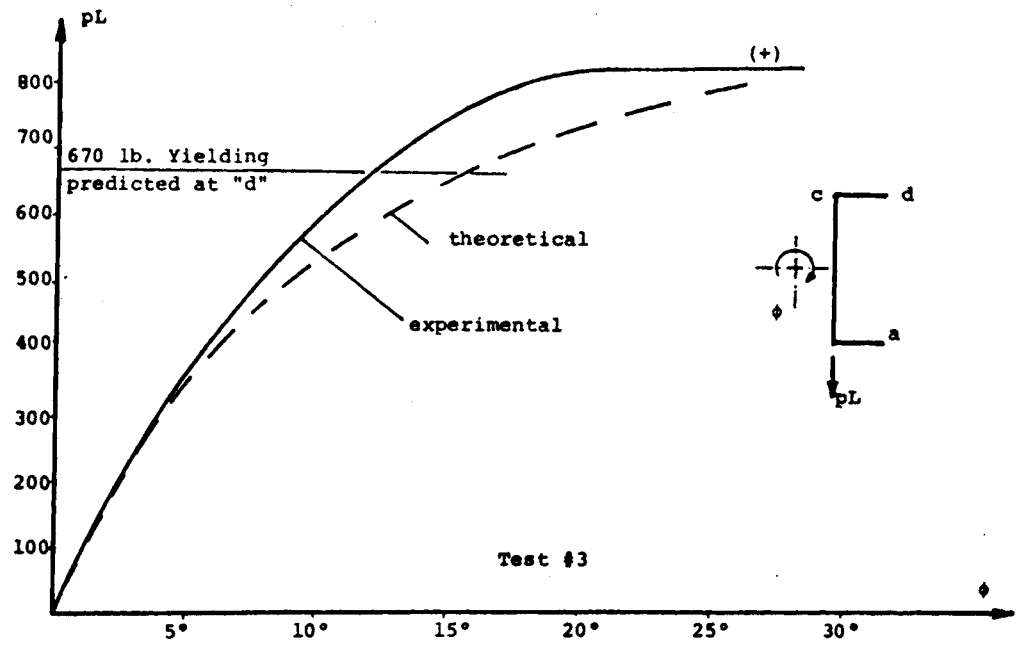

Figure 68a: Comparison of theoretical and test results for ϕ.
Uplift loading, Q = ∞, Channel Section

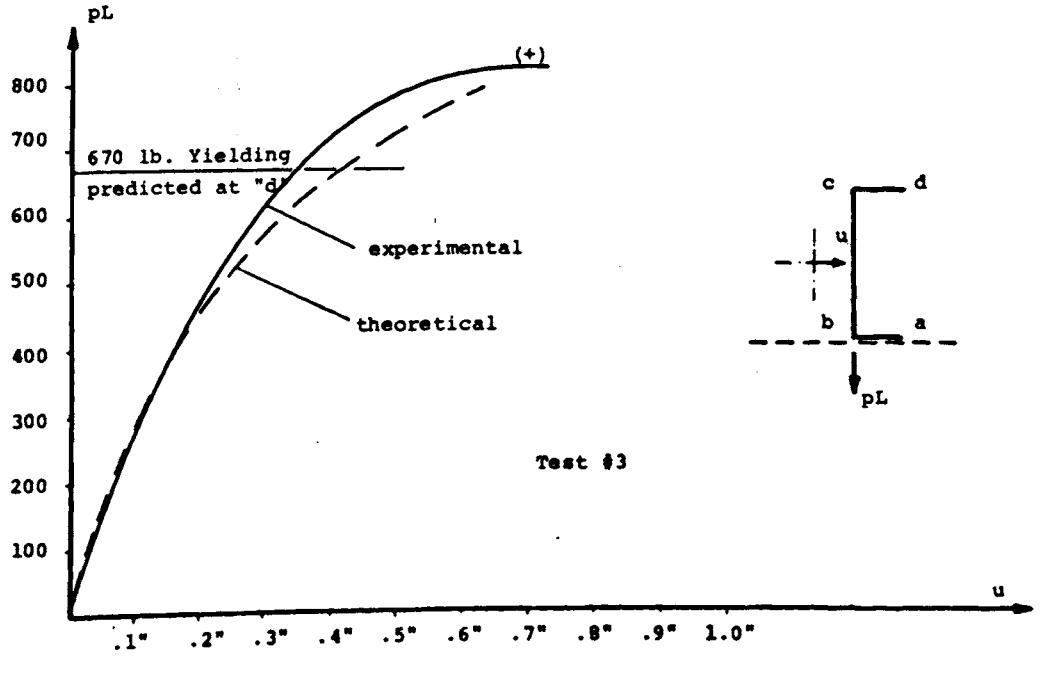

Figure 68b: Comparison of theoretical and test results for u.
Uplift loading, Q = ∞, Channel Section

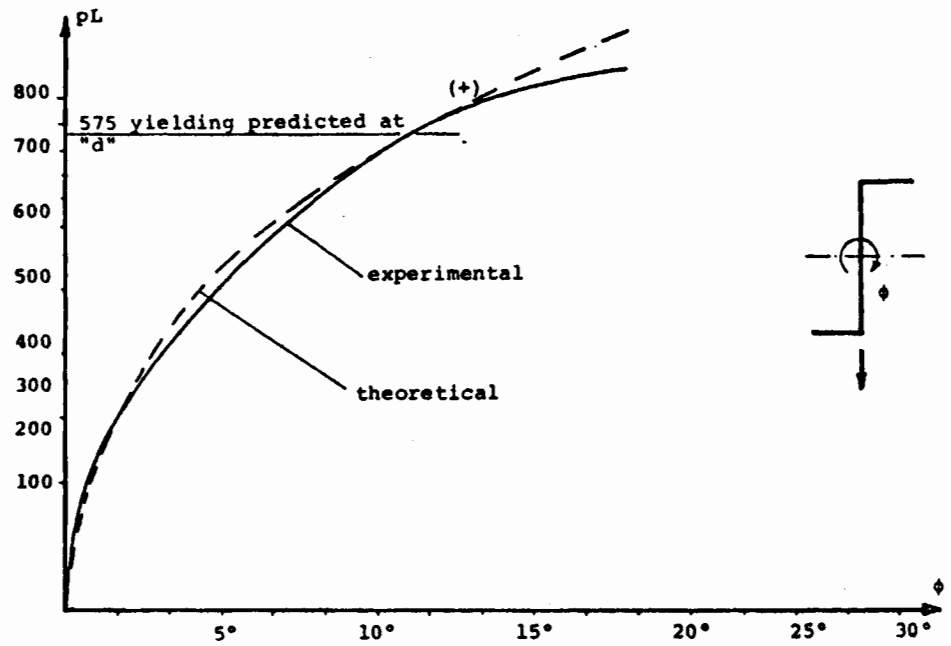

Figure 69: Comparison of theoretical and test results for ϕ.
Uplift loading, Q = ∞, Z-Section

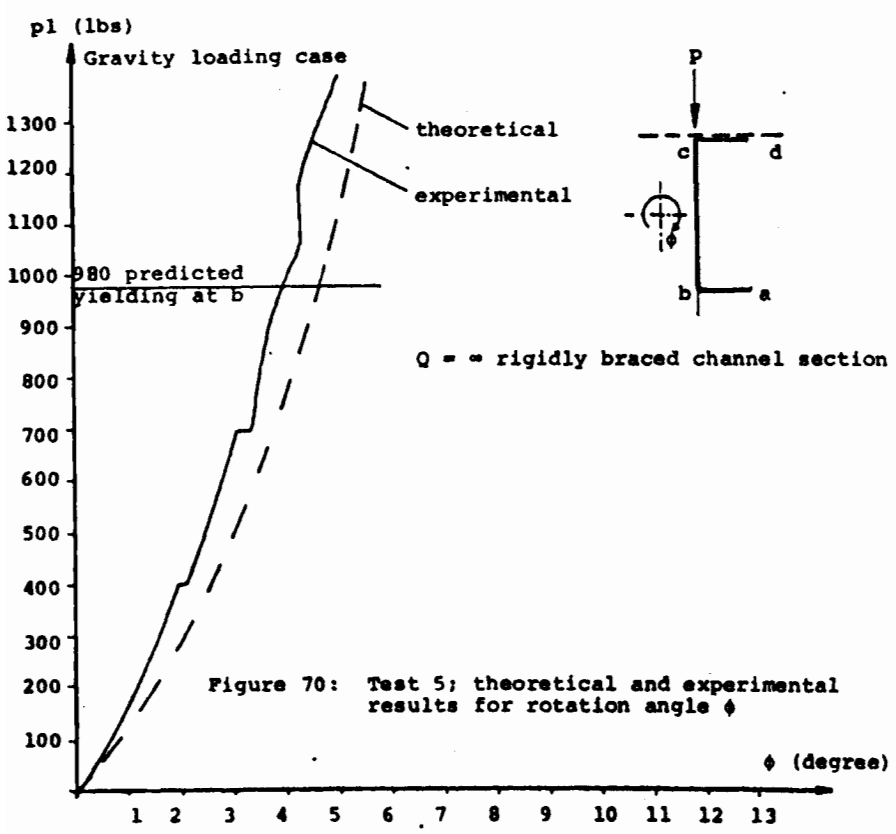

Figure 70: Test 5; theoretical and experimental results for rotation angle ϕ

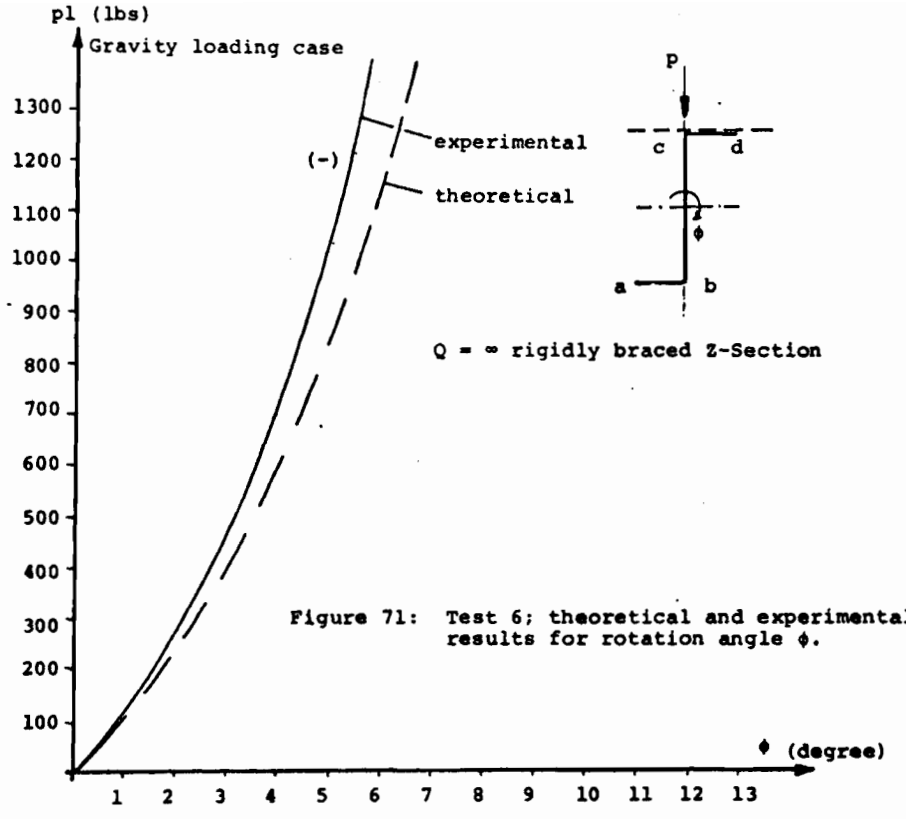

Figure 71: Test 6; theoretical and experimental results for rotation angle ϕ.

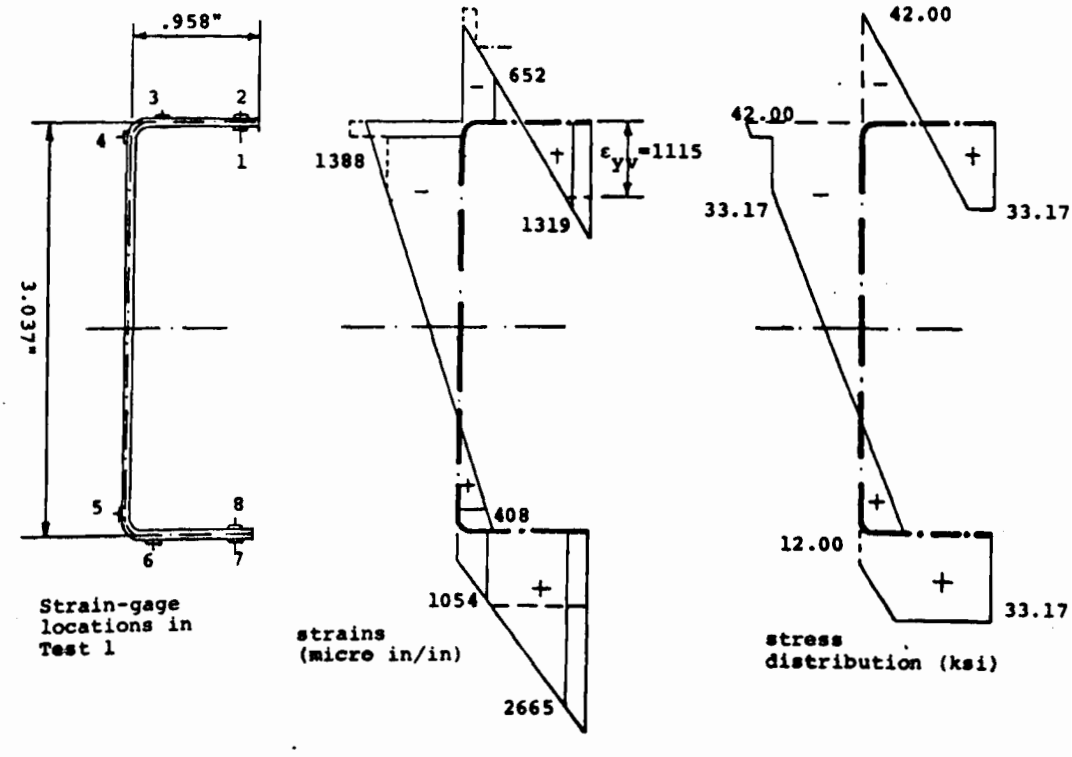

Figure 72: Strain and Stress Distribution at Midspan during failure.

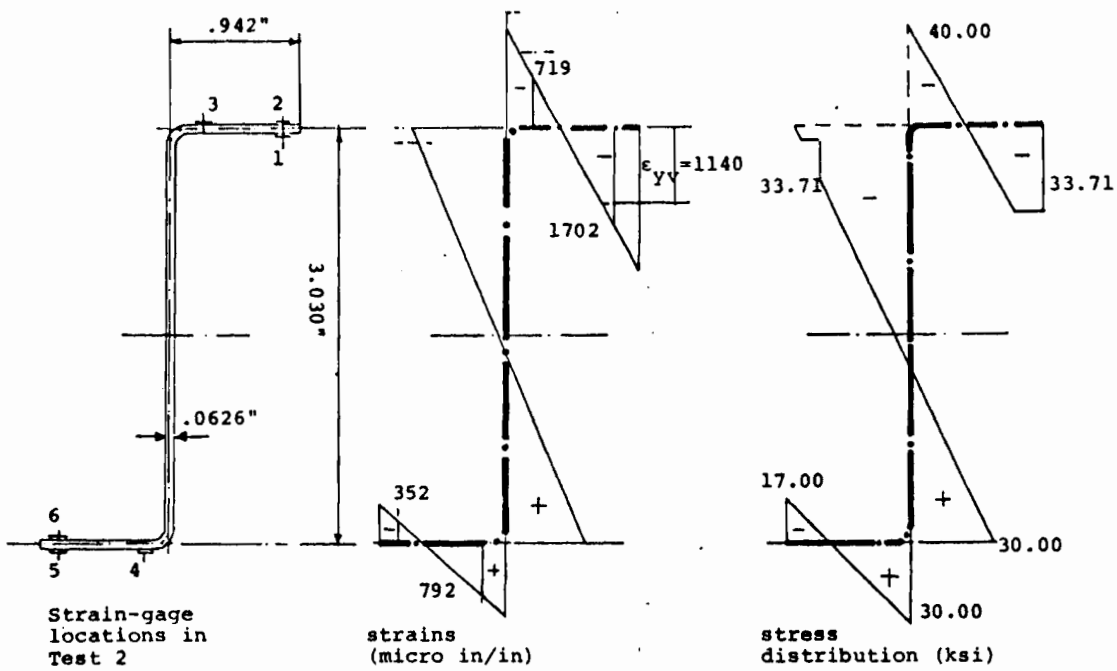

Figure 73: Strain and Stress Distribution at Midspan During Failure.

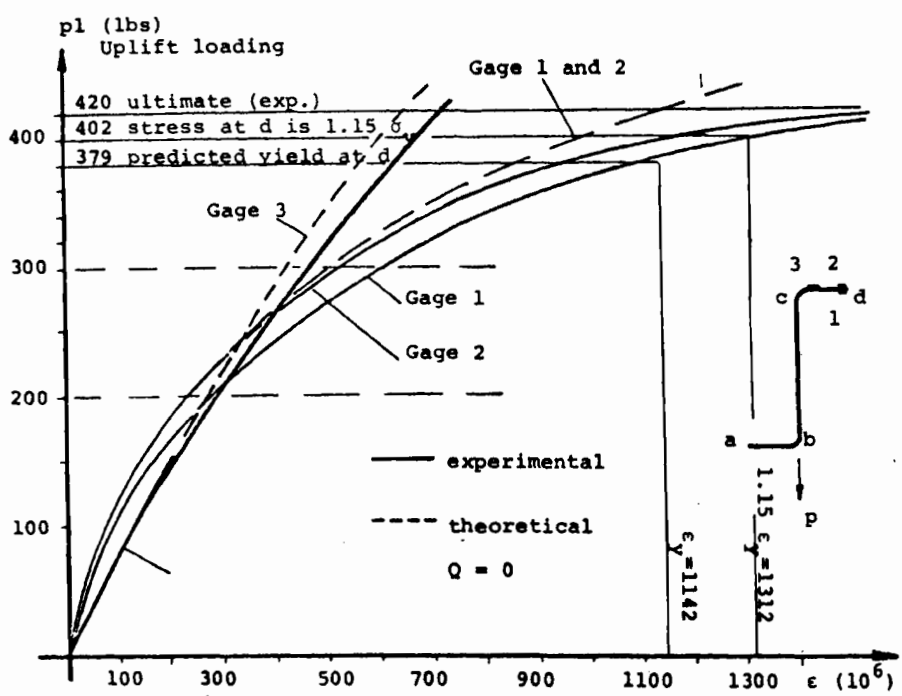

Figure 74: Test 2; Strain Measurements at Gages 1, 2 and 3.

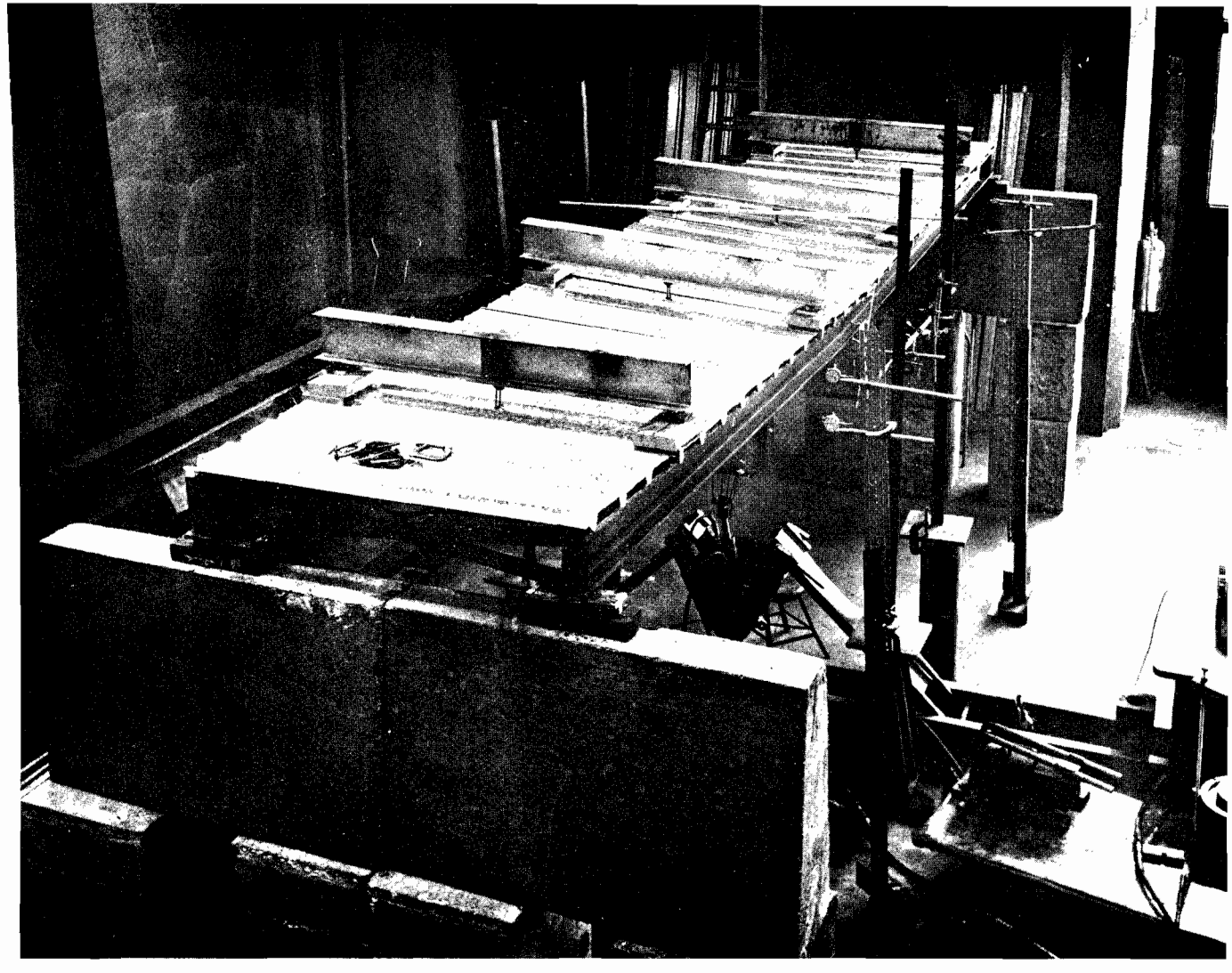

Figure 75. Full scale test for channel purlins under downward loading.

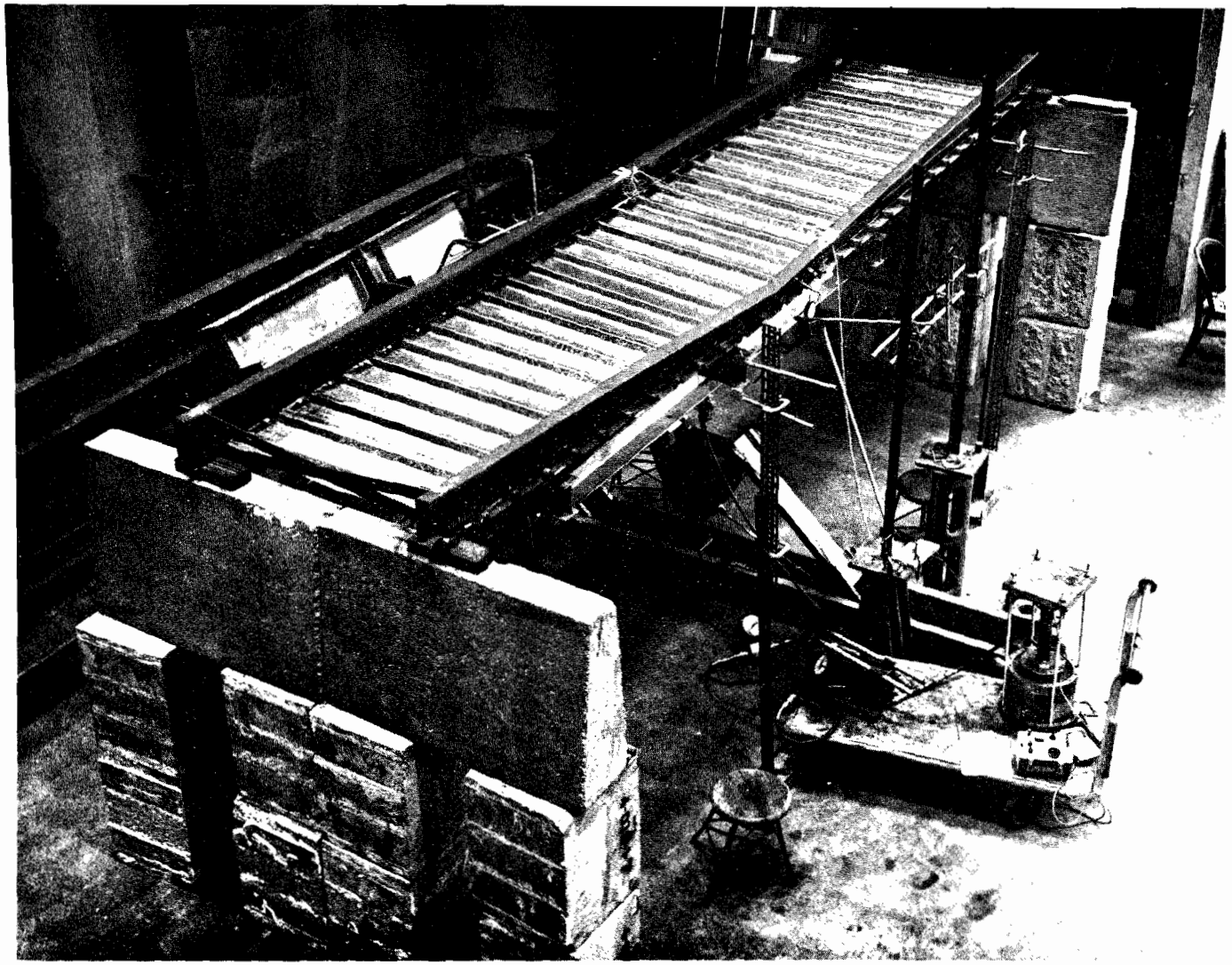

Figure 76. Full scale test for channel purlins under uplift loading.

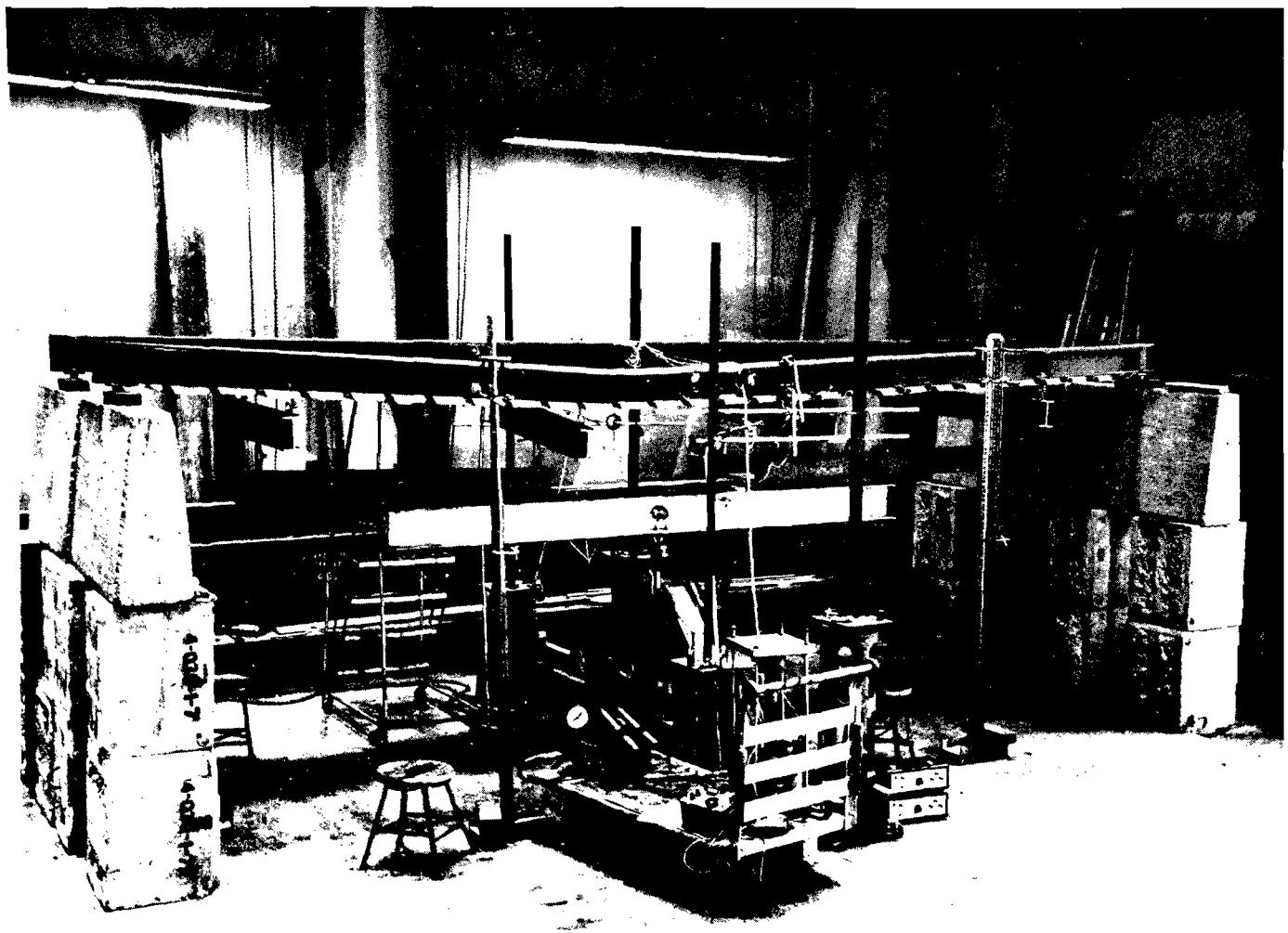

Figure 77. Loading arrangement for channel purlin test under uplift loads.

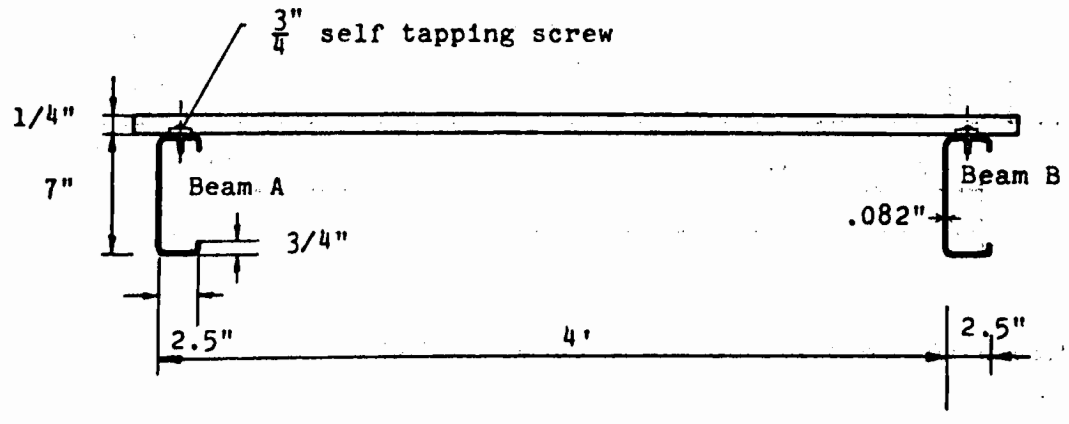

Figure 78 Full-scale test arrangement

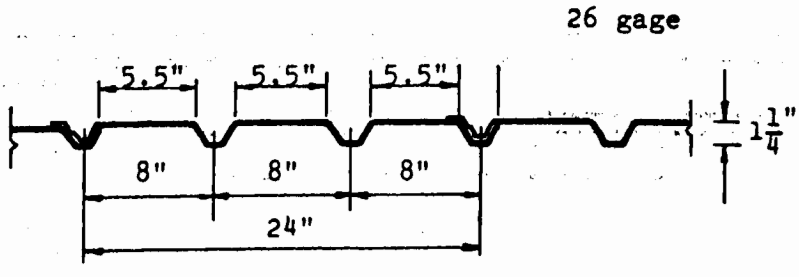

Figure 79 Deck Panel used in the Full scale Tests

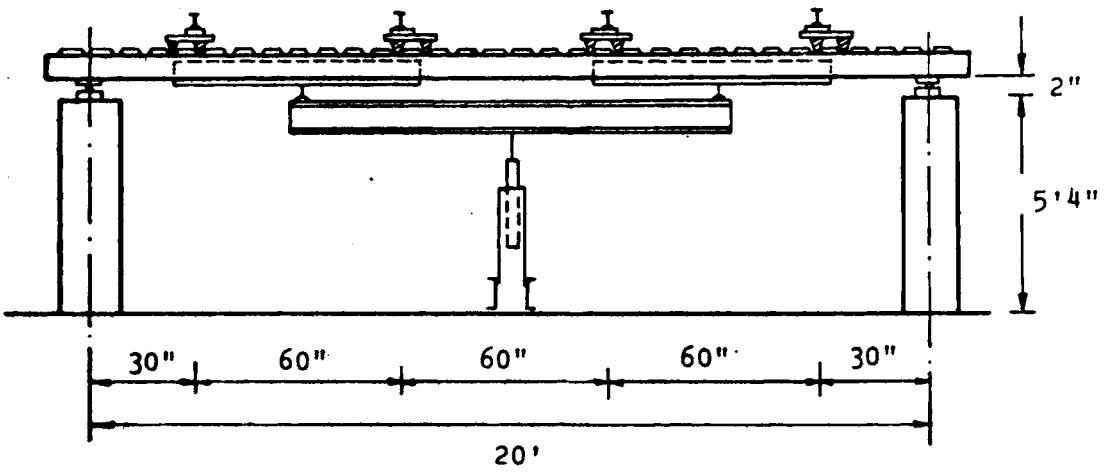

Figure 80 Test set-up for gravity loading

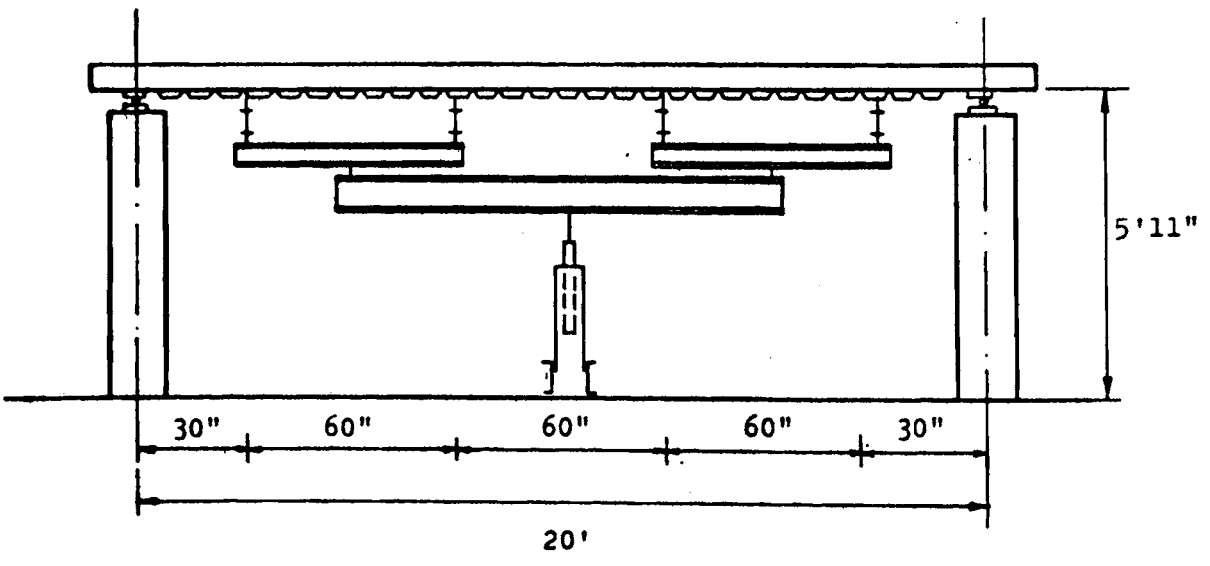

Figure 81 Test set-up for uplift loading

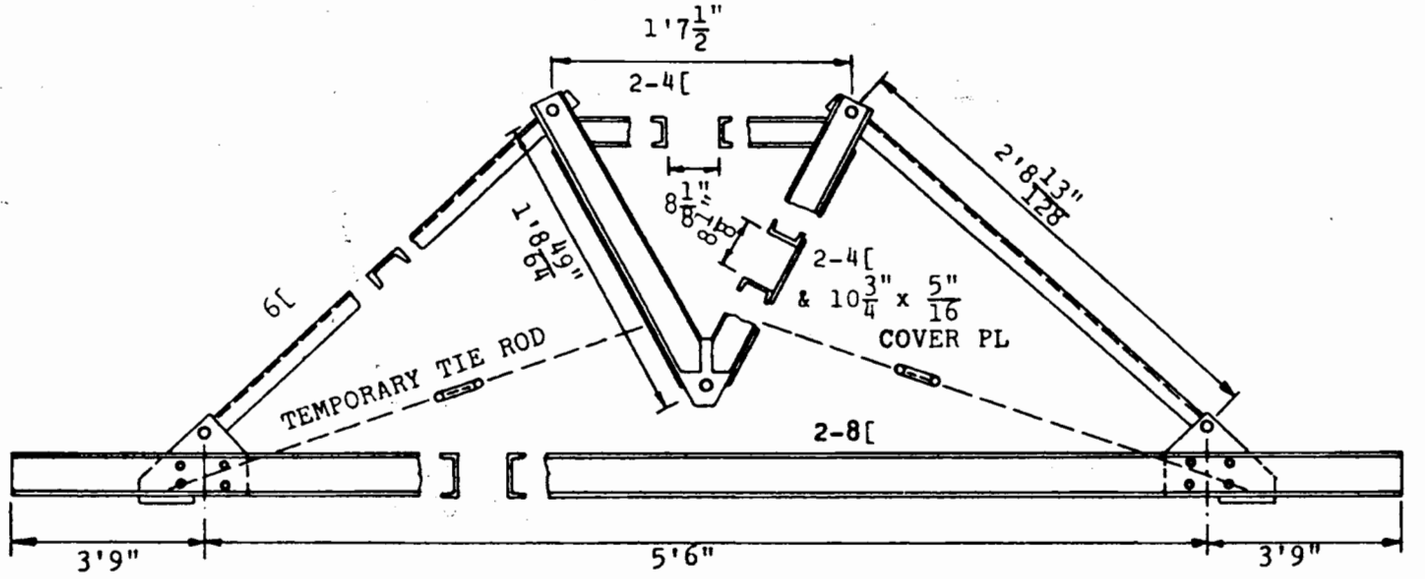

Figure 82 Gravity simulator

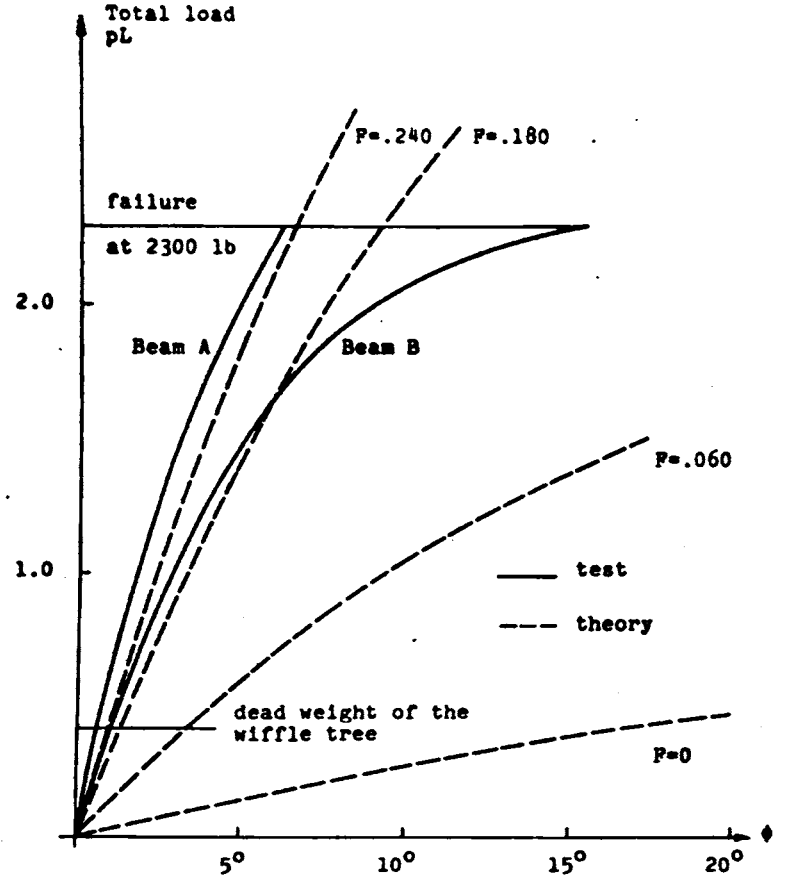

Figure 83 Angle of rotation ϕ at midspan for Test #F1
L. Channel, uplift loading

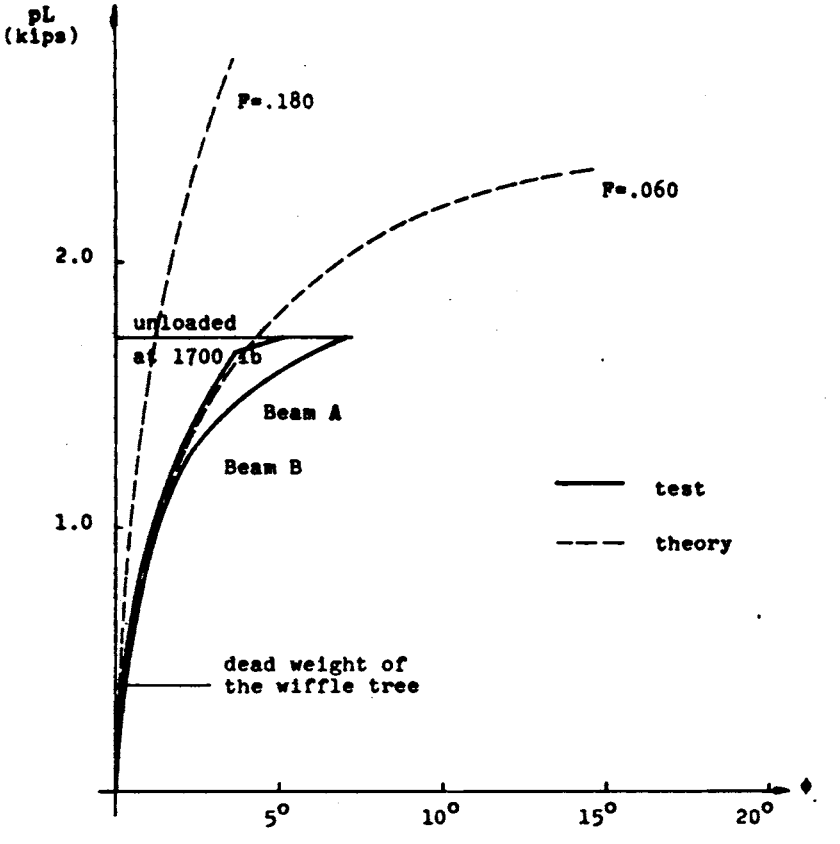

Figure 84 Angle of rotation ϕ at midspan for Test #F2
L. Z-section, uplift loading

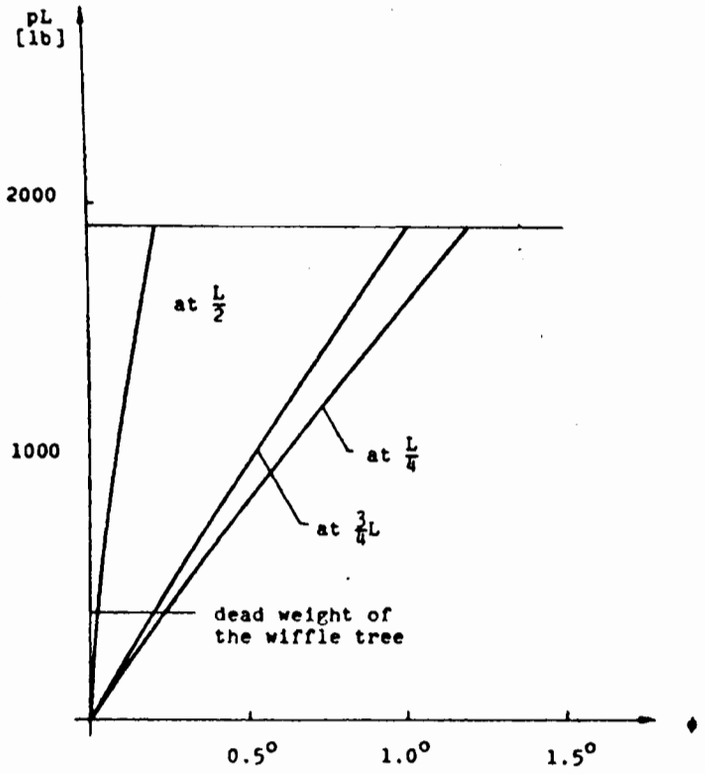

Figure 85 Angle of Rotation at $\frac{L}{4}$, $\frac{L}{2}$ and $\frac{3}{4}$L for Test #F3, Lipped Z-section with discrete brace at midspan, uplift loading

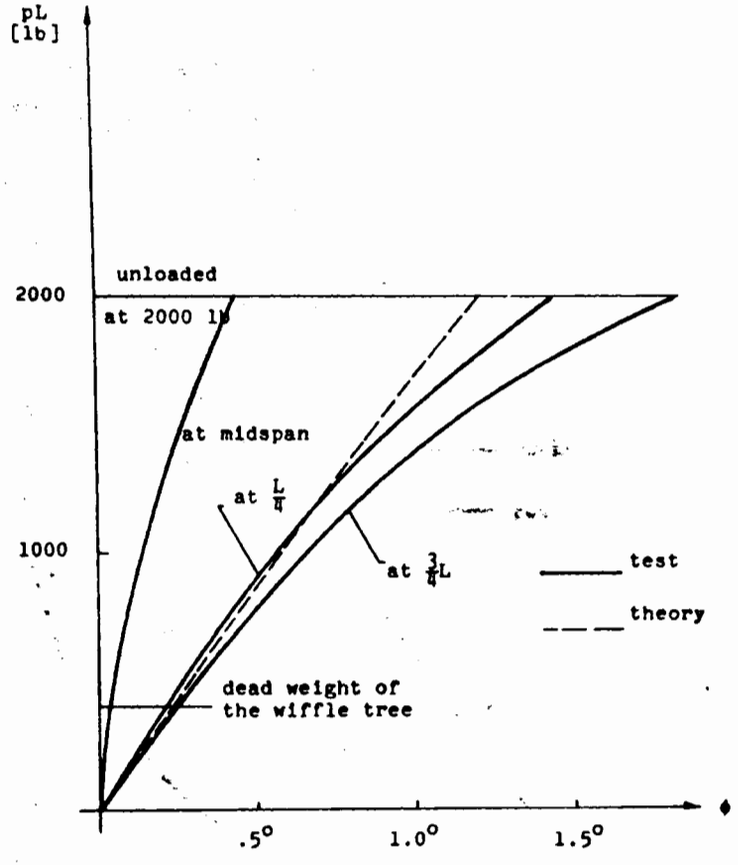

Figure 86 Angle of Rotation ϕ at $\frac{L}{4}$, $\frac{L}{2}$ and $\frac{3}{4}$L for Test #F4 L, Channel with discrete brace at midspan gravity loading

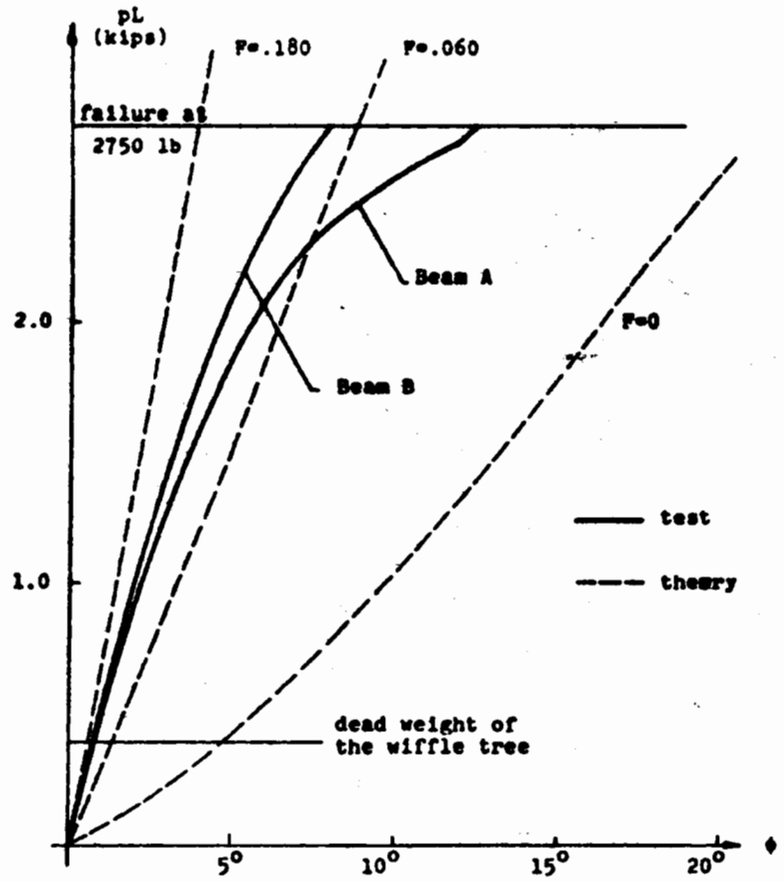

Figure 87 Angle of Rotation φ at midspan for #F5

L. Channel, gravity loading

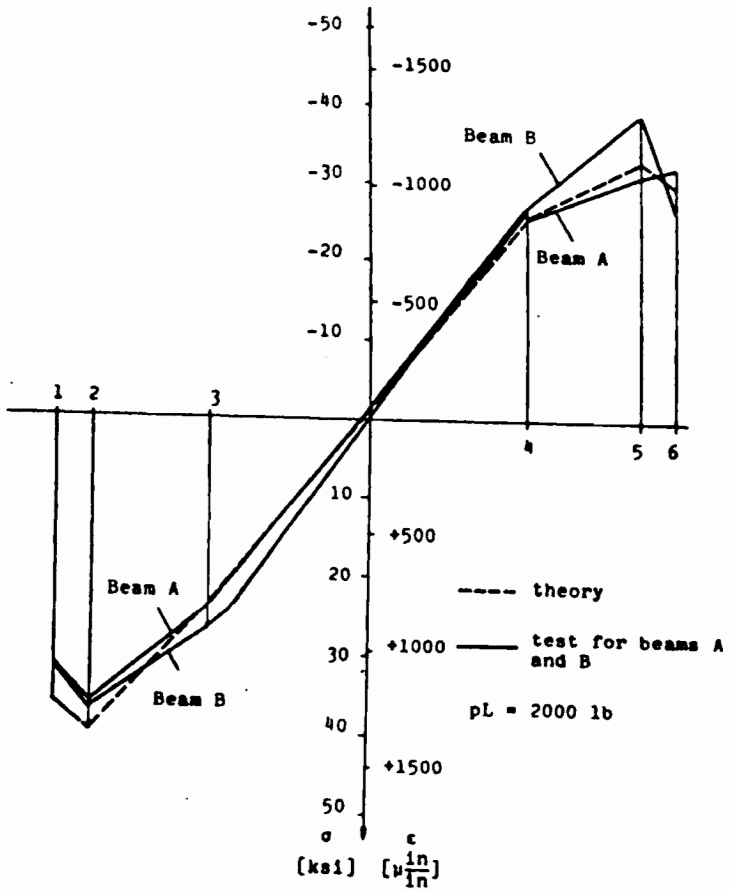

Figure 88 Strain distribution for Test #P4 at midspan

L. Channel, downward loading, discrete brace at midspan

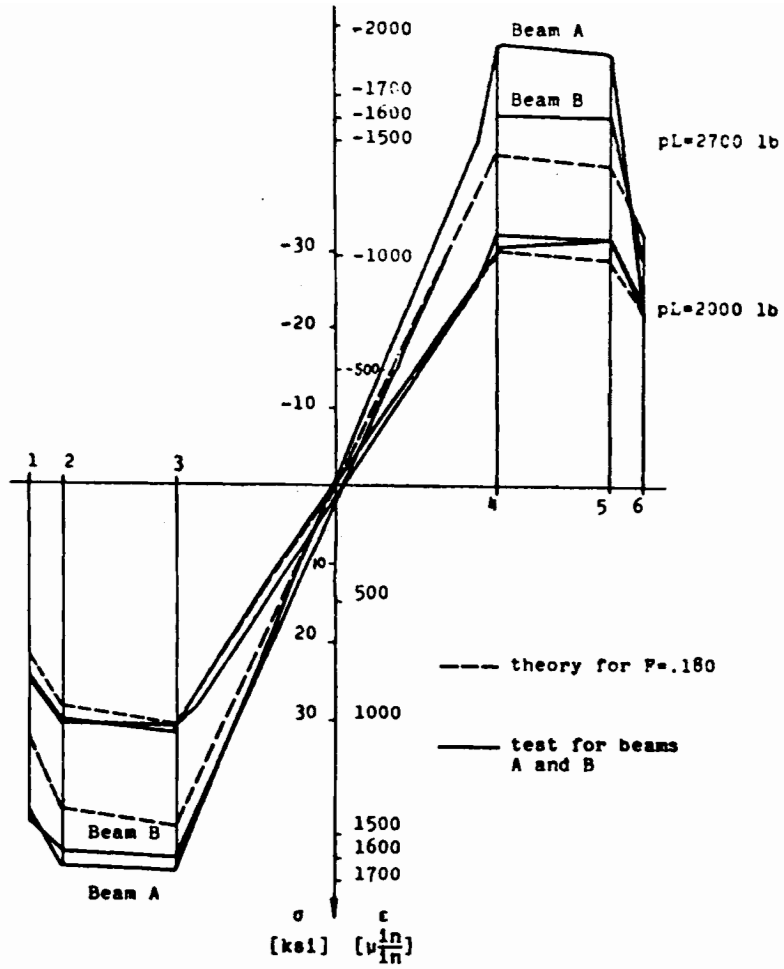

Figure 89 Strain distribution for Test #P5 at midspan

L. Channel, downward loading

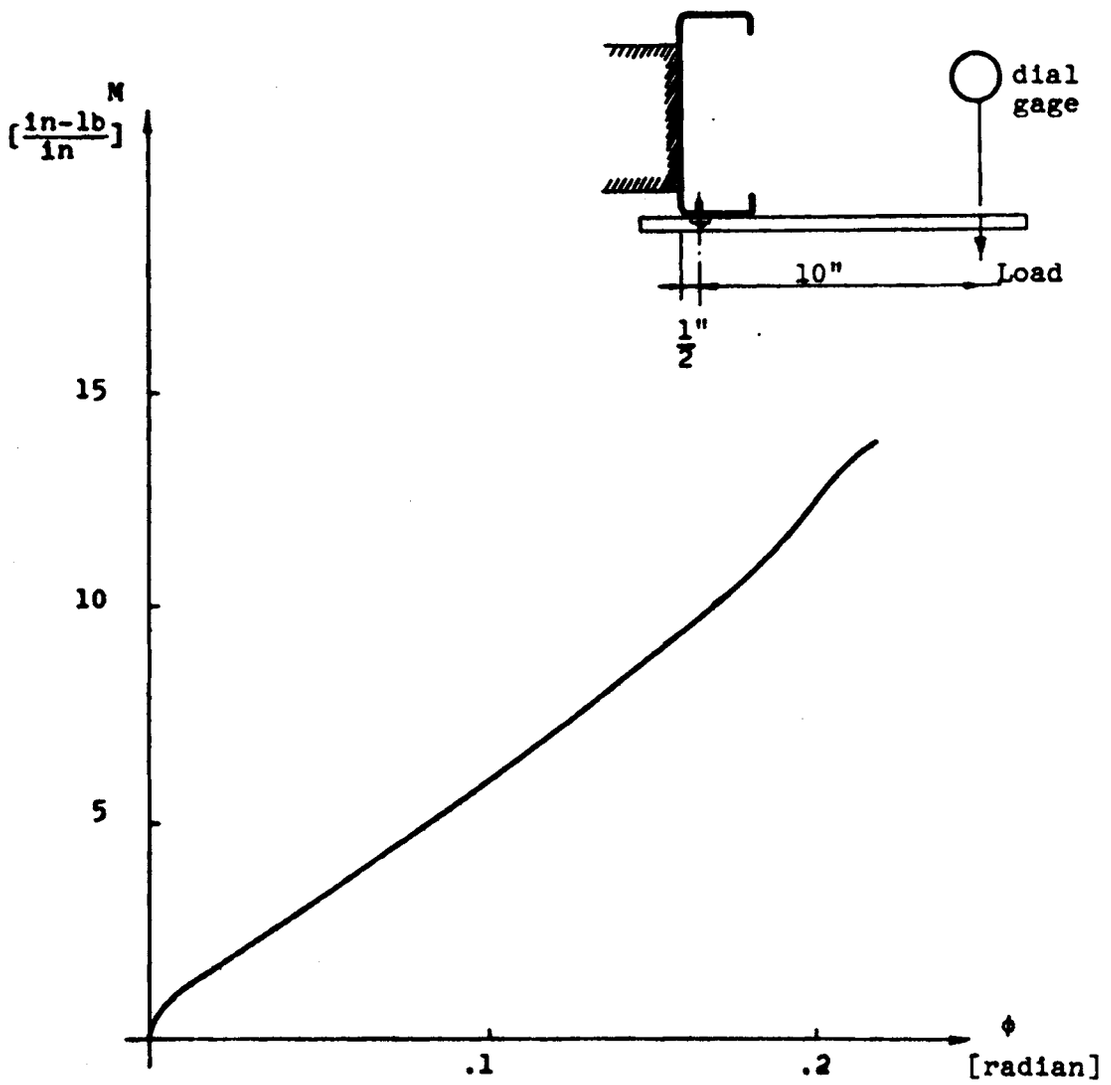

Figure 90 Test for determination of F
for gravity loading case

DESIGN TABLES FOR DIAPHRAGM BRACED CHANNEL AND Z-SECTION BEAMS

INTRODUCTION

The load carrying capacity of channel and Z-section purlins can be determined by the use of the attached tables prepared on the basis of Ref. 1. The load carrying capacity is determined by either the initiation of yielding or reaching a rotational deformation decided to be excessive.

These tables are for beams with depth h = 8 in. and have been prepared to cover a sizeable range of design parameters as discussed below.

The tables given here are for the purpose of illustrating the general principle of the design tables. Improvements such as extending the range of parameters and reducing the number of significant figures can be introduced by the user.

As an alternative for design use, the basic computer program can be modified to produce special tables for particular sections that each company may intend to use, for example, as purlins.

DIAPHRAGM BRACING

The two modes of bracing provided by diaphragms are shear bracing and bracing by torsional restraint. The parameters in the tables reflecting these two modes are

F = Torsional Restraint (in-k/in/rad). Values of F varying from 0 to 0.3 enable consideration of a variety of diaphragms.

Q = Shear Rigidity (kip/rad). Values of Q equal to 0, Q_L and infinity have been used. Q_L is defined as an efficient value of Q and is equal to 3.0 x M_{bend}/h. M_{bend} and h are defined in the following section.

BEAMS (Purlins)

Yield stress (SIG) values of 33 ksi and 55 ksi have been used.

The following parameters define the geometric cross-section properties.

b,h,c,t: Dimensions as shown in Fig. 1 below.

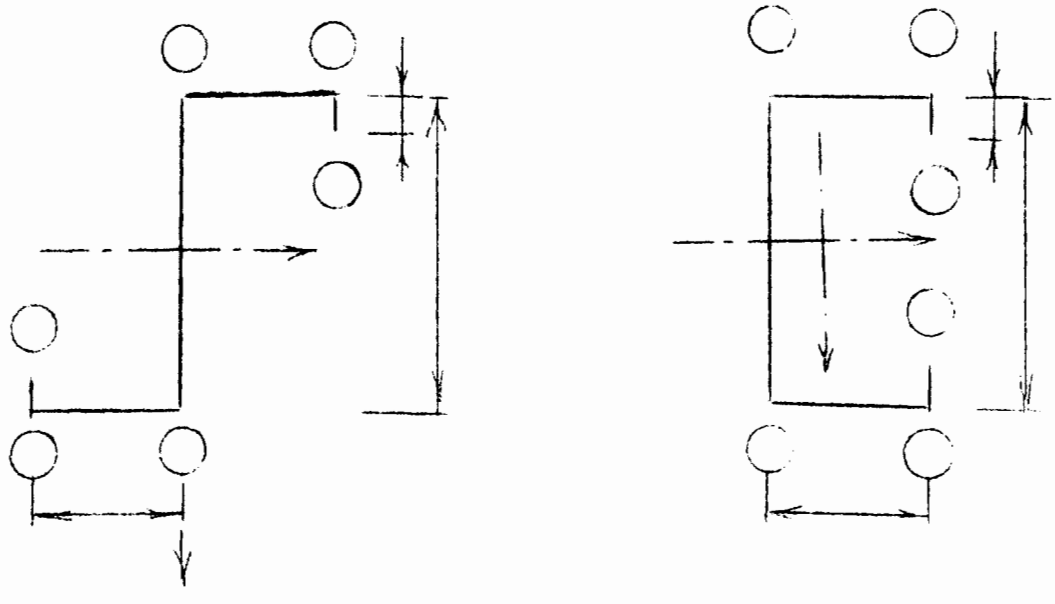

Fig. 1 Cross-sectional Geometry.

h: A value of 8 inches was used in the generation of these tables. For the sake of simplicity these tables do not contain all the geometric dimensionless parameters. The results given in the tables are sensitive to the value of h. Other tables produced for h = 6 in. are in good agreement with h = 8 in.

for the case of F = 0. For F not equal to zero, results differ by up to about 15% for gravity and by up to about 30% for uplift bonding (in both cases h = 8 inches results are conservative when used for h = 6 in.) Using the program provided here, similar tables can be readily generated for other typical purlin depths.

c: Again for simplicity this dimension was determined according to AISI Specifications. The value of c was taken equal to $2.8t \sqrt[6]{(b/t)^2 - 4000./SIG}$ but not less than 4.8t, and not to exceed $63.3/\sqrt{SIG}$.

R = $(b/t)/(b/t)_{lim}$ where $(b/t)_{lim}$ was taken as $171./\sqrt{SIG}$ (fully effective according to AISI Specifications).

Values of the ratio of purlin span L to depth h used were 20, 30, 40. An explanation of the representation of these values is given in the following section.

FURTHER EXPLANATION OF TABLES

A typical portion of a table is shown below

b/h \ R	1.0	0.80
	0.1144*6	0.1043*6
.2	0.0631*7	0.0550*7
	0.0426*7	0.0358*7
	0.3082*6	0.2828*6
.4	0.2162*7	0.1881*7
	0.1440*7	0.1210*7

The tabulated values are M/M_{bend}. M_{bend} is the hypothetical ment capacity if twist and lateral deflection were restrained

and is equal to $2(SIG.I_x)/h$. M is the moment capacity of the diaphragm braced beam.

As seen the results are given in groups of three numbers. In each group the first, second and third lines give the values of M/M_{bend} for L/h = 20, 30 and 40, respectively.

If the number appearing after the asterisk is 1 to 6, it indicates the corner at which yielding initiates. It is also an indication that the load carrying capacity (as given) is determined by the initiation of yielding and at that load the maximum notation does not exceed 30°. The corner rotation is given in Fig. 1. If the number after the asterisk is 7, it indicates that at the given value of M/M_{bend} the maximum rotation is 30° even though yielding is not yet reached. If the number is 8 it indicates that the numerical procedure used has not converged to a solution and the result given is meaningless.

COMPUTER PROGRAM

The entire computer program listing and the output that the tables were based upon are attached. The deck of cards for this program is being mailed under separate cover.

It should be emphasized that the tables and computer program give capacity moments (incipient yield moments) which must be divided by a safety factor for the purpose of calculating allowable loads.

REFERENCES

Celebi, N., "Diaphragm Braced Channel and Z-Section Beams", Report No. 344, Dept. of Structural Eng., Cornell University, Ithaca, New York, October, 1971.

LIPPED CHANNEL SECTION SIG=33.00

Q	b/h	F/E	0.00				0.15				0.30				TYPE OF LOADING
			1.00	0.80	0.60	0.40	1.00	0.80	0.60	0.40	1.00	0.80	0.60	0.40	
0.0	0.2		0.1144*6	0.1043*6	0.0948*6	0.0848*6	0.5412*2	0.5860*2	0.6475*2	0.7338*2	0.6998*2	0.7454*2	0.8003*2	0.8646*2	PLATE UNDER AXIAL LOAD
			0.0631*7	0.0550*7	0.0477*7	0.0408*7	0.5898*2	0.6418*2	0.7115*2	0.8057*2	0.7705*2	0.8192*2	0.8730*2	0.9262*2	
			0.0426*7	0.0358*7	0.0298*7	0.0244*7	0.6145*2	0.6694*2	0.7438*2	0.8436*2	0.8096*2	0.8597*2	0.9107*2	0.9532*2	
	0.4		0.3092*6	0.2828*6	0.2593*6	0.2352*6	0.4530*4	0.4736*4	0.5148*4	0.5953*4	0.5486*4	0.5861*4	0.6451*4	0.7382*4	
			0.2162*7	0.1881*7	0.1631*7	0.1395*7	0.5403*4	0.5940*4	0.6505*4	0.7374*2	0.6913*4	0.7423*4	0.7945*2	0.8481*2	
			0.1440*7	0.1210*7	0.1007*7	0.0827*7	0.6087*2	0.6503*2	0.7082*2	0.7870*2	0.7578*2	0.7965*2	0.8422*2	0.8944*2	
	0.6		0.3923*4	0.3687*4	0.3457*4	0.3216*4	0.4288*4	0.4196*4	0.4207*4	0.4455*4	0.4614*4	0.4632*4	0.4811*4	0.5333*4	
			0.3402*4	0.3003*6	0.2642*6	0.2304*6	0.4646*4	0.4743*4	0.5063*4	0.5800*4	0.5518*4	0.5802*4	0.6322*4	0.7219*4	
			0.2815*7	0.2341*7	0.1926*7	0.1552*7	0.5241*4	0.5521*4	0.6053*4	0.6986*4	0.6511*4	0.6931*4	0.7544*4	0.8389*4	
0.0	0.2		0.1890*1	0.1762*1	0.1635*1	0.1487*1	0.5415*5	0.5689*5	0.6082*5	0.6669*5	0.6533*5	0.6850*5	0.7270*5	0.7843*5	PLATE UNDER PURE BENDING
			0.1154*7	0.1045*7	0.0943*7	0.0837*7	0.5746*5	0.6142*5	0.6678*5	0.7429*5	0.7199*5	0.7599*5	0.8087*5	0.8666*5	
			0.0724*7	0.0644*7	0.0565*7	0.0487*7	0.5998*5	0.6453*5	0.7062*5	0.7898*5	0.7643*5	0.8074*5	0.8564*5	0.9080*5	
	0.4		0.3133*1	0.2920*1	0.2720*1	0.2519*1	0.4315*3	0.4497*3	0.4842*3	0.5501*3	0.5069*3	0.5385*3	0.5882*3	0.6697*3	
			0.2309*1	0.2541*1	0.2486*7	0.2172*7	0.5461*3	0.5805*3	0.6324*3	0.6859*5	0.6620*3	0.7042*3	0.7370*5	0.7796*5	
			0.2047*7	0.1764*7	0.1509*7	0.1275*7	0.6014*5	0.6280*5	0.6672*5	0.7256*5	0.7123*5	0.7417*5	0.7806*5	0.8326*5	
	0.6		0.2994*1	0.2788*1	0.2609*1	0.2460*1	0.3497*3	0.3424*3	0.3439*3	0.3654*3	0.3771*3	0.3789*3	0.3944*3	0.4395*3	
			0.3277*1	0.2943*1	0.2656*1	0.2407*1	0.4317*3	0.4411*3	0.4687*3	0.5307*3	0.5026*3	0.5273*3	0.5724*3	0.6525*3	
			0.3327*7	0.2790*7	0.2316*7	0.1895*7	0.5119*3	0.5352*3	0.5786*3	0.6556*3	0.6129*3	0.6489*3	0.7027*3	0.7798*5	

LIPPED CHANNEL SECTION SIG=33.00

Q	b/t	ρ	0.00				0.15				0.30				TYPE OF LOADING
			1.00	0.80	0.60	0.40	1.00	0.80	0.60	0.40	1.00	0.80	0.60	0.40	
Q_L	0.2		0.7465*4	0.7465*4	0.7483*4	0.7537*4	0.9494*4	0.9624*4	0.9753*4	0.9874*4	0.9762*4	0.9835*4	0.9901*4	0.9954*4	UNIFORM COMPRESSION
			0.7715*7	0.7585*7	0.7485*7	0.7426*7	0.9903*4	0.9934*4	0.9959*4	0.9978*4	0.9961*4	0.9973*4	0.9981*4	0.9987*4	
			0.7083*7	0.6948*7	0.6849*7	0.6799*7	0.9972*4	0.9979*4	0.9985*4	0.9990*4	0.9985*4	0.9988*4	0.9990*4	0.9992*4	
	0.4		0.5699*3	0.5631*3	0.5595*3	0.5619*3	0.6845*3	0.7094*3	0.7499*3	0.8116*4	0.7562*3	0.7894*3	0.8283*4	0.8828*4	
			0.6582*3	0.6452*3	0.6424*3	0.6708*7	0.8573*4	0.8813*4	0.9111*4	0.9467*4	0.9145*4	0.9344*4	0.9557*4	0.9771*4	
			0.6904*7	0.6509*7	0.6187*7	0.5963*7	0.9395*4	0.9546*4	0.9700*4	0.9848*4	0.9714*4	0.9802*4	0.9881*4	0.9944*4	
	0.6		0.5261*3	0.4907*3	0.4776*3	0.4683*3	0.5394*3	0.5368*3	0.5452*3	0.5786*3	0.5691*3	0.5764*3	0.5994*3	0.6557*3	
			0.5965*3	0.5465*3	0.5300*3	0.5200*3	0.6773*3	0.6948*3	0.7315*3	0.7969*4	0.7482*3	0.7775*3	0.8167*4	0.8734*4	
			0.6347*7	0.6824*7	0.6241*7	0.5766*7	0.8095*4	0.8310*4	0.8639*4	0.9108*4	0.8718*4	0.8951*4	0.9240*4	0.9573*4	
Q_L	0.2		0.1445*1	0.1716*1	0.1590*1	0.1446*1	0.7095*3	0.7630*3	0.8131*5	0.8703*5	0.8369*5	0.8665*5	0.8993*5	0.9357*5	DEEP BEAM
			0.1154*7	0.1051*7	0.0945*7	0.0839*7	0.8868*5	0.9187*5	0.9507*5	0.9788*5	0.9604*5	0.9742*5	0.9859*5	0.9950*5	
			0.0795*7	0.0656*7	0.0568*7	0.0489*7	0.9748*5	0.9792*2	0.9801*2	0.9948*2	0.9930*2	0.9966*2	0.9993*3	0.9979*3	
	0.4		0.2727*1	0.2480*1	0.2283*1	0.2104*1	0.4172*3	0.4343*3	0.4676*3	0.5345*3	0.4890*3	0.5208*3	0.5721*3	0.6596*3	
			0.2391*1	0.2435*1	0.2213*1	0.1994*1	0.5621*3	0.6047*3	0.6679*3	0.7630*3	0.6926*3	0.7417*3	0.8040*3	0.8810*5	
			0.2054*7	0.1797*7	0.1571*7	0.1362*7	0.7154*3	0.7657*3	0.8290*3	0.8993*5	0.8484*3	0.8885*3	0.9225*5	0.9516*5	
	0.6		0.3685*1	0.2901*1	0.2739*1	0.2593*1	0.3463*3	0.3402*3	0.3415*3	0.3597*3	0.3698*3	0.3713*3	0.3848*3	0.4247*3	
			0.3182*1	0.2895*1	0.2643*1	0.2414*1	0.4134*3	0.4226*3	0.4497*3	0.5132*3	0.4825*3	0.5078*3	0.5550*3	0.6413*3	
			0.3103*1	0.2979*7	0.2567*7	0.2191*7	0.5096*3	0.5377*3	0.5894*3	0.6809*3	0.6218*3	0.6643*3	0.7265*3	0.8159*3	

LIPPED CHANNEL SECTION SIG=33.00

Q	F / b/t	0.00				0.15				0.30				TYPE OF LOADING
		1.00	0.80	0.60	0.40	1.00	0.80	0.60	0.40	1.00	0.80	0.60	0.40	
THICKNESS	0.2	0.8876*3	0.8938*3	0.9012*3	0.9118*3	0.9628*3	0.9714*3	0.9802*3	0.9892*3	0.9795*3	0.9853*3	0.9908*3	0.9957*3	AXIAL
		0.9480*3	0.9511*3	0.9547*3	0.9597*3	0.9935*3	0.9954*3	0.9971*3	0.9985*3	0.9972*3	0.9981*3	0.9987*3	0.9991*3	
		0.9695*3	0.9712*3	0.9731*3	0.9758*3	0.9979*3	0.9984*3	0.9988*3	0.9991*3	0.9988*3	0.9990*3	0.9991*3	0.9993*3	
	0.4	0.6379*3	0.6411*3	0.6475*3	0.5609*3	0.7046*3	0.7249*3	0.7556*3	0.8059*3	0.7507*3	0.7773*3	0.8136*3	0.8657*3	
		0.7413*3	0.7451*3	0.7526*3	0.7631*3	0.8667*3	0.8881*3	0.9140*3	0.9455*3	0.9122*3	0.9310*3	0.9513*3	0.9729*3	
		0.8276*3	0.8313*3	0.8381*3	0.8513*3	0.9490*3	0.9610*3	0.9734*3	0.9859*3	0.9730*3	0.9809*3	0.9883*3	0.9948*3	
	0.6	0.5391*3	0.5335*3	0.5318*3	0.5357*3	0.5592*3	0.5619*3	0.5723*3	0.6003*3	0.5786*3	0.5871*3	0.6065*3	0.6494*3	
		0.6026*3	0.5962*3	0.5940*3	0.6000*3	0.6752*3	0.6912*3	0.7211*3	0.7759*3	0.7258*3	0.7507*3	0.7886*3	0.8466*3	
		0.6775*3	0.6710*3	0.6695*3	0.6784*3	0.8019*3	0.8246*3	0.8572*3	0.9028*3	0.8588*3	0.8829*3	0.9123*3	0.9474*3	
	0.2	0.1835*1	0.1707*1	0.1582*1	0.1440*1	0.7463*3	0.7997*3	0.8615*3	0.9309*3	0.8785*3	0.9159*3	0.9532*3	0.9863*3	PLATE
		0.1170*7	0.1052*7	0.0946*7	0.0839*7	0.9354*3	0.9725*3	0.9940*2	0.9685*2	0.9941*2	0.9801*2	0.9784*2	0.9876*2	
		0.0759*7	0.0657*7	0.0569*7	0.0489*7	0.9284*2	0.9387*2	0.9607*2	0.9877*2	0.9765*2	0.9867*2	0.9969*2	0.9984*3	
	0.4	0.3225*1	0.2848*1	0.2679*1	0.2490*1	0.4052*3	0.4211*3	0.4529*3	0.5191*3	0.4728*3	0.5040*3	0.5557*3	0.6459*3	
		0.2534*1	0.2397*1	0.2184*1	0.1972*1	0.5638*3	0.6150*3	0.6831*3	0.7832*3	0.7067*3	0.7584*3	0.8227*3	0.9002*3	
		0.2061*7	0.1803*7	0.1580*7	0.1374*7	0.7510*3	0.8019*3	0.8638*3	0.9355*3	0.8805*3	0.9182*3	0.9564*3	0.9899*3	
	0.6	0.3174*1	0.3010*1	0.2860*1	0.2706*1	0.3418*3	0.3369*3	0.3377*3	0.3517*3	0.3605*3	0.3615*3	0.3720*3	0.4046*3	
		0.3119*1	0.2858*1	0.2627*1	0.2409*1	0.3999*3	0.4085*3	0.4345*3	0.4977*3	0.4663*3	0.4914*3	0.5390*3	0.6288*3	
		0.3039*1	0.2686*1	0.2383*1	0.2081*7	0.5079*3	0.5381*3	0.5937*3	0.6922*3	0.6265*3	0.6721*3	0.7384*3	0.8320*3	

LIPPED CHANNEL SECTION SIG=55.00

Q	b/t	F \ R	0.00				0.15				0.30				TYPE OF LOADING
			1.00	0.80	0.60	0.40	1.00	0.80	0.60	0.40	1.00	0.80	0.60	0.40	
0.0	0.2		0.0925*7	0.0731*7	0.0631*7	0.0540*7	0.3200*6	0.3528*2	0.3953*2	0.4665*2	0.4461*2	0.4877*2	0.5446*2	0.6335*2	UNIFORM COMPRESSION
			0.0459*7	0.0388*7	0.0318*7	0.0258*7	0.3412*2	0.3745*2	0.4199*2	0.4941*2	0.4756*2	0.5206*2	0.5808*2	0.6760*2	
			0.0323*7	0.0263*7	0.0207*7	0.0159*7	0.3480*2	0.4164*5	0.4264*2	-0.0033*8	0.4847*2	0.5306*2	-0.0022*8	0.6920*2	
	0.4		0.2539*6	0.2270*6	0.1976*6	0.1715*6	0.3507*4	0.3533*4	0.3712*4	0.4244*4	0.4175*4	0.4367*4	0.4786*4	0.5625*4	
			0.1580*7	0.1331*7	0.1083*7	0.0877*7	0.3599*7	0.3850*7	0.4345*7	0.4992*2	0.4758*4	0.5151*4	0.5740*2	0.6544*2	
			0.1096*7	0.0891*7	0.0695*7	0.0534*7	0.3749*7	0.4104*7	0.4543*2	0.5319*2	0.5145*2	0.5554*2	0.6137*2	0.7043*2	
	0.6		0.3795*4	0.3480*4	0.3053*6	0.2677*6	0.4021*4	0.3801*4	0.3612*4	0.3647*4	0.4230*4	0.4093*4	0.4056*4	0.4350*4	
			0.3010*6	0.2641*7	0.2089*7	0.1647*7	0.3834*4	0.3721*4	0.3770*4	0.4212*4	0.4428*4	0.4492*4	0.4795*4	0.5555*4	
			0.2175*7	0.1746*7	0.1332*7	0.1001*7	0.3787*7	0.3824*7	0.4141*7	0.5036*7	0.4815*4	0.5051*4	0.5550*4	0.6486*4	
0.0	0.2		0.1555*7	0.1423*7	0.1268*7	0.1118*7	0.3708*5	0.3908*5	0.4186*5	0.4679*5	0.4668*5	0.4959*5	0.5343*5	0.5970*5	UNIFORM COMPRESSION
			0.0797*7	0.0705*7	0.0608*7	0.0519*7	0.3628*5	0.3907*5	0.4280*5	0.4902*5	0.4816*5	0.5192*5	0.5684*5	0.6460*5	
			0.0519*7	0.0447*7	0.0374*7	0.0307*7	0.3600*5	0.3902*5	0.4307*5	0.4981*5	0.4874*5	0.5286*5	0.5828*5	0.6690*5	
	0.4		0.3071*1	0.2811*1	0.2532*1	0.2273*1	0.3948*3	0.3895*3	0.4078*3	0.4524*3	0.4363*3	0.4534*3	0.4889*3	0.5553*3	
			0.2249*7	0.1941*7	0.1625*7	0.1355*7	0.4176*3	0.4353*3	0.4694*3	0.5112*5	0.5089*3	0.5401*3	0.5719*5	0.6213*5	
			0.1506*7	0.1260*7	0.1019*7	0.0814*7	0.4263*5	0.4447*5	0.4739*5	0.5288*5	0.5293*5	0.5579*5	0.5981*5	0.6642*5	
	0.6		0.3247*1	0.2959*1	0.2682*1	0.2455*1	0.3571*1	0.3402*1	0.3304*3	0.3375*3	0.3760*3	0.3662*3	0.3662*3	0.3936*3	
			0.3356*1	0.3145*7	0.2515*7	0.2004*7	0.3969*3	0.3902*3	0.3977*3	0.4359*3	0.4434*3	0.4503*3	0.4770*3	0.5389*3	
			0.2543*7	0.2061*7	0.1592*7	0.1213*7	0.4276*7	0.4302*7	0.4616*7	0.5036*3	0.4967*3	0.5161*3	0.5564*3	0.6262*5	

LIPPED CHANNEL SECTION SIG=55.00

Q	b/t	R	0.00				0.15				0.30				TYPE OF LOADING
			1.00	0.80	0.60	0.40	1.00	0.80	0.60	0.40	1.00	0.80	0.60	0.40	
0.0	0.2		0.0925*7	0.0731*7	0.0631*7	0.0540*7	0.3200*6	0.3528*2	0.3953*2	0.4665*2	0.4461*2	0.4877*2	0.5446*2	0.6335*2	UNIAXIAL COMPRESSION
			0.0459*7	0.0388*7	0.0318*7	0.0258*7	0.3412*2	0.3745*2	0.4199*2	0.4941*2	0.4756*2	0.5206*2	0.5808*2	0.6760*2	
			0.0323*7	0.0263*7	0.0207*7	0.0159*7	0.3480*2	0.4164*5	0.4264*2	-0.0033*8	0.4847*2	0.5306*2	-0.0022*8	0.6920*2	
	0.4		0.2539*6	0.2270*6	0.1976*6	0.1715*6	0.3507*4	0.3533*4	0.3712*4	0.4244*4	0.4175*4	0.4367*4	0.4786*4	0.5625*4	
			0.1580*7	0.1331*7	0.1083*7	0.0877*7	0.3599*7	0.3850*7	0.4345*7	0.4992*2	0.4758*4	0.5151*4	0.5740*2	0.6544*2	
			0.1096*7	0.0891*7	0.0695*7	0.0534*7	0.3749*7	0.4104*7	0.4543*2	0.5319*2	0.5145*2	0.5554*2	0.6137*2	0.7043*2	
	0.6		0.3795*4	0.3480*4	0.3053*6	0.2677*6	0.4021*4	0.3801*4	0.3612*4	0.3647*4	0.4230*4	0.4093*4	0.4056*4	0.4350*4	
			0.3010*6	0.2641*7	0.2089*7	0.1647*7	0.3834*4	0.3721*4	0.3770*4	0.4212*4	0.4428*4	0.4492*4	0.4795*4	0.5555*4	
			0.2175*7	0.1746*7	0.1332*7	0.1001*7	0.3787*7	0.3824*7	0.4141*7	0.5036*7	0.4815*4	0.5051*4	0.5550*4	0.6486*4	
	0.2		0.1555*7	0.1423*7	0.1268*7	0.1118*7	0.3708*5	0.3908*5	0.4186*5	0.4679*5	0.4668*5	0.4959*5	0.5343*5	0.5970*5	UPLIFT ORAVITY
			0.0797*7	0.0705*7	0.0608*7	0.0519*7	0.3628*5	0.3907*5	0.4280*5	0.4902*5	0.4816*5	0.5192*5	0.5684*5	0.6460*5	
			0.0519*7	0.0447*7	0.0374*7	0.0307*7	0.3600*5	0.3902*5	0.4307*5	0.4981*5	0.4874*5	0.5286*5	0.5828*5	0.6690*5	
0.0	0.4		0.3071*1	0.2811*1	0.2532*1	0.2273*1	0.3948*3	0.3895*3	0.4078*3	0.4524*3	0.4363*3	0.4534*3	0.4889*3	0.5553*3	
			0.2240*7	0.1941*7	0.1525*7	0.1355*7	0.4176*3	0.4353*3	0.4694*3	0.5112*5	0.5089*3	0.5401*3	0.5719*5	0.6213*5	
			0.1506*7	0.1260*7	0.1019*7	0.0814*7	0.4263*5	0.4447*5	0.4739*5	0.5288*5	0.5293*5	0.5579*5	0.5981*5	0.6642*5	
	0.6		0.3247*1	0.2959*1	0.2682*1	0.2455*1	0.3571*1	0.3402*1	0.3304*3	0.3375*3	0.3760*3	0.3662*3	0.3662*3	0.3936*3	
			0.3356*1	0.3145*7	0.2515*7	0.2004*7	0.3969*3	0.3902*3	0.3977*3	0.4359*3	0.4434*3	0.4503*3	0.4770*3	0.5389*3	
			0.2543*7	0.2061*7	0.1592*7	0.1213*7	0.4276*7	0.4302*7	0.4616*7	0.5036*3	0.4967*3	0.5161*3	0.5564*3	0.6262*5	

LIPPED CHANNEL SECTION SIG=55.00

Q	F / B/t	0.00				0.15				0.30				TYPE OF LOADING
		1.00	0.80	0.60	0.40	1.00	0.80	0.60	0.40	1.00	0.80	0.60	0.40	
Q_L	0.2	0.8095*7	0.7966*7	0.7874*7	0.7811*7	0.9254*4	0.9419*4	0.9613*4	0.9792*4	0.9601*4	0.9710*4	0.9823*4	0.9913*4	GRAVITY
		0.7103*7	0.6974*7	0.6902*7	0.6866*7	0.9823*4	0.9876*4	0.9927*4	0.9964*4	0.9924*4	0.9949*4	0.9969*4	0.9983*4	
		0.6569*7	0.6433*7	0.6365*7	0.6337*7	0.9949*4	0.9965*4	0.9979*4	0.9988*4	0.9978*4	0.9984*4	0.9989*4	0.9993*4	
	0.4	0.6137*3	0.6053*3	0.6048*3	0.6104*3	0.6864*3	0.7017*3	0.7386*3	0.7896*4	0.7393*3	0.7632*4	0.8010*4	0.8561*4	
		0.7029*7	0.6626*7	0.6305*7	0.6085*7	0.8300*4	0.8502*4	0.9835*4	0.9252*4	0.8840*4	0.9054*4	0.9340*4	0.9632*4	
		0.6102*7	0.5684*7	0.5373*7	0.5167*7	0.9135*4	0.9307*4	0.9528*4	0.9743*4	0.9525*4	0.9649*4	0.9784*4	0.9894*4	
	0.6	0.5443*3	0.5244*3	0.5071*3	0.4974*3	0.5649*3	0.5538*3	0.5537*3	0.5777*3	0.5839*3	0.5804*3	0.5936*3	0.6392*3	
		0.6235*3	0.5995*3	0.6461*7	0.5935*7	0.6906*3	0.6943*3	0.7224*3	0.7739*4	0.7403*3	0.7568*4	0.7896*4	0.8446*4	
		0.6504*7	0.5792*7	0.5165*7	0.4693*7	0.7938*4	0.8057*4	0.8358*4	0.8837*4	0.8441*4	0.8633*4	0.8963*4	0.9367*4	
Q_L	0.2	0.1563*7	0.1426*7	0.1269*7	0.1120*7	0.5317*3	0.5829*3	0.6562*3	0.7598*3	0.6933*3	0.7494*3	0.8202*5	0.8869*5	UPLIFT
		0.0819*7	0.0715*7	0.0611*7	0.0519*7	0.0007*8	0.0009*8	0.0012*8	0.8366*3	0.8194*3	0.0009*8	0.9539*5	0.9626*2	
		0.0558*7	0.0466*7	0.0360*7	0.0309*7	0.8837*2	0.9391*2	0.9810*5	0.9784*3	0.9814*5	0.8309*2	0.0022*8	0.9777*2	
	0.4	0.2247*1	0.2711*1	0.2451*1	0.2206*1	0.3729*3	0.3779*3	0.3973*3	0.4469*3	0.4241*3	0.4427*3	0.4828*3	0.5605*3	
		0.2267*7	0.1983*7	0.1695*7	0.1449*7	0.4788*7	0.5170*7	0.5366*3	0.6332*3	0.5704*3	0.6152*3	0.6861*3	0.7677*3	
		0.1505*7	0.1266*7	0.1042*7	0.0858*7	0.5572*7	0.6314*7	0.6798*3	0.7830*3	0.7183*3	0.7693*3	0.8382*3	0.9185*5	
	0.6	0.3243*1	0.2995*1	0.2738*1	0.2517*1	0.3496*3	0.3352*1	0.3253*3	0.3308*3	0.3644*3	0.3558*3	0.3556*3	0.3793*3	
		0.3212*1	0.2845*1	0.2486*1	0.2331*7	0.3832*3	0.3772*3	0.3863*3	0.4296*3	0.4310*3	0.4395*3	0.4709*3	0.5444*3	
		0.2577*7	0.2141*7	0.1725*7	0.1396*7	0.4320*7	0.4369*7	0.4788*7	0.6063*7	0.5289*3	0.5572*3	0.6150*3	0.7137*3	

LIPPED CHANNEL SECTION SIG=55.00

Q	P	R	0.00				0.15				0.30				TYPE OF LOADING
		b/t	1.00	0.80	0.60	0.40	1.00	0.80	0.60	0.40	1.00	0.80	0.60	0.40	
IMPERFECT	0.2		0.9228*3	0.9279*3	0.9367*3	0.9458*3	0.9620*3	0.9695*3	0.9787*3	0.9876*3	0.9758*3	0.9817*3	0.9883*3	0.9939*3	UNIFORM
			0.9645*3	0.9667*3	0.9705*3	0.9743*3	0.9909*3	0.9932*3	0.9955*3	0.9975*3	0.9953*3	0.9966*3	0.9978*3	0.9987*3	
			0.9778*3	0.9790*3	0.9811*3	0.9833*3	0.9965*3	0.9973*3	0.9981*3	0.9988*3	0.9981*3	0.9985*3	0.9989*3	0.9992*3	
	0.4		0.6822*3	0.6866*3	0.7017*3	0.7227*3	0.7236*3	0.7396*3	0.7715*3	0.8173*3	0.7555*3	0.7771*3	0.8148*3	0.8643*3	
			0.8325*3	0.8076*3	0.8227*3	0.8414*3	0.8727*3	0.8897*3	0.9156*3	0.9447*3	0.9069*3	0.9240*3	0.9465*3	0.9689*3	
			0.8901*3	0.8842*3	0.8949*3	0.9074*3	0.9465*3	0.9570*3	0.9703*3	0.9830*3	0.9672*3	0.9754*3	0.9845*3	0.9922*3	
	0.6		0.5679*3	0.5605*3	0.5602*3	0.5682*3	0.5820*3	0.5798*3	0.5895*3	0.6163*3	0.5952*3	0.5976*3	0.6151*3	0.6548*3	
			0.6555*3	0.6481*3	0.6521*3	0.6658*3	0.7001*3	0.7085*3	0.7367*3	0.7860*3	0.7346*3	0.7514*3	0.7885*3	0.8434*3	
			0.7445*3	0.7393*3	0.7470*3	0.7636*3	0.8157*3	0.8309*3	0.8621*3	0.9035*3	0.8567*3	0.8760*3	0.9070*3	0.9422*3	
	0.2		0.1566*7	0.1428*7	0.1270*7	0.1121*7	0.5755*3	0.6313*3	0.7079*3	0.8100*3	0.7434*3	0.7984*3	0.8668*3	0.9461*3	PARTIAL
			0.0822*7	0.0716*7	0.0612*7	0.0519*7	0.0007*8	0.0009*8	0.0012*8	0.8334*2	0.0007*8	0.9684*3	0.9065*2	0.9330*2	
			0.0561*7	0.0467*7	0.0381*7	0.0309*7	0.9544*2	0.9971*3	0.9710*3	0.8101*2	0.8042*2	1.3949*3	0.9195*2	0.9892*2	
	0.4		0.2830*1	0.2666*1	0.2417*1	0.2180*1	0.3662*3	0.3711*3	0.3906*3	0.4420*3	0.4166*3	0.4356*3	0.4775*3	0.5605*3	
			0.2270*7	0.1990*7	0.1707*7	0.1463*7	0.4895*7	0.5339*7	0.5613*3	0.6675*3	0.5940*3	0.6433*3	0.7196*3	0.8234*3	
			0.1505*7	0.1267*7	0.1044*7	0.0862*7	0.6001*7	0.6929*7	0.7288*3	0.8325*3	0.7657*3	0.8165*3	0.8836*3	0.9609*3	
	0.6		0.3243*1	0.3009*1	0.2763*1	0.2543*1	0.3428*3	0.3303*3	0.3202*1	0.3250*3	0.3558*3	0.3478*3	0.3470*3	0.3673*3	
			0.3147*1	0.2794*1	0.2450*1	0.2154*1	0.3768*3	0.3708*3	0.3801*3	0.4250*3	0.4248*3	0.4337*3	0.4666*3	0.5452*3	
			0.2584*7	0.2157*7	0.1751*7	0.1428*7	0.4330*7	0.4386*7	0.4838*7	0.6264*7	0.6045*7	0.5740*3	0.6379*3	0.7438*3	

LIPPED Z-SECTION SIG=33.00

Q	F	b/t	0.00				0.15				0.30				TYPE OF LOADING
			1.00	0.80	0.60	0.40	1.00	0.80	0.60	0.40	1.00	0.80	0.60	0.40	
0.0	0.2		0.1281*6	0.1172*6	0.1085*6	0.0983*6	0.3786*4	0.3993*4	0.4257*4	0.4611*4	0.4380*4	0.4558*4	0.4771*4	0.5044*4	UNIAXIAL COMPRESSION
			0.0577*7	0.0607*7	0.0542*7	0.0476*7	0.3786*4	0.3994*4	0.4257*4	0.4611*4	0.4383*4	0.4561*4	0.4777*4	0.5055*4	
			0.0434*7	0.0378*7	0.0327*7	0.0278*7	0.3772*4	0.3983*4	0.4253*4	0.4616*4	0.4383*4	0.4566*4	0.4787*4	0.5068*4	
	0.4		0.3329*4	0.3235*4	0.3132*4	0.2911*6	0.3690*4	0.3718*4	0.3788*4	0.3931*4	0.3871*4	0.3923*4	0.4010*4	0.4150*4	
			0.2192*6	0.2015*6	0.1843*6	0.1658*6	0.3503*4	0.3594*4	0.3732*4	0.3934*4	0.3829*4	0.3914*4	0.4026*4	0.4178*4	
			0.1574*7	0.1387*7	0.1216*7	0.1049*7	0.3486*4	0.3598*4	0.3748*4	0.3951*4	0.3842*4	0.3931*4	0.4043*4	0.4193*4	
	0.6		0.3692*4	0.3631*4	0.3569*4	0.3498*4	0.3733*4	0.3691*4	0.3663*4	0.3662*4	0.3765*4	0.3736*4	0.3724*4	0.3747*4	
			0.3216*4	0.3084*4	0.2942*4	0.2773*4	0.3489*4	0.3468*4	0.3485*4	0.3562*4	0.3628*4	0.3630*4	0.3663*4	0.3736*4	
			0.2690*4	0.2446*6	0.2203*6	0.1949*6	0.3379*4	0.3396*4	0.3456*4	0.3571*4	0.3603*4	0.3627*4	0.3677*4	0.3759*4	
0.0	0.2		0.2219*1	0.1920*1	0.1316*1	0.1685*1	0.4040*3	0.4200*3	0.4412*3	0.4708*3	0.4498*3	0.4648*3	0.4833*3	0.5079*3	BIAXIAL COMPRESSION
			0.1139*1	0.1061*1	0.0984*1	0.0913*7	0.3906*3	0.4091*3	0.4330*3	0.4657*3	0.4438*3	0.4604*3	0.4807*3	0.5072*3	
			0.0715*7	0.0650*7	0.0588*7	0.0524*7	0.3842*3	0.4040*3	0.4295*3	0.4643*3	0.4415*3	0.4591*3	0.4804*3	0.5078*3	
	0.4		0.3654*3	0.3623*3	0.3577*3	0.3522*3	0.3865*3	0.3886*3	0.3936*3	0.4041*3	0.3978*3	0.4017*3	0.4083*3	0.4196*3	
			0.2933*3	0.2818*1	0.2653*1	0.2462*1	0.3671*3	0.3736*3	0.3838*3	0.3998*3	0.3906*3	0.3973*3	0.4067*3	0.4201*3	
			0.2194*1	0.2033*1	0.1875*1	0.1705*1	0.3601*3	0.3689*3	0.3812*3	0.3989*3	0.3890*3	0.3966*3	0.4066*3	0.4205*3	
	0.6		0.3762*3	0.3714*3	0.3668*3	0.3624*3	0.3790*3	0.3753*3	0.3729*3	0.3727*3	0.3812*3	0.3784*3	0.3771*3	0.3787*3	
			0.3443*3	0.3357*3	0.3268*3	0.3170*3	0.3607*3	0.3583*3	0.3587*3	0.3636*3	0.3699*3	0.3693*3	0.3711*3	0.3766*3	
			0.3178*3	0.2946*3	0.2811*3	0.2659*3	0.3501*3	0.3502*3	0.3538*3	0.3622*3	0.3662*3	0.3674*3	0.3710*3	0.3776*3	

LIPPED Z-SECTION SIG=33.00

Q	b/h \ P	0.00				0.15				0.30				TYPE OF LOADING
		1.00	0.80	0.60	0.40	1.00	0.80	0.60	0.40	1.00	0.80	0.60	0.40	
Q_1	0.2	0.8964*3	0.9021*3	0.9088*3	0.9183*3	0.9021*4	0.9063*4	0.9114*4	0.9190*4	0.9004*4	0.9051*4	0.9107*4	0.9188*4	FLEXURAL
		0.9425*5	0.9189*5	0.8992*5	-0.0040*8	0.9496*4	0.9524*4	0.9556*4	0.9602*4	0.9497*4	0.9527*4	0.9560*4	0.9607*4	
		-0.0027*8	-0.0034*8	-0.0047*8	-0.0072*8	0.9701*4	0.9720*4	0.9741*4	0.9770*4	0.9706*4	0.9724*4	0.9745*4	0.9773*4	
	0.4	0.6234*3	0.6303*3	0.6394*3	0.6549*3	0.6390*3	0.6500*3	0.6644*3	0.6862*3	0.6466*3	0.6580*3	0.6722*3	0.6927*3	
		0.7491*3	0.7562*3	0.7657*3	0.7813*3	0.7742*3	0.7845*3	0.7963*3	0.8124*3	0.7785*3	0.7879*3	0.7987*3	0.8114*4	
		0.8390*3	0.8448*3	0.8522*3	0.8641*3	0.8555*4	0.8605*4	0.8666*4	0.8760*4	0.8530*4	0.8587*4	0.8656*4	0.8758*4	
	0.6	-0.0001*8	-0.0001*8	0.4982*3	0.5050*3	-0.0001*8	-0.0001*8	0.5064*3	0.5185*3	0.0001*8	-0.0001*8	-0.0002*8	0.5259*3	
		0.5792*3	0.5816*3	0.5862*3	0.5968*3	0.5963*3	0.6050*3	0.6180*3	0.6396*3	0.6048*3	0.6145*3	0.6278*3	0.6480*3	
		0.6699*3	0.6733*3	0.6792*3	0.6920*3	0.6976*3	0.7086*3	0.7225*3	0.7420*3	0.7049*3	0.7154*3	0.7279*3	0.7454*3	
Q_2	0.2	0.2501*1	0.2350*1	0.2201*1	0.2025*1	0.6970*3	0.7363*3	0.7825*3	0.8372*3	0.7878*3	0.8167*3	0.8478*3	0.8820*3	PLATE
		0.1471*7	0.1334*7	0.1209*7	0.1080*7	0.8365*3	0.8683*3	0.9027*3	0.9363*3	0.9080*3	0.9248*3	0.9401*3	0.9535*3	
		0.0959*7	0.0839*7	0.0733*7	0.0634*7	0.8976*3	0.9318*3	0.9582*3	0.9723*3	0.9594*3	0.9662*3	0.9712*3	0.9756*3	
	0.4	0.4212*3	0.4144*3	0.4078*3	0.4007*3	0.4726*3	0.4824*3	0.5008*3	0.5366*3	0.5059*3	0.5219*3	0.5467*3	0.5873*3	
		0.3613*3	0.3440*3	0.3211*1	0.2944*1	0.5558*3	0.5831*3	0.6223*3	0.6797*3	0.6280*3	0.6562*3	0.6917*3	0.7378*3	
		0.2949*7	0.2536*7	0.2256*7	0.1988*7	0.6671*3	0.7009*3	0.7428*3	0.7953*3	0.7461*3	0.7730*3	0.8032*3	0.8384*3	
	0.6	0.4151*3	0.4095*3	0.4044*3	0.3997*3	0.4233*3	0.4213*3	0.4222*3	0.4301*3	0.4304*3	0.4310*3	0.4358*3	0.4500*3	
		0.4024*3	0.3895*3	0.3768*3	0.3636*3	0.4493*3	0.4539*3	0.4677*3	0.4993*3	0.4797*3	0.4911*3	0.5119*3	0.5488*3	
		0.3816*3	0.3597*3	0.3380*3	0.3156*3	0.5053*3	0.5216*3	0.5508*3	0.6008*3	0.5616*3	0.5833*3	0.6143*3	0.6593*3	

LIPPED Z-SECTION SIG=33.00

Q	F / R / b/t	0.00				0.15				0.30				TYPE OF LOADING
		1.00	0.80	0.60	0.40	1.00	-0.80	0.60	0.40	1.00	0.80	0.60	0.40	
SIMPLE	0.2	0.8925*3	0.8976*3	0.9039*3	0.9134*3	0.9636*3	0.9718*3	0.9803*3	0.9891*3	0.9794*3	0.9851*3	0.9905*3	0.9954*3	UNIFORM
		0.9503*3	0.9529*3	0.9559*3	0.9605*3	0.9933*3	0.9953*3	0.9970*3	0.9983*3	0.9969*3	0.9978*3	0.9985*3	0.9990*3	
		0.9709*3	0.9722*3	0.9738*3	0.9762*3	0.9977*3	0.9983*3	0.9987*3	0.9990*3	0.9986*3	0.9988*3	0.9990*3	0.9992*3	
	0.4	0.6506*3	0.6520*3	0.6561*3	0.6663*3	0.7119*3	0.7303*3	0.7587*3	0.8064*3	0.7539*3	0.7788*3	0.8134*3	0.8639*3	
		0.7524*3	0.7544*3	0.7598*3	0.7725*3	0.8680*3	0.8883*3	0.9133*3	0.9442*3	0.9097*3	0.9282*3	0.9485*3	0.9706*3	
		0.8356*3	0.8390*3	0.8432*3	0.8542*3	0.9475*3	0.9593*3	0.9718*3	0.9846*3	0.9695*3	0.9779*3	0.9860*3	0.9932*3	
	0.6	0.5462*3	0.5425*3	0.5404*3	0.5418*3	0.5636*3	0.5669*3	0.5766*3	0.6019*3	0.5793*3	0.5883*3	0.6068*3	0.6471*3	
		0.6135*3	0.6072*3	0.6037*3	0.6066*3	0.6774*3	0.6929*3	0.7211*3	0.7735*3	0.7210*3	0.7455*3	0.7826*3	0.8398*3	
		0.6849*3	0.6821*3	0.6792*3	0.6848*3	0.7995*3	0.8217*3	0.8534*3	0.8985*3	0.8490*3	0.8736*3	0.9039*3	0.9405*3	
	0.2	0.2491*1	0.2510*1	0.2334*1	0.2134*1	0.8570*3	0.8947*3	0.9332*3	0.9700*3	0.9407*3	0.9609*3	0.9793*3	0.9941*3	SPLIT GRAVITY
		0.1536*7	0.1383*7	0.1246*7	0.1108*7	0.9676*3	0.9870*3	0.9988*2	0.9872*2	0.9992*2	0.9925*2	0.9915*2	0.9953*2	
		0.6994*7	0.0962*7	0.0749*7	0.0645*7	0.9632*2	0.9704*2	0.9827*2	0.9952*2	0.9902*2	0.9947*2	0.9950*2	0.9993*3	
	0.4	0.4694*3	0.4582*3	0.4484*3	0.4383*3	0.5610*3	0.5800*3	0.6153*3	0.6829*3	0.6278*3	0.6602*3	0.7099*3	0.7875*3	
		0.4003*3	0.3779*3	0.3514*1	0.3183*1	0.7036*3	0.7456*3	0.8045*3	0.8788*3	0.8155*3	0.8550*3	0.8995*3	0.9474*3	
		0.3022*7	0.2658*7	0.2340*7	0.2045*7	0.8440*3	0.8820*3	0.9238*3	0.9564*3	0.9292*3	0.9528*3	0.9750*3	0.9931*3	
	0.6	0.4483*3	0.4600*3	0.4521*3	0.4445*3	0.4876*3	0.4872*3	0.4929*3	0.5137*3	0.5053*3	0.5115*3	0.5278*3	0.5677*3	
		0.4515*3	0.4331*3	0.4154*3	0.3976*3	0.5380*3	0.5512*3	0.5822*3	0.6494*3	0.6008*3	0.6294*3	0.6780*3	0.7594*3	
		0.4284*3	0.3995*3	0.3708*3	0.3614*7	0.6347*3	0.6671*3	0.7211*3	0.8058*3	0.7354*3	0.7765*3	0.8308*3	0.8989*3	

LIPPED Z-SECTION SIG=55.00

Q	F / B/t	0.00				0.15				0.30				TYPE OF LOADING
		1.00	0.80	0.60	0.40	1.00	0.80	0.60	0.40	1.00	0.80	0.60	0.40	
0.0	0.2	0.0896*6	0.0827*7	0.0728*7	0.0635*7	0.2412*6	0.2585*6	0.2822*6	0.3203*6	0.3152*6	0.3382*6	0.3678*6	0.4104*4	UNIFORM COMPRESSION
		0.0474*7	0.0414*7	0.0352*7	0.0296*7	0.2426*6	0.2609*6	0.2846*6	0.3218*6	0.3174*6	0.3404*6	0.3692*4	0.4091*4	
		0.0314*7	0.0267*7	0.0219*7	0.0176*7	0.2419*6	0.2602*6	0.2840*6	0.3221*6	0.3169*6	0.3399*4	0.3682*4	0.4091*4	
	0.4	0.2744*6	0.2551*6	0.2305*6	0.2064*6	0.3120*4	0.3097*4	0.3114*4	0.3254*4	0.3339*4	0.3368*4	0.3450*4	0.3642*4	
		0.1685*6	0.1540*7	0.1315*7	0.1116*7	0.2720*4	0.2785*4	0.2918*4	0.3178*4	0.3150*4	0.3250*4	0.3404*4	0.3650*4	
		0.1129*7	0.0967*7	0.0801*7	0.0657*7	0.2633*4	0.2741*4	0.2909*4	0.3187*4	0.3130*4	0.3249*4	0.3414*4	0.3660*4	
	0.6	0.3525*4	0.3411*4	0.3255*4	0.3100*4	0.3567*4	0.3475*4	0.3369*4	0.3317*4	0.3603*4	0.3528*4	0.3453*4	0.3451*4	
		0.2871*4	0.2651*6	0.2334*6	0.2036*6	0.3120*4	0.3032*4	0.2971*4	0.3034*4	0.3285*4	0.3246*4	0.3243*4	0.3348*4	
		0.2218*6	0.2005*7	0.1639*7	0.1333*7	0.2866*4	0.2829*4	0.2845*4	0.2992*4	0.3159*4	0.3169*4	0.3218*4	0.3360*4	
0.0	0.2	0.1475*1	0.1385*1	0.1265*1	0.1141*1	0.2813*1	0.2952*1	0.3137*1	0.3454*1	0.3479*3	0.3649*3	0.3883*3	0.4225*3	PLATE BENDING
		0.0787*7	0.0716*7	0.0636*7	0.0558*7	0.2608*1	0.2773*1	0.2985*1	0.3329*1	0.3321*1	0.3517*3	0.3773*3	0.4147*3	
		0.0490*7	0.0436*7	0.0378*7	0.0324*7	0.2520*1	0.2693*1	0.2918*1	0.3285*1	0.3252*1	0.3457*3	0.3729*3	0.4124*3	
	0.4	0.3301*3	0.3215*3	0.3101*3	0.2931*1	0.3480*3	0.3463*3	0.3472*3	0.3560*3	0.3606*3	0.3621*3	0.3674*3	0.3808*3	
		0.2370*1	0.2197*1	0.1987*1	0.1783*1	0.3062*3	0.3097*3	0.3182*3	0.3370*3	0.3362*3	0.3430*3	0.3543*3	0.3739*3	
		0.1677*7	0.1491*7	0.1290*7	0.1111*7	0.2871*3	0.2947*3	0.3074*3	0.3302*3	0.3268*3	0.3361*3	0.3497*3	0.3712*3	
	0.6	0.3562*3	0.3577*3	0.3468*3	0.3375*3	0.3687*3	0.3615*3	0.3532*3	0.3494*3	0.3710*3	0.3647*3	0.3583*3	0.3575*3	
		0.3221*3	0.3080*3	0.2900*3	0.2727*3	0.3364*3	0.3289*3	0.3225*3	0.3249*3	0.3465*3	0.3421*3	0.3398*3	0.3459*3	
		0.2764*3	0.2574*3	0.2296*1	0.2128*7	0.3127*3	0.3079*3	0.3063*3	0.3152*3	0.3326*3	0.3314*3	0.3331*3	0.3432*3	

LIPPED Z-SECTION . SIG=55.00

Q	P / B	0.00				0.15				0.30				TYPE OF LOADING
		1.00	0.80	0.60	0.40	1.00	0.80	0.60	0.40	1.00	0.80	0.60	0.40	
Q_L	0.2	0.9319*3	0.9366*3	C.9449*3	0.9192*5	0.9336*4	0.9365*4	0.9418*4	0.9460*4	0.9311*4	0.9345*4	0.9407*4	0.9475*4	BENDING
		0.9859*4	1.0236*4	-0.0012*8	0.9291*4	0.9658*4	0.9677*4	0.9710*4	0.9747*4	0.9656*4	0.9677*4	0.9712*4	0.9751*4	
		1.0487*4	0.9505*4	0.8227*7	0.8050*7	0.9795*4	0.9809*4	0.9830*4	0.9854*4	0.9798*4	0.9812*4	0.9834*4	0.9857*4	
	0.4	0.6967*3	0.6949*3	0.7115*3	0.7326*3	0.6981*3	0.7098*3	0.7312*3	0.7576*3	0.7049*3	0.7174*3	0.7388*3	0.7640*3	
		0.8163*3	0.8254*3	0.8393*3	0.8556*3	0.8326*3	0.8421*3	0.8570*3	0.8729*3	0.8361*3	0.8450*3	0.8589*3	0.8707*4	
		0.8421*3	0.8972*3	C.9066*3	0.9174*3	0.8998*3	0.9043*4	C.9109*4	0.9188*4	0.8972*4	0.9015*4	0.9092*4	0.9182*4	
	0.6	0.5374*3	0.5386*3	0.5447*3	C.5565*3	0.5405*3	0.5433*3	0.5527*3	0.5706*3	0.5432*3	0.5471*3	0.5586*3	C.5793*3	
		0.6491*3	0.6515*3	C.6626*3	0.6797*3	0.6600*3	0.6689*3	0.6883*3	0.7157*3	0.6673*3	0.6779*3	0.6983*3	0.7247*3	
		0.7495*3	C.7542*3	C.7667*3	0.7837*3	0.7656*3	0.7763*3	0.7949*3	0.8164*3	0.7717*3	0.7824*3	0.7999*3	0.8194*3	
Q_L	0.2	C.1901*1	0.1751*1	0.1573*1	0.1433*7	0.5513*3	0.5970*3	0.6611*3	0.7465*3	0.6872*3	0.7317*3	0.7879*3	0.8534*3	SHEAR
		C.1037*7	0.0913*7	0.0786*7	0.0673*7	0.0007*8	0.0009*8	0.0012*8	0.0019*8	0.7755*3	0.8159*3	0.0012*8	0.9424*3	
		0.0710*7	0.0597*7	0.0492*7	0.0402*7	0.8602*2	0.9019*2	0.9492*2	0.9871*4	0.9458*2	0.9698*2	0.9889*4	0.9825*3	
	0.4	C.3923*3	0.3794*3	0.3640*3	C.3447*1	0.4358*3	0.4390*3	0.4526*3	0.4981*3	0.4691*3	0.4813*3	0.5081*3	0.5587*3	
		C.3123*7	0.2790*7	C.2430*7	C.2113*7	0.4796*3	0.5020*3	0.5456*3	0.6199*3	0.5669*3	0.5992*3	0.6503*3	0.7209*3	
		C.2274*7	C.1781*7	0.1495*7	0.1252*7	0.5671*3	0.6031*3	C.6585*3	0.7366*3	0.6826*3	0.7196*3	0.7700*3	0.8315*3	
	0.6	0.4149*3	0.4044*3	0.3919*3	0.3811*3	0.4219*3	0.4148*3	0.4091*3	0.4124*3	0.4283*3	0.4240*3	0.4236*3	0.4360*3	
		C.3921*3	0.3709*3	0.3459*3	0.3221*3	0.4302*3	0.4256*3	0.4309*3	0.4602*3	0.4596*3	0.4645*3	0.4836*3	0.5286*3	
		C.3750*7	C.3215*7	0.2673*7	0.2223*7	0.4541*3	0.4701*3	0.4951*3	0.5530*3	0.5257*3	0.5446*3	0.5830*3	C.6468*3	

LIPPED Z-SECTION SIG=55.00

Q	b/h	F	0.00				0.15				0.30				TYPE OF LOADING
			1.00	0.80	0.60	0.40	1.00	0.80	0.60	0.40	1.00	0.80	0.60	0.40	
MAXIMUM	0.2		0.9273*3	0.9315*3	0.9390*3	0.9470*3	0.9634*3	0.9703*3	0.9790*3	0.9875*3	0.9761*3	0.9817*3	0.9881*3	0.9937*3	UNIFORM
			0.9666*3	0.9684*3	0.9716*3	0.9749*3	0.9910*3	0.9931*3	0.9954*3	0.9973*3	0.9949*3	0.9963*3	0.9975*3	0.9985*3	
			0.9791*3	0.9801*3	0.9818*3	0.9837*3	0.9964*3	0.9972*3	0.9980*3	0.9987*3	0.9978*3	0.9983*3	0.9987*3	0.9991*3	
	0.4		0.6993*3	0.7017*3	0.7126*3	0.7290*3	0.7354*3	0.7490*3	0.7768*3	0.8188*3	0.7630*3	0.7823*3	0.8164*3	0.8632*3	
			0.8154*3	0.8186*3	0.8301*3	0.8456*3	0.8765*3	0.8919*3	0.9157*3	0.9436*3	0.9061*3	0.9223*3	0.9440*3	0.9665*3	
			0.8993*3	0.8910*3	0.8994*3	0.9099*3	0.9460*3	0.9560*3	0.9689*3	0.9817*3	0.9640*3	0.9724*3	0.9820*3	0.9904*3	
	0.6		0.5772*3	0.5728*3	0.5721*3	0.5765*3	0.5877*3	0.5883*3	0.5970*3	0.6199*3	0.5975*3	0.6023*3	0.6185*3	0.6543*3	
			0.6699*3	0.6638*3	0.6655*3	0.6745*3	0.7060*3	0.7148*3	0.7400*3	0.7852*3	0.7334*3	0.7502*3	0.7849*3	0.8374*3	
			0.7589*3	0.7541*3	0.7589*3	0.7710*3	0.8167*3	0.8314*3	0.8602*3	0.8998*3	0.8492*3	0.8687*3	0.8992*3	0.9351*3	
	0.2		0.2053*7	0.1875*7	0.1647*1	0.1479*7	0.6817*3	0.7373*3	0.8071*3	0.8894*3	0.8391*3	0.8820*3	0.9295*3	0.9755*3	
			0.1075*7	0.0940*7	0.0804*7	0.0685*7	1.2293*2	0.0009*8	0.0012*8	0.9872*3	1.0670*2	0.9695*3	0.9472*2	0.9682*2	
			0.0732*7	0.0611*7	0.0500*7	0.0407*7	0.9752*2	0.9993*3	0.9890*3	0.8376*2	0.8318*2	3.7641*3	0.9514*2	0.9957*2	
	0.4		0.4325*3	0.4160*3	0.3966*3	0.3755*1	0.4991*3	0.5067*3	0.5311*3	0.5907*3	0.5530*3	0.5756*3	0.6225*3	0.7068*3	
			0.3304*7	0.2919*7	0.2520*7	0.2175*7	0.5811*3	0.6167*3	0.6815*3	0.7817*3	0.7061*3	0.7531*3	0.8195*3	0.8980*3	
			0.2190*7	0.1856*7	0.1541*7	0.1280*7	0.7025*3	0.7488*3	0.8137*3	0.8964*3	0.8396*3	0.8801*3	0.9288*3	0.9770*3	
	0.6		0.4584*3	0.4458*3	0.4305*3	0.4167*3	0.4710*3	0.4643*3	0.4606*3	0.4713*3	0.4829*3	0.4814*3	0.4876*3	0.5167*3	
			0.4343*3	0.4078*3	0.3773*3	0.3483*3	0.4925*3	0.4911*3	0.5063*3	0.5603*3	0.5396*3	0.5545*3	0.5940*3	0.6766*3	
			0.3930*7	0.3327*7	0.2736*7	0.2256*7	0.5501*3	0.5654*3	0.6098*3	0.7015*3	0.6415*3	0.6706*3	0.7395*3	0.8314*3	

```
PEKOZ,T                   ***START*** OS18 CJ5939  (1886) 71.348  09.35.10  JOB DEST = UPSON      PEKOZ,T
PEKOZ,T                   ***START*** OS18 CJ5939  (1886) 71.348  09.35.10  JOB DEST = UPSON      PEKOZ,T
PEKOZ,T                   ***START*** OS18 CJ5939  (1886) 71.348  09.35.10  JOB DEST = UPSON      PEKOZ,T
PEKOZ,T                   ***START*** OS18 CJ5939  (1886) 71.348  09.35.10  JOB DEST = UPSON      PEKOZ,T
PEKOZ,T                   ***START*** OS18 CJ5939  (1886) 71.348  09.35.10  JOB DEST = UPSON      PEKOZ,T
PEKOZ,T                   ***START*** OS18 CJ5939  (1886) 71.348  09.35.10  JOB DEST = UPSON      PEKOZ,T
PEKOZ,T                   ***START*** OS18 CJ5939  (1886) 71.348  09.35.10  JOB DEST = UPSON      PEKOZ,T
PEKOZ,T                   ***START*** OS18 CJ5939  (1886) 71.348  09.35.10  JOB DEST = UPSON      PEKOZ,T
PEKOZ,T                   ***START*** OS18 CJ5939  (1886) 71.348  09.35.10  JOB DEST = UPSON      PEKOZ,T
PEKOZ,T                   ***START*** OS18 CJ5939  (1886) 71.348  09.35.10  JOB DEST = UPSON      PEKOZ,T
PEKOZ,T                   ***START*** OS18 CJ5939  (1886) 71.348  09.35.10  JOB DEST = UPSON      PEKOZ,T
PEKOZ,T                   ***START*** OS18 CJ5939  (1886) 71.348  09.35.10  JOB DEST = UPSON      PEKOZ,T
PEKOZ,T                   ***START*** OS18 CJ5939  (1886) 71.348  09.35.10  JOB DEST = UPSON      PEKOZ,T
PEKOZ,T                   ***START*** OS18 CJ5939  (1886) 71.348  09.35.10  JOB DEST = UPSON      PEKOZ,T
PEKOZ,T                   ***START*** OS18 CJ5939  (1886) 71.348  09.35.10  JOB DEST = UPSON      PEKOZ,T
PEKOZ,T                   ***START*** OS18 CJ5939  (1886) 71.348  09.35.10  JOB DEST = UPSON      PEKOZ,T
PEKOZ,T                   ***START*** OS18 CJ5939  (1886) 71.348  09.35.10  JOB DEST = UPSON      PEKOZ,T
PEKOZ,T                   ***START*** OS18 CJ5939  (1886) 71.348  09.35.10  JOB DEST = UPSON      PEKOZ,T
PEKOZ,T                   ***START*** OS18 CJ5939  (1886) 71.348  09.35.10  JOB DEST = UPSON      PEKOZ,T
PEKOZ,T                   ***START*** OS18 CJ5939  (1886) 71.348  09.35.10  JOB DEST = UPSON      PEKOZ,T
```

```
PEKOZ,T          ***START*** OS18 CJ5939  (1886) 71.348  09.35.10  JOB DEST = UPSON        PEKOZ,T
PEKOZ,T          ***START*** OS18 CJ5939  (1886) 71.348  09.35.10  JOB DEST = UPSON        PEKOZ,T
PEKOZ,T          ***START*** OS18 CJ5939  (1886) 71.348  09.35.10  JOB DEST = UPSON        PEKOZ,T
PEKOZ,T          ***START*** OS18 CJ5939  (1886) 71.348  09.35.10  JOB DEST = UPSON        PEKOZ,T
PEKOZ,T          ***START*** OS18 CJ5939  (1886) 71.348  09.35.10  JOB DEST = UPSON        PEKOZ,T
PEKOZ,T          ***START*** OS18 CJ5939  (1886) 71.348  09.35.10  JOB DEST = UPSON        PEKOZ,T
PEKOZ,T          ***START*** OS18 CJ5939  (1886) 71.348  09.35.10  JOB DEST = UPSON        PEKOZ,T
PEKOZ,T          ***START*** OS18 CJ5939  (1886) 71.348  09.35.10  JOB DEST = UPSON        PEKOZ,T
PEKOZ,T          ***START*** OS18 CJ5939  (1886) 71.348  09.35.10  JOB DEST = UPSON        PEKOZ,T
PEKOZ,T          ***START*** OS18 CJ5939  (1886) 71.348  09.35.10  JOB DEST = UPSON        PEKOZ,T
PEKOZ,T          ***START*** OS18 CJ5939  (1886) 71.348  09.35.10  JOB DEST = UPSON        PEKOZ,T
PEKOZ,T          ***START*** OS18 CJ5939  (1886) 71.348  09.35.10  JOB DEST = UPSON        PEKOZ,T
PEKOZ,T          ***START*** OS18 CJ5939  (1886) 71.348  09.35.10  JOB DEST = UPSON        PEKOZ,T
PEKOZ,T          ***START*** OS18 CJ5939  (1886) 71.348  09.35.10  JOB DEST = UPSON        PEKOZ,T
PEKOZ,T          ***START*** OS18 CJ5939  (1886) 71.348  09.35.10  JOB DEST = UPSON        PEKOZ,T
PEKOZ,T          ***START*** OS18 CJ5939  (1886) 71.348  09.35.10  JOB DEST = UPSON        PEKOZ,T
PEKOZ,T          ***START*** OS18 CJ5939  (1886) 71.348  09.35.10  JOB DEST = UPSON        PEKOZ,T
PEKOZ,T          ***START*** OS18 CJ5939  (1886) 71.348  09.35.10  JOB DEST = UPSON        PEKOZ,T
PEKOZ,T          ***START*** OS18 CJ5939  (1886) 71.348  09.35.10  JOB DEST = UPSON        PEKOZ,T
PEKOZ,T          ***START*** OS18 CJ5939  (1886) 71.348  09.35.10  JOB DEST = UPSON        PEKOZ,T
```

```
JOB ORIGIN FROM REMOTE STP TERMINAL=XUPS
//CJ5939 JOB P4MZZZZ,'PEKOZ,T                '.PRTY=7,CLASS=L,REGION=135K  DEST=UPS
/*MAIN LINES=9
/*FORTG REGION=130K                                                    STMT0001
/*COPY TABL                                                            STMT0002
/*LINKFORT REGION=110K                                                 STMT0003
/*GOFORT TIME=6 REGION=65K                                             STMT0004
/*COPY DATH NOSEQ                                                      STMT0005
/*
```

CMS11 END OF CDS TABL REACHED ON STMT0002

JOB CJ5939 71.349 CLASS L PRIORITY 07 TIMES AND CHARGES (OCS RATES IN EFFECT AS OF 26 JULY 1971)

#	STEP NAME	TIME STAMP	JOB-STEP TIMES CPU-SEC	I/O SEC	SEC IN CORE	CHARGES AS RUN $-CPU	$-I/O	$-CORE	CHARGES- BEST CLASS $-CPU	$-I/O	I/O OPS	CORE USED
1	FORT	33950.42	23.69	26.82	50.51 @ 130K	.95	1.44	2.19	1.06	1.20 B	894	130K
2	LKED	33959.12	1.22	6.00	7.22 @ 110K	.04	.32	.30	.06	.24 A	200	10CK
CMS11 END OF CDS DATH REACHED ON STMT0005												
3	GO	34500.67	242.96	2.79	245.65 @ 60K	9.83	.15	9.33	9.83	.15 C	93	52K
	UNIT TOTALS:		267.77	35.61	303.38						1187	
	DOLLAR TOTALS:		$10.84	$1.92	$11.82							

DEDICATED DEVICE CHARGE: $.30 NO. OF DEVICES: 0
JOB TIME STAMP: 34501.22

BEST CLASS FOR JOB WOULD BE | C | CHARGE IN BEST CLASS WOULD BE | $24.58 | JOB EXECUTION CHARGE AS RUN | $24.58 |

ADDITIONAL CHARGES:
SETUP - $ .00

(ABOVE DOES NOT INCLUDE CHARGES FOR CARDS READ,CARDS PUNCHED, OR LINES PRINTED)

```
************************* * * N E W S   F L A S H * * *************************
*                                                                             *
* DECEMBER 3      ARCHIVE PACK 62 WILL EXPIRE ON WEDNESDAY, DECEMBER 22.      *
* DECEMBER 3   ARCHIVE PACK 53 WILL NOT EXPIRE UNTIL AFTER MONDAY, JANUARY 24. *
* NOVEMBER 29     JOBS REQUESTING MORE THAN 450K OF CORE WILL BE CANCELLED.   *
*                  SEE OCS MEMO AN-37 FOR MORE INFORMATION.                   *
*******************************************************************************
```

```
//CJ5939 JOB P4MZ135,'PEKOZ,T              ',                       *DEST=UPS
// MSGCLASS=A,PRTY=06,MSGLEVEL=(1,1)
//FORTG    EXEC FORTG,                                              * SIMJCL
// REGION=130K                                                        SIMJCL
[illegible]
**SYSPRINT DD UNIT=(CTC,,DEFER),LABEL=(1,NL),                       X0004000
**            DCB=(LRECL=120,RECFM=FBA,BUFNO=1,BLKSIZE=960)          00040000
**SYSPUNCH DD UNIT=(CTC,,DEFER),LABEL=(1,NL)                         00040000
[illegible] UNIT [illegible] (CYL,(2,1)),                            [illegible]
[illegible]
```

```
JOB ORIGIN FROM REMOTE STP TERMINAL=XUPS
//CJ5939 JOB P44ZZZZ,'PEKOZ,T              ',PRTY=7,CLASS=L,REGION=135K  DEST=UPS
/*MAIN LINES=9
/*FORTG REGION=130K                                                    STMT0001
/*COPY TABL                                                            STMT0002
/*LINKFORT REGION=110K                                                 STMT0003
/*GOFORT TIME=6 REGION=65K                                             STMT0004
/*COPY DATH NOSEQ                                                      STMT0005
/*
```

```
CMS11 END OF CDS TABL      REACHED ON STMT0002
      JOB CJ5939   71.348  CLASS L  PRIORITY   07          TIMES AND CHARGES (OCS RATES IN EFFECT AS OF 26 JULY 1971)
```

#	STEP NAME	TIME STAMP	JOB-STEP TIMES: CPU-SEC	I/O SEC	SEC IN CORE	CHARGES AS RUN: $-CPU	$-I/O	$-CORE	CHARGES- BEST CLASS: $-CPU	$-I/O	I/O OPS	CORE USED
1	FORT	33950.42	23.69	26.82	50.51 @ 130K	.95	1.44	2.19	1.06	1.20 B	894	130K
2	LKED	33989.12	1.22	6.00	7.22 @ 110K	.04	.32	.30	.06	.24 A	200	100K

```
CMS11 END OF CDS DATH      REACHED ON STMT0005
```

#	STEP NAME	TIME STAMP	CPU-SEC	I/O SEC	SEC IN CORE	$-CPU	$-I/O	$-CORE	$-CPU	$-I/O	I/O OPS	CORE USED
3	GO	34500.67	242.86	2.79	245.65 @ 60K	9.83	.15	9.33	9.83	.15 C	93	52K
	UNIT TOTALS:		267.77	35.61	303.38						1187	
	DOLLAR TOTALS:		$10.84	$1.92	$11.82							

```
      DEDICATED DEVICE CHARGE:    $.30      NO. OF DEVICES:   0
      JOB TIME STAMP:          34501.22

  BEST CLASS FOR JOB WOULD BE  | C |     CHARGE IN BEST CLASS WOULD BE  | $24.58 |     JOB EXECUTION CHARGE AS RUN  | $24.58 |

  ADDITIONAL CHARGES:
        SETUP - $      .00

                  (ABOVE DOES NOT INCLUDE CHARGES FOR CARDS READ,CARDS PUNCHED, OR LINES PRINTED)

                  ********************** * * N E W S  F L A S H  * * **********************
                  *                                                                      *
                  * DECEMBER 3      ARCHIVE PACK 62 WILL EXPIRE ON WEDNESDAY, DECEMBER 22.  *
                  * DECEMBER 3   ARCHIVE PACK 63 WILL NOT EXPIRE UNTIL AFTER MONDAY, JANUARY 24. *
                  * NOVEMBER 29     JOBS REQUESTING MORE THAN 450K OF CORE WILL BE CANCELLED.  *
                  *                  SEE OCS MEMO AN-37 FOR MORE INFORMATION.            *
                  ************************************************************************

//CJ5939 JOB P440135,'PEKOZ,T              ',                          *DEST=UPS
// MSGCLASS=A,PRTY=04,MSGLEVEL=(1,1)
//FO=TG    EXEC FORTG,                                                 *  SIMJCL
//  REGION=130K                                                          SIMJCL
XX*SYSPRINT DD   UNIT=(CTC,,DEFER),LABEL=(1,NL),                      X0004000
XX               DCB=(L=ECL=120,REC=M=FBA,BUFNO=1,BLKSIZE=960)
X*SYSPUNCH DD    UNIT=(CTC,,DEFER),LABEL=(1,NL)                       X0005000
XXSYSUT1 DD      UNIT=(CTC,,DEFER),LABEL=(1,SL),SPACE=(CYL,(2,1)),    X0006000
XX               DCB=(M,BLKSIZE=3200)                                 X0007000
```

```
IEF237I 451   ALLOCATED TO SYSPRINT
IEF237I 457   ALLOCATED TO SYSPUNCH
IEF237I 230   ALLOCATED TO SYSLIN
IEF237I 452   ALLOCATED TO SYSIN
IEF285I   SYS71348.T091429.RV000.CJ5939.R0000052        DELETED
IEF285I   VOL SER NOS= ASP451.
IEF285I   SYS71348.T091429.RV000.CJ5939.LOADSET         PASSED
IEF285I   VOL SER NOS= DSCRX2.
IEF285I   CJ5939.ASP01                                  DELETED
IEF285I   VOL SER NOS= 011886.
STEP RETURN CODE IS     0

//LKED    EXEC LINKFORT,                                    *  SIMJCL
//  REGION=110K                                               SIMJCL
XX        PROC  PROG=IEWLF880
XXLKED    EXEC  PGM=&PROG,PARM='MAP,LIST',COND=(4,LT)
IEF653I SUBSTITUTION JCL - PGM=IEWLF880,PARM='MAP,LIST',COND=(4,LT)
XXSYSPRINT DD  UNIT=(CTC,,DEFER),LABEL=(1,NL),
XX             DCB=(BUFNO=1,BLKSIZE=968)
XXSYSLIB   DD  DISP=SHR,DSN=SYS1.FORTLIB
XX         DD  DISP=SHR,DSN=SYS1.FORTAUX
XX         DD  DISP=SHR,DSN=SYS1.ADLIB
XXSYSLIN   DD  DSNAME=&LOADSET,DISP=(OLD,DELETE)
IEF653I SUBSTITUTION JCL - DSNAME=&LOADSET,DISP=(OLD,DELETE)
XX         DD  DDNAME=SYSIN
XXSYSUT1   DD  UNIT=SYSSC,SEP=SYSLIN,SPACE=(CYL,(2,1))
XXSYSLMOD  DD  UNIT=(SYSSC,,SEP=SYSLIN),SEP=SYSUT1,DSNAME=&GOSET(GO),    X00180000
IEF653I SUBSTITUTION JCL - UNIT=(SYSSC,,SEP=SYSLIN),SEP=SYSUT1,DSNAME=&GOSET(GO),
XX             DISP=(MOD,PASS),SPACE=(CYL,(2,1,1))
IEF236I ALLOC. FOR CJ5939   LKED    LKED
IEF237I 451   ALLOCATED TO SYSPRINT
IEF237I 140   ALLOCATED TO SYSLIB
IEF237I 140   ALLOCATED TO
IEF237I 140   ALLOCATED TO
IEF237I 230   ALLOCATED TO SYSLIN
IEF237I 130   ALLOCATED TO SYSUT1
IEF237I 231   ALLOCATED TO SYSLMOD
IEF285I   SYS71348.T091429.RV000.CJ5939.R0000054        DELETED
IEF285I   VOL SER NOS= ASP451.
IEF285I   SYS1.FORTLIB                                  KEPT
IEF285I   VOL SER NOS= DSYS71.
IEF285I   SYS1.FORTAUX                                  KEPT
IEF285I   VOL SER NOS= DSYS71.
IEF285I   SYS1.ADLIB                                    KEPT
IEF285I   VOL SER NOS= DSYS71.
IEF285I   SYS71348.T091429.RV000.CJ5939.LOADSET         DELETED
IEF285I   VOL SER NOS= DSCRX2.
IEF285I   SYS71348.T091429.RV000.CJ5939.R0000055        DELETED
IEF285I   VOL SER NOS= DSCRX1.
IEF285I   SYS71348.T091429.RV000.CJ5939.GOSET           PASSED
IEF285I   VOL SER NOS= DSCRZZ.
STEP RETURN CODE IS     0

//GO.FORT   EXEC GOFORT,                                  *  SIMJCL
//  TIME=5                                                  SIMJCL
XXGO      EXEC  PGM=*.LKED.LKED.SYSLMOD,COND=(4,LT)       00020000
XXFT05F001 DD   UNIT=(CTC,,DEFER),LABEL=(1,NL),DCB=(RECFM=F,BLKSIZE=80)  00040000
XXFT06F001 DD   UNIT=(CTC,,DEFER),LABEL=(1,NL),           X00060000
XX              DCB=(LRECL=133,BLKSIZE=1064,RECFM=FB,BUFNO=1)  00080000
XXFT05F001 DD   DDNAME=SYSIN                            00100000
//SYSIN DD UNIT=(CTC,,DEFER),DSNAME=CJ5939.ASP02,       *
//            VOL=SER=DSCRZZ,DCB=(LRECL=80,BLKSIZE=80,RECFM=F)
//
```

```
IEF237I 458   ALLOCATED TO FT06F001
IEF237I 459   ALLOCATED TO FT05F001
IEF285I   SYS71348.T091429.RV000.CJ5939.GOSET                    PASSED
IEF285I   VOL SER NOS= DSCRZZ.
IEF285I   SYS71348.T091429.RV000.CJ5939.R0000057                 DELETED
IEF285I   VOL SER NOS= ASP458.
IEF285I   CJ5939.ASP02                                           DELETED
IEF285I   VOL SER NOS= 021886.
STEP RETURN CODE IS    0

IEF285I   SYS71348.T091429.RV000.CJ5939.GOSET                    DELETED
IEF285I   VOL SER NOS= DSCRZZ.
ACCOUNT P4M  ACCOUNTING # E770080899     ACCT MGR CELERI NURI

                          TOTAL USAGE                          TOTAL USAGE
  TIME(SECONDS*100)          86550   TERMINAL TIME                      0
  LINES PRINTED              39437   CARDS PUNCHED                   1562
  ACCESSES                      57   CARDS FILED                     3102
  TOTAL CHARGE             $145.48   NON-EXECUTION CHARGE           $52.70
  CARDS READ                  3228
                             LIMITS
  MAX CARDS IN CDS'S          5000   PRIORITY LIMIT                     8
  TOTAL CHARGES             $200.00

   CUT-OFF DATE  72.181  CREATION DATE  68.043  LAST ALTERED  71.347

 CDS NAME  EDITION  CARDS   BLOCKS  ARCHIVE
 BEAM      00014    00609   00031   063
 DATA      00013    00019   00002   064
 HIRO      00003    00130   00007   051*
 EIGN      00007    00656   00026   051*
 COMB      00001    00029   00001   048*
 MASA      00003    00734   00028   063
 DATH      00002    00020   00002   064
 TABL      00001    00735   00028   064
* - ARCHIVE HAS EXPIRED

CURRENT ARCHIVE PACK IS 064
```

PEKOZ,T SYSPRINT • 0518 CJ5939 (1886) 71.348 09.35.25 JOB DEST = UPSON PEKOZ,T

```
      IMPLICIT REAL * 8 (A-H,O-Z)                                       TAB10001
      COMMON /CMT/ CMAT(6,6),DSP(6)                                     TAB10002
      DIMENSION UCR(2),WCR(2),VCN(2,7),NIY(7)                           TAB10003
      DIMENSION CC(3,3),DSM(6),STR(6),STE(6),PRM(6),                    TAB10004
     *          SG(6,2),WG(6,2),          W(6),SV(6),SU(6),WW(6),WK(6),TAB10005
     *DF1(6),DF(6),NPA(6),NL(6),                                        TAB10006
     *          Z(3),PCR(2),HLH(6),LLD(2,2),                            TAB10007
     *          HAY(27, 2,12),NAY(27, 2,12)                             TAB10008
      DIMENSION Z1(3),Z9(3),Z101(3),Z3(3,3),Z6(3,3),ZS(3,3),            TAB10009
     *          FO(3),F2(3),FE(3),SN(3)                                 TAB10010
C                                                                       TAB10011
C   JOB  ** >135<  **    >138 <  **                                     TAB10012
C                                                                       TAB10013
C   UCR(1),WCR(1)  ,    CURVATURE FROM  F2(N)  (MIDSPAN)                TAB10014
C   UCR(2),WCR(2)  ,    CURVATURE FROM  FE(N)  (SUPPORT)                TAB10015
C   IY=1           ,    YIELDING AT MIDSPAN                             TAB10016
C   IY=2           ,    YIELDING AT SUPPORT                             TAB10017
C   NIY(N8R)       ,    INITIALIZATION OF  IY. SEE  READ  AND  NO 4510  TAB10018
C   N8R=1,2,3      ,    HINGED,FLEXURALLY HINGED-FIXED,FIXED  RESPECTIVETAR10019
C   VCN(IY,N4R)    ,    CONSTANT FOR BENDING MOMENT                     TAB10020
C                                                                       TA910021
   99 FORMAT ( 8I10)                                                    TAB10022
   99 FORMAT (7F10.5 )                                                  TAB10023
  109 FORMAT ('1')                                                      TAB10024
  110 FORMAT (1X/    )                                                  TAB10025
  111 FORMAT (1X )                                                      TAB10026
  112 FORMAT (1X//  )                                                   TAB10027
  190 FORMAT (13,11F11.5 )                                              TAB10028
C                                                                       TAB10029
  191 FORMAT(30X,'CHANNEL  SECTION',3X,'IO=',I2, 3X,'SIG=',F5.2)        TA910030
  192 FORMAT(30X,'LIPPED CHANNEL SECTION'                               TAB10031
     *,3X,'IO=',I2, 3X,'SIG=',F5.2)                                     TAB10032
  193 FORMAT(30X,'Z-SECTION',3X,'IO=',I2,3X,'SIG=',F5.2)                TAB10033
  194 FORMAT(30X,'LIPPED Z-SECTION'                                     TAB10034
     *,3X,'IO=',I2,3X,'SIG=',F5.2)                                      TAB10035
C                                                                       TAB10036
  195 FORMAT (61X,'M/4BEAM'/)                                           TAB10037
  196 FORMAT (54X,'ANGLE  OF  ROTATION ' ,/     )                       TAB10038
  197 FORMAT (52X,'DOWNWARD LOADING' ,3X,'A/3=',F5.2  )                 TAB10039
  198 FORMAT(// 53X,'UPLIFT LOADING ',3X,'A/3=',F5.2  )                 TAB10040
  200 FORMAT ( 56X,'HINGE) END.')                                       TAB10041
C                                                                       TAB10042
  201 FORMAT (2X,'IO=',I2,' ,N4R=',I2,' ,NIC=',I2,' ,N=',I2,' , IY=',I2,TAB10043
     *,',N2=',I2,',I4=',I2,',',13X,'IOF=',I2,',L=',I2,',ISS=',I2,',IA=',TAB10044
     *I2,',IT=',I2,',NJ=',I2,',MP=',I2  )                               TAB10045
  205 FORMAT (1X,'SG  ',6F9.3,3X,6F9.3,'    NG'  )                      TAB10046
C                                                                       TAB10047
  211 FORMAT (6F15.7)                                                   TAB10048
  215 FORMAT (3F25.15)                                                  TA910049
  281 FORMAT (7F17.7 )                                                  TAB10050
C                                                                       TAB10051
  291 FORMAT (1X,'LENGTH',2X,'DEPTH',2X,'WIDTH',19X,'N2=',16X,'ANGLE OF TAB10052
     *ROTATION' / ,5( F6.1,4F13.4, 5X,F13.4 / ),/                       TAB10053
     *          25X,     'SHEAR RIGIDITY G',47X,'LATERAL DISPLACEMENT U'/TAB10054
     *    5( F6.1,4F13.4, 5X,F13.4 )./                                  TAB10055
     *  23X,'SLOPE UPON AT SUPPORT'    ,44X,'VERTICAL DISPLACEMENT V' /  TAB10056
     *    5( F6.1,4F13.4, 5X,F13.4 )./     )                          TAB10057
                                                                        TAB10058
```

```
0001          IMPLICIT REAL * 8 (A-H,O-Z)                                      TAB10001
0002             COMMON /CMT/ CMAT(6,6),DSP(6)                                 TAB10002
0003             DIMENSION UCR(2),WCR(2),VCN(2,7),NIY(7)                       TAB10003
0004             DIMENSION CC(3,3),DSM(6),STR(6),STE(6),PRM(6),                TAB10004
                *       SG(6,2),WG(6,2),          W(6),SV(6),SU(6),WW(6),WK(6),TAB10005
                *DF1(6),DF(6),NPA(6),NL(6),                                   TAB10006
                *       Z(3),PCR(2),HLH(6),LLD(2,2),                          TAB10007
                *       HAY(27, 2,12),NAY(27, 2,12)                           TAB10008
0005             DIMENSION Z1(3),Z9(3),Z101(3),Z3(3,3),Z6(3,3),ZS(3,3),        TAB10009
                *       F0(3),F2(3),FE(3),SN(3)                               TAB10010
                C                                                             TAB10011
                C   J03  ** >135<  **    >138 <  **                           TAB10012
                C                                                             TAB10013
                C   UCR(1),WCR(1)  ,    CURVATURE FROM  F2(N)  (MIDSPAN)     TAB10014
                C   UCR(2),WCR(2)  ,    CURVATURE FROM  FE(N)  (SUPPORT)     TAB10015
                C   IY=1           ,    YIELDING AT MIDSPAN                  TAB10016
                C   IY=2           ,    YIELDING AT SUPPORT                  TAB10017
                C   NIY(NBR)       ,    INITIALIZATION OF  IY. SEE  READ  AND  NO 4510  TAB10018
                C   NBR=1,2,3      ,    HINGED,FLEXURALLY HINGED-FIXED,FIXED  RESPECTIVETAB10019
                C   VCN(IY,NBR)    ,    CONSTANT FOR BENDING MOMENT          TAB10020
                C                                                             TAB10021
0006            98 FORMAT ( 8I10)                                             TAB10022
0007            99 FORMAT (7F10.5 )                                           TAB10023
0008           109 FORMAT ('1')                                               TAB10024
0009           110 FORMAT (1X/     )                                          TAB10025
0010           111 FORMAT (1X )                                               TAB10026
0011           112 FORMAT (1X//  )                                            TAB10027
0012           190 FORMAT (I3,11F11.5 )                                       TAB10028
                C                                                             TAB10029
0013           191 FORMAT(30X,'CHANNEL  SECTION',3X,'ID=',I2, 3X,'SIG=',F5.2) TAB10030
0014           192 FORMAT(30X,'LIPPED CHANNEL SECTION'                        TAB10031
                  *,3X,'ID=',I2, 3X,'SIG=',F5.2)                              TAB10032
0015           193 FORMAT(30X,'Z-SECTION',3X,'ID=',I2,3X,'SIG=',F5.2)         TAB10033
0016           194 FORMAT(30X,'LIPPED Z-SECTION'                              TAB10034
                  *,3X,'ID=',I2,3X,'SIG=',F5.2)                               TAB10035
                C                                                             TAB10036
0017           195 FORMAT (61X,'M/MBEND'/)                                    TAB10037
0018           196 FORMAT (54X,'ANGLE  OF  ROTATION ' ,/     )                TAB10038
0019           197 FORMAT (52X,'DOWNWARD LOADING' ,3X,'A/3=',F5.2  )          TAB10039
0020           198 FORMAT(// 53X,'UPLIFT LOADING ',3X,'A/3=',F5.2  )          TAB10040
0021           200 FORMAT ( 56X,'HINGED BND.')                                TAB10041
                C                                                             TAB10042
0022           201 FORMAT (2X,'ID=',I2,' ,NR=',I2,' ,NIC=',I2,' ,N=',I2,' , IY=',I2,TAB10043
                  *',NP2=',I2,',I4=',I2,',',13X,'IDE=',I2,',L=',I2,',ISS=',I2,',IA=',TAB10044
                  *I2,',IT=',I2,',MJ=',I2,',MP=',I2  )                        TAB10045
0023           205 FORMAT (1X,'SG  ',6F9.3,3X,6F9.3,'     SG'  )              TAB10046
                C                                                             TAB10047
0024           211 FORMAT (6F15.7)                                            TAB10048
0025           214 FORMAT (3F25.15 )                                          TAB10049
0026           251 FORMAT (7F17.7 )                                           TAB10050
                C                                                             TAB10051
0027           291 FORMAT (1X,'LENGTH',2X,'PENDU.,  MOMENT',19X,'AM2=',16X,'ANGLE OF TAB10052
                  *F/F0 RATI' /  , 5( F6.1,4F13.4, 5X,4F13.4 / ),/            TAB10053
                  *       25X,     'SLOPE',19X,'DEFLECTION',47X,'LATERAL DISPLACEMENT U'// TAB10054
                  *    5( F6.1,4F13.4, 5X,4F13.4 /),/                         TAB10055
                  *  23X,'SLOPE DRAW AT SUPPORT'    ,44X,'VERTICAL DISPLACEMENT V' /  TAB10056
                  *    5( F6.1,4F13.4, 5X,4F13.4 /),/     )                   TAB10057
                C                                                             TAB10058
```

```
0001                IMPLICIT REAL * 8 (A-H,O-Z)                                    TAB10001
0002                COMMON /CMT/ CMAT(6,6),DSP(6)                                  TAB10002
0003                DIMENSION UCR(2),WCR(2),VCN(2,7),NIY(7)                        TAB10003
0004                DIMENSION CC(3,3),DSM(6),STR(6),STE(6),PRM(6),                 TAB10004
                   *        SG(6,2),WG(6,2),          W(6),SV(6),SU(6),WW(6),WK(6),  TAB10005
                   *DF1(6),DF(6),NPA(6),NL(6),                                    TAB10006
                   *        Z(3),PCR(2),HLH(6),LLD(2,2),                          TAB10007
                   *        HAY(27, 2,12),NAY(27, 2,12)                           TAB10008
0005                DIMENSION Z1(3),Z9(3),Z101(3),Z3(3,3),Z6(3,3),ZS(3,3),         TAB10009
                   *        FO(3),F2(3),FE(3),SN(3)                               TAB10010
                C                                                                  TAB10011
                C  JOB  ** >135<  **    >138 <  **                                 TAB10012
                C                                                                  TAB10013
                C  UCR(1),WCR(1)  ,    CURVATURE FROM  F2(N)  (MIDSPAN)            TAB10014
                C  UCR(2),WCR(2)  ,    CURVATURE FROM  FE(N)  (SUPPORT)            TAB10015
                C  IY=1           ,    YIELDING AT MIDSPAN                         TAB10016
                C  IY=2           ,    YIELDING AT SUPPORT                         TAB10017
                C  NIY(NBR)       ,    INITIALIZATION OF  IY. SEE  READ  AND  NO 4510  TAB10018
                C  NBR=1,2,3      ,    HINGED,FLEXURALLY HINGED-FIXED,FIXED  RESPECTIVETAB10019
                C  VCN(IY,N+R)    ,    CONSTANT FOR BENDING MOMENT                 TAB10020
                C                                                                  TAB10021
0006                98 FORMAT ( 8I10)                                              TAB10022
0007                99 FORMAT (7F10.5 )                                            TAB10023
0008               109 FORMAT ('1')                                                TAB10024
0009               110 FORMAT (1X/    )                                            TAB10025
0010               111 FORMAT (1X )                                                TAB10026
0011               112 FORMAT (1X//  )                                             TAB10027
0012               190 FORMAT (I3,11F11.5 )                                        TAB10028
                C                                                                  TAB10029
0013               191 FORMAT(30X,'CHANNEL  SECTION',3X,'IO=',I2, 3X,'SIG=',F5.2)  TAB10030
0014               192 FORMAT(30X,'LIPPED CHANNEL SECTION'                         TAB10031
                     *,3X,'IO=',I2, 3X,'SIG=',F5.2)                                TAB10032
0015               193 FORMAT(30X,'Z-SECTION',3X,'IO=',I2,3X,'SIG=',F5.2)          TAB10033
0016               194 FORMAT(30X,'LIPPED Z-SECTION'                               TAB10034
                     *,3X,'IO=',I2,3X,'SIG=',F5.2)                                 TAB10035
                C                                                                  TAB10036
0017               195 FORMAT (61X,'M/4SEC')')                                     TAB10037
0018               196 FORMAT (54X,'ANGLE OF  ROTATION ' ,/    )                   TAB10038
0019               197 FORMAT (52X,'DOWNWARD LOADING' ,3X,'A/3=',F5.2  )           TAB10039
0020               198 FORMAT(// 53X,'UPLIFT LOADING ',3X,'A/3=',F5.2  )           TAB10040
0021               200 FORMAT ( 56X,'HINGED END.')                                 TAB10041
                C                                                                  TAB10042
0022               201 FORMAT (2X,'IO=',I2,' ,N+R=',I2,' ,NIC=',I2,' ,N=',I2,' , IY=',I2,TAB10043
                     *','M2=',I2,',I4=',I2,',',13X,'IDF=',I2,',L=',I2,',ISS=',I2,',IA=',TAB10044
                     *I2,',IT=',I2,',M4=',I2,',MP=',I2  )                          TAB10045
0023               205 FORMAT (1X,'SG  ',6F9.3,3X,6F9.3,'    +G'  )                TAB10046
                C                                                                  TAB10047
0024               211 FORMAT (6F15.7)                                             TAB10048
0025               214 FORMAT (6E15.14 )                                           TAB10049
0026               251 FORMAT (7I17.7 )                                            TAB10050
                C                                                                  TAB10051
0027               291 FORMAT (1X,'LENGTH',2X,'RESIDUAL MOMENT',19X,'M*2=',15X,'ANGLE OF TAB10052
                     *F/D= ',I1,' /  , 5( F6.1,4F13.4, 3X,4F13.4 / ),/              TAB10053
                     *        25X,     'SHEAR RIGIDITY G',47X,'LATERAL DISPLACEMENT U'/ TAB10054
                     *    5( F6.1,4F13.4, 3X,4F13.4 /),/                            TAB10055
                     *  23X,'SLOPE UPON AT SUPPORT' ,44X,'VERTICAL DISPLACEMENT V' /  TAB10056
                     *    5( F6.1,4F13.4, 3X,4F13.4 /),/    )                       TAB10057
                C                                                                  TAB10058
```

```
      IMPLICIT REAL * 8 (A-H,O-Z)                                       TAB10001
      COMMON /CMT/ CMAT(6,6),DSP(6)                                     TAB10002
      DIMENSION UCR(2),WCR(2),VCN(2,7),NIY(7)                           TAB10003
      DIMENSION CC(3,3),DSM(6),STR(6),STE(6),PRM(6),                    TAB10004
     *     SG(6,2),WG(6,2),          W(6),SV(6),SU(6),WW(6),WK(6),      TAB10005
     *DF1(6),DF(6),NPA(6),NL(6),                                        TAB10006
     *     Z(3),PCR(2),HLH(6),LLD(2,2),                                 TAB10007
     *     HAY(27, 2,12),NAY(27, 2,12)                                  TAB10008
      DIMENSION Z1(3),Z9(3),Z101(3),Z3(3,3),Z6(3,3),ZS(3,3),            TAB10009
     *     FO(3),F2(3),FE(3),SN(3)                                      TAB10010
C                                                                       TAB10011
C   JOB  ** >135<  **    >138 <  **                                     TAB10012
C                                                                       TAB10013
C   UCR(1),WCR(1)  ,    CURVATURE FROM  F2(N)  (MIDSPAN)                TAB10014
C   UCR(2),WCR(2)  ,    CURVATURE FROM  FE(N)  (SUPPORT)                TAB10015
C   IY=1           ,    YIELDING AT MIDSPAN                             TAB10016
C   IY=2           ,    YIELDING AT SUPPORT                             TAB10017
C   NIY(NBR)       ,    INITIALIZATION OF  IY. SEE  READ  AND  NO 4510  TAB10018
C   NBR=1,2,3      ,    HINGED,FLEXURALLY HINGED-FIXED,FIXED  RESPECTIVETAB10019
C   VCN(IY,NBR)    ,    CONSTANT FOR BENDING MOMENT                     TAB10020
C                                                                       TAB10021
   98 FORMAT ( 8I10)                                                    TAB10022
   99 FORMAT (7F10.5 )                                                  TAB10023
  109 FORMAT ('1')                                                      TAB10024
  110 FORMAT (1X/    )                                                  TAB10025
  111 FORMAT (1X )                                                      TAB10026
  112 FORMAT (1X//  )                                                   TAB10027
  190 FORMAT (I3,11F11.5 )                                              TAB10028
C                                                                       TAB10029
  191 FORMAT(30X,'CHANNEL  SECTION',3X,'IO=',I2, 3X,'SIG=',F5.2)        TAB10030
  192 FORMAT(30X,'LIPPED CHANNEL SECTION'                               TAB10031
     *,3X,'I2=',I2, 3X,'SIG=',F5.2)                                     TAB10032
  193 FORMAT(30X,'Z-SECTION',3X,'IO=',I2,3X,'SIG=',F5.2)                TAB10033
  194 FORMAT(30X,'LIPPED Z-SECTION'                                     TAB10034
     *,3X,'IO=',I2,3X,'SIG=',F5.2)                                      TAB10035
C                                                                       TAB10036
  195 FORMAT (61X,'M/4BD'/)                                             TAB10037
  196 FORMAT (54X,'ANGLE  OF  ROTATION ' ,/    )                        TAB10038
  197 FORMAT (52X,'DOWNWARD LOADING' ,3X,'A/B=',F5.2  )                 TAB10039
  198 FORMAT(// 53X,'UPLIFT LOADING ',3X,'A/B=',F5.2  )                 TAB10040
  200 FORMAT ( 56X,'HINGED BND.')                                       TAB10041
C                                                                       TAB10042
  201 FORMAT (2X,'IO=',I2,' ,NR=',I2,' ,NIC=',I2,' ,N=',I2,' , IY=',I2,TAB10043
     *',NP=',I2,',IH=',I2,',',13X,'IDF=',I2,',L=',I2,',ISS=',I2,',IA=',TAB10044
     *I2,',IT=',I2,',NU=',I2,',MP=',I2  )                               TAB10045
  205 FORMAT (1X,'SG  ',5F9.3,3X,5F9.3,'    NG'  )                      TAB10046
C                                                                       TAB10047
  211 FORMAT (6F15.7)                                                   TAB10048
  219 FORMAT (3F25.15 )                                                 TAB10049
  251 FORMAT (7F17.7 )                                                  TAB10050
C                                                                       TAB10051
  291 FORMAT (1X,'LENGTH',2X,'DEPTH',2X,'WIDTH',19X,'NU2=',16X,'ANGLE OF TAB10052
     *F',I2,' /  ', 5( F6.1,4F13.4, 3X,4F13.4 / ),/                     TAB10053
     *        25X,     'SHEAR STIFFNESS G',4X,'LATERAL DISPLACEMENT U' TAB10054
     *    5( F6.1,4F13.4, 3X,4F13.4 /),/                                 TAB10055
     *  23X,'SLOPE UPON AT SUPPORT'   ,44X,'VERTICAL DISPLACEMENT V' /   TAB10056
     *    5( F6.1,4F13.4, 3X,4F13.4 /),/     )                         TAB10057
C                                                                       TAB10058
```

```
0028          294 FORMAT (1X,2(4F10.4,5X),4F10.4)                                    TAB10059
0029          295 FORMAT ( 3X, 4(F8.4,'*',I1),5X,4(F8.4,'*',I1),5X,4(F8.4,'*',I1)) TAB10060
0030          296 FORMAT(I3,          4(F8.4,'*',I1),5X,4(F8.4,'*',I1),5X,          TAB10061
                 *                                  4(F8.4,'*',I1) )              TAB10062
              C                                                                     TAB10063
              C                                                                     TAB10064
              C                                                                     TAB10065
              CC  INPUT, WHICH IS SAME FOR ALL CASES.                               TAB10066
0031            READ 98,NIY(1),NIY(2),NIY(3)                                        TAB10067
0032            READ 99,VCN(1,1),VCN(2,1),VCN(1,2),VCN(2,2),VCN(1,3),VCN(2,3)       TAB10068
0033            READ 211, E,G,PI,PI2                                                TAB10069
              C                                                                     TAB10070
              C   INPUT, CONCERNING THE DEFINITE INTEGRALS DUE TO GALERKINS METHOD. TAB10071
              C         CHANGES WITH BOUNDARY CONDITION.                          TAB10072
0034            N1=1                                                                TAB10073
0035            N2=3                                                                TAB10074
0036            READ  219,(SN(I),I=N1,N2)                                           TAB10075
0037            READ  219,(FO(I),I=N1,N2)                                           TAB10076
0038            READ  219,(F2(I),I=N1,N2)                                           TAB10077
0039            READ  219,(FE(I),I=N1,N2)                                           TAB10078
0040            READ  219,(Z10(I),I=N1,N2)                                          TAB10079
0041            READ  219,(Z9(I),I=N1,N2)                                           TAB10080
0042            READ  219,(Z1(I),I=N1,N2)                                           TAB10081
0043            READ 219,((Z3(I,J),J=1,3),I=N1,N2)                                  TAB10082
0044            READ 219,((Z6(I,J),J=1,3),I=N1,N2)                                  TAB10083
0045            READ 219,((Z5(I,J),J=1,3),I=N1,N2)                                  TAB10084
              C                                                                     TAB10085
              CC  INPUT, WHICH CHANGES FROM CASE TO CASE.                           TAB10086
0046            READ  98, NPRB, NNRB, NNIC, NOF, IOM, IHM, NMCS, MM2                TAB10087
              C                                                                     TAB10088
              C          NPRB :    NUMBER OF CROSS-SECTIONS                       TAB10089
              C          NNRB :    NUMBER OF BOUNDARY CONDITIONS  (NOT INCLUDED IN TAB10090
              C                    THE PRESENT FORM).                             TAB10091
              C          NNIC :    NUMBER OF CASES CONCERNING  IC  AND  HA        TAB10092
              C          NOF :     NUMBER OF ROTATIONAL RESTRAINTS CONSIDERED     TAB10093
              C          IOM :     NUMBER OF SHEAR RIGIDITIES CONSIDERED.         TAB10094
              C          IHM :     NUMBER OF SPAN LENGTHS CONSIDERED.             TAB10095
              C          NMCS :    NUMBER OF CASES WITH DIFFERENT  MM2            TAB10096
              C          MM2 :     TOTAL NUMBER OF SERIES TERMS. ( IN THE PRESENT TAB10097
              C          FORM, WHERE THERE IS A DO LOOP WITH  NMCS DEFINING  MM2, TAB10098
              C          INCLUSION OF  MM2 IN THE INPUT IS SUPERFLUS).           TAB10099
              C                                                                  TAB10100
              C          SIG :     YIELD STRESS                                  TAB10101
              C          ACCRCT :  ACCURACY OF LINEAR INTERPOLATION PROCEDURE USED TAB10102
              C                    IN DETERMINING THE FAILURE LOAD, PROVIDED THAT TAB10103
              C                    THE NUMBER OF ITERATIONS ARE LESS THAN 10.     TAB10104
              C                                                                  TAB10105
              C                                                                  TAB10106
              C                                                                  TAB10107
              CC  PRINTING OF SOME OF THE INPUT PARAMETERS                       TAB10108
0047            PRINT 98, NPRB, NNRB, NNIC, NOF, IOM, IHM, NMCS, MM2             TAB10109
              C                                                                  TAB10110
0048            ACCRCT = 0.00000010+00                                           TAB10111
0049            A = 8.0D+00                                                      TAB10112
              C                                                                  TAB10113
              C                                                                  TAB10114
0050              DO  11   ISIG = 1,2                                            TAB10115
              C   ..  ..   ....   ...                                            TAB10116
```



```
              C                                                                  TAB10117
0051            SIG = 33.0+00                                                    TAB10118
0052            IF  (ISIG.EQ.2)  SIG = 55.00+00                                  TAB10119
              C                                                                  TAB10120
```

```
                C                                                                       TAB10117
0051                  SIG = 33.D+00                                                     TAB10118
0052                  IF  (ISIG.EQ.2)  SIG = 55.0D+00                                   TAB10119
                C                                                                       TAB10120
                C                                                                       TAB10121
0053                       DO   12  ISEC = 2,4,2                                        TAB10122
                C          ..   ..  .... . .....                                        TAB10123
                C                                                                       TAB10124
                C                                                                       TAB10125
                C                                                                       TAB10126
                CC  INPUT, THE CROSS-SECTION DIMENSIONS, TYPE, AND THE INDICES OF THE   TAB10127
                C          "EDGE" CORNERS, WHERE :                                      TAB10128
                C                    ISEC=1  FOR CHANNEL                                TAB10129
                C                    ISEC=2  FOR L. CHANNEL                             TAB10130
                C                    ISEC=3  FOR Z-SECTION                              TAB10131
                C                    ISEC=4  FOR L. Z-SECTION                           TAB10132
0054                  GO TO (4005,4006,4005,4006),ISEC                                  TAB10133
0055             4005 LSA = 2                                                           TAB10134
0056                  LSB = 5                                                           TAB10135
0057                  GO TO 4007                                                        TAB10136
0058             4006 LSA = 1                                                           TAB10137
0059                  LSB = 6                                                           TAB10138
0060             4007 CONTINUE                                                          TAB10139
                C                                                                       TAB10140
                C                                                                       TAB10141
0061                       DO   13   IB = 1,3                                           TAB10142
                C          ..   ..   ..   ...                                           TAB10143
                C                                                                       TAB10144
0062                  BOA = IB                                                          TAB10145
0063                  BOA = BOA*2.D-01                                                  TAB10146
0064                  B = A*BOA                                                         TAB10147
                C                                                                       TAB10148
                C                                                                       TAB10149
0065                       DO   14   IFACT = 1,4                                        TAB10150
                C          ..   ..   .....   ...                                        TAB10151
                C                                                                       TAB10152
0066                  FACTOR = IFACT                                                    TAB10153
0067                  FACTOR = (6.D+00 -FACTOR)*.2D+00                                  TAB10154
0068                  T = ( (B*DSQRT(SIG))/171.D+00)*FACTOR                             TAB10155
0069                  C = 2.8D+00*T*((18/T)**2 - 400C.D+00/SIG)**(1./6.)                TAB10156
0070                  CMIN = 4.*B+00*T                                                  TAB10157
0071                  IF  (C.LT.CMIN)  C= CMIN                                          TAB10158
0072                  CMAX=(68.3D+00/DSQRT(SIG))*T                                      TAB10159
0073                  IF  (C.GT.CMAX)  C= CMAX                                          TAB10160
0074                     BOA=B/A                                                        TAB10161
0075                     COB=C/B                                                        TAB10162
0076                     BOT=B/T                                                        TAB10163
0077                     COT=C/T                                                        TAB10164
0078                  HE=(A+T)/2.                                                       TAB10165
0079                  AA=(A+2.*B+2.*C)                                                  TAB10166
0080                  APEA=AA*T                                                         TAB10167
0081                  TU=  (AA*T**3)/3.                                                 TAB10168
0082                  XI=T*(B**3/12.+B*A**2/2.+C**3/6.0+C*(A-C)**2/2.)                  TAB10169
0083                  GO TO (4111,4111,4113,4113),ISEC                                  TAB10170
0084             4111 YI=B*B*T*(2.*A*B+B*B+2.*C*(2.*B+3.*A))/(3.*AA)                    TAB10171
0085                  XY=0.0                                                            TAB10172
0086                  HA=T*0*(6.*T*T+4.*A+2.*B*A*A-B.*C**3)/(12.*XI)                    TAB10173
0087                  C=T*B*A*((1./3.+A)*HA**2+(B+C-HA)*(-1.+HA)**2+2.*C*((-B+HA-2.*(B+HTAB10174
```

```
                *A)*C/A)*(-B+HA-(B+HA)*C/A)))/6.                                  TAB10175
0088            XBAR=-  B*(B+2.*C)/AA                                             TAB10176
0089            XO=XBAR-HA                                                        TAB10177
0090            W(1)=-0.5*A*(B-HA)-(HA+B)*C                                       TAB10178
0091            W(2)=-0.5*A*(B-HA)                                                TAB10179
0092            W(3)= 0.5*A*HA                                                    TAB10180
0093            W(4)=-W(3)                                                        TAB10181
0094            W(5)=-W(2)                                                        TAB10182
0095            W(6)=-W(1)                                                        TAB10183
0096            SU(1)=B+XBAR+0.5*T*(ISEC-1)                                       TAB10184
0097            SU(2)=SU(1)                                                       TAB10185
0098            SU(3)=XBAR-T/2.                                                   TAB10186
0099            SU(4)=XBAR-T/2.                                                   TAB10187
0100            SU(5)=SU(1)                                                       TAB10188
0101            SU(6)=SU(1)                                                       TAB10189
0102            GO TO 4115                                                        TAB10190
0103      4113  YI=2.*T*B**2*(B/3.+C)                                             TAB10191
0104            XY=-T*B*(B*A/2.+C*(A-C))                                          TAB10192
0105            CW= T*B*B*(2.*B*A**3 +8*A*B*A +2.*C*A*A*(3.*A+2.*B) +12.*A*C*C*(A+TAB10193
                *B) +8.*C**3*(A+2.*B) +4.*C**4) /(12.*AA)                         TAB10194
0106            XBAR=0.0                                                          TAB10195
0107            XO=0.0                                                            TAB10196
0108            HA=C.0                                                            TAB10197
0109            SU(1)=-B-0.5*T*(ISEC-3)                                           TAB10198
0110            SU(2)=SU(1)                                                       TAB10199
0111            SU(3)=0.0                                                         TAB10200
0112            SU(4)=0.0                                                         TAB10201
0113            SU(5)=-SU(1)                                                      TAB10202
0114            SU(6)=-SU(1)                                                      TAB10203
0115            W(3)=-B*(B*A/2.+C*(A+C))/AA                                       TAB10204
0116            W(2)=W(3)+B*A/2.                                                  TAB10205
0117            W(1)=W(2)+H*C                                                     TAB10206
0118            W(6)=W(1)                                                         TAB10207
0119            W(5)=W(2)                                                         TAB10208
0120            W(4)=W(3)                                                         TAB10209
0121      4115  SV(1)=A/2.-C                                                      TAB10210
0122            SV(2)= HE                                                         TAB10211
0123            SV(3)= HE                                                         TAB10212
0124            SV(4)=-HE                                                         TAB10213
0125            SV(5)=-HE                                                         TAB10214
0126            SV(6)=-A/2.+C                                                     TAB10215
0127            HAA=HA                                                            TAB10216
          C           HAA = HA  :  THE DISTANCE OF WEB FROM THE SHEAR CENTER.     TAB10217
          C                        HA  WILL BE LATER REDEFINED AS THE HORIZONTAL  TAB10218
          C                        DISTANCE OF LOAD FROM SHEAR CENTER.           TAB10219
0128            HS = HE                                                           TAB10220
          C           HS :      THE VERTICAL DISTANCE OF THE LOAD FROM  S.C.     TAB10221
          C                     IN THE PRESENT FORM  HS = HE  .                   TAB10222
          C           HE        DISTANCE OF THE DIAPHRAGM FROM S.C.               TAB10223
0129            CWW=CW*(XI*YI-XY*XY)*HE*HE/XI                                     TAB10224
0130            ALAM=(HA*XI+HE*XY)/CWW                                            TAB10225
0131            DO 4120 I=1,6                                                     TAB10226
0132            WW(I)=XY*HE*SV(I)/XI-HE*SU(I)+W(I)                                TAB10227
0133      4120  WX(I)=ALAM*WW(I)/SV(I)                                           TAB10228
0134            NBR = 1                                                           TAB10229
          C                                                                       TAB10230
          C                                                                       TAB10231
          C---->  DO LOOP FOR THE # OF CASES CONCERNING  IC  AND  HA              TAB10232
```



```
0135            DO  3  NIC = 1, NNIC                                              TAB10233
          C                                                                       TAB10234
0136            HAOB = 0.0                                                        TAB10235
0137            HA = HAA                                                          TAB10236
```

```
0135                DO  3  NIC = 1, NNIC                                    TAB10233
                C                                                           TAB10234
0136            HAOB = 0.0                                                  TAB10235
0137            HA = HAA                                                    TAB10236
0138            GO TO (491,492),NIC                                         TAB10237
0139        491 IC=1                                                        TAB10238
0140            GO TO 497                                                   TAB10239
0141        492 IC=2                                                        TAB10240
0142            GO TO ( 493, 493, 494, 494), ISEC                           TAB10241
0143        493 HAOB = .5                                                   TAB10242
0144            HA = HAA + B/2.D 00                                         TAB10243
0145        494 CONTINUE                                                    TAB10244
0146        497 CONTINUE                                                    TAB10245
            C                                                               TAB10246
            C---->    DO LOOP  FOR  F                                       TAB10247
0147                  DO  5  IQF = 1, NQF                                   TAB10248
0148            F = .15*(IQF-1)                                             TAB10249
            C                                                               TAB10250
            C                                                               TAB10251
            C---->    DO LOOP  FOR  Q                                       TAB10252
0149                  DO  6   IQ = 1, IQM                                   TAB10253
0150            L = 3                                                       TAB10254
            C           L :       IN GENERAL INDICATES THE CORNER WHERE YIELDING TAB10255
            C                     IS EXPECTED.                              TAB10256
            C                                                               TAB10257
            C                                                               TAB10258
            C---->    DO LOOP  FOR  THE SPAN LENGTH  HL                     TAB10259
0151                  DO  7   IH = 1, IHM                                   TAB10260
0152            HL = IH*10                                                  TAB10261
0153            HL = (HL+10.D 00)*A                                         TAB10262
0154            HL2 = HL*HL                                                 TAB10263
0155            PKA=E*(XI*YI-XY*XY)/(XI*HL2)                                TAB10264
0156            PKD=E*CW/HL2                                                TAB10265
            C         HERE PART  1                                          TAB10266
            C   THESE CONSTANTS CORRESPOND TO THAT OF IN APPENDIX C OF THE REPORT TAB10267
            C   FOR  MM2 = 2, FOR HINGED BOUNDARY CONDITIONS.               TAB10268
0157            T1=.5*PI2*PI2                                               TAB10269
0158            T2=-.5*PI2                                                  TAB10270
0159            T5=-(0.125+PI2/24.)                                         TAB10271
0160            T9=.5                                                       TAB10272
0161            T101=2./PI                                                  TAB10273
0162            SN2=PI2                                                     TAB10274
0163            F2P=1.0                                                     TAB10275
            C         ADDITION TO PART 1  **                                TAB10276
            C                                                               TAB10277
0164            IY=NIY(NBR)                                                 TAB10278
0165            AKP=1./VCN(IY,NBR)                                          TAB10279
0166            AKD = DABS (AKP)                                            TAB10280
0167            BEND = XI*SIG/ HL*(AKP/AKD)                                 TAB10281
            C         BEND :    MBEND, THE HYPOTETICAL BENDING CAPACITY, TWIST TAB10282
            C                   AND LATERAL DEFLECTION RESTRAINED.          TAB10283
0168            BENR=-BEND*(-1.)**IC                                        TAB10284
            C         BENR :    BEND WITH SIGN, PLUS INDICATING GRAVITY.    TAB10285
0169            PBEN = BENP*AKD/ HL2                                        TAB10286
0170            T2P=T2/T9                                                   TAB10287
0171            T5P=T5/T9                                                   TAB10288
0172            T101P=T101/T9                                               TAB10289
0173            AK1=AKP*T5P/T2P                                             TAB10290
```

```
0174              PX=E*SN2*XI/HL2                                                TAB10291
0175              PY=E*SN2*(XI*YI-XY*AY)/(XI*HL2)                                TAB10292
0176              PO=E*SN2*CW/HL2-T2P*G*TJ/SN2+F*HL2/SN2                         TAB10293
0177              PYO=PY*HE*HE+PO                                                TAB10294
0178              QL = BEND*AK1/HE                                               TAB10295
                  C          QL :      THE SO CALLED LIMITING SHEAR RIGIDITY.    TAB10296
                  C                    BY THE CONSERVATIVE EQUATION 4.37 .      TAB10297
                  C                                                             TAB10298
                  C   DEFINE  SHEAR  RIGIDTY                                    TAB10299
0179              PBEN = BENR*AKD/ HL2                                           TAB10300
0180              T2P=T2/T9                                                      TAB10301
0181              T5P=T5/T9                                                      TAB10302
0182              T101P=T101/T9                                                  TAB10303
0183              AK1=AKP*T5P/T2P                                                TAB10304
0184              PX=E*SN2*XI/HL2                                                TAB10305
0185              PY=E*SN2*(XI*YI-XY*AY)/(XI*HL2)                                TAB10306
0186              PO=E*SN2*CW/HL2-T2P*G*TJ/SN2+F*HL2/SN2                         TAB10307
0187              PYO=PY*HE*HE+PO                                                TAB10308
0188              QL = BEND*AK1/HE                                               TAB10309
0189              GO TO (501,502,504,504),IQ                                     TAB10310
0190           501 Q=0.0                                                         TAB10311
0191               GO TO 507                                                    TAB10312
0192           502 Q=QL                                                         TAB10313
0193               GO TO 507                                                    TAB10314
0194           503 Q=QL*2.                                                      TAB10315
0195               GO TO 507                                                    TAB10316
0196           504 Q=1000.                                                      TAB10317
0197           507 CONTINUE                                                     TAB10318
                  C                                                             TAB10319
                  C              END   OF   ADDITION                            TAB10320
                  C                                                             TAB10321
0198              TA=-T5*T5                                                      TAB10322
0199              TB=Q*HE*T2*(2.*T5+T9)-PKA*T1*HE*T9                             TAB10323
0200              TC=(PKA*T1-Q*T2)*(PKQ*T1-G*TJ*T2+F*HL2*T9)-PKA*T1*Q*HE*HE*T2   TAB10324
0201              DSC=DSQRT(TB*TB-4.*TA*TC)                                      TAB10325
0202              RT1=0.5*(-TB+DSC)/TA                                           TAB10326
0203              RT2=0.5*(-TB-DSC)/TA                                           TAB10327
0204              IF (RT1.GT.0.0) GO TO 514                                      TAB10328
0205              PCR(1)=RT2/HL2                                                 TAB10329
0206              PCR(2)=RT1/HL2                                                 TAB10330
0207              GO TO 4510                                                     TAB10331
0208           514 PCR(1)=RT1/HL2                                                TAB10332
0209              PCR(2)=RT2/HL2                                                 TAB10333
                  C          PCR (1) : THE CRITICAL LOAD FOR  MM2 = 2,  PCR(1) IS FOR   TAB10334
                  C                    GRAVITY AND  PCR(2) IS FOR UPLIFT CASES.        TAB10335
0210           4510 CONTINUE                                                    TAB10336
                  C $$      INITIALIZATION :                                    TAB10337
0211              MM = 1                                                         TAB10338
0212              IY=AIY(MM)                                                     TAB10339
0213           4511 ISS=0                                                       TAB10340
0214           4512 AKAP = SIG/E                                                TAB10341
0215              GO TO 4514                                                     TAB10342
0216           4513 ISS = ISS+ 1                                                TAB10343
                  C                                                             TAB10344
                  C $$      CHECK :                                             TAB10345
0217           4514 IF (ISS.GT.3)  GO TO 519                                    TAB10346
                  C                                                             TAB10347
                  C $$      FURTHER INITIALIZATION :                            TAB10348
```



```
0218              MJ = 1                                                         TAB10349
0219              IA=0                                                           TAB10350
0220              IT=0                                                           TAB10351
0221              DEN1=0.0                                                       TAB10352
```

```
0218              MJ = 1                                                        TAB10349
0219              IA=0                                                          TAB10350
0220              IT=0                                                          TAB10351
0221              DFN1=0.0                                                      TAB10352
0222              DO 4520 I=LSA,LSB                                             TAB10353
0223         4520 DF1(I)=0.0                                                    TAB10354
0224              DNN1=0.0                                                      TAB10355
                  C                                                             TAB10356
                  C $$     DECIDE ON THE BEGINNING VALUE FOR  P  AND THE INCR.  TAB10357
0225              DLAM = .56*PBEN                                               TAB10358
0226              ALAM=PCR(IC) *0.5                                             TAB10359
0227              IF(DABS(ALAM).LT.DABS(DLAM)) DLAM=ALAM                        TAB10360
0228              ALAM=DLAM                                                     TAB10361
                  C                                                             TAB10362
                  C              END  OF  PART  1                               TAB10363
0229              M=MM2                                                         TAB10364
0230              MM=(M+1)/2                                                    TAB10365
                  C                                                             TAB10366
0231         2110 P=ALAM                                                        TAB10367
                  C                                                             TAB10368
0232         2111 CONTINUE                                                      TAB10369
                  C $$     DETERMINE THE COEFFICIENT MATRIX FOR  THE DEFORMATION AMPLITUDETAB10370
                  C                                                             TAB10371
                  CCC      SUBROUTINE CFFS                                      TAB10372
0233              PKG=G*TJ+Q*HE*HE                                              TAB10373
0234                 DO 15 I=1,MM                                               TAB10374
0235              GO TO ( 301, 302, 302, 302,302,302,302),NBR                   TAB10375
0236         301  AI=2*I-1                                                      TAB10376
0237              PM2=PI2*AI*AI                                                 TAB10377
0238              T4=-PM2/2.                                                    TAB10378
0239              T5=-.125-PM2/24.                                              TAB10379
0240              T101=2./(PI*AI)                                               TAB10380
0241              CC(I,1)=-Q*HE*T4+P*HL2*T5                                     TAB10381
0242              GO TO 309                                                     TAB10382
0243         302  T101=Z101(I)                                                  TAB10383
0244         309  DSP12*I-1)=-P*HL2*T101*XY/XI                                  TAB10384
0245              DSP12*I)  = P*HL2*HA*T101                                     TAB10385
0246                 DO 15 J=1,MM                                               TAB10386
0247              GO TOI 311, 312, 313,312,313,312,313),NBR                     TAB10387
0248         311  IF (I.EQ.J) GO TO 15                                         TAB10388
0249              AJ=2*J-1                                                      TAB10389
0250              AMN=   (AI*AI-AJ*AJ)**2                                       TAB10390
0251              T5=2.*AJ*AI**3/AMN                                            TAB10391
0252              T4=6.CO+CO                                                    TAB10392
0253              GO TO 319                                                     TAB10393
0254         312  T5=Z6(J,I)                                                    TAB10394
0255              GO TO 318                                                     TAB10395
0256         313  T5=ZS(J,I)                                                    TAB10396
0257         318  T4=Z3(I,J)                                                    TAB10397
0258         319  CC(I,J)=-Q*HE*T4+P*HL2*T5                                     TAB10398
0259          15     CONTINUE                                                   TAB10399
0260                 DO 16 I=1,MM                                               TAB10400
0261                 DO 16 J=1,MM                                               TAB10401
0262              IF (I-J) 330,320,330                                          TAB10402
0263         320  GO TO (321,322,322,322,322,322,322),NBR                      TAB10403
0264         321  AI=2*I-1                                                      TAB10404
0265              PM2=PI2*AI**2                                                 TAB10405
0266              T1=PM2*PM2/2.                                                 TAB10406
```

```
0267            T2=-PM2/2.                                                  TAB10407
0268            T9=.5                                                       TAB10408
0269            GO TO 338                                                   TAB10409
0270          322 T1=Z1(I)                                                  TAB10410
0271            T9=Z9(I)                                                    TAB10411
0272            T2=Z3(I,I)                                                  TAB10412
0273            GO TO 338                                                   TAB10413
0274          330 T1=0.0D+00                                                TAB10414
0275            T9=0.0D+00                                                  TAB10415
0276            GO TO (331,332,332),NBR                                     TAB10416
0277          331 T2=0.0D+00                                                TAB10417
0278            GO TO 338                                                   TAB10418
0279          332 T2=Z3(I,J)                                                TAB10419
0280          338 CMAT(2*I-1,2*J-1)=PKA*T1-Q*T2                             TAB10420
              CC  CMAT(2*I  ,2*J  )=PKD*T1-PKG*T2+(-P*HE+F)*HL2*T9          TAB10421
0281              CMAT(2*I  ,2*J-1)=PKD*T1-PKG*T2+(-P*HS+F)*HL2*T9          TAB10422
0282              CMAT(2*I-1,2*J)=CC(I,J)                                   TAB10423
0283              CMAT(2*I,2*J-1)=CC(J,I)                                   TAB10424
0284           16   CONTINUE                                               TAB10425
              C                                                             TAB10426
              C $$    FIND THE SOLUTION                                     TAB10427
0285            CALL SLTN(M)                                                TAB10428
              C                                                             TAB10429
              C $$    DETERMINE DEFLECTIONS AND CURVATURES                  TAB10430
0286              DO 22 I=1,M                                               TAB10431
0287            J=(I+1)/2                                                   TAB10432
0288              GO TO (341,342,342),NBR                                   TAB10433
0289          341 AI=2*J-1                                                  TAB10434
0290              AMN=(-1)**((I+3)/2)                                       TAB10435
0291              PRM(I)=DSP(I)*AI/HL                                       TAB10436
0292              DSM(I)=DSP(I)*AMN                                         TAB10437
0293              STR(I)=-DSP(I)*AI*AI*AMN*PI2                              TAB10438
0294              GO TO 22                                                  TAB10439
0295          342 DSM(I)=DSP(I)*EQ(J)                                       TAB10440
0296              STR(I)=DSP(I)*EZ(J)*SN(J)*SN(J)                           TAB10441
0297              STR(I)=DSP(I)*EE(J)*SN(J)*SN(J)                           TAB10442
0298           22   CONTINUE                                               TAB10443
0299              U=0.0                                                     TAB10444
0300              PHI=0.0                                                   TAB10445
0301              GAM=0.0                                                   TAB10446
0302              U1=0.0                                                    TAB10447
0303              PHI1=0.0                                                  TAB10448
0304              UE=0.0                                                    TAB10449
0305              PHIE=0.0                                                  TAB10450
0306              M1=(M+1)/2                                                TAB10451
0307              M2=M/2                                                    TAB10452
0308              DO 23 I=1,M1                                              TAB10453
0309              J=(I+1)/2                                                 TAB10454
0310              U1=U1+DSM(2*I-1)                                          TAB10455
0311              PHI1=PHI1+STR(2*I-1)                                      TAB10456
0312              GO TO (351,352,352),NBR                                   TAB10457
0313          351 GAM=GAM+PRM(2*I-1)*PI                                     TAB10458
0314              UE=UE+DSM(2*I)                                            TAB10459
0315              GO TO 23                                                  TAB10460
0316          352 PHIE=PHIE+STR(2*I-1)                                      TAB10461
0317           23 CONTINUE                                                  TAB10462
0318              UPR(1)=U1                                                 TAB10463
0319              UPR(2)=UE                                                 TAB10464
```

FORTRAN IV G LEVEL 20 MAIN DATE = 71348 09/24/22 PAGE 0009

```
0320              PHI=PHI+DSM(2*I)                                          TAB10465
0321              PHI1=PHI1+STR(2*I)                                        TAB10466
0322              GO TO (341,362,362),NBR                                   TAB10467
0323          361 GAM=GAM+PRM(2*I-1)*PI*HL                                  TAB10468
```

```
0320              PHI=PHI+ DSM(2*I)                                          TAB10465
0321              PHI1=PHI1+STR(2*I)                                         TAB10466
0322               GO TO (361,362,362),NBR                                   TAB10467
0323          361 GAM=GAM+PRM(2*I  )*PI*HE                                   TAB10468
0324              PHIE=0.0D+00                                               TAB10469
0325              GO TO 24                                                   TAB10470
0326          362 PHIE=PHIE+STE(2*I)                                         TAB10471
0327           24 CONTINUE                                                   TAB10472
0328              WCR(1)=PHI1                                                TAB10473
0329              WCR(2)=PHIE                                                TAB10474
                  C                                                          TAB10475
                  C      HERE   PART   2                                     TAB10476
                  C                                                          TAB10477
                  C $$      DESICION  ON  FLOW          (SEE FLOWCHART)      TAB10478
                  C                                                          TAB10479
0330              GO TO (25,1530,1536),MJ                                    TAB10490
0331           25 DNUN=PI/6.0-DABS(PHI)                                      TAB10481
                  C  25 DNUN=PI/9.0-DABS(PHI)                                TAB10482
                  C  25 DNUN=PI/18.-DABS(PHI)                                TAB10483
0332              SYGN=DNUN*DNN1                                             TAB10484
0333              GO TO (41,40,43,40,45),MP                                  TAB10485
0334           41 IF (SYGN) 1633, 448, 448                                   TAB10486
0335          448 CONTINUE                                                   TAB10487
                  C C C PRINT 98,IA,IT,IL,ISS,NL(1),NL(2),NL(3),MP           TAB10488
0336              IF (DNUN)  28,  28, 450                                    TAB10489
0337           28 MP=5                                                       TAB10490
0338              GO TO 30                                                   TAB10491
0339           43 IF (SYGN) 1638,1635,1635                                   TAB10492
0340           45 IF (SYGN) 1633,  27,  27                                   TAB10493
0341           40 AKAP1=HL2*SV(L)*VCN( IY,NBR)/(XI*E)                        TAB10494
0342              DFUN=AKAP1*P-((SU(L)-XY*SV(L)/XI)*UCR(IY)+W(L)*WCR(IY))/HL2 TAB10495
0343              DFUN=AKAP-DABS(DFUN)                                       TAB10496
0344              SIGN=DFUN*DFN1                                             TAB10497
0345              GO TO (519, 42,519, 44,519),MP                             TAB10498
0346           42 IF (SIGN) 1649,1645,1645                                   TAB10499
0347           44 IF (SIGN) 1642,  29,  29                                   TAB10500
                  C                                                          TAB10501
                  C                                                          TAB10502
                  CCCCCCCCC  BOUNDS ON THE ROOTS    CCCCC                    TAB10503
                  C                                                          TAB10504
0348          450 DNN1=DNUN                                                  TAB10505
0349              DO 446 I=1,6                                               TAB10506
0350          446 NL(I)=0.0                                                  TAB10507
0351              IL=0                                                       TAB10508
0352              DO 455 L=LSA,LSB                                           TAB10509
0353              AKAP1=HL2*SV(L)*VCN( IY,NBR)/(XI*E)                        TAB10510
0354              DFUN=AKAP1*P-((SU(L)-XY*SV(L)/XI)*UCR(IY)+W(L)*WCR(IY))/HL2 TAB10511
0355              DFUN=AKAP-DABS(DFUN)                                       TAB10512
0356              SIGN=DFUN*DF(L)                                            TAB10513
0357              IF (SIGN)  451, 452, 452                                   TAB10514
0358          451 IL=IL+1                                                    TAB10515
0359              NL(IL)=L                                                   TAB10516
0360          452 DF(L)=DFUN                                                 TAB10517
0361          455 CONTINUE                                                   TAB10518
0362              IF (IL-1)  456, 458, 470                                   TAB10519
0363          456 DO 457 I=LSA,LSB                                           TAB10520
0364          457 DF1(I)=DF(I)                                               TAB10521
0365              GO TO 30                                                   TAB10522
```

```
                C                                                                   TAB10523
0364              29 DFN1=DFUN                                                      TAB10524
                C  27 PRINT 99,IA,IT,IL,ISS,MP                                    TAB10525
0367              27 CONTINUE                                                       TAB10526
                C                                                                   TAB10527
0368              30 IA=IA+1                                                        TAB10528
                C C C PRINT 190,IA,PDEN,ALAM,DLAM,DFN1,DFUN,DNN1,DNUN,SIGN,SYGN,U,PHI TAB10529
                C                                                                   TAB10530
                C $$     CHECK  THE NUMBER OF ITERATIONS  IA                        TAB10531
0369              IF (IA-4)  35,  35,519                                            TAB10532
0370           35 DLAM=DLAM/2.                                                      TAB10533
0371              ALM1=ALAM                                                         TAB10534
0372              GO TO (  37, 519, 519,  37,  38),MP                               TAB10535
0373           37 IF (DFUN) 1618, 529,1619                                          TAB10536
0374         1618 ALAM=ALAM-DLAM                                                    TAB10537
0375              GO TO 2110                                                        TAB10538
0376         1619 ALAM=ALAM+DLAM                                                    TAB10539
0377              GO TO 2110                                                        TAB10540
0378           38 DNN1=DNUN                                                         TAB10541
0379              IF (DNUN) 1618,529,1619                                           TAB10542
0380          458 L=NL(I)                                                          TAB10543
0381          459 DFUN=DF(L)                                                       TAB10544
0382              DFN1=DF1(L)                                                       TAB10545
0383              GO TO 1642                                                        TAB10546
0384          470 ALM4=1000.*                                                      TAB10547
0385              DO 471 I=1,LL                                                     TAB10548
0386              L=NL(I)                                                           TAB10549
0387              DFUN=DF(L)                                                        TAB10550
0388              DFN1=DF1(L)                                                       TAB10551
0389              ALM3=(ALM1*DFUN-ALAM*DFN1)/(DFUN-DFN1)                            TAB10552
0390              IF ( DABS(ALM4).LT.DABS(ALM3) )  GO TO 471                        TAB10553
0391              LM=NL(I)                                                          TAB10554
0392              ALM4=ALM3                                                         TAB10555
0393          471 CONTINUE                                                         TAB10556
0394              L=LM                                                              TAB10557
0395              GO TO 459                                                         TAB10558
                C                                                                   TAB10559
                C                                                                   TAB10560
                CCCCCCCCC  LINEAR INTERPOLATION    CCCCCCCCCC                       TAB10561
                C                                                                   TAB10562
0396          1642 MP=2                                                           TAB10563
                C C C PRINT 111                                                   TAB10564
0397              GO TO 1649                                                        TAB10565
0398          1645 IF(IT.GT.2) GO TO 1646                                          TAB10566
0399              ALM1=ALM2                                                         TAB10567
0400              DFN1=DFN2                                                         TAB10568
0401          1646 ALM3=(ALM1*DFUN-ALAM*DFN1)/(DFUN-DFN1)                           TAB10569
                C C C PRINT 191,L,LM1,ALAM,DF(L),DFUN,DNN1,DNUN,ALM3              TAB10570
0402              DF(L)=DF(L)                                                       TAB10571
0403              DF1(L)=DFUN                                                       TAB10572
0404              DFUN=DABS(DFUN)                                                   TAB10573
0405              IF (DFUN-1.E-5) 1649,1649,1645                                    TAB10574
0406          1649 MP=3                                                           TAB10575
                C C C PRINT 111                                                   TAB10576
0407              GO TO 1635                                                        TAB10577
0408          1646 IF(IT.GT.2) GO TO 1648                                          TAB10578
0409              ALM1=ALM2                                                         TAB10579
0410              DFN1=DFN2                                                         TAB10580
```



```
0411          1648 ALM2=(ALM1*DFUN-ALAM*DFN1)/(DFUN-DFN1)                       TAB10581
                C C C PRINT 191,L,LM1,ALAM,DF(L),DFUN,DNN1,DNUN,ALM3            TAB10582
0412              DF(L)=DFUN                                                    TAB10583
0413              DF1(L)=DFUN                                                   TAB10584
0414              DFUN=DABS(DFUN)                                               TAB10585
```

```
0411        1638 ALM3=(ALM1*DNUN-ALAM*DNN1)/(DNUN-DNN1)                    TAB10581
            C C C PRINT 281,ALM1,ALAM,DFN1,DFUN,DNN1,DNUN,ALM3             TAB10582
0412              DNN2=DNN1                                                TAB10583
0413              DNN1=DNUN                                                TAB10584
0414              DUN=DABS(DNUN)                                           TAB10585
0415        1630  IT=IT+1                                                  TAB10586
0416              ALM2=ALM1                                                TAB10587
0417              ALM1=ALAM                                                TAB10588
0418              DAM=DABS(ALM3-ALAM)*1000.                                TAB10589
0419              ALAM=ALM3                                                TAB10590
0420              IF (IT.GT.10) GO TO 529                                  TAB10591
0421              IF(DAM.LT.ACCROT.OR.DUN.LT.ACCROT)GO TO 529              TAB10592
0422              GO TO 2110                                               TAB10593
            C                                                              TAB10594
0423          529 MJ=2                                                     TAB10595
            C C C PRINT 281,ALM2,ALAM,DFN2,DFUN,DNN2,DNUN,ALM3             TAB10596
0424              GO TO 2110                                               TAB10597
            C                                                              TAB10598
0425        1530  SGM1=0.0                                                 TAB10599
            C     PRINT 281,PCR(1),PCR(2),P,U1,PHI1,UE,PHIE                TAB10600
            C     PRINT 281,PCR(1),PCR(2),P,ALAM ,U1,PHI1                  TAB10601
            C                                                              TAB10602
            C                                                              TAB10603
            C                END OF PART 2                                 TAB10604
            C                                                              TAB10605
            C $$      DETERMINE STRESSES :                                 TAB10606
0426                  DO 1533 J= 1, IY                                     TAB10607
0427                DO 1533 I=LSA,LSB                                      TAB10608
0428                SGMV=(P*HL2*VCR(J,MAR)+XY*UCR(J)*E/HL2)*SV(I)/XI       TAB10609
0429                SGMU=-E*SU(I)*UCR(J)/HL2                               TAB10610
0430                SGMW=-E* W(I)*WCR(J)/HL2                               TAB10611
0431                SGM =SGMV+SGMU+SGMW                                    TAB10612
0432                SG(I,J)=SGM                                            TAB10613
            C           SG(I,J)  : TOTAL STRESS                            TAB10614
0433                WG(I,J)=SGMU+SGMW                                      TAB10615
            C           WG(I,J)  : STRESS DUE TO TWIST AND LATERAL DEFLECTION. TAB10616
0434                IF(SGM1.GT.DABS(SGM)) GO TO 1533                       TAB10617
0435                SGM1=DABS(SGM)                                         TAB10618
0436                LS=I                                                   TAB10619
0437                IYY=J                                                  TAB10620
0438        1533  CONTINUE                                                 TAB10621
            C     HERE PART 3                                              TAB10622
            C                                                              TAB10623
            C $$      FINAL CHECK                                          TAB10624
0439                GO TO ( 519,1650,1649),MP                              TAB10625
0440          1649  SGM1=(SGM1-ACCROT*E)/1.15                              TAB10626
0441                IF (SGM1-SIG) 1334,1334,1651                           TAB10627
0442          1650  CONTINUE                                               TAB10628
0443                IF (IYY-IY) 1651,2650,1651                             TAB10629
0444          2650  IF(LS.EQ.L) GO TO 1653                                 TAB10630
0445          1651  L=LS                                                   TAB10631
0446                IY=IYY                                                 TAB10632
0447                ISS=ISS+1                                              TAB10633
0448                MP=4                                                   TAB10634
0449                GO TO 4512                                             TAB10635
0450          1653  DNUN=DNUN+ACCROT                                       TAB10636
0451                IF (DNUN) 1654,1534,1534                               TAB10637
0452          1654  MP=5                                                   TAB10638
```

```
                ISS=ISS+1                                                       TAB10639
                GO TO 4514                                                      TAB10640
          519 P=-C.00001                                                        TAB10641
                L=8                                                             TAB10642
                GO TO 1534                                                      TAB10643
         1334 L=7                                                               TAB10644
C                                                                               TAB10645
 1534 CONTINUE                                                                  TAB10646
                II = IIOF-33*4                                                  TAB10647
                I = IH +(IP-1)*3 +(IO-1)*9                                      TAB10648
                NAY(I,IC,IFACT+II) = L                                          TAB10649
                HAY(I,IC,IFACT+II) = P*HL2 *VCN(IY,NBR) /BENR                   TAB10650
         1536 CONTINUE                                                          TAB10651
          520 CONTINUE                                                          TAB10652
            9     CONTINUE                                                      TAB10653
            7     CONTINUE                                                      TAB10654
            6     CONTINUE                                                      TAB10655
C<----------------                                                             TAB10656
C                                                                               TAB10657
C                                                                               TAB10658
C                                                                               TAB10659
            5   CONTINUE                                                        TAB10660
C<----------------                                                             TAB10661
C                                                                               TAB10662
            3     CONTINUE                                                      TAB10663
C<----------------                                                             TAB10664
C                                                                               TAB10665
C........                                                                       TAB10666
C-PR.....FINAL  PRINTOUT     THE SUMMARY TABLE INCLUDES :                       TAB10667
C                                                                               TAB10668
C                    1) THE RATIO OF FAILURE MOMENT TO  MBENR                   TAB10669
C                                                                               TAB10670
C                    2) THE INDEX OF THE CORNER WHERE YIELDING OCCUPED.         TAB10671
C                       IF THE INDEX IS  7  THEN ANGLE OF ROT. GOVERNS.         TAB10672
C                       IF THE INDEX IS 8.  THE ATTEMP TO FIND THE FAILURE      TAB10673
C                       LOAD WAS UNSUCCESFUL. CHANGES IN THE BEGINNING          TAB10674
C                       VALUES FOR  P  AND THE INCREMENT  MAY HELP.             TAB10675
C                                                                               TAB10676
            14 CONTINUE                                                         TAB10677
            13 CONTINUE                                                         TAB10678
               DO  761  I2=1,3                                                  TAB10679
               PRINT 109                                                        TAB10680
               GO TO (7061,7062,7063,7064),ISEC                                 TAB10681
          7061 PRINT 101,I2,SIG                                                 TAB10682
               GO TO 7065                                                       TAB10683
          7062 PRINT 102,I2,SIG                                                 TAB10684
               GO TO 7065                                                       TAB10685
          7063 PRINT 103,I2,SIG                                                 TAB10686
               GO TO 7065                                                       TAB10687
          7064 PRINT 104,I2,SIG                                                 TAB10688
          7065 CONTINUE                                                         TAB10689
               DO  761  IC = 1,2                                                TAB10690
               GO TO (7071,7072),IC                                             TAB10691
          7071 PRINT 105                                                        TAB10692
               GO TO 7073                                                       TAB10693
          7072 PRINT 106                                                        TAB10694
          7073 CONTINUE                                                         TAB10695
               DO  761  I=1,3                                                   TAB10696
```



```
               PRINT 111                                                        TAB10697
               DO  761  IH=1,NW                                                 TAB10698
               I = IH +(IP-1)*3 +(IO-1)*9                                       TAB10699
          761  PRINT 108,    (HAY(I,IC,J), HAY(I,IC,J), J=1,12)                TAB10700
```

COMMON BLOCK /CMT / MAP SIZE 150

SYMBOL	LOCATION	SYMBOL	LOCATION	SYMBOL	LOCATION	SYMBOL	LOCATION	SYMBOL	LOCATION
CMAT	0	DSP	120						

SUBPROGRAMS CALLED

SYMBOL	LOCATION	SYMBOL	LOCATION	SYMBOL	LOCATION	SYMBOL	LOCATION	SYMBOL	LOCATION
I9COM#	484	FDXPD#	488	FRXPI#	48C	SLTN	490	FIXPI#	494
DSQRT	498								

SCALAR MAP

SYMBOL	LOCATION	SYMBOL	LOCATION	SYMBOL	LOCATION	SYMBOL	LOCATION	SYMBOL	LOCATION
E	4F8	G	500	PI	508	PI2	510	ACCROT	518
A	52C	SIG	528	BOA	530	B	538	FACTOR	540
T	548	C	550	CMIN	558	CMAX	560	COB	568
BOT	570	COT	578	HE	580	AA	588	AREA	590
TJ	598	XI	5A0	YI	5A8	XY	5B0	HA	5B8
CW	5C0	XBAR	5C8	XO	5D0	HAA	5D8	HS	5E0
CWW	5E8	ALAM	5F0	HAOB	5F8	F	600	HL	608
HL2	610	PKA	618	PKD	620	T1	628	T2	630
T5	638	T9	640	T101	648	SN2	650	F2P	658
AKP	660	AKD	668	BEND	670	BENR	678	PBEN	680
T2P	688	T5P	690	T101P	698	AK1	6A0	PX	6A8
PY	6B0	PQ	6B8	PYO	6C0	QL	6C8	Q	6D0
TA	6D8	T8	6E0	TC	6E8	DSC	6F0	RT1	6F8
RT2	700	AKAP	708	DEN1	710	DNN1	718	DLAM	720
P	728	PKS	730	AI	738	PM2	740	T4	748
AJ	750	AM4	758	U	760	PHI	768	GAM	770
U1	778	PHI1	780	UE	788	PHIE	790	DNUN	798
SYGN	7A0	AKAP1	7A8	DEUN	7B0	SIGN	7B8	ALM1	7C0
ALM4	7C8	ALM3	7D0	ALM2	7D8	DEN2	7E0	DUN	7E8
DNN2	7F0	DAM	7F8	SGM1	800	SGMV	808	SGMU	810
SGMW	818	SGM	820	N1	828	N2	82C	I	830
J	834	NPSB	838	NNRB	83C	NNIC	840	NQF	844
IDM	848	IHM	84C	NMCS	850	MM2	854	ISIG	858
ISEC	85C	LSA	860	LSB	864	IB	868	IFACT	86C
NBR	870	NIC	874	IC	878	IQF	87C	IQ	880
L	884	IH	888	IY	88C	MP	890	ISS	894
MJ	898	IA	89C	IT	8A0	M	8A4	MM	8A8
M1	8AC	M2	8B0	IL	8B4	LM	8B8	LS	8BC
IYY	8C0	II	8C4						

ARRAY MAP

SYMBOL	LOCATION	SYMBOL	LOCATION	SYMBOL	LOCATION	SYMBOL	LOCATION	SYMBOL	LOCATION
UCR	8C8	VCR	8D8	VCN	8E8	NIY	958	CC	978
DSM	9C0	STA	9F0	STE	A20	PKM	A50	SG	A80
WJ	A50	W	940	SV	B70	SU	BA0	WW	BD0
WK	C00	DF1	C30	DF	C60	NPA	C90	NL	CA8
Z	C00	BCP	C08	MLH	CE8	LLD	D18	HAY	D28
HAY	21D8	Z1	2888	Z9	2940	Z1C1	2868	Z3	28D0
Z5	2C18	Z9	2CA0	FC	2CA8	F2	2CC0	FE	2CD8
SW	2CF0								

FORMAT STATEMENT MAP

FORTRAN IV G LEVEL 20 [illegible] DATE = 71348 09/24/22 PAGE 0015

LOCATION	SYMBOL	LOCATION	SYMBOL	LOCATION	SYMBOL	LOCATION
	109	2015	110	2018	111	201F
	191	2032	192	205C	193	208C
	197	2082	198	2523		

SYMBOL	LOCATION	SYMBOL	LOCATION	SYMBOL	LOCATION	SYMBOL	LOCATION	SYMBOL	LOCATION
98	2D08	99	2DCE	109	2D15	110	2D1A	111	2D1F
112	2D23	190	2D29	191	2D32	192	2D5C	193	2D8C
194	2DAF	195	2DD9	196	2DE7	197	2E02	198	2E23
200	2E45	201	2E56	205	2ED5	211	2EF3	219	2EFA
281	2F01	291	2F08	294	2FE4	295	2FF7	296	3020

```
*OPTIONS IN EFFECT*   NOID,EBCDIC,SOURCE,NOLIST,NODECK,LOAD,MAP
*OPTIONS IN EFFECT*   NAME = MAIN     , LINECNT =      60
*STATISTICS*     SOURCE STATEMENTS =      498,PROGRAM SIZE =    23658
*STATISTICS*   NO DIAGNOSTICS GENERATED
```

```
0001            SUBROUTINE SLTN(NV)                                     TAB10705
0002            IMPLICIT REAL * 8 (A-H,O-Z)                             TAB10706
0003               COMMON /CMT/ CMAT(6,6),DSP(6)                        TAB10707
0004            IDG=1                                                   TAB10708
0005          100 IF (IDG.EQ.NV) GO TO 200                              TAB10709
0006          110 K=IDG+1                                               TAB10710
0007              DO 160 I=K,NV                                         TAB10711
0008              HOLD=CMAT(I,IDG)/CMAT(IDG,IDG)                        TAB10712
0009              DO 130 J=K,NV                                         TAB10713
0010          130 CMAT(I,J)=CMAT(I,J)-CMAT(IDG,J)*HOLD                  TAB10714
0011              DSP(I)=DSP(I)-DSP(IDG)*HOLD                           TAB10715
0012          160 CONTINUE                                              TAB10716
0013              IDG=IDG+1                                             TAB10717
0014              GO TO 100                                             TAB10718
                C                                                       TAB10719
                C  BACK SUBSTITUTION                                    TAB10720
                C                                                       TAB10721
0015          200 HOLD=CMAT(NV,NV)                                      TAB10722
0016              DSP(NV)=DSP(NV)/HOLD                                  TAB10723
0017              I=NV                                                  TAB10724
0018              K=NV-1                                                TAB10725
0019          220 HOLD=CMAT(K,K)                                        TAB10726
0020              SUM=0.0                                               TAB10727
0021              DO 230 L=I,NV                                         TAB10728
0022          230 SUM=SUM+CMAT(K,L)*DSP(L)                              TAB10729
0023              DSP(K)=(DSP(K)-SUM)/HOLD                              TAB10730
0024              I=I-1                                                 TAB10731
0025              K=K-1                                                 TAB10732
0026              IF(I.NE.1) GO TO 220                                  TAB10733
0027              RETURN                                                TAB10734
0028              END                                                   TAB10735
```


COMMON BLOCK /CMT / MAP SIZE 150

SYMBOL	LOCATION	SYMBOL	LOCATION	SYMBOL	LOCATION	SYMBOL	LOCATION	SYMBOL	LOCATION

COMMON BLOCK /CMT / MAP SIZE 150

SYMBOL	LOCATION	SYMBOL	LOCATION	SYMBOL	LOCATION	SYMBOL	LOCATION	SYMBOL	LOCATION
CMAT	0	DSP	120						

SCALAR MAP

SYMBOL	LOCATION	SYMBOL	LOCATION	SYMBOL	LOCATION	SYMBOL	LOCATION	SYMBOL	LOCATION
HOLD	C0	SUM	C8	IDG	D0	NV	D4	K	D8
I	DC	J	E0	L	E4				

```
    *OPTIONS IN EFFECT*   NOID,EBCDIC,SOURCE,NOLIST,NODECK,LOAD,MAP
    *OPTIONS IN EFFECT*   NAME = SLTN     , LINECNT =      60
    *STATISTICS*     SOURCE STATEMENTS =        28,PROGRAM SIZE =       948
    *STATISTICS*   NO DIAGNOSTICS GENERATED

    *STATISTICS*   NO DIAGNOSTICS THIS STEP 0
```

MODULE MAP

CONTROL SECTION NAME	ORIGIN	LENGTH	ENTRY NAME	LOCATION	NAME	LOCATION	NAME	LOCATION	NAME	LOCATION
MAIN	00	5C6A								
SLTN	5C70	384								
IHCLSQRT*	6028	158								
			DSQRT	6029						
IHCFDXPD*	6188	1A0								
			FDXPD#	6188						
IHCFIXPI*	6328	14F								
			FIXPI#	6328						
IHCFRXPI*	6478	141								
			FRXPI#	6478						
IHCECOMH*	65C0	F49								
			IBCOM#	65C0	FDIOCS#	667C	INTSWTCH	74EE		
IHCCOMH2*	7510	651								
			SEQDASD	787C						
IHCFCVTH*	7868	119D								
			ADCON#	7868	FCVAOUTP	7C12	FCVLOUTP	7CA2	FCVZOUTP	7DF2
			FCVIOUTP	81A0	FCVEOUTP	86A2	FCVCOUTP	88BC	INT6SWCH	88A3
IHCEFNTH*	8D08	512								
			ARITH#	8D08	ADJSWTCH	9074				
IHCLEXP *	9220	288								
			DEXP	9220						
IHCLLOG *	94A8	200								
			DLOG10	94A8	DLOG	94C0				
IHCEFIOS*	96A8	1368								
			FIOCS#	96A8	FIOCSREP	96AE				
IHCERRM *	AA10	58C								
			ERRMON	AA10	IHCERRE	AA28				
IHCUOPT *	AFD0	300								
IHCETRCH*	B2D0	28E								
			IHCTRCH	B2D0	ERRTRA	B2D8				
IHCUATBL*	B560	638								
CMT	B898	150								

ENTRY ADDRESS 00
TOTAL LENGTH BCE8

****GO DOES NOT EXIST BUT HAS BEEN ADDED TO DATA SET

PEKOZ,T FT06F001 * 0S18 CJ5939 (1886) 71.348 09.36.34 JOB DEST = UPSON PEKOZ,T

LIPPED CHANNEL SECTION IQ= 1 SIG=33.00

DOWNWARD LOADING A/B=

0.1144*6	0.1043*6	0.0948*6	0.0848*6	0.5412*2	0.5860*2	0.6475*2	0.7338*2	0.6998*2	0.7454*2	0.8003*2	0.8646*2
0.0531*7	0.0550*7	0.0477*7	0.0408*7	0.5898*2	0.6418*2	0.7115*2	0.8057*2	0.7705*2	0.8192*2	0.8730*2	0.9262*2
0.0426*7	0.0358*7	0.0298*7	0.0244*7	0.6145*2	0.6694*2	0.7438*2	0.8436*2	0.8096*2	0.8597*2	0.9107*2	0.9532*2
0.3092*6	0.2828*6	0.2593*6	0.2352*6	0.4530*4	0.4736*4	0.5148*4	0.5953*4	0.5486*4	0.5861*4	0.6451*4	0.7382*4
0.2162*7	0.1881*7	0.1631*7	0.1395*7	0.5403*4	0.5940*4	0.6505*4	0.7374*2	0.6913*4	0.7423*4	0.7945*2	0.8481*2
0.1440*7	0.1210*7	0.1007*7	0.0827*7	0.6087*2	0.6503*2	0.7082*2	0.7870*2	0.7578*2	0.7965*2	0.8422*2	0.8944*2
0.3923*4	0.3687*4	0.3457*4	0.3216*4	0.4288*4	0.4196*4	0.4207*4	0.4455*4	0.4614*4	0.4632*4	0.4811*4	0.5333*4
0.3432*4	0.3003*6	0.2642*6	0.2304*6	0.4646*4	0.4743*4	0.5063*4	0.5800*4	0.5518*4	0.5802*4	0.6322*4	0.7219*4
0.2815*7	0.2341*7	0.1926*7	0.1552*7	0.5241*4	0.5521*4	0.6053*4	0.6986*4	0.6511*4	0.6931*4	0.7544*4	0.8389*4

UPLIFT LOADING A/B=

0.1890*1	0.1762*1	0.1635*1	0.1487*1	0.5415*5	0.5689*5	0.6082*5	0.6669*5	0.6533*5	0.6850*5	0.7270*5	0.7843*5
0.1154*7	0.1045*7	0.0943*7	0.0837*7	0.5746*5	0.6142*5	0.6678*5	0.7429*5	0.7199*5	0.7599*5	0.8087*5	0.8666*5
0.0729*7	0.0644*7	0.0565*7	0.0487*7	0.5998*5	0.6453*5	0.7062*5	0.7898*5	0.7643*5	0.8074*5	0.8564*5	0.9080*5
0.3139*1	0.2920*1	0.2720*1	0.2519*1	0.4315*3	0.4497*3	0.4842*3	0.5501*3	0.5069*3	0.5385*3	0.5882*3	0.6697*3
0.2302*1	0.2541*1	0.2486*7	0.2172*7	0.5461*3	0.5805*3	0.6324*3	0.6859*5	0.6620*3	0.7042*3	0.7370*5	0.7796*5
0.2047*7	0.1764*7	0.1509*7	0.1275*7	0.6014*5	0.6290*5	0.6672*5	0.7256*5	0.7123*5	0.7417*5	0.7806*5	0.8326*5
0.2994*1	0.2788*1	0.2609*1	0.2460*1	0.3497*3	0.3424*3	0.3439*3	0.3654*3	0.3771*3	0.3789*3	0.3944*3	0.4395*3
0.3270*1	0.2943*1	0.2656*1	0.2407*1	0.4317*3	0.4411*3	0.4687*3	0.5307*3	0.5026*3	0.5273*3	0.5724*3	0.6525*3
0.3327*7	0.2790*7	0.2316*7	0.1895*7	0.5119*3	0.5352*3	0.5786*3	0.6556*3	0.6129*3	0.6489*3	0.7027*3	0.7798*5

LIPPED CHANNEL SECTION IO= 2 SIG=33.00

DOWNWARD LOADING A/B=

0.7465*4	0.7465*4	0.7483*4	0.7537*4	0.9494*4	0.9624*4	0.9753*4	0.9874*4	0.9762*4	0.9835*4	0.9901*4	0.9954*4
0.7715*7	0.7585*7	0.7485*7	0.7426*7	0.9903*4	0.9934*4	0.9959*4	0.9978*4	0.9961*4	0.9973*4	0.9981*4	0.9987*4
0.7383*7	0.6948*7	0.6849*7	0.6799*7	0.9972*4	0.9979*4	0.9985*4	0.9990*4	0.9985*4	0.9988*4	0.9990*4	0.9992*4
0.5699*3	0.5631*3	0.5595*3	0.5619*3	0.6845*3	0.7094*3	0.7499*3	0.8116*4	0.7562*3	0.7894*3	0.8283*4	0.8826*4
0.6580*3	0.6482*3	0.6424*3	0.7108*7	0.8573*4	0.8813*4	0.9111*4	0.9467*4	0.9145*4	0.9344*4	0.9557*4	0.9771*4
0.6904*7	0.6509*7	0.6187*7	0.5963*7	0.9395*4	0.9546*4	0.9700*4	0.9848*4	0.9714*4	0.9802*4	0.9881*4	0.9944*4
0.5361*3	0.4907*3	0.4776*3	0.4683*3	0.5394*3	0.5368*3	0.5452*3	0.5786*3	0.5691*3	0.5764*3	0.5994*3	0.6557*3
0.5665*3	0.5465*3	0.5300*3	0.5200*3	0.6773*3	0.6948*3	0.7315*3	0.7969*4	0.7482*3	0.7775*3	0.8167*4	0.8734*4
0.5347*3	0.6824*7	0.6241*7	0.5766*7	0.8095*4	0.8310*4	0.8639*4	0.9108*4	0.8718*4	0.8951*4	0.9240*4	0.9573*4

UPLIFT LOADING A/B=

0.1645*1	0.1716*1	0.1590*1	0.1446*1	0.7095*3	0.7630*3	0.8131*5	0.8703*5	0.8369*5	0.8665*5	0.8993*5	0.9357*5
0.1154*7	0.1051*7	0.0945*7	0.0839*7	0.8868*5	0.9187*5	0.9507*5	0.9788*5	0.9604*5	0.9742*5	0.9859*5	0.9950*5
0.0755*7	0.0656*7	0.0568*7	0.0489*7	0.9748*5	0.9792*2	0.9801*2	0.9948*2	0.9930*2	0.9966*2	0.9993*3	0.9979*3
0.3073*1	0.2880*1	0.2698*1	0.2504*1	0.4172*3	0.4343*3	0.4676*3	0.5345*3	0.4890*3	0.5208*3	0.5721*3	0.6590*3
0.2591*1	0.2435*1	0.2213*1	0.1994*1	0.5621*3	0.6047*3	0.6679*3	0.7630*3	0.6926*3	0.7417*3	0.8040*3	0.9810*5
0.2059*7	0.1797*7	0.1571*7	0.1362*7	0.7154*3	0.7657*3	0.8290*3	0.8993*5	0.8494*3	0.8885*3	0.9225*5	0.9516*5
0.3085*1	0.2901*1	0.2739*1	0.2593*1	0.3463*3	0.3402*3	0.3415*3	0.3597*3	0.3698*3	0.3713*3	0.3848*3	0.4247*3
0.3182*1	0.2995*1	0.2643*1	0.2414*1	0.4134*3	0.4226*3	0.4497*3	0.5132*3	0.4825*3	0.5078*3	0.5550*3	0.6413*3
0.3103*1	0.2979*7	0.2567*7	0.2191*7	0.5096*3	0.5377*3	0.5894*3	0.6809*3	0.6218*3	0.6643*3	0.7265*3	0.8159*3

LIPPED CHANNEL SECTION IO= 3 SIG=33.00

DOWNWARD LOADING A/B=

0.8876*3	0.8938*3	0.9012*3	0.9118*3	0.9628*3	0.9714*3	0.9802*3	0.9892*3	0.9795*3	0.9853*3	0.9908*3	0.9957*3
0.9480*3	0.9511*3	0.9547*3	0.9597*3	0.9935*3	0.9954*3	0.9971*3	0.9985*3	0.9972*3	0.9981*3	0.9987*3	0.9991*3
0.9695*3	0.9712*3	0.9731*3	0.9758*3	0.9979*3	0.9984*3	0.9988*3	0.9991*3	0.9988*3	0.9990*3	0.9991*3	0.9993*3
0.6379*3	0.6411*3	0.6475*3	0.6609*3	0.7046*3	0.7249*3	0.7556*3	0.8059*3	0.7507*3	0.7773*3	0.8136*3	0.8657*3
0.7413*3	0.7451*3	0.7526*3	0.7631*3	0.8667*3	0.8881*3	0.9140*3	0.9455*3	0.9122*3	0.9310*3	0.9513*3	0.9729*3
0.8276*3	0.8313*3	0.8381*3	0.8513*3	0.9490*3	0.9610*3	0.9734*3	0.9859*3	0.9730*3	0.9809*3	0.9883*3	0.9948*3
0.5391*3	0.5335*3	0.5318*3	0.5357*3	0.5592*3	0.5619*3	0.5723*3	0.6003*3	0.5786*3	0.5871*3	0.6065*3	0.6494*3
0.6025*3	0.5962*3	0.5940*3	0.6000*3	0.6752*3	0.6912*3	0.7211*3	0.7759*3	0.7258*3	0.7507*3	0.7856*3	0.8460*3
0.6775*3	0.6710*3	0.6695*3	0.6784*3	0.8019*3	0.8246*3	0.8572*3	0.9028*3	0.8588*3	0.8829*3	0.9123*3	0.9474*3

UPLIFT LOADING A/B=

0.1835*1	0.1707*1	0.1582*1	0.1440*1	0.7463*3	0.7997*3	0.8615*3	0.9309*3	0.8785*3	0.9159*3	0.9532*3	0.9863*3
0.1170*7	0.1052*7	0.0946*7	0.0839*7	0.9354*3	0.9725*3	0.9940*2	0.9895*2	0.9941*2	0.9801*2	0.9784*2	0.9876*2
0.0759*7	0.0657*7	0.0569*7	0.0489*7	0.9284*2	0.9387*2	0.9607*2	0.9877*2	0.9765*2	0.9867*2	0.9969*2	0.9984*3
0.3025*1	0.2848*1	0.2679*1	0.2490*1	0.4052*3	0.4211*3	0.4529*3	0.5191*3	0.4728*3	0.5040*3	0.5557*3	0.6459*3
0.2534*1	0.2397*1	0.2194*1	0.1972*1	0.5638*3	0.6150*3	0.6831*3	0.7832*3	0.7067*3	0.7584*3	0.8227*3	0.9002*3
0.2061*7	0.1803*7	0.1580*7	0.1374*7	0.7510*3	0.8019*3	0.8638*3	0.9355*3	0.8805*3	0.9182*3	0.9564*3	0.9899*3
0.3174*1	0.3010*1	0.2860*1	0.2706*1	0.3418*3	0.3369*3	0.3377*3	0.3517*3	0.3605*3	0.3615*3	0.3720*3	0.4046*3
0.3114*1	0.2854*1	0.2627*1	0.2409*1	0.3999*3	0.4085*3	0.4345*3	0.4977*3	0.4663*3	0.4914*3	0.5390*3	0.6286*3
0.3039*1	0.2686*1	0.2383*1	0.2281*7	0.5079*3	0.5381*3	0.5937*3	0.6922*3	0.6265*3	0.6721*3	0.7384*3	0.8320*3

LIPPED Z-SECTION IQ= 1 SIG=33.00

DOWNWARD LOADING A/B=

0.1261*6	0.1172*6	0.1085*6	0.0983*6	0.3786*4	0.3993*4	0.4257*4	0.4611*4	0.4380*4	0.4558*4	0.4771*4	0.5044*4
0.0577*7	0.0607*7	0.0542*7	0.0476*7	0.3786*4	0.3994*4	0.4257*4	0.4611*4	0.4383*4	0.4561*4	0.4777*4	0.5055*4
0.0434*7	0.0378*7	0.0327*7	0.0278*7	0.3772*4	0.3983*4	0.4253*4	0.4616*4	0.4383*4	0.4566*4	0.4787*4	0.5068*4
0.3329*4	0.3235*4	0.3132*4	0.2911*6	0.3690*4	0.3718*4	0.3788*4	0.3931*4	0.3871*4	0.3923*4	0.4010*4	0.4150*4
0.2192*6	0.2015*6	0.1843*6	0.1658*6	0.3503*4	0.3594*4	0.3732*4	0.3934*4	0.3829*4	0.3914*4	0.4026*4	0.4178*4
0.1574*7	0.1387*7	0.1216*7	0.1049*7	0.3486*4	0.3598*4	0.3748*4	0.3951*4	0.3842*4	0.3931*4	0.4043*4	0.4193*4
0.3692*4	0.3631*4	0.3569*4	0.3498*4	0.3733*4	0.3691*4	0.3663*4	0.3662*4	0.3765*4	0.3736*4	0.3724*4	0.3747*4
0.3216*4	0.3084*4	0.2942*4	0.2773*4	0.3489*4	0.3468*4	0.3485*4	0.3562*4	0.3628*4	0.3630*4	0.3663*4	0.3736*4
0.2490*4	0.2446*6	0.2203*6	0.1949*6	0.3379*4	0.3396*4	0.3456*4	0.3571*4	0.3603*4	0.3627*4	0.3677*4	0.3759*4

UPLIFT LOADING A/B=

0.2019*1	0.1920*1	0.1816*1	0.1685*1	0.4040*3	0.4200*3	0.4412*3	0.4708*3	0.4498*3	0.4648*3	0.4833*3	0.5079*3
0.1139*1	0.1061*1	0.0984*1	0.0913*7	0.3906*3	0.4091*3	0.4330*3	0.4657*3	0.4438*3	0.4604*3	0.4807*3	0.5072*3
0.0715*7	0.0650*7	0.0588*7	0.0524*7	0.3842*3	0.4040*3	0.4295*3	0.4643*3	0.4415*3	0.4591*3	0.4804*3	0.5078*3
0.3663*3	0.3623*3	0.3577*3	0.3522*3	0.3865*3	0.3886*3	0.3936*3	0.4041*3	0.3978*3	0.4017*3	0.4083*3	0.4196*3
0.2939*3	0.2818*1	0.2653*1	0.2462*1	0.3671*3	0.3736*3	0.3838*3	0.3998*3	0.3906*3	0.3973*3	0.4067*3	0.4201*3
0.2194*1	0.2033*1	0.1875*1	0.1705*1	0.3601*3	0.3689*3	0.3812*3	0.3989*3	0.3890*3	0.3966*3	0.4066*3	0.4205*3
0.3762*3	0.3714*3	0.3668*3	0.3624*3	0.3790*3	0.3753*3	0.3729*3	0.3727*3	0.3812*3	0.3784*3	0.3771*3	0.3787*3
0.3443*3	0.3357*3	0.3268*3	0.3170*3	0.3607*3	0.3583*3	0.3587*3	0.3636*3	0.3699*3	0.3693*3	0.3711*3	0.3766*3
0.3078*3	0.2946*3	0.2811*3	0.2659*3	0.3501*3	0.3502*3	0.3538*3	0.3622*3	0.3662*3	0.3674*3	0.3710*3	0.3776*3

LIPPED Z-SECTION ID= 2 SIG=33.00

DOWNWARD LOADING A/B=

0.9964*3	0.9021*3	0.9098*3	0.9183*3	0.9021*4	0.9063*4	0.9114*4	0.9190*4	0.9004*4	0.9051*4	0.9107*4	0.9182*4
0.9425*5	0.9189*5	0.8992*5	-0.0040*8	0.9496*4	0.9524*4	0.9556*4	0.9602*4	0.9497*4	0.9527*4	0.9569*4	0.9627*4
0.0027*8	-0.0034*8	-0.0047*8	-0.0072*8	0.9701*4	0.9720*4	0.9741*4	0.9770*4	0.9706*4	0.9724*4	0.9745*4	0.9773*4
0.6234*3	0.6303*3	0.6394*3	0.6549*3	0.6390*3	0.6500*3	0.6644*3	0.6862*3	0.6466*3	0.6580*3	0.6722*3	0.6927*3
0.7491*3	0.7562*3	0.7657*3	0.7813*3	0.7742*3	0.7845*3	0.7963*3	0.8124*3	0.7785*3	0.7879*3	0.7987*3	0.8114*4
0.8390*3	0.8448*3	0.8522*3	0.8641*3	0.8555*4	0.8605*4	0.8666*4	0.8760*4	0.8530*4	0.8587*4	0.8656*4	0.8758*4
-0.0001*8	-0.0001*8	0.4982*3	0.5050*3	-0.0001*8	-0.0001*8	0.5064*3	0.5185*3	-0.0001*8	-0.0001*8	-0.0002*8	0.5259*3
0.5792*3	0.5816*3	0.5862*3	0.5968*3	0.5963*3	0.6050*3	0.6180*3	0.6396*3	0.6048*3	0.6145*3	0.6278*3	0.6490*3
0.6599*3	0.6733*3	0.6792*3	0.6920*3	0.6976*3	0.7086*3	0.7225*3	0.7420*3	0.7049*3	0.7154*3	0.7279*3	0.7454*3

UPLIFT LOADING A/B=

0.2571*1	0.2350*1	0.2201*1	0.2025*1	0.6970*3	0.7363*3	0.7825*3	0.8372*3	0.7878*3	0.8167*3	0.8478*3	0.8920*3
0.1471*7	0.1334*7	0.1209*7	0.1080*7	0.8365*3	0.8683*3	0.9027*3	0.9363*3	0.9080*3	0.9248*3	0.9401*3	0.9535*3
0.0959*7	0.0839*7	0.0733*7	0.0634*7	0.8976*3	0.9318*3	0.9582*3	0.9723*3	0.9594*3	0.9662*3	0.9712*3	0.9756*3
0.4212*3	0.4144*3	0.4078*3	0.4007*3	0.4726*3	0.4824*3	0.5008*3	0.5366*3	0.5059*3	0.5219*3	0.5467*3	0.5873*3
0.3610*3	0.3440*3	0.3211*1	0.2944*1	0.5558*3	0.5831*3	0.6223*3	0.6797*3	0.6280*3	0.6562*3	0.6917*3	0.7378*3
0.2849*7	0.2536*7	0.2256*7	0.1988*7	0.6671*3	0.7009*3	0.7428*3	0.7953*3	0.7461*3	0.7730*3	0.8032*3	0.8384*3
0.4151*3	0.4095*3	0.4044*3	0.3997*3	0.4233*3	0.4213*3	0.4222*3	0.4301*3	0.4304*3	0.4310*3	0.4358*3	0.4500*3
0.4024*3	0.3895*3	0.3768*3	0.3636*3	0.4493*3	0.4539*3	0.4677*3	0.4993*3	0.4797*3	0.4911*3	0.5119*3	0.5488*3
0.3916*3	0.3597*3	0.3380*3	0.3156*3	0.5053*3	0.5216*3	0.5508*3	0.6008*3	0.5616*3	0.5833*3	0.6143*3	0.6593*3

LIPPED Z-SECTION IQ= 3 SIG=33.00

DOWNWARD LOADING A/B=

0.8925*3	0.8976*3	0.9035*3	0.9134*3	0.9636*3	0.9718*3	0.9803*3	0.9891*3	0.9794*3	0.9851*3	0.9905*3	0.9954*3
0.9503*3	0.9529*3	0.9559*3	0.9605*3	0.9933*3	0.9953*3	0.9970*3	0.9983*3	0.9969*3	0.9978*3	0.9985*3	0.9990*3
0.9709*3	0.9722*3	0.9738*3	0.9762*3	0.9977*3	0.9983*3	0.9987*3	0.9990*3	0.9986*3	0.9988*3	0.9990*3	0.9992*3
0.6505*3	0.6520*3	0.6561*3	0.6663*3	0.7119*3	0.7303*3	0.7587*3	0.8064*3	0.7539*3	0.7768*3	0.8134*3	0.8639*3
0.7524*3	0.7544-3	0.7598*3	0.7725*3	0.8680*3	0.8883*3	0.9133*3	0.9442*3	0.9097*3	0.9282*3	0.9485*3	0.9706*3
0.8355*3	0.8390*3	0.8432*3	0.8542*3	0.9475*3	0.9593*3	0.9718*3	0.9846*3	0.9695*3	0.9779*3	0.9860*3	0.9932*3
0.5462*3	0.5425*3	0.5404*3	0.5418*3	0.5636*3	0.5669*3	0.5766*3	0.6019*3	0.5793*3	0.5883*3	0.6068*3	0.6471*3
0.6135*3	0.6072*3	0.6037*3	0.6066*3	0.6774*3	0.6929*3	0.7211*3	0.7735*3	0.7210*3	0.7455*3	0.7826*3	0.8398*3
0.6839*3	0.6821*3	0.6792*3	0.6848*3	0.7995*3	0.8217*3	0.8534*3	0.8985*3	0.8490*3	0.8736*3	0.9039*3	0.9405*3

UPLIFT LOADING A/B=

0.2691*1	0.2510*1	0.2334*1	0.2134*1	0.8570*3	0.8947*3	0.9332*3	0.9700*3	0.9407*3	0.9609*3	0.9793*3	0.9941*3
0.1534*7	0.1343*7	0.1246*7	0.1108*7	0.9676*3	0.9870*3	0.9988*2	0.9872*2	0.9992*2	0.9925*2	0.9915*2	0.9953*2
0.6994*7	0.6962*7	0.6749*7	0.6645*7	0.9632*2	0.9704*2	0.9827*2	0.9952*2	0.9902*2	0.9947*2	0.9990*2	0.9993*3
0.4684*3	0.4592*3	0.4484*3	0.4383*3	0.5610*3	0.5800*3	0.6153*3	0.6829*3	0.6278*3	0.6602*3	0.7099*3	0.7875*3
0.4023*3	0.3779*3	0.3514*1	0.3183*1	0.7036*3	0.7466*3	0.8045*3	0.8788*3	0.8155*3	0.8550*3	0.8996*3	0.9474*3
0.3022*7	0.2658*7	0.2340*7	0.2046*7	0.8440*3	0.8820*3	0.9238*3	0.9564*3	0.9292*3	0.9528*3	0.9750*3	0.9931*3
0.4493*3	0.4600*3	0.4521*3	0.4445*3	0.4876*3	0.4872*3	0.4929*3	0.5137*3	0.5053*3	0.5115*3	0.5278*3	0.5677*3
0.4515*3	0.4331*3	0.4154*3	0.3976*3	0.5380*3	0.5512*3	0.5822*3	0.6494*3	0.6008*3	0.6294*3	0.6780*3	0.7594*3
0.4294*3	0.3995*3	0.3708*3	0.3614*7	0.6347*3	0.6671*3	0.7211*3	0.8058*3	0.7354*3	0.7765*3	0.8308*3	0.8988*3

LIPPED CHANNEL SECTION IQ= 1 SIG=55.00

DOWNWARD LOADING A/B=

0.0925*7	0.0731*7	0.0631*7	0.0540*7	0.3200*6	0.3528*2	0.3953*2	0.4665*2	0.4461*2	0.4877*2	0.5446*2	0.6335*2
0.0459*7	0.0383*7	0.0318*7	0.0258*7	0.3412*2	0.3745*2	0.4199*2	0.4941*2	0.4756*2	0.5206*2	0.5809*2	0.6760*2
0.0323*7	0.0263*7	0.0207*7	0.0159*7	0.3480*2	0.4164*5	0.4264*2	-0.0033*8	0.4847*2	0.5306*2	-0.0022*8	0.6920*2
0.2530*6	0.2270*6	0.1976*6	0.1715*6	0.3507*4	0.3533*4	0.3712*4	0.4244*4	0.4175*4	0.4367*4	0.4786*4	0.5625*4
0.1580*7	0.1331*7	0.1083*7	0.0877*7	0.3599*7	0.3850*7	0.4345*7	0.4992*2	0.4758*4	0.5151*4	0.5740*2	0.6544*2
0.1096*7	0.0891*7	0.0695*7	0.0534*7	0.3749*7	0.4104*7	0.4543*2	0.5319*2	0.5145*2	0.5554*2	0.6137*2	0.7043*2
0.3795*4	0.3480*4	0.3053*6	0.2677*6	0.4021*4	0.3801*4	0.3612*4	0.3647*4	0.4230*4	0.4093*4	0.4056*4	0.4350*4
0.3010*6	0.2641*7	0.2089*7	0.1647*7	0.3834*4	0.3721*4	0.3770*4	0.4212*4	0.4428*4	0.4492*4	0.4795*4	0.5555*4
0.2175*7	0.1746*7	0.1332*7	0.1001*7	0.3787*7	0.3824*7	0.4141*7	0.5036*7	0.4815*4	0.5051*4	0.5550*4	0.6486*4

UPLIFT LOADING A/B=

0.1555*7	0.1423*7	0.1268*7	0.1118*7	0.3708*5	0.3908*5	0.4186*5	0.4679*5	0.4668*5	0.4959*5	0.5343*5	0.5970*5
0.0797*7	0.0705*7	0.0608*7	0.0518*7	0.3628*5	0.3907*5	0.4280*5	0.4902*5	0.4816*5	0.5192*5	0.5684*5	0.6460*5
0.0519*7	0.0447*7	0.0374*7	0.0307*7	0.3600*5	0.3902*5	0.4307*5	0.4981*5	0.4874*5	0.5286*5	0.5828*5	0.6690*5
0.3071*1	0.2811*1	0.2532*1	0.2273*1	0.3948*3	0.3895*3	0.4078*3	0.4524*3	0.4363*3	0.4534*3	0.4889*3	0.5553*3
0.2240*7	0.1941*7	0.1625*7	0.1355*7	0.4176*3	0.4353*3	0.4694*3	0.5112*5	0.5089*3	0.5401*3	0.5719*5	0.6213*5
0.1506*7	0.1260*7	0.1019*7	0.0814*7	0.4263*5	0.4447*5	0.4739*5	0.5288*5	0.5293*5	0.5579*5	0.5981*5	0.6642*5
0.3247*1	0.2959*1	0.2682*1	0.2455*1	0.3571*1	0.3402*1	0.3304*3	0.3375*3	0.3760*3	0.3662*3	0.3662*3	0.3936*3
0.3356*1	0.3145*7	0.2515*7	0.2004*7	0.3969*3	0.3902*3	0.3977*3	0.4358*3	0.4434*3	0.4503*3	0.4770*3	0.5389*3
0.2540*7	0.2061*7	0.1592*7	0.1213*7	0.4276*7	0.4302*7	0.4616*7	0.5036*3	0.4967*3	0.5161*3	0.5564*3	0.6262*5

LIPPED CHANNEL SECTION IO= 2 SIG=55.00

DOWNWARD LOADING A/B=

0.8095*7	0.7966*7	0.7874*7	0.7311*7	0.9254*4	0.9419*4	0.9613*4	0.9792*4	0.9601*4	0.9710*4	0.9823*4	0.9913*4
0.7103*7	0.6974*7	0.6902*7	0.6366*7	0.9823*4	0.9876*4	0.9927*4	0.9964*4	0.9924*4	0.9949*4	0.9969*4	0.9983*4
0.6569*7	0.6433*7	0.6365*7	0.6337*7	0.9949*4	0.9965*4	0.9979*4	0.9988*4	0.9978*4	0.9984*4	0.9989*4	0.9993*4
0.6137*3	0.6053*3	0.6048*3	0.6104*3	0.6864*3	0.7017*3	0.7386*3	0.7896*4	0.7393*3	0.7632*4	0.8010*4	0.8561*4
0.7029*7	0.6626*7	0.6305*7	0.6085*7	0.8300*4	0.8502*4	0.9835*4	0.9252*4	0.8840*4	0.9054*4	0.9340*4	0.9632*4
0.6102*7	0.5684*7	0.5373*7	0.5167*7	0.9135*4	0.9307*4	0.9528*4	0.9743*4	0.9525*4	0.9649*4	0.9784*4	0.9894*4
0.5443*3	0.5244*3	0.5071*3	0.4974*3	0.5649*3	0.5538*3	0.5537*3	0.5777*3	0.5839*3	0.5804*3	0.5936*3	0.6392*3
0.6235*3	0.5995*3	0.6461*7	0.5935*7	0.6906*3	0.6943*3	0.7224*3	0.7739*4	0.7403*3	0.7568*4	0.7896*4	0.8446*4
0.6504*7	0.5792*7	0.5165*7	0.4693*7	0.7938*4	0.8057*4	0.8358*4	0.8837*4	0.8441*4	0.8633*4	0.8963*4	0.9367*4

UPLIFT LOADING A/B=

0.1543*7	0.1426*7	0.1269*7	0.1120*7	0.5317*3	0.5829*3	0.6562*3	0.7598*3	0.6933*3	0.7494*3	0.8202*3	0.8869*3
0.0913*7	0.0715*7	0.0611*7	0.0519*7	0.0007*8	0.0009*8	0.0012*8	0.8366*3	0.8194*3	0.0009*8	0.9539*3	0.9626*2
0.0555*7	0.0466*7	0.0380*7	0.0309*7	0.8837*2	0.9391*2	0.9810*3	0.9784*3	0.9814*3	0.8309*2	0.0022*8	0.9777*2
0.2947*1	0.2711*1	0.2451*1	0.2206*1	0.3729*3	0.3779*3	0.3973*3	0.4469*3	0.4241*3	0.4427*3	0.4828*3	0.5605*3
0.2267*7	0.1983*7	0.1695*7	0.1449*7	0.4788*7	0.5170*7	0.5366*3	0.6332*3	0.5704*3	0.6152*3	0.6861*3	0.7877*3
0.1505*7	0.1266*7	0.1042*7	0.0858*7	0.5572*7	0.6314*7	0.6798*3	0.7830*3	0.7183*3	0.7693*3	0.8382*3	0.9185*3
0.3249*1	0.2995*1	0.2738*1	0.2517*1	0.3496*3	0.3352*1	0.3253*3	0.3308*3	0.3644*3	0.3558*3	0.3556*3	0.3793*3
0.3212*1	0.2845*1	0.2486*1	0.2331*7	0.3832*3	0.3772*3	0.3863*3	0.4296*3	0.4310*3	0.4395*3	0.4709*3	0.5444*3
0.2577*7	0.2141*7	0.1725*7	0.1396*7	0.4320*7	0.4369*7	0.4788*7	0.6063*7	0.5289*3	0.5572*3	0.6150*3	0.7137*3

LIPPED CHANNEL SECTION IQ= 3 SIG=55.00

DOWNWARD LOADING A/B=

0.9229*3	0.9279*3	0.9367*3	0.9458*3	0.9620*3	0.9695*3	0.9787*3	0.9876*3	0.9758*3	0.9817*3	0.9883*3	0.9935*3
0.9645*3	0.9667*3	0.9705*3	0.9743*3	0.9909*3	0.9932*3	0.9955*3	0.9975*3	0.9953*3	0.9966*3	0.9978*3	0.9987*3
0.9779*3	0.9790*3	0.9811*3	0.9833*3	0.9965*3	0.9973*3	0.9981*3	0.9988*3	0.9981*3	0.9985*3	0.9989*3	0.9992*3
0.6822*3	0.6866*3	0.7017*3	0.7227*3	0.7236*3	0.7396*3	0.7715*3	0.8173*3	0.7555*3	0.7771*3	0.8148*3	0.8643*3
0.8325*3	0.8076*3	0.8227*3	0.8414*3	0.8727*3	0.8897*3	0.9156*3	0.9447*3	0.9069*3	0.9240*3	0.9465*3	0.9689*3
0.9301*3	0.8842*3	0.8949*3	0.9074*3	0.9465*3	0.9570*3	0.9703*3	0.9830*3	0.9672*3	0.9754*3	0.9845*3	0.9922*3
0.5679*3	0.5605*3	0.5602*3	0.5682*3	0.5820*3	0.5798*3	0.5895*3	0.6163*3	0.5952*3	0.5976*3	0.6151*3	0.6548*3
0.6553*3	0.6481*3	0.6521*3	0.6658*3	0.7001*3	0.7045*3	0.7367*3	0.7860*3	0.7346*3	0.7514*3	0.7885*3	0.8434*3
0.7445*3	0.7393*3	0.7470*3	0.7636*3	0.8157*3	0.8309*3	0.8621*3	0.9035*3	0.8567*3	0.8760*3	0.9070*3	0.9422*3

UPLIFT LOADING A/B=

0.1566*7	0.1428*7	0.1270*7	0.1121*7	0.5755*3	0.6313*3	0.7079*3	0.8100*3	0.7434*3	0.7984*3	0.8668*3	0.9461*3
0.0822*7	0.0716*7	0.0612*7	0.0519*7	0.0007*8	0.0009*8	0.0012*8	0.8334*2	0.0007*8	0.9684*3	0.9065*2	0.9330*2
0.0561*7	0.0467*7	0.0381*7	0.0309*7	0.9544*2	0.9971*3	0.9710*3	0.8101*2	0.8042*2	1.3949*3	0.9195*2	0.9392*2
0.2830*1	0.2666*1	0.2417*1	0.2180*1	0.3662*3	0.3711*3	0.3906*3	0.4420*3	0.4166*3	0.4356*3	0.4775*3	0.5605*3
0.2270*7	0.1990*7	0.1707*7	0.1463*7	0.4895*7	0.5339*7	0.5613*3	0.6675*3	0.5940*3	0.6433*3	0.7195*3	0.8234*3
0.1505*7	0.1267*7	0.1044*7	0.0862*7	0.6001*7	0.6929*7	0.7288*3	0.8325*3	0.7657*3	0.8165*3	0.8836*3	0.9609*3
0.3243*1	0.3009*1	0.2763*1	0.2543*1	0.3428*3	0.3303*3	0.3202*1	0.3250*3	0.3558*3	0.3478*3	0.3470*3	0.3673*3
0.3147*1	0.2794*1	0.2450*1	0.2154*1	0.3768*3	0.3708*3	0.3801*3	0.4250*3	0.4248*3	0.4337*3	0.4666*3	0.5452*3
0.2584*7	0.2157*7	0.1751*7	0.1428*7	0.4330*7	0.4386*7	0.4838*7	0.6264*7	0.6045*7	0.5740*3	0.6379*3	0.7438*3

LIPPED Z-SECTION IQ= 1 SIG=55.00

DOWNWARD LOADING A/B=

0.0396*6	0.0827*7	0.0728*7	0.0635*7	0.2412*6	0.2585*6	0.2822*6	0.3203*6	0.3152*6	0.3382*6	0.3678*6	0.4104*4
0.2474*7	0.0414*7	0.0352*7	0.0296*7	0.2426*6	0.2609*6	0.2846*6	0.3218*6	0.3174*6	0.3404*6	0.3692*4	0.4091*4
0.0314*7	0.0267*7	0.0219*7	0.0176*7	0.2419*6	0.2602*6	0.2840*6	0.3221*6	0.3169*6	0.3399*4	0.3682*4	0.4091*4
0.2744*6	0.2551*6	0.2305*6	0.2064*6	0.3120*4	0.3097*4	0.3114*4	0.3254*4	0.3339*4	0.3369*4	0.3450*4	0.3642*4
0.1595*6	0.1540*7	0.1315*7	0.1116*7	0.2720*4	0.2785*4	0.2918*4	0.3178*4	0.3150*4	0.3250*4	0.3404*4	0.3650*4
0.1129*7	0.0967*7	0.0801*7	0.0657*7	0.2633*4	0.2741*4	0.2909*4	0.3187*4	0.3130*4	0.3249*4	0.3414*4	0.3660*4
0.3525*4	0.3411*4	0.3255*4	0.3100*4	0.3567*4	0.3475*4	0.3369*4	0.3317*4	0.3603*4	0.3528*4	0.3453*4	0.3451*4
0.2471*4	0.2651*6	0.2334*6	0.2036*6	0.3120*4	0.3032*4	0.2971*4	0.3034*4	0.3285*4	0.3246*4	0.3243*4	0.3348*4
0.2219*6	0.2005*7	0.1639*7	0.1333*7	0.2866*4	0.2829*4	0.2845*4	0.2992*4	0.3159*4	0.3169*4	0.3218*4	0.3360*4

UPLIFT LOADING A/B=

0.1475*1	0.1385*1	0.1265*1	0.1141*1	0.2813*1	0.2952*1	0.3137*1	0.3454*1	0.3479*3	0.3649*3	0.3883*3	0.4225*3
0.0787*7	0.0716*7	0.0636*7	0.0558*7	0.2608*1	0.2773*1	0.2985*1	0.3329*1	0.3321*1	0.3517*3	0.3773*3	0.4147*3
0.0490*7	0.0436*7	0.0378*7	0.0324*7	0.2520*1	0.2693*1	0.2918*1	0.3285*1	0.3252*1	0.3457*3	0.3729*3	0.4124*3
0.3301*3	0.3215*3	0.3101*3	0.2931*1	0.3480*3	0.3463*3	0.3472*3	0.3560*3	0.3606*3	0.3621*3	0.3674*3	0.3808*3
0.2370*1	0.2197*1	0.1987*1	0.1783*1	0.3062*3	0.3097*3	0.3182*3	0.3370*3	0.3362*3	0.3430*3	0.3543*3	0.3739*3
0.1677*7	0.1491*7	0.1290*7	0.1111*7	0.2871*3	0.2947*3	0.3074*3	0.3302*3	0.3268*3	0.3361*3	0.3497*3	0.3712*3
0.3562*3	0.3577*3	0.3468*3	0.3375*3	0.3687*3	0.3615*3	0.3532*3	0.3494*3	0.3710*3	0.3647*3	0.3583*3	0.3575*3
0.3221*3	0.3080*3	0.2900*3	0.2727*3	0.3364*3	0.3289*3	0.3225*3	0.3249*3	0.3465*3	0.3421*3	0.3398*3	0.3459*3
0.2784*3	0.2574*3	0.2296*1	0.2128*7	0.3127*3	0.3079*3	0.3063*3	0.3152*3	0.3326*3	0.3314*3	0.3331*3	0.3432*3

LIPPED Z-SECTION IQ= 2 SIG=55.00

DOWNWARD LOADING A/B=

0.9319*3	0.9366*3	0.9449*3	0.9192*5	0.9336*4	0.9365*4	0.9418*4	0.9480*4	0.9311*4	0.9345*4	0.9407*4	0.9475*4
0.9859*4	1.0236*4	-0.0012*8	0.9291*4	0.9658*4	0.9677*4	0.9710*4	0.9747*4	0.9656*4	0.9677*4	0.9712*4	0.9751*4
1.0497*4	0.9505*4	0.8227*7	0.8050*7	0.9795*4	0.9809*4	0.9830*4	0.9854*4	0.9798*4	0.9812*4	0.9834*4	0.9857*4
0.6967*3	0.6945*3	0.7115*3	0.7326*3	0.6981*3	0.7098*3	0.7312*3	0.7576*3	0.7049*3	0.7174*3	0.7388*3	0.7640*3
0.9153*3	0.8254*3	0.8393*3	0.8556*3	0.8326*3	0.8421*3	0.8570*3	0.8729*3	0.8361*3	0.8450*3	0.8599*3	0.8707*4
0.8921*3	0.8972*3	0.9066*3	0.9174*3	0.8998*3	0.9043*4	0.9109*4	0.9188*4	0.8972*4	0.9015*4	0.9092*4	0.9192*4
0.5374*3	0.5386*3	0.5447*3	0.5565*3	0.5405*3	0.5433*3	0.5527*3	0.5706*3	0.5432*3	0.5471*3	0.5586*3	0.5793*3
0.6491*3	0.6515*3	0.6626*3	0.6797*3	0.6600*3	0.6689*3	0.6883*3	0.7157*3	0.6673*3	0.6779*3	0.6983*3	0.7247*3
0.7495*3	0.7542*3	0.7667*3	0.7837*3	0.7656*3	0.7763*3	0.7949*3	0.8164*3	0.7717*3	0.7824*3	0.7999*3	0.8194*3

UPLIFT LOADING A/B=

0.1901*1	0.1751*1	0.1573*1	0.1433*7	0.5513*3	0.5970*3	0.6611*3	0.7465*3	0.6872*3	0.7317*3	0.7879*3	0.8534*3
0.1037*7	0.0913*7	0.0786*7	0.0673*7	0.0007*8	0.0009*8	0.0012*8	0.0019*8	0.7755*3	0.8159*3	0.0012*8	0.9424*3
0.0710*7	0.0597*7	0.0492*7	0.0402*7	0.8602*2	0.9019*2	0.9492*2	0.9871*4	0.9458*2	0.9698*2	0.9889*4	0.9925*3
0.3923*3	0.3794*3	0.3640*3	0.3447*1	0.4358*3	0.4390*3	0.4526*3	0.4881*3	0.4691*3	0.4913*3	0.5081*3	0.5587*3
0.3128*7	0.2790*7	0.2430*7	0.2113*7	0.4796*3	0.5020*3	0.5456*3	0.6199*3	0.5669*3	0.5992*3	0.6503*3	0.7209*3
0.2074*7	0.1781*7	0.1495*7	0.1252*7	0.5671*3	0.6031*3	0.6585*3	0.7366*3	0.6826*3	0.7196*3	0.7700*3	0.8315*3
0.4149*3	0.4044*3	0.3919*3	0.3811*3	0.4219*3	0.4148*3	0.4091*3	0.4124*3	0.4283*3	0.4240*3	0.4236*3	0.4360*3
0.3921*3	0.3709*3	0.3459*3	0.3221*3	0.4302*3	0.4256*3	0.4309*3	0.4602*3	0.4596*3	0.4645*3	0.4836*3	0.5286*3
0.3750*7	0.3215*7	0.2673*7	0.2223*7	0.4641*3	0.4701*3	0.4951*3	0.5530*3	0.5257*3	0.5446*3	0.5830*3	0.6448*3

LIPPED Z-SECTION IQ= 3 SIG=55.00

DOWNWARD LOADING A/B=

0.9273*3	0.9315*3	0.9390*3	0.9470*3	0.9634*3	0.9703*3	0.9790*3	0.9875*3	0.9761*3	0.9817*3	0.9861*3	0.9937*3
0.9656*3	0.9684*3	0.9716*3	0.9749*3	0.9910*3	0.9931*3	0.9954*3	0.9973*3	0.9949*3	0.9963*3	0.9975*3	0.9985*3
0.9791*3	0.9801*3	0.9818*3	0.9837*3	0.9964*3	0.9972*3	0.9980*3	0.9987*3	0.9978*3	0.9983*3	0.9987*3	0.9991*3
0.6993*3	0.7017*3	0.7126*3	0.7290*3	0.7354*3	0.7490*3	0.7768*3	0.8188*3	0.7630*3	0.7823*3	0.8164*3	0.8632*3
0.8154*3	0.8186*3	0.8301*3	0.8456*3	0.8765*3	0.8919*3	0.9157*3	0.9436*3	0.9061*3	0.9223*3	0.9440*3	0.9665*3
0.8993*3	0.8910*3	0.8994*3	0.9099*3	0.9460*3	0.9560*3	0.9689*3	0.9817*3	0.9640*3	0.9724*3	0.9820*3	0.9904*3
0.5772*3	0.5728*3	0.5721*3	0.5765*3	0.5877*3	0.5883*3	0.5970*3	0.6199*3	0.5975*3	0.6023*3	0.6185*3	0.6543*3
0.6699*3	0.6638*3	0.6655*3	0.6745*3	0.7060*3	0.7148*3	0.7400*3	0.7852*3	0.7334*3	0.7502*3	0.7849*3	0.8374*3
0.7589*3	0.7541*3	0.7589*3	0.7710*3	0.8167*3	0.8314*3	0.8602*3	0.8998*3	0.8492*3	0.8687*3	0.8992*3	0.9351*3

UPLIFT LOADING A/B=

0.2053*7	0.1875*7	0.1647*1	0.1479*7	0.6817*3	0.7373*3	0.8071*3	0.8894*3	0.8391*3	0.8820*3	0.9295*3	0.9755*3
0.1075*7	0.0940*7	0.0804*7	0.0685*7	1.2293*2	0.0009*8	0.0012*8	0.9872*3	1.0676*2	0.9695*3	0.9472*2	0.9682*2
0.0732*7	0.0611*7	0.0500*7	0.0407*7	0.9752*2	0.9993*3	0.9990*3	0.8376*2	0.8318*2	3.7641*3	0.9514*2	0.9957*2
0.4326*3	0.4160*3	0.3966*3	0.3755*1	0.4991*3	0.5067*3	0.5311*3	0.5907*3	0.5530*3	0.5758*3	0.6225*3	0.7065*3
0.3306*7	0.2919*7	0.2520*7	0.2175*7	0.5811*3	0.6167*3	0.6815*3	0.7817*3	0.7061*3	0.7531*3	0.8195*3	0.8980*3
0.2190*7	0.1856*7	0.1541*7	0.1280*7	0.7025*3	0.7488*3	0.9137*3	0.8964*3	0.8396*3	0.8901*3	0.9288*3	0.9770*3
0.4584*3	0.4458*3	0.4305*3	0.4167*3	0.4710*3	0.4663*3	0.4606*3	0.4713*3	0.4829*3	0.4814*3	0.4876*3	0.5167*3
0.4343*3	0.4078*3	0.3773*3	0.3483*3	0.4925*3	0.4911*3	0.5063*3	0.5603*3	0.5396*3	0.5545*3	0.5940*3	0.6766*3
0.3930*7	0.3327*7	0.2736*7	0.2256*7	0.5501*3	0.5654*3	0.6098*3	0.7015*3	0.6415*3	0.6706*3	0.7395*3	0.8314*3

```
PEKOZ,T                 ****END**** OS17 CJ5939  (1886) 71.348  09.37.01  JOB DEST = UPSON      PEKOZ,T
PEKOZ,T                 ****END**** OS17 CJ5939  (1886) 71.348  09.37.01  JOB DEST = UPSON      PEKOZ,T
PEKOZ,T                 ****END**** OS17 CJ5939  (1886) 71.348  09.37.01  JOB DEST = UPSON      PEKOZ,T
PEKOZ,T                 ****END**** OS17 CJ5939  (1886) 71.348  09.37.01  JOB DEST = UPSON      PEKOZ,T
PEKOZ,T                 ****END**** OS17 CJ5939  (1886) 71.348  09.37.01  JOB DEST = UPSON      PEKOZ,T
PEKOZ,T                 ****END**** OS17 CJ5939  (1886) 71.348  09.37.01  JOB DEST = UPSON      PEKOZ,T
PEKOZ,T                 ****END**** OS17 CJ5939  (1886) 71.348  09.37.01  JOB DEST = UPSON      PEKOZ,T
PEKOZ,T                 ****END**** OS17 CJ5939  (1886) 71.348  09.37.01  JOB DEST = UPSON      PEKOZ,T
PEKOZ,T                 ****END**** OS17 CJ5939  (1886) 71.348  09.37.01  JOB DEST = UPSON      PEKOZ,T
PEKOZ,T                 ****END**** OS17 CJ5939  (1886) 71.348  09.37.01  JOB DEST = UPSON      PEKOZ,T
PEKOZ,T                 ****END**** OS17 CJ5939  (1886) 71.348  09.37.01  JOB DEST = UPSON      PEKOZ,T
PEKOZ,T                 ****END**** OS17 CJ5939  (1886) 71.348  09.37.01  JOB DEST = UPSON      PEKOZ,T
PEKOZ,T                 ****END**** OS17 CJ5939  (1886) 71.348  09.37.01  JOB DEST = UPSON      PEKOZ,T
PEKOZ,T                 ****END**** OS17 CJ5939  (1886) 71.348  09.37.01  JOB DEST = UPSON      PEKOZ,T
PEKOZ,T                 ****END**** OS17 CJ5939  (1886) 71.348  09.37.01  JOB DEST = UPSON      PEKOZ,T
PEKOZ,T                 ****END**** OS17 CJ5939  (1886) 71.348  09.37.01  JOB DEST = UPSON      PEKOZ,T
PEKOZ,T                 ****END**** OS17 CJ5939  (1886) 71.348  09.37.01  JOB DEST = UPSON      PEKOZ,T
PEKOZ,T                 ****END**** OS17 CJ5939  (1886) 71.348  09.37.01  JOB DEST = UPSON      PEKOZ,T
PEKOZ,T                 ****END**** OS17 CJ5939  (1886) 71.348  09.37.01  JOB DEST = UPSON      PEKOZ,T
PEKOZ,T                 ****END**** OS17 CJ5939  (1886) 71.348  09.37.01  JOB DEST = UPSON      PEKOZ,T
```

```
JOB OPTION FROM REMOTE SYS TERMINAL=UPS
//CJ5672 JOB P44ZZZZ,'PEKOZ,T              ',PRTY=7,CLASS=B,REGION=100K  DEST=UPS
/*CREATE DATH                                                          STMT0001
/*

CMSO2 LISTING OF CDS DATH      EDITION - 001
 00001          1          1          2
 00002  .125     .0      .125       .0      .041666667-.08333333
 00003  29500.          11600.          3.14159265359  9.86960440109
 00004   0.3141592653589790 01   0.9424777960769380 01   0.1570796326794900 02
 00005   0.1000000000000000 01  -0.1000000000000000 01   0.1000000000000000 01
 00006  -0.1000000000000000 01   0.1000000000000000 01  -0.1000000000000000 01
 00007   0.0000000000000000 00   0.0000000000000000 00   0.0000000000000000 00
 00008   0.6366197723675810 00   0.2122065907891940 00   0.1273239544735160 00
 00009   0.5000000000000000 00   0.5000000000000000 00   0.5000000000000000 00
 00010   0.4870454551700120 02   0.3945068186877100 04   0.3044034094812580 05
 00011  -0.4934802200544680 01  -0.0000000000000000 00  -0.0000000000000000 00
 00012  -0.0000000000000000 00  -0.4441321980490210 02  -0.0000000000000000 00
 00013  -0.0000000000000000 00  -0.0000000000000000 00  -0.1233700550136170 03
 00014  -0.5362335167120570 00   0.8437500000000000 00   0.4340277777777780 00
 00015   0.9375000000000000-01  -0.3826101650408510 01   0.2929687500000000 01
 00016   0.1736111111111110-01   0.1054687500000000 01  -0.1040583791780140 02
 00017  -0.5362335167120570 00   0.8437500000000000 00   0.4340277777777780 00
 00018   0.9375000000000000-01  -0.3826101650408510 01   0.2929687500000000 01
 00019   0.1736111111111110-01   0.1054687500000000 01  -0.1040583791780140 02
 00020        0         0         2         3         3         3         0         6
```

JOB CJ5672 71.347 CLASS B PRIORITY 07 TIMES AND CHARGES (OCS RATES IN EFFECT AS OF 26 JULY 1971)

#	STEP NAME	TIME STAMP	JOB-STEP TIMES: CPU-SEC	JOB-STEP TIMES: I/O SEC	JOB-STEP TIMES: SEC IN CORE	CHARGES AS RUN: $-CPU	CHARGES AS RUN: $-I/O	CHARGES AS RUN: $-CORE	CHARGES- BEST CLASS: $-CPU	CHARGES- BEST CLASS: $-I/O	I/O OPS	CORE USED
1	COSFUNC	51501.23	.11	.33	.44 @ 100K	.00	.01	.01	.00	.01 A	11	18K
	UNIT TOTALS:		.11	.33	.44						11	
	DOLLAR TOTALS:		$.00	$.01	$.01							

DEDICATED DEVICE CHARGE: $.00 NO. OF DEVICES: 0
JOB TIME STAMP: 51501.26

BEST CLASS FOR JOB WOULD BE	CHARGE IN BEST CLASS WOULD BE	JOB EXECUTION CHARGE AS RUN
A	$.02	$.02

ADDITIONAL CHARGES:
SETUP - $ .00

(ABOVE DOES NOT INCLUDE CHARGES FOR CARDS READ,CARDS PUNCHED, OR LINES PRINTED)

```
********************** * * N E W S   F L A S H * * **********************
*                                                                        *
* DECEMBER 9      ARCHIVE PACK 62 WILL EXPIRE ON WEDNESDAY, DECEMBER 22. *
* DECEMBER 15     ARCHIVE PACK 63 WILL NOT EXPIRE UNTIL AFTER MONDAY, JANUARY 24. *
* DECEMBER 31     JOBS REQUESTING MORE THAN 450K OF CORE WILL BE CANCELLED. *
*                 SEE OCS MEM AN-37 FOR MORE INFORMATION.                *
**************************************************************************
```